Dissolution Rate Enhancement of Poorly Water-Soluble Drugs using Lyophilisation Technology

A thesis submitted to The University of Strathclyde for the degree of Doctor of Philosophy in the

Faculty of Science

October 2010

By

Heba Fathy Mansour

Strathclyde Institute of Pharmacy and Biomedical Sciences,
University of Strathclyde,

Glasgow, United Kingdom

DECLARATION OF AUTHOR'S RIGHTS

This thesis is dedicated to the memory of my father,

Who did his best for me to spread my wings and experience new pastures;

For all his love, kindness, encouragement and support throughout my life.

ACKNOWLEDGEMENTS

Studying for a Ph.D has been one of the most significant academic challenges I have ever faced. Without the support, patience and guidance of the following people, this study would not have been completed. It is to them that I owe my deepest gratitude.

Prof Alex Mullen who undertook to act as my supervisor despite his many other academic and professional commitments. His wisdom, knowledge and commitments to the highest standards inspired and motivated me.

Dr Fiona McInnes whose encouragement, supervision and support throughout enabled me to develop an understanding and perspective in research.

Prof Alastair Florence and his students especially Ryan Taylor and Scott McKellar for assistance in the experimental part of XRPD study.

Anne Goudie and Steve Steer for excellent technical help.

Lee Ann Hodges for her assistance in the in-vivo study.

Manal Alsaadi for her assistance in the HPLC study.

My colleagues, Mohamed Qadir, Issraa Abed-Alrahman, Utsana Puapermpoonsrir, Hibah Al-Dawsari, Jagdishbhai Italia, Vivekanand Bhardwaj, for making SIPBS 218 a great place to work.

Love and thanks to my mother, Inas Abd El-Aal who gave me the moral support I required throughout my study.

My heartfelt thanks and deep appreciation to my husband, Mohamed Osman, without whom, this effort would have been worth nothing. His love, support and constant patience have taught me so much about sacrifice, discipline and compromise.

Lastly, I offer my regards and blessings to all of those who supported me in any respect during the completion of the project.

ABSTRACT

Glibenclamide, spironolactone and ketoconazole are hydrophobic drugs that have poor oral bioavailability. Lyophilisation and different water-soluble excipients (SLS, mannitol, PEG 6000, gelatin, tromethamine, citric acid, fumaric acid) were employed to enhance their rate and extent of dissolution. In-vitro dissolution studies for the lyophilised formulations revealed that lyophilisation significantly enhanced the dissolution rate of glibenclamide and ketoconazole (in the first few minutes only) and negatively affected that of spironolactone. The dissolution rates of all three drugs from their lyophilised mixtures with the water-soluble excipients (except citric acid) were further enhanced compared to the lyophilised drugs alone. Solid state characterisation (XRPD, FT-IR, DSC and TGA) of the lyophilised systems revealed the transformation of the drugs to amorphous forms. Enteric or non-enteric coatings were applied to capsules containing selected lyophilised systems. The coating process did not alter the stability of the amorphous forms of glibenclamide or ketoconazole, while that of spironolactone showed a low incidence of recrystallisation. The coated formulations were stored under different conditions; 25ºC/75% RH, 25ºC/65% RH, 25ºC/0% RH, 37ºC/0% RH and 50ºC/0% RH for up to 90 days. The stored samples were physically characterised and tested for dissolution. The amorphous form of glibenclamide was maintained during storage while spironolactone exhibited recrystallisation during storage at 65% or 75% RH. Ketoconazole showed a complete change in its colour and consistency under different storage conditions, suggesting drug degradation. In-vivo performance of the lyophilised formulation of glibenclamide/SLS was investigated in two male beagle dogs. The lyophilised system achieved significantly higher C_{max} and AUC_{0-360} and lower T_{max} values than that achieved by the commercial tablets, suggesting a higher rate and extent of glibenclamide absorption. This enhancement in the drug absorption was attributed to the higher rate and extent of dissolution of the drug from these formulations compared to the commercial tablets.

PUBLICATIONS

Mansour, H, McInnes, F, Florence, A. and Mullen, A. (2009) The role of lyophilisation in the enhancement of glibenclamide release from hard gelatin capsules. J. Pharm. Pharmacol., 61: A38-A39, Meeting abstract:50.

Mansour, H., McInnes, F. and Mullen, A. (2010) In situ lyophilisation for release enhancement of ketoconazole from hard gelatin capsules. UKICRS Symposium.

Mansour, M., McInnes, F., Hodges, L. A., Alsaadi, M., Mullen, A. In-vivo performance of lyophilised glibenclamide capsule formulations following oral administration to beagle dogs. (In preparation).

CONTENTS

Chapter 1

1. Introduction

1.1 Overview

Drug delivery aims to permit the safe and efficacious delivery of pharmaceutical compounds to humans or animals. The most common methods of drug delivery include oral, nasal, pulmonary, topical, parenteral and rectal routes. Oral drug delivery is the most predominant route and has the highest degree of patient compliance. Due to higher stability, ease of production and accuracy of dosage, solid oral dosage forms have several advantages over other dosage forms. Therefore, most of the new active pharmaceutical ingredients under development are likely to be formulated as a solid dosage form that will provide high bioavailability after oral administration (Ikegami et al., 2006; Charman & Charman, 2003).

According to the Biopharmaceutical Classification System (BCS), drugs are categorised into four groups (Figure 1.1) depending on their solubility and permeability characteristics (Amidon et al., 1995):

- **Class I** compounds have both high aqueous solubility and gastrointestinal permeability and greater than 90 % of an administered dose would get absorbed.

- **Class II** compounds have high permeability and low aqueous solubility in relation to the administered dose. These compounds have been reported to account for at least 40% of new chemical entities (Lai et al., 2009). They have poor bioavailability after oral administration (Charman & Charman, 2003) which potentially decreases their clinical efficacy (Pouton, 2006).

- **Class III** compounds have high aqueous solubility but low permeability through the gastrointestinal membrane thereby limiting possible drug bioavailability.

- **Class IV** compounds have neither good aqueous solubility nor gastrointestinal permeability for absorption to be complete.

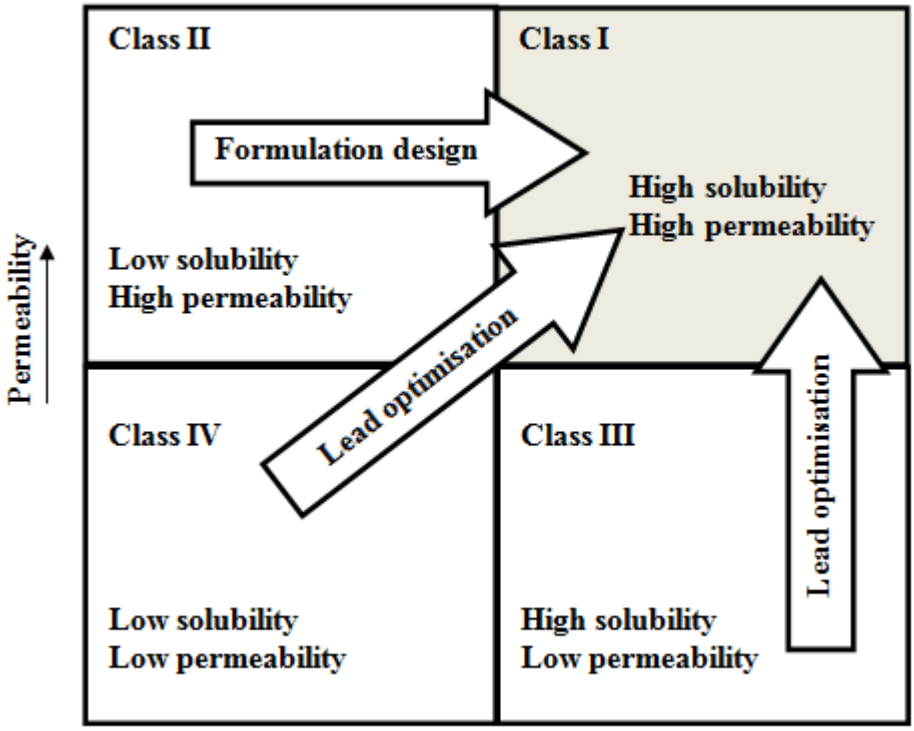

Figure 1.1: A typical representation of the biopharmaceutical classification system (Pouton, 2006).

The bioavailability of both Class III and IV compounds that have low gastrointestinal permeability is often difficult to improve by formulation strategies as this usually necessitates altering, often permanently, the permeability of the gastrointestinal tract which is undesirable. A good approach to improve the bioavailability of such compounds is to go back to the discovery lead optimisation phase (chemical approaches) and design drugs with better physicochemical properties (Figure.1.1 Pouton, 2006). This however is not always possible without compromising structure-activity relationships. Improving formulation design can, however, lead to enhancement of the solubility of Class II compounds and so achieve bioavailability similar to those of Class I compounds. Many promising drugs are absorbed only in the uppermost part of the small intestine, in spite of their high permeability, showing a narrow absorption window. Consequently, if such Class II compounds are not fully released and dissolved in this gastrointestinal region, they will exhibit a low bioavailability (Streubel et al., 2006). Thus, approaches that enhance the water solubility of Class II drugs are considered by the pharmaceutical industry to be one

of the most useful approaches for optimisation of Class II compounds, which is the approach this thesis will focus on. These approaches will be discussed in detail later after considering the anatomy and variable physiological conditions within the gastrointestinal tract (GIT) that may affect formulation behaviour and drug absorption.

1.2 Gastrointestinal tract

1.2.1 Anatomy and function

The GIT is a hollow tube starting from the mouth to anus (Figure. 1.2). Based on function, it is divided into the following sections: oesophagus, stomach, small intestine, colon, rectum, and anus.

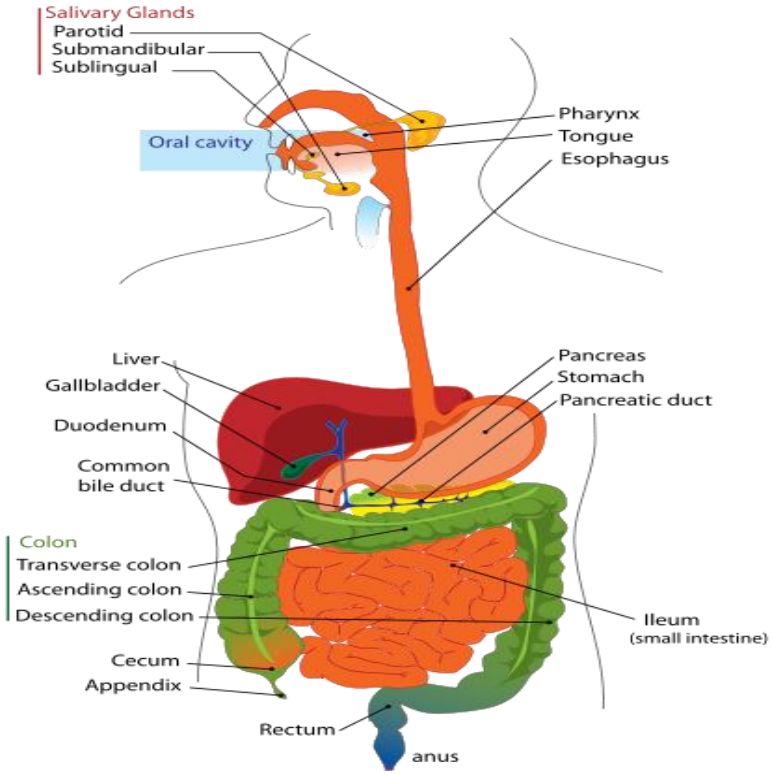

Figure 1.2: Anatomical structure of the gastrointestinal tract (retrieved from http://www.dentalarticles.com/visual/d/gastrointestinaltract.php, October 2010).

The walls of the GIT are organised into a number of distinct layers. These layers are the mucosa (the inner coating), submucosa (layer below the mucosa), muscle layer and serosa (Stendal, 1997). The most important layer is the mucosa through which drug absorption takes place.

1.2.1.1 Oesophagus

The main function of the oesophagus is to transfer food to the stomach. It consists of muscular tube, about 25 cm long with two sphincters. The upper sphincter controls the entry of material to the oesophagus while the lower one controls the exit of material (Stendal, 1997). Generally, transit time of a dosage form through the oesophagus is about 5-15 seconds, depending on posture and concurrent water ingestion at administration time (Wilson, 2000).

1.2.1.2 Stomach

The stomach is a 'J' shaped region of the GIT, connected to the oesophagus from the upper part and to the duodenum from the lower part. It has four main areas: the cardia, fundus, body, and pylorus. The stomach has five main functions: food reservoir; grinding and mixing of food; chemical break down of food; eradication of ingested microbes; and controlling of emptying of gastric contents into the duodenum (Stendal, 1997). Several minutes after food passage into the stomach, mechanical digestion starts. Food is macerated and mixed with the secretions from gastric glands by peristaltic movements, mild mixing, waves that start every 20 seconds. Food mixed with gastric secretions forms a thin liquid known as chyme. Gastric emptying takes place when peristaltic movements push chyme to the duodenum through the pyloric sphincter. The major process of chemical digestion in the stomach is the start of protein digestion by the enzyme pepsin (Tortora & Grabowski, 2003).

The stomach pH differs depending on the presence or absence of food. In the presence of food, the pH is initially between 3-7 followed by decrease to pH 1-2

within 3-4 hours as a result of gastric HCL acid secretion (Dressman et al., 1998; Horter & Dressman, 2001).

The retention times of formulations in the stomach are dependent on the size of the formulations (Gröning et al., 2007) and whether or not the formulation is consumed with a meal (Doran, et al., 1998). Multiparticulate dosage forms also empty more slowly in the presence of food. Because the dosage forms mix uniformly with the food, passage into the small intestine will be influenced by the composition of the ingested food. An appreciation of these factors can allow prediction of when drug release may be realised and/or started.

1.2.1.3 Small intestine

The small intestine has a diameter of 2.5 cm and a length of about 6 m (Tortora & Grabowski, 2003). It is divided into three segments: the duodenum (20-30 cm long), the jejunum (2.5 m long), and the ileum (2.5 m long).

The main function of the small intestine is to permit absorption of the digested food released from the stomach into the systemic circulation through the epithelial lining. Most of the absorption takes place in the duodenum and jejunum. Before absorption, incompletely digested proteins, fats and carbohydrates are broken down to monosaccharides, fatty acids and amino acids in the small intestine.

The acidic gastric contents (chyme) are emptied through the pyloric sphincter into the duodenum which forms a 'C' shape around the head of the pancreas. The pancreas secrets proteases, lipases and amylase into the duodenum as a result of the presence of food. Furthermore, the pancreas secrets mucus which contains bicarbonate to neutralise the acidic gastric chyme (Tortora & Grabowski, 2003). On the other hand, liver secrets bile that is stored and concentrated in the gall bladder and discharged through the bile duct into the duodenum. Bile is necessary for absorption of dietary fat and augments the absorption of lipophilic drugs. It consists of bile acids, bile pigments, cholesterol, phospholipids and plasma electrolytes.

The pH of the small intestine varies across its length and increases from pH 5 to 6.5 at the duodenum to the ileum. Acidic chyme initially lowers the pH (in the duodenum) which is re-established by the pancreatic bicarbonate secretion (Horter & Dressman, 2001). Intestinal contents are continually mixed by short, stationary segmental contractions. A small-intestinal transit time in healthy volunteers has been reported to be about 3.5 – 4.5 h (Wilson, 2000).

Most of drug absorption takes place in the small intestine rather than the stomach or the large intestine due to large surface area available for absorption as a result of the presence of numerous villi and microvilli that increase the surface area by several folds. In the GIT, drugs have to pass through a monolayer epithelium to the systemic circulation. Thus, the permeability of the GIT membranes or the lipophilicity of drugs is the major determinant for the extent of oral drug absorption. It is known that drug lipophilicity is dependent on octanol-water partition coefficients (log P) and according to Lipinski's Rule of Five, the orally active drugs (lipophilic) should have log P values less than 5 (Pang, 2004).

Drugs can transport across the GIT membranes by trancellular (across cells) or paracellular (between cells) transport. Most drugs transport to the systemic circulation through trancellular pathway, which include passive diffusion and carrier-mediated (active) transport. Low molecular weight hydrophilic drugs can cross the GIT membranes through paracellular pathway or tight junctions. Tight junctions are continuous strands of junctional membrane proteins that connect adjacent cells and contain slight gates or pores filled with water. These pores can open and close regulating parcellular transport of a drug depending on its size, shape and charge. In addition, the small intestine has various apical cationic and anionic transporters known as P-glycoproteins (membrane-associated proteins). These are present within the enterocytes that are abundant at the tips of the villi. These proteins are known as ABC or ATP-binding cassette and act as transporters for different molecules across extra- and intra-cellular membranes (Pagliara et al., 1999).

1.2.1.4 Large intestine

The large intestine is the last part of the GIT. It is divided into four principal regions: caecum, colon (ascending, transverse, descending, and sigmoid), rectum, and anal canal. There are two types of motility in the colon; segmental and propulsive which are responsible for movement within the colon and mixing of the colonic contents respectively. The main functions of the large intestine are the absorption of electrolyte, absorption of water from the undigested food, secretion of mucus, production of certain vitamins, formation of faeces and the expulsion of faeces from the body.

Transit through the large intestine is variable between humans and can be as short as a few hours to a number of days. In fact, the large intestine is inhabited by several species of bacteria that perform different functions. These bacteria metabolise undigested polysaccharides (fibres) resulting in formation of short-chain fatty acids that are absorbed by passive diffusion across the colonic mucosa. The large intestine secrets bicarbonate that neutralise the increased acidity resulting from fatty acid formation. Furthermore, these bacteria produce some vitamins such as vitamin K and biotin, which are absorbed into the blood circulation. On the other hand, bacterial fermentation of the undigested polysaccharides produces mixture of gases such as nitrogen and carbon dioxide along with trace amounts of hydrogen, methane and hydrogen sulphide.

1.2.2 Factors affecting drug absorption in gastrointestinal tract

1.2.2.1 Dissolution

Drug dissolution in the GI tract is a prerequisite for absorption after oral administration and the rate-limiting step in the intestinal absorption of class II compounds (Fagerholm, 2007; Wilding, 1999). The dissolution rate is highly affected by the physicochemical characteristics of the drug and by the physiological conditions of the GI tract (Dahan & Amidone, 2008). According to Noyes-Whitney equation (Eq. 1.1), the dissolution rate is directly proportional to saturation solubility of the drug in solvent.

$dm/dt = KA(Cs-C)$ (Equation.1.1)

Where:

- m is the mass (mg) of drug passed into solution in time t (min) while dm/dt is the dissolution rate (mg/min);
- A is the surface area available for dissolution (cm^2);
- Cs is the saturation solubility of the drug in solvent at experimental temperature (mg/ml);
- C is the concentration of solute (mg/ml);
- K is the intrinsic dissolution rate constant (cm^2 $seconds^{-1}$ ml^{-1}) whereas $K= D/Vh$ (Equation.1.2)
- D is the diffusion coefficient of the drug in dissolution medium (cm^2/second);
- h is the thickness of the boundary layer adjacent to the dissolving drug surface (cm);
- V is the volume of dissolution media (ml).

According to Noyes-Whitney equation, as the surface area of the solute decreases, the dissolution rate decreases. The volume of dissolution medium should be sufficient to avoid reaching zero value for (C_s-C) in a certain system. Thus, sink conditions should be attained. These conditions can be achieved in practice if the dissolved solute is removed from the bulk solution at a faster rate than it is dissolved. This takes place in-vivo when the drug is absorbed more rapidly than it dissolves in the GIT fluids.

The majority of drugs are absorbed across gastrointestinal membrane by passive diffusion, so the absorption rate depends on the concentration gradient across the two sides of the membrane. An increase in the dissolution rate leads to increase in the concentration gradient and subsequently increase in the absorption rate. If the dissolution rate is lower than the absorption rate, dissolution will be the rate-determining step for the gastrointestinal absorption. In this situation, drug particle size has an essential role in drug absorption through GIT.

As the dissolution rate is the main limiting step to absorption of Class II drugs, correlation of in-vivo results with in-vitro dissolution data (IVIVC) is a promising approach (Dressman & Reppas, 2000). According to the definition by Food and Drug Administration (FDA), IVIVC is a predictive mathematical model describing the relationship between an in-vitro property of a dosage form and an in-vivo response. In general, the in-vitro property is the rate and extent of drug dissolution while the in-vivo response is the concentration of drug in plasma or the amount of drug absorbed.

The most important role of establishing IVIVC is to use in-vitro dissolution test as a substitute for in-vivo studies. The advantage of this is to reduce the number of bioequivalence studies carried out during the early approval process and during the scaling-up and post-approval changes.

1.2.2.2 Particle size

The particle size of drug powder has a highly significant effect on its dissolution rate. The smaller the particle size, the higher the surface area, and the faster the dissolution rate (Dressman et al., 2007; Lobenberg et al., 2000). Furthermore, it is worth to know that the surface area available to the dissolution medium (wetted surface) is the important factor and not the actual particle size. This is very important in the case of a very poorly water-soluble drug in a dissolution fluid that has poor wetting characteristics, as a decrease in particle size may actually decrease the dissolution rate due to agglomeration of the drug particles (Kostewicz et al., 2002, Takano et al., 2006).

1.2.2.3 Polymorphism and amorphous formation

Several drugs can crystallise in different physical forms or polymorphs that have different arrangement of molecules in the crystal lattice. These different polymorphs have different lattice free energies and hence exhibit different physicochemical properties, such as melting point, heat of fusion, density, and refractive index. In addition, the flow of powders is variable between different crystalline forms (Singhal

& Curatalo, 2004). As the lattice free energies or the forces between molecules are different among polymorphs, their solubility is also different. Consequently, the dissolution rate and bioavailability is different for different polymorphs. However, the polymorph that has high free energy is unstable and tends to transform into the more stable crystalline form with time. This is considered a serious disadvantage of using a more unstable (water-soluble) polymorph of a drug substance in formulations. For example, the HIV protease inhibitor, ritonavir, formulated using the less stable but more soluble polymorph, converts to the more stable but less soluble polymorph during storage (Bauer et al., 2001).

Amorphous forms of solids (will be discussed later in Section 1.2.3.7) are characterised by lack of long range three dimensional structure of crystals leading to high free energies and subsequently high solubility. However, the amorphous form is thermodynamically unstable and tends to transform to the stable crystalline form in response to different stresses such as moisture and temperature (Strydom et al., 2009). Therefore, determination of the solubility of amorphous powders is complicated (Hancock & Parks, 2000).

1.2.2.4 Ionisation pK_a of drugs

Several poorly water-soluble drugs are either weak acids or bases. The degree of ionisation and consequently the aqueous solubility of acidic or basic drugs are influenced by GIT pH. The percent of drug molecules ionised at a given pH can be described by the Henderson-Hasselbach equation (Eqs. 1.3, 1.4).

$$pH = pK_a + \log \frac{[A^-]}{[HA]} \qquad \text{(Equation 1.3)}$$

$$pH = pK_w - pK_b + \log \frac{[B]}{[BH^+]} \qquad \text{(Equation 1.4)}$$

Where:

- pK_a is the negative logarithm of dissociation constant of acid K_a.
- pK_b is the negative logarithm of dissociation constant of base K_b.
- pK_w is the negative logarithm of dissociation constant of water K_w.

- pH is the negative logarithm of the concentration of hydrogen ions.
- $[A^-]$ and [HA] is the concentration of ionised and unionised acid respectively.
- [B] and $[BH^+]$ is the concentration of unionised and ionised base respectively.

According to the Henderson-Hasselbach equation, it can be concluded that the degree of ionisation and consequently the solubility of weakly acidic drugs increase in basic media (above the pK_a) while those of weakly basic drugs increase in acidic media (below the pK_a).

1.2.2.5 Bile secretion

Bile is secreted by liver hepatocytes and it consists of high percentage of natural bile salts. Bile salts are the salts of bile acids such as cholic, deoxycholic, chenodeoxycholic, and lithocholic acids, which in turn may conjugate to glycine or taurine. Bile is stored in the gall bladder before being released into the small intestine. The presence of fatty foods in the small intestine induces the release of cholecystokinin hormone, which stimulates contraction of the gall bladder resulting in the release of bile into the duodenum. Bile salts act as powerful surfactants and hence may increase the bioavailability of hydrophobic drugs by dissolution enhancement via increased wettability and solubility through micellar solubilisation (Luner, 2000; Luner & Kamp, 2001; Sheng et al., 2006). However, the enhanced dissolution rate may be drug specific. Whilst bile salts enhance the solubility of many drugs e.g. ketoconazole and griseofulvin (Calafato & Picó), it lower the solubility of others e.g. pafenolol, by formation of poorly soluble complexes (Lennernas & Reghard, 1993).

Most of the excreted bile acids are reabsorbed in the terminal ileum by active transport mechanisms and are transported back to the liver and the gall bladder through enterohepatic circulation. This permits a low rate of daily production and high discharge into the digestive system.

1.2.2.6 Gastrointestinal pH

The solubilisation/dissolution of nonionisable drugs is not affected by changes in pH along the GI tract, while the dissolution of ionisable compounds is (Balakrishnan et al., 2004). In general, aqueous solubility is directly proportional to the number of hydrogen bonds, which can be formed with water. Thus, ionisable drugs generally exhibit more aqueous solubility than do unionisable drug molecules. Along the GI tract, a drug is exposed to a wide range of pHs that can further vary in response to the presence of food (see Section 1.2.1.2). Generally, the pH values within the stomach are lower than those within the small intestine. Moreover, the pH within the small intestine is much less dependent on food intake and rises slowly from the proximal to the distal segments exhibiting a range of 4.4 - 7.4 (Dressman et al., 1998; Kalantzi et al., 2006).

Weakly basic drugs ionise and dissolve quickly in the acidic medium of the stomach. As a drug passes from the stomach to the duodenum, the degree of the drug ionisation decreases as a consequence of increased intraluminal pH, that may lead to drug precipitation and consequently decreased absorption (Galia et al., 1998; Kalantzi et al., 2006 b). On the other hand, weakly acidic drugs ionise in the small intestine resulting in rapid dissolution and improved bioavailability (see Section 1.2.2.4).

1.2.2.7 Gastrointestinal transit

Gastrointestinal transit includes gastric residence time or gastric emptying, and the intestinal transit time. As the dissolution rate of class II drugs is expected to be slower than the time taken for gastric emptying, this factor has no significant effect on the intestinal absorption of this group of compounds. Intestinal transit on the other hand, significantly affects absorption of this group. Long transit time of a hydrophobic drug in the main absorption site allows for more dissolution and hence, absorption increases. The average small intestinal transit time ranges between 3 and 4 hours (Yu & Amidon, 1999; Yu et al., 1996). It has been reported that the intestinal transit time is fixed and independent on food intake or the physical

characteristics of the administered formulation (Kenyonet al., 1995; Clarke et al., 1995). However, a recent study revealed that the small intestinal transit time of a model placebo tablet formulation when administered 45 minutes before food was significantly shorter than that administered in the fed (directly after food) or fasted state (Fadda et al., 2009).

1.2.2.8 Volume of fluid in the gastrointestinal tract

The volume of the dissolution medium in the GI tract depends on the volume of fluid that is co-administered with the medication and the net balance of water in the gut following gastrointestinal secretion and resorption processes. As the volume of the dissolution medium increases, more drug as a percentage dissolves. In the stomach, the fluid volume can range from 300 - 500 ml in the fasting-state to 800 – 900 ml in the fed-state; in the small intestine, the fluid volume can range from 500 ml in the fasting-state to 900-1000 ml in the fed-state (Dressman et al., 1998; Custodio et al., 2008; Dressman & Reppas, 2000). Mixing of chyme with an administered dosage form in the gastrointestinal tract influences the thickness of the fluid layer surrounding drug particles and consequently affects the drug dissolution rate and absorption. In addition, the viscosity of the luminal fluid increases by the presence of food and hence, the dissolution rate and bioavailability of a drug may also be reduced.

1.2.2.9 Presence of food

Food may affect the drug bioavailability and can either enhance, delay or reduce drug absorption. Presence of food in the stomach results in increased gastric secretion, prolonged residence time and delayed gastric emptying. Gastric residence time depends on the volume and contents of chyme. It increases by increasing chyme volume and in the presence of chyme of low pH and high osmolarity (Winstanley & Orme, 1989). Thus, when a drug is administered with a meal, the rate of its absorption will be lower than that in the case of fasted state. The bioavailability of some drugs can be increased by the presence of food as it increases fluid volume

and gastric residence time resulting in complete drug dissolution before passage into the small intestine which has the highest surface area for drug absorption. Particularly, some hydrophobic drugs such as griseofulvin and mebendazole, when administered as solid dosage forms may not dissolve readily in the stomach. However, the bioavailability of these drugs can be improved when they are taken with a very fatty meal due to formation of drug solution in the dietary oil (Winstanley & Orme, 1989). On the other hand, the bioavailability of acid labile drugs can be reduced by the effect of food due to prolonged exposure to the acidic gastric secretion.

Moreover, it has been reported that the effect of the drug particle size on its dissolution rate is dependent on food intake. For example, smaller particle size of DPC 961, a reverse transcriptase inhibitor (BCS class II), had a great enhancing effect on its dissolution rate in the fasting state while it had no effect in the fed state. This might be because of differences in the capacities of solubilisation in the fed and fasting states (Aungst et al., 2002).

1.3 Approaches for enhancement of dissolution rate and gastrointestinal absorption of hydrophobic drugs

The free energy of a solid compound establishes the capability of the solid to dissolve in a solvent system. For a solid to dissolve, its free energy should be higher than the solvent free energy. When the free energies of both the solvent and the solid becomes the same, saturation equilibrium is achieved (Grant & Brittain, 1995). Thus, the solubility of a hydrophobic drug can be enhanced by increasing the drug free energy at constant pressure and temperature. This can be achieved by several approaches such as alteration of the polymorphic form; formation of an amorphous form; and reduction of drug particle size that increase the equilibrium solubility (Grant & Brittain, 1995). Other approaches for dissolution and bioavailability enhancement include adjustment of pH; use of a co-solvent system; use of a prodrug; formation of salt, formation of a solid dispersions, complexation with cyclodextrins and use of polymers and surfactants.

1.3.1 Prodrug

A prodrug is a derivative of an active compound that transforms in the body to the parent drug by metabolic processes. The enhanced solubility of the prodrug and high membrane permeability of the parent drug are considered the driving force for bioavailability improvement (Dahan & Hoffman., 2007). For example, it has been reported that the aqueous solubility and bioavailability of a poorly water-soluble drug amprenavir, a HIV protease inhibitor, were significantly enhanced by the formation of the phosphate ester prodrug (Brouwers et al., 2007). The prolonged time spent in the development stages of the prodrug and the further studies required to assess its toxicity and pharmacokinetics are considered the main disadvantages of this strategy (Kim & Park 2004). Also, the rapid transformation of the water-soluble prodrug in the biological media of the GI tract to the insoluble form can limit its absorption. Hence, the enhanced solubility achieved by this approach does not always lead to bioavailability enhancement (Fleisher et al., 1996). Consequently, the water-soluble prodrug strategy is seldom employed for improving the oral delivery of hydrophobic compounds.

1.3.2 Co-solvents

The solubility of non polar drugs in an aqueous medium can be improved by the addition of water-miscible solvents to the aqueous system. Most of the co-solvents have hydrogen accepting and donating functional groups which induce miscibility with water through hydrogen bonding formation (Yalkowsky, 1999). The mechanism of solubilising ability of co-solvent system is the modification of solution polarity and interference with hydrogen bonding between water molecules (Millard et al., 2002). Co-solvents are either liquids or solids that have high water solubility such as polyethylene glycols and polyvinylpyrrolidone (Yalkowsky, 1999). The most frequently used solvents are the water soluble solvents such as polyethylene glycol 400 and ethanol or water insoluble organic solvents such as long and medium chain triglycerides. Hydrophobic drugs can be dissolved employing one (binary), two (tertiary) or more organic solvents.

1.3.3 pH adjustment

Adjustment of pH is considered one of the most simplest means of enhancing solubility of ionisable drugs. Weakly acidic drugs ionise and can form water-soluble salts at pH above their pK_a values while weakly basic drugs ionise and can form water-soluble salts at pH below their pK_b values (discussed in Section 1.2.2.1.4). It has been reported that one unit increase in pH results in a ten-fold increase in the solubility of a monovalent acid, one hundered-fold for a divalent acid and one thousand-fold for a trivalent acid (Yalkowsky, 1999). The probability of tissue damage by very high or low pH and the precipitation of drugs upon mixing or dilution with other liquids are considered the main limitations of this approach. Furthermore, some buffers can not be used for pH adjustment in human due to their toxicity.

1.3.4 Particle size reduction

According to the Noyes-Whitney equation (Section 1.2.2.2), dissolution rate and consequently bioavailability of hydrophobic drugs can be increased by increasing the surface area which is subjected to the biological fluids in the gastrointestinal tract. This can be achieved by reduction of the particle sizes of these poorly water-soluble drugs. It has been reported that this approach was used to enhance the bioavailability of many drugs. These drugs include griseofulvin, digoxin, nitrofurantoin, tolbutamide, naproxen and ibuprofen (Ashford, 2002). Micronization which involves the disruption of large crystals is considered one of the earliest methods designed to achieve reduced particle size. The air-jet milling has been used for many years for micronization of drug crystals to particle size ranging from 2 -5 µm (Pouton, 2006). Other methods include ball milling (Merisko-Liversidge et al., 2003) and high-pressure homogenisation (Lai et al., 2009). However, all these methods have many drawbacks, due to the process of mechanical disruption and heat generation that can lead to changes in the drug surface properties (Mackin et al., 2002; Ticehurst et al., 2000). These changes include phase transitions such as polymorphic transitions and dehydration (Zhang et al., 2004). Milled powders can exhibit particle agglomeration and poor wettability. Therefore, the increase in the

dissolution rate may not be as high as expected from the increase in the surface area (Rasenack & Müller, 2002).

1.3.5 Solid dispersion

Poor water solubility and related problems of slow dissolution and low bioavailability can be overcome by the technique of solid dispersion formation. The word 'solid dispersion' has been used to explain a group of dosage forms in which the drug is dispersed in an inert carrier. The carrier may be either amorphous or crystalline and the drug can be dispersed either in an amorphous or crystalline form (van Drooge et al., 2004a). Chiou and Riegelman (1971) specifically defined these structures as 'the dispersion of one or more active ingredients in an inert carrier matrix at solid-state prepared by the melting (fusion) or solvent method'. Corrigan (1985) recommended the meaning to be 'product formed by converting a fluid drug-carrier combination to the solid state'. Practically, these dosage forms have been generally employed for enhancement of in-vitro release and bioavailability of hydrophobic drugs relative to usual dosage forms (Vasconcelos et al., 2007; Ahuja et al., 2007; Newa et al., 2008; Zahedi & Lee, 2007; Modi & Tayade, 2006; Laitinen, et al., 2009; Fukushima et al., 2007). Commonly used carriers are sugars and water-miscible or water-soluble polymers such as polyethylene glycols (PEGs) and polyvinylpyrrolidone (PVP). However, the definition of solid dispersion has been recently expanded to include water insoluble carriers such as Gelucires and Eudragits.

Solid dispersion technique has been employed extensively by several researchers for dissolution and bioavailability enhancement. It has been reported that the dissolution rate of indomethacin was enhanced through formation of a fully amorphous solid dispersion of the drug with porous silica (Takeuchi et al., 2005). Furthermore, some previous studies showed that solid dispersions are suitable for tablet formulations for delivery of Delta(9)-tetrahydrocannabinol to the GI tract (van Drooge et al., 2004b) and for preparation of sublingual tablets (van Drooge et al., 2005). The expected bioavailability improvement due to solid dispersion formation was supported by many in-vivo studies using different drugs such as carbamazepin and albendazole

(El-Zein et al., 1998; Kohri et al., 1999). Solid dispersions can be classified into simple eutectic mixtures and solid solutions.

1.3.5.1 Simple eutectic mixtures

A simple eutectic mixture is described as a mixture of two substances that have very restricted miscibility in the solid state but totally miscible in the liquid state (one component is soluble in the melt of the other). In this system, both the drug and the carrier exist in a crystalline state refering to a crystalline solid dispersion. The melting point of an eutectic solid dispersion is below the melting points of individual components. They are generally prepared by quick cooling of the co-melt of both substances which crystallise out concurrently giving a physical mixture of very fine crystals of the two components. When a eutectic mixture, consisting of a hydrophobic drug and a water-soluble carrier is introduced into an aqueous medium, the carrier dissolves fast, releasing very fine drug crystals (Leuner & Dressman, 2000). The resultant suspension has large surface area leading to enhanced dissolution rate and hence, better bioavailability. The bioavailability of ABT-963 (a cyclooxygenase-2 inhibitor) has been improved by the formation of a eutectic mixture with Pluronic F-68 (Chen et al., 2004). Also, the dissolution rate and bioavailability of ibuprofen have been enhanced from the binary solid dispersion with poloxamer 188 due to eutectic formation (Newa et al., 2007). The eutectic solid dispersions of ibuprofen, fenofibrate and flurbiprofen with PEG (3350, 8000 or 20000) have been investigated. It was found that the dissolution rate of flurbiprofen increased as the molecular weight of PEG decrease, due to increase of the drug/carrier interactions (Vippagunta et al., 2007).

1.3.5.2 Solid solutions

A solid solution is similar to a liquid solution as it consists of only one phase corresponding to the number of components. In a solid solution, a drug particle size is considerably reduced to its absolute minimum and the dissolution rate of the drug is dependent on the carrier dissolution rate. By careful choice of the carrier, a drug dissolution rate can be considerably increased. According to the miscibility of the

components, solid solutions can be categorised to continuous and non-continuous solid solutions. Moreover, they can be categorised according to the way of distribution of solvate molecules within the solution to substitutional, interstitial or amorphous solid solutions (Leuner & Dressman, 2000).

- **Continuous solid solutions**

A continuous solid solution is characterised by complete miscibility of the components. hypothetically, this means that the interaction between the solution components is stronger than the bonding between the molecules of individual components. Furthermore, on the molecular level, this type of solid solution has a homogeneous structure as only one phase exists (van, Drooge et al., 2006). PVP-diazepam solid solution prepared by fusion and inulin-diazepam solid solution prepared by spray freeze drying are examples of this group of solid solutions (van, Drooge et al., 2006). Moreover, it has been reported that perphenazine was molecularly dispersed within PVP K30 or PEG 8000 which resulted in a marked dissolution rate enhancement of the drug (Laitinen et al., 2009).

- **Discontinuous solid solutions**

A discontinuous solid solution is characterised by limited solubility of the components in each other. On the molecular level, the resultant solution does not have homogeneous composition, but it is separated into two phases. In this type of solid solution, the communal solubilities of the components should be more than 5% and if the temperature decreases below a definite limit, the communal solubilities decrease (Leuner & Dressman, 2000). Solid solutions of carbamazepine or nifedipine with PEG 1500 are examples of this type of solid dispersion and have been reported to exhibit significant dissolution rate enhancement for both drugs (Bley et al., 2010).

- **Substitutional crystalline solid solutions**

A substitutional crystalline solid solutions are traditional solid solutions with a crystalline structure. In this system, drug molecules either replace carrier molecules or fit into the spaces between the carrier molecules in the crystal lattice. For

substitution to take place, the size of the drug molecules should not differ by more than 15% from that of the carrier molecules (Leuner & Dressman, 2000). This class of solid solutions is represented by the solid solutions of iron–copper hexacyanoferrates (Schwudke et al., 2000).

- **Interstitial crystalline solid solutions**

In this class of solid solutions, the drug molecules reside in the spaces between the carrier molecules in the crystal lattice. Similar to substitutional crystalline solid solution, the relative molecular size is a critical measure for categorising the solid solution type. In this type of solid solutions, the diameter of drug molecules should not be more than 59% of the diameter of carrier molecules. Moreover, the volume of the drug molecule should not exceed 20% of that of the carrier molecule (Leuner & Dressman, 2000). Solid solutions of rofecoxib with each of urea, mannitol or sorbitol represent this class of solid solutions and has been reported to enhance the drug dissolution rate (Ahuja et al., 2007).

- **Amorphous solid solutions**

In this class, the drug molecules are molecularly but unevenly dispersed within the amorphous carrier. The first amorphous solid solution was prepared by Chiou and Riegelman (1969) using grisofulvin in citric acid. Urea and sugars such as sucrose, dextrose and galactose are examples of other carriers that were used in earlier studies. As polymers often have amorphous nature, these carriers are suitable for formation of amorphous solid solutions. Polymers such as polyvinylpyrrolidone (PVP), polyethylene glycols (PEGs) and different cellulose derivatives have been recently employed for preparation of this type of solid solutions. Konno and Taylor (2008) have investigated the dissolution rate enhancement of felodipine through formation of an amorphous solid dispersion of the drug with PVP, hydroxypropyl methylcellulose (HPMC) or hydroxypropyl methylcellulose acetate succinate (HPMCAS). Representing this class, Irbesartan-tartaric acid solid solution has been reported to enhance the solubility of irbesartan by 9.5 times over that of the crystalline drug (Chawla & Bansal, 2008). Celecoxib-polymethacrylate amorphous

solid solution has been reported to significantly enhance the drug dissolution rate (Albers et al., 2008).

1.3.5.3 Mechanisms of dissolution enhancement of hydrophobic drugs by solid dispersion technique

Solid dispersions represent the maximum particle size reduction for hydrophobic drugs and consequently, large surface area leading to dissolution enhancement and hence, bioavailability improvement (Vasconcelos, 2007). Moreover, the solubility enhancement of drugs in solid dispersion formulations is strongly related to the improvement of the drug wettability achieved by this technique (Karavas et al., 2006). Drug particles in solid dispersion have also been reported to have a highly porous structure that greatly enhances the drug release rate (Vasconcelos, 2007). In addition, by selection of carriers, amorphous solid dispersions can be obtained. This amorphous structure can be stabilised by specific interactions such as hydrogen bonding between poorly water-soluble drugs and carriers (Vippagunta et al., 2007). These amorphous states of the hydrophobic drugs tend to have higher solubility and bioavailability (Pokharkar et al., 2006). However, solid dispersion strategies resulting in amorphous formation are not widely used in commercial products, as the amorphous state of a drug may undergo recrystallisation due to the effect of temperature and humidity during storage (Pokharkar et al., 2006, Mooteret al., 2006, Chauhan et al., 2005). This may lead to decreased drug solubility and dissolution rate (Mooteret al., 2006, Wang et al., 2005).

1.3.6 Cyclodextrins

Cyclodextrins (CDs) are cyclic oligosaccharides which consist of six, seven or eight α-(1-4)-linked glucopyranose units representing α, β and γ cyclodextrins respectively (Figure. 1.3). They are hollow cones having an external hydrophilic surfaces and internal hydrophobic cavities. The external surface enhances the absorption rate through gastrointestinal tract while the internal cavity provides a suitable environement for hydrophobic compounds. Cyclodextrins can interact with drug

molecules forming inclusion complexes. Complexation of hydrophobic drugs with cyclodextrins results in: increased water solubility and bioavailability (Klein et al., 2009; Taneri et al., 2002; Abosehmah-Albidy et al., 1997); improved physical and chemical stability (Stella & He, 2008); long shelf life; decreased side effects and ease of powder handling and preparation of liquids and aqueous injectable solutions of poorly soluble drugs (Szejtli, 1997).

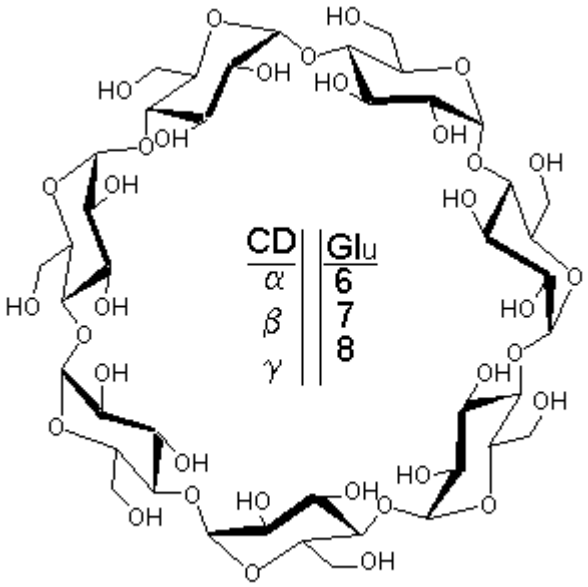

Figure 1.3: Structure of cyclodextrins (retrived from http://jindrich.org/ projects/cyclodextrins.html, October 2010).

Various studies have shown that cyclodextrins have potential in the development of sublingual delivery of low solubility peptides (Mannila et al., 2009). Also, intraoral formulations of low molecular weight lipophilic compounds as Δ^9-tetrahydrocannabinol, cannabidiol have been developed using (β-CD) (Mannila et al., 2007, 2006). Moreover, hydroxypropyl-β-CD has been reported to enhance sublingual absorption of insulin (Cui et al., 2005).

Some drugs are not suitable for complexation with cyclodextrins such as inorganic compounds. Generally, very small or very large molecules (proteins, peptides,

enzymes, and polysaccharides) can not form complexes with cyclodextrins. To form a useful complex with CDs, a drug should have the following features (Szejtli, 1997):

- A drug molecule should consist of more than five atoms or less than five condensed rings.
- Melting point should be below 250ºC (if not, cohesive forces between the molecules will be very strong).
- The molecular weight should be between 100 and 400 as in the case of smaller molecules, the complex drug content will be too low while large molecules do not fit within the CD cavity.

Another restraining factor for complexation with CDs is the dose of the drug that has to be administered orally. To form a successful inclusion complex between a drug moleule and a cyclodextrin molecule, a molar ratio should be employed to calculate the required amount of cyclodextrin which is often 1:1 (drug:cyclodextrin, Stella & He, 2008). As the molecular weights of the drugs to be complexed are low relative to those of cyclodextrins (972, 1132 and 1297 for α, β and γ-CD, respectively) and the weight of an oral tablet should not be more than 500 mg, the correlation between a drug dose and its molecular weight determines the viability of the drug for oral administration as a complex with CDs.

Toxicity issue of CDs should be also considered. It has been reported that both α- and β-cyclodextrins as well as a number of alkylated CDs can cause renal toxicity and disruption of biological membranes. However, γ-CD and some of its derivatives, as well as hydroxypropyl β-CD have been reported to be much safer (Stella & He, 2008). Furthermore, the prices of CDs and their derivatives are high relative to other carriers which is considered another limitation for their routine use.

1.3.7 Surfactants

Surfactants are compounds that have low to moderate molecular weights and, act as wetting agents. They decrease the surface tension of liquids (dissolution media) resulting in improved dissolution of hydrophobic powders. They have amphiphilic

nature as a surfactant molecule consists of one hydrophilic polar part and another hydrophobic one. According to the charge of the polar head group, they are classified into anionic (negatively charged) and cationic (positively charged) surfactants while those having both negatively and positively charged head group components are referred as zwitterionic surfactants. Uncharged surfactants are known as non-ionic surfactants. Surfactants have the ability to self-associate in aqueous solution to form micelles that consist of surfactant molecules packed together in a specific manner forming hydrophobic cores (Figure. 1.4). Therefore, surfactants can solubilize hydrophobic drugs in the cores of their micelles, thus decreasing their hydrolytic degradation and toxicity and improving their bioavailability.

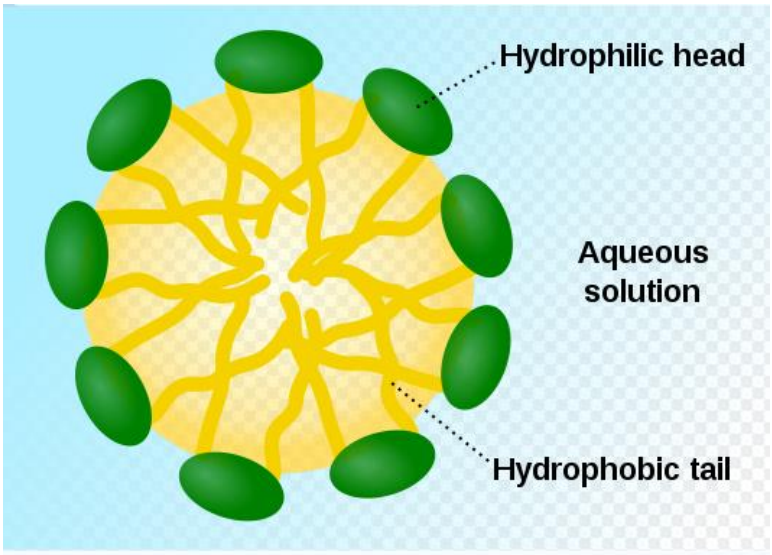

Figure 1.4: Schematic structure of a micelle and a surfactant molecule (retrieved from http://en.wikipedia.org/wiki/Surfactant, October 2010).

Many studies have investigated the effect of surfactants in enhancing dissolution rtae of poorly water soluble drugs. For example, it has been reported that sodium dodecyl sulfate (SDS) and sodium taurocholate (STC) as anionic surfactants, cetyl trimethyl ammonium bromide (CTAB) as a cationic surfactant and Tween 80 as a

non-ionic surfactant enhanced the dissolution rtae of a new phosphate salt of carvedilol (alpha and beta blocker, Chakraborty et al., 2009).

1.3.8 Polymorphism

Polymorphism occurs when a drug molecule can exist in different crystalline forms (discussed in Section 1.2.2.3). These multiple forms have different physicochemical properties such as melting point, solubility, heat of fusion, density, and refractive index. Polymorphism is very important in industry as the presence of different forms of a drug can greatly affect its dissolution rate, solubility and hence, bioavailability (Pudipeddi & Serajuddin, 2004). Modification of polymorphs can be achieved by heat, mechanical stress and by the effect of solvents. For example, it has been reported that crystallisation of glibenclamide from different solvents resulted in formation of two polymorphs and two solvates (Suleiman & Najib, 1989). In another study, sublimation of the quickly cooled melt of glibenclamide gave a new insoluble polymorph of the drug (Panagopoulou-Kaplani & Malamataris 2000). Berbenni et al. (1999) have reported the formation of different polymorphic forms of spironolactone with different physicochemical characterisations by crystallisation from different solvents. In a recent study, the α-polymorph of indomethacin exhibited a higher dissolution rate than do the γ polymorph of the drug (Aceves-Hernandez et al., 2009).

1.3.9 Amorphous form

Formation of amorphous, high energy forms has been reported to be an effective approach to improve the bioavailability of active pharmaceutical ingredients through enhanced dissolution (Lakshman et al., 2008). The solubility of amorphous forms can be as much as 10-1600 folds higher than that of the crystalline forms (Hancock & Parks 2000). In spite of the pronounced ability of the amorphous form in enhancing dissolution rate and bioavailability of poorly water-soluble drugs, it has the disadvantage of being thermodynamically unstable with a tendency to transform to the more stable, lower energy crystalline form (Yoshioka & Stella, 2000; Bhugra & Pikal, 2008; Zhou et al., 2007; Gao, 2008). Transformation of an amorphous form

to a crystalline form is accelerated by certain stresses such as temperature or moisture that can be sorbed from the atmosphere during storage, unless it is controlled by the addition of certain ingredients in the formulations or the packaging. Imperfect manufacturing processes that leave trace amounts of drug crystals may also accelerate the transformation process by acting as nucleation centres (Lakshman et al., 2008).

One of the strategies for stabilization of amorphous materials is by incorporating them into solid dispersions where they are protected in polymeric carriers (Vasanthavada et al., 2008). Furthermore, their transformation to crystalline forms can be adjusted by the use of carriers that could manipulate hygroscopicity or provide functional groups for specific interactions with the amorphous molecules such as hydrogen bonding (Telang et al., 2009).

Several techniques can be used for amorphous formation. These techniques include precipitation from a solution by spray drying (Alhalaweh at al., 2009); lyophilisation (Margulis-Goshen & Magdassi, 2009; Laitinen et al., 2009); spin-coating (Strydom et al., 2009); and decompression of supercritical fluids (Kang et al., 2008). Rapid cooling of the melt (Német et al., 2008; Savolainen et al., 2007); mechanical disruption of the crystal lattice by milling (Petterson, et al., 2005); wet granulation (Rodriguez et al., 2002) and desolvation (Fukushima et al., 2007) are considered other methods for obtaining amorphous form of crystalline compounds.

Hot-melt extrusion (HME) is another technique that can be applied for amorphous formation. This approache is a practical method to prepare several drug delivery systems such as granules, sustained release tablets, transdermal and transmucosal drug delivery systems. Compared to traditional processing techniques, HME has the advantages of absence of solvents; fewer processing procedures; no need for the compressibility of the active ingredients; powerful mixing and agitation during processing lead to deaggregation of drug particles suspended in the molten polymer, resulting in a more uniform dispersion of very small particles; and drug bioavailability may be enhanced by solubilization or dispersion at the molecular level in HME dosage forms (Mididoddi & Repka, 2007).

On the large scale, lyophilisation is frequently prefered than other methods for production of glass-state amorphous solid formulations which contain thermally unstable compounds (Kadoya et al., 2008).

1.4 Lyophilisation

Lyophilisation, or freeze-drying, is a simple process used in the manufacture of different pharmaceutical products. Some examples include parenteral drugs, in-vitro diagnostic products, blood serum, plasma, antibiotics, and vaccines. It involves the removal of water or other solvents from a frozen product by a process called sublimation. Sublimation occurs when a solid goes directly to the gaseous state without passing through the liquid phase.

1.4.1 Advantages of lyophilisation

Lyophilisation has been reported to have the following advantages (Murgatroyd, 1997):

- **Retention of activity**

The process of lyophilisation is a mild technique of drying and thus protects biologically active molecules such as proteins. The 'mildness' of lyophilisation process is due to a number of reasons including:

1. Low temperature applied during the process protects heat labile species.
2. Freezing causes immobilization of molecules avoiding chemical reaction between formulation components.
3. It provides low temperature at which enzymes and bacteria cannot be active.
4. Avoidance of oxidation reactions due to absence of oxygen as a result of application of a vacuum.

- **Ease of reconstitution**

In a drug aqueous solution, water freezes as branched crystals between which the concentrated solution freezes. Thus, sublimation of the branched ice crystals from

around drug molecules results in formation of a lyophilised product with a highly porous structure. This structure is characterised by large surface area that leads to rapid dissolution.

- **Long shelf life**

The moisture content of the lyophilised products is less than 2% allowing good storage stability. This leads to ease of manufacture, distribution and storage that decrease the cost of the final products.

- **Accurate dosing**

To be lyophilised, a material should be introduced as a liquid fill in its final container. For that reason, the dose can be accurately measured compared to the powder fill. As in the case of mixtures, the components should be milled to get accurate particle size and should be homogenously mixed.

1.4.2 Disadvantages of lyophilisation

On the other hand, lyophilisation has some disadvantages (Murgatroyd, 1997).

- **Speed**

Lyophilisation is a time consuming process. It takes several hours for a drying cycle to finish. In addition, defrosting, cleaning and sometimes equipment sterilisation after process completion is prolonged reducing batch throughput.

- **Operating costs**

Costs of operation are high because it is not efficient in the consumption of energy. That is because many tonnes of stainless steel, silicone oil and glass go through a large temperature cycles to apply or remove heat for drying of wet product weighing less than 1 kg.

1.4.3 Basic Principles

To optimize the lyophilisation process, critical properties of the formulation should be known and applied correctly to the process design. These properties are the stability of the drug; collapse temperature of the formulation; and properties of the excipients included. The macroscopic collapse temperature of a formulation (T_c) is the temperature above which the lyophilised product loses macroscopic structure and collapses during lyophilisation process (Tang & Pikal, 2004). T_c is frequently about 2ºC higher than the glass transition temperature (T_g); the temperature at which an amorphous material transforms from a glass to rubber state. If the solute crystallises in the frozen solution, T_c is the same as the eutectic temperature (T_{eu}); the temperature at which the eutectic system solidifies and it is lower than the solidification temperatures of individual components of the mixture. For production of a suitable lyophilised product, the formulation should be lyophilised at a temperature below its T_c (Tang & Pikal, 2004).

Mainly, lyophilisation process consists of three basic stages. These stages include freezing of the product; primary drying; and final or secondary drying that are discussed in details in the following paragraphs.

1.4.4 Stages of lyophilisation

1.4.4.1 Freezing

Freezing is the initial step of lyophilisation, in which the system goes through separation into multiple phases. In this stage, interfaces arise between the drug phase and the frozen solvent. The aim of this stage is the immobilization of molecules before the drying stages and so size, shape and structure of the products are fixed and maintained during the lyophilisation process, unless damage or loss happens to the product. The porous structure and surface area of the final product, that can greatly affect reconstitution of the product, are established throughout this stage. Thus, freezing is considered one of the most essential steps of lyophilisation. There are two mechanisms by which a true solution freezes. First, the solvent will supercool,

followed by formation of nuclei and crystals. Consequently, the critical concentration of the solute above which its concentration cannot increase, is reached. At this critical concentration and at the appropriate temperature, the concentrated solution goes through either eutectic freezing or a glass transition. Eutectic freezing takes place through crystallisation. On the other hand, a glass transition results in a massive increase in solution viscosity that makes the solution appear as a fragile solid, while in fact it is a super cooled solution that maintains elastic characteristics (Murgatroyd, 1997).

If the system consists of more than one solute, the freezing cycle can be more problematic. One solute may experience crystallisation and go through eutectic freezing whilst other may be amorphous and go through a glass transition. In addition, it is probable that the freezing point in such circumstances may not be clearly defined, or there may be more than two freezing points achieved from the mixture of water and solute.

Commonly used refrigerants to cool samples during small scale freeze drying include liquid carbon dioxide, liquid nitrogen, dry ice or an acetone/dry ice combination and standard ammonia. Freon refrigeration units are more commonly used for industrial scale processing.

1.4.4.2 Primary Drying

Primary drying follows the freezing stage. Throughout this stage, product temperature (T_p) should be optimised, and maintained a few degrees lower than T_c, to obtain a dry product with a satisfactory appearance. The difference between T_p and T_c is known as the temperature safety margin. Higher product temperature can accelerate the drying process as with each 1ºC rise in the temperature, drying time can be decreased by around 13 %. Therefore, an ideal lyophilisation process takes place with the product temperature elevated to the maximum level that can be safely held below T_c. However, if the product temperature is held too near to T_c, then the possibility of collapse increases (Tang & Pikal, 2004).

Primary drying takes place under low pressure to increase the rate of ice sublimation. The chamber pressure (P_c) affects both heat and mass transfer during the lyophilisation process and consequently, the ice sublimation rate. Thus, P_c should be lower than the ice vapour pressure at the target product temperature for achieving a high rate of sublimation (Tang & Pikal, 2004).

The composition of the formulation at the beginning of the drying cycle depends upon both the properties of the solutes and the method of freezing. It may consist of ice and crystallised solute; ice and freeze-concentrated glassy solution; or ice and a mixture of crystallised solute and freeze-concentrated glassy solution. Practically, if freezing is properly performed, an amorphous glassy product will be obtained during the freeze concentration stage. If the formulation does not give rise to crystalline product (eutectic behaviour), the temperature should be maintained below T_g throughout the primary drying process to prevent melt back of ice into the frozen mixture. The main driving force for ice sublimation is the difference between vapour pressure of the ice surface and that of condenser surface (ΔG_s). As vapour pressure is directly proportional to temperature, the exact driving force is the temperature difference between the condenser and ice surfaces. This explains why ΔG_s can be increased to its maximum by choosing a formulation having a high T_g and a condenser that has the ability to run at lower temperature ranges (Felix, 2007).

Tertiary butyl alcohol (TBA) (as a solvent in the formulation) has been reported to accelerate primary drying rate due to its high vapour pressure (Kasraian & DeLuca, 1995). The particular mechanism of TBA in accelerating ice sublimation rate depends on alteration of the ice crystal habit. The presence of TBA in the formulation to be lyophilised, leads to the formation of needle-shaped crystals. These types of crystals are characterised by large surface areas available for sublimation. This increase in the specific surface area is associated with decrease in the resistance of the dried cake to mass transfer of the solvent. In addition, because of its high vapour pressure, its sublimation takes place simultaneously with ice sublimation leaving no residue in the dried amorphous cake.

At the end of primary drying, the sublimation process stops as there is no ice left in the product. Consequently, no ice vapour exists in the lyophilisation chamber and the product temperature increases to that of the shelf temperature (Felix, 2007).

1.4.4.3 Secondary Drying

Secondary drying is the final stage of lyophilisation process in which any residual, unfrozen water is removed from the solute phase by desorption. Directly after the end of primary drying, an amorphous product still has residual water on the surface of the dried solid. The amount of this residual water is 5-20% w/w depending on the formulation (Tang & Pikal 2004). On the other hand, the amount of residual water in the case of crystalline systems is much lower than that of amorphous systems and is present as a thin layer adsorbed onto the crystal surfaces. An exception is crystalline hydrates, where water molecules are hydrogen bonded to each other or to solute molecules. These types of crystalline systems contain water molecules that are not entirely removed during the sublimation processes that occur during the primary drying stage. However, the aim of secondary drying is to decrease the remaining moisture content to a level optimal for long-term stability. This is usually around 0.5-3% w/w residual moisture. The point that should be seriously considered during this stage is that, even as ice sublimation reaches completion, an amorphous product should be kept at a temperature close to T_g. If the product temperature, at any time, gets higher than T_g, the delicate composition of the dried cake will start to collapse. This usually happens due to a rapid reduction in the solid matrix viscosity as a result of raising product temperature above T_g (Felix, 2007).

The product must be maintained at a sufficiently elevated temperature for enough time to allow water desorption. Frequently, it is better to use an elevated shelf temperature for a short period than using a low temperature for a long time (Pikal & Shah, 1990). It is more difficult for amorphous products to be dry than crystalline products, therefore, longer periods at higher temperatures are required for the removal of the adsorbed water.

Many researchers have employed lyophilisation technology to improve pharmaceutical dosage forms. For example, long-term stability and applicability of liposomal vaccines have been improved by formulating the systems as lyophilised products (Mohammed et al., 2006). Dry powder influenza vaccine has been prepared by lyophilisation for nasal delivery (Garmise et al., 2006). Nicotine lyophilised nasal inserts have been reported to display significantly extended nicotine release profile over the conventional formulations (McInnes et al., 2005). Lyophilised sporozoites exhibited better storage stability between -20 and 5ºC than non-lyophilised sporozoites kept under the same conditions (Marcotty et al., 2003). Lyophilised complex of ibuprofen/β-hydroxypropyl-cyclodextrin has been reported to meet the desired solubility requirements to be considered as a possible injectable product (Kagkadis et al., 1996). It has been reported that lyophilisation technology was used to formulate fast dissolving ketoprofen tablets that had a significantly enhanced dissolution rate (Ahmed & Nafadi, 2006).

The main objective of a commercial pharmaceutical lyophilisation process is to deliver a product that has a suitable shelf life and one that can be easily reconstituted when required. The dried products may be either amorphous, crystalline or a combination of both states. These products should be protected in dosage forms that guarantee long-term stability and therapeutic efficacy. Thus, coating pharmaceutical dosage forms with protective films is a useful approach to prolong their shelf life.

1.5 Film Coating

Film coating is the application of a coating material to the outer surface of a solid dosage form for the following purposes (Hogan, 2002):

- Protection of drugs from the environment, especially from light and moisture.
- Masking of an unpleasant drug taste.
- Masking variations in the appearance of raw materials between batches.
- Identification of marketing brands by application of colour or gloss.
- Ease of handling.
- Ease of of swallowing.

- Release modification e.g. polymer coating for enteric or sustained release purposes.

Generally, there are three types of coatings; film coating, sugar coating and press coating. Film coating is the most recent and most commonly used technology for coating of solid dosage forms. In the process of film coating, a thin film of polymer is applied onto the surface of the solid dosage form, usually by use of a spray technique. The coating system consists of a polymer in an appropriate solvent in addition to other ingredients as plasticizers and pigments. In the process of film coating, there are four principal criteria to be satisfied (Sakellariou & Rowe 1995):

- The film should have an even thickness, particularly if it is designed for controlling drug release.
- The film should be coherent and have no defects or fractures to avoid early drug release.
- The film should exhibit sufficient adherence to the substrate.
- The film should have stability upon handling and storage to prevent any change in the drug release kinetics with time.

1.5.1 Film coating raw materials

1.5.1.1 Polymers

The polymer should have adequate solubility in water to permit the dissolution of the active ingredients from the dosage form. However, polymers with low water solubility are required if the release has to be modified. Generally, polymer solutions should have low viscosity to facilitate application using the available film coating instruments. Polymers employed for coating of solid dosage forms can generally be classified into three groups (Sakellariou & Rowe 1995):

- **Immediate release water-soluble polymers**

This group includes polymers that are soluble in the GIT and hence do not affect drug release. They are frequently water-soluble cellulose ethers such as methylcellulose, hydroxypropyl cellulose, hydroxypropyl methylcellulose,

hydroxyethyl cellulose and hydroxyethyl methylcellulose. This group also includes water-soluble vinyl derivatives such as polyvinyl alcohol and polyvinyl pyrrolidone. High molecular weight polyethylene glycols and certain acrylic copolymers can also be employed.

- **Enteric coating polymers**

This group includes polymers that are only soluble at pH above 5.0-5.5 (that found in the small intestine). Examples of these polymers are cellulose acetate phthalate and hydroxypropyl methylcellulose phthalate.

- **Insoluble coating polymers**

This group includes water-insoluble polymers that control the release rate of drugs. Examples of these polymers include ethyl cellulose, polyvinyl acetate and certain acrylates.

1.5.1.2 Plasticizers

The function of plasticizers is to lower the glass transition temperatures (T_g) of the polymer. In addition, they modify the physical properties of the polymer to make it more suitable for application, for example, increasing the flexibility of the coating, reduction of cracking risk and improving film adhesion to the substrate. Plasticiser characteristics such as molecular weight, chemical structure and concentration affect its ability to lower the T_g of the polymer. The plasticizer should be highly compatible with the polymer incorporated in the coating system. Generally, a water-soluble plasticizer is compatible with a water-soluble polymer whereas a water-insoluble plasticizer is compatible with a water-insoluble polymer. Commonly used plasticizers include; polyols such as polyethylene glycol 400; organic esters such as diethyl phthalate; and oils/glycerides such as fractionated coconut oil.

1.5.1.3 Colourants

It is preferred to use water-insoluble colorants rather than water-soluble colorants. That is because water-insoluble colorants are more chemically stable against light;

give higher opacity and covering ability; and enhance the impermeability of the film to water vapour. Examples of colorants include iron oxide pigments, titanium dioxide, and aluminium lakes (Hogan, 2002).

1.5.1.4 Solvents

At the start of film coating technology, organic solvents were commonly employed to dissolve polymers. However, modern approaches tend to use water as a solvent to avoid the drawbacks associated with the use of organic solvents. The organic solvents have the following disadvantages (Hogan, 2002):

- Release of the vapour of organic solvent to the environment is unsafe, and efficient removal of solvent vapour is expensive.
- Organic solvents are unsafe as they can cause explosion, toxic hazards and fire.
- Organic solvents are relatively expensive, and the cost of the storage and quality control is high.

A combination of two solvents is commonly used to improve the processing and the quality of the final film coating. Common combinations include ethanol/water, acetone/water, methylene chloride/ethanol, acetone/methylene chloride, acetone/ethanol/isopropanol and acetone/ethanol/methylene chloride (Avis et al., 1999).

1.5.2 Organic coating

In this type of coating, the film is formed from organic polymer solution by evaporation of the organic solvent. Following solvent evaporation, the polymer concentration increases and an intermediate gel-like phase is obtained. Further evaporation of the solvent results in formation of a solvent free polymeric film (Wesseling & Bodmeier, 1999). There are numerous problems associated with organic coating (discussed in the above Section). Therefore, the focus of scientists has been directed towards the aqueous based coating.

1.5.3 Aqueous based coating

The word aqueous here does not mean total avoidance of organic solvents from the coating systems but it means a significant decrease in their use, and the use of the more pharmaceutically suitable solvents such as ethyl acetate and butanone in water-based system. There are two major classes of aqueous-based coating; latex and pseudolatex.

1.5.3.1 Latexes

Latexes are mainly produced by an emulsion-polymerisation process. In this process, the polymers used for coating are directly synthesised from the monomers. This method is employed for monomers that can polymerise in aqueous media. Monomers are activated to form polymers by the addition of free radical initiators. The toxic effect of residual monomers and initiators is the main disadvantage of this system. Therefore, the focus has been shifted to development of pseudolatexes.

1.5.3.2 Pseudolatexes

In contrast to latexes, pseudolatexes are prepared by emulsification of organic polymer solutions in water, followed by removal of the organic solvent by vacuum. Pseudolatexes are classically prepared by an emulsification–evaporation technique. In this technique, a solution of the polymer in a water-immiscible organic solvent is emulsified in an aqueous phase by the aid of emulsifiers (stabilisers) (Vanderhoff, 1993). Subsequently, this emulsion is exposed to a high-energy source such as ultrasound radiation, homogenizers, high-pressure dispersers, or colloid mills. The resultant emulsion of the polymer is very stable and the size of the polymer droplets is less than 0.5 µm. After completion of the emulsification process, organic solvent is removed by vacuum steam distillation, producing a fine aqueous dispersion of polymeric particles ranging from 0.1 to 0.3 µm. The role of emulsifiers is to facilitate emulsion formation and to prevent coalescence and agglomeration of the dispersed polymer particles in the stage of solvent evaporation and during storage.

Quintanar-Guerrero et al. (1999) recommended another technique known as the emulsification–diffusion for preparation of nanoparticles from preformed polymers. In this method, a solution of a polymer in a partially water-miscible solvent (saturated with water) is emulsified in an aqueous phase (saturated with the solvent) containing a stabiliser. Then, water is added to the system, which leads to diffusion of the solvent into the external phase leaving aggregation of the polymer in the form of nanoparticles. However, to get a high polymer concentration in the final system, solvent and a considerable amount of water should be removed. This process has the following advantages:

- It does not need high energy source as in Vanderhoff's method
- It has high efficiency
- It is reproducible and easy to develop

Most of the aqueous-based film coating processes are performed using fluidised bed coaters. In this type of coaters, the aqueous dispersion of a polymer is sprayed onto the surfaces of the solid dosage forms while water evaporates. A curing stage of thermal treatment at high temperature is recommended directly after the coating process. This process accelerates the film formation by enhancing the coalescence of the polymer particles. In addition, it plays a role in enhancing film stability during storage (Wesseling & Bodmeier, 1999).

1.5.4 Dry powder coating

Aqueous based coating systems are not suitable for water-sensitive dosage forms. In addition, spray nozzles may be blocked if a highly viscous coating solution (high polymer concentration) is used to decrease the coating time. To overcome these limitations and for further reduction in costs, dry coating was developed. In this method, neither organic solvent nor water is used. The powders of the coating polymer and the plasticiser are directly applied, under heated air, to the dosage form to form the coating film (Obara et al., 1999). Synchronisation of the delivery rates of both components is essential to permit the two processes to start and finish at the same time. As in the case of aqueous coatings, a curing process is required to

enhance coalescence of polymeric particles and hence formation of a smooth uniform film. This curing process involves spraying water onto the surface and subsequent drying of the product. This is due to water evaporation providing a driving force for fusion of polymeric particles (Obara et al., 1999). Thus, dry coating is not absolutely free from water, but rather, only a relatively small amount of water is still required. The costs of this type of coating are noticeably low because the processing time is short and no need for preparation of coating dispersions or solutions.

1.5.5 Basic requirements for film coating

There are essential requirements for the film coating process (Hogan, 2002). These requirements include:

- Good atomization of the spray system for application to the surface of the substrates.
- Enough mixing and agitation of the substrates being coated during the spraying process.
- Adequate input of hot drying air to allow sufficient evaporation for solvents especially in case of aqueous based systems.
- Adequate facilities to remove exhaust air and dust.

1.5.6 Coating equipment

Most film coating processes are carried out by techniques that involve spraying or atomizing the coating system onto the surface of the substrates to be coated e.g. pan coater and fluidised bed coater.

1.5.6.1 Pan coater

In the case of pan coating, the spray nozzle is designed to produce uniform spray droplets of adequately small diameter. All the sprayed droplets contact the substrates in the same status, allowing for the same heat, mass transfer and drying time for all droplets. This supports the formation of a homogeneous film on all substrates and

avoid over wetting. Film formation proceeds by droplet spreading, coalescence, adhesion and by solvent evaporation (Mehta, 2008). There are two types of pan coaters:

- **Conventional pan coater**

The conventional pan coater is the first type used for early sugar coating processes. In this type, hot drying air is directed onto the tumbling substrates from the back opening while the spray gun established at the front opening. Because the exhaust air is also removed from the back opening, there is considerable loss of drying power leading to reduced heat and mass transfer. Subsequently, the coating finish may not be as good as required. Therefore, this type of pan coaters was not proficient in the removal of the water-based solvent because the heat required for evaporation of water is far more than that required for organic solvent removal. Adjustment of the production of the hot air and exhaust utensils improved the process for application with organic solvents.

- **Perforated pan coater**

The steady change from organic-based to aqueous-based coating required modifications of the pan coater for efficient solvent removal. It is known that the latent heat required of water evaporation is much more than that required for evaporation of usual organic solvents such as ethanol (Mehta, 2008). This fact should be considered in planning suitable coating parameters such as drying time, pan speed and air flow. This is because over wetting may lead to clustering of the substrate and may also affect hygroscopic or water-sensitive drugs or excipients included in the formulations. Compared to the conventional pan coater that pushes hot air onto the bed surface of the substrate, the perforated pan coater drives the drying air through the substrate bed. In addition, positions of the heat supply as well as the exhaust ducts and vents can be changed to give the most efficient drying. The main advantage of the perforated pan is its capability to attain a processing speed similar to that of fluidised bed coater while keeping the mild tumbling movement of the pan coater. This advantage is highly important in the case of delicate substrates such as friable tablets and liquid filled gelatin capsules (Mehta, 2008).

1.5.6.2 Fluidised-bed coater

The process of fluidised bed coating has been employed for a long time in pharmaceutical production. It is the process in which an ascending flow of gas pass through a bed of tiny solid particles at a high rate maintaining these particles suspended and agitated. There are three basic modes (Mehta, 2008) for film coating using this technology (Figure 1.5).

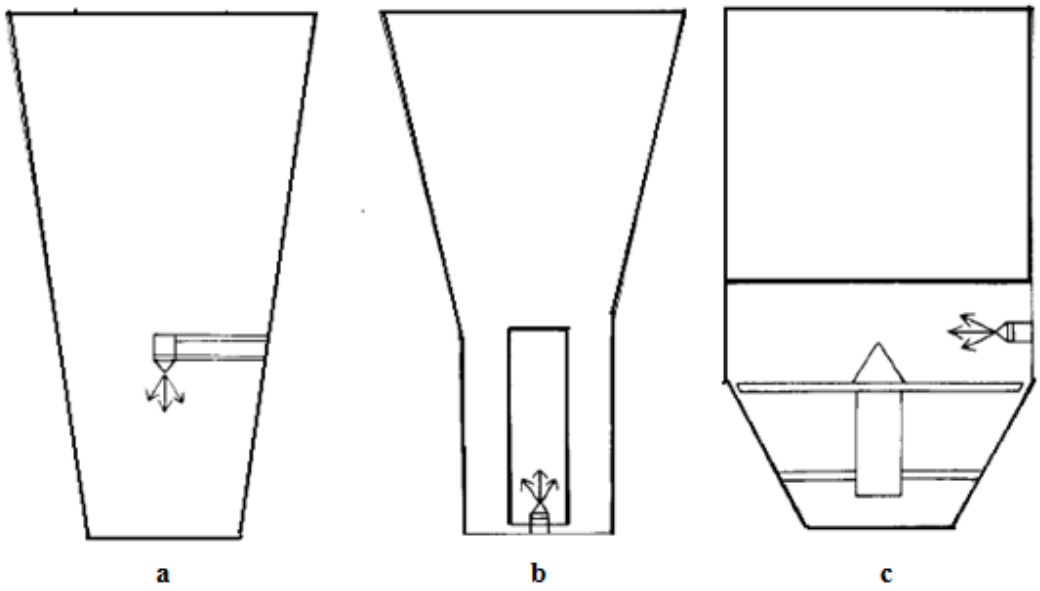

Figure 1.5: Different modes of fluidised bed technology: top spray (a), bottom spray (b), tangential spray (c) (Shirley et al., 1992).

- **Top spray or granulator mode**

This mode is usually used to coat small particles effectively. The resultant film is not highly uniform. Therefore, it is only a feasible and simple method when the release from the dosage forms does not depend on the membrane thickness or perfections. In this mode, the processing chamber has an elongated, conical shape to allow high fluidisation and decrease the speed of particles in the upper area. The spray nozzle is located in the top and sprays the coating system counter-current to the fluidised air current. It is commonly used for taste-masking coatings.

- **Bottom-spray or Wurster mode**

This mode is suitable for modified-release coatings. In this process, the spray nozzle is located in the bottom and the coating system is sprayed concurrently with the fluidised air current. The processing chamber is narrow at the product-containing area in the lower region while it is wider in the upper region. In the upper, wider area, the particles lose their regular circulatory movement. Hence, in the Wurster chamber, a cylindrical part is placed in the centre over the gas distributer to obtain a more organised particle movement. On the other hand, the movement of particles in the lower area is well-organised and thus results in reproducible coating. The bottom spray mode enhances collision between particles and droplets of the coating liquid leading to a great efficacy and reduction of dust formation.

- **The rotor or tangential spray mode**

This mode is suitable for modified release coating process. In this mode, the spray nozzle placed at the side of the processing chamber and thus, the coating system is sprayed peripherally to a rotating bed of particles. The combined effects of the fluidisation air and a rotating disk in the processing chamber enhance the efficiency of the machine.

1.6 The Aim of Work

Lyophilisation is often considered a method for alteration of the physical forms of many pharmaceutical compounds. The objectives of the present thesis were to employ lyophilisation technology to enhance the dissolution rate and extent of three exemplars of poorly water-soluble drugs; glibenclamide, spironolactone and ketoconazole. Water-soluble excipients were also used in the lyophilised formulations for further enhancement of the dissolution rates of these drugs.

Chapter 2

2. Materials and methods

2.1 Materials

2.1.1 Drugs

Glibenclamide	Medex, Naseby, Northants, NN6 7DF, U.K.
Spironolactone	Medex, Naseby, Northants, NN6 7DF, U.K.
Ketoconazole	Medex, Naseby, Northants, NN6 7DF, U.K.
Glibenclamide commercial tablets	APS, Leeds, LS27 0JG, UK.
Spironolactone commercial tablets	Norton Healthcare Ltd, London, E16 2QJ, UK.
Ketoconazole 200 mg tablets (Nizoral®)	Janssen-Clilag Ltd, Buckinghamshire HP14 4HJ, UK.

2.1.2 Excipients

D-mannitol, minimum 98%	Sigma-Aldrich Co. Ltd., Poole, Dorset, UK.
Sodium lauryl sulphate (SLS)	Sigma-Aldrich Co. Ltd., Poole, Dorset, UK.
Polyethylene glycol (PEG) 6000	Fluka (Sigma-Aldrich Chemie GmbH, Steinheim, Germany)
Gelatin from bovine skin, type B	Sigma-Aldrich Co. Ltd., Poole, Dorset, UK.
Tromethamine	Sigma-Aldrich Co. Ltd., Poole, Dorset, UK
Fumaric acid	Sigma-Aldrich Co. Ltd., Poole, Dorset, UK.
Citric acid	Sigma-Aldrich Co. Ltd., Poole, Dorset, UK.

2.1.3 Chemicals

Potassium dihydrogen phosphate (KH_2PO4)	Sigma-Aldrich Co. Ltd., Poole, Dorset, UK.
Sodium hydroxide pellets	Sigma-Aldrich Co. Ltd., Poole, Dorset, UK
Hydrochloric acid	Sigma-Aldrich Co. Ltd., Poole, Dorset, UK
Sodium nitrite	Sigma-Aldrich Co. Ltd., Poole, Dorset, UK.
Sodium chloride	BDH, Poole, UK
Opadry®	Colorcon Limited, Kent, DA2 60D, UK.
Opadry® enteric	Colorcon Limited, Kent, DA2 60D, UK.
Ammonia solution SP. gr 88%	VWR international Ltd., Poole, England.
Lactose monohydrate (Fast-flo)	Pfizer Ltd., Kent, UK
Technetium-99m diethylenetriaminepenta-acetic acid (^{99m}Tc-DTPA)	Radiopharmacy, Western Infirmary, Glasgow, UK).
Bone cement	Heraeus Medical, UK

2.1.4 Solvents

Tertiary butyl alcohol (TBA)	Sigma-Aldrich Co. Ltd., Poole, Dorset, UK.
Ethanol	Sigma-Aldrich Co. Ltd., Poole, Dorset, UK.
Methanol HPLC grade	Fisher Scientific, Leicestershire, LE11 5RG, UK.

Chloroform HPLC grade	Fisher Scientific, Leicestershire, LE11 5RG, UK.
Formic acid 99-100 %	VWR international Ltd., Poole, England.

2.1.5 Consumables

Hard gelatin capsule	Capsugel, Bornem, Belgium
Syringe driven filter units, 0.22 µm	Millex GP, Millipore, Ireland.
Aluminum crucibles with lids (40 µl)	Mettler-Toledo Ltd.,Leicester,UK.
Lithium heparin beaded monovette blood sample tubes	Sarstedt, Leicester, UK.
Polypropylene eppendorf tubes, 2 ml	Fisher Scientific, Leicestershire, LE11 5RG, UK.
Autosampler vials with screw caps, 1.5 ml	Phenomenex, Macclesfield Cheshire, SK10 2BN, UK.
Autosampler vial inserts	Phenomenex, Macclesfield Cheshire, SK10 2BN, UK

2.2 Equipment

2.2.1 Manufacturing equipment

Sartorius balance	Sartorius AG, goettingen, Germany.
Magnetic stirrer	Bibby Sterlin Ltd., Stone, UK.
- 86 ^{o}C Heraeus Freezer	HFU 586 Basic, Germany
Lyophiliser	Martin Christ Gefriertrocknungsanlagen GmbH, An der Unteren Söse 50, 37520 Osterode, Germany
Microprocessor pH meter	Hanna pH 211, UK
Electrical stirrer	Stuart Scientific, SS 10, UK.

Mini coater/drier	Caleva Process Solutions Ltd., Dorset UK.

2.2.2 Analytical equipment

Dissolution apparatus	Copley Scientific Limited, Nottingham, NG4 2JY, UK.
Unicam (UV1) spectrophotometer	Unicam UV-Visible spectrophotometry, Cambridge, UK.
Crucible sealing press	Mettler-Toledo Ltd., Leicester,UK.
Differential scanning calorimeter (**DSC;** DSC 822^{e} module; TA controller TC15)	Mettler-Toledo Ltd., Leicester,UK.
Thermogravimetric analysis system (**TGA**/SDTA 851^{e})	Mettler-Toledo Ltd., Leicester,UK.
Fourier transform infrared spectrometer (Jasco **FT/IR** – 4200)	Jasco Ltd., Essex,CM6 1XN, UK.
X-ray powder diffraction (**XRPD;** Bruker-AXS D8)	Bruker AXS GmbH, Karlsruhe, Germany.
Gamma camera	Scintron, MIE, Germany.
Gamma counter	J&P Engineering MS310 ratemeter, reading UK.
Blood glucose meter + test strips (**Accu-Chek Aviva**)	Boots Pharmacy, Uk.
Centrifuge (Heraeus instruments)	Fisher scientific, Loughborogh, UK.
Evaporative centrifuge (Speedvac SPD121P)	Thermo Savant, Holbrook, NY 11741-4306 USA

HPLC system	Gynkoteck, P580 LPG, D82110, Germering, Germany
HPLC column (Luna 3 µm C_{18} (2) 100 Å, 150 × 4.60 mm	Phenomenex, Macclesfield Cheshire, SK10 2BN, UK.

2.3 PC software

Differential scanning calorimeter software STAR^e system	Mettler-Toledo Ltd.,Leicester,UK.
FT/IR software	Jasco Ltd., Essex, CM6 1XN, UK.
X-ray software (EVA 9.0.0.2)	Socabim, Germany.
Gamma image analysis	MIE, Seth, Germany.
HPLC software (Chromeleon)	D82110,Germering, Germany

2.4 Analytical techniques

2.4.1 In-vitro release studies

In-vitro release studies were carried out using the USP type II paddle method. Glibenclamide dissolution was performed using 1000 ml of 0.2 M phosphate buffer solution (pH 7.4, Bachhav & Patravale, 2009) maintained at 37 ± 0.5ºC and stirred at 100 rpm. Spironolactone dissolution was carried out using 1000 ml of 0.1N HCL containing 0.1% w/v SLS as a dissolution medium (Hamid et al., 2010), maintained at 37 ± 0.5ºC and stirred at 50 rpm. Ketoconazole dissolution was conducted in 1000 ml of 0.5% w/v SLS aqueous solution (Elder et al., 2003), maintained at 37 ± 0.5ºC and stirred at 100 rpm. A gastro-resistance study of glibenclamide enteric coated capsule formulations was conducted in 1000 ml of 0.1N HCL maintained at 37 ± 0.5ºC and stirred at 50 rpm for 2 h (He et al., 2009). Methylene blue was included in the capsule formulations and the resistance of the enteric coat to the acid medium was evaluated by visual inspection for any release of the blue dye in the dissolution medium. For dissolution of glibenclamide enteric coated capsule formulations, the above dissolution medium and conditions for glibenclamide dissolution were employed.

Six dissolution pots were used for each dissolution run. Tested capsules were attached with a few turns of wire helix to prevent floating on the surface of the dissolution medium. Samples (5 ml) were collected periodically and replaced with the same volume of fresh dissolution medium. After filtration through a syringe driven filter unit (0.22 μm), drug concentrations were determined spectrophotometrically at 240 nm, 242 nm and 291 nm for glibenclamide, spironolactone and ketoconazole respectively.

2.4.2 Statistical analysis

In-vitro release data were statistically analysed using difference factor (f_1) and similarity factor (f_2) (Shah et al., 1998). The comparison was performed between reference and test dissolution profiles.

If (U_{r1} , U_{r2},....., U_{rp}) are the percentage dissolution at p time points on the reference profile, and (U_{t1} , U_{t2},....., U_{tp}) are the percentage dissolution at the same time points on the test profile, the difference between the two profiles at these time points is equal to (U_{r1} - U_{t1}, U_{r2}, - U_{t2}....., U_{rp} - U_{tp}). The difference at the p time points can be explained as D_1 = [(U_{r1} - U_{t1})+ (U_{r2}, - U_{t2}) + ...+(U_{rp} - U_{tp})] . The f_1 value represents the cumulative difference between the two profiles at all time points and is explained by the following equation:

$$f_1 = \left\{\left[\sum_{i=1}^{p}[\mu_{ti} - \mu_{ri}]\right] / \left[\sum_{i=1}^{p}\mu_{ri}\right]\right\} \times 100 \qquad \text{(Equation. 2.1)}$$

Where *p* is the time points for sampling, μ_{ti} is the percentage dissolution of the test formulation at any time point, μ_{ri} is the percentage dissolution of the reference formulation at the same time point. Generally, f_1 values in the range 0-15 represent non significant differences between the test and reference formulation. The f_2 value measures the similarity in the percentage dissolution of the two profiles. It is equivalent to the reciprocal of the mean square-root transform of the sum of square distances at all time intervals and explained by the following equation:

$$f_2 = 50 \times \log\left\{\left[1 + (1/p)\sum_{i=1}^{p}(\mu_{ti} - \mu_{ri})^2\right]^{-1/2} \times 100\right\} \qquad \text{(Equation. 2.2)}$$

The values of f_2 range from 0 to 100 and the higher the value the more similarity between the two dissolution curves. If the difference between test and reference dissolution profiles is less than 10%, f_2 values are more than 50 and this indicates no significant difference between the test and reference formulations.

2.4.3 Ultraviolet spectroscopy

The photonic energy of ultraviolet (UV) or visible light going through solutions excites the movement of electrons within molecules to higher energy levels. UV/visible spectrophotometry is used to measure this excitation as an absorption – wavelength spectrum. The concentrations of chemical solutions can be determined by spectrophotometers according to the Beer Lambert law. This law showed that the amount of incident light absorbed by a sample is directly related to the number of absorbing molecules and hence to solution concentration. Also, it states that the amount of the absorbed incident light is independent of the intensity of the light source (equation 2.1).

$$A = \log [I_o / I_t] = \varepsilon.b.c \qquad \text{(Equation. 2.3)}$$

Where A is the measured absorbance, I_o and I_t are the intensities of the incident and the transmitted light respectively, ε is the molar extinction coefficient, b is the path length (cm) of the cell containing the solution to be measured (usually equal 1 cm), and c is the concentration (mol/L).

As ε and b are constant, so $A_1 / A_2 = C_1 / C_2$ (Equation. 2.4)

Where A_1 and A_2 are the absorbance of solution 1 and 2, and C_1 and C_2 are the corresponding concentrations. This equation is used to determine the concentration of a solution, knowing its absorbance from the UV spectrophotometer.

2.4.4 Attenuated total reflectance Fourier-transform infrared spectroscopy (ATR FT-IR)

Infra-red (IR) spectroscopy is the study of scattering, absorption, reflection or transmission of IR radiation in the spectral range 12500 to 10 cm^{-1}. The most commonly used region for drug analysis is the middle region of the spectrum in the range 4000 to 400 cm^{-1}. At room temperature, a molecule exists in its ground vibrational state. IR radiation stimulates the molecular vibrations and hence molecular rotations. Two types of vibrations can happen to molecules, stretching vibrations that lead to alteration of the length of bonds and bending vibrations that

involve alteration of bond angles. At an incident IR radiation of an appropriate energy (wave length, wave number), resonance absorption excites the molecule to a higher state of vibration. This transition produces an absorption spectrum that is characteristic for each compound. The electromagnetic radiation energy is calculated by Plank's equation:

$E = hc / \lambda$ (Equation. 2.5)

Where E is the energy, h is the Plank's constant, c is the velocity of light and λ is the wave length of light.

The relationship between wave length and wave number is given by the following equation:

$W\ (cm^{-1}) = 1/ \lambda$ (Equation. 2.6)

Where W is the wave number and λ is the wave length in cm. Alteration in the wave number of a band can be an indication for changes in the structural environment of the molecule.

The original infra-red spectrometers were of the dispersive type (Figure 2.1). In these instruments, IR radiation from an appropriate source passes through the sample and then through a slit into a monochromator. The monochromator has optics that focus the light beam on a prism or a grating which disperses light into spectrum of its constituent wave numbers before being detected.

The total light energy that strikes the detector is small as the slit only allows a narrow portion of wave numbers to pass to the detector. The prism or grating rotates to permit different wave number portions to pass through the slit and be detected. The intensity is plotted against wave number producing IR spectra.

Modern infra-red, FT-IR, spectrometers, employ a beam splitter that divides the incoming infra-red beam into two beams (Figure 2.2). One beam falls on a stationary mirror while the other falls on a short distance moving mirror. Beams reflected from both mirrors recombine together before passing through the sample and then to the detector.

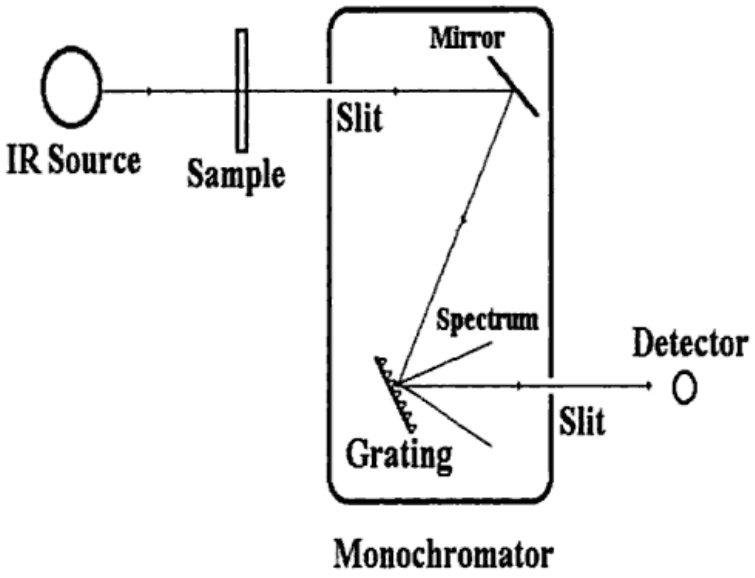

Figure 2.1: Dispersive infra-red spectrometer (Smith, 2000)

By a computer connected to the instrument, the resulting signal is subjected to a mathematical procedure called fourier transform that plots the light intensity against the wave number. It has no slit so the wave number range that strikes the detector is not restricted and the intensity of radiation is not reduced. Furthermore, this type of spectrometer detects all wave numbers simultaneously rather than individually as in the case of dispersive type providing a big enhancement of the signal-to-noise ratio (Grant & Brittain, 1995). It can also detect the spectrum much faster than the dispersive type which allows the instrument to do multiple scans for the same sample and adds them together, which increase the resolution of the spectrum. FT-IR spectrometers have the following advantages over the dispersive models:

- The sample is located next to the detector which decreases heat effects resulting from having the sample near the source of IR radiation.
- It is an accurate method that needs no external calibration
- It is a fast method, collecting a scan every second
- It has improved sensitivity as the scans of one second can be added together to decrease signal to noise level
- It has higher optical throughput

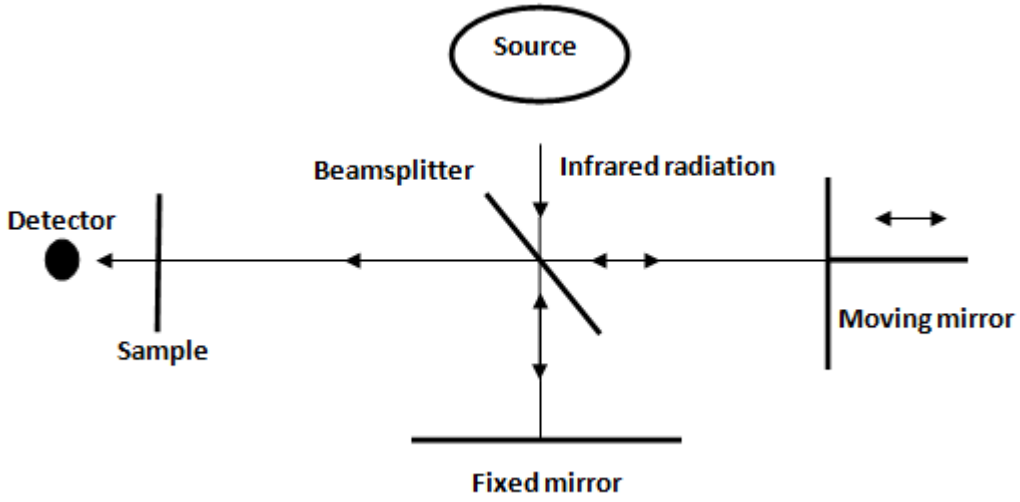

Figure 2.2: Fourier transform infra-red spectrometer (Smith, 2000)

In the traditional FT-IR sampling by transmission, the sample has to be diluted with an IR transparent salt and pressed into a pellet or thin film before analysis to prevent totally absorbing IR bands and subsequent high intensity spectra.

In the attenuated total reflectance Fourier-transform infrared spectrometer (ATR-FT-IR), light arrives at a suitable angle to the boundary between two media m_1 (ATR crystal) and m_2 (sample) having different refractive indexes n_1, n_2. In principle, a single rhomboid prism made from a suitable optical material is used as m_1. If m_2 has absorption properties, the reflected beam has an attenuated intensity, the attenuated total reflectance (ATR). Subsequently, the intensities of the spectra are of lower absorbance than the corresponding transmission spectra and can be detected as a plot of the intensity versus wave number.

Generally, a powder sample (m_2) without sample preparation is placed on the prism surface where it is compressed by a plunger. Powders, liquids, films, etc., can be easily measured with no pre-treatment. This device give rise to excellent results and flat base line as the technique is independent of light scattering (Drake, 2004).

In the present thesis, ATR-FTIR spectra were collected using Jasco FTIR – 4200 Fourier transform infrared spectrometer. Typically, samples of 2-5 mg were used. The spectra of samples were taken at 650–4000 cm^{-1} wavenumber.

2.4.5 Differential scanning calorimetry (DSC)

Differential scanning calorimetry is a thermal analytical technique in which the reference and sample are heated to a temperature above the melting point of the sample. The reference and sample temperatures are screened and constantly maintained at the same level or at isothermal conditions ($T_S = T_R$). When the sample absorbs or emits energy, isothermal conditions are kept constant by comparison of the signals coming from identical temperature sensors placed in the sample and reference holders. The automatic and continuous adjustment of heater power (energy per unit time) to attain these conditions gives rise to different electrical signals that are recorded. The sample requires more or less power to be maintained at the same temperature as that of the reference. This differential power is represented as a plot between temperature and the peak area or the energy of transition. Furthermore, different heat flow is expressed as exothermic or endothermic events.

DSC as a thermal method of analysis has the following advantages (Hatakeyama, 1999):

- It is a quick analytical method
- It requires simple sample preparation
- It applies a wide temperature range
- It requires small quantities of sample
- It is suitable for solids, liquids or semisolids
- It has excellent quantitative and qualitative ability

Furthermore, this technique has an important role in the determination of melting points, desolvation and glass transition temperatures, purity and polymorphic transformation.

Two types of DSC systems are commonly used (Figure 2.3). The first type is the power compensation DSC in which the sample and reference temperatures are controlled separately by identical furnaces. The second one is the heat flux DSC in which the sample and reference are enclosed together in a single furnace and their temperatures are controlled by a single temperature sensor.

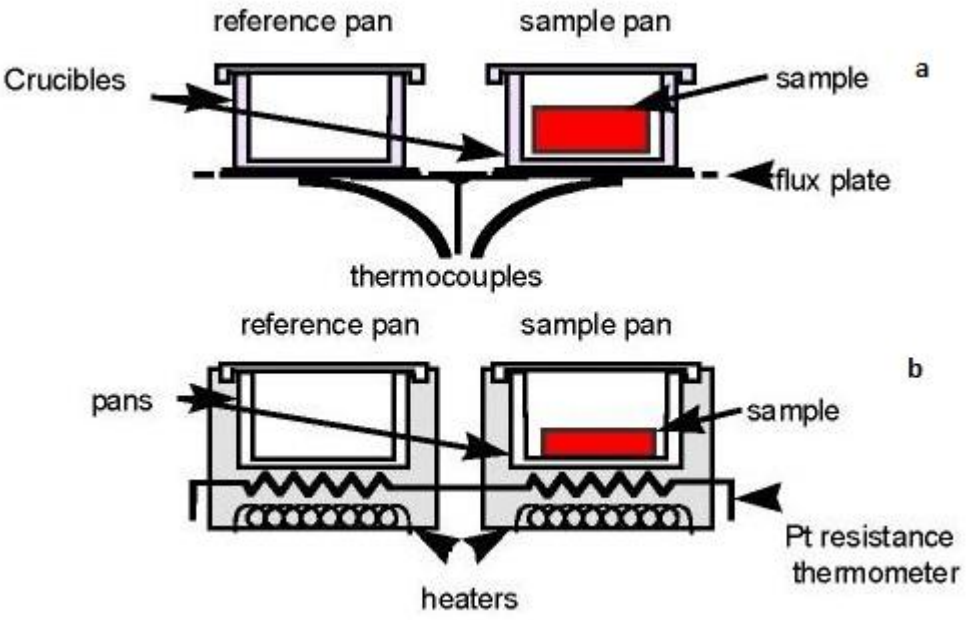

Figure 2.3: (a) Heat flux DSC; (b) power compensation DSC (retrieved from http://materials.npl.co.uk/matsol/dpscdtsc.jpg**, 15/4/2010).**

In the present thesis, Mettler Toledo star^{e} DSC 822^{e} system (based on the heat flux principle) was used. The system consists of a TA controller (TC 15) and a measuring cell (DSC 822^{e} module) that was cooled under a purge of nitrogen at a flow rate of 50 ml/min.

Aluminium standard crucible pans (40 µl) were used. Each crucible was weighed before loading of the sample. A sample of (1-5 mg) was weighed in the crucible by difference. A crucible sealing press was used to seal the pan with a pierced lid to allow gas exchange during heating. Then, the sealed crucible was put in the DSC instrument.

Glibenclamide and ketoconazole samples were heated from 30 to 230ºC at a rate of 10ºC / min while spironolactone samples were heated from 25 to 210ºC at a rate of 10ºC / min. The resulting DSC thermograms were normalised versus the weight of each sample.

2.4.6 Thermogravimetric analysis (TGA)

TGA is a type of analysis that is used to determine weight changes relative to temperature change. TGA is usually utilised to determine degradation temperatures; content of absorbed moisture; the ratio of organic and inorganic contents in materials; decomposition temperatures; and solvent residues.

The instrument consists of a highly accurate balance that is capable of detecting weight changes in micron range. The sample is loaded on a platinum pan which is located in a tiny, electrically heated oven connected to a thermometer to precisely determine the temperature (Figure 2.4). An inert gas such as nitrogen is usually used to purge the atmosphere to avoid oxidation or other unwanted reactions and to remove gaseous products resulting from heating of samples. The gas flow rate is about 30-40 ml/min. Analysis is performed by gradual increase of the temperature and plotting the weight of the sample versus temperature by a computer connected to the instrument.

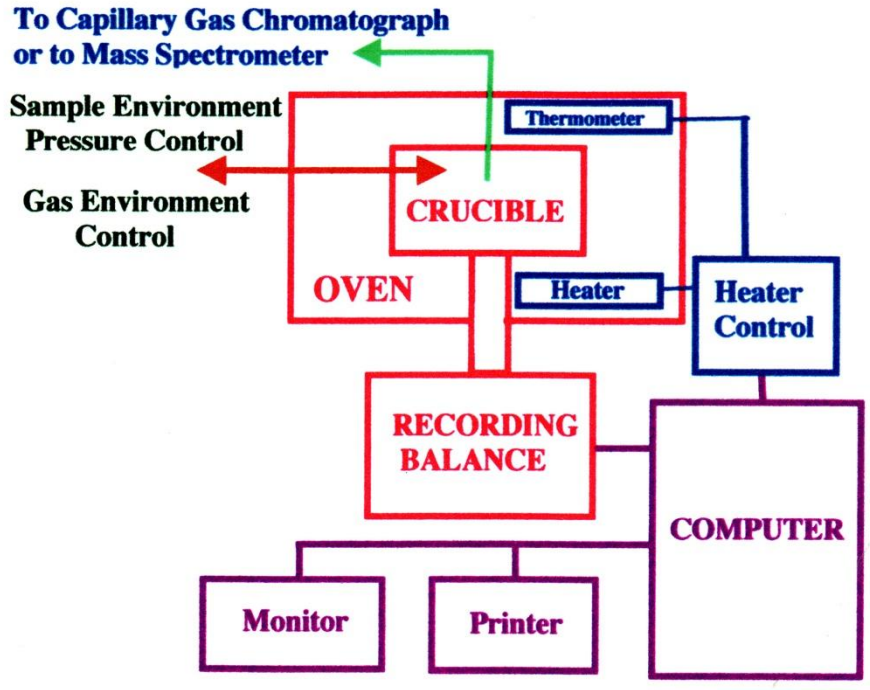

Figure 2.4: A Block Diagram of a Modern Thermo-Gravimetric Analysis Instrument (retrieved from http://physicalchemistryresources.com/Book5_sections/TA_Thermogravimetric %20 AnalysisHTML_1.htm**, 15/4/2010).**

In the present thesis, samples of 2-10 mg were loaded into uncovered aluminium crucibles and subjected to a 25-240ºC heating cycle. The obtained data were analysed to establish the weight loss of the sample in relation to temperature changes during the heating cycle.

2.4.7 X-Ray powder diffraction (XRPD)

X rays are quite short-wave length, high-energy beams of electromagnetic radiation. They lie in the wave length region between 0.1 and 100 Å (1 Å (angstrom) = 10^{-10} m) bordered by the γ-ray region to the short-wave length side and the vacuum ultraviolet region to the long-wave length side. Interaction of x-rays with the sample leads to the creation of secondary diffracted beams in the form of cones. These secondary beams are related to the interplanner spacing in the crystalline powder according to Bragg's equation:

$$n\lambda = 2\,d\sin\theta \qquad \text{(Equation 2.7)}$$

Where n is an integer, λ is the wavelength of the X-rays, d is the interplanner spacing generating the diffraction and θ is the diffraction angle. The unit of λ and d is angstrom. Diffraction maxima or peaks are measured through the 2θ diffractometer circle for the powder samples having a statistically unlimited amount of randomly arranged crystallites.

Figure 2.5 represents the operating principle of the powder diffraction system. The diffraction angle (2θ) is dependent on the interplanner spacing while the diffraction maximum intensity is dependent on the strength of those diffractions in the sample.

There are two basic types of Powder diffractometers; θ-θ in which the X-ray tube and detector move concurrently or θ-2θ in which the X-ray tube is fixed, and the sample moves at half the rate of the detector to keep the θ-2θ geometry. The diffraction angles and intensities are recorded electronically through a detector, electronics and a particular software resulting in a plot of 2θ (x axis) against intensity (y axis) for the sample.

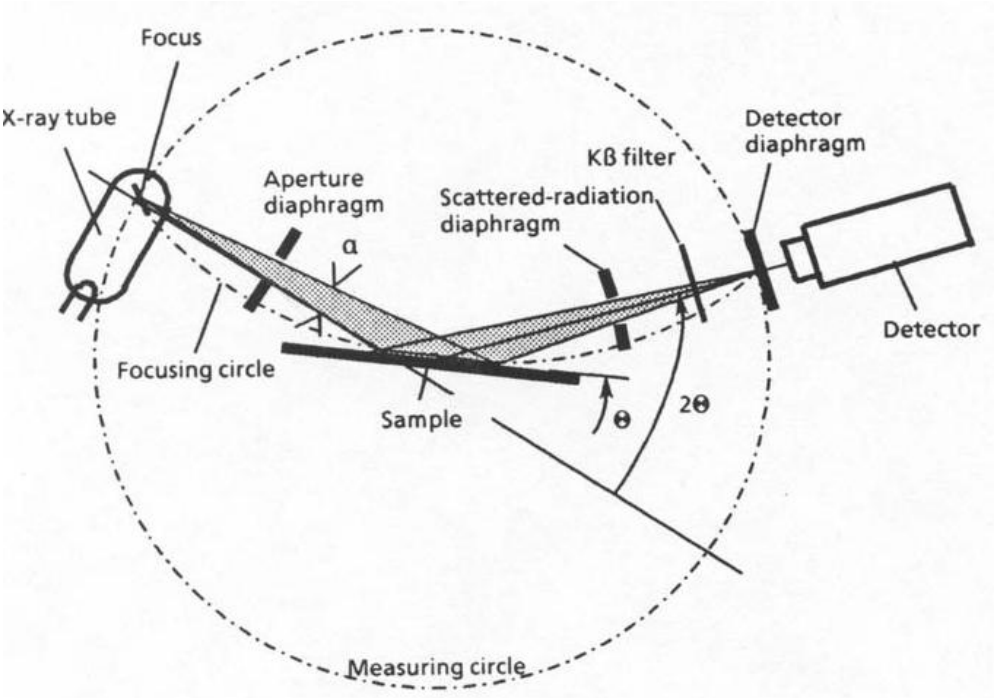

Figure 2.5: Operating principle of powder diffraction system (retrieved from http://epswww.unm.edu/xrd/xrdclass/01-XRD-Intro.pdf**, 15/4/2010).**

In the present thesis, samples of 10-50 mg with an even flat surface were mounted on a 28 position sample plate supported on a polyimide (Kapton, 7.5 µm thickness) film. The samples were analyzed at room temperature using transmission foil XRPD data collected on a Bruker AXS D8-Advance transmission diffractometer equipped with θ-2θ geometry. The source of radiation was monochromatic copper (Cu K_{a1}), λ was 1.54056 Å. Data was collected in the range from 4º to 35º 2θ with 2θ step and 1 second step $^{-1}$ count time.

2.5 Capsule spray coating

A bench-top minicoater, Caleva (Figure 2.6) was used for the coating process as it provides a suitable means of coating a small number of capsules. The spray head of the coater has one input for the coating solution/suspension and another one for the compressed air to ideally aerosolise the coating system into spray droplets. The coating system was stirred during the whole coating process to prevent precipitation of the coating raw materials. Capsule formulations were weighed before and after

coating and the average percentage weight gain was calculated. The percentage weight gain was kept within the specified range by adjusting and unifying the volume of the coating suspension per capsule. More details of this process will be discussed in Chapter 5.

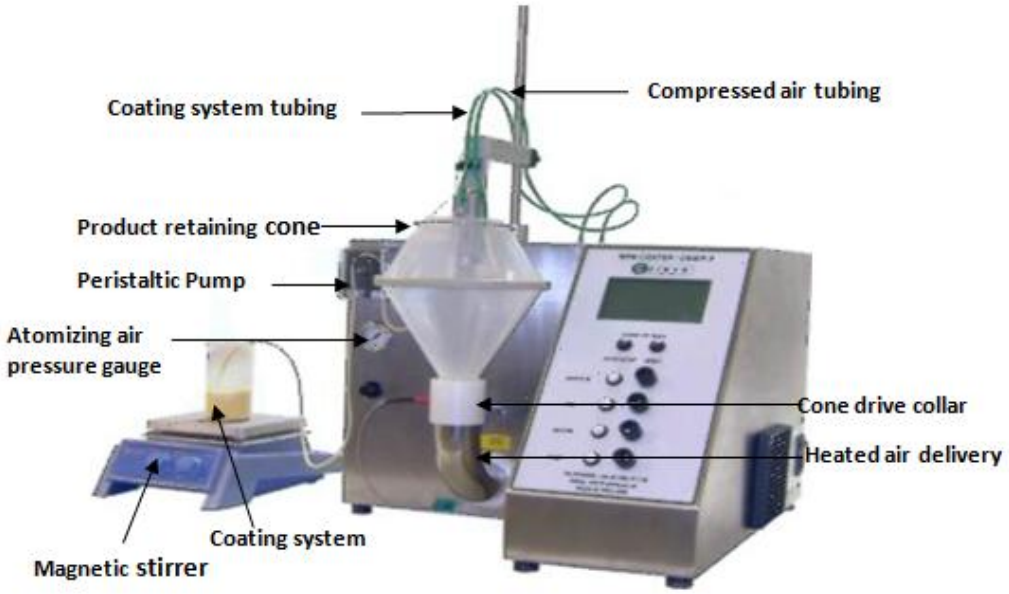

Figure 2.6: bench-top Caleva minicoater (retrieved from http://www.laboratory-tablet-coater.com/**, 15/4/2010)**

2.6 Stability studies

Stability studies for the coated capsule formulations were carried out under five different storage conditions; 25ºC/75% relative humidity (RH), 25ºC/65% RH, 25ºC/0% RH, 37ºC/0% RH and 50ºC/0% RH. More details of this study will be discussed in Section 6.3.2

2.8 In-vivo dog study

The study was carried out according to Laboratory Animal Care Principles and under a valid UK Home Office Animals (Scientific Procedures) Project Licence. Two male beagle dogs weighing from 11 to 15 kg were given 5 mg of glibenclamide as either commercial tablets or lyophilised glibenclamide-SLS capsule formulations with a

one week washout period between studies. Greater details of this study are provided in Section 7.3.2.

2.7.1 Gamma-scintigraphic study

Gamma-scintigraphy has been widely used in research as a useful non-invasive technique for imaging the performance of pharmaceutical dosage forms in-vivo (McInnes et al., 2008, Ghimire et al., 2007). In addition, it presents important information about the location of a dosage form at the time of any pharmacokinetic occasion in the plasma profiles. This facilitates analysis of pharmacokinetic profiles depending on location and performance of the dosage form at particular time points.

Figure 2.7 represents a schematic diagram of gamma-scintigraphy camera. A source [S] emits gamma radiation which is then absorbed by sodium iodide (NaI) crystals [C]. All gamma emissions are filtered by a parallel-hole collimator (PHC) that is located between the source and the crystals. This collimator has holes that act as a path for gamma radiation to reach the crystals. It allows only the passage of gamma radiations that are parallel to the holes and prevent all others reaching the crystals.

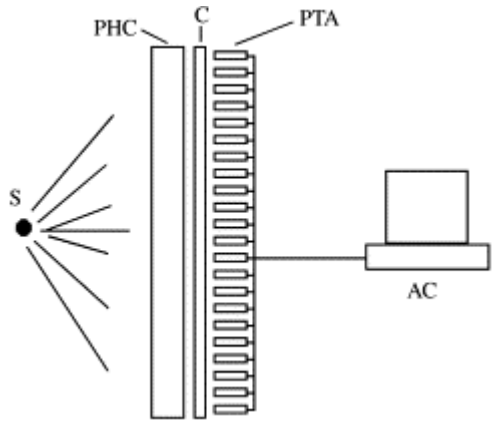

Figure 2.7: Schematic diagram of gamma-camera (Webb et al., 2002)

Gamma radiations stimulate sodium ions to release photons having different wavelengths. The position, energy and intensity of these photons are detected by

photomultiplier tubes (PTA). The signals from each tube are transmitted by a summation circuitry to the acquisition computer for more analysis. For dosage form evaluation by gamma scintigraphy camera, radioactive isotopes should be included in the dosage form so that it can be traced by the camera. The radioactive isotopes are chosen depending on different factors such as half life, radiation energy and extent, cost, and availability (Wilding et al., 2001). There are two methods for incorporating a radioactive material in a dosage form; neutron activation technique or standard labelling procedure (Digenis et al., 1998). In the technique of neutron activation, a non-radioactive material such as Samarium-152 and Erbium-170 is added to the dosage form followed by neutron irradiation process to generate gamma emitting isotopes ^{153}Sm and ^{171}Er . Although this method decreases the worker exposure to radiation during production, it is expensive and the generated heat during the process of irradiation can induce changes in the performance of the polymeric contents of the formulations (Maggi et al., 2004; Marvola et al., 2004). In the standard labelling technique, a radioactive isotope such as ^{99m}Tc or ^{111}In is directly incorporated in the dosage form.

Table 2.1 shows examples of the commonly used radioactive isotopes. In the present study, Technitium-99m was selected.

Table 2.1: Examples of commonly used radioactive isotopes

Radioactive isotope	Half life
Technetium-99m (^{99m}Tc)	6 hours
Indium-111 (^{111}In)	2.5 days
Erbium-171 (^{171}Er)	7.5 hours
Samarium-153 (^{153}Sm)	47 hours
Chromium-51 (^{51}Cr)	28 days

Technitium-99m is considered the most widely used radioisotope for Gamma scintigraphy studies. It is characterised by adaptable chemistry, low energy (140 keV) and low radiation dose (Wilding et al., 2001). Its half-life is six hours which is short enough to minimise the radiation dose to the animal. It is also inexpensive and can be easily produced (Guan et al., 2010).

2.7.2 Chromatographic analysis of glibenclamide by HPLC

Glibenclamide was assayed using a Dionex HPLC system incorporating a reverse phase column (150 × 4.60 mm Phenomenex, 3 µm C_{18} (2) 100 Å column fitted with a Phenomenex guard column). An isocratic mobile phase consisting of 70% v/v methanol and 30% v/v formic acid (0.1% v/v) was eluted through the column at a flow rate of 1 ml/min. The injection volume was 20 µl and the UV detection wavelength was 240 nm. Details of the HPLC analysis method will be discussed in Section 7.3.4.

2.7.3 Dog blood glucose levels during the in-vivo study

Blood glucose levels were assessed directly after sample collection using One Touch test strips analysed using an Accu-Chek® Aviva Nano.

Chapter 3

3. Effect of lyophilisation process and excipient manipulation on the dissolution rate of poorly water-soluble drugs

3.1 Introduction

Glibenclamide, spironolactone and ketoconazole were used in the present thesis as three models of poorly water-soluble drugs belonging to BCS class II (see Section 1.1). These drugs have poor gastrointestinal absorption after oral administration due to their poor water-solubility and subsequent low dissolution rate which negatively affects their therapeutic efficacy (Charman & Charman, 2003). It is well-known for these drugs that an increase in their dissolution rate could lead to great enhancement in their oral bioavailability (Onoue et al., 2009).

Different hydrophilic excipients have been reported to enhance the dissolution rate of poorly water-soluble drugs. Some of these excipients on this basis were adopted in this work to enhance the dissolution rate of glibenclamide, spironolactone and ketoconazole. These excipients include mannitol, Sodium lauryl sulfate (SLS), polyethylene glycol (PEG) 6000, tromethamine, gelatin, citric acid and fumaric acid.

Mannitol (Figure 3.1) is considered a non-reducing sugar which is commonly used as an excipient in lyophilised formulations due to its excellent cake-forming properties. It is also used as a bulking agent in lyophilised protein formulations (Pyne et al., 2002). Furthermore, mannitol as a hydrophilic excipient has been employed in pharmaceutical formulations for dissolution enhancement of hydrophobic drugs (Ahuja et al., 2007).

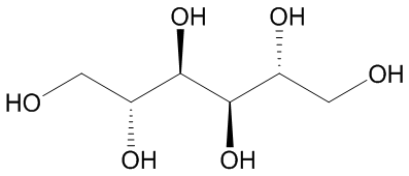

Figure 3.1: Chemical structure of mannitol

SLS (Figure 3.2) is an anionic surfactant which acts by decreasing the surface tension of dissolution medium leading to drug dissolution enhancement. It has been

reported to enhance the dissolution rate of active pharmaceutical ingredients such as the phosphate salt of carvedilol (Chakraborty et al., 2009).

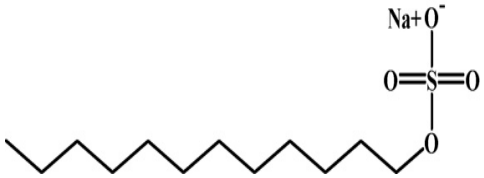

Figure 3.2: Chemical structure of sodium lauryl sulfate

PEG 6000 (Figure 3.3) is a hydrophilic polymer that has been used by many researchers to enhance the dissolution rate of hydrophobic drugs through solid dispersion formation (Asyarie & Rashmawati, 2007; Ahuja et al., 2007).

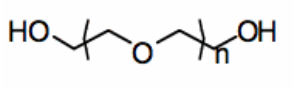

Figure 3.3: Chemical structure of polyethylene glycols

Tromethamine (Figure 3.4) is an organic amine proton acceptor that has been used recently as a pharmaceutical excipient for dissolution rate enhancement of acidic hydrophobic drugs. It acts as an alkalinizing agent that increases the pH of the diffusion layer surrounding drug particles in the dissolution medium (Abdelkader et al., 2007).

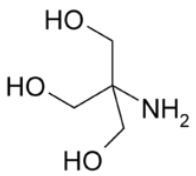

Figure 3.4: Chemical structure of tromethamine

Gelatin (Figure 3.5) is a combination of water soluble proteins derived from collagen. It has been reported that water soluble gelatin has mild surface activity and can enhance the dissolution rate of several poorly water-soluble drugs (Kallinteri & Antimisiaris, 2001).

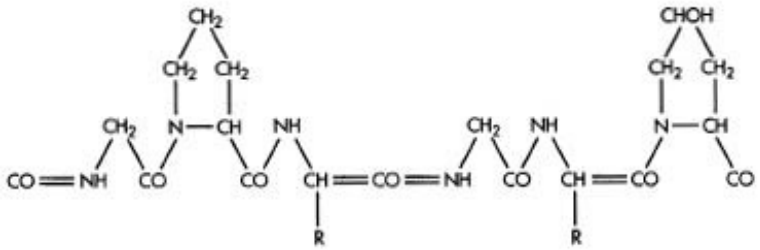

Figure 3.5: Chemical structure of gelatin

Fumaric acid (Figure 3.6) and citric acid (Figure 3.7) are water-soluble organic acids that act as pH modifiers. They can be used to lower the pH of the microenvironment of dosage forms leading to dissolution enhancement of poorly water-soluble drugs (Tran et al., 2010).

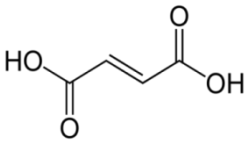

Figure 3.6: Chemical structure of fumaric acid

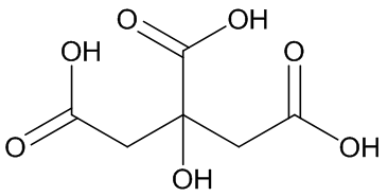

Figure 3.7: Chemical structure of citric acid

3.1.1 Glibenclamide

Glibenclamide is an oral hypoglycaemic agent that is used for the treatment of non insulin-dependent diabetes mellitus (Type II). Glibenclamide belongs to the second generation sulfonylureas (Figure. 3.8) which are characterised by poor water solubility that leads to low dissolution rate and subsequently, erratic absorption (Kumar et al., 2001; Tashtoush et al., 2004; Valleri et al., 2004).

Glibenclamide is a weak acidic drug with a pK_a of 5.3 and has very poor water solubility. It also has restricted solubility in organic solvents such as ethanol, methanol and chloroform. As a white crystalline powder, glibenclamide has a reported melting temperature of 172-174ºC (Klein et al., 2009).

Glibenclamide's oral bioavailability depends on its particle size and crystallinity (Wei et al., 2008). Therefore, some commercial tablet formulations contain a micronized form of the drug to enhance the oral bioavailability (Klein et al., 2009). Timmins et al. (2006) and Balan et al. (2000) have reported that a controlled particle size and size distribution of glibenclamide decreased the variability in its bioavailability.

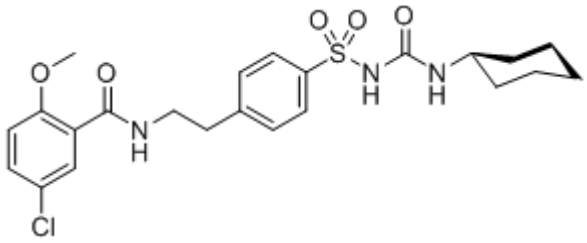

Figure 3.8: Chemical structure of glibenclamide.

The recommended human daily dose of glibenclamide is typically 2.5–5 mg which can be increased up to 15 mg if necessary. To develop a reliable and safe oral hypoglycaemic treatment, many strategies have been investigated to enhance dissolution and consequently oral bioavailability of glibenclamide and other sulfonylureas drugs.

It has been reported that glibenclamide undergoes polymorphism. Suleiman and Najib. (1989) obtained two polymorphs (form I and II crystallised from dioxane and acetonitrile respectively) and two pseudo-polymorphs (pentanol and toluene solvates) of glibenclamide. It was found that the rank aqueous solubility was: pentanol solvate > Form II > toluene solvate > form I which was the most stable and showed the lowest solubility. Panagopoulou-Kaplani and Malamataris (2000) investigated the formation of another insoluble polymorphic form of glibenclamide by sublimation of the drug glassy state at 130-160ºC.

Tashtoush et al. (2004) investigated the improvement of the dissolution rate and bioavailability of glibenclamide processed as a solid dispersion formation with Gelucire 44/14 and polyethylene glycol 6000 employing fusion method compared to Daonil® tablets (Hoechst). Glibenclamide dissolution, bioavailability and efficacy have been enhanced by formation of solid dispersion of the drug with microcrystalline cellulose by solvent deposition techniques (Dastmalchi et al., 2005). Zerrouk et al. (2006) has reported that the aqueous solubility of glibenclamide was increased 40 times in the presence of 25 mM hydroxypropyl-β-cyclodextrin, 25 times in the presence of 13 mM β-cyclodextrin and just 3 times in the presence of 0.5% w/v chitosan. Moreover, it was found that simultaneous presence of chitosan and cyclodextrin resulted in significant reduction in the solubilising effect of cyclodextrin due to competition between the drug and the polymer for interaction with the cyclodextrin cavity. In contrast, it was revealed from permeation studies that chitosan was more effective than cyclodextrins in enhancing glibenclamide permeability through a Caco-2 cell layer (a colon rectal adenocarcinoma cell line of human origin; an in-vitro tool for permeability studies). A 5.5-fold enhancement of glibenclamide dissolution over marketed drug tablets, has been reported by Cirri et al. (2007) who investigated the formation of ternary solid dispersion of glibenclamide/PEG 6000/SLS in the ratio 10/80/10. This ternary system was found to achieve 100% glibenclamide dissolution after 20 minutes. The dissolution performance and solubility of glibenclamide has been significantly improved through complexation with hydroxybutenyl-β-cyclodextrin (Klein et al., 2009). Furthermore, Cirri et al. (2009) have developed glibenclamide fast dissolving tablets using ternary solid dispersion of the drug with hydroxypropyl β-cyclodextrin and

polyvinylpyrrolidone. These formulations achieved 100% glibenclamide dissolution within the first 15 minutes. It was found that preparation of solid dispersion of glibenclamide with polyglycolized glycerides carriers using a spray drying technique with the aid of silicon dioxide as adsorbent resulted in burst drug dissolution in the first 10 minutes as well as enhancement in the drug dissolution rate and extent. Furthermore, from an in-vivo study, it was found that the blood glucose level in Swiss Albino mice, after administration of the glibenclamide solid dispersion, was reduced to 139 ± 2.3 mg/dl after 60 minutes in comparison to 250 ± 5.3 mg/dl in the case of the unprocessed drug (Chauhan et al., 2005). This finding revealed the enhancement of glibenclamide therapeutic efficacy from the solid dispersion over the unprocessed drug. Self-microemulsifying drug delivery system (SMEDDS) or anhydrous state of microemulsion of glibenclamide has been developed to improve in-vitro drug dissolution compared to unprocessed drug and its commercial tablets (Bachhav & Patravale, 2009). Dora et al. (2010) have developed nanoparticle formulations of glibenclamide with Eudragit L100 for oral administration. This formulation achieved dissolution and bioavailability enhancement and consequently higher activity in diabetic rabbit model relative to plain glibenclamide.

3.1.2 Spironolactone

Spironolactone is a synthetic steroidal aldosterone antagonist (Figure 3.9) that is used as a potassium sparing diuretic. It is primarily used for treatment of ascites associated with liver cirrhosis, heart failure and hypertension. Spironolactone is practically insoluble in water, soluble in alcohol, and freely soluble in benzene and chloroform. It has a melting point of 198-207ºC. It also undergoes extensive first pass metabolism and enterohepatic circulation (Moffat et al., 2004). Thus, this diuretic is characterised by unpredictable and low oral bioavailability (Absosehmah-Albidy et al., 1997) which has been reported as being about 75% (Abshagen et al., 1976). Commercial tablets contain 25, 50, or 100 mg of drug. Spironolactone has been reported to recrystallise into different polymorphic forms from different solvents and to go through structural rearrangements upon heating (Neville et al., 1994; Berbenni et al., 1999). Beckstead et al. (1993) investigated the preparation of

five solvates of spironolactone by crystallisation from absolute methanol, acetonitrile, absolute ethanol, ethyl acetate, and benzene. Agafonov et al. (1991) investigated two polymorphic forms and four solvates of spironolactone by crystallisation from acetone, dioxane, chloroform, acetonitrile, ethanol, methanol and ethyl acetate.

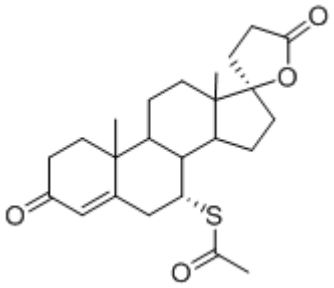

Figure 3.9: Chemical structure of spironolactone.

Some methods have been reported to improve the dissolution rate and bioavailability of spironolactone. Soliman et al. (1997) investigated complex formation of spironolactone with different types of cyclodextrins (CDs); β-CD, γ-CD, hydroxypropyl β-CD and hydroxypropyl γ-CD employing spray drying technique. The obtained complexes were amorphous and exhibited higher dissolution rate than the unprocessed spironolactone powder especially in the case of hydroxypropyl CDs. It has been reported that spironolactone nanoparticles produced by an antisolvent precipitation technique had a significantly faster dissolution rate than the unprocessed drug (Dong et al., 2009). Dong et al. (2010) investigated antisolvent precipitation of spironolactone nanoparticles using a continuous and highly effective static mixing process. The resultant lyophilised spironolactone nanoparticles exhibited 6.6 folds faster dissolution rate than the lyophilised raw drug. In another study, solid dispersion of spironolactone with porous silica has been investigated. It was found that the drug transformed to an amorphous form in the solid dispersion and hence, exhibited remarkable improvement in the drug dissolution rate compared with the unprocessed spironolactone powder (Uchino et al., 2007). Furthermore,

Yassin et al. (2009) studied the formation of solid dispersion of spironolactone with Gelucire (G44, G50) and Aerosil® 200 by spray drying technique. Dissolution rate was significantly enhanced relative to the physical mixture and the unprocessed spironolactone. DSC studies revealed the transformation of spironolactone to an amorphous form in the solid dispersion.

3.1.3 Ketoconazole

Ketoconazole is a broad spectrum imidazole derivative antifungal drug used for the treatment of superficial and systemic mycosis (Figure 3.10). It is a weak base with two pK_a values of 2.94 and 6.15. It displays strongly pH dependent solubility; it is readily soluble in acidic water (pH < 3) and has a very low solubility (less than 4-6.7 µg/ml) in water at or beyond neutral pH (Zhou et al., 2005). It is soluble in methanol, freely soluble in methylene chloride and sparingly soluble in ethanol (European Pharmacopoeia, 1997). If not properly formulated, ketoconazole may exhibit degradation through oxidation or hydrolysis, particularly in aqueous media (Skiba et al., 2000). Furthermore, bioavailability studies of ketoconazole have revealed that its oral absorption in humans is erratic and dependent on pH (Zhou et al., 2005).

Different methods have been investigated to improve the dissolution rate of ketoconazole. Complexation of ketoconazole with β-cyclodextrin and 2-hydroxypropyl-β-cyclodextrin has been reported to enhance the drug dissolution rate (Esclusa-Diaz, 1996). Taneri et al. (2002) investigated the enhancement of the dissolution rate of ketoconazole by complexation of the drug with hydroxypropyl-β-cyclodextrin or methyl-β-cyclodextrin by kneading or spray drying technique. Improved dissolution rate and bioavailability of ketoconazole by more than two times that of the commercial tablets have been reported by controlled precipitation of the drug (Elder et al., 2007). In another study, a distinctly enhanced dissolution rate of ketoconazole was achieved by micronization of the drug by the aid of controlled crystallisation technique (Rasenack & Müller, 2002). Heo et al. (2005) investigated the enhancement of ketoconazole dissolution rate by incorporating different excipients of a self microemulsifying drug delivery system (oils, fatty acids and

surfactant) in the solid dispersion of the drug with PEG 6000 using the fusion method. The resultant system showed significant improvement in the dissolution rate and more than two folds maximum plasma concentration and area under the plasma concentration-time curve compared to the unprocessed drug. Basa et al. (2008) developed a new tablet formulation containing ketoconazole nanoparticles layered onto water-soluble excipients. This tablet formulation exhibited a significantly faster dissolution rate of ketoconazole than that of the commercially available tablets.

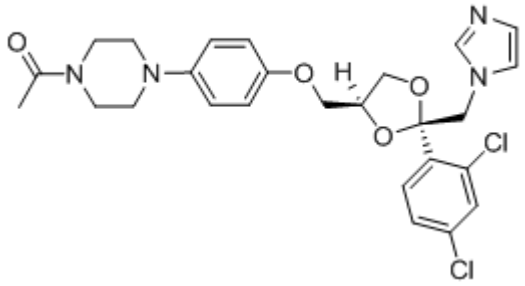

Figure 3.10: Chemical structure of ketoconazole.

3.2 Aims and objectives

The aim of this chapter is to enhance the dissolution rate of glibenclamide, spironolactone and ketoconazole through lyophilisation process. The effect of co-lyophilisation of these drugs with different excipients on their dissolution rates was also studied.

3.3 Methods

3.3.1 Construction of calibration curves

Drugs (~50 mg) were individually dissolved in 10 ml methanol. 1 ml of the resulting drug solutions were used to prepare stock solutions using the in-vitro dissolution media to be used in dissolution studies. Serial dilutions were prepared from these stock solutions. The drug solutions were scanned between 200 and 350 nm to obtain

UV spectra. This was used to identify λ_{max} for analysis runs. At the selected wave length for individual drugs, the absorbance of a given solution was measured. The measured absorbance values were plotted against concentrations. From this plot, a linear relationship between absorbance and concentration was obtained and used for further dissolution studies to determine the concentrations of drugs in solutions.

3.3.2 Preparation of lyophilised formulations

3.3.2.1 Glibenclamide

40 mg of glibenclamide, alone or as mixtures with different excipients, were dissolved in 8 ml of a co-solvent system consisting of 50% v/v t-butyl alcohol, 12.5% v/v ammonia solution (88% w/w) and 37.5% v/v distilled water. A magnetic stirrer was used to facilitate the dissolution of the drug and excipients into the co-solvent system. Solutions were frozen at -80ºC for 3 hours and lyophilised overnight using a Christ type lyophiliser set at a shelf temperature of 25ºC and a vacuum pressure of 0.035 mbar. Lyophilised powders equivalent to 5 mg of glibenclamide, were filled into hard gelatin capsules and used for dissolution studies. Different excipients and their concentrations that were used in glibenclamide formulation development are listed in Table 3.1.

Table 3.1: Different excipients used in glibenclamide formulation development

Excipient	Concentrations
Mannitol	83, 91, 95 % w/w
SLS	85, 91, 93 % w/w
PEG 6000	33, 50, 80 % w/w
Tromethamine	33, 50, 80 % w/w
Gelatin	28, 50, 66 % w/w

3.3.2.2 Spironolactone

200 mg of spironolactone, alone or as mixtures with different excipients were dissolved in 8 ml co-solvent system consisting of 60% v/v t-butyl alcohol and 40%

v/v distilled water. The procedures mentioned in Section 3.3.2.1 were followed to obtain the lyophilised products. Lyophilised powders equivalent to 25 mg spironolactone, were filled into hard gelatin capsules and used for dissolution studies. Different excipients and their concentrations that were used in spironolactone formulation development are listed in Table 3.2.

Table 3.2: Different excipients used in spironolactone formulation development

Excipient	Concentrations
Mannitol	50, 67, 80 % w/w
SLS	55, 67, 74 % w/w
PEG 6000	50, 67, 80 % w/w
Fumaric acid	55, 67, 74 % w/w
Citric acid	55, 67, 74 % w/w

3.3.2.3 Ketoconazole

1.6 g ketoconazole or equivalent mixtures with different excipients were dissolved in 16 ml co-solvent system of 50% v/v t-butyl alcohol, 40% v/v distilled water and 10% v/v 0.2 N hydrochloric acid. In the case of mixtures of ketoconazole with excipients, solution volumes equivalent to 100 mg of ketoconazole were filled into hard gelatin capsule bodies for lyophilisation. The solution of ketoconazole alone was lyophilised in glass vials to avoid loss of the product through overflow (observed during method development) during the lyophilisation process. The procedures mentioned in Section 3.3.2.1 were followed to obtain the lyophilised products. 200 mg of ketoconazole powder (lyophilised alone) was filled into hard gelatin capsules. The resultant capsules were capped and then used for dissolution studies (two capsules of the lyophilised mixtures, equivalent to the dose of 200 mg, were used). Different excipients and their concentrations that were used in ketoconazole formulation development are listed in Table 3.3.

Table 3.3: Different excipients used in ketoconazole formulation development

Excipient	Concentrations
Mannitol	11, 20, 33 % w/w
SLS-mannitol	9-30, 14-28, 19-27 % w/w
PEG 6000-mannitol	40-20, 25-25, 14-28 % w/w

3.3.3 Preparation of physical mixtures

Physical mixtures corresponding to the lyophilised products achieving the highest dissolution rate were prepared by trituration using a mortar and a pestle with gentle mixing for approximately 5 minutes avoiding compression. Physical mixtures corresponding to 5 mg glibenclamide, 25 mg spironolactone or 200 mg ketoconazole were used for dissolution studies.

Table 3.4: Summary of physical mixtures of drugs with different excipients

Drug	Excipient concentrations in the Physical mixtures
Glibenclamide	93% w/w SLS, 91% w/w mannitol, 50% w/w gelatin, 80% w/w PEG 6000, 50% w/w tromethamine.
Spironolactone	67% w/w SLS, 67% w/w mannitol, 55% w/w citric acid, 74% w/w fumaric acid, 80% w/w PEG 6000.
Ketoconazole	33% w/w mannitol, 14% w/w SLS + 28% w/w mannitol, 14% w/w PEG 6000 + 28% w/w mannitol.

3.3.4 In-vitro dissolution studies

The in-vitro dissolution studies were performed for the lyophilised formulations and the physical mixtures. The details of the in-vitro dissolution studies were summarised in Section 2.4.1. In-vitro dissolution data were statistically analysed using similarity factor (f_2) (Section 2.4.2).

3.4 Results and discussion

3.4.1 Calibration curves

Figures 3.11-3.13 show calibration curves for glibenclamide, spironolactone and ketoconazole in phosphate buffer solution (pH 7.4); 0.1N HCL (containing 0.1% w/v SLS); and 0.5% w/v SLS solution respectively. Linear relationships were obtained as a result of plotting absorbance versus concentration.

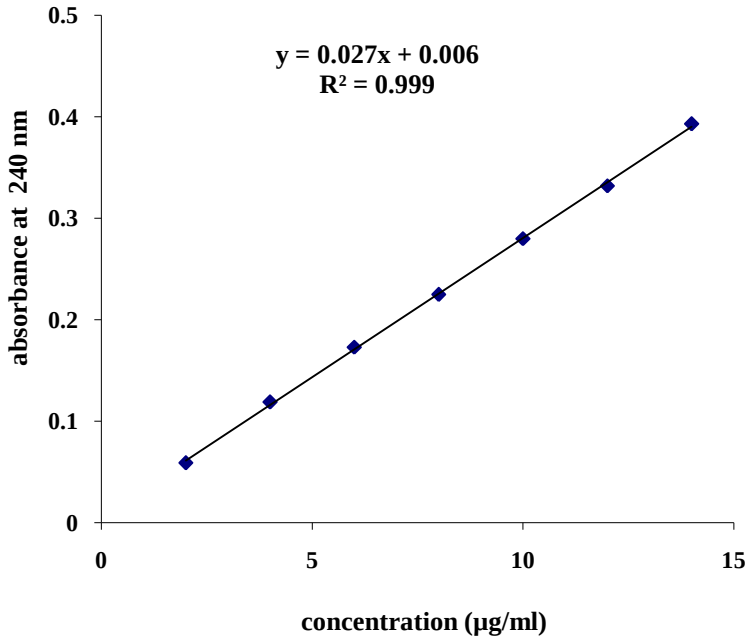

Figure 3.11: Calibration curve of glibenclamide in phosphate buffer solution (pH 7.4).

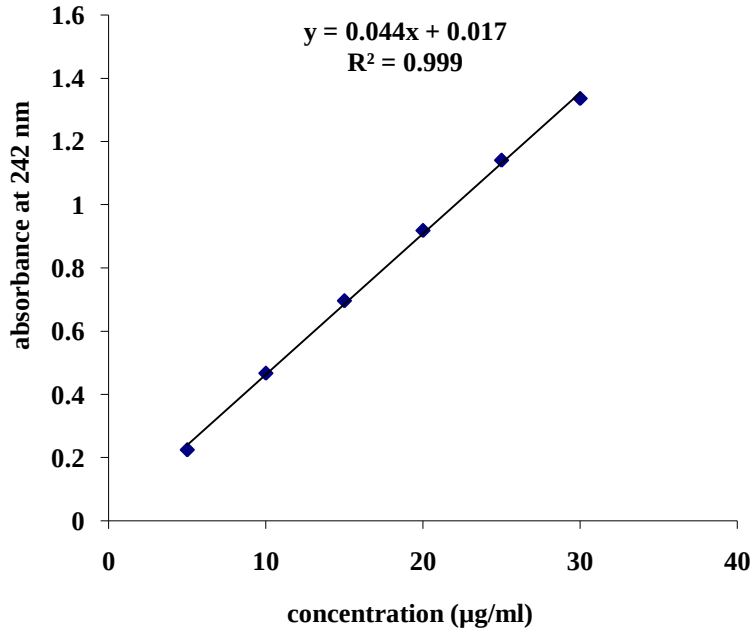

Figure 3.12: Calibration curve of spironolactone in 0.1 N HCL containing 0.1% w/v SLS.

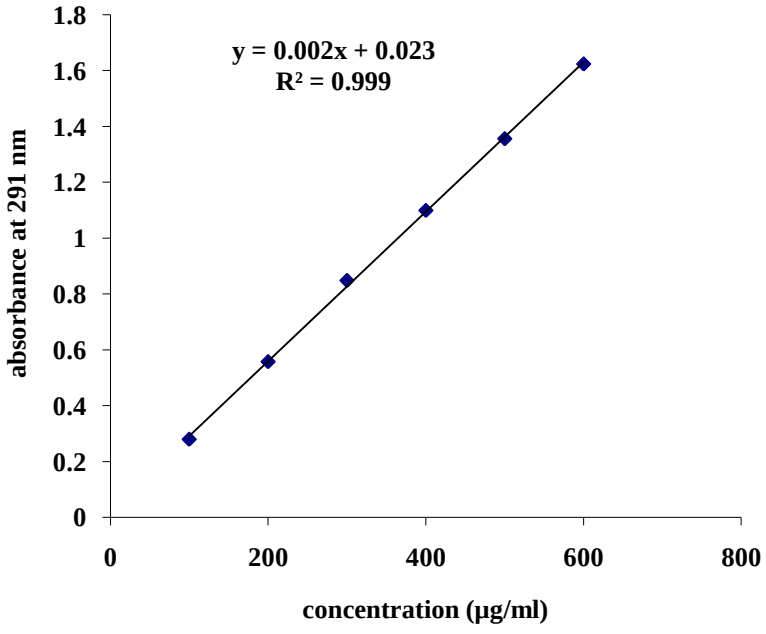

Figure 3.13: Calibration curve of ketoconazole in 0.5% w/v SLS aqueous solution.

3.4.2 In-vitro dissolution studies

3.4.2.1 Lyophilised glibenclamide

Dissolution profile obtained from the lyophilised glibenclamide filled into hard gelatin capsules is shown in Figure 3.14. Dissolution performance of the lyophilised glibenclamide is better than that of the commercial tablets. The percentages of glibenclamide dissolved from the unprocessed glibenclamide capsules and the commercial tablets were 40% and 52% respectively within the first 60 minutes. On the other hand, the percentage of glibenclamide dissolved from the lyophilised formulations was 82% within the same time period. Statistical analysis showed a significant difference between the dissolution profiles of lyophilised glibenclamide and those of the unprocessed drug (f_2 = 17.2) and the commercial tablets (f_2 = 26.2).

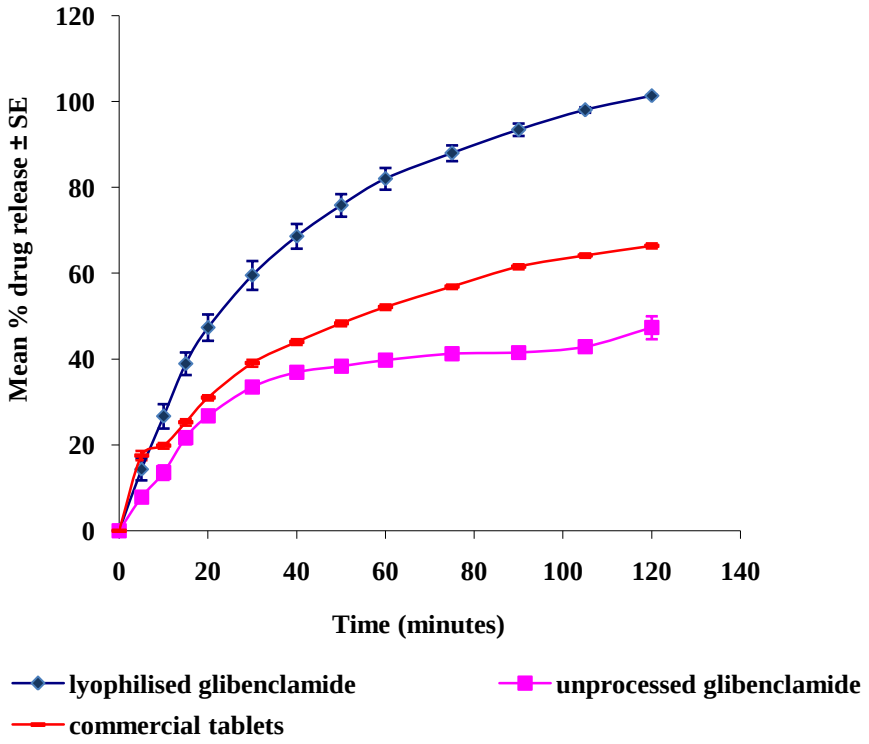

Figure 3.14: Effect of lyophilisation on the dissolution profile of glibenclamide (n=6).

Dissolution rate enhancement of the lyophilised drug may be attributed to change in the polymorphic form or amorphous formation during the lyophilisation process (see

Section 4.4.1.1). It has been reported by many researchers that lyophilisation may result in changes in the physical structure of the processed ingredients (Takada et al., 2009; Kadoya et al., 2008; Abdul-Fattah et al., 2007; Haque and Roos, 2005). Dissolution rate enhancement of hydrophobic drugs due to amorphous formation during lyophilisation process has been reported in many literatures (Hodges et al., 2006; Ahmed & Nafadi, 2006; Laitinen et al., 2009).

3.4.2.2 Lyophilised glibenclamide-mannitol mixture

The effect of different concentrations of mannitol on the dissolution profile of lyophilised glibenclamide is illustrated in Figure 3.15. It was found that mannitol in all concentrations enhanced the dissolution rate of the drug. Statistical analysis showed significant differences between individual dissolution profiles of lyophilised glibenclamide with different concentrations of mannitol and that of the lyophilised drug alone (f_2= 41.6, 42.2, 42.4 for 83%, 91%, 93% w/w mannitol respectively).

Physical mixture of glibenclamide with 91% w/w mannitol was tested for dissolution behaviour and compared with the corresponding lyophilised mixture, commercial tablets and unprocessed drug. Figure 3.16 shows marked increase in the dissolution rate and extent of glibenclamide from the lyophilised mixture compared with other formulations.

The percentage of glibenclamide dissolved after 30 minutes (D_{30}) and the time for dissolution of 50% of the initial amount ($T_{50\%}$) were represented in Table 3.5. Lyophilisation of glibenclamide with mannitol decreased $T_{50\%}$ from 54.3 minutes (commercial tablets) and more than 120 minutes (unprocessed drug) to 22.2 minutes while that of the physical mixture was 114.2 minutes. Furthermore, After 30 minutes, almost 76.7% of drug dissolved from the lyophilised mixture while for the physical mixture, commercial tablets and unprocessed drug only 40.5%, 39.1% and 33.5% respectively dissolved.

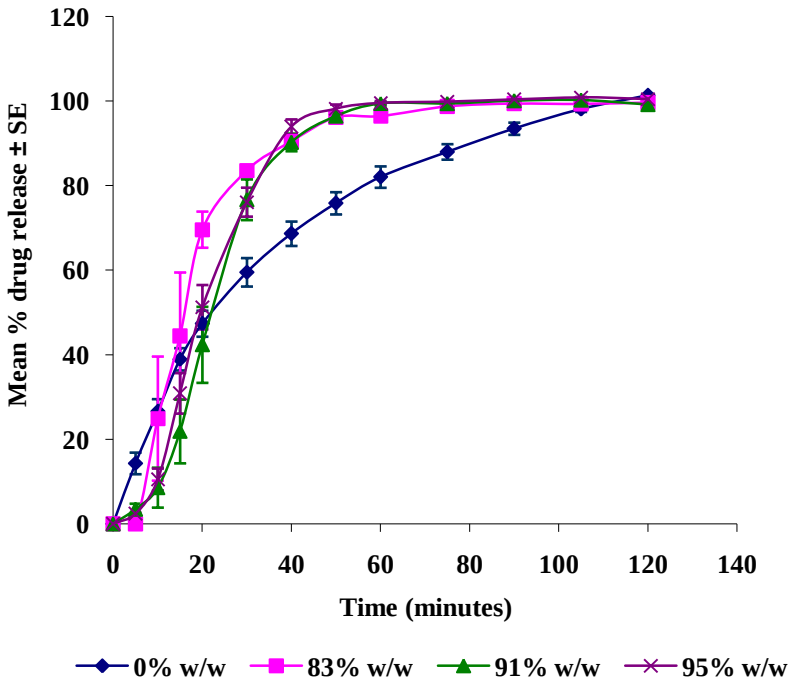

Figure 3.15: Effect of different concentrations of mannitol on the dissolution profile of lyophilised glibenclamide (n=6).

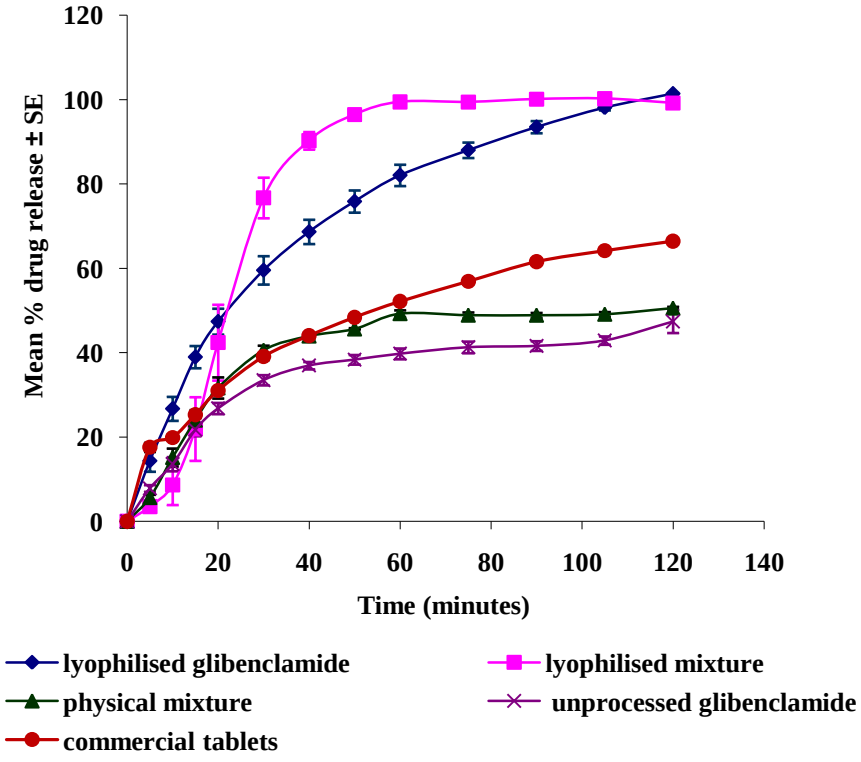

Figure 3.16: Dissolution profiles of lyophilised and physical mixtures of glibenclamide with 91% w/w mannitol (n=6).

Table 3.5: Dissolution properties of lyophilised and physical mixtures of glibenclamide with 91% w/w mannitol compared to the unprocessed drug and commercial tablets.

Sample	D_{30} ± SE	$T_{50\%}$ (minutes)
Lyophilised mixture	76.7 ± 4.8	22.2
Physical mixture	40.5 ± 1.1	114.2
Commercial tablets	39.1± 0.5	54.3
Unprocessed glibenclamide	33.5 ± 1.2	> 120

The exhibited dissolution enhancement may be attributed to the formation of drug solid dispersion throughout the water soluble excipient, mannitol, during the lyophilisation process. Typical mechanisms for enhancement of dissolution properties of drugs by solid dispersions are formation of smaller particle size of the drug (Karavas et al., 2005); alteration of drug polymorphic form (Karavas et al., 2006); enhancement of drug wettability (Zajc et al., 2005); prevention of drug particle aggregation by excipients; and finally the combination of these mechanisms. Another explanation for the produced dissolution enhancement of glibenclamide is the transformation of the drug to an amorphous form in the produced solid dispersion (see Section 4.4.1.2). Solubility and dissolution enhancement of glibenclamide from the drug solid dispersion with polyglycolized glycerides (Gelucire 50/13, 44/14) has been explained on the basis of formation of amorphous form of the drug in the solid dispersion (Chauhan et al., 2005). Ahuja et al. (2007) have studied the enhancement of a poorly water-soluble drug, rofecoxib, through formation of a solid dispersion with mannitol. Also, solid dispersion formation of a hydrophobic drug, meloxicam, with mannitol has been reported to increase the solubility and dissolution rate of the drug (Pathak et al., 2008).

3.4.2.3 Lyophilised glibenclamide-SLS mixture

The effect of different concentrations of SLS on the dissolution characteristics of lyophilised glibenclamide is illustrated in Figure 3.17. The lyophilised mixtures of

glibenclamide with SLS exhibited marked improvement in the dissolution rate and extent especially with higher concentrations of the excipient. Statistical analysis showed a significant difference between dissolution profiles of the lyophilised glibenclamide-SLS formulations and that of the lyophilised drug alone (f_2= 42, 28.3, 23 for 85%, 91%, 93% w/w SLS respectively).

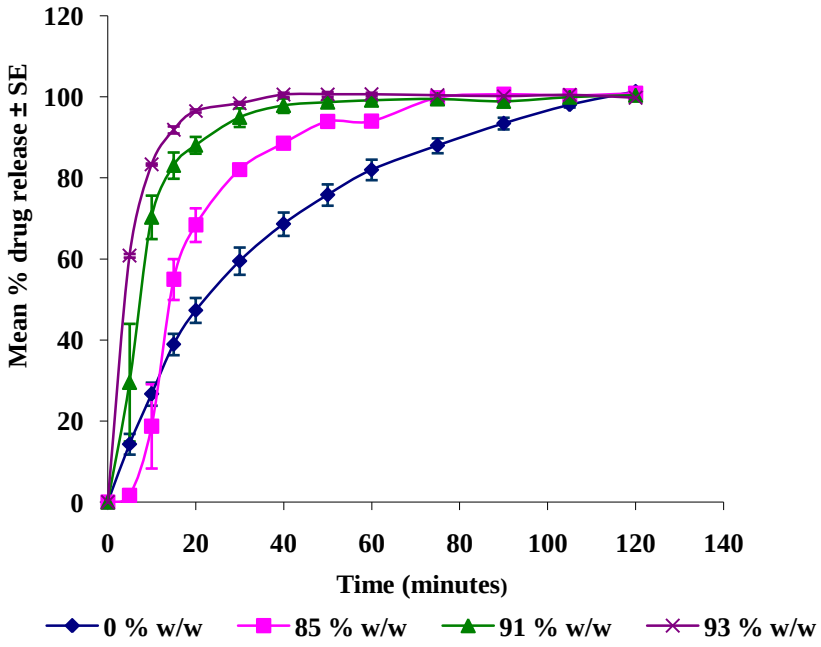

Figure 3.17: Effect of different concentrations of sodium lauryl sulfate on the dissolution profile of lyophilised glibenclamide (n=6).

The dissolution behaviour of the physical mixture of glibenclamide with 93% w/w SLS was investigated and compared with the corresponding lyophilised mixture, commercial tablets and unprocessed drug (Figure 3.18). The lyophilised mixture of glibenclamide with SLS exhibited marked improvement in the dissolution rate and extent of the drug. Statistical analysis showed significant differences between dissolution profile of the lyophilised mixture and those of the corresponding physical mixture, commercial tablets and unprocessed drug with f_2 values of 13.4, 14.2 and 7.8 respectively.

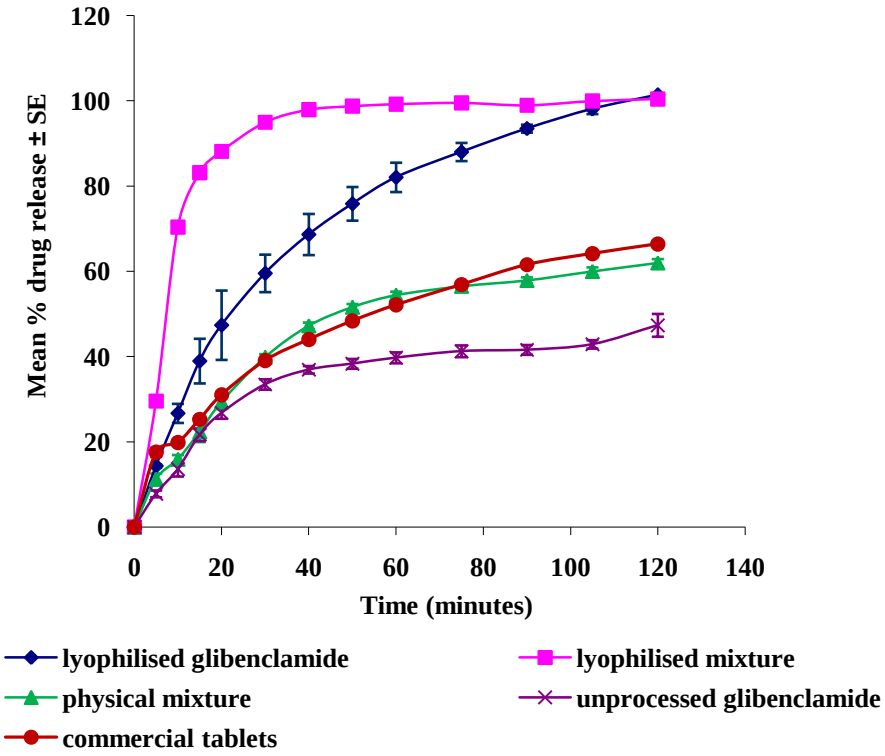

Figure 3.18: Dissolution profiles of lyophilised and physical mixtures of glibenclamide with 93% w/w sodium lauryl sulfate (n=6).

Table 3.6 shows $T_{50\%}$ and D_{30} of glibenclamide from different formulations. Lyophilisation of glibenclamide with SLS resulted in a marked decrease in $T_{50\%}$ relative to the commercial tablets, unprocessed drug and physical mixture. Furthermore, after 30 minutes, almost all the drug content of the lyophilised mixture dissolved while the physical mixture, commercial tablets and unprocessed glibenclamide showed less than 50% drug dissolution.

The improvement in the dissolution properties of glibenclamide may be attributed to formation of amorphous state of the drug in the lyophilised matrix of the water soluble fast dissolving excipient (see Section 4.4.1.3). Furthermore, sodium lauryl sulphate surfactant activity in solution aiding drug wetting, solubilisation and dissolution is another contributing factor. Another possible explanation for the dissolution enhancement exhibited by SLS is the formation of solid dispersion with the drug during the lyophilisation process which in turn enhances dissolution through the previously mentioned mechanisms (Section 3.4.2.2). Chakraborty et al. (2009)

has reported that carvedilol solubility was enhanced by increasing SLS concentrations in a basic dissolution medium. Also, Fukushima et al. (2007) has reported dissolution enhancement of atazanavir from its amorphous solid dispersion with SLS. Similar results have been obtained by Kennedy et al. (2008) who reported 12-fold dissolution enhancement of AMG 517 from its amorphous solid dispersion containing SLS compared with that without surfactant.

Table 3.6: Dissolution properties of lyophilised and physical mixtures of glibenclamide with 93% w/w sodium lauryl sulphate compared to the unprocessed drug and commercial tablets.

Sample	D_{30} ± SE	$T_{50\%}$ (minutes)
Lyophilised mixture	98.5 ± 0.3	4.1
Physical mixture	39.8 ± 0.7	46.3
Commercial tablets	39.1± 0.5	54.3
Unprocessed glibenclamide	33.5 ± 1.2	> 120

3.4.2.4 Lyophilised glibenclamide-PEG 6000 mixture

The effect of different concentrations of PEG 6000 on the dissolution characteristics of lyophilised glibenclamide is illustrated in Figure 3.19. It was found that only the lyophilised mixture of glibenclamide with 80% w/w PEG 6000 exhibited marked improvement in the dissolution rate and extent. Statistical analysis showed significant difference between the dissolution profile of the lyophilised glibenclamide-80% w/w PEG 6000 and that of the lyophilised drug alone (f_2 = 31.2).

The dissolution performance of the physical mixture of glibenclamide with 80% w/w PEG 6000 was investigated (Figure 3.20). The lyophilised mixture exhibited marked improvement in the drug dissolution rate and extent. Statistical analysis showed significant differences between the dissolution profile of the lyophilised mixture and those of the corresponding physical mixture, commercial tablets and unprocessed glibenclamide (f_2 =14.7, 17.7, 10.1 respectively).

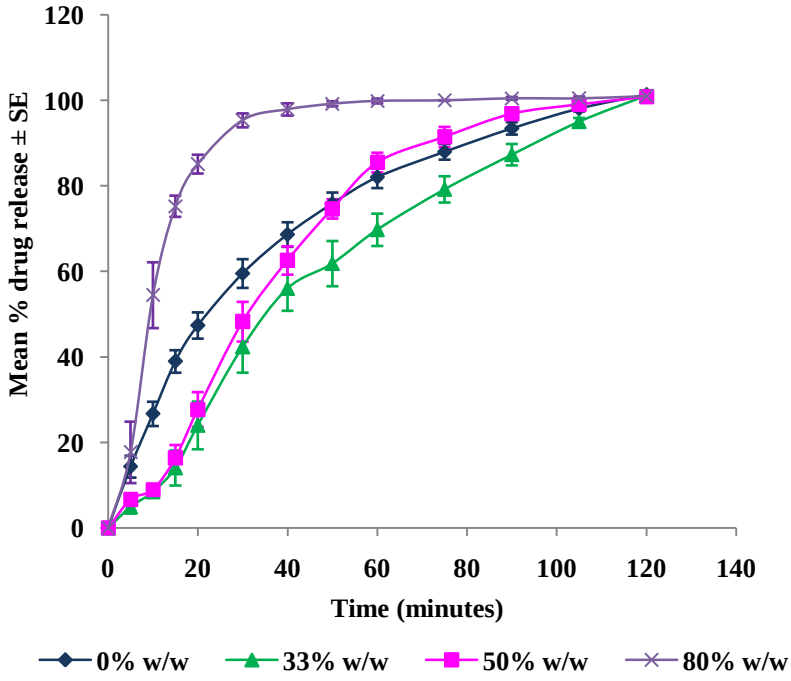

Figure 3.19: Effect of different concentrations of polyethylene glycol 6000 on the dissolution profile of lyophilised glibenclamide (n=6).

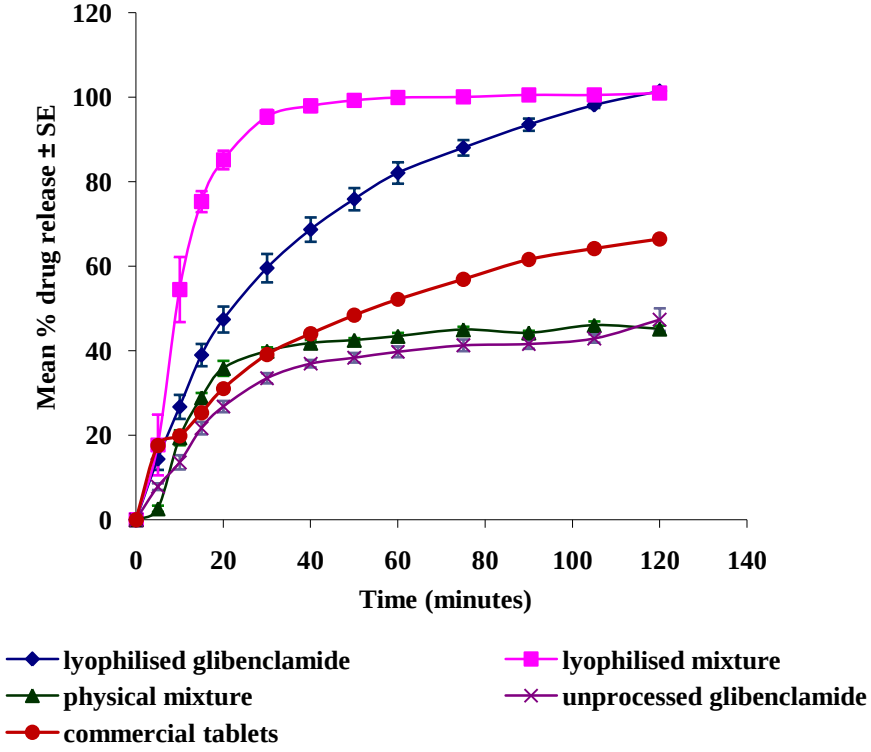

Figure 3.20: Dissolution profiles of lyophilised and physical mixtures of glibenclamide with 80% w/w PEG 6000 (n=6).

Lyophilisation of glibenclamide with 80% w/w PEG 6000 significantly decreased $T_{50\%}$ of glibenclamide in comparison with commercial tablets and unprocessed drug. Furthermore, D_{30} of the drug from the lyophilised mixture was found to be more than 2-fold those from the physical mixture, commercial tablets and the unprocessed drug (Table 3.7).

Table 3.7: Dissolution properties of lyophilised and physical mixtures of glibenclamide with 80% w/w PEG 6000 compared to the unprocessed drug and commercial tablets

Sample	D_{30} ± SE	$T_{50\%}$ (minutes)
Lyophilised mixture	95.6 ± 1.6	9.4
Physical mixture	39.8 ± 0.8	> 120
Commercial tablets	39.1± 0.5	54.3
Unprocessed glibenclamide	33.5 ± 1.2	> 120

The possible mechanism of increased dissolution rate by PEG 6000 may be the formation of solid dispersion during lyophilisation resulting in reduction of the particle size of the drug; improvement of drug wettability; disaggregation of drug particles and dissolution of the drug in the hydrophilic excipient. Also, formation of an amorphous form of the drug in the solid dispersion is another explanation for the dissolution rate enhancement (see Section 4.4.1.4). Law et al. (2001) investigated the dissolution rate enhancement of ritonavir, a human immunodeficiency virus (HIV) protease inhibitor, by the formation of an amorphous form of the drug in its solid dispersion with PEG 8000. Additionally, the solubilisation effect of PEG itself might play an important role in the improvement of the dissolution characteristics of glibenclamide. These results are in agreement with Asyarie and Rashmawati (2007) who found that the dissolution and solubility of gliclazide were enhanced through formation of a solid dispersion of the drug with PEG 6000. Also, it was found that PEG 6000 enhanced the dissolution rate of rofecoxib as a model of poorly water-soluble drug (Ahuja et al., 2007).

3.4.2.5 Lyophilised glibenclamide-gelatin mixture

The effect of different concentrations of water soluble gelatin on the dissolution rate of lyophilised glibenclamide is illustrated in Figure 3.21. It is clear from the Figure that 50% and 66% w/w gelatin retarded the dissolution rate of glibenclamide during the first 40 minutes. Statistical analysis showed a significant difference between the dissolution profile of lyophilised glibenclamide alone and those of lyophilised glibenclamide with 50% and 66% w/w gelatin with f_2 values of 47 and 45 respectively. On the other hand, the dissolution profile of the lyophilised drug with 28% w/w gelatin showed no significant difference from that of the lyophilised glibenclamide alone $f_2 = 57$.

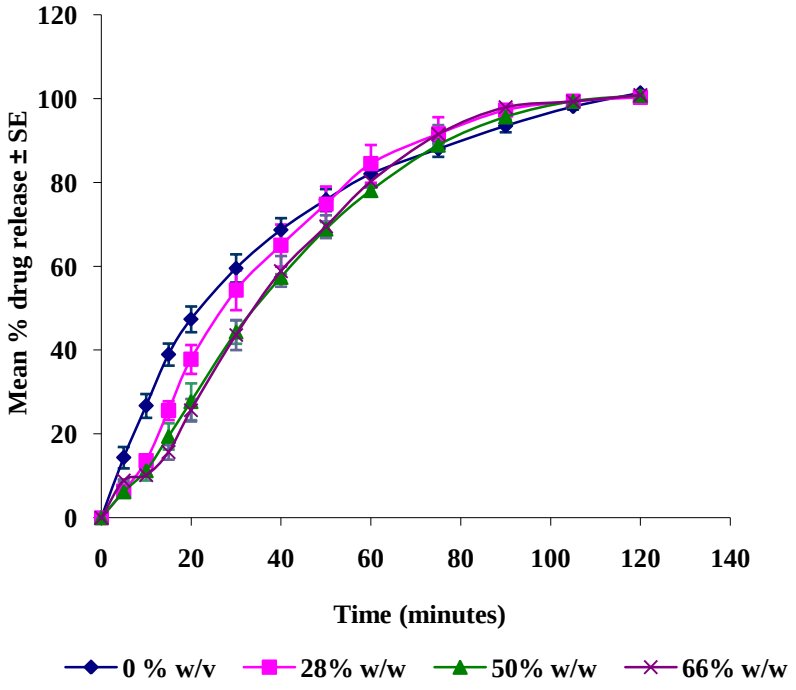

Figure 3.21: Effect of different concentrations of gelatin on the dissolution profile of lyophilised glibenclamide (n=6).

The dissolution performance of the physical mixture of glibenclamide with 50% w/w gelatin was investigated and compared with the corresponding lyophilised mixture, commercial tablets and unprocessed drug. Figure 3.22 shows that after the first 30

minutes, the lyophilised mixture of glibenclamide with the excipient exhibited marked improvement in the dissolution rate and extent over the corresponding physical mixture, unprocessed drug and commercial tablets.

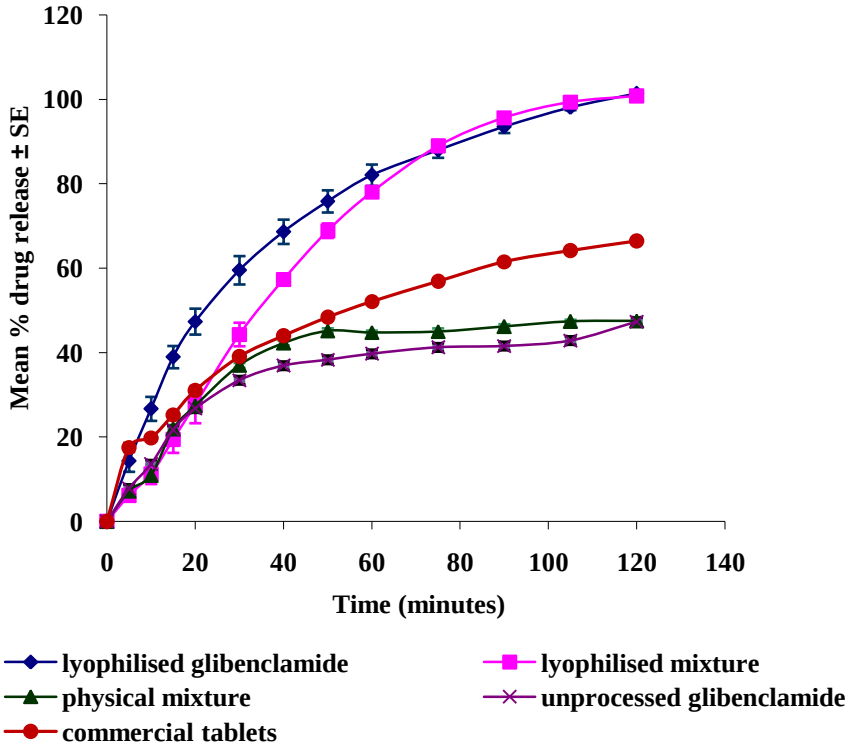

Figure 3.22: Dissolution profiles of lyophilised and physical mixtures of glibenclamide with 50% w/w gelatin (n=6).

$T_{50\%}$ of glibenclamide and the percentage dissolved after 60 minutes (D_{60}) are shown in Table 3.8. Lyophilisation of glibenclamide with gelatin decreased $T_{50\%}$ from 54.3 minutes (commercial tablets) and more than 120 minutes (unprocessed drug) to 40 minutes while that of the physical mixture was more than 120 minutes. Furthermore, after 60 minutes, almost 78% of glibenclamide dissolved from the lyophilised mixture, while only 44.8%, 52.1% and 39.7% of the drug dissolved from the physical mixture, commercial tablets and unprocessed glibenclamide respectively.

Table 3.8: Dissolution properties of lyophilised and physical mixtures of glibenclamide with 50% w/w gelatin compared to unprocessed drug and commercial tablets.

Sample	D_{60} ± SE	$T_{50\%}$ (minutes)
Lyophilised mixture	78 ±1.2	32.8
Physical mixture	44.8 ± 0.4	> 120
Commercial tablets	52.1± 0.6	54.3
Unprocessed glibenclamide	39.7 ±1.2	> 120

The enhanced dissolution rate and extent of glibenclamide from the lyophilised mixture with gelatin over the commercial tablets, physical mixture and unprocessed drug may be attributed to transformation of the drug to an amorphous form during the lyophilisation process with the amorphous excipient (see Section 4.4.1.6). This is in agreement with Chono et al. (2008) who found that the dissolution rate and gastrointestinal absorption of pranlukast as a model poorly water-soluble drug were enhanced by grinding with gelatin. Kallinteri and Antimisiaris (2001) found that the solubility of seven drugs (nitrofurantoin, chlorothiazide, phenobarbital, prednisolone, griseofulvin, diazepam and piroxicam) was significantly enhanced in the presence of gelatin. Also, formation of a solid dispersion of the drug in the hydrophilic excipient during lyophilisation can be considered another explanation for the dissolution rate enhancement. On the other hand, retardation effect of high concentrations of gelatin on the dissolution rate compared to lyophilised glibenclamide alone could be due to the increase in the viscosity of the diffusion layer surrounding the formulation which retards diffusion of water into the drug particles. Similar results have been reported for carbamazepine as its dissolution rate from liquisolid formulations was higher in the presence of lower concentrations of hydroxypropyl methylcellulose than higher concentrations that form gel around the drug particles (Javadzadeh et al., 2007).

3.4.2.6 Lyophilised glibenclamide-tromethamine mixture

The effect of different concentrations of tromethamine (33%, 50% and 80% w/w) on the dissolution rate of lyophilised glibenclamide is illustrated in Figure 3.23. The lyophilised mixtures were characterised by marked dissolution rate enhancement. Statistical analysis showed significant differences between dissolution profiles of the lyophilised glibenclamide-tromethamine formulations and that of the lyophilised drug alone (f_2= 36.7, 40.3, 48.3 for 80%, 50%, 33% w/w tromethamine respectively).

Figure 3.24 shows the performance of the physical mixture of glibenclamide with 50% w/w tromethamine. The lyophilised mixture was characterised by a marked enhancement in the dissolution rate and extent over the corresponding physical mixture, unprocessed drug and commercial tablets.

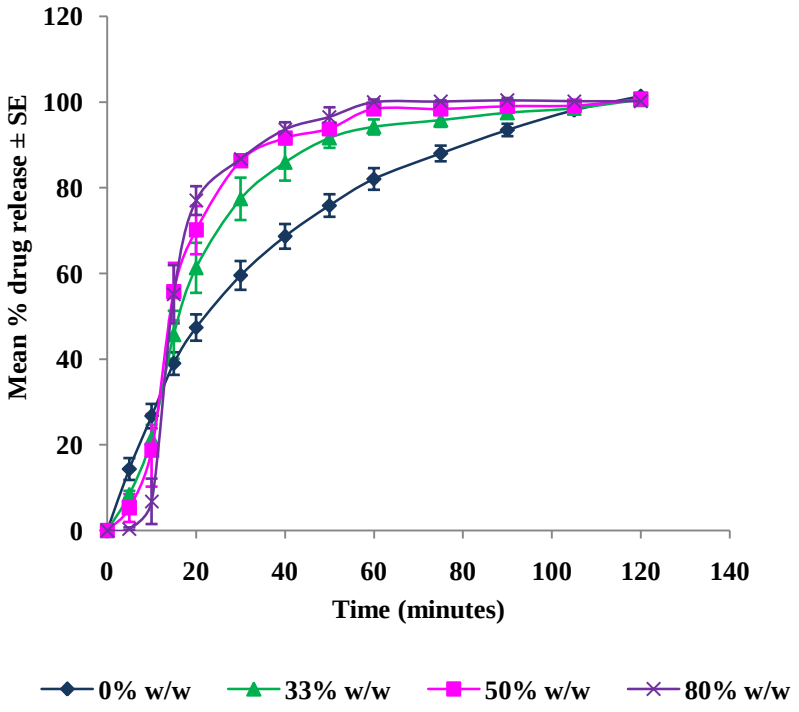

Figure 3.23: Effect of different concentrations of tromethamine on the dissolution profile of lyophilised glibenclamide (n=6).

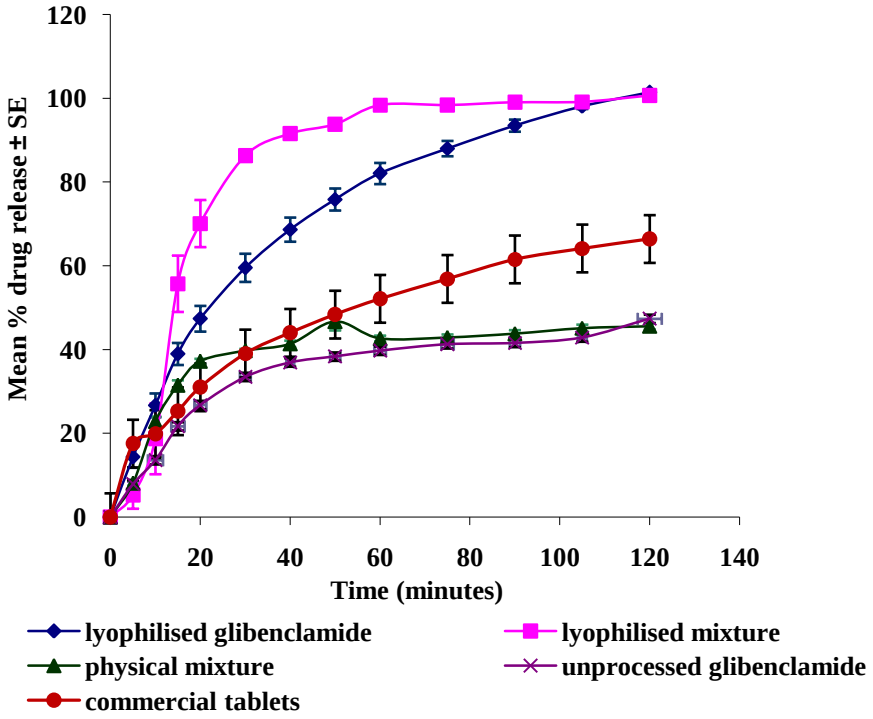

Figure 3.24: Dissolution profiles of lyophilised and physical mixtures of glibenclamide with 50% w/w tromethamine (n=6).

$T_{50\%}$ and D_{30} of glibenclamide from different formulations are shown in Table 3.9. The dissolution rate of glibenclamide could be ranked: lyophilised mixture > commercial tablets > physical mixture or unprocessed drug. Moreover, after 30 minutes, the percentage of glibenclamide dissolved from the lyophilised mixture, was more than 2-fold those dissolved from the physical mixture, commercial tablets and unprocessed drug.

Table 3.9: Dissolution properties of lyophilised and physical mixtures of glibenclamide with 50% w/w tromethamine compared to unprocessed drug and commercial tablets.

Sample	D_{30} ± SE	$T_{50\%}$ (minutes)
lyophilised mixture	86.3 ± 1.3	14.2
Physical mixture	39.7 ± 0.4	> 120
Commercial tablets	39.1 ± 0.5	54.3
Unprocessed glibenclamide	35.5 ± 1.2	> 120

The enhanced dissolution of glibenclamide from its lyophilised mixture with tromethamine may be attributed to formation of an amorphous form of the drug during the lyophilisation process (see Section 4.4.1.5) and solid dispersion formation. Another contributing factor is the increased wettability of the drug particles due to the solubilising effect of tromethamine which acts as an alkalinizing agent that increased the pH in the immediate diffusion layer surrounding glibenclamide particles. This finding is in agreement with Abdelkader et al. (2007) who found that the dissolution rate and analgesic effect of nimesulide, a poorly water-soluble acidic drug, were enhanced by formation of solid dispersion with tromethamine. Salt formation through interaction between the acidic drug and basic excipient could be another mechanism of dissolution enhancement. McGloughlin and Corrigan (1992) investigated dissolution enhancement (22-fold) of benzoic acid, a model acidic drug, from its mixture with tromethamine due to salt formation.

3.4.2.7 Lyophilised spironolactone

Dissolution profile obtained from the lyophilised spironolactone filled into hard gelatin capsules is shown in Figure 3.25. In contrast to glibenclamide, lyophilisation process had a negative effect on the dissolution performance of spironolactone. It was found that the dissolution rates of spironolactone commercial tablets and the unprocessed powder were superior to that of the lyophilised drug alone during the first 60 minutes. Statistical analysis showed significant differences between the dissolution profiles of the commercial tablets or the unprocessed powder and that of the lyophilised drug alone wit f_2 values of 45 and 32 respectively. The decrease of the dissolution rate of the lyophilised spironolactone is attributable to poor wettability of the lyophilised powder. This poor wettability might be attributed to the lyophilisation process which was visually observed (during weighing) to induce an electrostatic charge on the spironolactone powder, such that it self-associated and remained floating on the surface of the dissolution medium for a prolonged time. Similar results were obtained by Laitinen et al. (2009) who found that the lyophilised perphanazine/PVP solid dispersion remained floating on the surface of the dissolution medium which subsequently decreased the drug dissolution rate.

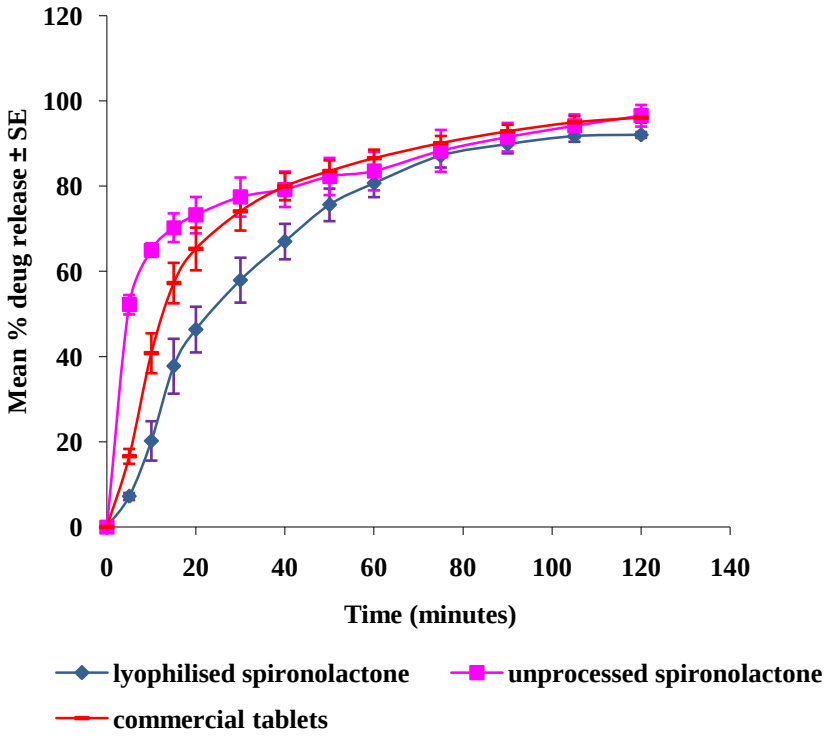

Figure 3.25: Effect of lyophilisation on the dissolution profile of spironolactone (n=6).

3.4.2.8 Lyophilised spironolactone-mannitol mixture

The effect of different concentrations of mannitol on the dissolution profile of lyophilised spironolactone is illustrated in Figure 3.26. It was found that mannitol in all concentrations enhanced the dissolution rate of spironolactone. Statistical analysis showed significant differences between individual dissolution profiles of lyophilised spironolactone with different concentrations of mannitol, and that of the lyophilised drug alone (f_2= 42.8, 30.7, 29.1 for 50%, 67%, 80% w/w mannitol respectively).

Physical mixtures of spironolactone with 67% w/w mannitol were tested for dissolution behaviour and compared with the corresponding lyophilised mixture, commercial tablets and unprocessed drug. Figure 3.27 showed marked increase in the rate and extent of dissolution of spironolactone from the lyophilised mixture. Statistical analysis showed significant differences between the dissolution profile of the lyophilised spironolactone alone and those of commercial tablets, physical mixture and the unprocessed drug with f_2 values of 42.5, 36.6 and 37.3 respectively.

Also, it was found that the physical mixture had a superior dissolution rate over that of the commercial tablets. Statistical analysis showed a significant difference between their dissolution profiles (f_2=36).

The percentage of spironolactone dissolved after 30 minutes (D_{30}) and the time for dissolution of 50% of the initial amount ($T_{50\%}$) were represented in Table 3.10. Lyophilisation with mannitol was found to decrease the initial dissolution rate of spironolactone relative to that of the physical mixture and unprocessed drug. After 30 minutes, the percentage of the drug dissolved from the lyophilised mixture was higher than those dissolved from the physical mixture, commercial tablets and unprocessed drug suggesting the absence of correlation between the dissolution rate and extent of spironolactone.

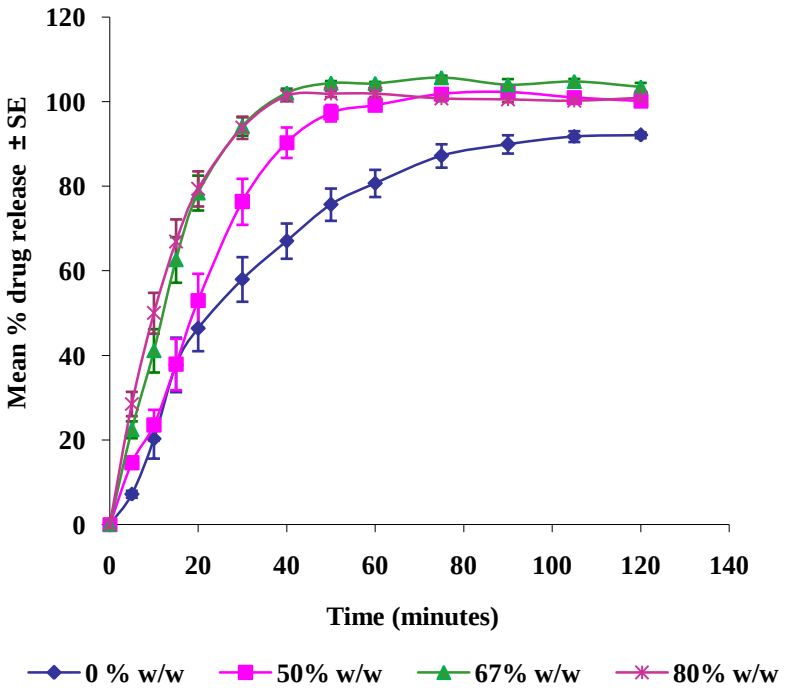

Figure 3.26: Effect of different concentrations of mannitol on the dissolution profile of lyophilised spironolactone (n=6).

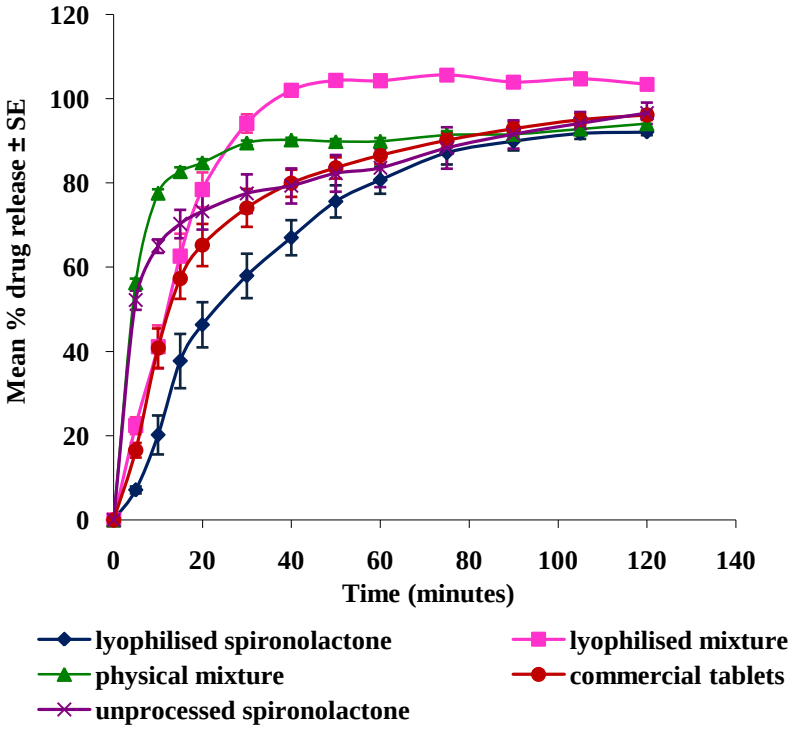

Figure 3.27: Dissolution profiles of lyophilised and physical mixtures of spironolactone with 67% w/w mannitol (n=6).

Table 3.10: Dissolution properties of lyophilised and physical mixtures of spironolactone with 67 % w/w mannitol compared to the unprocessed drug and commercial tablets.

Sample	D_{30} ± SE	$T_{50\%}$ (minutes)
Lyophilised mixture	94.2 ± 2.1	12.1
Physical mixture	89.5 ± 1.4	4.4
Commercial tablets	74.1 ± 4.5	12.8
Unprocessed spironolactone	77.5 ± 4.5	4.8

The exhibited dissolution enhancement by mannitol compared with lyophilised spironolactone alone may be attributed to the formation of solid dispersion of spironolactone with mannitol during lyophilisation process. Typical mechanisms for enhancement of dissolution properties of drugs by solid dispersions were discussed in Section 3.4.2.2. Furthermore, the drug might transform to an amorphous form in

the matrix of the lyophilised water-soluble excipient (see Section 4.4.2.2). The dissolution enhancement noticed for the spironolactone physical mixture might be due to the close contact of the drug with the hydrophilic excipient during dry mixing which resulted in increased wettability and dispersibility of spironolactone. On the other hand, increasing of the $T_{50\%}$ of the lyophilised mixture of spironolactone might be attributable to floating of the powder that was noticed at the beginning of the dissolution period. This floating behaviour was due to poor wettability caused by the lyophilisation process which could electrically charge the spironolactone powder. In a similar study, Arias et al. (1994) investigated the enhancement of dissolution rate and oral absorption of triamterene, a sparing potassium diuretic by formation of a solid dispersion with mannitol.

3.4.2.9 Lyophilised spironolactone-SLS mixture

The effect of different concentrations of SLS on the dissolution characteristics of lyophilised spironolactone is illustrated in Figure 3.28. The lyophilised mixtures of spironolactone with SLS exhibited marked enhancement in the the extent and rate of drug dissolution. Statistical analysis showed significant differences between dissolution profiles of spironolactone lyophilised with 67% and 74% w/w SLS and that of the lyophilised drug alone with f_2 values of 22.5 and 19 respectively.

The dissolution behaviour of the physical mixture of spironolactone with 67% w/w SLS was investigated. It can be observed from Figure 3.29 that the lyophilised mixture of spironolactone was characterised by higher extent and rate of drug dissolution. Statistical analysis showed significant differences between the dissolution profiles of the lyophilised mixture of spironolactone and those of the commercial tablets, physical mixture and unprocessed drug with f_2 values of 29, 49.5 and 40 respectively.

$T_{50\%}$ and D_{30} of spironolactone are represented in Table 3.11. The dissolution rate of spironolactone from different formulations could be ranked: lyophilised mixture > physical mixture > unprocessed drug > commercial tablets. The extent of dissolution did not appear to correlate with dissolution rate.

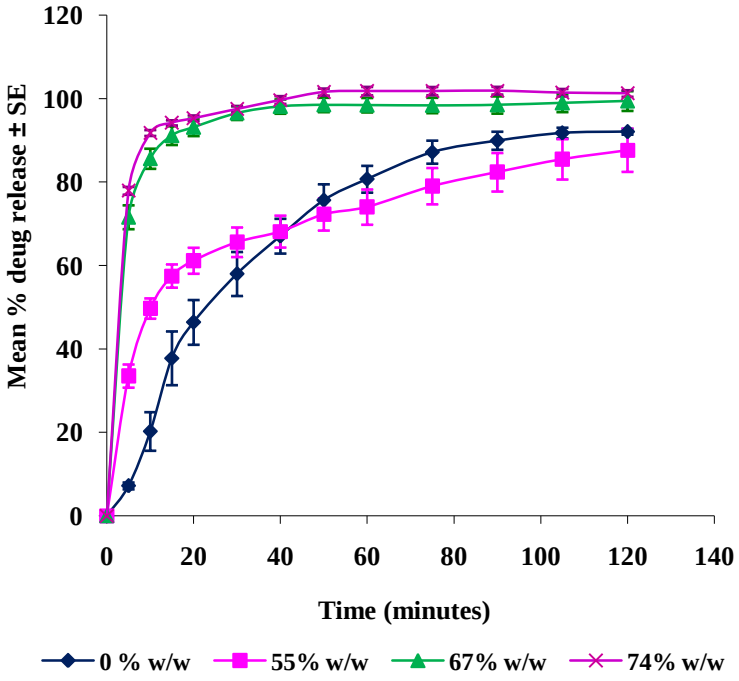

Figure 3.28: Effect of different concentrations of sodium lauryl sulfate on the dissolution profile of lyophilised spironolactone (n=6).

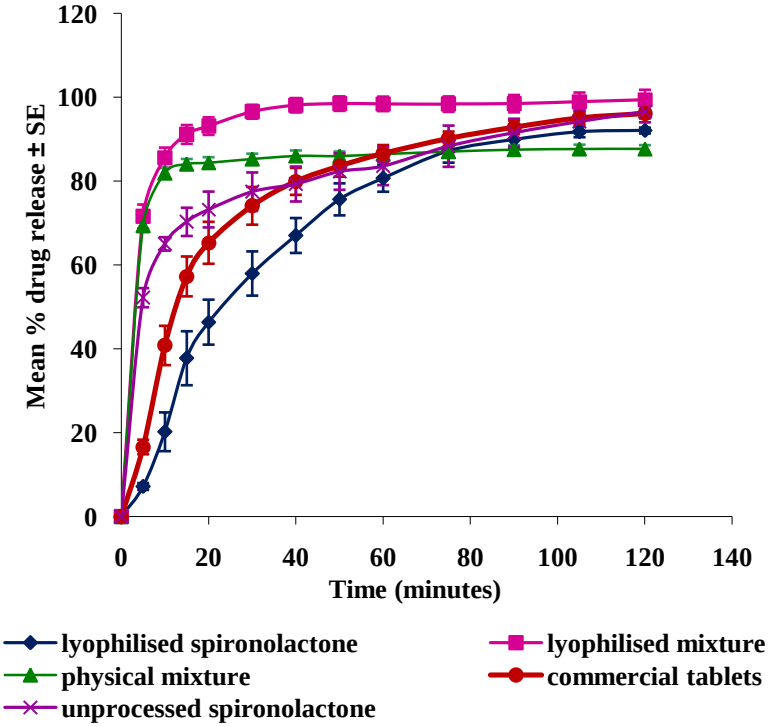

Figure 3.29: Dissolution profiles of lyophilised and physical mixtures of spironolactone with 67% w/w sodium lauryl sulfate (n=6).

Table 3.11: Dissolution properties of lyophilised and physical mixtures of spironolactone with 67% w/w sodium lauryl sulphate compared to the unprocessed drug and commercial tablets.

Sample	D_{30} ± SE	$T_{50\%}$ (minutes)
Lyophilised mixture	96.6 ± 1.6	3.5
Physical mixture	85.3 ± 1.2	3.6
Commercial tablets	74.1 ± 4.5	12.8
Unprocessed spironolactone	77.5 ± 4.5	4.8

The marked improvement in the dissolution properties of spironolactone from its lyophilised mixtures with SLS may be attributed to formation of an amorphous state of the drug in the lyophilised matrix of SLS (see Section 4.4.2.3). This is in agreement with Dong et al. (2010) who reported that the amorphous form of spironolactone contained in a nanoparticle formulation had a role in the dissolution rate enhancement of the drug. Other explanations for the mechanism of drug dissolution rate enhancement by SLS were explained in Section 3.4.2.3. Patel and Joshi (2008) also reported that SLS had a significant effect in enhancing the dissolution rate of aceclofenac, a poorly water-soluble drug, when mixed with another surfactant from the alkyl polyglucoside class (C10APG, C12APG and C12/14APG).

3.4.2.10 Lyophilised spironolactone-PEG 6000 mixture

The effect of different concentrations of PEG 6000 on the dissolution characteristics of lyophilised spironolactone is illustrated in Figure 3.30. The different concentrations of the water-soluble excipient had an obvious enhancing effect on the dissolution properties of spironolactone. Statistical analysis showed significant differences between the dissolution profile of the lyophilised spironolactone alone and those of the lyophilised mixtures of the drug with 50%, 67% and 80% w/w of PEG 6000, with f_2 values of 46, 34 and 35 respectively.

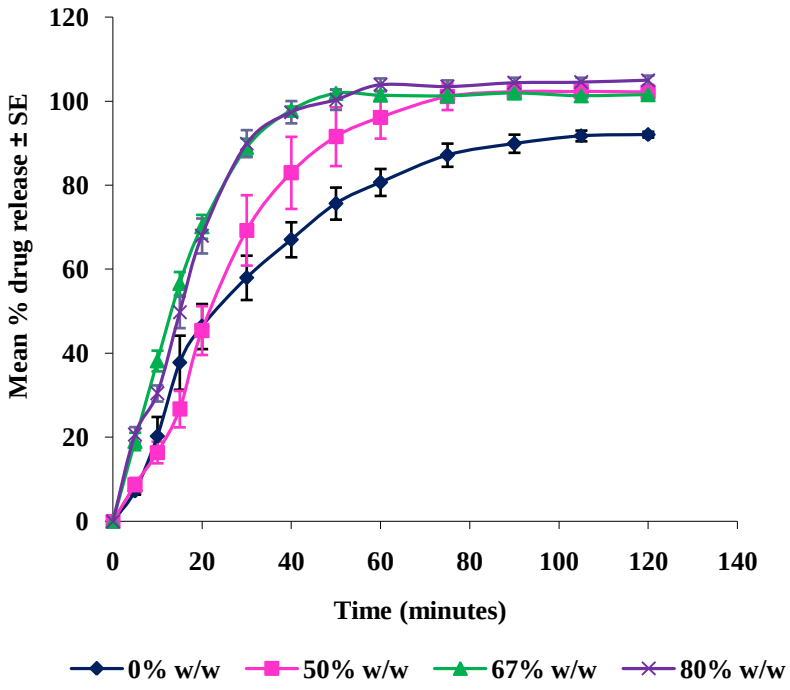

Figure 3.30: Effect of different concentrations of polyethylene glycol 6000 on the dissolution profile of lyophilised spironolactone (n=6).

The dissolution performance of the physical mixture of spironolactone with 67% w/w PEG 6000 was investigated and compared with the corresponding lyophilised mixture, commercial tablets and unprocessed drug (Figure 3.31). The lyophilised mixture of spironolactone exhibited slower dissolution rate than that of the physical mixture and similar dissolution rate to that of the commercial tablets during the first twenty minutes. After that, the dissolution rate of the drug from the lyophilised mixture exceeded that of the physical mixture and commercial tablets. Moreover, the dissolution profile of the physical mixture was significantly different from that of the commercial tablets (f_2= 44.7) showing higher dissolution rate.

Table 3.12 shows $T_{50\%}$ and D_{30} of spironolactone from different formulations. Lyophilisation of the drug with PEG 6000 resulted in an apparent increase in $T_{50\%}$ suggesting slower dissolution rate of spironolactone from the lyophilised mixture compared with the physical mixture, commercial tablets and unprocessed drug. After 30 minutes, the percentage of the drug dissolved from the lyophilised mixture was higher than those dissolved from the other formulations suggesting the absence of correlation between the dissolution rate and extent of spironolactone.

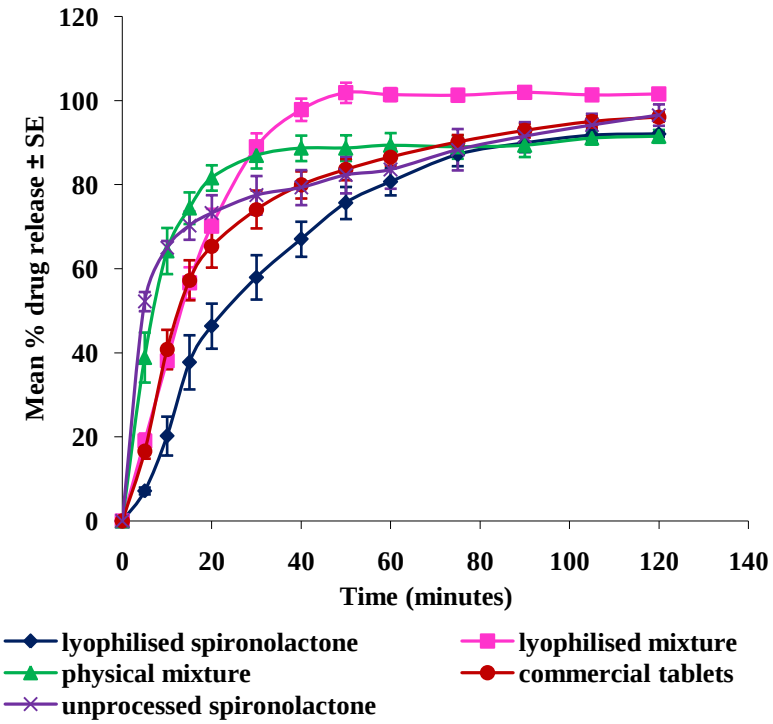

Figure 3.31: Dissolution profiles of lyophilised and physical mixtures of spironolactone with 67% w/w polyethylene glycol 6000 (n=6).

Table 3.12: Dissolution properties of lyophilised and physical mixtures of spironolactone with 67% w/w PEG 6000 compared to the unprocessed drug and commercial tablets.

Sample	D_{30} ± SE	$T_{50\%}$ (minutes)
Lyophilised mixture	89 ± 2.1	13.2
Physical mixture	87 ± 3.1	7.2
Commercial tablets	74.1 ± 4.5	12.8
Unprocessed spironolactone	77.5 ± 4.5	4.8

The initial, slow dissolution rate of spironolactone from its lyophilised mixture with PEG 6000 and the increase in $T_{50\%}$ were attributed to the transient floating of the lyophilised powder on the surface of the dissolution medium at the beginning of the dissolution run due to the effect of the lyophilisation process on spironolactone (see Section 3.4.2.7). The possible mechanism for subsequent dissolution rate

enhancement may be the solubilisation effect of PEG 6000 in addition to the formation of a solid solution of the drug with PEG 6000 during the lyophilisation process that led to reduction of the drug particle size and/or improvement of its wettability. Also, the formation of an amorphous state of spironolactone may play an important role in the observed drug dissolution enhancement (see Section 4.4.2.4). The improvement in spironolactone dissolution rate from the physical mixture during the first twenty minutes was attributed to the close contact of the drug with the hydrophilic excipient during dry mixing which resulted in increased wettability and dispersibility of spironolactone. In a similar study, the solubility and dissolution rate of lamotrigine were reported to be enhanced by solid dispersion formation with PEG 6000 using solvent evaporation technique. Physical characterisation of the solid dispersion revealed that the drug was converted to an amorphous form (Shinde et al., 2008). PEG 6000 has also been reported to enhance the dissolution rate of carbamazepine either in the solid dispersion formulation or the corresponding physical mixture with the drug (Zerrouk et al., 2001).

3.4.2.11 Lyophilised spironolactone-citric acid mixture

The effect of different concentrations of citric acid on the dissolution rate of lyophilised spironolactone is shown in Figure 3.32. The excipient had a marked retardation effect on the dissolution rate and extent of the drug from the lyophilised mixtures. Furthermore, it was found that as the concentration of citric acid decreases, the rate and extent of dissolution of spironolactone decreases. Statistical analysis showed significant difference in the extent and rate of dissolution between the lyophilised formulations with f_2 values < 50. At the end of the dissolution period, the amount of the drug dissolved from the lyophilised mixtures of the drug with 55%, 67% and 74% w/w citric acid was 41%, 57% and 70% respectively while that of the lyophilised drug alone was 92%.

The dissolution performance of the physical mixture of spironolactone with 55% w/w citric acid was investigated. It is obvious from Figure 3.33 that the lyophilised mixture exhibited a markedly reduced extent and rate of dissolution than the corresponding physical mixture, commercial tablets and unprocessed drug.

Table 3.13 shows $T_{50\%}$ and D_{30} of spironolactone from different formulations. Lyophilisation of the drug with citric acid increased $T_{50\%}$ to more than 2 hours relative to the physical mixture and unprocessed drug suggesting massive decrease in the dissolution rate of spironolactone from the lyophilised mixture. Furthermore, after 30 minutes, the percentage drug dissolved from the lyophilised mixture was less than 20% while those dissolved from the physical mixture, commercial tablets and unprocessed drug were more than 70%.

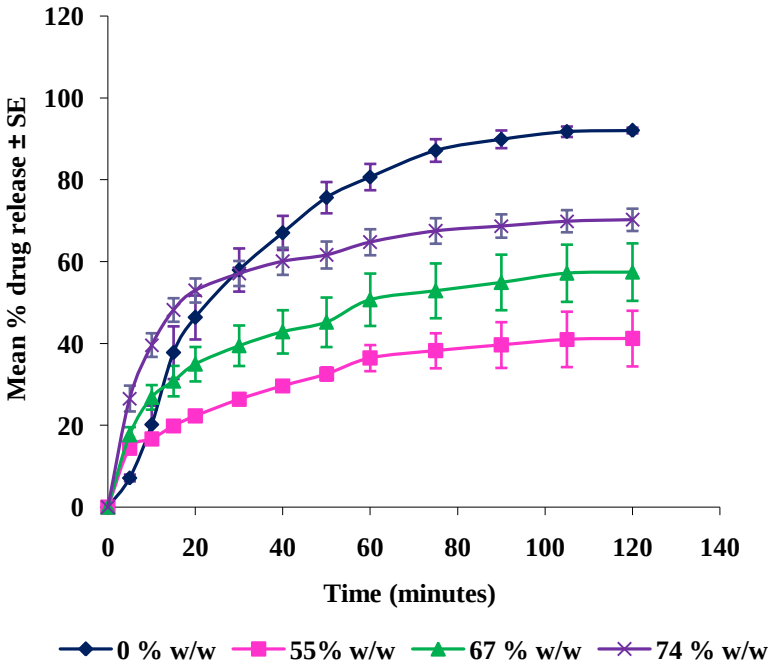

Figure 3.32: Effect of different concentrations of citric acid on the dissolution profile of lyophilised spironolactone (n=6).

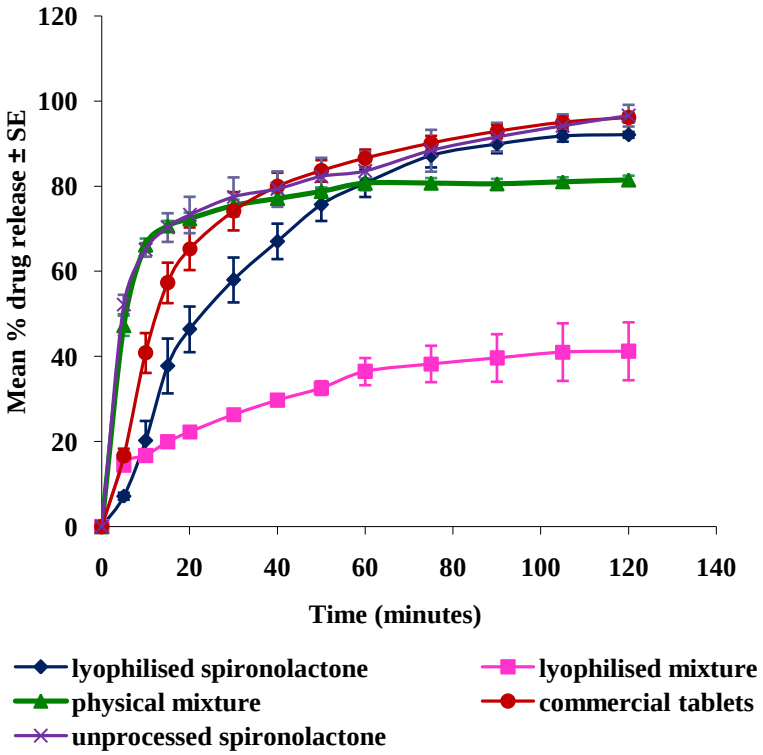

Figure 3.33: Dissolution profiles of lyophilised and physical mixtures of spironolactone with 55% w/w citric acid (n=6).

Table 3.13: Dissolution properties of lyophilised and physical mixtures of spironolactone with 55% w/w citric acid compared to unprocessed drug and commercial tablets.

Sample	D_{30} ± SE	$T_{50\%}$ (minutes)
lyophilised mixture	17.3 ± 1.3	>120
Physical mixture	75.4 ± 1.7	5.7
Commercial tablets	74.1± 4.5	12.8
Unprocessed spironolactone	77.5 ± 4.5	4.8

The retardation of spironolactone dissolution from its lyophilised mixture with citric acid may be attributable to the high hygroscopicity of citric acid that affected the structural integrity of the lyophilised mixture. This led to formation of aggregated sticky particles upon addition to aqueous dissolution media that were seen sinking as a mass to the bottom of the the vessel where they remained throughout. Similar

findings have been reported by Hodges et al. (2006) who found that citric acid hygroscopicity had a negative effect on the structural integrity of the lyophilised spironolactone-mannitol-SLS system. In the case of higher concentrations of citric acid, the faster dissolution rate might be explained on the basis of improved wettability by alteration of the chemical environment (pH and hydrogen bonding) surrounding the drug particles.

3.4.2.12 Lyophilised spironolactone-fumaric acid mixture

The effect of different concentrations of fumaric acid on the dissolution rate of lyophilised spironolactone is shown in Figure 3.34. The lyophilised mixtures of the drug with high concentrations of fumaric acid (67%, 74% w/w) showed marked improvement in the dissolution rate of spironolactone. There was a significant difference between the dissolution profile of the lyophilised mixture of spironolactone with 74% w/w fumaric acid (superior dissolution rate) and that of lyophilised mixture of the drug with 67% fumaric acid w/w (f_2 = 48.4).

Figure 3.35 shows the performance of the physical mixture of spironolactone with 74% w/w fumaric acid. Both the lyophilised and physical mixtures exhibited greater rate and extent of drug dissolution compared with that of the commercial tablets and the unprocessed drug with no significant difference between their dissolution profiles (f_2 = 55.65).

The time for dissolution of 50% of the initial amount of spironolactone and the percentage dissolved after 30 minutes are shown in Table 3.14. Mixing of spironolactone with fumaric acid either in the lyophilised or physical mixture decreased $T_{50\%}$ compared with the commercial tablets. Furthermore, After 30 minutes, the percentage drug dissolved from the lyophilised or physical mixture was more than 85% while those dissolved from the commercial tablets and unprocessed drug were less than 80%.

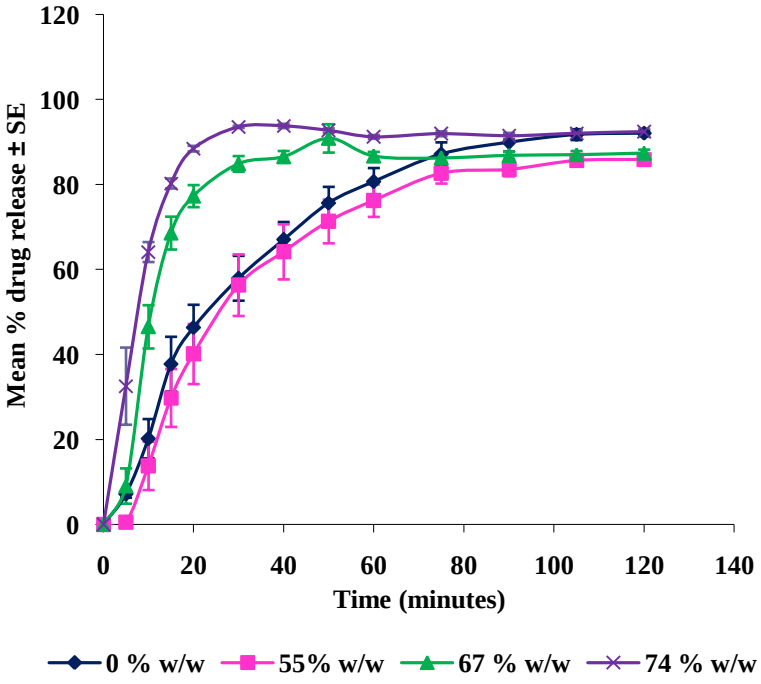

Figure 3.34: Effect of different concentrations of fumaric acid on the dissolution profile of lyophilised spironolactone (n=6).

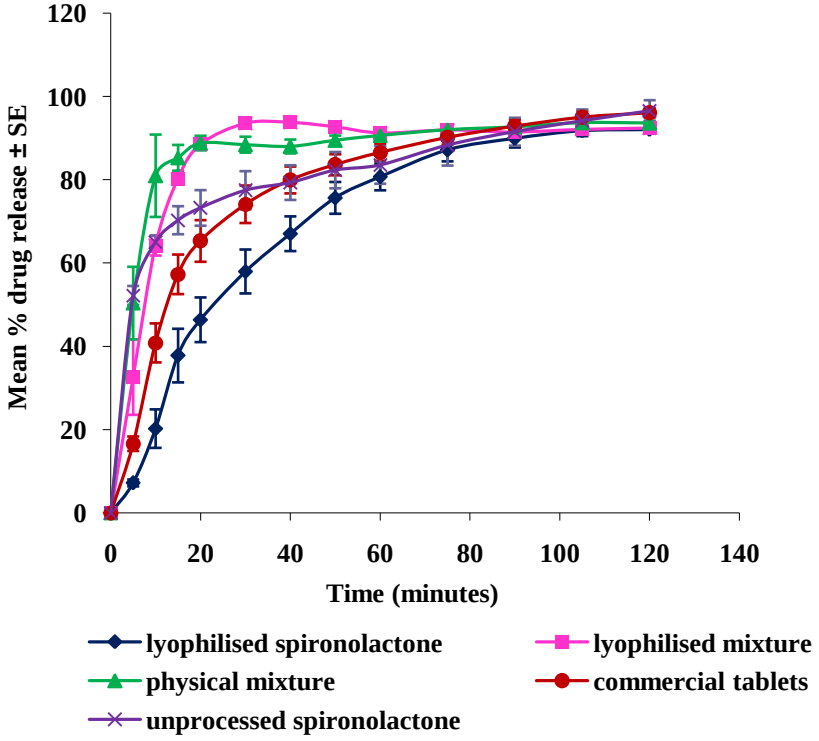

Figure 3.35: Dissolution profiles of lyophilised and physical mixtures of spironolactone with 74% w/w fumaric acid (n=6).

Table 3.14: Dissolution properties of lyophilised and physical mixtures of spironolactone with 74% w/w fumaric acid compared to unprocessed drug and commercial tablets.

Sample	D_{30} ± SE	$T_{50\%}$ (minutes)
lyophilised mixture	93.6 ± 0.3	7.6
Physical mixture	88.4 ± 2.3	4.9
Commercial tablets	74.1± 1.6	12.8
Unprocessed spironolactone	77.5 ± 2.3	4.8

The enhanced dissolution of spironolactone from the lyophilised mixture with fumaric acid may be attributed to solid dispersion formation during the process of lyophilisation. Formation of an amorphous form of spironolactone is another possible explanation (see Section 4.4.2.6). In addition, alteration of the chemical environment surrounding spironolactone particles by fumaric acid might contribute to the dissolution enhancement of the drug from the lyophilised and physical mixtures. This is in agreement with Tran et al. (2010) who found that fumaric acid greatly enhanced the dissolution of isradipine from its solid dispersion with PVP. The enhancement was attributed to pH change of the drug microenvironment for extended time and maintenance of the amorphous structure through intermolecular interactions between the drug and fumaric acid.

3.4.2.13 Lyophilised ketoconazole

Dissolution profile of the lyophilised ketoconazole filled into hard gelatin capsules is shown in Figure 3.36. The lyophilised ketoconazole showed improvement in the dissolution rate in the first 15 minutes compared with the commercial tablets and unprocessed drug. A marked reduction in the rate and extent of ketoconazole dissolution was observed from the lyophilised formulation after the first 15 minutes until the end of the dissolution experiment.

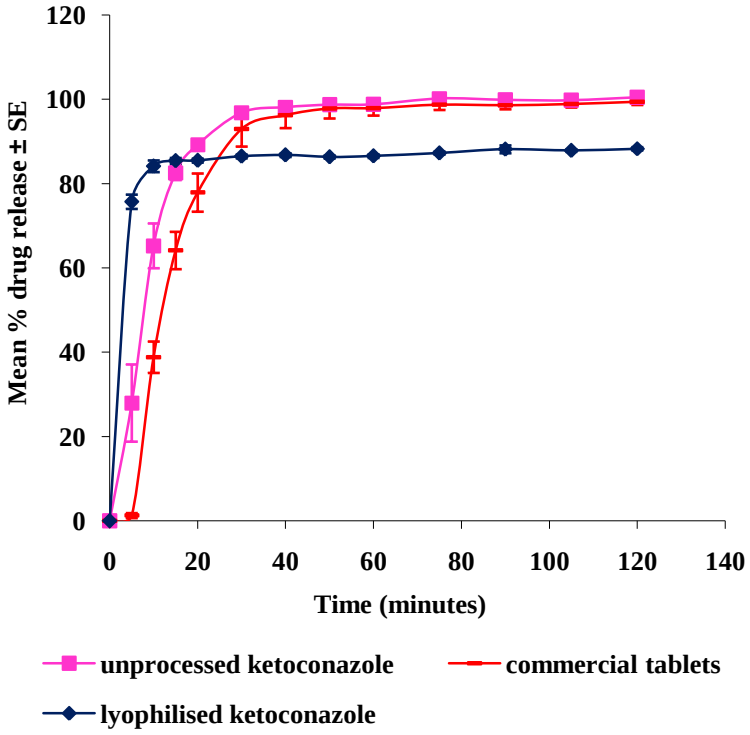

Figure 3.36: Effect of lyophilisation on the dissolution profile of ketoconazole (n=6).

The initial improvement of ketoconazole dissolution rate compared to the unprocessed drug and the commercial tablets may be due to formation of an amorphous form of the drug during the lyophilisation process (see Section 3.4.3.1). As the lyophilised ketoconazole was highly hygroscopic, it absorbed ambient moisture during filling into gelatin capsules that led to formation of aggregated sticky particles that were very difficult to handle under normal laboratory conditions. These aggregated sticky particles clumped upon addition to dissolution media and sank to the bottom of the flask. This explains the lower rate and extent of ketoconazole dissolution after the first 15 minutes.

3.4.2.14 Lyophilised ketoconazole-mannitol mixture

The effect of different concentrations of mannitol on the dissolution profile of lyophilised ketoconazole is illustrated in Figure 3.37. Statistical analysis showed no significant differences between the dissolution profile of the lyophilised

ketoconazole alone and those of the lyophilised drug with 11%, 20% and 33% w/w mannitol (f_2 = 51.5, 54.8, 57.3 respectively).

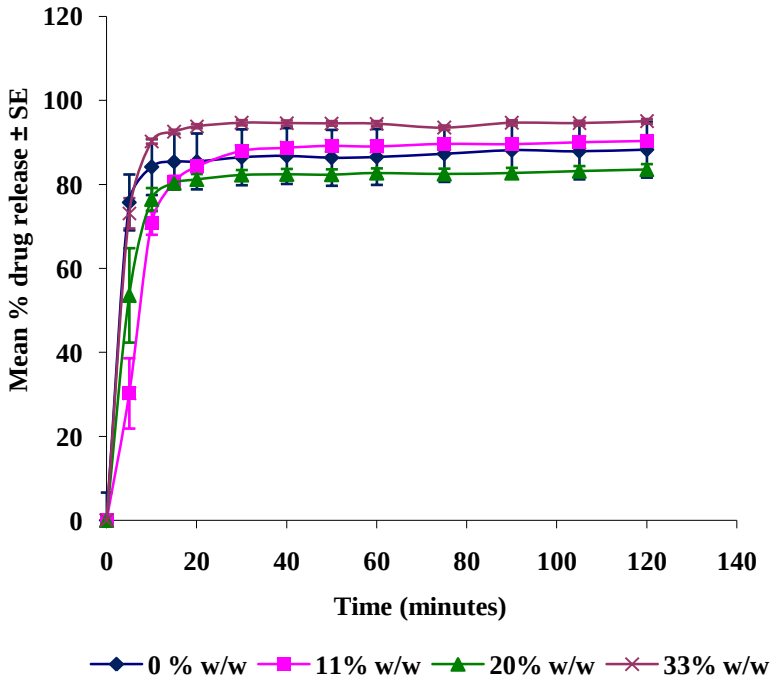

Figure 3.37: Effect of different concentrations of mannitol on the dissolution profile of lyophilised ketoconazole (n=6).

Physical mixture of ketoconazole with 33% w/w mannitol was tested for dissolution behaviour and compared with the corresponding lyophilised mixture, commercial tablets and unprocessed drug (Figure 3.38). Statistical analysis showed no significant difference between the dissolution profiles of the lyophilised and physical mixtures with an f_2 value of 51. On the other hand, there were significant differences between the dissolution profile of the lyophilised mixture and those of the commercial tablets and unprocessed drug (f_2 = 29 and 40.1 respectively) as the lyophilised ketoconazole-mannitol mixture exhibited superior dissolution rate during the first 20 minutes.

Table 3.15 shows the percentage of ketoconazole dissolved after 15 minutes (D_{15}) and the time for dissolution of 50% of the initial amount ($T_{50\%}$). Lyophilisation of ketoconazole with mannitol decreased $T_{50\%}$ of the drug relative to the physical

mixture, commercial tablets and unprocessed drug. After 15 minutes, the percentage of ketoconazole dissolved from the lyophilised mixture exceeded those dissolved from the the other formulations.

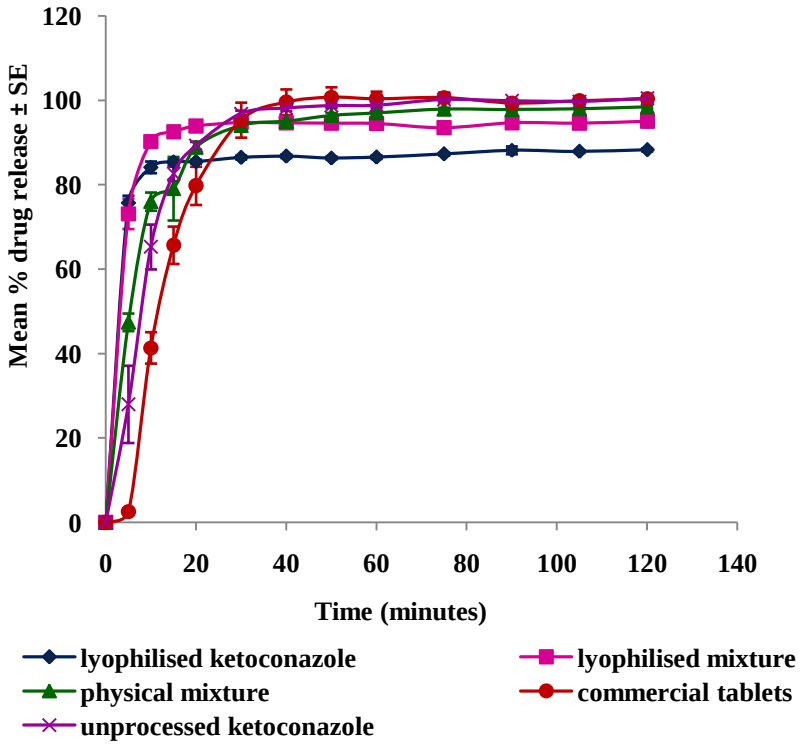

Figure 3.38: Dissolution profiles of lyophilised and physical mixtures of ketokonazole with 33% w/w mannitol (n=6).

Table 3.15: Dissolution properties of lyophilised and physical mixtures of ketoconazole with 33% w/w mannitol compared to the unprocessed drug and commercial tablets.

Sample	D_{15} ± SE	$T_{50\%}$ (minutes)
Lyophilised mixture	92.5 ± 0.6	3.6
Physical mixture	79.1 ± 1.5	5.4
Commercial tablets	65.6 ± 2.1	12.2
Unprocessed ketoconazole	82.6 ± 2.1	8

The initial dissolution rate enhancement of ketoconazole from the lyophilised mixture with mannitol (relative to the unprocessed drug and commercial tablets) is attributed to the formation of a solid dispersion of the drug with the water soluble excipient during the lyophilisation process. The mechanisms for enhancement of dissolution rate of a drug by solid dispersion were discussed in Section 3.4.2.2. Transformation of ketoconazole to an amorphous state during lyophilisation may be another important contributing factor for the dissolution rate enhancement (see Section 4.4.3.2).

3.4.2.15 Lyophilised ketoconazole-mannitol-SLS mixture

The effect of different concentrations of SLS-mannitol mixture on the dissolution characteristics of the lyophilised ketoconazole is illustrated in Figure 3.39. The lyophilised mixtures containing high concentrations of SLS showed marked improvement in ketoconazole dissolution rate compared the lyophilised drug alone. Statistical analysis revealed significant differences between the dissolution profile of the lyophilised ketoconazole alone and those of the lyophilised mixture of the drug with 14/28% and 19/27% w/w SLS-mannitol with f_2 values of 43.4 and 39.5 respectively.

The dissolution behaviour of the physical mixture of ketoconazole with 14% w/w SLS and 28% w/w mannitol was investigated. It can be observed from Figure 3.40 that the lyophilised mixture exhibited marked dissolution rate improvement in the first 30 minutes of the dissolution period. Statistical analysis showed significant differences between the dissolution profile of the lyophilised mixture and those of the corresponding physical mixture, commercial tablets and unprocessed drug with f_2 values of 24.7, 24.3 and 35 respectively.

D_{15} and $T_{50\%}$ of ketoconazole from the lyophilised mixture, commercial tablets, physical mixture and raw drug are presented in Table 3.16. The lyophilised mixture of ketoconazole with 14% w/w SLS and 28% w/w mannitol showed the highest dissolution rate and displayed the maximum percentage of drug dissolved after 15 minutes relative to the other formulations.

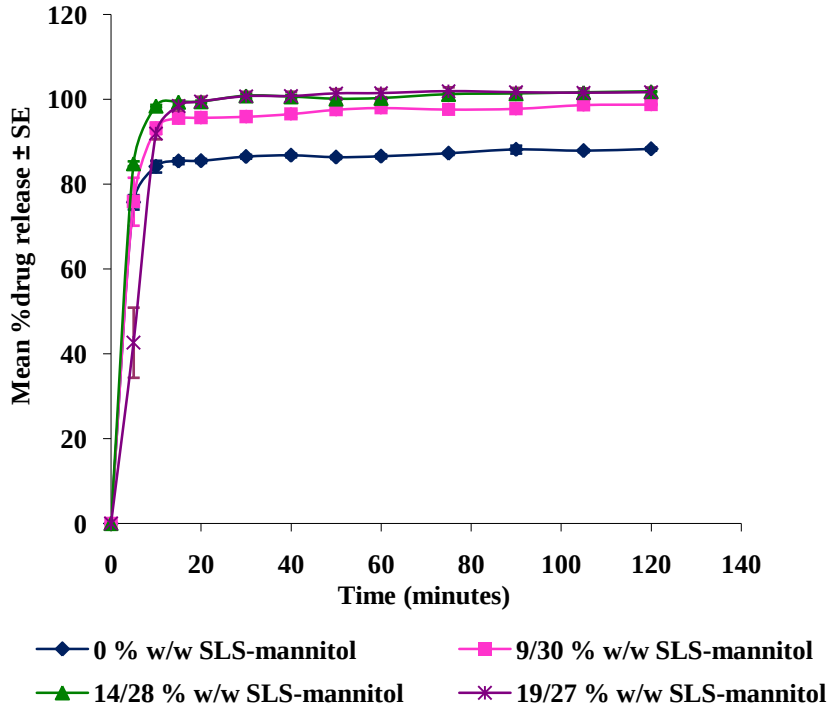

Figure 3.39: Effect of different concentrations of sodium lauryl sulfate and mannitol on the dissolution profile of lyophilised ketoconazole (n=6).

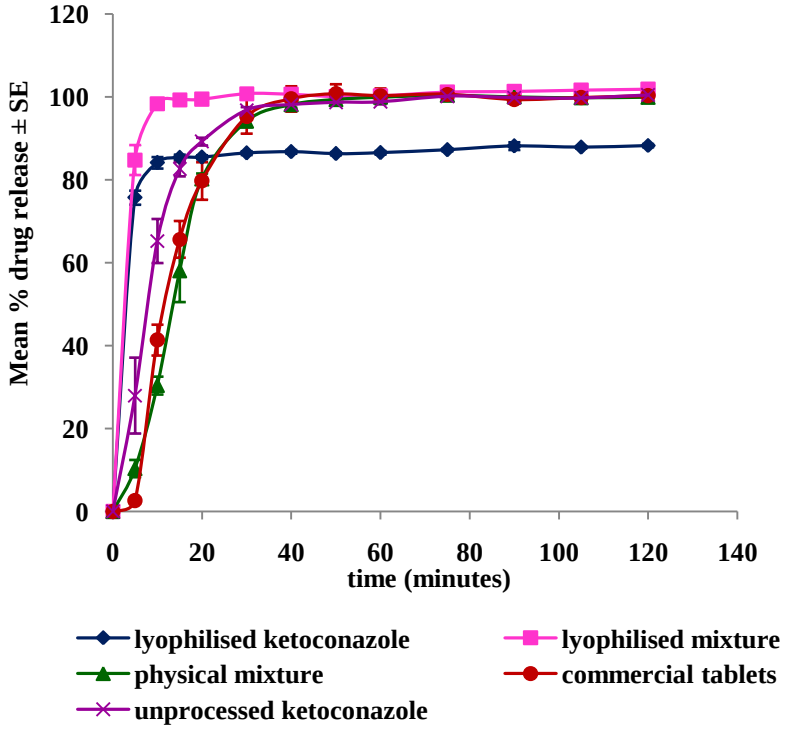

Figure 3.40: Dissolution profiles of lyophilised and physical mixtures of ketoconazole with 14% w/w sodium lauryl sulfate and 28% w/w mannitol (n=6).

The marked improvement in the dissolution rate of ketoconazole from the lyophilised mixture may be attributed to transformation of the crystalline form of ketoconazole to an amorphous form during the lyophilisation process (see Section 4.4.3.3). Furthermore, SLS surfactant activity and solid dispersion formation might have an important role in the dissolution rate enhancement (see Section 3.4.2.3).

Table 3.16: Dissolution properties of lyophilised and physical mixtures of ketoconazole with 14% w/w sodium lauryl sulphate and 28% w/w mannitol compared to the unprocessed drug and commercial tablets.

Sample	D_{15} ± SE	$T_{50\%}$ (minutes)
Lyophilised mixture	99.3 ± 0.3	2.9
Physical mixture	58 ± 0.6	12.1
Commercial tablets	64.2 ± 2.1	12.2
Unprocessed ketoconazole	82.6 ± 2.1	8

3.4.2.16 Lyophilised ketoconazole-mannitol-PEG 6000 mixture

The effect of different concentrations of PEG 6000-mannitol mixture on the dissolution characteristics of lyophilised ketoconazole is illustrated in Figure 3.41. The excipient mixtures had an enhancing effect on the dissolution rate of the drug. Statistical analysis showed significant differences between the dissolution profile of the lyophilised ketoconazole alone and those of the lyophilised mixture of the drug with 40/20%, 25/25% and 14/28% w/w PEG 6000-mannitol giving f_2 values of 42.6, 47.7 and 46.3 respectively.

The dissolution performance of physical mixture of ketoconazole with 14% w/w PEG 6000 and 28% w/w mannitol was investigated and compared with the corresponding lyophilised mixture, commercial tablets and unprocessed drug. Figure 3.42 shows that the lyophilised mixture exhibited the highest dissolution rate relative to the other formulations. Statistical analysis showed significant differences between the dissolution profile of the lyophilised mixture and those of the physical mixture,

commercial tablets and unprocessed ketoconazole with f_2 values of 41, 28.7 and 42.2 respectively.

Table 3.17 shows D_{15} and $T_{50\%}$ of ketoconazole from different formulations. The dissolution rate of the drug from these formulations could be ranked: lyophilised mixture > physical mixture or unprocessed drug > commercial tablets. Also, it can be concluded from the table that the extent of spironolactone dissolution correlates with its dissolution rate.

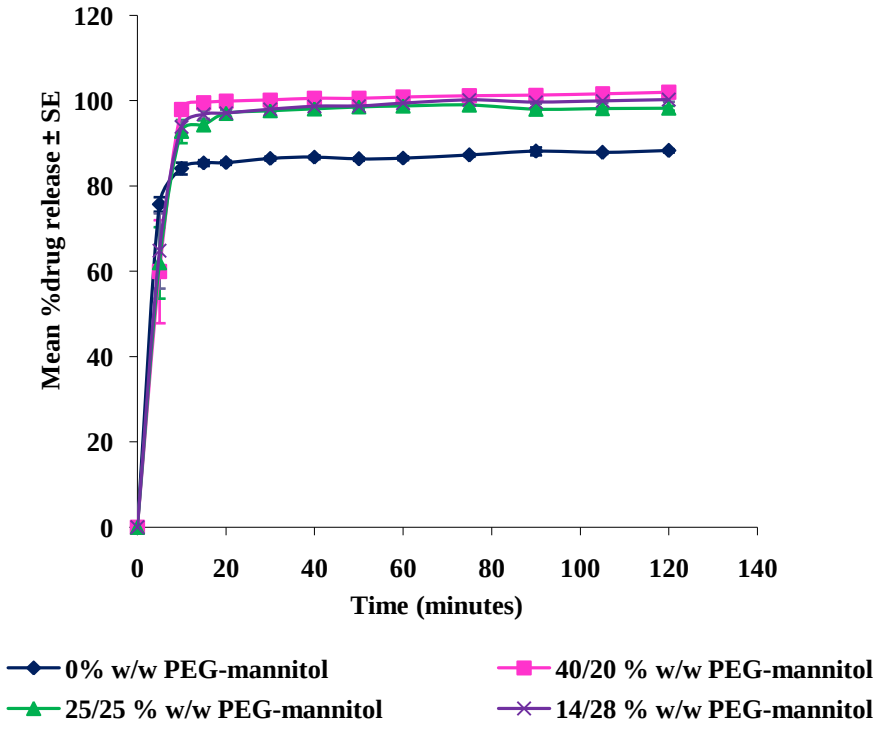

Figure 3.41: Effect of different concentrations of polyethylene glycol and mannitol on the dissolution profile of lyophilised ketoconazole (n=6).

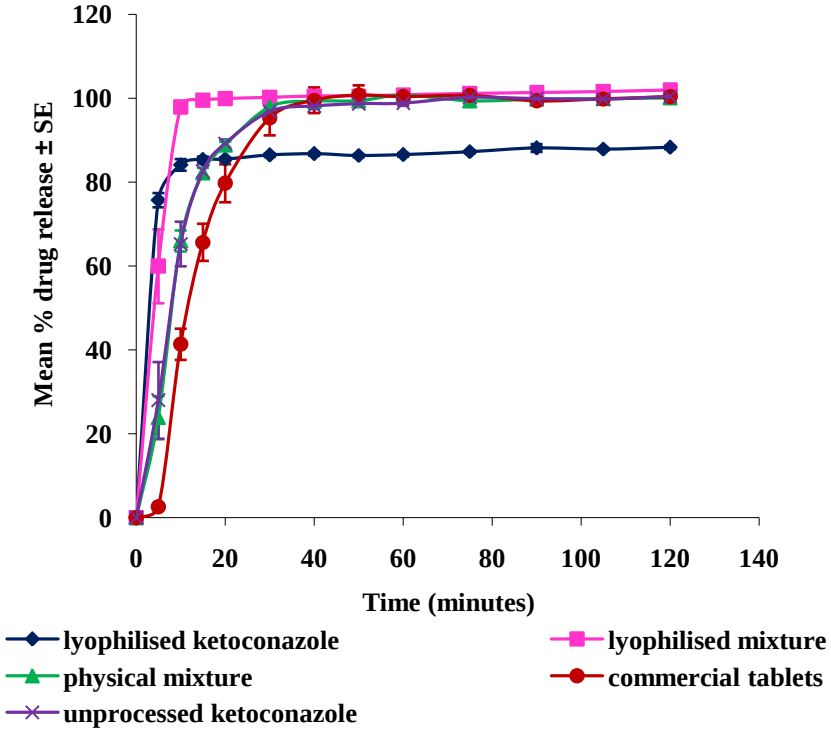

Figure 3.42: Dissolution profiles of lyophilised and physical mixtures of ketoconazole with 14% w/w polyethylene glycol 6000 and 28% w/w mannitol (n=6).

Table 3.17: Dissolution properties of lyophilised and physical mixtures of ketoconazole with 14% w/w PEG 6000 and 28% w/w mannitol compared to the unprocessed drug and commercial tablets.

Sample	D_{15} ± SE	$T_{50\%}$ (minutes)
lyophilised mixture	99.5 ±1.5	3.65
Physical mixture	82.2±3.1	8.1
Commercial tablets	64.2 ± 2.1	12.2
Unprocessed ketoconazole	82.6 ± 2.1	8

The increased dissolution rate of ketoconazole from the lyophilised mixture may be due to the formation of an amorphous form of the drug in the solid dispersion post-lyophilisation (see Section 4.4.3.4). Also, the solubilisation effect of PEG 6000 might play an important role in the observed ketoconazole dissolution rate

enhancement. It has been reported that the dissolution rate of ketoconazole was enhanced from its solid dispersion with PEG 6000 containing various excipients of a self microemulsifying drug delivery system such as oils, fatty acids and surfactant (Heo et al. 2005).

From dissolution study results, the lyophilised mixtures of ketoconazole with mannitol, mannitol-SLS or mannitol-PEG 6000, provide extensive dissolution rate enhancement. The time necessary for dissolution of 50% of ketoconazole was 3-4 minutes while 84% of drug dissolved in the first 5 minutes. It has been reported that the dissolution rate of ketoconazole was improved by solid dispersion with polyvinylpyrrolidone K25 (Wuyts, as cited by Van den Mooter et al., 2001) and the time necessary for dissolution of 50% of the drug was 10 minutes. Esclusa-Díaz et al. (1996) has reported 80% ketoconazole dissolution at 5 minutes from the spray-dried complex of the drug with hydroxypropyle β-cyclodextrin. Therefore the results of the present work are generally superior to previously reported formulation approaches.

3.5 Summary of the in-vitro dissolution results

Drug	Results
glibenclamide	• Lyophilisation enhanced glibenclamide dissolution rate and extent compared to the unprocessed drug and commercial tablets. • Mannitol, SLS, PEG 6000 and tromethamine achieved further dissolution enhancement when co-lyophilised with the drug. • Co-lyophilisation of glibenclamide with high concentrations of gelatin significantly retarded the drug dissolution rate. • Lyophilised mixtures of glibenclamide with 93% w/w SLS, 91% w/w mannitol, 80% w/w PEG 6000, 50% w/w gelatin or 50% w/w tromethamine exhibited higher dissolution rate than the corresponding physical mixtures, unprocessed drug and commercial tablets.

spironolactone	• Lyophilisation retarded spironolactone dissolution rate compared to the unprocessed drug and commercial tablets. • Mannitol, SLS, PEG 6000 and fumaric acid achieved dissolution rate enhancement for spironolactone when co-lyophilised with the drug. • Citric acid retarded the dissolution rate and extent of spironolactone when co-lyophilised with the drug. • Lyophilised mixtures of spironolactone with 67% w/w SLS, 67% w/w mannitol, 67% w/w PEG 6000, or 74% w/w fumaric acid exhibited higher dissolution rate than the corresponding physical mixtures, unprocessed drug and commercial tablets.
ketoconazole	• Compared to the unprocessed drug and commercial tablets, lyophilisation enhanced the dissolution rate of ketoconazole in the first 15 minutes only while reduced the drug dissolution rate and extent after that. • Compared to the lyophilised drug alone, mannitol had no enhancing effect on the dissolution rate of ketoconazole when co-lyophilised with the drug. • Co-lyophilisation of ketoconazole with mannitol and SLS or PEG 6000 enhanced the dissolution rate and extent of the drug compared to the lyophilised drug alone. • Lyophilised mixtures of ketoconazole with 28% w/w mannitol and 14% w/w SLS or PEG 6000 exhibited higher dissolution rate than the corresponding physical mixtures, unprocessed drug and commercial tablets.

3.6 Conclusion

It can be concluded from this chapter that:

- Lyophilisation had variable effects on the dissolution rate of drug alone depending on their physicochemical properties. Lyophilisation significantly enhanced the dissolution rate of glibenclamide compared to the commercial tablets and unprocessed drug. On the other hand, it had a negative effect on the dissolution rate of spironolactone. Furthermore, lyophilisation enhanced the initial dissolution rate of ketoconazole but decreased the total extent of drug dissolution.
- The different excipients used (with the exception of citric acid) significantly enhanced the dissolution rate of the drugs from their lyophilised mixtures compared to the lyophilised drugs alone. This may be attributable to the formation of solid dispersions and a change in the physical state of the drugs after lyophilisation. On the other hand, citric acid had a negative effect on the dissolution rate of lyophilised spironolactone due its hygroscopic nature.
- SLS exhibited the greatest enhancement of the dissolution rates of glibenclamide, spironolactone and ketoconazole. Thus, the lyophilised mixtures of the model drugs with SLS were subsequently employed for coating and stability studies and glibenclamide in-vivo study.

Chapter 4

4. Physicochemical characterisation of lyophilised and physical mixtures of glibenclamide, spironolactone and ketoconazole with water-soluble excipients

4.1 Introduction

Solid oral dosage forms are characterised by low production costs, ease of use and handling and good physical and chemical stability. In solid dosage forms, active pharmaceutical entities and excipients may be present in crystalline or amorphous forms. Depending upon the prevailing physical conditions experienced during preparation of solid formulations, drug and/or excipients may undergo a number of phase transitions including polymorphic, solvate, hydrate or amorphous formation. Heating, solvent exposure, milling and drying processes such as lyophilisation and spray drying can present suitable conditions for phase transformation during pharmaceutical manufacturing.

Physicochemical characteristics of the solid state are influenced by phase transitions such as polymorphism or amorphous formation. The major characteristics influenced are melting points, crystal shape, solid state reactions, hygroscopicity, heat capacity, colour, solubility, dissolution rate and stability (Zhang et al., 2004). Thus, properties of solid state drug substances and excipients should be identified in order to guarantee reliable product performance.

Thermal analysis of drug substances and excipients is principally important for investigation of the physical structure of a formulation and is regularly used as a quality control procedure as well as in preformulation studies. Thermal analytical techniques including differential scanning calorimetry (DSC), thermogravimetric analysis (TGA) and combined techniques such as Fourier-transform infrared spectroscopy (FT-IR) and X-ray powder diffraction (XRPD) support analysis of substances in the solid state.

4.2 Aims and objectives

The aim of this chapter is to employ a number of analytical techniques such as DSC, FT-IR and XRPD to characterise lyophilised glibenclamide, spironolactone and ketoconazole systems and their corresponding physical mixtures.

4.3 Methods

Analytical techniques and sample preparation are described in detail in Chapter 2. Preparation of lyophilised and physical mixtures of the investigated drugs with different water-soluble excipients is provided in Sections 3.3.2 and 3.3.3. All mixtures were freshly prepared and evaluated by DSC, TGA, FT-IR and XRPD.

4.4 Results and discussion

4.4.1 Glibenclamide

4.4.1.1 Lyophilised glibenclamide

Figure 4.1 shows the DSC thermograms of the unprocessed and lyophilised glibenclamide. The unprocessed glibenclamide was characterised by a single sharp endothermic peak at 175ºC corresponding to the known melting point of the drug crystals (Panagopoulou-Kaplani & Malamataris, 2000). In contrast, the thermogram of the lyophilised drug lacked the drug melting endotherm, indicating the formation of an amorphous form of glibenclamide during the lyophilisation process. Furthermore, the thermogram showed a shallow, broad endotherm starting from 55ºC to 85ºC followed by another small endotherm around 105ºC corresponding to removal of residual solvent. These broad endotherms might overlap the endotherm corresponding to T_g of the produced amorphous form of glibenclamide as it has been reported at 84.8ºC (Chauhan et al., 2005). TGA results showed weight loss in the temperature range 40-105°C supporting the above DSC results (Figure 4.2).

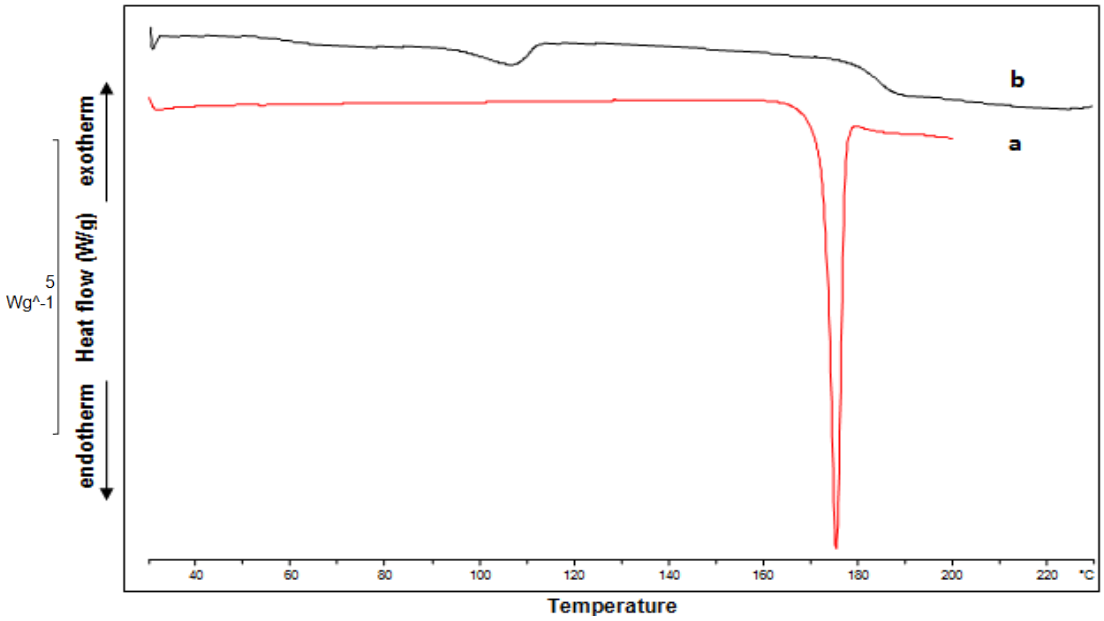

Figure 4.1: DSC of unprocessed glibenclamide (a) and lyophilised glibenclamide (b) powders.

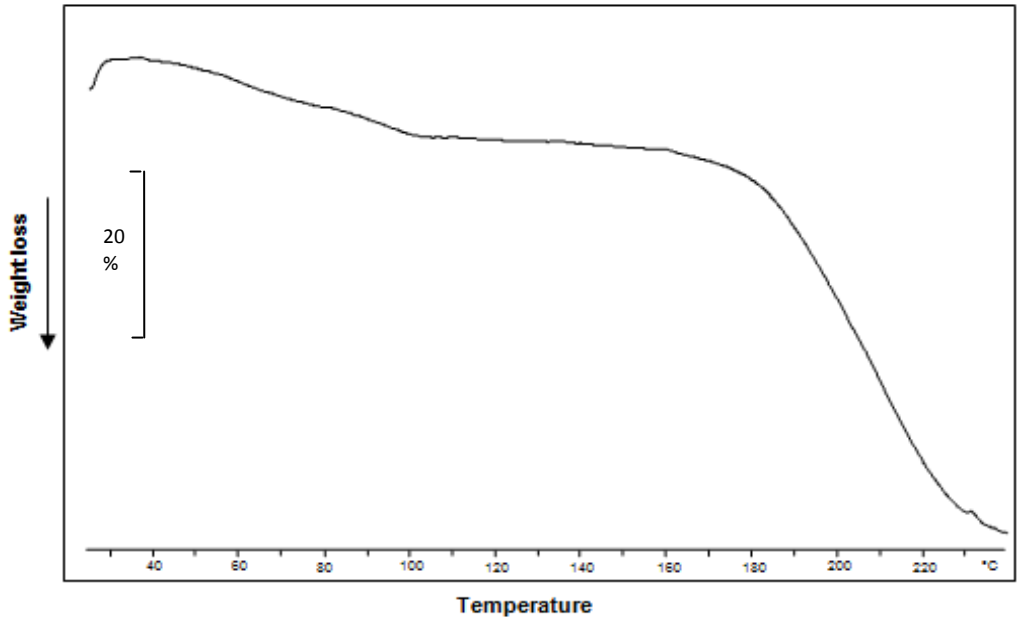

Figure 4.2: TGA of lyophilised glibenclamide powder.

The corresponding XRPD patterns are compared in Figure 4.3. The unprocessed drug exhibited high crystallinity as indicated by numerous sharp distinctive peaks as previously reported (Hassan et al., 1991; Chauhan et al., 2005). On the other hand, the XRPD pattern of the lyophilised drug exhibited an extensive decrease in the number and intensity of peaks suggesting that the majority of glibenclamide converted to an amorphous form during the lyophilisation process. The diffractogram also showed the appearance of new peaks at 13.5º, 16.5º, 17.2º, 20.3º and 21.5º 2θ (highlighted by * in Figure 4.2) which may correspond to solvates of glibenclamide. It has been previously reported that glibenclamide crystallised into pseudo-polymorphic forms; pentanol and toluene solvates by slowly cooling the solutions of the drug in these solvents (Suleiman & Najib, 1989).

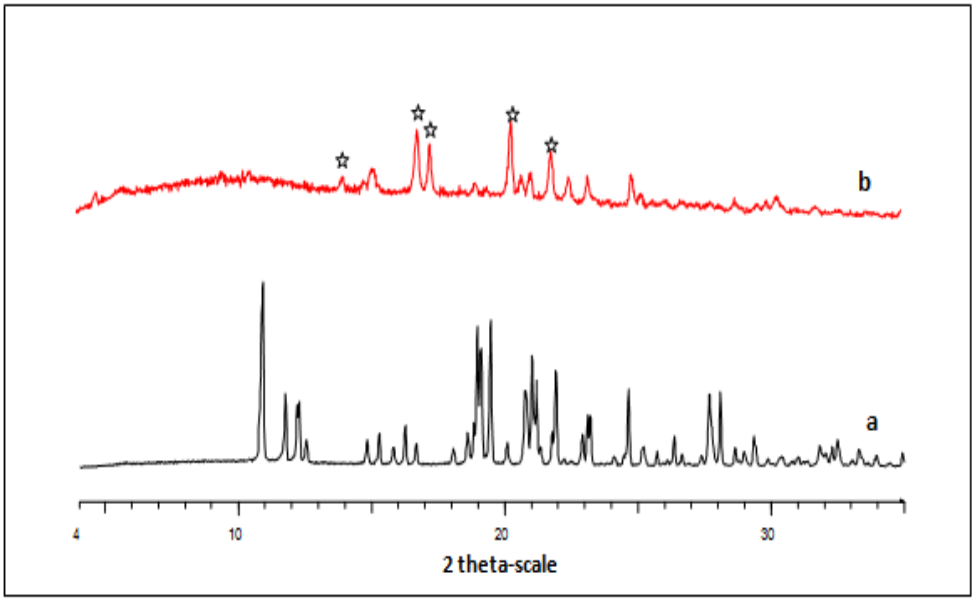

Figure 4.3: XRPD of unprocessed glibenclamide (a) and lyophilised glibenclamide (b) powders (* highlights new peaks).

The corresponding FT-IR spectra are shown in Figure 4.4. The unprocessed glibenclamide showed the characteristic amide peaks at 3366, 3312, 3117 and 1713 cm^{-1}, urea carbonyl stretching vibrations at 1615 and 1519 cm^{-1}, SO_2 stretching vibrations at 1155 and 1340 cm^{-1}. Noticeable differences in FT-IR spectrum of the

lyophilised glibenclamide were observed and these are summarised in Table 4.1. These differences may be due to intermolecular hydrogen bonding and partial transformation of glibenclamide from the keto- to enol form (Panagopoulou-Kaplani et al., 2000) provoked during the lyophilisation process.

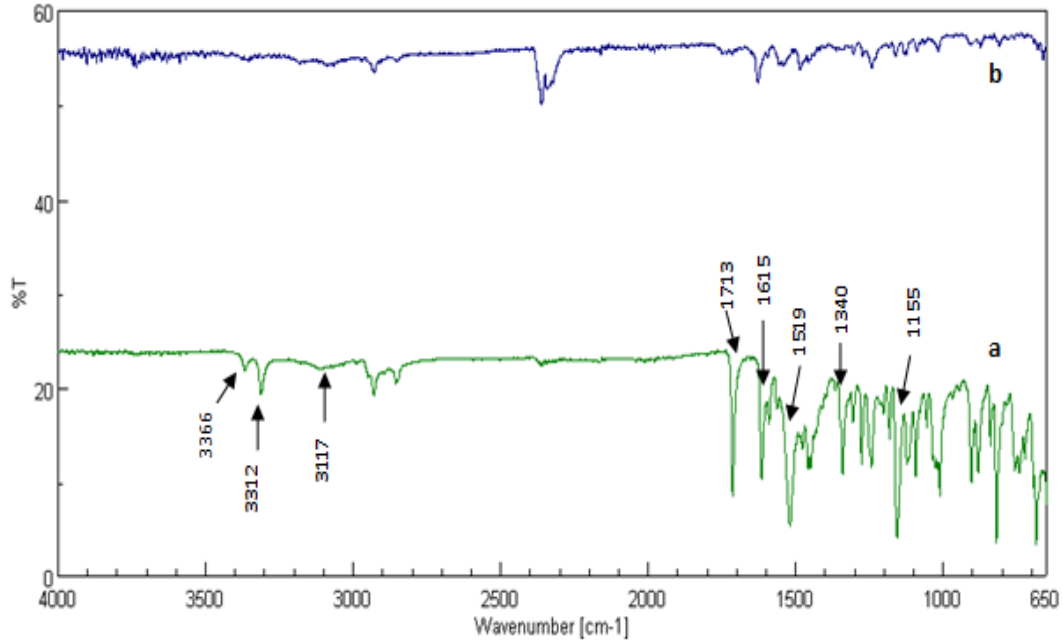

Figure 4.4: FT-IR of unprocessed glibenclamide (a) and lyophilised glibenclamide (b) powders.

In general, the absorption peaks of the lyophilised drug seemed to be less sharp than those of the unprocessed powder pointing to formation of an amorphous form of glibenclamide during the lyophilisation process which was supported by the DSC and XRPD results. Similar results have been obtained by Laitinen et al. (2009) who reported that the FT-IR spectrum of lyophilised perphenazine was less sharp compared to the unprocessed drug due to formation of an amorphous form of the drug during the lyophilisation process. Similarly, Chauhan et al. (2005) studied the FT-IR of an amorphous glibenclamide produced by spray drying process and the results revealed the disappearance of two characteristic amide peaks of

glibenclamide and the simultaneous shift of glibenclamide urea carbonyl stretching vibrations to higher frequencies due to intermolecular hydrogen bonding.

This alteration in the physical structure of glibenclamide explains the major improvement in glibenclamide dissolution compared to the unprocessed drug and the commercial tablet formulations (Section 3.4.2.1).

Table 4.1: Wave numbers of FT-IR absorption bands where differences were detected between unprocessed and lyophilised glibenclamide

Wave number (cm^{-1})	Corresponding bond or functional group	Spectral change in lyophilised glibenclamide
3366	Amide	Disappeared
3312	Amide	Disappeared
3117	Amide	Disappeared
1713	Amide	Decreased intensity
1615	urea carbonyl	Shift to 1628 cm^{-1}
1519	urea carbonyl	Disappeared
1340	SO_2	Disappeared
1155	SO_2	Decreased intensity and shift to 1161 cm^{-1}

4.4.1.2 Lyophilised glibenclamide-mannitol mixture

The physical state of unprocessed glibenclamide, mannitol, and their physical and lyophilised mixtures (91% w/w mannitol) were investigated by DSC and their

thermograms are shown in Figure 4.5. The unprocessed glibenclamide exhibited a sharp melting endotherm at 175ºC whereas the unprocessed mannitol exhibited its melting endotherm at 168ºC which is characteristic for the β polymorph of mannitol (Izutsu et al., 2004). The thermogram of the physical and lyophilised mixtures showed the melting endotherm of mannitol while the melting endotherm of glibenclamide disappeared. It is possible that glibenclamide may have dissolved in the melt of mannitol during the DSC measurement thereby abolishing its melting point.

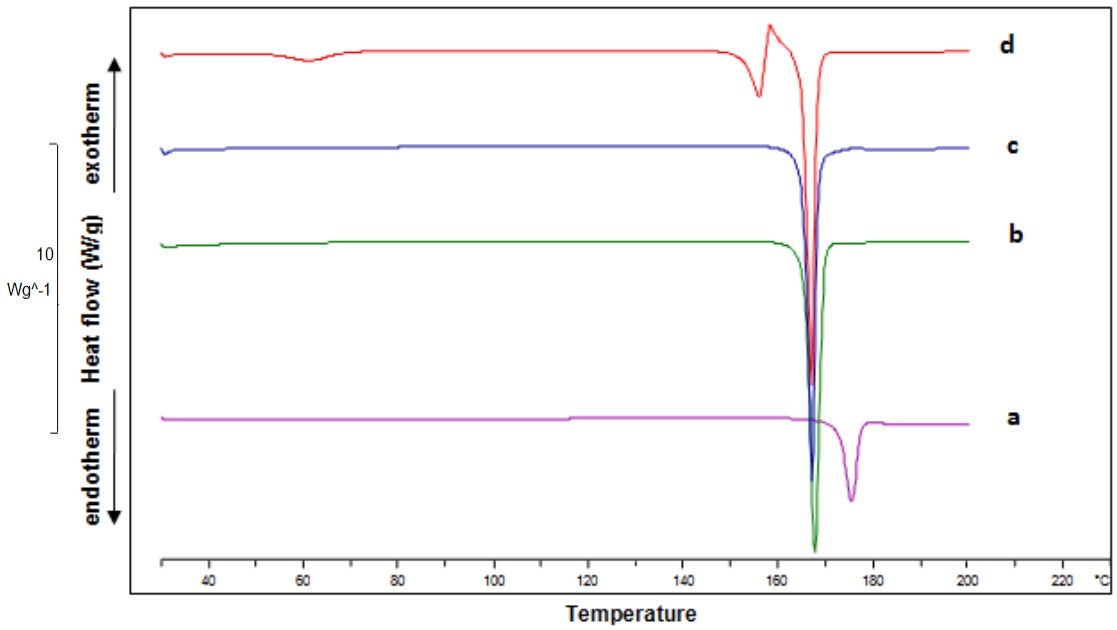

Figure 4.5: DSC of unprocessed glibenclamide (a), unprocessed mannitol (b), glibenclamide-mannitol physical mixture (c) and glibenclamide-mannitol lyophilised mixture (d).

The thermogram of the lyophilised mixture also exhibited different thermal transitions: broad endotherm around 60ºC; endothermic peaks at 154ºC and 168ºC; and an exothermic peak at 158ºC. The broad endotherm around 60ºC may represent removal of residual moisture as confirmed by the weight loss observed in TGA starting from 48ºC (Figure 4.6). This broad endotherm may also represent dehydration of mannitol hydrate that might be formed during lyophilisation (Nunes

et al., 2004). The melting endotherm at 154ºC represents the melting point of the δ polymorph of mannitol that was produced during the lyophilisation process (Izutsu et al., 2004). The exotherm at 158ºC represents melt-recrystallisation of the δ polymorph to the more stable β and/or α polymorph of mannitol by addition of heat during the DSC analysis while the endotherm at 168ºC represents the melting point of the produced β and/or α polymorph of mannitol (Takada et al., 2009).

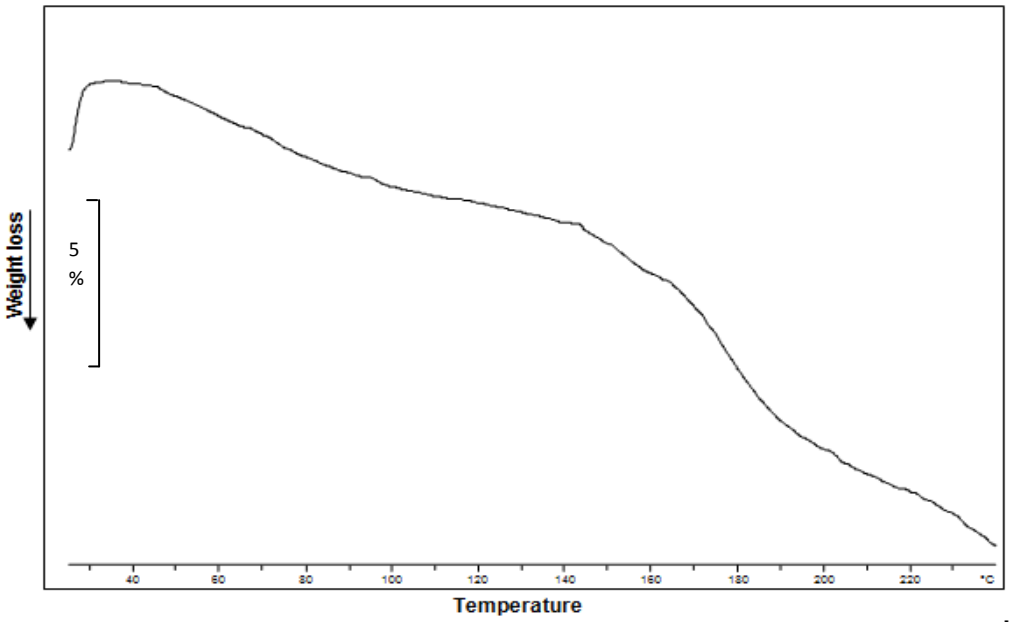

Figure 4.6: TGA of lyophilised glibenclamide-mannitol mixture.

The corresponding XRPD patterns are shown in Figure 4.7. The diffractogram of the unprocessed mannitol displayed several sharp peaks at 10.5º 14.6º, 16.8º, 18.8º and 23.4º 2θ that are characteristic for the β polymorph of mannitol (Hawe & Frieß, 2006) indicating the high crystallinity of the excipient. The diffractogram of the physical mixture represented the addition pattern of unprocessed glibenclamide (Section 4.4.1.1) and mannitol. Moreover, the intensity of the characteristic peaks of glibenclamide was reduced due to dilution with excipient. The lyophilised mixture showed the disappearance of all the characteristic peaks of the drug suggesting that glibenclamide could be dispersed in an amorphous form in the water-soluble excipient. The diffractogram also showed the disappearance of the characteristic

peaks of mannitol and the appearance of new crystal peaks at 9.7º and 20.4º 2θ (highlighted by * in Figure 4.7). These peaks are characteristic for the δ polymorphic form of mannitol (Hawe & Frieß, 2006) which was supported by the DSC results. These results are in agreement with Kim et al. (1998) who reported the formation of the δ polymorph of mannitol by lyophilisation of its rapidly frozen solution. The absence of the characteristic peak at 19.7º 2θ omits the possibility of presence of mannitol hydrate (Hawe & Frieß, 2006) as suggested by the DSC results.

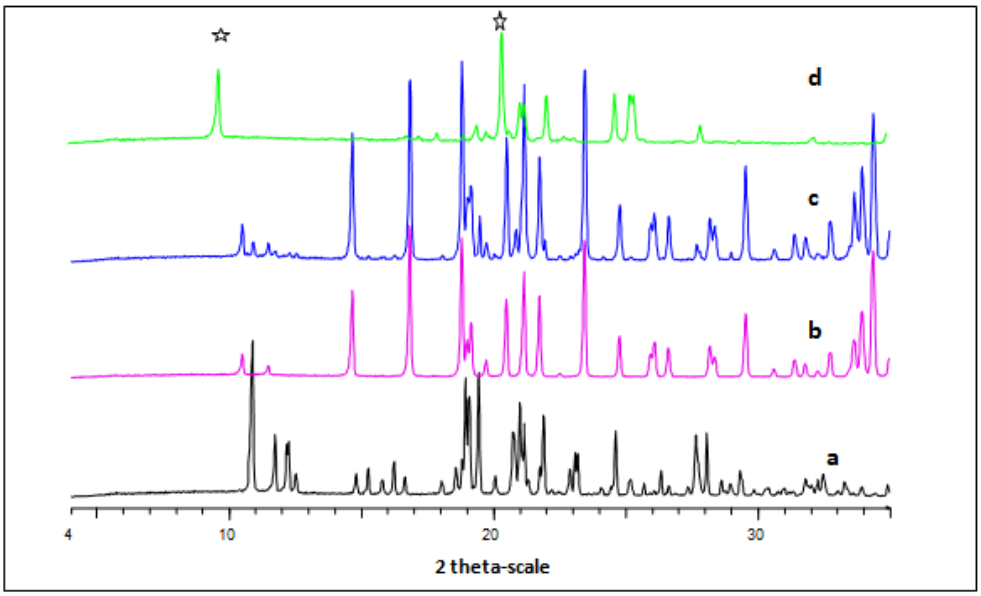

Figure 4.7: XRPD of unprocessed glibenclamide (a), unprocessed mannitol (b), glibenclamide-mannitol physical mixture (c) and glibenclamide-mannitol lyophilised mixture (d) (* highlights new peaks).

The corresponding FT-IR spectra are shown in Figure 4.8. The characteristic absorption bands of glibenclamide were previously discussed (Table 4.1). The mannitol spectrum is characterised by OH stretching vibration peaks at 3392 and 3289 cm^{-1} and C-O stretching vibration peaks at 1082 and 1020 cm^{-1} (Juppo et al., 2003). The spectrum of the physical mixture showed all the characteristic peaks of mannitol and exhibited disappearance of the characteristic peaks of glibenclamide. This might be attributed to high concentration of the excipient that swamped the drug absorption peaks or drug-excipient interaction (hydrogen bonding) during

preparation of the mixture. Similar observation has been reported by Chauhan et al. (2005) who found that SO_2 characteristic peaks of glibenclamide disappeared in the spectrum of its physical mixture with Gelucire 50/13 or 44/14 and Aerosil® 200 due to weak hydrogen bonding between the glibenclamide SO_2 group and the silanol groups of Aerosil® 200 during preparation of the physical mixture.

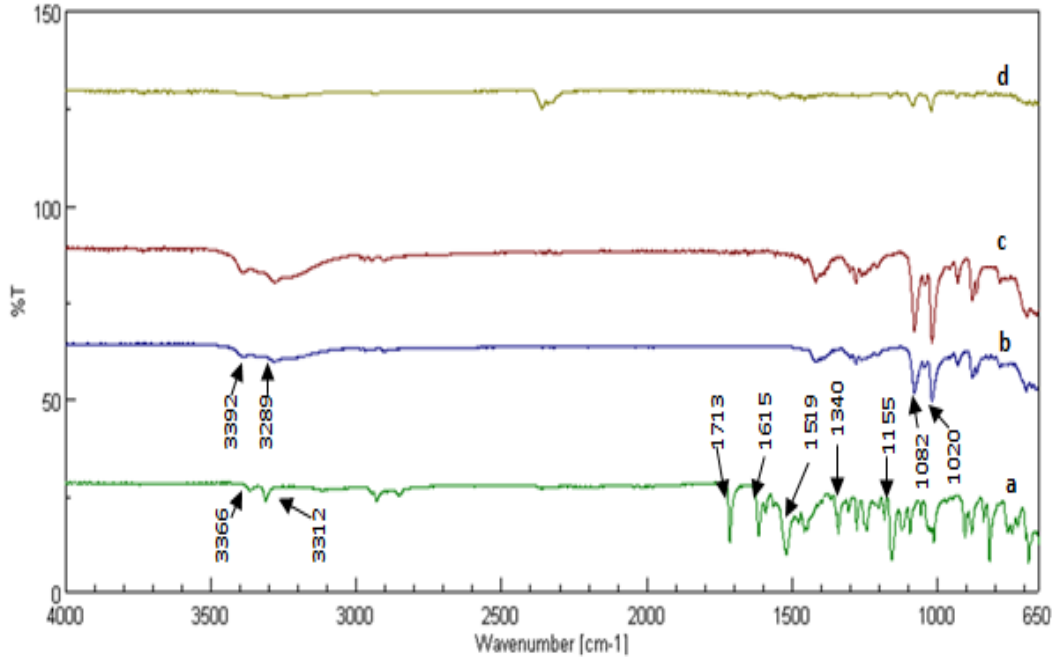

Figure 4.8: FTIR of unprocessed glibenclamide (a), unprocessed mannitol (b), glibenclamide-mannitol physical mixture (c) and glibenclamide-mannitol lyophilised mixture (d).

Noticeable changes in FT-IR spectrum of the lyophilised mixture were observed and these are summarised in Table 4.2. These changes suggest formation of hydrogen bonding between carbonyl, amide and SO_2 groups of glibenclamide and OH groups of mannitol. Generally, the spectrum of the lyophilised mixture has fewer and less sharp absorption bands compared to that of the physical mixture suggesting crystal disturbance of glibenclamide and mannitol molecules during lyophilisation and supporting the XRPD and DSC results. Thus, it can be concluded that drug-excipient interactions and alterations in the physical structure of glibenclamide, in the lyophilised mixture, are most likely the main mechanisms of glibenclamide dissolution rate enhancement observed (Section 3.4.2.2). Similar results have been

reported by Juppo et al. (2003) who reported that the interactions between 2, 6-dimethyl-8-(2-ethyl-6-methylbenzylamino)-3-hydroxymethylimidazo-[1,2-a]pyridine mesylate and mannitol and the changes in the drug crystalline structure enhanced the dissolution rate of the drug from its solid dispersion with mannitol.

Table 4.2: Wave numbers of FT-IR absorption bands where changes were detected in lyophilised glibenclamide-mannitol mixture, compared to unprocessed components

Wave number (cm^{-1})	Corresponding bond or functional group	Spectral change in lyophilised system
3366	Amide (glibenclamide)	Disappeared
3312	Amide (glibenclamide)	Disappeared
1713	Amide (glibenclamide)	Disappeared
1615	urea carbonyl (glibenclamide)	Disappeared
1519	urea carbonyl (glibenclamide)	Disappeared
1340	SO_2 (glibenclamide)	Disappeared
1155	SO_2 (glibenclamide)	Disappeared
3392	OH (mannitol)	Disappeared
3289	OH (mannitol)	Disappeared

4.4.1.3 Lyophilised glibenclamide-SLS mixture

The thermal properties of unprocessed glibenclamide, SLS, their physical and lyophilised mixtures (93% w/w SLS) are shown in Figure 4.9. SLS exhibited a sharp

melting endotherm at 199ºC which is close to that reported by Waard et al. (2008). It also showed another shallow endotherm around 105ºC (Brown et al., 1999) which corresponds to evaporation of the water content typically present within SLS (2% w/w).

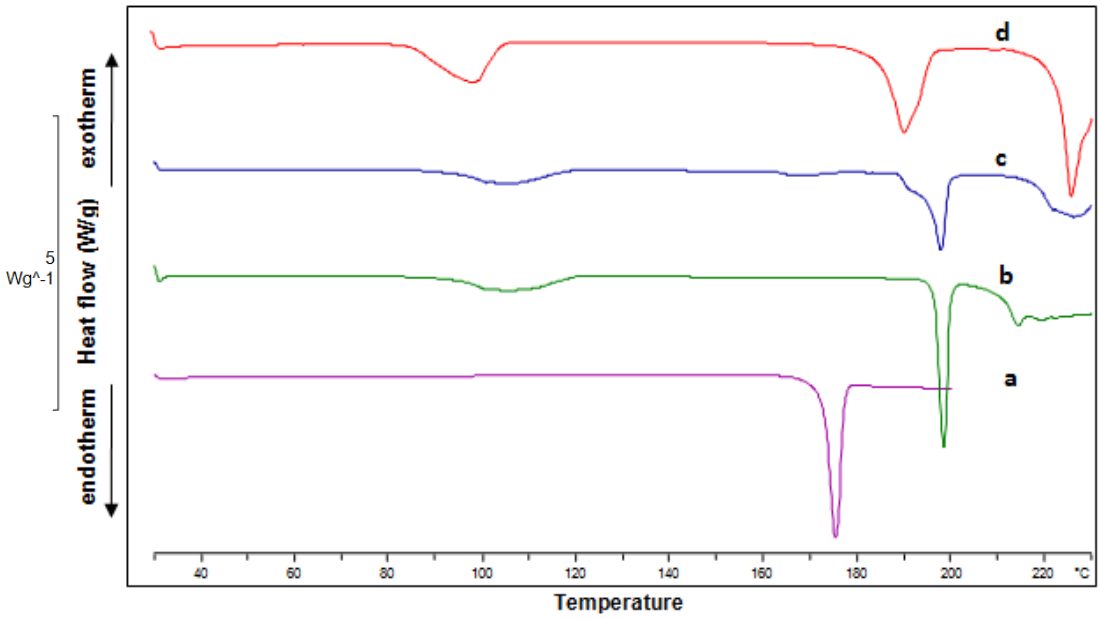

Figure 4.9: DSC of unprocessed glibenclamide (a), unprocessed SLS (b), glibenclamide-SLS physical mixture (c) and glibenclamide-SLS lyophilised mixture (d).

The thermogram of the physical mixture showed the disappearance of the glibenclamide melting endotherm that might be attributed to high concentration of SLS relative to glibenclamide which swamped the drug melting peak. It also displayed both endotherms of SLS with decreased intensity of the melting endotherm at 199ºC due to disturbance in the crystalline structure of SLS in the physical mixture. A similar behaviour was observed in the case of the lyophilised mixture along with a shift of the SLS endotherms to 99ºC and 192ºC, suggesting formation of solid dispersion and interactions between glibenclamide and SLS. Waard et al. (2008) has reported the incidence of interactions between SLS and each of inulin and diazepam in their solid dispersion leading to enhancement of the dissolution rate of diazepam.

The corresponding XRPD patterns are shown in Figure 4.10. In addition to the high crystallinity of the drug, SLS also, is characterised by obvious crystallinity. The XRPD pattern of the physical mixture showed the characteristic peaks of SLS while the characteristic peaks of glibenclamide disappeared due to lower concentration of the drug relative to the excipient in the physical mixture.

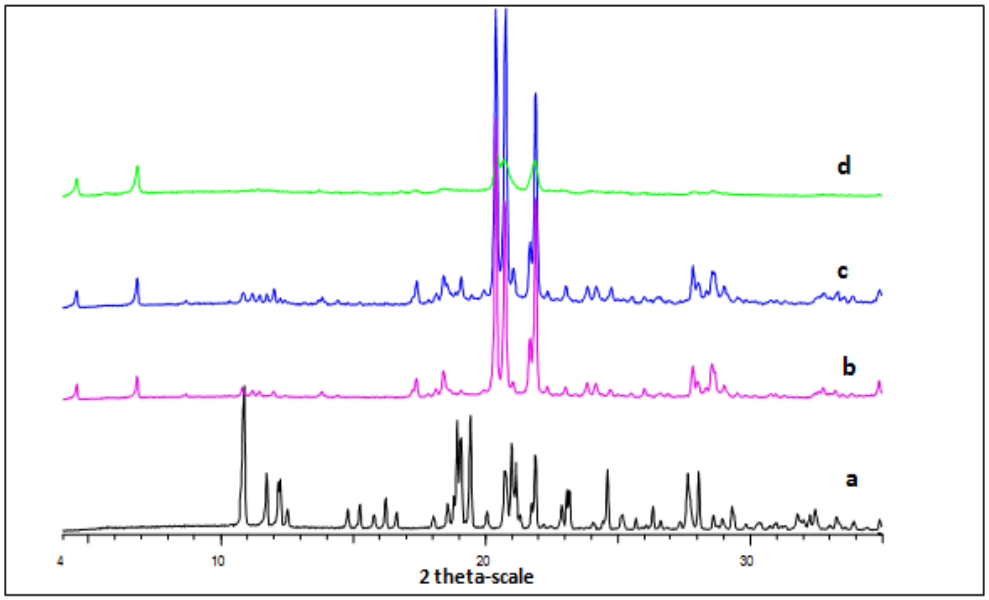

Figure 4.10: XRPD of unprocessed glibenclamide (a), unprocessed SLS (b), glibenclamide-SLS physical mixture (c) and glibenclamide-SLS lyophilised mixture (d).

The lyophilised mixture showed the disappearance of all the characteristic peaks of glibenclamide. This finding suggests that glibenclamide was dispersed as an amorphous form in the SLS matrix. Moreover, some of the distinctive SLS peaks disappeared while the intensity of the other peaks extensively decreased, suggesting partial transformation of SLS to an amorphous form. This mechanism explains the dissolution rate enhancement of glibenclamide from its lyophilised mixture with SLS (Section 3.4.2.3). Similar results have been reported by Fukushima et al. (2007) who found that the HIV protease inhibitor, atazanavir, could be dispersed homogenously in an amorphous form in its solid dispersion with SLS.

The corresponding FT-IR spectra are shown in Figure 4.11. The SLS spectrum showed peaks at 2915 and 2849 cm^{-1} assigned to the C-H stretching vibrations of long chain fatty alkyl group of surfactants (Patel & Joshi, 2008). It also, showed C-H bending, C-O stretching, and S=O stretching vibrations at 1467, 1216 and 1080 cm^{-1} respectively. The spectrum of the physical mixture showed all the characteristic peaks of SLS while the drug peaks disappeared due to the high concentration of the excipient relative to the drug.

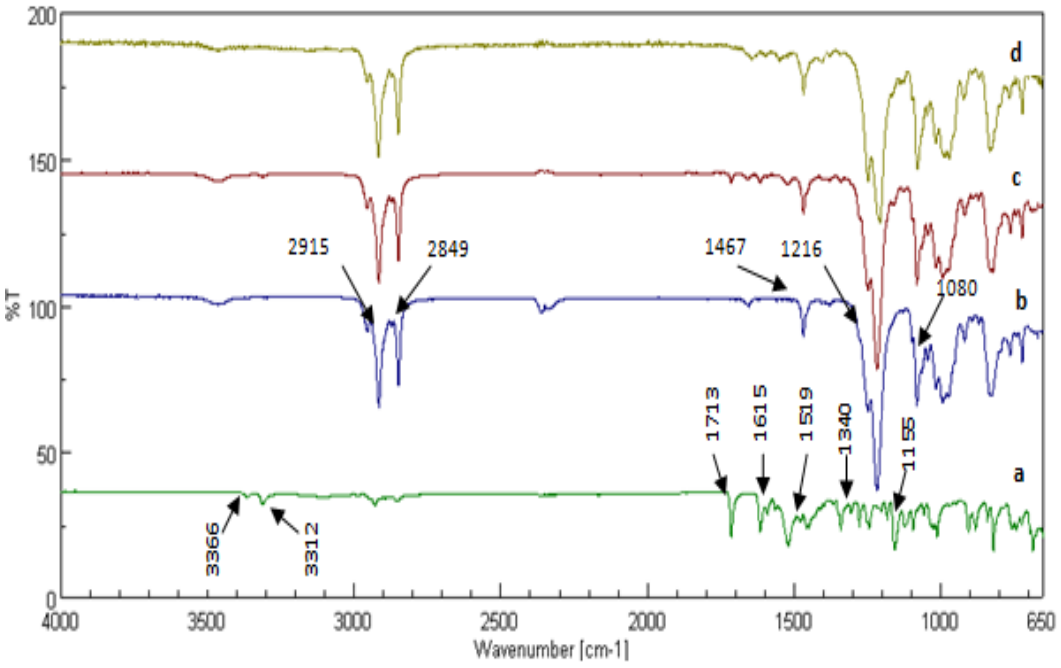

Figure 4.11: FT-IR of unprocessed glibenclamide (a), unprocessed SLS (b), glibenclamide-SLS physical mixture (c) and glibenclamide-SLS lyophilised mixture (d).

Noticeable changes in FT-IR spectrum of the lyophilised mixture were observed and these are summarised in Table 4.3. These changes suggest the incidence of drug-excipient interactions and support the DSC results. Possible interactions could be hydrogen bonding between the N–H groups of the drug and the $SO3^-$ group of SLS (Patel & Joshi, 2008) or between CH_2–O of SLS and SO_2 or carbonyl group of glibenclamide.

Table 4.3: Wave numbers of FT-IR absorption bands where changes were detected in lyophilised glibenclamide-SLS mixture, compared to unprocessed components

Wave number (cm^{-1})	Corresponding bond or functional group	Spectral change in lyophilised system
3366	Amide (glibenclamide)	Disappeared
3312	Amide (glibenclamide)	Disappeared
1713	Amide (glibenclamide)	Disappeared
1615	urea carbonyl (glibenclamide)	Shift to 1628 cm^{-1}
1519	urea carbonyl (glibenclamide)	Disappeared
1340	SO_2 (glibenclamide)	Disappeared
1155	SO_2 (glibenclamide)	Disappeared
2915	Long chain alkyl group (SLS)	Decreased intensity
2849	Long chain alkyl group (SLS)	Decreased intensity
1467	C-H (SLS)	Decreased intensity
1216	C-O (SLS)	Increased intensity of the shoulder
1080	S=O (SLS)	Shift to 1083 cm^{-1}

4.4.1.4 Lyophilised glibenclamide-PEG 6000 mixture

The DSC thermograms of unprocessed glibenclamide, PEG 6000, their physical and lyophilised mixtures (80% w/w PEG 6000) are illustrated in Figure 4.12. While the

glibenclamide melting endotherm appeared at 175ºC, the endothermic peak corresponding to the PEG 6000 melting temperature appeared at 64ºC, which is close to that previously reported by Yamashita et al. (2003).

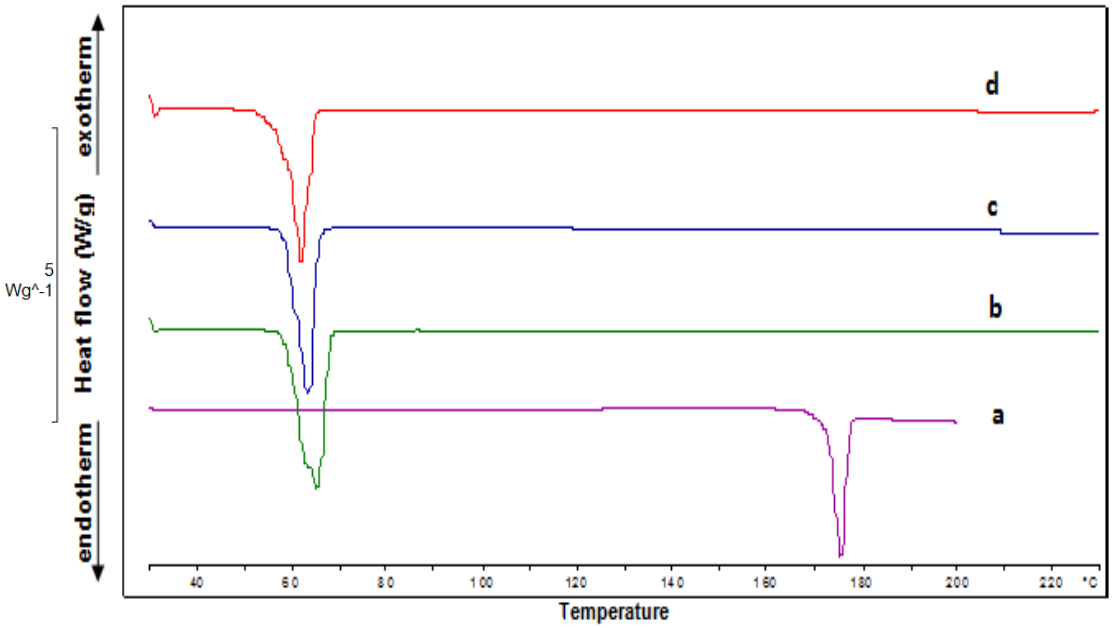

Figure 4.12: DSC of unprocessed glibenclamide (a), unprocessed PEG 6000 (b), glibenclamide-PEG 6000 physical mixture (c) and glibenclamide-PEG 6000 lyophilised mixture (d).

No apparent differences were detected between DSC thermograms of the physical and lyophilised mixtures. Both thermograms exhibited disappearance of the melting endotherm of glibenclamide and appearance of one endotherm at 64ºC corresponding to the fusion temperature of PEG 6000. This absolute disappearance of the drug melting peak was attributed to dissolution of glibenclamide in the melt of PEG 6000 before reaching its melting temperature during DSC analysis. This finding is in agreement with Asyarie and Rashmawati (2007) who found that the melting endotherms of gliclazide disappeared in the DSC thermograms of both the physical mixtures and solid dispersions of the drug with PEG 6000. Similar results have been

reported for the solid dispersion of tacrolimus with PEG 6000 **(**Yamashita et al., 2003).

The corresponding XRPD patterns are shown in Figure 4.13. PEG 6000 diffraction pattern showed two high, distinctive peaks at 19º and 23º 2θ (Asyarie & Rashmawati, 2007) indicating the semi-crystalline nature of the polymer (Wang et al., 2004, Zhu et al., 2010). The diffraction pattern of the physical mixture is equivalent to the addition pattern of the drug and the polymer with decreased intensity of glibenclamide peaks due to dilution from the presence of excipient.

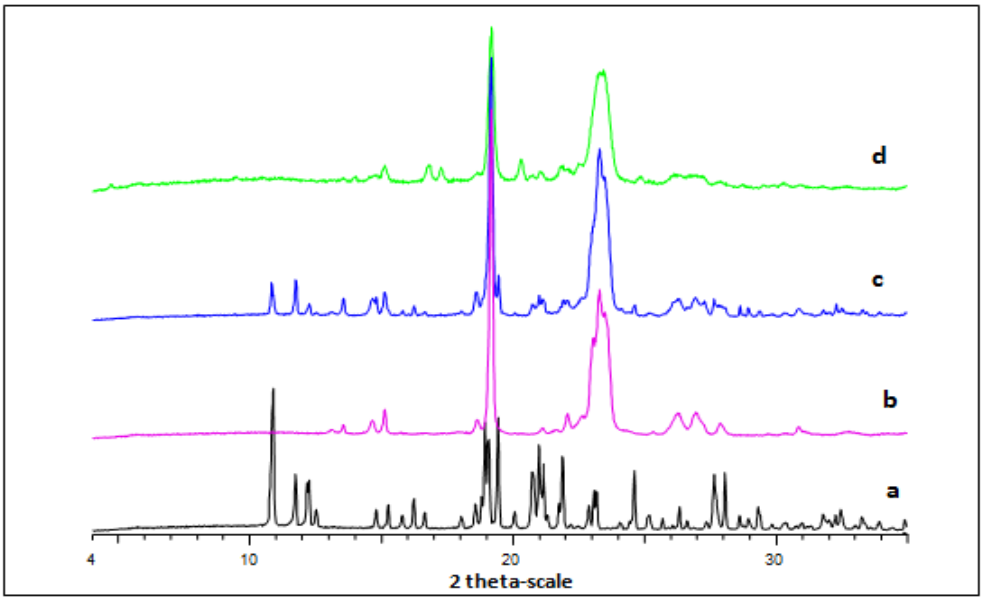

Figure 4.13: XRPD of unprocessed glibenclamide (a), unprocessed PEG 6000 (b), glibenclamide-PEG 6000 physical mixture (c) and glibenclamide-PEG 6000 lyophilised mixture (d).

The diffractogram of the lyophilised mixture showed the characteristic peaks of PEG 6000 with the disappearance of glibenclamide peaks. This finding suggests that PEG 6000 maintained its physical state in the lyophilised mixture while the drug dispersed as an amorphous form in the polymer matrix. Similar results have been reported for perphenazine as the XRPD pattern of its solid dispersion with PEG 8000 exhibited

disappearance of the drug peaks with maintenance of the polymer peaks (Laitinen et al., 2009).

The corresponding FT-IR spectra are shown in Figure 4.14. The spectrum of PEG 6000 showed characteristic absorption bands at 3400, 2880, and 1095 cm^{-1} representing OH, C-H, and C-O stretching vibrations respectively. The spectrum of the physical mixture displayed the addition spectra of the drug and the polymer. Noticeable changes in FT-IR spectrum of the lyophilised mixture were observed and these are summarised in Table 4.4. These changes suggest the incidence of drug-excipient interactions such as hydrogen bonding in the produced solid dispersion. The possible interaction could take place between the amide hydrogen of glibenclamide and the loan pairs of oxygen atoms of PEG 6000 or between amide group, SO2, or carbonyl group of the drug and OH groups of PEG 6000.

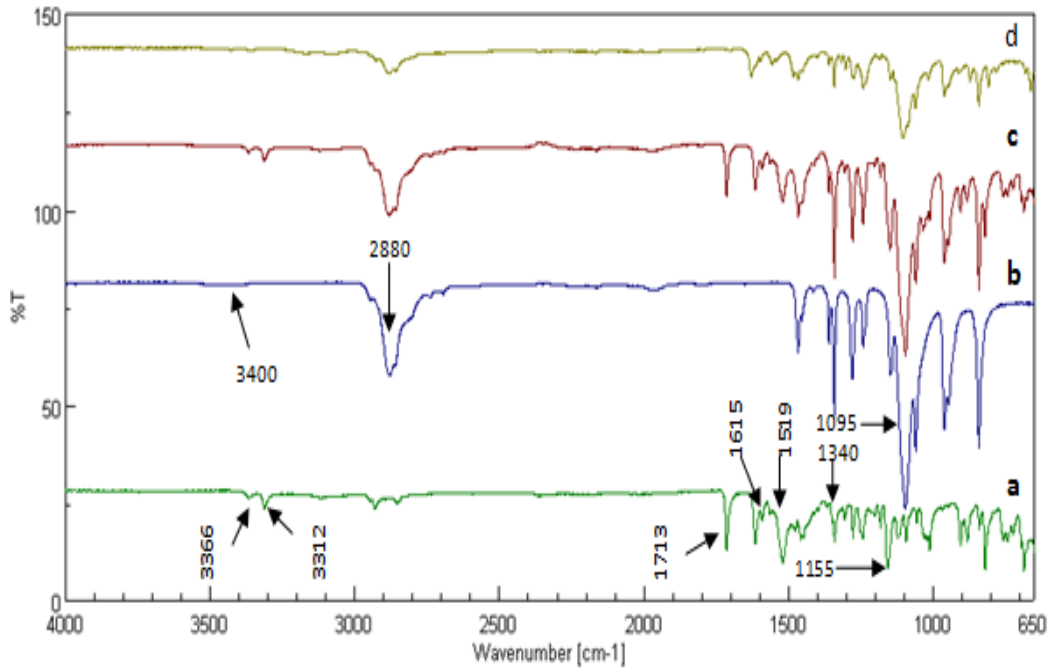

Figure 4.14: FT-IR of unprocessed glibenclamide (a), unprocessed PEG 6000 (b), glibenclamide-PEG 6000 physical mixture (c) and glibenclamide-PEG 6000 lyophilised mixture (d).

Table 4.4: Wave numbers of FT-IR absorption bands where changes were detected in lyophilised glibenclamide-PEG 6000 mixture, compared to unprocessed components

Wave number (cm^{-1})	Corresponding bond or functional group	Spectral change in lyophilised system
3366	Amide (glibenclamide)	Disappeared
3312	Amide (glibenclamide)	Disappeared
1713	Amide (glibenclamide)	Disappeared
1615	urea carbonyl (glibenclamide)	Shift to 1627 cm^{-1}
1519	urea carbonyl (glibenclamide)	Shift to 1540 cm^{-1}
1340	SO_2 (glibenclamide)	Disappeared
1155	SO_2 (glibenclamide)	Disappeared
3400	OH (PEG 6000)	Disappeared
2880	C-H (PEG 6000)	Shift to 2883 cm^{-1}
1095	C-O (PEG 6000)	Shift to 1100 cm^{-1}

4.4.1.5 Lyophilised glibenclamide-tromethamine mixture

The DSC thermograms of unprocessed glibenclamide, tromethamine, and their physical and lyophilised mixtures with 50% w/w tromethamine are illustrated in Figure 4.15. Unprocessed tromethamine displayed one endotherm at 139ºC and another endotherm at 172ºC. It has been reported that the former endotherm corresponds to solid-solid transition of the metastable polymorph of tromethamine

while the later endotherm corresponds to the melting temperature of tromethamine crystals (Abdelkader et al., 2007). The thermograms of the physical and lyophilised mixtures showed the disappearance of the characteristic melting endotherm of glibenclamide and the appearance of a single endotherm at 135ºC and 131ºC respectively. These endotherms most probably represent eutectic peaks suggesting complexation between the drug and the excipient and formation of eutectic system. Verma and Garg (2005) and Abdelkader et al. (2007) have reported similar results for the mixtures of glipizide-tromethamine and nimesulide-tromethamine respectively.

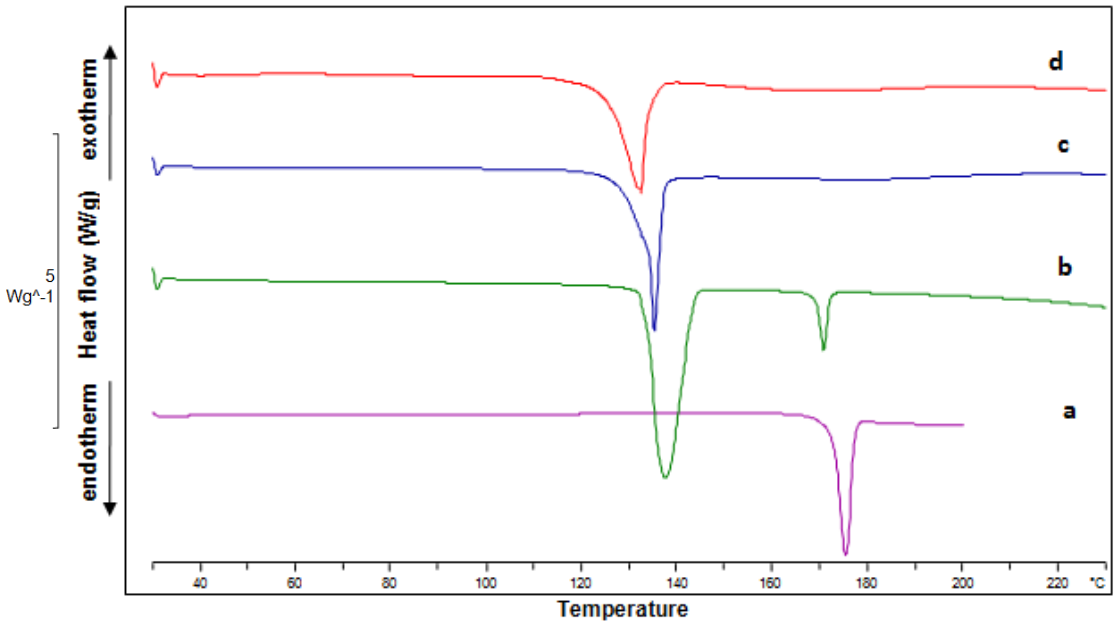

Figure 4.15: DSC of unprocessed glibenclamide (a), unprocessed tromethamine (b), glibenclamide-tromethamine physical mixture (c) and glibenclamide-tromethamine lyophilised mixture (d).

The corresponding XRPD patterns are compared in Figure 4.16. The tromethamine diffraction pattern showed several distinctive peaks. The diffraction pattern of the physical mixture showed the characteristic peaks of both drug and excipient with decreased intensity as a result of dilution effects in the mixture. On the other hand, the diffraction pattern of the lyophilised mixture exhibited disappearance of all the

characteristic peaks of glibenclamide. This indicates the transformation of the drug into an amorphous form in its solid dispersion with the excipient. In addition, the intensities of the characteristic peaks of tromethamine were strongly decreased suggesting the transformation of the majority of the excipient into an amorphous form in the lyophilised mixture.

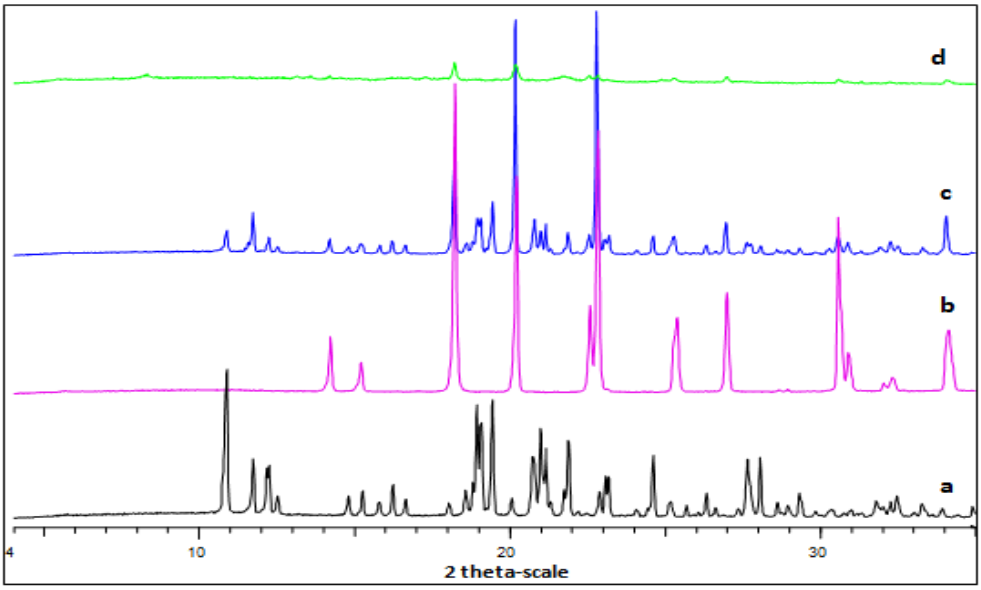

Figure 4.16: XRPD of unprocessed glibenclamide (a), unprocessed tromethamine (b), glibenclamide-tromethamine physical mixture (c) and glibenclamide-tromethamine lyophilised mixture (d).

The corresponding FT-IR spectra are shown in Figure 4.17. The spectrum of tromethamine showed absorption bands at 3346 and 3287 cm^{-1} presenting N-H and O-H stretching vibrations respectively. It also showed two absorption bands at 1585 and 1019 cm^{-1} that are characteristic to N-H bending and C-N stretching vibrations respectively. The spectrum of the physical mixture displayed all the characteristic absorption bands of glibenclamide and tromethamine. Noticeable changes in FT-IR spectrum of the lyophilised mixture were observed and these are summarised in Table 4.5. Generally, the spectrum of the lyophilised mixture showed significant changes in the peak appearance. There is strong evidence of intermolecular

hydrogen bonding between the proton donor; glibenclamide (acidic drug) and the proton acceptor; tromethamine (basic excipient) which might result in salt formation. Tromethamine has been reported to form a salt with Benzoic acid as a model acidic drug (McGloughlin and Corrigan,1992).

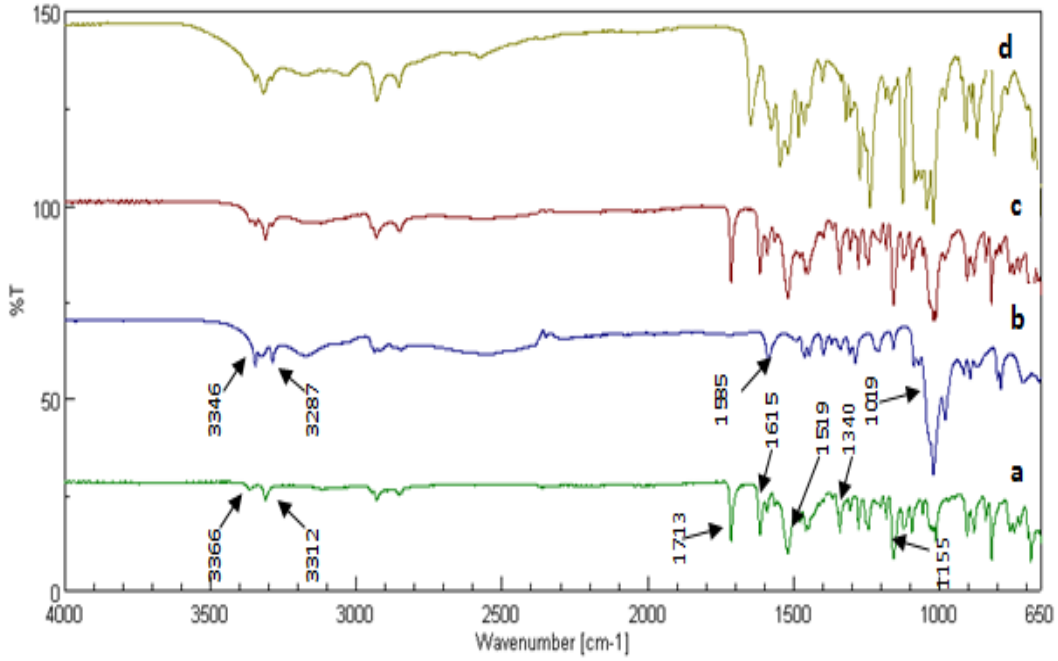

Figure 4.17: FT-IR of unprocessed glibenclamide (a), unprocessed tromethamine (b), glibenclamide-tromethamine physical mixture (c) and glibenclamide-tromethamine lyophilised mixture (d).

Table 4.5: Wave numbers of FT-IR absorption bands where changes were detected in lyophilised glibenclamide-tromethamine mixture, compared to unprocessed components

Wave number (cm^{-1})	Corresponding bond or functional group	Spectral change in lyophilised system
3366	Amide (glibenclamide)	Disappeared
1713	Amide (glibenclamide)	Disappeared
1615	urea carbonyl (glibenclamide)	Shift to 1646 cm^{-1}
1340	SO_2 (glibenclamide)	Disappeared
1155	SO_2 (glibenclamide)	Decreased intensity and shift to 1166 cm^{-1}
1585	N-H (tromethamine)	Shift to 1576 cm^{-1}

From the above discussion, it can be concluded that the main factor contributing to the dissolution rate enhancement of glibenclamide from its lyophilised mixture with tromethamine (Section 3.4.2.6) is the dispersion of the drug in an amorphous form in the excipient matrix. Also, drug-excipient interactions that might lead to salt formation could be another possible explanation.

4.4.1.6 Lyophilised glibenclamide-gelatin mixture

The thermal behaviours of the unprocessed glibenclamide, gelatin, and their physical and lyophilised mixtures (50% w/w gelatin) are presented in Figure 4.18. The thermogram of gelatin displayed no melting endotherm indicating the amorphous nature of the excipient (Chono et al., 2008). The thermogram of the physical mixture showed that the melting endotherm of glibenclamide appeared less sharp and less intense, with an enthalpy of fusion 146.16 mJ compared to that of the unprocessed

drug with an enthalpy of fusion 227 mJ. This could be attributed to decreased concentration of the drug in the mixture or to disturbance of the crystalline structure of glibenclamide in its physical mixture with the amorphous excipient. On the other hand, the thermogram of the lyophilised mixture showed complete disappearance of glibenclamide melting endotherm. This finding suggests that the drug was dispersed as an amorphous form in the matrix of the amorphous excipient. This result explains the drastic enhancement in the dissolution rate of glibenclamide observed from its lyophilised mixture with gelatin (Section 3.4.2.5). In a similar study, it was found that tablets containing lyophilised ketoprofen with suitable excipients including gelatin, exhibited enhanced drug dissolution as a result of formation of an amorphous form of the drug in its solid dispersion with the excipients (Ahmed & Nafadi, 2006).

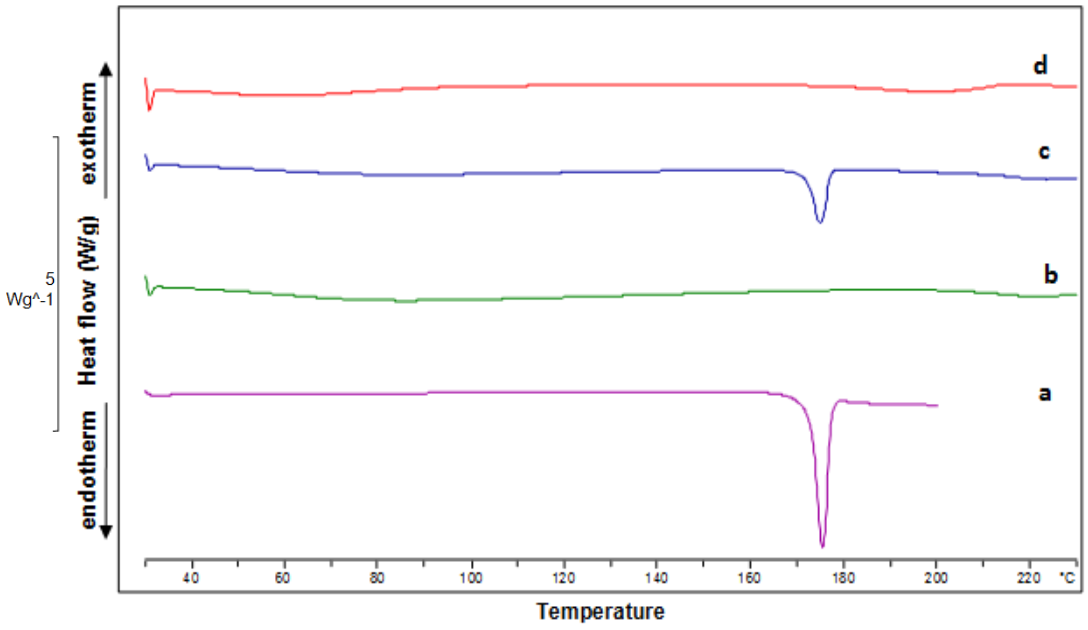

Figure 4.18: DSC of unprocessed glibenclamide (a), unprocessed gelatin (b), glibenclamide-gelatin physical mixture (c) and glibenclamide-gelatin lyophilised mixture (d).

The corresponding XRPD patterns are compared in Figure 4.19. The gelatin diffraction pattern showed a hump pattern that is characteristic for amorphous substances. The diffraction pattern of the physical mixture showed the characteristic peaks of the drug with apparent decrease in their intensity as a result of dilution effect of the drug by the amorphous excipient. On the other hand, the diffraction pattern of the lyophilised mixture exhibited disappearance of all the characteristic peaks of glibenclamide and displayed a hump pattern suggesting dispersion of the drug in an amorphous form in the matrix of the amorphous excipient. This observation was supported by the disappearance of the drug melting endotherm in the DSC thermogram of glibenclamide-gelatin lyophilised mixture.

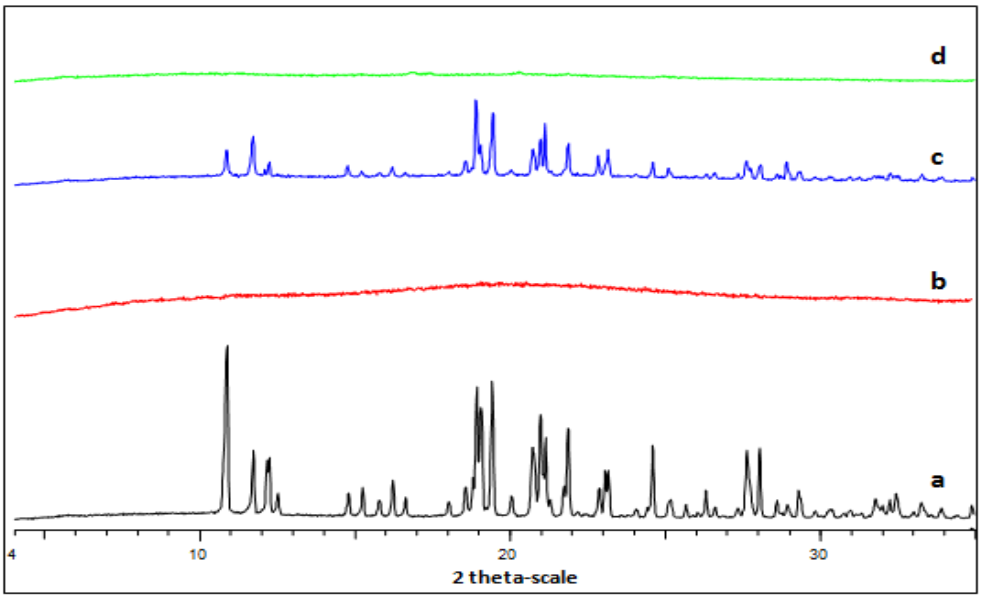

Figure 4.19: XRPD of unprocessed glibenclamide (a), unprocessed gelatin (b), glibenclamide-gelatin physical mixture (c) and glibenclamide-gelatin lyophilised mixture (d).

The corresponding FT-IR spectra are shown in Figure 4.20. The spectrum of gelatin showed absorption bands at 1630 and 1517 cm^{-1} assigned to C=O and N-H bending vibrations respectively (Mi, 2005). The spectrum of the physical mixture displayed all the characteristic absorption bands of glibenclamide at the same wave numbers. Noticeable differences in FT-IR spectrum of the lyophilised mixture were observed and these are summarised in Table 4.6. These observed changes may be attributable to the incidence of intermolecular hydrogen bonding between glibenclamide and gelatin in the solid dispersion produced during the lyophilisation process. Moreover, the change in the appearance of the peaks and the decrease in their number and sharpness compared to the spectrum of the physical mixture support the DSC and XRPD results suggesting the dispersion of glibenclamide in an amorphous form in gelatin matrix.

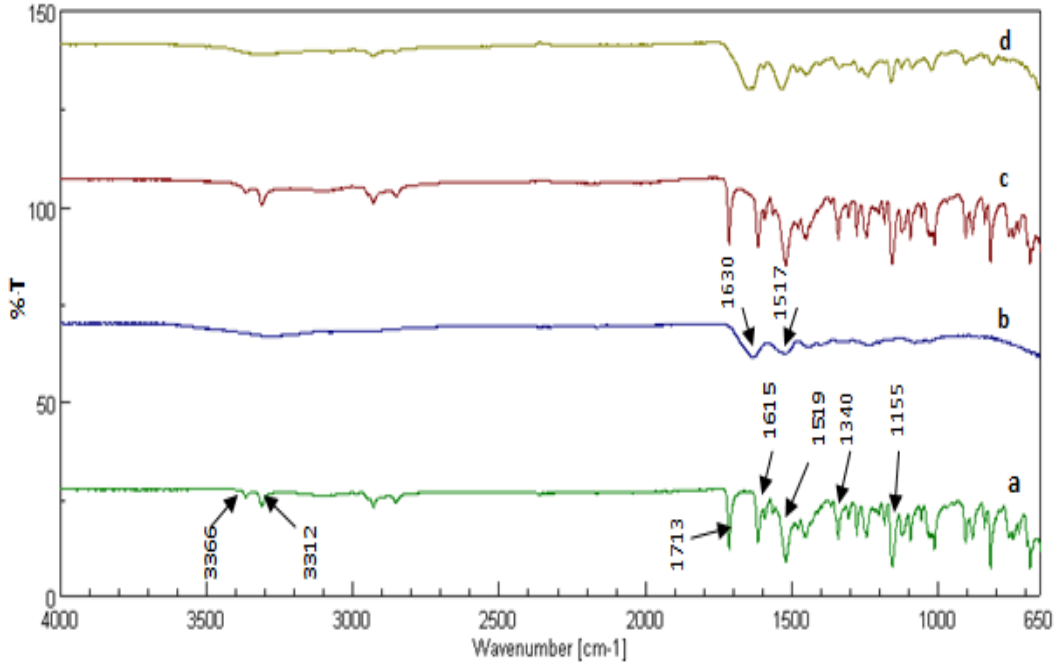

Figure 4.20: FT-IR of unprocessed glibenclamide (a), unprocessed gelatin (b), glibenclamide-gelatin physical mixture (c) and glibenclamide-gelatin lyophilised mixture (d).

Table 4.6: Wave numbers of FT-IR absorption bands where changes were detected in lyophilised glibenclamide-gelatin mixture, compared to unprocessed components

Wave number (cm^{-1})	Corresponding bond or functional group	Spectral change in lyophilised system
3366	Amide (glibenclamide)	Disappeared
3312	Amide (glibenclamide)	Disappeared
1713	Amide (glibenclamide)	Disappeared
1615	urea carbonyl (glibenclamide)	Disappeared
1519	urea carbonyl (glibenclamide)	Shift to 1532 cm^{-1} and broadening
1340	SO_2 (glibenclamide)	Decreased intensity and shift to 1338 cm^{-1}
1155	SO_2 (glibenclamide)	Decreased intensity and shift to 1160 cm^{-1}
1630	C=O (gelatin)	Shift to 1645 cm^{-1}
1517	N-H (gelatin)	Shift to 1532 cm^{-1}

4.4.2 Spironolactone

4.4.2.1 Lyophilised spironolactone

The physical states of the unprocessed and lyophilised spironolactone were investigated by DSC and their thermograms are illustrated in Figure 4.21. The unprocessed spironolactone exhibited a sharp melting endotherm at 208ºC which is in accordance with that reported in the literature (Dong et al., 2009). This melting temperature seems to be in agreement more closely with that of the polymorphic

form II (210ºC) of spironolactone than form I (205ºC) reported by Agafonov et al. (1991). On the other hand, the thermogram of the lyophilised drug showed an exothermic recrystallisation peak at 113ºC followed by melting endotherm at 208ºC. This finding points to the amorphous nature of the lyophilised spironolactone that recrystallised during the application of heat during the DSC analysis to the same crystalline structure of the unprocessed drug powder. It has been reported that spironolactone molecules can undergo structural rearrangement by the application of heat (Neville et al., 1994; Beakstead et al., 1993; Berbenni et al., 1999). Similar thermogram have been obtained by Hodges et al. (2006) who reported dissolution enhancement of spironolactone by lyophilisation due to transformation of the drug to an amorphous form.

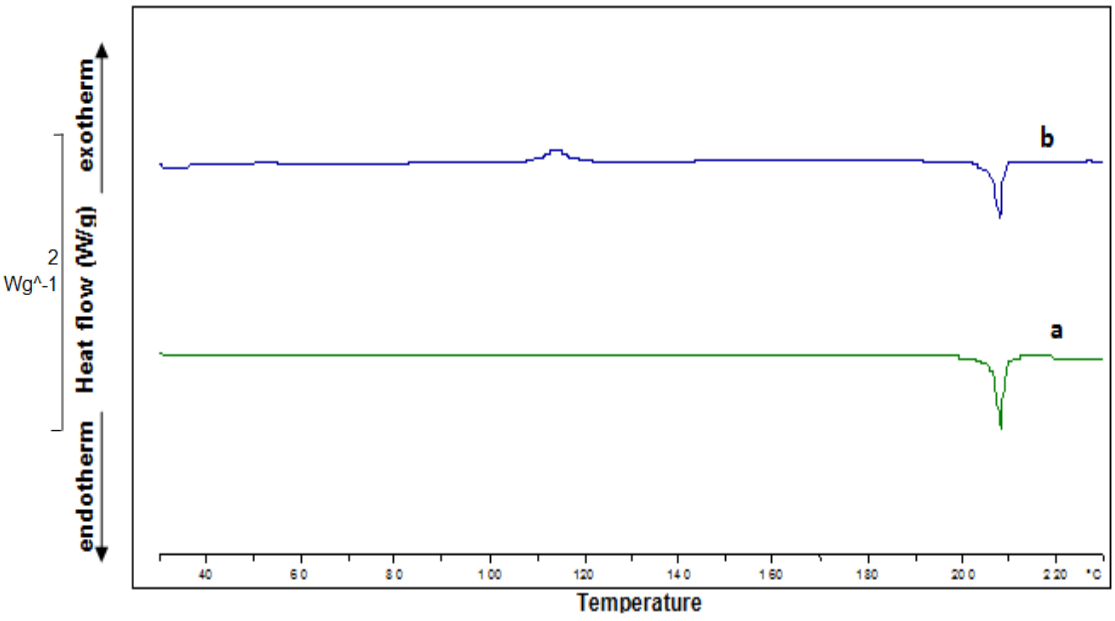

Figure 4.21: DSC of unprocessed spironolactone (a) and lyophilised spironolactone (b) powders.

The corresponding XRPD patterns are shown in Figure 4.22. The diffractogram of the unprocessed spironolactone contained numerous sharp peaks indicating high crystallinity of the drug which has been reported by Dong et al. (2010). In contrast, the diffractogram of the lyophilised drug showed the disappearance of its characteristic peaks and the appearance of a hump pattern. These data revealed that

spironolactone was transformed to an amorphous form by the lyophilisation process which was supported by the DSC results.

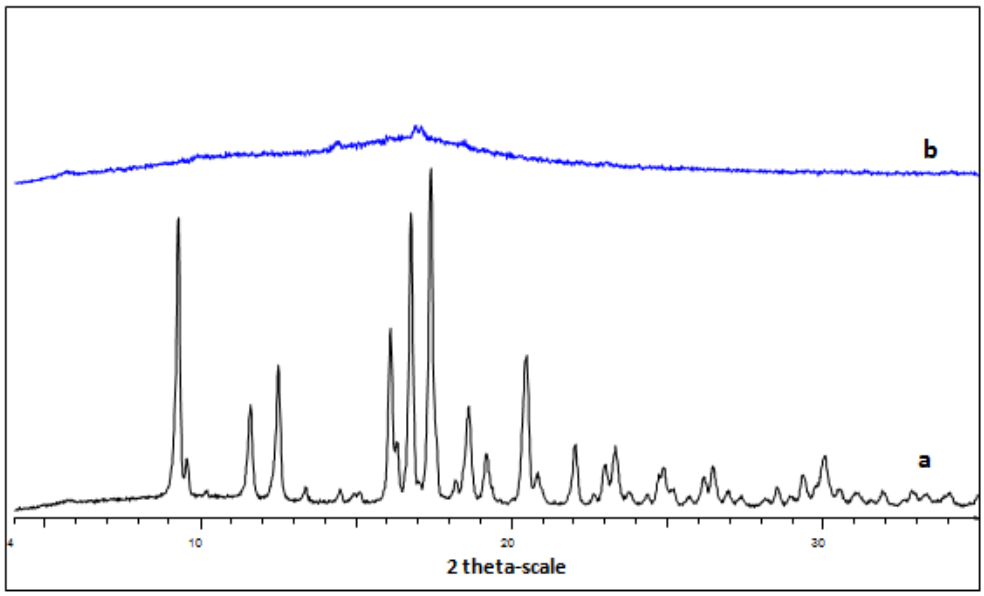

Figure 4.22: XRPD of unprocessed spironolactone (a) and lyophilised spironolactone (b) powders.

The corresponding FT-IR spectra are shown in Figure 4.23. The spectrum of the unprocessed spironolactone revealed the existence of four characteristic bands at 1764, 1689, 1672 and 1616 cm^{-1} corresponding to C=O stretching of the lactone ring; C=O stretching of the thioacetyl group; C=O stretching of the C_6-ring; and C=C stretching respectively (Rajabi et al., 2008). The changes in FT-IR spectrum of the lyophilised spironolactone are summarised in Table 4.7. Generally, the absorption peaks of the lyophilised drug appeared to be far less sharp than those of the unprocessed drug. These changes could be attributed to changes in the physical structure of spironolactone during lyophilisation process and formation of an amorphous form of the drug which was in accordance with the DSC and XRPD results.

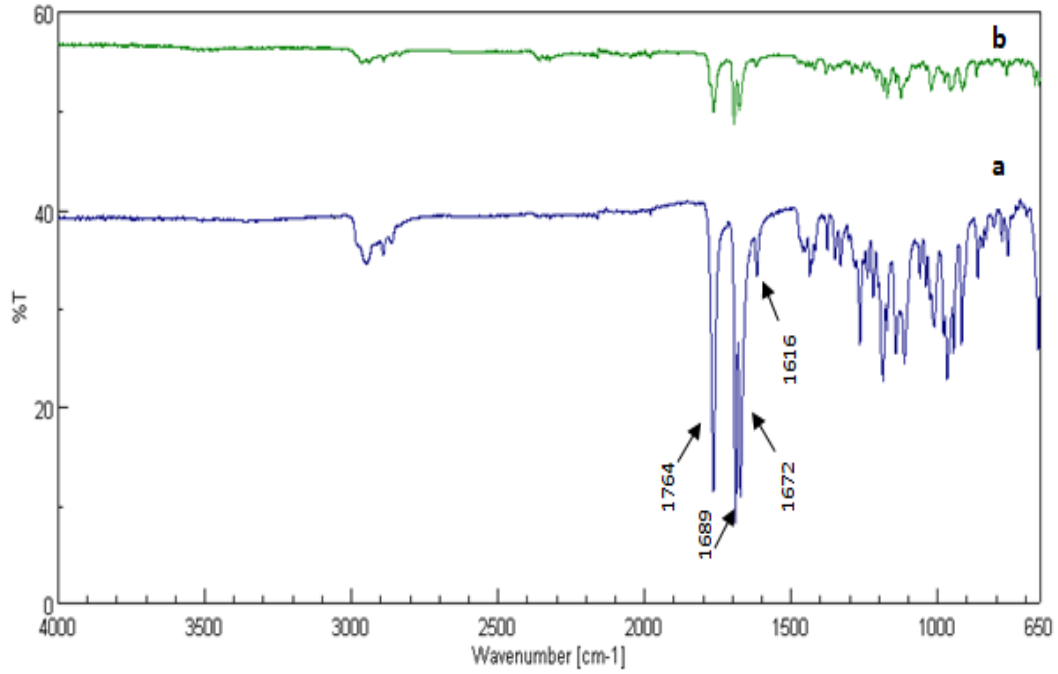

Figure 4.23: FTIR of unprocessed spironolactone (a) and lyophilised spironolactone (b) powders.

Table 4.7: Wave numbers of FT-IR absorption bands where differences were detected between unprocessed and lyophilised spironolactone

Wave number (cm^{-1})	Corresponding bond or functional group	Spectral change in lyophilised spironolactone
1764	C=O of lactone ring	Decreased intensity and insignificant shift to 1765 cm^{-1}
1689	C=O of thioacetyl group	Decreased intensity and insignificant shift to 1694 cm^{-1}
1672	C=O of C_6-ring	Decreased intensity and insignificant shift to 1676 cm^{-1}
1616	C=C	Decreased intensity and insignificant shift to 1619 cm^{-1}

4.4.2.2 Lyophilised spironolactone-mannitol mixture

The physical state of unprocessed spironolactone, mannitol, and their physical and lyophilised mixtures (67% w/w mannitol) were investigated by DSC and their thermograms are shown in Figure 4.24. Spironolactone showed a sharp melting endotherm at 208ºC whereas unprocessed mannitol exhibited a melting endotherm at 168ºC, which is characteristic for the β polymorph of mannitol (Izutsu et al., 2004).

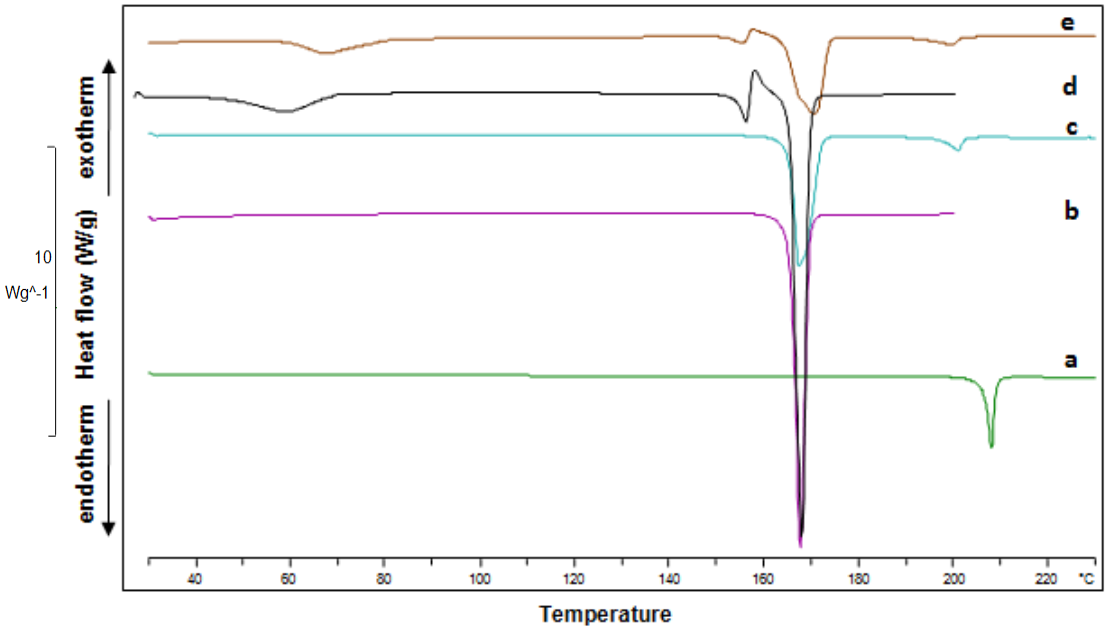

Figure 4.24: DSC of unprocessed spironolactone (a), unprocessed mannitol (b), spironolactone-mannitol physical mixture (c) lyophilised mannitol (d) and spironolactone-mannitol lyophilised mixture (e).

The thermogram of the physical mixture showed a shift of the spironolactone melting endotherm to 201ºC, while the melting endotherm of mannitol was maintained at 168ºC. In addition, the intensity of both melting endotherms was decreased. The shift in the drug melting endotherm could be due to the mixing process that decreases the purity of the drug in the mixture and may not necessarily suggest drug/excipient interaction. The reduction in the intensity of the peaks might be attributed to disturbance in the crystalline structures of both the drug and excipient or due to the decrease in their concentrations in the physical mixture. The thermogram of the

lyophilised mixture demonstrated broadening and severe reduction in the intensity of the spironolactone melting endotherm suggesting transformation of the majority of the drug to an amorphous form. The melting endotherms of spironolactone and mannitol shifted to 201ºC and 170ºC respectively suggesting drug-excipient interactions. The shift in the melting endotherm of spironolactone may also suggest transformation of spironolactone to another polymorphic form (form I, see Section 4.4.2.1). The thermogram also showed an endotherm at 156ºC, followed by exotherm at 159ºC corresponding to mannitol thermal transition that has been discussed in Section 4.4.1.2. A broad, shallow endotherm was observed in the temperature range 58-80ºC representing removal of residual moisture or dehydration of mannitol hydrate that might be produced during lyophilisation (Nunes et al., 2004). This finding is supported by the appearance of the same endotherm in the thermogram of the lyophilised mannitol.

The corresponding XRPD patterns are compared in Figure 4.25. The diffractograms of unprocessed drug and excipient revealed their crystalline nature as evidenced by numerous diffraction peaks.

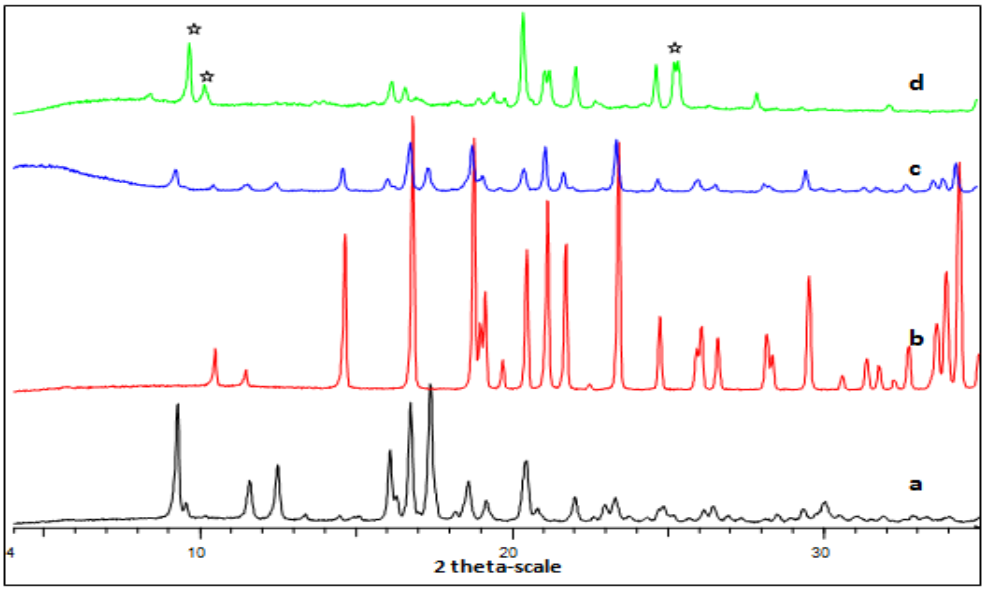

Figure 4.25: XRPD of unprocessed spironolactone (a), unprocessed mannitol (b), spironolactone-mannitol physical mixture (c) and spironolactone-mannitol lyophilised mixture (d) (* highlights new peaks).

The diffractogram of the physical mixture displayed the characteristic peaks of both spironolactone and mannitol with decreased intensity due to dilution effect upon mixing. The diffractogram of the lyophilised mixture showed the disappearance of the characteristic peaks of spironolactone. Supporting the DSC results, this was attributed to transformation of the drug to an amorphous form. Also, new diffraction peaks were observed (highlighted by * in Figure 4.25) at 9.7º, 10.1º and 25.2º 2θ. The peak at 9.7º 2θ has been reported to be characteristic for the δ polymorph of mannitol (Hawe & Frieß, 2006) while the others may present another spironolactone polymorphic form. The absence of the characteristic peak at 19.7º 2θ omits the possibility of presence of mannitol hydrate (Hawe & Frieß, 2006) as suggested by the DSC results.

The corresponding FT-IR spectra are illustrated in Figure 4.26. The characteristic absorption bands of unprocessed mannitol and spironolactone were previously discussed in Sections 4.4.1.2 and 4.4.2.1.

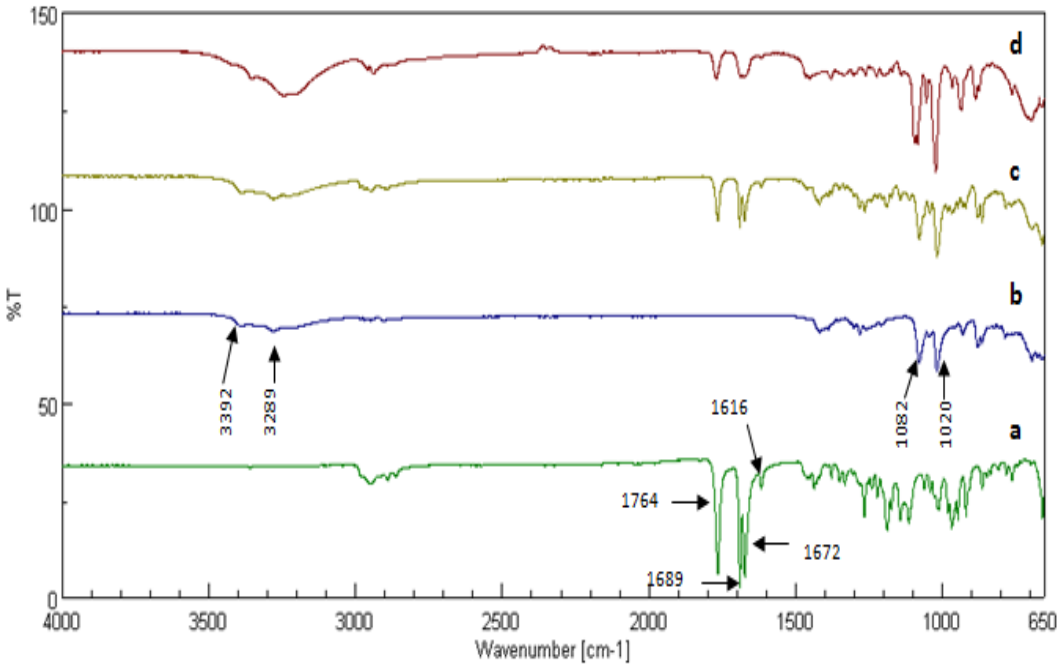

Figure 4.26: FT-IR of unprocessed spironolactone (a), unprocessed mannitol (b), spironolactone-mannitol physical mixture (c) and spironolactone-mannitol lyophilised mixture (d) (* highlights new peaks).

The spectrum of the physical mixture seemed to be equivalent to the addition spectra of spironolactone and mannitol. Noticeable differences in FT-IR spectrum of the lyophilised mixture were observed and these are summarised in Table 4.8. A broad absorption band was observed in the range 3000-3600 cm^{-1} (OH stretching vibrations of water) highlighting interaction with water which was supported by the appearance of a broad endothermic peak in the DSC thermogram in the temperature range 58-80^{o}C representing a dehydration step. These observed changes suggest the incidence of intermolecular hydrogen bonding between the drug and the excipient as supported by the DSC results. The possible interaction could occur between carbonyl groups of the drug and hydroxyl groups of the excipient. Similar interactions have been reported between mannitol and a model of poorly water-soluble drug, 2, 6-dimethyl-8-(2-ethyl-6-methylbenzylamino)-3-hydroxymethylimidazo-[1, 2-a] pyridi-nemesylate, in the solid dispersion of the drug in mannitol (Juppo et al., 2003).

Table 4.8: Wave numbers of FT-IR absorption bands where changes were detected in lyophilised spironolactone-mannitol mixture, compared to unprocessed components

Wave number (cm^{-1})	Corresponding bond or functional group	Spectral change in lyophilised system
1764	C=O of lactone ring (spironolactone)	Decreased intensity , broadening and shift to 1770 cm^{-1}
1689	C=O of thioacetyl group (spironolactone)	Decreased intensity , broadening and shift to 1686 cm^{-1}
1672	C=O of C_6-ring (spironolactone)	Disappeared or merged with the peak at 1686 cm^{-1}
1616	C=C (spironolactone)	Disappeared
3289	OH (mannitol)	Disappeared
1082	C-O (mannitol)	Split and insignificant shift to 1083 cm^{-1}
1020	C-O (mannitol)	Insignificant shift to 1022 cm^{-1}

4.4.2.3 Lyophilised spironolactone-SLS mixture

The thermal behaviour of unprocessed spironolactone, SLS, and their physical and lyophilised mixtures (67% w/w SLS) are shown in Figure 4.27. The melting endotherms of spironolactone and SLS were observed at 208ºC and 199ºC respectively. The thermogram of the physical mixture demonstrated broadening and shift in both spironolactone and SLS melting endotherms to 204ºC and 193ºC respectively. This shift suggests the presence of solid-state interaction between the drug and the excipient. On the other hand, the decreased intensity and sharpness of peaks might be attributed to disturbance in the crystalline structures of both the drug and excipient in the physical mixture or due to dilution effect.

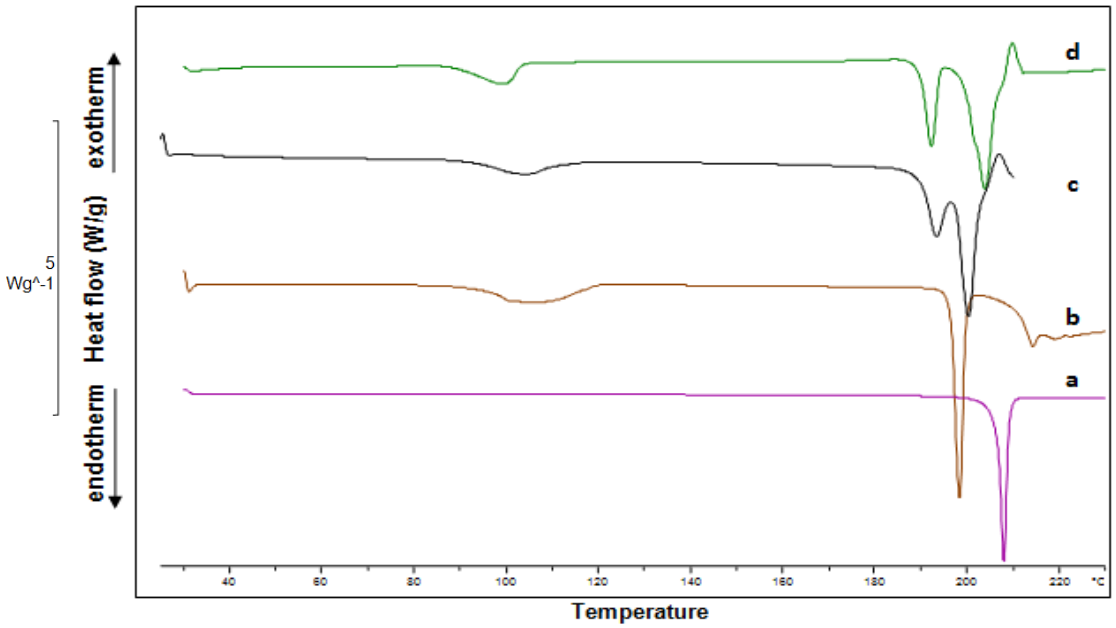

Figure 4.27: DSC of unprocessed spironolactone (a), unprocessed SLS (b), spironolactone-SLS physical mixture (c) and spironolactone-SLS lyophilised mixture (d).

The thermogram of the lyophilised mixture exhibited similar behaviour to that of the physical mixture. The spironolactone and SLS melting endotherms shifted to 204ºC and 192ºC respectively. This is explained on the basis of drug-excipient interactions. Similar interaction between SLS and diazepam in their solid dispersion has been

reported by Waard et al. (2008). Furthermore, the endothermic shift was accompanied with a decrease in the intensity and broadening of the melting endotherms of spironolactone and SLS. This might be attributable to partial transformation of spironolactone and SLS to amorphous forms in their solid dispersion. The maintenance of the melting endotherm of spironolactone in the DSC thermogram of the lyophilised mixture contradicted the following XRPD results that showed the disappearance of all the characteristic peaks of spironolactone. This finding suggests that the heat introduced during DSC analysis may initiate molecular rearrangement of the drug molecules and recrystallisation of its amorphous form (see Sections 3.4.2.2 and 4.4.2.1).

The corresponding XRPD patterns are illustrated in Figure 4.28. The diffractograms of unprocessed spironolactone and SLS displayed the high crystalline nature of the drug and the excipient as indicated by numerous distinctive peaks. The diffractogram of the physical mixture showed dramatic reduction in the intensity of the characteristic peaks of spironolactone and SLS as a result of dilution effect in the mixture.

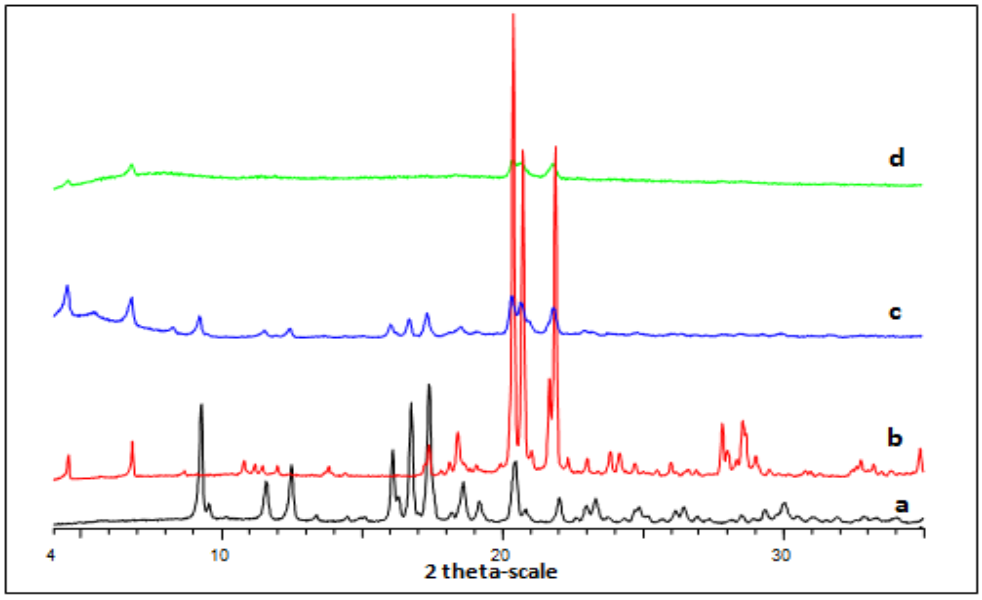

Figure 4.28: XRPD of unprocessed spironolactone (a), unprocessed SLS (b), spironolactone-SLS physical mixture (c) and spironolactone-SLS lyophilised mixture (d).

The diffractogram of the lyophilised mixture showed the disappearance of most of the characteristic peaks of SLS suggesting partial transformation to an amorphous form. In addition, the diffractogram lacked all the characteristic peaks of spironolactone suggesting the formation of an amorphous form of the drug in the SLS matrix. This finding is most probably the main factor of the dissolution rate enhancement observed for spironolactone from its lyophilised mixture with SLS (Section 3.4.2.9).

The corresponding FT-IR spectra are shown in Figure 4.29. The absorption bands of unprocessed spironolactone and SLS were previously discussed in Sections 4.4.2.1 and 4.4.2.3. The spectrum of the physical mixture displayed all the characteristic peaks of spironolactone and SLS with apparent reduction in the intensity as a result of dilution effect.

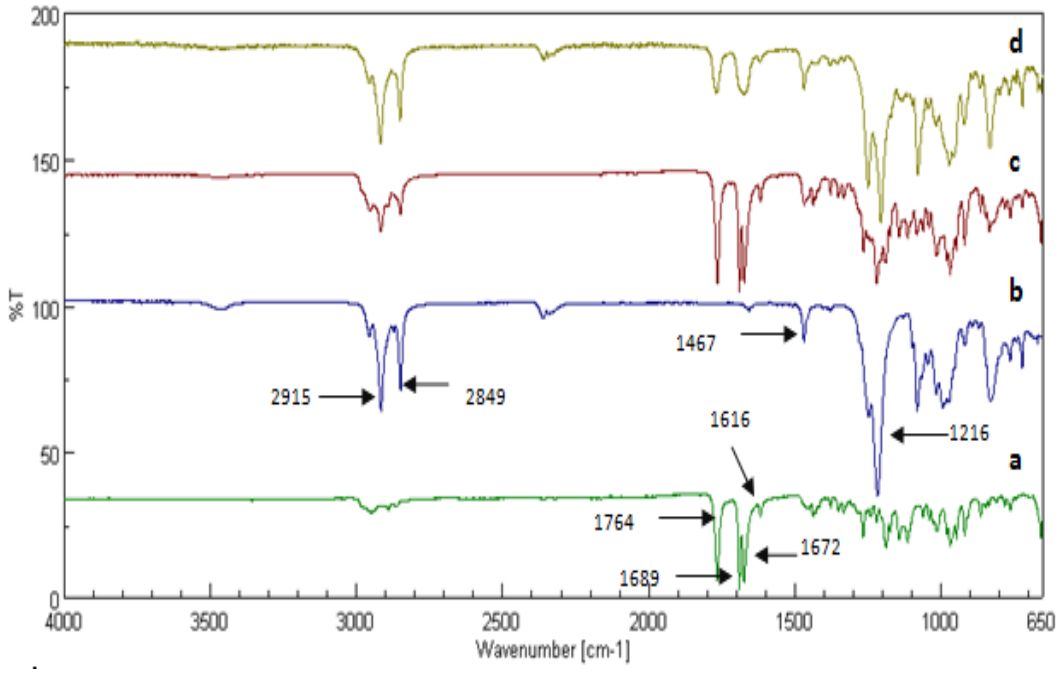

Figure 4.29: FT-IR of unprocessed spironolactone (a), unprocessed SLS (b), spironolactone-SLS physical mixture (c) and spironolactone-SLS lyophilised mixture (d).

Noticeable differences in FT-IR spectrum of the lyophilised mixture were observed and these are summarised in Table 4.9. These changes suggest incidence of interactions between spironolactone and SLS. The possible interactions are hydrogen bonding between the proton acceptors; carbonyl groups of the drug and CH_2-O group of SLS.

Table 4.9: Wave numbers of FT-IR absorption bands where changes were detected in lyophilised spironolactone-SLS mixture, compared to unprocessed components

Wave number (cm^{-1})	Corresponding bond or functional group	Spectral change in lyophilised system
1764	C=O of lactone ring (spironolactone)	Decreased intensity , broadening and shift to 1767 cm^{-1}
1689	C=O of thioacetyl group (spironolactone)	Disappeared or merged with the peak at 1672 cm^{-1}
1672	C=O of C_6-ring (spironolactone)	Decreased intensity , broadening and shift to 1674 cm^{-1}
1616	C=C (spironolactone)	Decreased intensity
1216	C-O (SLS)	Shift to 1204 cm^{-1} and icreased intensity of the shoulder
1080	S=O (SLS)	shift to 1078 cm^{-1}

4.4.2.4 Lyophilised spironolactone-PEG 6000 mixture

The DSC thermograms of unprocessed spironolactone, PEG 6000, and their physical and lyophilised mixtures (67% w/w PEG 6000) are shown in Figure 4.30. While spironolactone exhibited its melting endotherm at 208ºC, the endothermic peak corresponding to the PEG 6000 melting point appeared at 64ºC. The thermograms of the physical and lyophilised mixtures exhibited disappearance of the spironolactone melting endotherm. This may be attributed to dissolution of spironolactone in the

PEG 6000 melt during the DSC analysis before reaching its melting temperature. This finding is in agreement with Asyarie and Rashmawati (2007) and Yamashita et al. (2003). The thermogram of the physical mixture showed one endotherm at 64ºC corresponding to the fusion temperature of PEG 6000. On the other hand, the melting temperature of PEG was displayed at 56ºC in the case of the lyophilised mixture. This can be explained on the basis of transformation of the polymer to a different crystal form during lyophilisation process. Depression of the melting temperature of the polymer as a result of solid dispersion formation with the drug during the lyophilisation process is another possible explanation. Similar results have been reported by Wang et al. (2004) who found that the melting temperature of PEG 6000 in its solid dispersion with 80% w/w itraconazole was not around 63ºC, but at 58ºC.

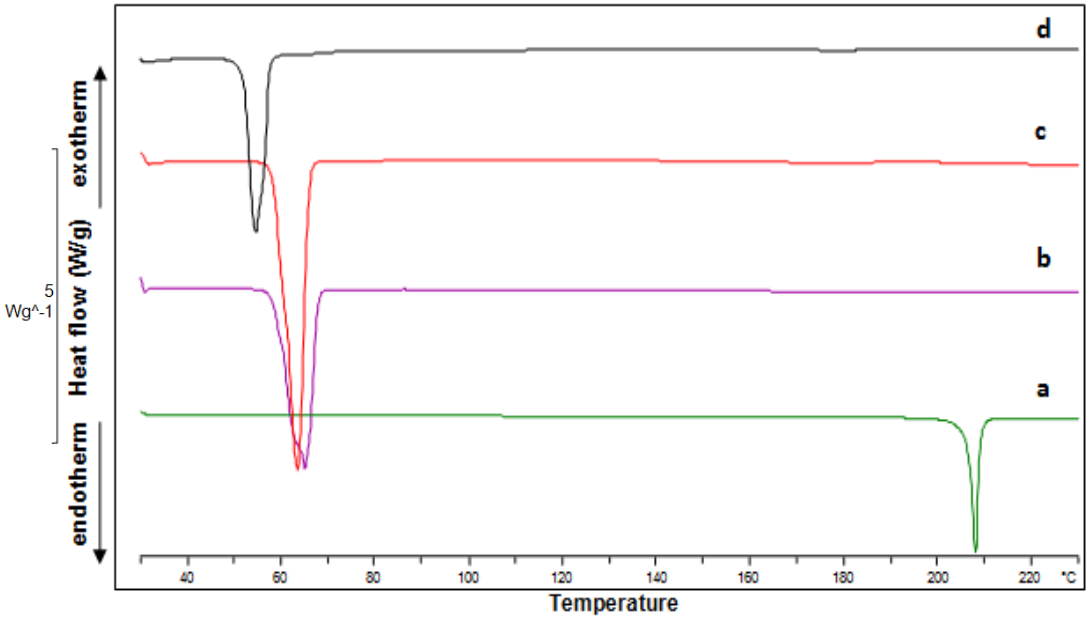

Figure 4.30: DSC of unprocessed spironolactone (a), unprocessed PEG 6000 (b), spironolactone-PEG 6000 physical mixture (c) and spironolactone-PEG 6000 lyophilised mixture (d).

The corresponding XRPD patterns are compared in Figure 4.31. The diffractogram of unprocessed spironolactone and PEG 6000 reflected their crystalline nature (see

Sections 4.4.2.1 and 4.4.1.4). The diffractogram of the physical mixture is equivalent to the addition pattern of the drug and the polymer with decreased intensity of their characteristic peaks due to decreased concentration of the drug and excipient in the mixture. On the other hand, the diffractogram of the lyophilised mixture exhibited complete disappearance of all spironolactone XRPD peaks and severe reduction in the intensity of the characteristic diffraction peaks of PEG 6000. This finding suggests the transformation of the drug and the majority of the polymer to an amorphous form in the solid dispersion produced during the lyophilisation process.

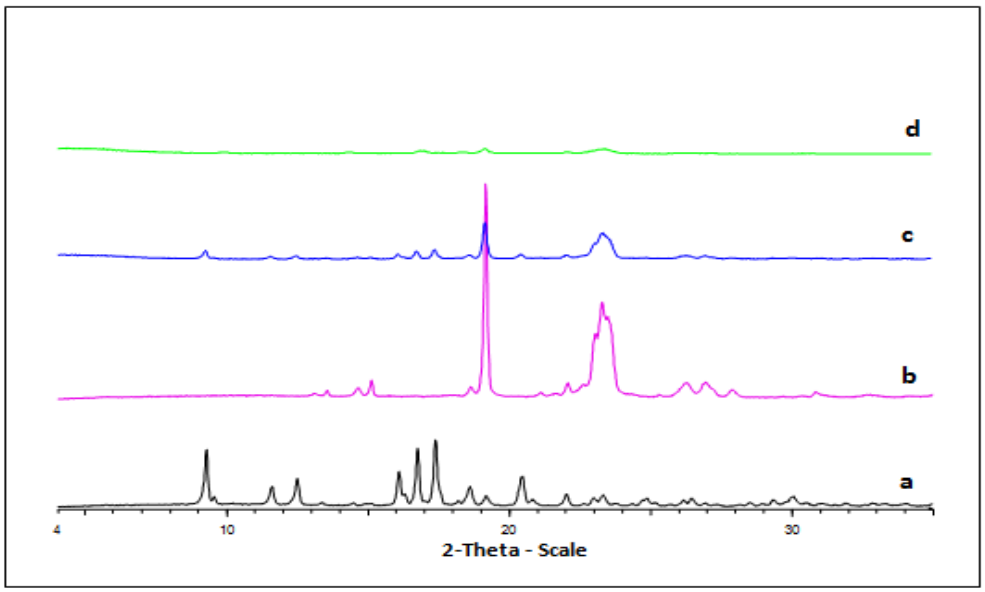

Figure 4.31: XRPD of unprocessed spironolactone (a), unprocessed PEG 6000 (b), spironolactone-PEG 6000 physical mixture (c) and spironolactone-PEG 6000 lyophilised mixture (d).

The corresponding FT-IR spectra are shown in Figure 4.32. The absorption bands of unprocessed spironolactone and PEG 6000 were discussed in Sections 4.4.2.1 and 4.4.1.4. The spectrum of the physical mixture displayed all the characteristic peaks of the drug and the polymer. Noticeable differences in FT-IR spectrum of the lyophilised mixture were observed and these are summarised in Table 4.10. These

changes suggest the incidence of strong interactions between spironolactone and PEG 6000 in the produced solid dispersion. The possible interactions are intermolecular hydrogen bonding between carbonyl groups of spironolactone and hydroxyl groups of PEG 6000. This finding is in a good agreement with Waghmare et al. (2008) who reported incidence of interactions between PEG 6000 and zaleplon in their solid dispersion. However, it is obvious that the spectrum of the lyophilised mixture is smoothened highlighting formation of an amorphous form of spironolactone which supports the XRPD results.

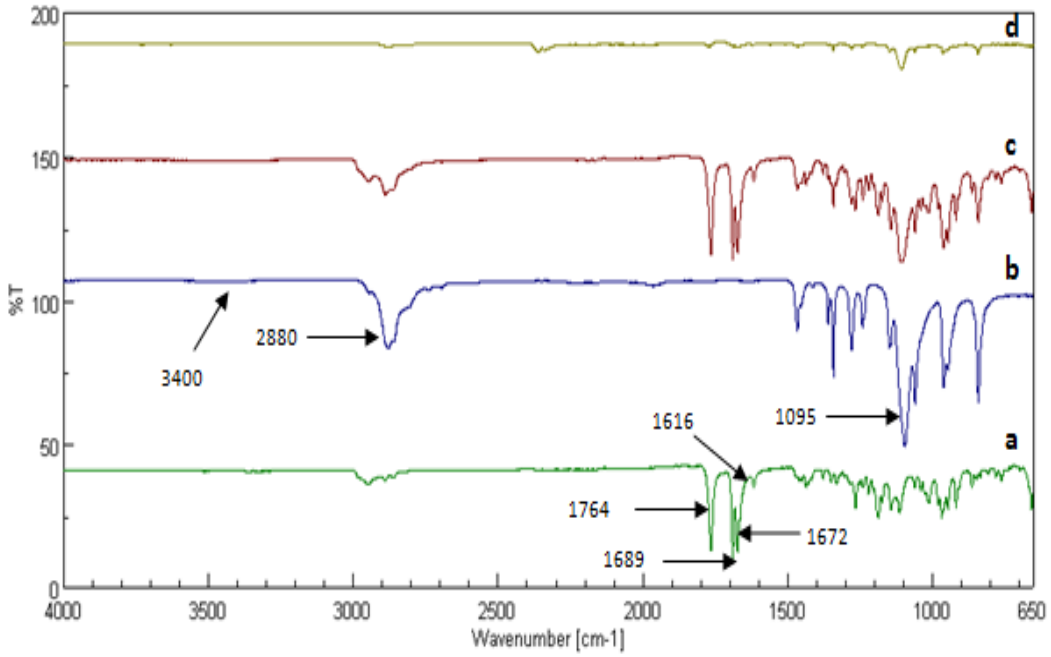

Figure 4.32: FT-IR of unprocessed spironolactone (a), unprocessed PEG 6000 (b), spironolactone-PEG 6000 physical mixture (c) and spironolactone-PEG 6000 lyophilised mixture (d).

Table 4.10: Wave numbers of FT-IR absorption bands where changes were detected in lyophilised spironolactone-PEG 6000 mixture, compared to unprocessed components

Wave number (cm^{-1})	Corresponding bond or functional group	Spectral change in lyophilised system
1764	C=O of lactone ring (spironolactone)	Disappeared
1689	C=O of thioacetyl group (spironolactone)	Disappeared
1672	C=O of C_6-ring (spironolactone)	Disappeared
1616	C=C (spironolactone)	Disappeared
3400	OH (PEG 6000)	Disappeared
2880	C-H (PEG 6000)	Disappeared
1095	C-O (PEG 6000)	Shift to 1106 cm^{-1}

4.4.2.5 Lyophilised spironolactone-citric acid mixture

The DSC thermograms of unprocessed spironolactone, citric acid, and their physical and lyophilised mixtures (55% w/w citric acid) are shown in Figure 4.33. Citric acid exhibited a sharp endotherm at 157ºC corresponding to its melting temperature. The thermogram of the physical mixture exhibited disappearance of spironolactone melting peak. This is most likely due to dissolution of the drug crystals in the melt of the excipient before reaching its fusion temperature. On the other hand, the citric acid melting endotherm was maintained in the thermogram although it was broader, less sharp and less intense compared to that of the unprocessed powder. This may be attributed to disturbance of the excipient crystalline structure during preparation of the physical mixture. Similarly, the thermogram of the lyophilised mixture lacked the melting endotherm of spironolactone whilst it displayed that of citric acid which

was dramatically reduced in intensity, broadened and shifted to 150ºC. These results suggest transformation of the mixture components to amorphous forms in the produced solid dispersion as well as possible drug-excipient interactions. Kadoya et al. (2008) have reported similar results for the lyophilised binary system of citric acid and 1,3-diamino-2-hydroxy-propane as it showed amorphous component and strong interactions between the drug and citric acid.

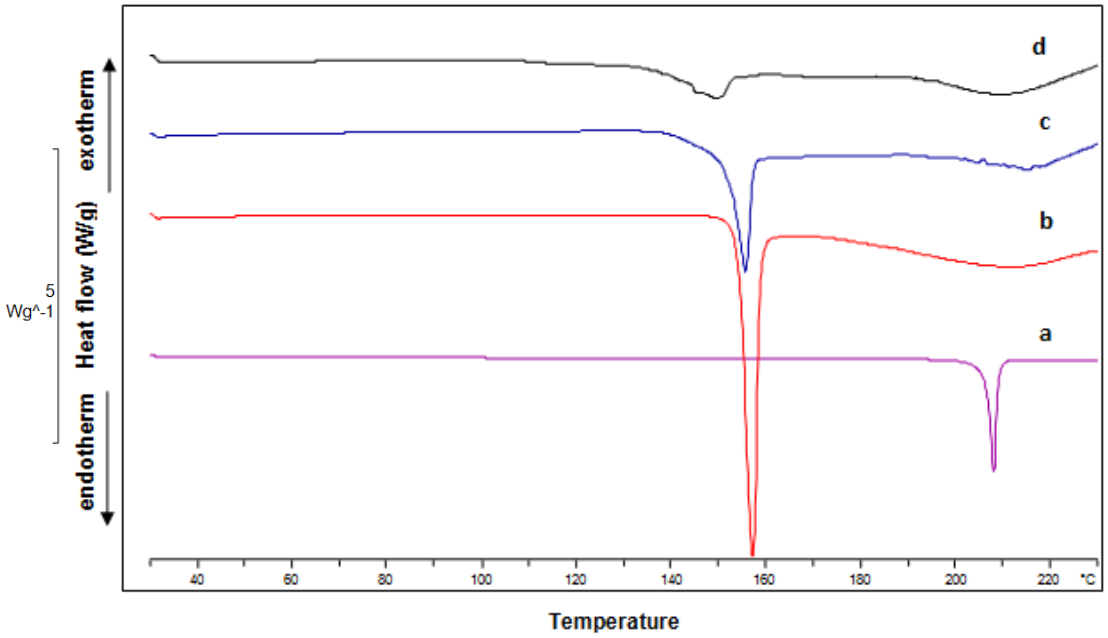

Figure 4.33: DSC of unprocessed spironolactone (a), unprocessed citric acid (b), spironolactone-citric acid physical mixture (c) and spironolactone-citric acid lyophilised mixture (d)

The corresponding XRPD patterns are compared in Figure 4.34. The diffratogrames of unprocessed spironolactone and citric acid reflected their crystalline nature as indicated by numerous distinctive peaks. The diffractogram of the physical mixture showed traces of spironolactone peaks in the XRPD pattern but lacked almost all the XRPD peaks of citric acid. This might be attributed to dilution effect and decreased crystallinity of the components in the physical mixture. On the other hand, the diffraction pattern of the lyophilised mixture exhibited complete disappearance of all spironolactone and citric acid XRPD peaks and the appearance of a halo pattern that

is characteristic for amorphous state. This finding confirms the complete transformation of spironolactone and citric acid to an amorphous form in the solid dispersion produced during the lyophilisation process which was supported by the DSC results.

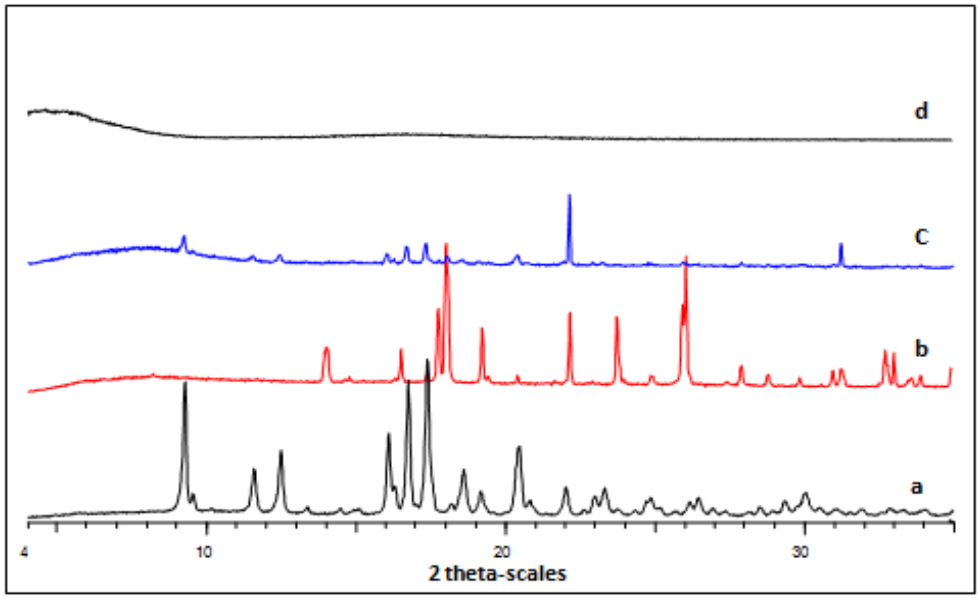

Figure 4.34: XRPD of unprocessed spironolactone (a), unprocessed citric acid (b), spironolactone-citric acid physical mixture (c) and spironolactone-citric acid lyophilised mixture (d)

The corresponding FT-IR spectra are shown in Figure 4.35. The absorption bands of unprocessed spironolactone were discussed in Section 4.4.2.1. The spectrum of citric acid showed characteristic absorption bands of O-H stretching vibrations of carboxylic acid at 3492 and 3282 cm^{-1} and C=O stretching vibrations at 1740 and 1690 cm^{-1} (Hoppu et al., 2007). The spectrum of the physical mixture showed all the characteristic peaks of spironolactone whilst it exhibited disappearance of the characteristic peaks of citric acid at 3492 and 3282 cm^{-1}. In addition, the characteristic peak of citric acid at 1740 cm^{-1} vanished and that at 1690 cm^{-1} disappeared or overlapped spironolactone absorption bands at 1689 cm^{-1}. This may be attributable to drug-excipient interactions such as hydrogen bonding during

preparation of the physical mixture. On the other hand, noticeable differences in FT-IR spectrum of the lyophilised mixture were observed and these are summarised in Table 4.11.

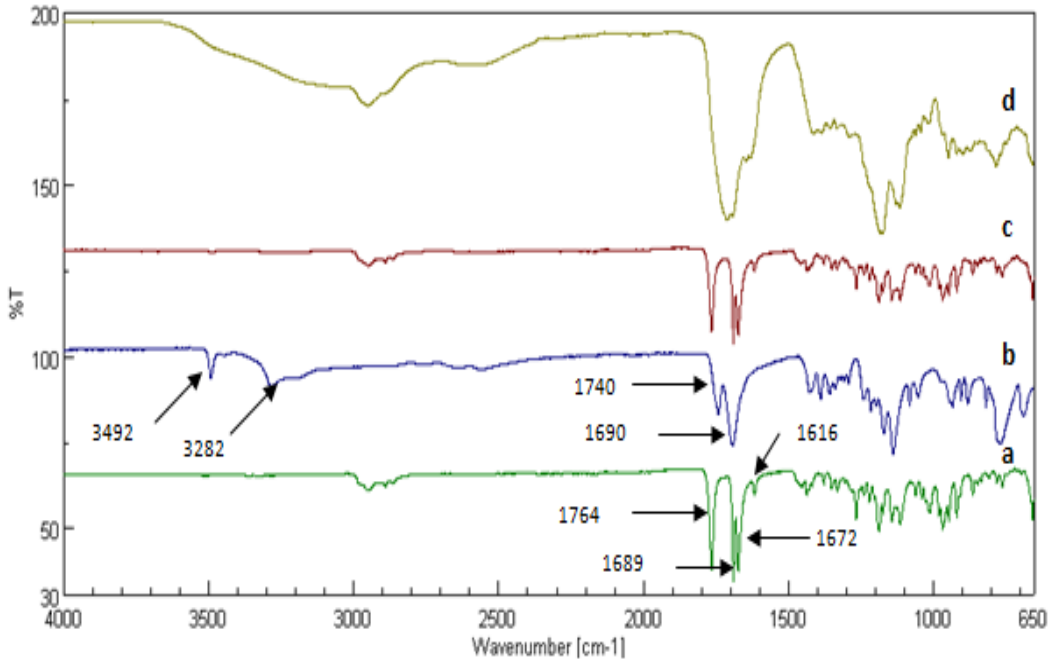

Figure 4.35: FT-IR of unprocessed spironolactone (a), unprocessed citric acid (b), spironolactone-citric acid physical mixture (c) and spironolactone-citric acid lyophilised mixture (d).

The spectrum of the lyophilised mixture showed that the absorption bands in the range 1616-1764 cm^{-1} merged into a broad band at 1713 cm^{-1} with no obvious peaks. Similar performance was observed at the band region around 1200 cm^{-1}, where all the peaks had merged into a single broad forked band. These changes suggest strong drug-excipient interactions in the solid dispersion produced during the lyophilisation process and support the DSC and XRPD results. These changes in the spectrum of the lyophilised mixture are in agreement with the changes in the FT-IR spectrum of the melt-quenched blend of paracetamol and citric acid investigated by Hoppu et al. (2007). The possible interactions could be intermolecular hydrogen bonding between the carbonyl groups of spironolactone and OH or COOH groups of

citric acid. In addition, the spectrum of the lyophilised mixture showed a very broad peak in the region 2400-3700 cm^{-1}. This peak points to high residual water and it is typical for amorphous solids and considered as evidence of interaction with water which suggests the high hygroscopicity of the amorphous solid dispersion formed during the lyophilisation process. Similar absorption band has been obtained by Laitinen et al. (2009) in the FT-IR spectrum of the amorphous form of perphenazine produced by lyophilisation process. Similarly, it has been reported that the lyophilised binary system of citric acid and 1,3-diamino-2-hydroxy-propane had a relatively high residual water (Kadoya et al., 2008).

Table 4.11: Wave numbers of FT-IR absorption bands where changes were detected in lyophilised spironolactone-citric acid mixture, compared to unprocessed components

Wave number (cm^{-1})	Corresponding bond or functional group	Spectral change in lyophilised system
1764	C=O of lactone ring (spironolactone)	Merged with other peaks in the vicinity
1689	C=O of thioacetyl group (spironolactone)	Merged with other peaks in the vicinity
1672	C=O of C_6-ring (spironolactone)	Merged with other peaks in the vicinity
1616	C=C (spironolactone)	Merged with other peaks in the vicinity
3492	O-H (citric acid)	Disappeared
3282	O-H (citric acid)	Disappeared
1740	C=O (citric acid)	Merged with other peaks in the vicinity
1690	C=O (citric acid	Merged with other peaks in the vicinity

From the above results that confirmed the formation of an amorphous solid dispersion of spironolactone and citric acid, it was expected that the dissolution rate of the drug from this solid dispersion is enhanced. In contrast, the spironolactone dissolution exhibited marked retardation compared to that of the physical mixture, unprocessed drug, and commercial tablets. As discussed in Section 3.4.2.11 and supported by the above discussion, this was attributed to the high hygroscopicity of the lyophilised system that absorbed water and consequently transformed into a clump that sank to the bottom of the dissolution flask where it remained intact over the experimental period.

4.4.2.6 Lyophilised spironolactone-fumaric acid mixture

The DSC thermograms of unprocessed spironolactone, fumaric acid, and their physical and lyophilised mixtures (74% w/w fumaric acid) are shown in Figure 4.36. The thermogram of fumaric acid displayed an endotherm at 291ºC corresponding to its melting temperature. It also showed another small endotherm at 205ºC, corresponding to transformation of prismatic fumaric acid to monoclinic fumaric acid, after which fumaric acid starts to sublime (Temesvàri et al., 1971). The thermal behaviour of the physical mixture demonstrated shift of the melting endotherms of spironolactone and fumaric acid to 183ºC and 275ºC respectively as well as reduction in their intensities. The observed shift could be attributed to the mixing process or it may suggest intensive solid-state interactions between the drug and the excipient in the the physical mixture. The observed reduction in the intensity of the melting endotherms might be due to disturbance in the crystalline structure of the drug and the excipient during preparation of the physical mixture. The thermogram of the lyophilised mixture showed similar performance to that of the physical mixture with further shift of the spironolactone and fumaric acid melting endotherms to 181ºC and 269ºC respectively suggesting strong interactions between the drug and the excipient. Also, the intensity of the spironolactone melting peak was dramatically reduced compared to its corresponding peak in the physical mixture. This finding suggests the transformation of the majority of the drug to an amorphous form during the lyophilisation process.

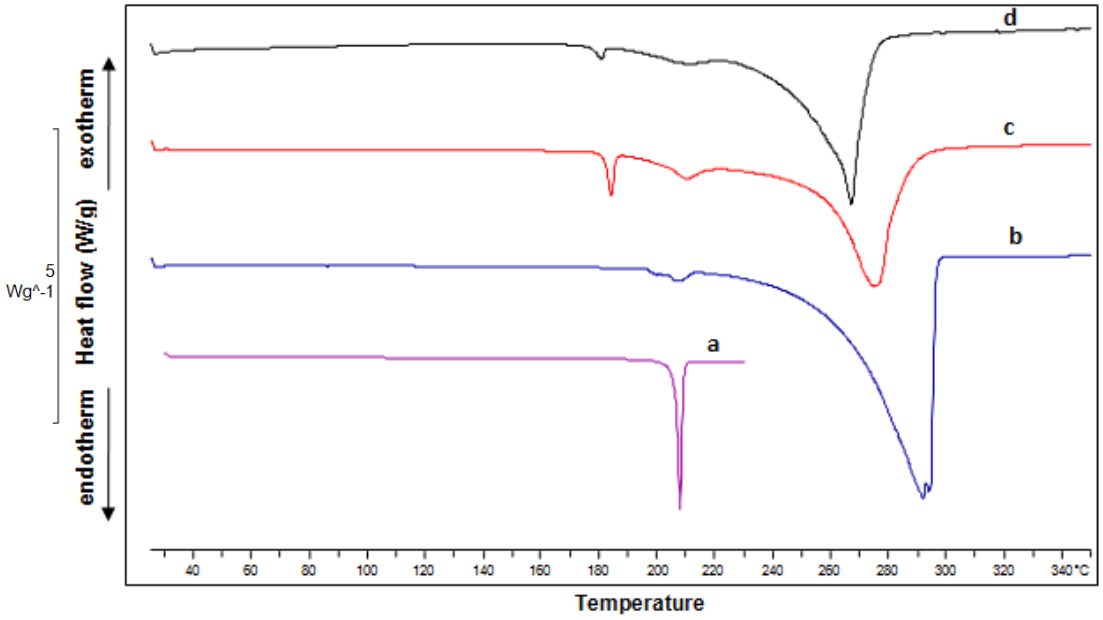

Figure 4.36: DSC of unprocessed spironolactone (a), unprocessed fumaric acid (b), spironolactone-fumaric acid physical mixture (c) and spironolactone-fumaric acid lyophilised mixture (d).

The corresponding XRPD patterns are compared in Figure 4.37. The diffratograms of unprocessed spironolactone and fumaric acid reflected their crystalline nature as indicated by numerous distinctive peaks. The diffraction pattern of the physical mixture presented the addition pattern of the drug and the excipient with apparent reduction in the intensity of the peaks due to dilution effect in the physical mixture. On the other hand, the diffraction pattern of the lyophilised mixture exhibited disappearance of all spironolactone XRPD peaks and most of the excipient peaks. This finding suggests the transformation of spironolactone and the majority of fumaric acid to amorphous forms in the solid dispersion produced during the lyophilisation process which was supported by the DSC results.

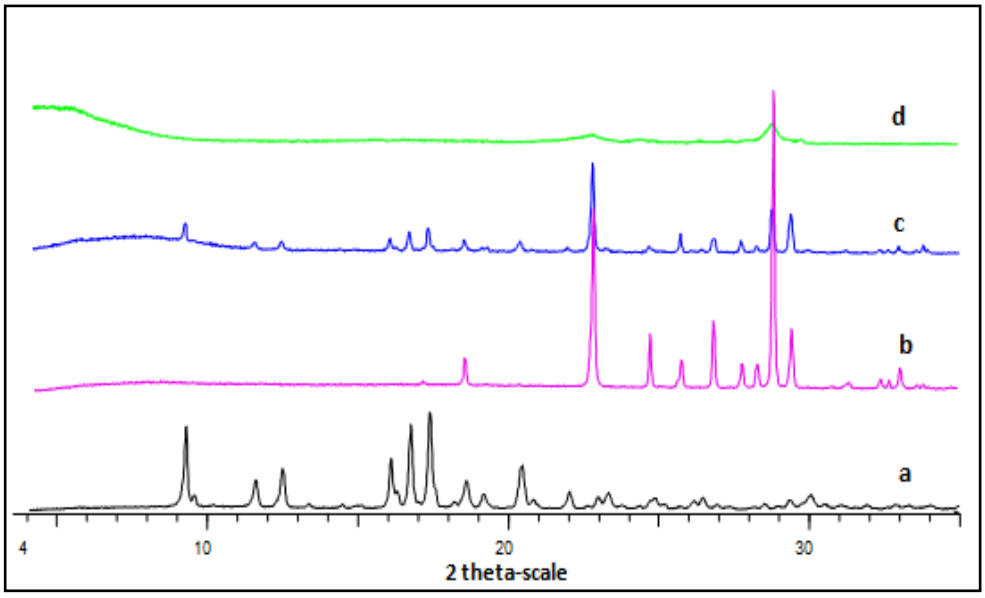

Figure 4.37: XRPD of unprocessed spironolactone (a), unprocessed fumaric acid (b), spironolactone-fumaric acid physical mixture (c) and spironolactone-fumaric acid lyophilised mixture (d).

The corresponding FT-IR spectra are shown in Figure 4.38. The spectrum of the unprocessed spironolactone was previously discussed in Section 4.4.2.1. The spectrum of fumaric acid showed characteristic OH (carboxylic acid) streching vibrations around 3000 cm^{-1} and C=O stretching vibrations at 1653 cm^{-1}. The spectrum of the physical mixture showed all the characteristic absorption bands of spironolactone whilst it exhibited disappearance of the characteristic peak of fumaric acid at 1653 cm^{-1} which might be overlapped with the drug peaks. On the other hand, noticeable differences in FT-IR spectrum of the lyophilised mixture were observed and these are summarised in Table 4.12. These changes may be attributed to intensive drug-excipient interactions such as intermolecular hydrogen bonding which were supported by the DSC and XRPD results.

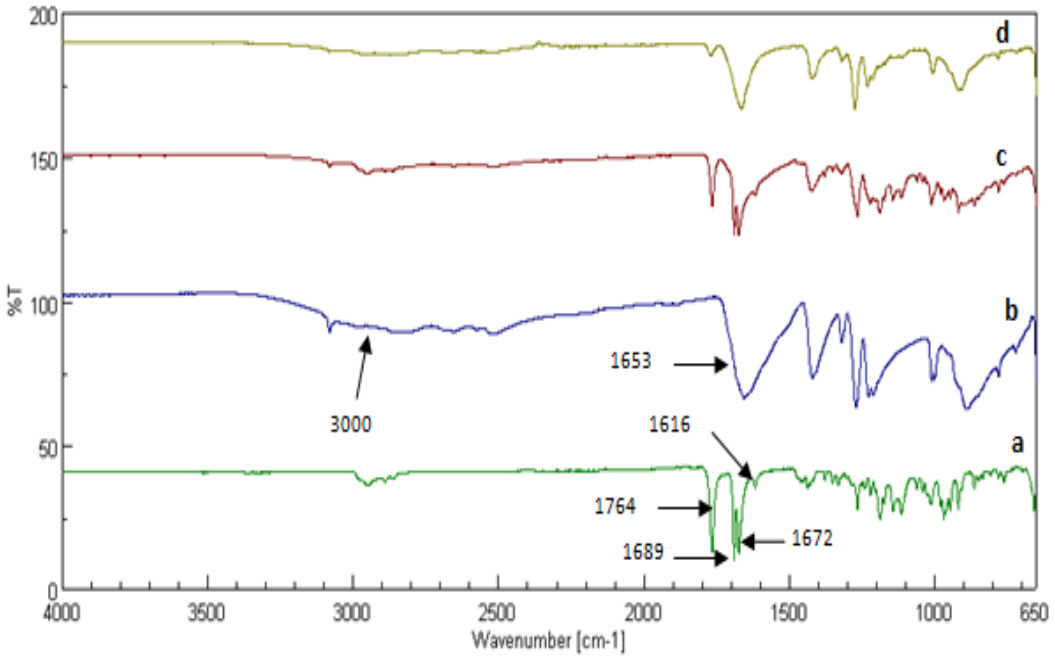

Figure 4.38: FT-IR of unprocessed spironolactone (a), unprocessed fumaric acid (b), spironolactone-fumaric acid physical mixture (c) and spironolactone-fumaric acid lyophilised mixture (d).

Table 4.12: Wave numbers of FT-IR absorption bands where changes were detected in lyophilised spironolactone-fumaric acid mixture, compared to unprocessed components

Wave number (cm^{-1})	**Corresponding bond or functional group**	**Spectral change in lyophilised system**
1764	C=O of lactone ring (spironolactone)	Decreased intensity, broadening and shift to 1769 cm^{-1}
1689	C=O of thioacetyl group (spironolactone)	Merged with other peaks in the vicinity
1672	C=O of C_6-ring (spironolactone)	Merged with other peaks in the vicinity
1616	C=C (spironolactone)	Merged with other peaks in the vicinity
3000	OH (fumaric acid)	Disappeared
1653	C=O (fumaric acid)	Shift to 1663 cm^{-1}

4.4.3 Ketoconazole

4.4.3.1 Lyophilised ketoconazole

The physical states of unprocessed ketoconazole and its lyophilised powder were investigated by DSC and their thermograms are shown in Figure 4.39. The unprocessed ketoconazole exhibited a sharp melting endotherm at 150ºC which is in accordance with published literature (Taneri et al., 2002). In contrast, the thermogram of the lyophilised drug showed the disappearance of the melting peak of ketoconazole and appearance of a broad endotherm in the temperature range 33 to 85ºC. This result suggests the formation of an amorphous form of ketoconazole during the lyophilisation process. The broad endotherm deemed to be attributable to the removal of residual moisture as confirmed by the weight loss observed in TGA in the same temperature range (Figure 4.40). This broad endotherm might overlap the endotherm corresponding to T_g of the produced amorphous form of ketoconazole as it has been reported at 44.5ºC (Van den Mooter et al., 2001).

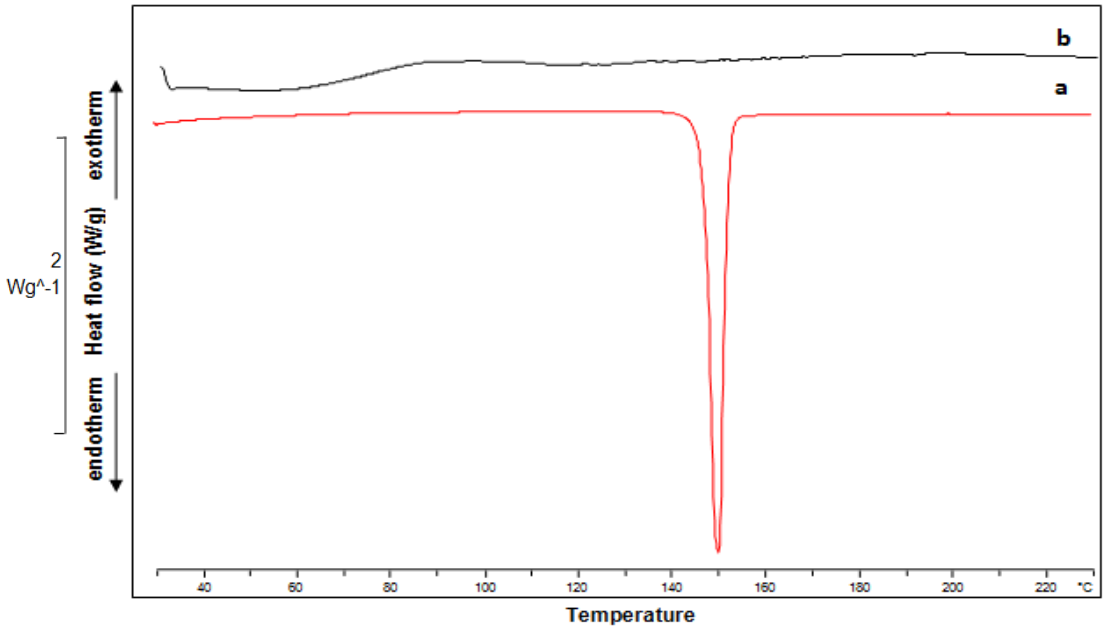

Figure 4.39: DSC of unprocessed ketoconazole (a) and lyophilised ketoconazole (b) powders.

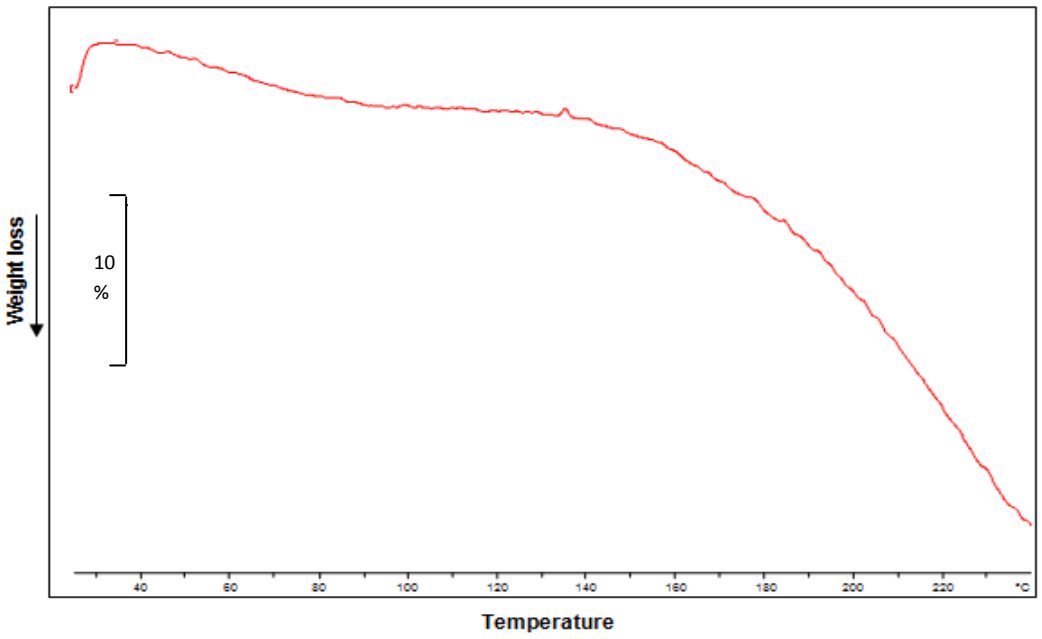

Figure 4.40: TGA of lyophilised ketoconazole powder.

The corresponding XRPD patterns are shown in Figure 4.41. The thermogram of the unprocessed ketoconazole showed numerous sharp peaks highlighting the crystalline nature of the drug (Viseras et al., 1995). In contrast, the diffractogram of the lyophilised drug exhibited disappearance of all the characteristic peaks of the drug and appearance of a hump pattern that is characteristic for amorphous state. This finding revealed that ketoconazole transformed into an amorphous form by lyophilisation which was supported by the DSC results.

The corresponding FT-IR spectra are shown in Figure 4.42. The unprocessed ketoconazole showed characteristic absorption bands at 1645, 1510, 1258, 1243, and 1222 cm^{-1} corresponding to C=O stretch of amide, C=C stretch of aromatic ring, C-H stretch of alkyl, aromatic C-O, and C-N respectively. The spectrum also showed dioxalan ring stretch at 1208 cm^{-1}, methylene rock coupled to deformation of dichlorophenyl C-H bonds at 1130 cm^{-1} and immidazole ring stretch at 1016 cm^{-1} (Dunmire et al., 2005). Noticeable differences in FT-IR spectrum of the lyophilised ketoconazole were observed and these are summarised in Table 4.13.

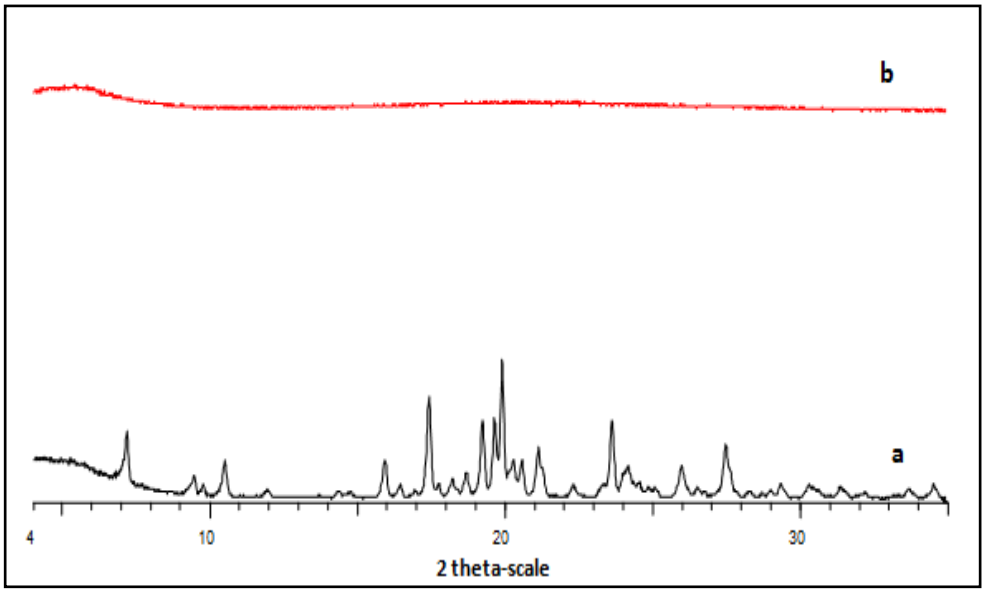

Figure 4.41: XRPD of unprocessed ketoconazole (a) and lyophilised ketoconazole (b) powders.

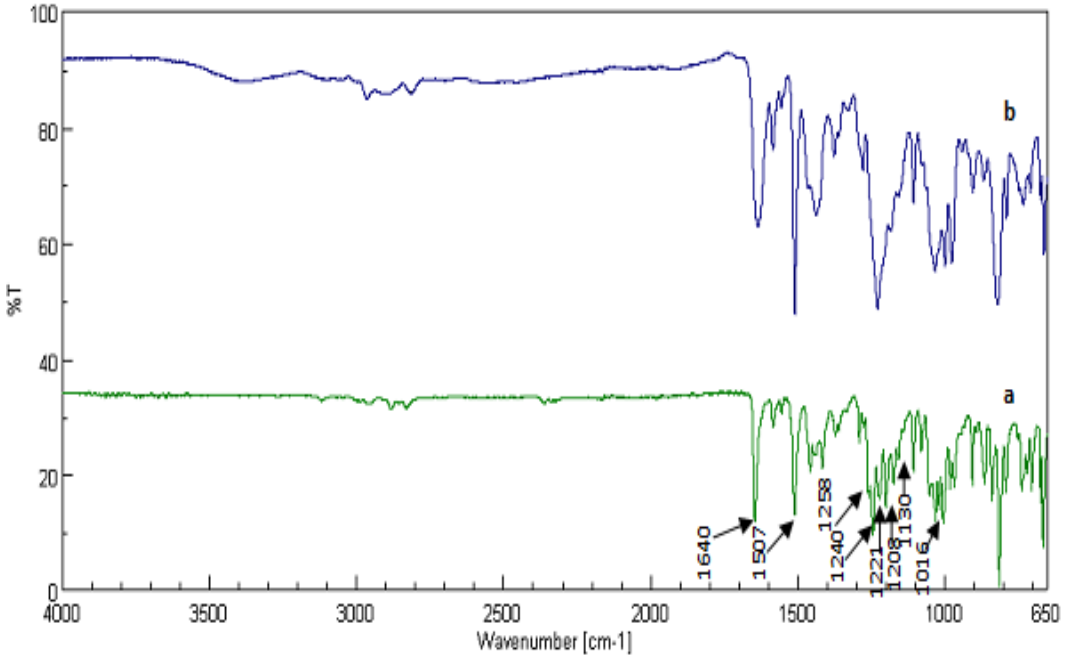

Figure 4.42: FT-IR of unprocessed ketoconazole (a) and lyophilised ketoconazole (b) powders.

The FT-IR spectrum of the lyophilised ketoconazole exhibited appearance of a large broad absorption band in the region 3200-3600 cm^{-1}. This band is typical for amorphous solids and points to interaction with water suggesting the high hygroscopicity of the amorphous ketoconazole produced during the lyophilisation process. Thus, these changes in the spectrum confirm the transformation of ketoconazole to an amorphous form during the lyophilisation process and support the DSC and XRPD results.

Table 4.13: Wave numbers of FT-IR absorption bands where differences were detected between unprocessed and lyophilised ketoconazole.

Wave number (cm^{-1})	Corresponding bond or functional group	Spectral change in lyophilised ketoconazole
1645	C=O of amide	Shift to 1634 cm^{-1}
1258	C-H of alkyl	Disappeared
1243	Aromatic C-O	Disappeared
1222	C-N	Shift to 1228 cm^{-1}
1208	Dioxalan ring	Disappeared
1130	C-H bonds	Disappeared
1016	Imidazole ring	Shift to 998 cm^{-1}

4.4.3.2 Lyophilised ketoconazole-mannitol mixture

The physical state of unprocessed ketoconazole, mannitol, and their physical and lyophilised mixtures (33% w/w mannitol) were investigated by DSC and their thermograms are shown in Figure 4.43. The unprocessed ketoconazole powder exhibited a sharp melting endotherm at 150ºC whereas the unprocessed mannitol exhibited a melting endotherm at 168ºC which is characteristic for the β polymorph of mannitol (Izutsu et al., 2004).

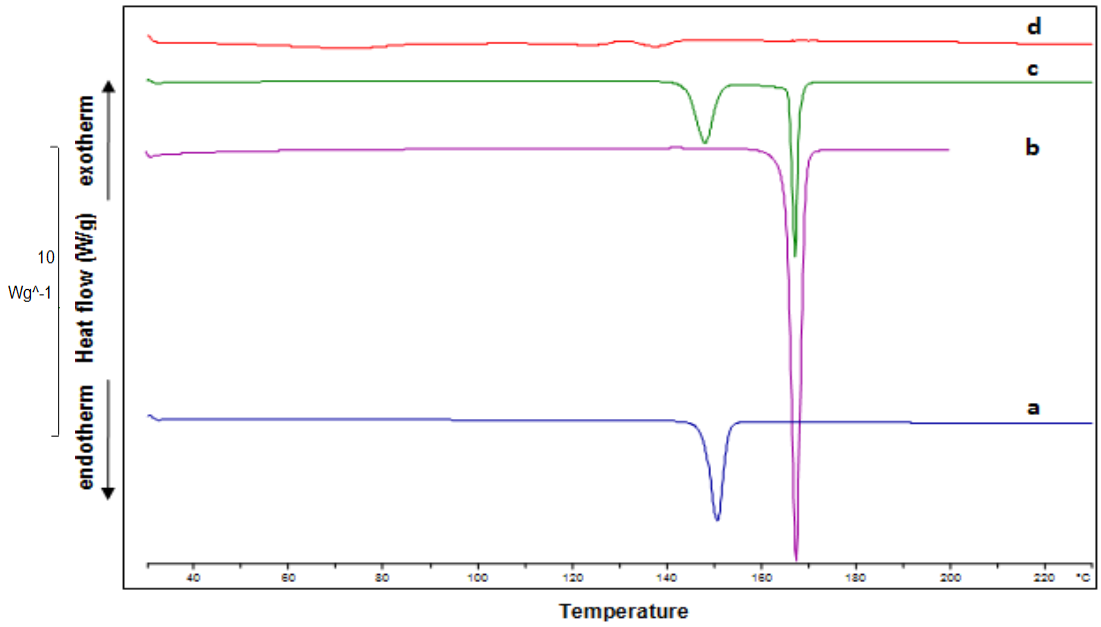

Figure 4.43: DSC of unprocessed ketoconazole (a), unprocessed mannitol (b), ketoconazole-mannitol physical mixture (c) and ketoconazole-mannitol lyophilised mixture (d).

The thermogram of the physical mixture showed both melting endotherms of the drug and excipient with an obvious decrease in their intensity. This may be attributed to disturbance in the crystalline structure of the drug and the excipient in the physical mixture or due to decreased concentration of the drug and excipient in the mixture. The thermogram of the lyophilised mixture exhibited disappearance of the mannitol melting endotherm and a dramatic decrease in the intensity of ketoconazole melting endotherm along with shift to 138ºC. This presumably is

attributed to transformation of the mixture components to amorphous forms. The shift in the ketoconazole melting endotherm suggests the incidence of drug-excipient interactions in the solid dispersion produced during the lyophilisation process.

The corresponding XRPD patterns are compared in Figure 4.44. The diffratograms of unprocessed ketoconazole and mannitol reflected their high crystalline nature as indicated by numerous distinctive peaks. The diffractogram of the physical mixture showed all the characteristic peaks of ketoconazole with reduced intensities as a result of dilution with mannitol in the mixture. Furthermore, the characteristic XRPD peaks of mannitol almost vanished. This is attributed to its lower concentration relative to ketoconazole in the mixture. On the other hand, the diffractogram of the lyophilised mixture exhibited disappearance of almost all XRPD peaks of the drug and the excipient suggesting the transformation of the mixture components to amorphous forms during the lyophilisation process which was supported by the DSC results.

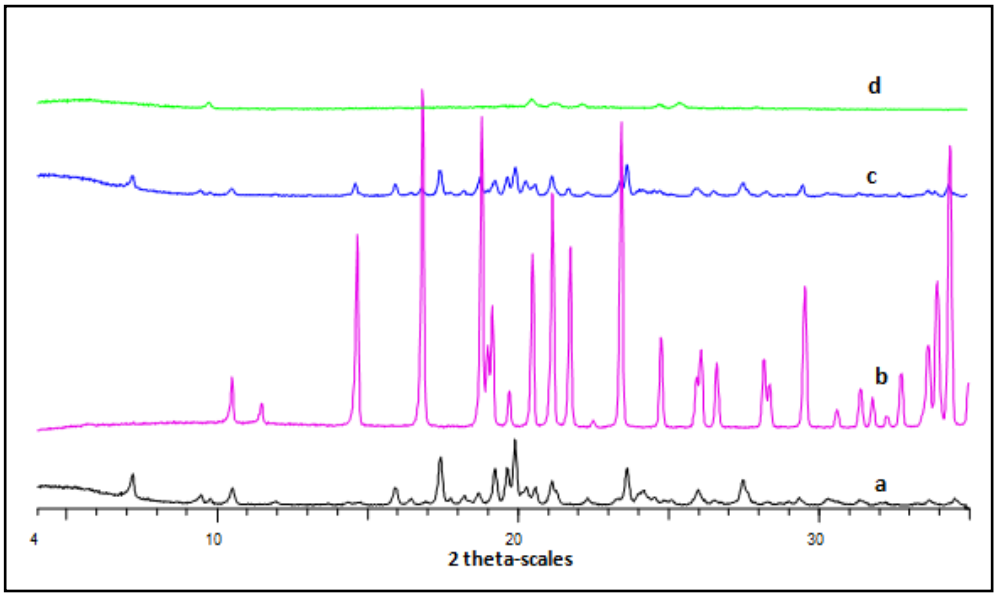

Figure 4.44: XRPD of unprocessed ketoconazole (a), unprocessed mannitol (b), ketoconazole-mannitol physical mixture (c) and ketoconazole-mannitol lyophilised mixture (d).

The corresponding FT-IR spectra are illustrated in Figure 4.45. The characteristic absorption bands of ketoconazole and mannitol were previously discussed in Sections 4.4.3.1 and 4.4.1.2. The spectrum of the physical mixture seemed to be equivalent to the addition spectrum of ketoconazole and mannitol. On the other hand, noticeable differences in FT-IR spectrum of the lyophilised mixture were observed and these are summarised in Table 4.14. In addition, the spectrum of the lyophilised mixture showed a broad band at 3000-3400 cm^{-1} which is typical for amorphous solids and points to interaction with water. These observed changes suggest the incidence of ketoconazol-mannitol interactions such as intermolecular hydrogen bonding between carbonyl group of ketoconazole and hydroxyl groups of mannitol.

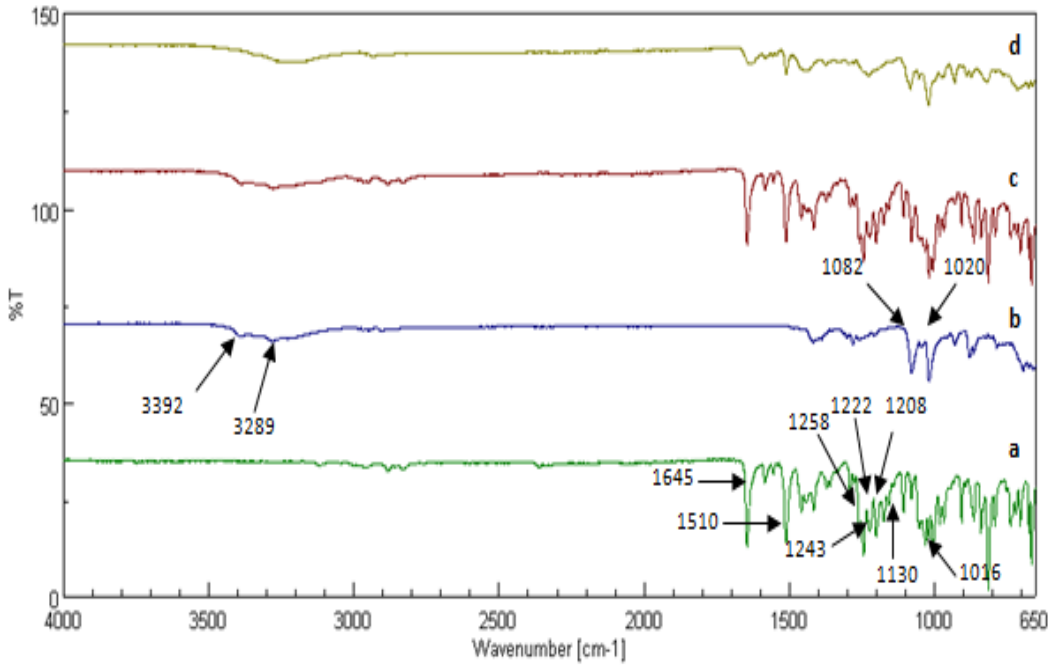

Figure 4.45: FT-IR of unprocessed ketoconazole (a), unprocessed mannitol (b), ketoconazole-mannitol physical mixture (c) and ketoconazole-mannitol lyophilised mixture (d).

Table 4.14: Wave numbers of FT-IR absorption bands where differences were detected in lyophilised ketoconazole-mannitol mixture, compared to unprocessed components

Wave number (cm^{-1})	Corresponding bond or functional group	Spectral change in lyophilised system
1645	C=O of amide (ketoconazole)	Decreased intensity, broadening and Shift to 1636 cm^{-1}
1258	C-H of alkyl (ketoconazole)	Disappeared or Merged with other peaks in the vicinity
1243	Aromatic C-O (ketoconazole)	Disappeared or Merged with other peaks in the vicinity
1222	C-N (ketoconazole)	Disappeared or Merged with other peaks in the vicinity
1208	Dioxalan ring (ketoconazole)	Disappeared or Merged with other peaks in the vicinity
1130	C-H (ketoconazole)	Disappeared
3392	OH (mannitol)	Disappeared
3289	OH (mannitol)	Disappeared

4.4.3.3 Lyophilised ketoconazole-mannitol-SLS mixture

The thermal behaviours of unprocessed ketoconazole, mannitol, SLS, and their physical and lyophilised mixtures (28% w/w mannitol and 14% w/w SLS) were investigated by DSC and their thermograms are shown in Figure 4.46. Unprocessed ketoconazole, SLS and mannitol exhibited sharp melting endotherms at 150ºC, 199ºC and 168ºC respectively. The thermogram of the physical mixture displayed the melting endotherms of ketoconazole and mannitol with broadening and decreased intensities which might be due to disturbance in their crystalline structures or the dilution of both components in the physical mixture. Furthermore, the thermogram lacked the melting endotherm of SLS which might be due to dissolution of the

excipient in the melt of ketoconazole or mannitol before reaching its fusion temperature. In contrast, the thermogram of the lyophilised mixture exhibited disappearance of mannitol and SLS melting endotherms and appearance of the ketoconazole melting endotherm as a very small, broad peak. These results suggest the transformation of the mixture components to amorphous forms in the solid dispersion produced during the lyophilisation process. In addition, the ketoconazole melting endotherm shifted to lower temperature (144ºC) suggesting the possibility of drug-excipient interactions.

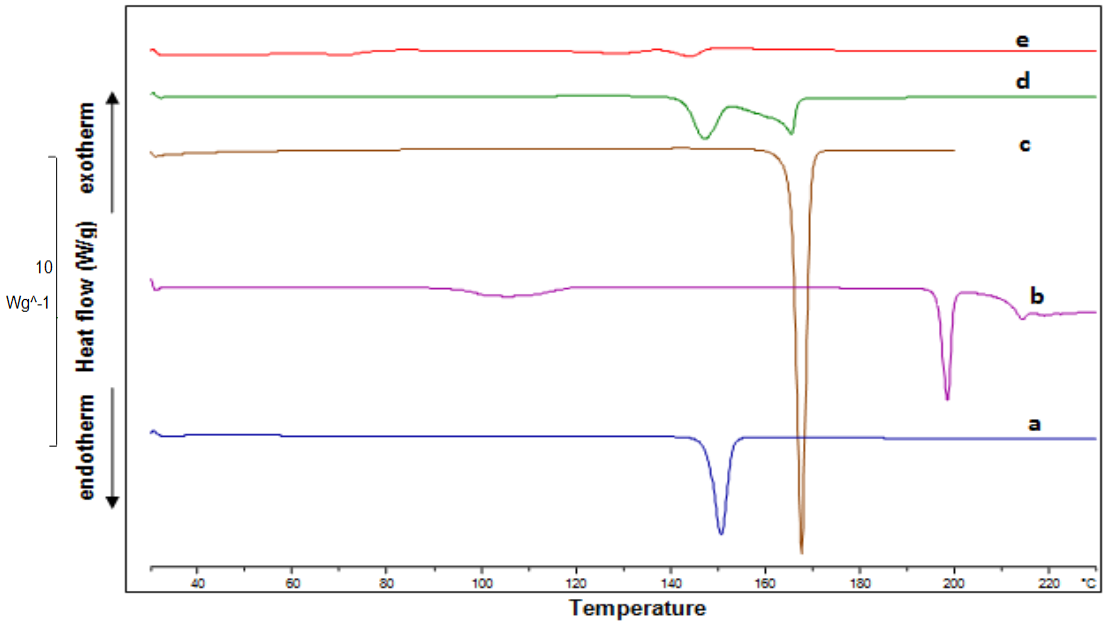

Figure 4.46: DSC of unprocessed ketoconazole (a), unprocessed SLS (b), unprocessed mannitol (c), ketoconazole-mannitol physical mixture (d) and ketoconazole-mannitol lyophilised mixture (e).

The corresponding XRPD patterns are compared in Figure 4.47. The diffratograms of ketoconazole, mannitol, and SLS displayed their crystalline nature as indicated by numerous distinctive peaks. The diffractogram of the physical mixture demonstrated appearance of most of the characteristic XRPD peaks of ketoconazole, mannitol and SLS. Disappearance or decreased intensity of some peaks in the thermogram of the physical mixture was noticeable and might be attributed to dilution of the components in the mixture. On the other hand, the diffraction pattern of the

lyophilised mixture exhibited disappearance of all the XRPD peaks and appearance of a halo pattern suggesting the complete transformation of the mixture components to amorphous state during the lyophilisation process which was supported by the DSC results.

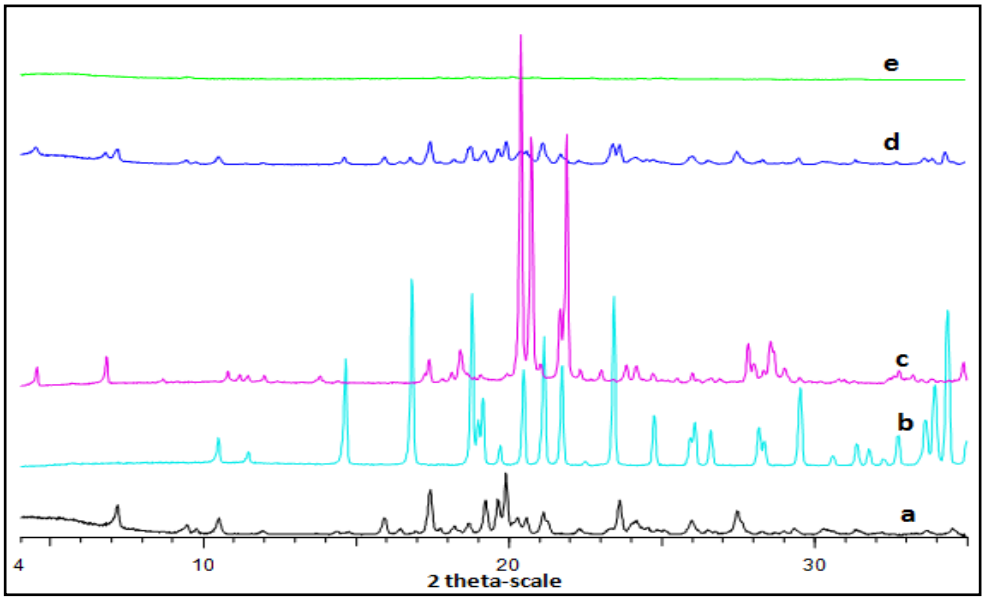

Figure 4.47: XRPD of unprocessed ketoconazole (a), unprocessed mannitol (b), unprocessed SLS (c), ketoconazole-mannitol physical mixture (d) and ketoconazole-mannitol lyophilised mixture (e).

The corresponding FT-IR spectra are illustrated in Figure 4.48. The characteristic absorption bands of the drug and excipients were discussed in Sections 4.4.3.1, 4.4.1.2 and 4.4.1.3. The spectrum of the physical mixture showed all the characteristic peaks of the drug whereas it lacked all the characteristic peaks of SLS as well as the mannitol characteristic peaks at 3392 and 3289 cm^{-1}. This finding might be due to low SLS and mannitol concentrations in the physical mixture relative to the drug. On the other hand, noticeable differences in FT-IR spectrum of the lyophilised mixture were observed and these are summarised in Table 4.15. In the spectrum of the lyophilised mixture, all ketoconazole characteristic peaks around 1200 cm^{-1} merged into a broad peak at 1228 cm^{-1}. The spectrum also showed the

appearance of a large broad peak in the region 3000-3500 cm^{-1} which is typical for amorphous solids. These observed changes suggest the incidence of intermolecular hydrogen bonding between the components of the amorphous solid dispersion produced during the lyophilisation process. According to the DSC, XRPD and FT-IR results, it can be concluded that the major dissolution rate enhancement observed from the lyophilised mixture of ketoconazole with mannitol and SLS (Section 3.4.2.15) was primarily attributed to formation of an amorphous solid dispersion of the drug in the amorphous lyophilised matrix of the excipients.

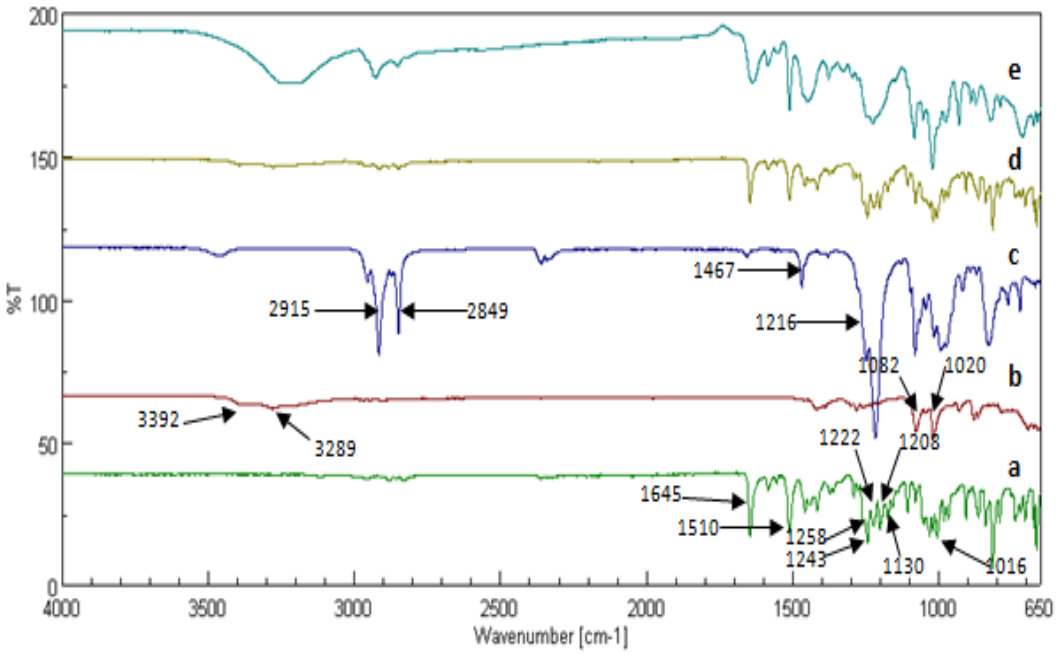

Figure 4.48: FT-IR of unprocessed ketoconazole (a), unprocessed mannitol (b), unprocessed SLS(c), ketoconazole-mannitol physical mixture (d) and ketoconazole-mannitol lyophilised mixture (e).

Table 4.15: Wave numbers of FT-IR absorption bands where differences were detected in lyophilised ketoconazole-mannitol-SLS mixture, compared to unprocessed components

Wave number (cm^{-1})	Corresponding bond or functional group	Spectral change in lyophilised system
1645	C=O of amide (ketoconazole)	Decreased intensity, broadening and Shift to 1634 cm^{-1}
1258	C-H of alkyl (ketoconazole)	Merged with other peaks in the vicinity
1243	Aromatic C-O (ketoconazole)	Merged with other peaks in the vicinity
1222	C-N (ketoconazole)	Merged with other peaks in the vicinity
1208	Dioxalan ring (ketoconazole)	Merged with other peaks in the vicinity
1130	C-H bonds (ketoconazole)	Disappeared
3392	OH (mannitol)	Disappeared
3289	OH (mannitol)	Disappeared
2915	Long chain alkyl group (SLS)	Decreased intensity
2849	Long chain alkyl group (SLS)	Decreased intensity
1467	C-H (SLS)	Broadening and shift to 1449 cm^{-1}
1216	C-O (SLS)	Merged with other peaks in the vicinity
1080	S=O (SLS)	Shift to 1083 cm^{-1}

4.4.3.4 Lyophilised ketoconazole-mannitol-PEG 6000 mixture

The physical states of unprocessed ketoconazole, mannitol, PEG 6000, and their physical and lyophilised mixtures (28% w/w mannitol and 14% w/w PEG 6000) were investigated by DSC and their thermograms are shown in Figure 4.49. Unprocessed ketoconazole, mannitol and PEG 6000 exhibited sharp melting endotherms at 150ºC, 168ºC and 64ºC respectively. The thermogram of the physical mixture displayed all three melting endotherms of the drug and excipients with apparent decrease in their intensities due to disruption of the crystalline structure of the components of the physical mixture during preparation or due to dilution effect.

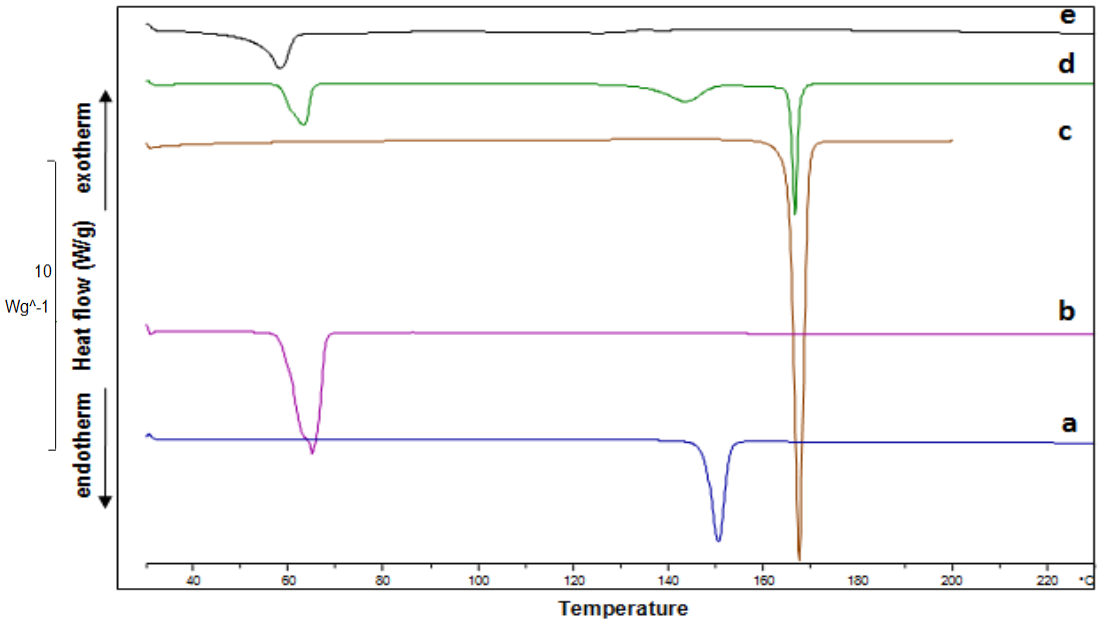

Figure 4.49: DSC of unprocessed ketoconazole (a), unprocessed PEG 6000 (b), unprocessed mannitol (c), ketoconazole-mannitol-PEG 6000 physical mixture (d) and ketoconazole-mannitol-PEG 6000 lyophilised mixture (e).

The thermogram of the lyophilised mixture exhibited complete disappearance of both ketoconazole and mannitol melting endotherms. In addition, PEG 6000 melting endotherm shifted to 58ºC C and its intensity was obviously reduced. This finding suggests that both ketoconazole and mannitol were completely transformed into

amorphous state while PEG 6000 partially transformed to an amorphous form in the produced solid dispersion. The observed shift of the PEG 6000 melting endotherm may be due to transformation of the polymer to a different crystal form during the lyophilisation process or due to depression of the melting temperature of the polymer as a result of solid dispersion formation. Similar results have been reported by Wang et al. (2004) who found that the melting temperature of PEG 6000 in its solid dispersion with 80% w/w itraconazole shifted to 58ºC.

The corresponding XRPD patterns are compared in Figure 4.50. The diffratograms of unprocessed ketoconazole, mannitol, and PEG 6000 reflected their crystalline nature as indicated by numerous distinctive peaks. The diffractogram of the physical mixture showed appearance of some peaks indicating the crystalline nature of the mixture. Disappearance of some peaks in the thermogram of the physical mixture and decreased intensities of others were obvious and might be attributed to a dilution effect in the mixture. On the other hand, the diffractogram of the lyophilised mixture exhibited disappearance of all peaks of the drug and mannitol while it showed traces of PEG 6000 peaks suggesting the transformation of the mixture components to amorphous state during the lyophilisation process which was supported by the DSC results.

The corresponding FT-IR spectra are illustrated in Figure 4.51. The characteristic absorption bands of the drug and the excipients were discussed in Sections 4.4.3.1, 4.4.1.2 and 4.4.1.4. The spectrum of the physical mixture showed all the characteristic peaks of the drug whereas it exhibited disappearance of some of the characteristic peaks of PEG 6000 and mannitol due to their low concentrations in the mixture. On the other hand, noticeable differences in FT-IR spectrum of the lyophilised mixture were observed and these are summarised in Table 4.16. The spectrum of the lyophilised mixture also exhibited appearance of a large broad peak in the region 3000-3500 cm^{-1} (explained previously). All ketoconazole characteristic peaks around 1200 cm^{-1} were found merged into a broad peak at around 1228 cm^{-1}. These changes suggest intensive intermolecular hydrogen bonding between the components of the amorphous solid dispersion produced during the lyophilisation process.

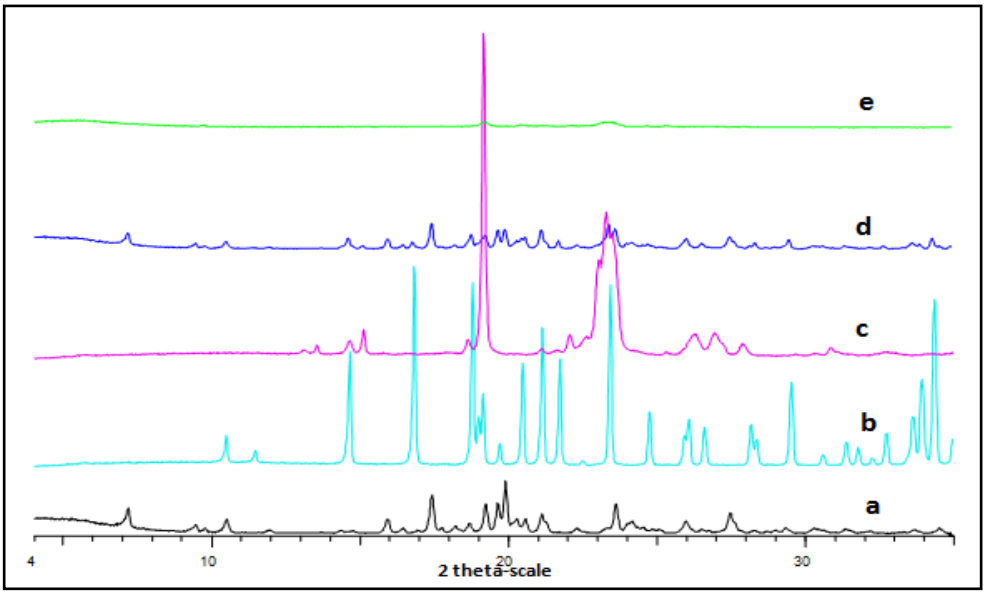

Figure 4.50: XRPD of unprocessed ketoconazole (a), unprocessed mannitol (b), unprocessed PEG 6000 (c), ketoconazole-mannitol-PEG 6000 physical mixture (d) and ketoconazole-mannitol-PEG 6000 lyophilised mixture (e).

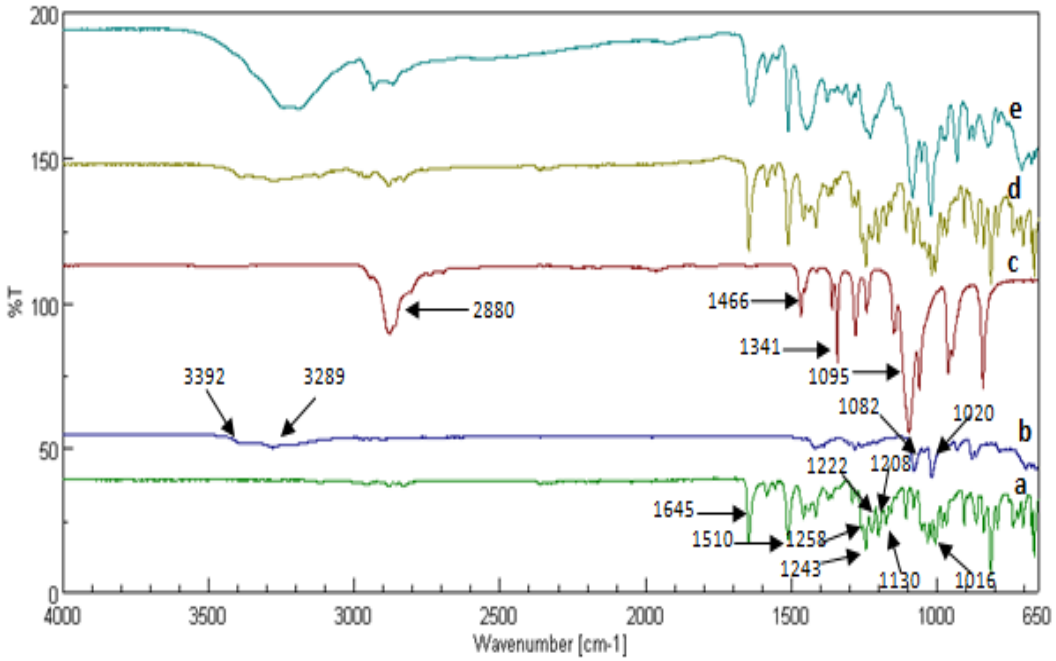

Figure 4.51: FT-IR of unprocessed ketoconazole (a), unprocessed mannitol (b), unprocessed PEG 6000(c), ketoconazole-mannitol-PEG 6000 physical mixture (d) and ketoconazole-mannitol-PEG 6000 lyophilised mixture (e).

Table 4.16: Wave numbers of FT-IR absorption bands where differences were detected in lyophilised ketoconazole-mannitol-PEG 6000 mixture, compared to unprocessed components

Wave number (cm^{-1})	Corresponding bond or functional group	Spectral change in lyophilised system
1645	C=O of amide (ketoconazole)	Decreased intensity, broadening and Shift to 1639 cm^{-1}
1258	C-H of alkyl (ketoconazole)	Merged with other peaks in the vicinity
1243	Aromatic C-O (ketoconazole)	Merged with other peaks in the vicinity
1222	C-N (ketoconazole)	Merged with other peaks in the vicinity
1208	Dioxalan ring (ketoconazole)	Merged with other peaks in the vicinity
1130	C-H bonds (ketoconazole)	Disappeared
3392	OH (mannitol)	Disappeared
3289	OH (mannitol)	Disappeared
2880	C-H (PEG 6000)	Shift to 2868 cm^{-1}
1466	C-H (PEG 6000)	Decreased intensity,broadening and shift to 1447 cm^{-1}
1095	C-O (PEG 6000)	Shift to 1081 cm^{-1}

4.5 Conclusion

It can be concluded from this chapter that:

- Lyophilisation of glibenclamide, spironolactone or ketoconazole alone or with different excipients resulted in transformation of the drugs to an amorphous state. This finding explains the dissolution enhancement observed for these drugs from their solid dispersions with the excipients (Chapter 3). FT-IR spectra of the lyophilised mixtures suggest the incidence of intermolecular hydrogen bonding between the drugs and the excipients.
- In the case of spironolactone, some XRPD patterns contradicted the corresponding DSC thermograms as the former displayed the amorphous nature of spironolactone in the lyophilised system while the later showed the melting endothermic peak of the drug. This could be due to the flexibility of spironolactone molecules that can go through molecular rearrangement by the application of heat experienced during the DSC analysis.
- The appearance of new XRPD peaks in the case of the lyophilised mixture of spironolactone with mannitol may suggest formation of a new polymorphic form of the drug during the lyophilisation process.
- Citric acid is not a good excipient in lyophilisation process as the lyophilised mixture of spironolactone with citric acid was characterised by high hygroscopicity as evident from the FT-IR results. This explains the transformation of the lyophilised product to a clump that sank to the bottom of the dissolution flask where it remained intact over the experimental period leading to retardation of the dissolution rate of spironolactone (Chapter 3).
- The lyophilised systems of ketoconazole were highly hygroscopic in nature as indicated by the appearance of a broad absorption band in the range 3000-3500 cm^{-1} (characteristic for OH of water molecules) in their FT-IR spectra.

Chapter 5

5. Spray coating of lyophilised glibenclamide, spironolactone and ketoconazole capsule formulations

5.1 Introduction

It is well known that the amorphous form has higher free energy, free volume and molecular mobility compared to the crystalline form, leading to physical instability, greater chemical reactivity, and water vapour absorption (Crowley & Zografi, 2002). The temperature at which the amorphous form transforms from glass to rubber (glass transition temperature, T_g) is considered a critical property of the amorphous material. Major changes in viscosity and molecular mobility occur at T_g. Chemical reactivity and crystallisation rates increase at temperatures above and directly below T_g (Guo et al., 2000). Stability of the amorphous form of drugs is the main obstacle in the successful exploitation and realisation of its advantageous physicochemical properties. The stability of the amorphous solid is further challenged by different stresses such as temperature, gases, and liquid vapours (Gupta & Bansal, 2005). Moreover, moisture has a plasticization effect on the amorphous material which increases the molecular mobility and decreases T_g resulting in increased tendency for transformation to the crystalline form (Strydom et al., 2009; Ambike et al., 2004; Andronis & Zografi, 1998; Andronis et al., 1997). Therefore, drugs dispersed in amorphous forms are liable to recrystallisation into different polymorphic forms upon storage, especially when they are subjected to high temperature and humidity.

Capsules, as pharmaceutical dosage forms represent many advantages compared to other traditional oral dosage forms. Capsules are easily formulated and can be filled with powders, granules, liquids or semi-solids (Marques et al., 2009). Capsules also have a number of patient advantages including ease of swallowing and masking of active pharmaceutical ingredient or excipient taste and odour (Jones, 2004). The percentage of moisture in the shell of hard gelatin capsule ranges between 13% and 16% w/w (Chang et al., 1998). This moisture content acts as a plasticizer to provide flexibility to the capsule shell. During storage, variation in moisture content of the shell can result in undesirable physical properties such as shell fragility or stickiness. Moisture can move from the capsule contents to the shell leading to softening

problems. On the other hand, moisture can transfer from the shell to the capsule contents during storage (Chang et al., 1998). The exchange of moisture between the capsule shell and the capsule contents is considered a disadvantage of hard gelatin capsules. When the filled capsules are kept in a closed container, the moisture redistributes until equilibrium is achieved. The high permeability of the capsule shell to water vapour is therefore another limitation of gelatin capsules. When capsules are stored in an open atmosphere, their contents have the potential to capture moisture from the environment until equilibrium is reached. This can have a detrimental effect on both the capsule and its contents. The transfer of moisture to the capsule contents can result in agglomeration or chemical degradation with a loss in function, biological activity, and change in toxicity of the active ingredients (Yoshioka & Stella, 2000).

Many drugs are unstable under the effect of air, light, heat or moisture. Thus, pharmaceutical dosage forms are commonly provided with polymeric coatings to extend their shelf life (Petereit & Weisbord, 1999). Furthermore, the destructive effect of the gastric acid and enzymes on drugs can be avoided by enteric coating which also prevents stomach irritation induced by some drugs (Long & Chen, 2009). Enteric coatings are selected to control the location of the drug release in the gastrointestinal tract. The majority of drug absorption takes place in the small intestine (see Section 1.2.1.3). Thus, the enteric coating which resists acidic environment of the stomach and disrupts in the small intestine (at higher pH), would be useful to ensure maintenance of a high drug concentration within the absorption point before dispersion. Thus, enteric coating has both the advantages of controlling the site of drug delivery whilst potentially protecting drug from the environment during storage of the dosage form. Enteric coating is used for protecting many drugs such as omeprazole (He et al., 2009), flubiprofen (Hashmat et al., 2007), acetylsalicylic acid, theophylline, paracetamol, propranolol hydrochloride, isoniazid, ranitidine hydrochloride and procainamide hydrochloride (Pina et al., 1997).

5.2 Aims and objectives

The present chapter aims to investigate the application of film coatings to various drug formulations; non-enteric film coating (glibenclamide, spironolactone and ketoconazole) or enteric film coating (glibenclamide), to the hard gelatin capsules containing the selected lyophilised formulations to overcome the disadvantages of moisture permeability of hard gelatin capsules. Before the coating process, the effect of certain process parameters such as the type of solvent system, the volume of solvent and drying time on the physicochemical stability of the drug formulations contained in the hard gelatin capsules were investigated.

5.3 Methods

The effect of two types of solvent systems on the physicochemical properties of the lyophilised formulations contained in hard gelatin capsules was investigated. These solvent systems were acetone/isopropyl alcohol (50% v/v) and ethanol/water (90/10% v/v).

5.3.1 Acetone/isopropyl alcohol solvent system

This system is a non aqueous solvent system that can be used for ethyl cellulose coating (see Section 1.5.1.1). It consisted of 50% v/v acetone and isopropyl alcohol. It was used for spraying capsules containing lyophilised formulations of either glibenclamide (93% w/w SLS); spironolactone (67% w/w SLS) or ketoconazole (14% w/w SLS and 28% w/w mannitol). The solvent system was applied to the capsules by a bench-top minicoater, Caleva using the parameters listed in Table 5.1.

5.3.1.1 Effect of application of different volumes of the solvent system

8 capsules were sprayed with 16, 32 or 64 ml (2, 4, or 8 ml per capsule) of 50% v/v acetone/isopropyl alcohol system using the minicoater parameters listed in Table 5.1. The resultant capsules had their dissolution performance evaluated (Section 2.4.1) and the contents removed for physical characterisation by DSC, XRPD and FT-IR.

Table 5.1: Minicoater experimental parameters for Acetone/isopropyl alcohol solvent system

Parameter	Value
Cone agitator speed (H_Z)	17.5
Air flow temperature (°C)	30
Drying temperature (°C)	30
Atomising air pressure (bar)	1
Inlet air flow (m/s)	7
Speed of the pump (r/m)	3
Height of spray head (mm)	150
Drying time (mins)	10

5.3.1.2 Effect of process drying time

8 capsules were sprayed with 32 ml (4 ml per capsule) of the 50% v/v acetone/isopropyl alcohol system using the minicoater parameters listed in Table 5.1. Capsules were allowed to dry for varying times post-spraying (10, 25, 40 and 60 minutes). The resultant capsule contents were physically characterised by DSC, XRPD and FT-IR.

5.3.2 Ethanol/water solvent system

This solvent system was employed in the present thesis as a solvent system for the enteric or non-enteric coating systems. It consisted of 90% v/v ethanol and 10% v/v water. It was used for spraying the selected capsule formulations (see Section 5.3.1). The solvent system was sprayed by a bench-top minicoater, Caleva applying the parameters listed in Table 5.2.

5.3.2.1 Effect of application of different volumes of the solvent system

8 capsules were sprayed with 16, 32 and 64 ml (2, 4, or 8 ml per capsule) of the solvent system of 90% v/v ethanol and 10% v/v water using the minicoater parameters listed in Table 5.2. The resultant capsules were tested for dissolution and the contents were physically characterised by DSC, XRPD and FT-IR.

5.3.2.2 Effect of process drying time

8 capsules were sprayed with 64 ml (8 ml per capsule) of the solvent system of 90% v/v ethanol and 10% v/v water using the minicoater parameters listed in Table 5.2. Capsules were allowed to dry for 20, 60 or 90 minutes. The resultant capsule contents were physically characterised by DSC, XRPD and FT-IR.

Table 5.2: Minicoater experimental parameters for ethanol/water solvent system.

Parameter	Value
Cone agitator speed (H_Z)	17.5
Air flow temperature (°C)	40
Drying temperature (°C)	40
Atomising air pressure (bar)	1
Inlet air flow (m/s)	7
Speed of the pump (r/m)	3
Height of spray head (mm)	150
Drying time (mins)	20

5.3.3 Application of coating systems

5.3.3.1 Non-enteric coating system

Opadry was used as a non-enteric coating system. It consists of hydroxylpropyl cellulose (HPC), hydroxylpropyl methyl cellulose (HPMC) as polymers and titanium dioxide as a colouring agent. Opadry coating dispersion (5% w/v) was prepared by mixing the desired amount of Opadry powder with a solvent system consisting of 90% v/v absolute ethanol and 10% v/v distilled water. The following mixing procedures were followed for optimum preparation of the coating system:

1. The required amount of the Opadry coating system was weighed.
2. The required volume of the solvent system was measured into a mixing vessel.
3. The solvent system was stirred using a propeller (1000 rpm) in the centre and as close to the bottom of the mixing vessel as possible to form a vortex.
4. Opadry powder was gradually but quickly added to the vortex avoiding floating on the solvent surface.
5. After addition of the entire amount of powder, the mixer speed was reduced (500 rpm) to remove the vortex and then the system was mixed for 45 minutes prior to use for coating the selected formulations of glibenclamide, spironolactone or ketoconazole formulations (see Section 5.3.1).

5.3.3.2 Enteric coating system

Opadry enteric was used as an enteric coating system. It consists of polyvinyl acetate phthalate as a polymer, stearic acid, triethyl citrate as plasticizers and titanium dioxide as a colouring agent. Opadry enteric coating dispersion systems (10% w/v) were prepared using the same solvent system and mixing procedures as those employed in the case of Opadry non-enteric coating system and used for coating glibenclamide formulations.

8 capsules were sprayed with 16 ml (2 ml per capsule) of the dispersion of the coating system (either enteric or non-enteric) using a bench-top minicoater, Caleva. The applied minicoater experimental parameters for enteric and non-enteric coating

are listed in Table 5.3. Capsules were weighed before and after coating and the percentage weight gain was calculated. The weight gain in the case of non-enteric coating was 5-7% while in the case of enteric coating, the weight gain was 8-12% .

Table 5.3: Minicoater experimental parameters for non-enteric and enteric coating.

Parameter	Non-enteric coat	Enteric coat
Cone agitator speed (H_Z)	17.5	17.5
Air flow temperature (ºC)	40	25
Drying temperature (ºC)	40	25
Atomising air pressure (bar)	1	1
Inlet air flow (m/s)	7	7
Speed of the pump (r/m)	3	1.5
Height of spray head (mm)	150	150
Drying time (mins)	20	20

5.4 Results and discussion

5.4.1 Acetone/isopropyl alcohol (50/50% w/w) solvent system

5.4.1.1 Effect of application of different volumes of solvent on dissolution profiles of lyophilised glibenclamide, spironolactone and ketoconazole formulations

The dissolution profiles of glibenclamide, spironolactone and ketoconazole capsule formulations after spraying with different volumes of 50% v/v acetone/isopropyl alcohol solvent system are illustrated in Figures 5.1-5.3 respectively. For all three drugs, there were no significant differences between the dissolution profiles of the systems ($f_2 > 50$). This finding suggests the stability of the solid dispersion formulations of the drugs after application of the solvent system.

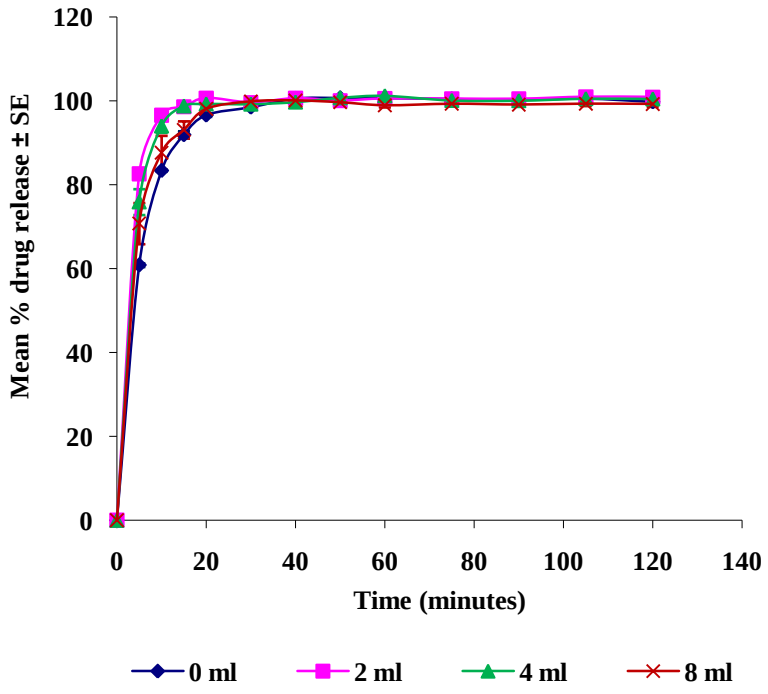

Figure 5.1: Effect of spraying different volumes of acetone/isopropyl alcohol (50/50% v/v) solvent system on the dissolution profiles of lyophilised glibenclamide-SLS formulations (n=6).

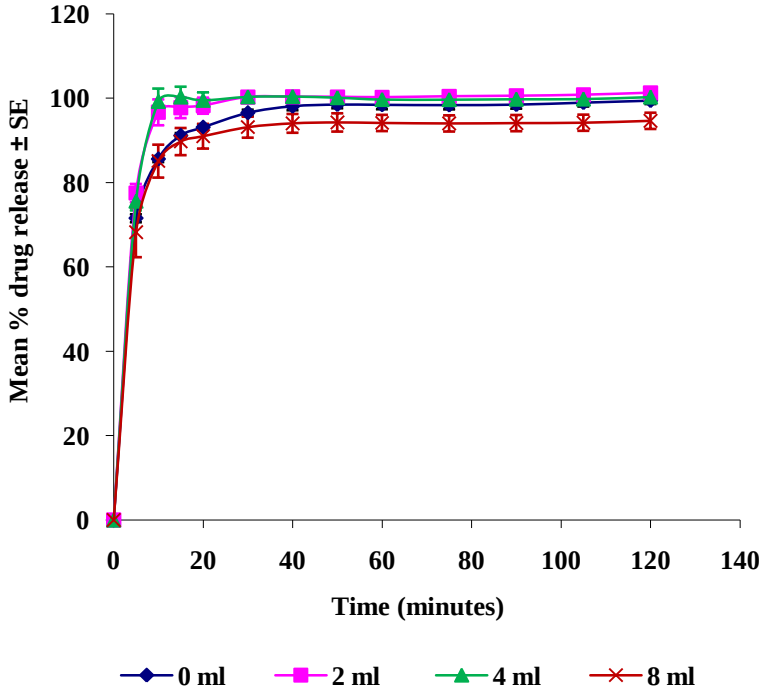

Figure 5.2: Effect of spraying different volumes of acetone/isopropyl alcohol (50/50% v/v) solvent system on the dissolution profiles of lyophilised spironolactone-SLS formulations (n=6).

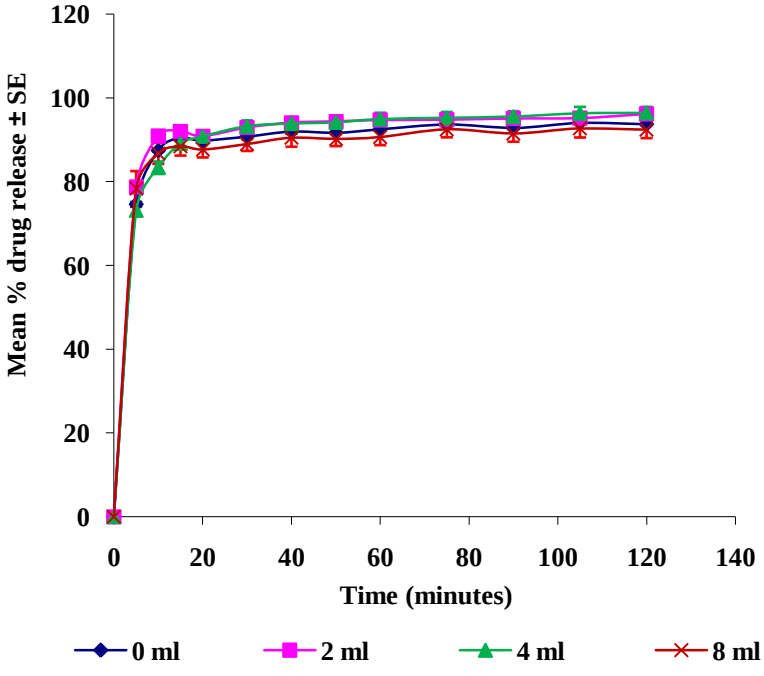

Figure 5.3: Effect of spraying different volumes of acetone/isopropyl alcohol (50/50% v/v) solvent system on the dissolution profiles of lyophilised ketoconazole-mannitol-SLS formulations (n=6).

5.4.1.2 Physical characterisation of lyophilised glibenclamide, spironolactone and ketoconazole formulations that received different volumes of acetone/isopropyl alcohol (50/50% v/v) solvent system

The DSC thermograms of glibenclamide, spironolactone and ketoconazole formulations after spraying of capsules with different volumes of 50% v/v acetone/isopropyl alcohol solvent system are illustrated in Figures 5.4-5.6. The thermograms of the sprayed glibenclamide formulations were identical. There were no difference between the thermograms of the sprayed formulations and that of the non-sprayed samples except for the appearance of a very small, shallow endotherm at 57ºC representing solvent evaporation. For spironolactone and ketoconazole, the thermograms of the sprayed formulations were also similar to each other and to those of the corresponding non-sprayed formulations.

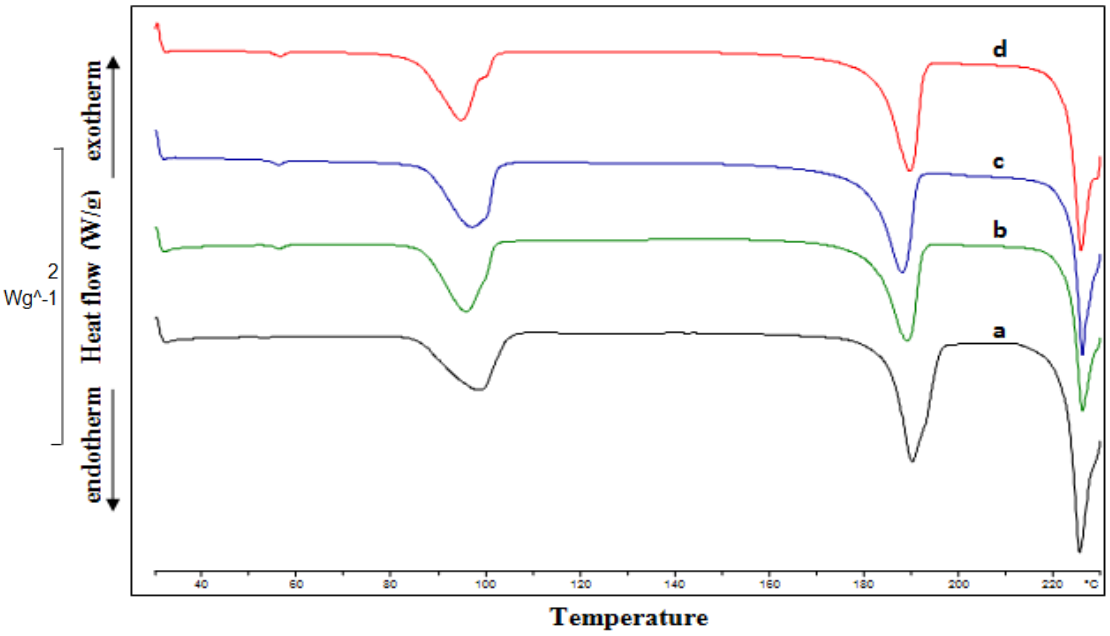

Figure 5.4: DSC of lyophilised glibenclamide-SLS formulations sprayed with different volumes of acetone/isopropyl alcohol (50/50% v/v) solvent system 0 ml (a); 2 ml (b); 4 ml (c); or 8 ml (d).

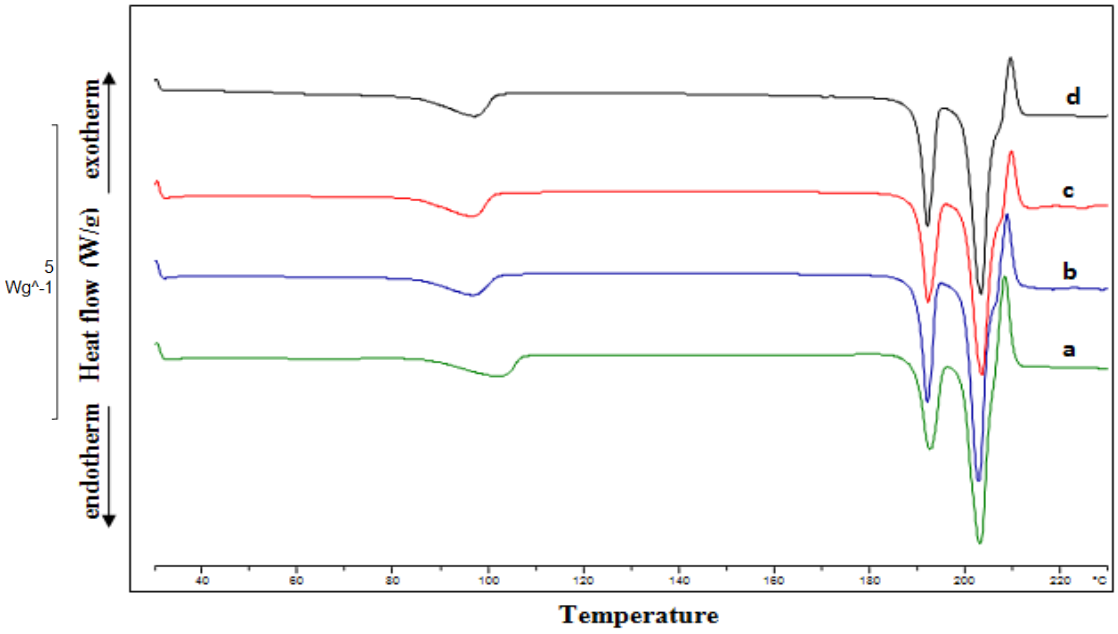

Figure 5.5: DSC of lyophilised spironolactone-SLS formulations sprayed with different volumes of acetone/isopropyl alcohol (50/50% v/v) solvent system 0 ml (a); 2 ml (b); 4 ml (c); or 8 ml (d).

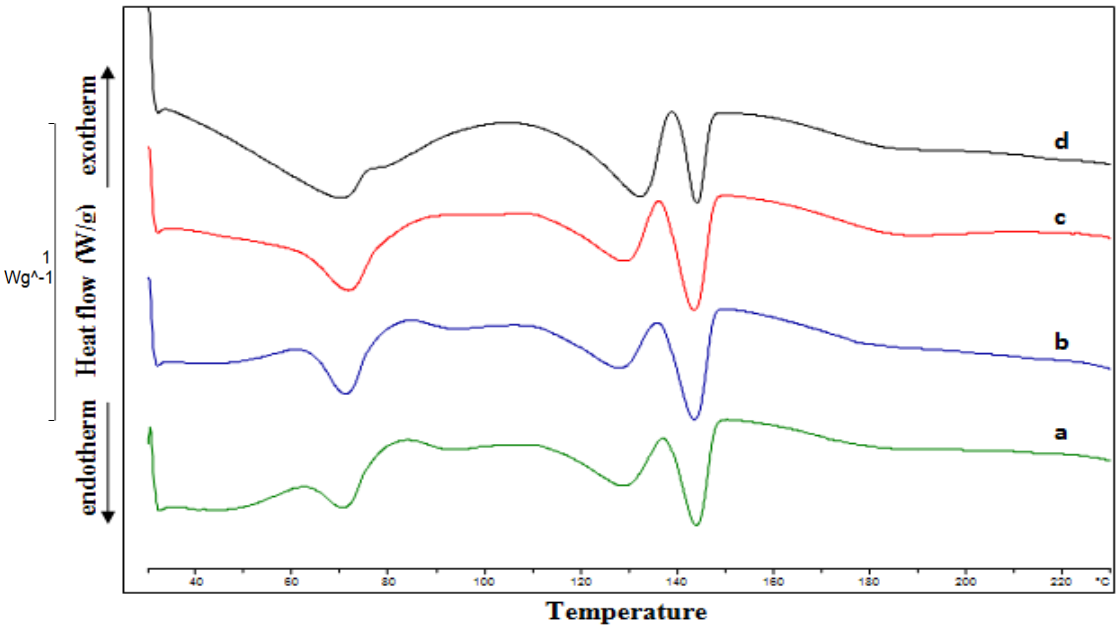

Figure 5.6: DSC of lyophilised ketoconazole-mannitol-SLS formulations sprayed with different volumes of acetone/isopropyl alcohol (50/50% v/v) solvent system 0 ml (a); 2 ml (b); 4 ml (c); or 8 ml (d).

The corresponding XRPD patterns of the systems are represented in Figures 5.7-5.9. The diffractograms of the sprayed formulations of glibenclamide and ketoconazole were identical to those of the corresponding non-sprayed samples supporting the DSC results and suggesting the stability of the amorphous forms of both drugs in their solid dispersions on being sprayed with different volumes of the solvent system. The diffractograms of the sprayed formulations of spironolactone showed recrystallisation peaks (Figure 5.8). This may be attributed to exposure of the formulations to the solvent vapour during the coating process. Adsorption of solvent molecules on the surface of the amorphous formulations may lead to an increase in the mobility of the drug molecules leading to their reorganisation and recrystallisation. Brinkmann et al. (1997) have reported that the exposure of an amorphous phthalocyanine film to the vapour of acetone induced significant alteration in the morphology and crystalline structure of the film. However, the absence of changes in the DSC thermograms or dissolution profiles of sprayed formulations of spironolactone compared to those of the corresponding non-sprayed samples suggests that the observed recrystallisation was minimal.

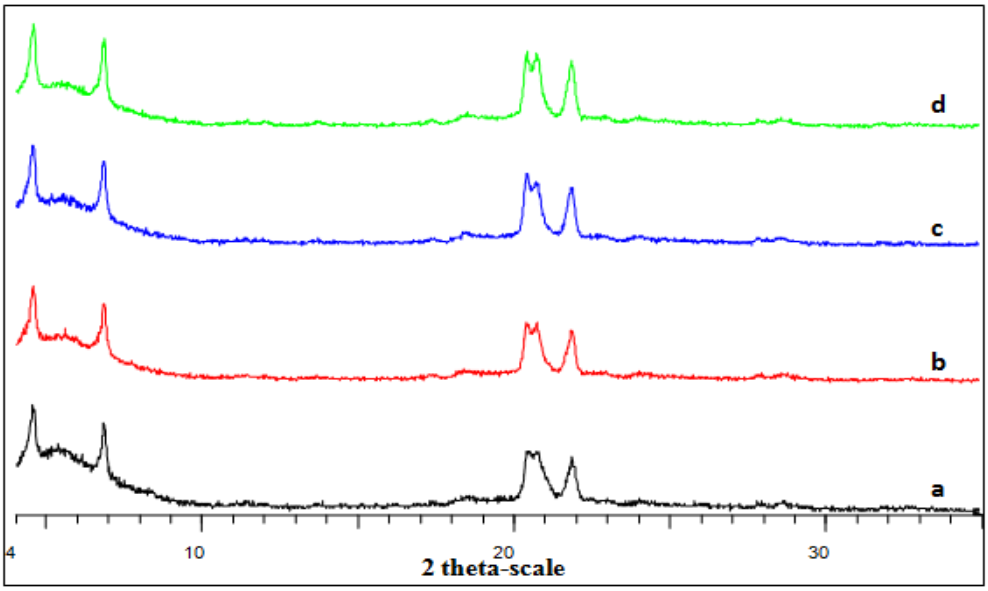

Figure 5.7: XRPD of lyophilised glibenclamide-SLS formulations sprayed with different volumes of acetone/isopropyl alcohol (50/50% v/v) solvent system 0 ml (a); 2 ml (b); 4 ml (c); or 8 ml (d).

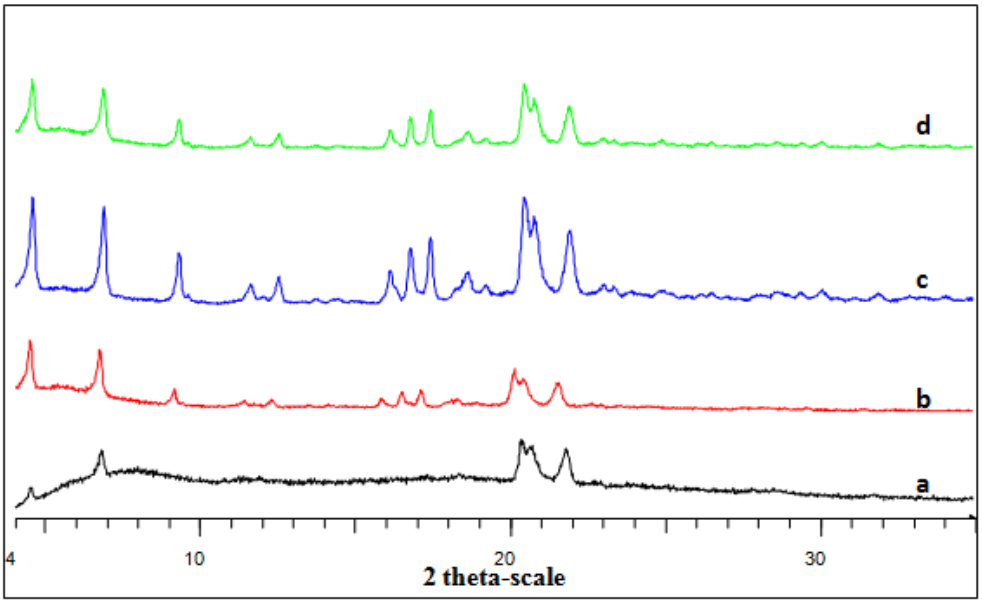

Figure 5.8: XRPD of lyophilised spironolactone-SLS formulations sprayed with different volumes of acetone/isopropyl alcohol (50/50% v/v) solvent system 0 ml (a); 2 ml (b); 4 ml (c); or 8 ml (d).

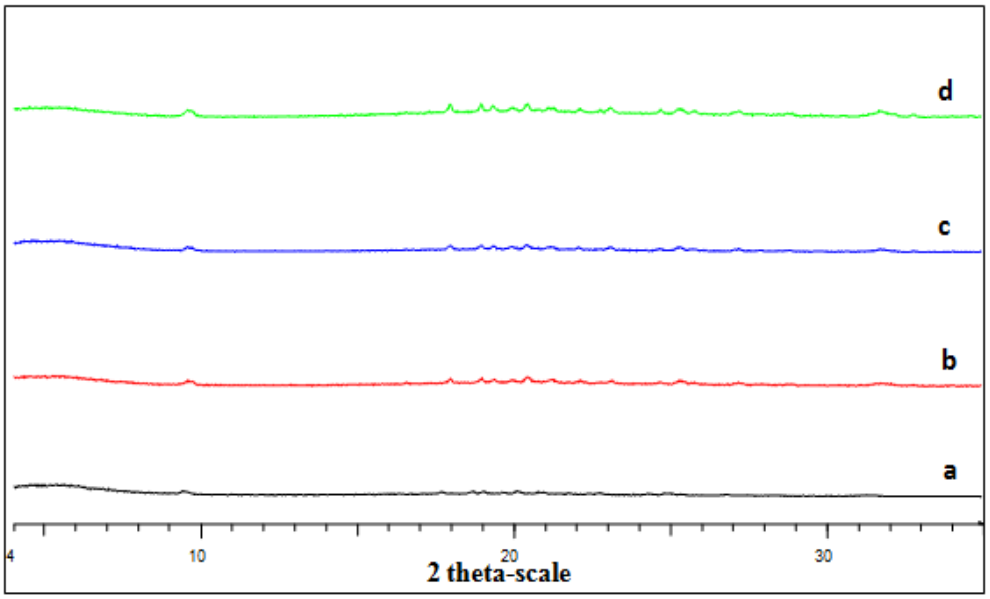

Figure 5.9: XRPD of lyophilised ketoconazole-mannitol-SLS formulations sprayed with different volumes of acetone/isopropyl alcohol (50/50% v/v) solvent system 0 ml (a); 2 ml (b); 4 ml (c); or 8 ml (d).

Figures 5.10-5.12 show the corresponding FT-IR spectra of the systems. For all three drugs, the absorption spectra of the sprayed formulations were identical to those of the corresponding non-sprayed samples with no differences between different volumes of the solvent system observed. This finding confirms that spraying with different volumes of the solvent system did not affect the stability of the solid dispersions of the drugs with the excipients supporting the DSC results. This stability explains the maintenance of dissolution rate of glibenclamide, spironolactone and ketoconazole formulations after the spraying process.

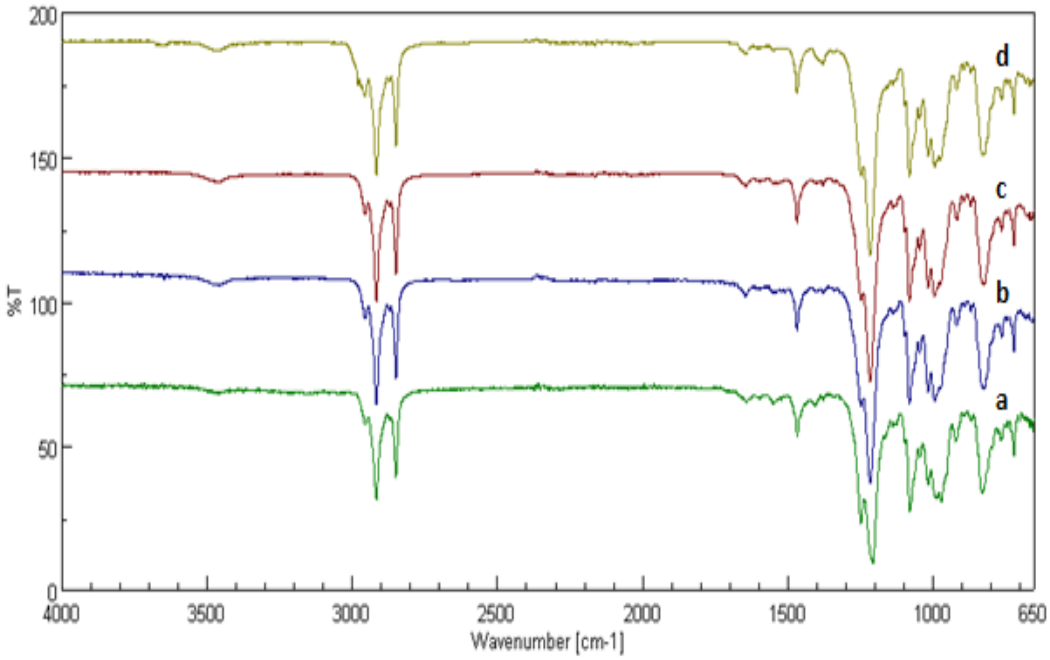

Figure 5.10: FT-IR of lyophilised glibenclamide-SLS formulations sprayed with different volumes of acetone/isopropyl alcohol (50/50% v/v) solvent system 0 ml (a); 2 ml (b); 4 ml (c); or 8 ml (d).

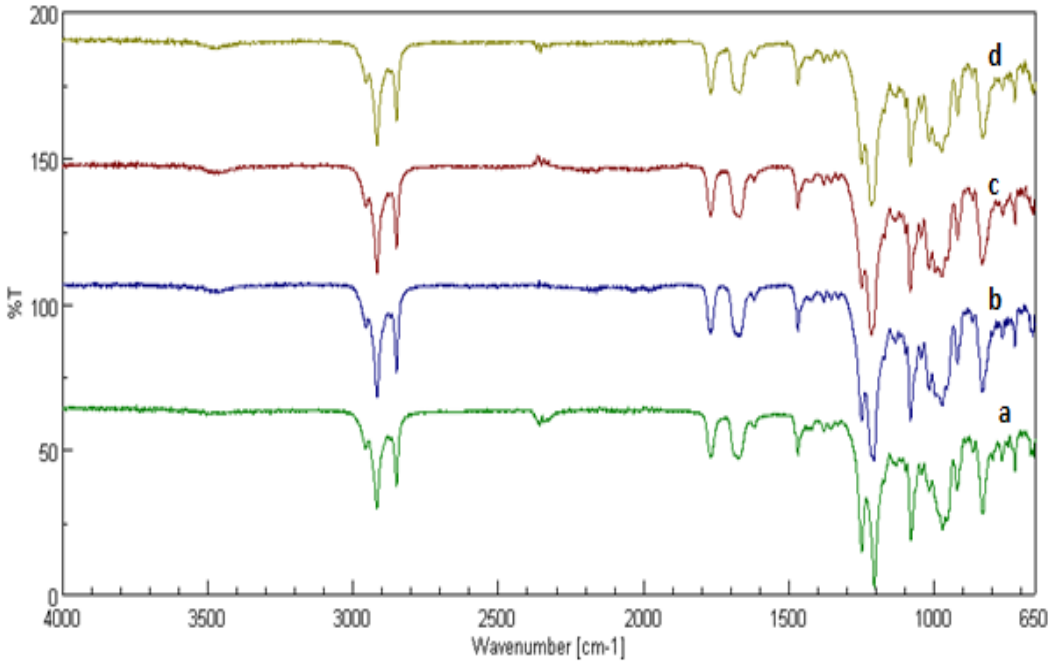

Figure 5.11: FT-IR of lyophilised spironolactone-SLS formulations sprayed with different volumes of acetone/isopropyl alcohol (50/50% v/v) solvent system 0 ml (a); 2 ml (b); 4 ml (c); or 8 ml (d).

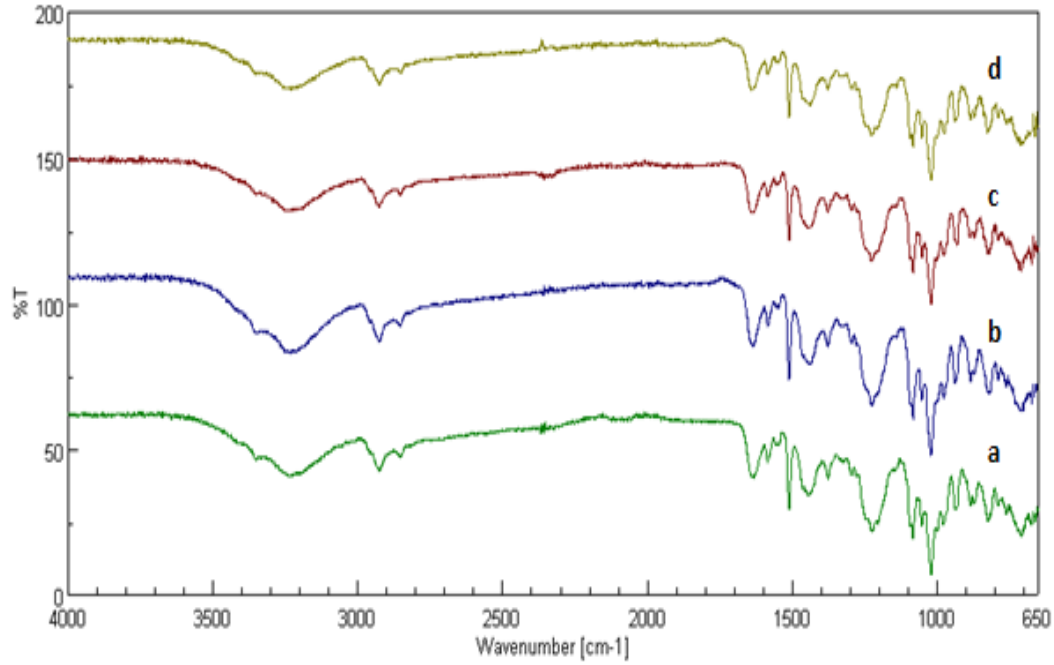

Figure 5.12: FT-IR of lyophilised ketoconazole-mannitol-SLS formulations sprayed with different volumes of acetone/isopropyl alcohol (50/50% v/v) solvent system 0 ml (a); 2 ml (b); 4 ml (c); or 8 ml (d).

5.4.1.3 Effect of process drying time on physical characteristics of lyophilised glibenclamide, spironolactone and ketoconazole capsule formulations sprayed with 50% v/v acetone/isopropyl alcohol solvent system

The DSC thermograms of glibenclamide, spironolactone and ketoconazole formulations after spraying of capsules with 4 ml (per each capsule) of 50% v/v acetone/isopropyl alcohol solvent system and drying for 10, 25, 40 and 60 minutes are illustrated in Figures 5.13-5.15. For all three drugs, the thermograms of the formulations dried for different times are identical to those of the corresponding non-sprayed samples. This finding suggests the stability of all three drug solid dispersions on being dried for different times after spraying of the solvent system.

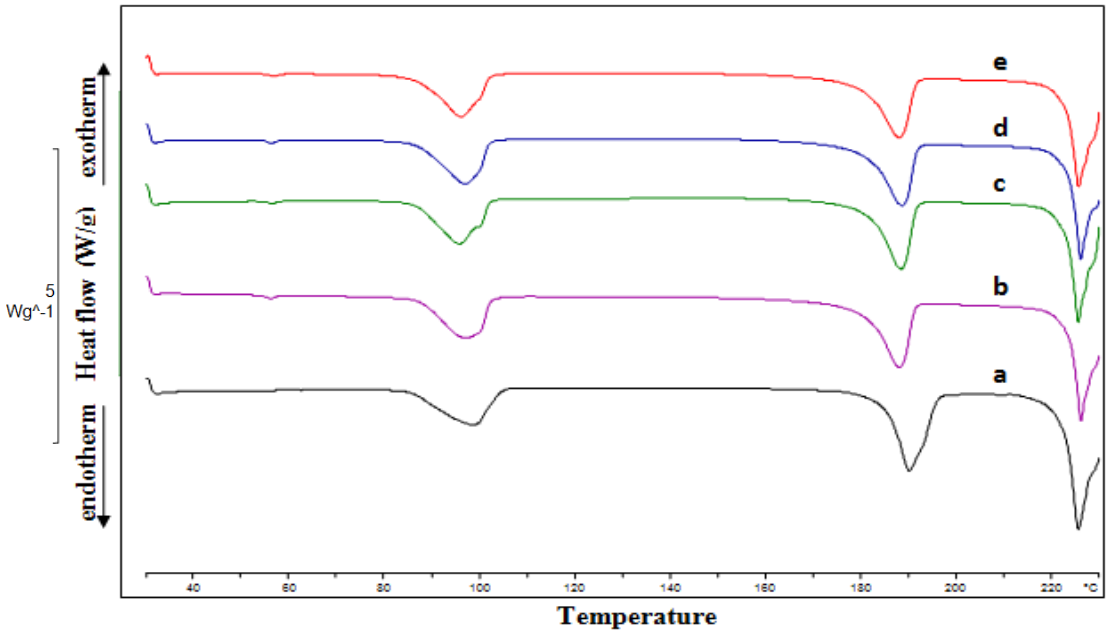

Figure 5.13: DSC of lyophilised glibenclamide-SLS formulations sprayed with 4 ml of acetone/isopropyl alcohol (50/50% v/v) solvent system and dried for different times non-sprayed (a); 10 (b); 25 (c); 40 (d); 60 (e) minutes.

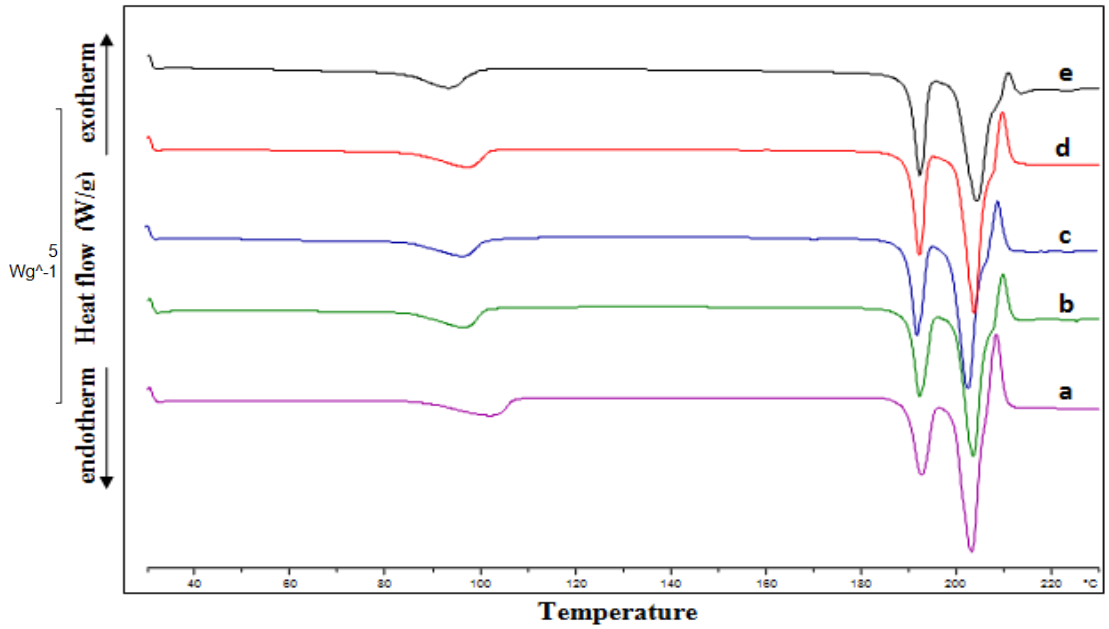

Figure 5.14: DSC of lyophilised spironolactone-SLS formulations sprayed with 4 ml of acetone/isopropyl alcohol (50/50% v/v) solvent system and dried for different times non-sprayed (a); 10 (b); 25 (c); 40 (d); 60 (e) minutes.

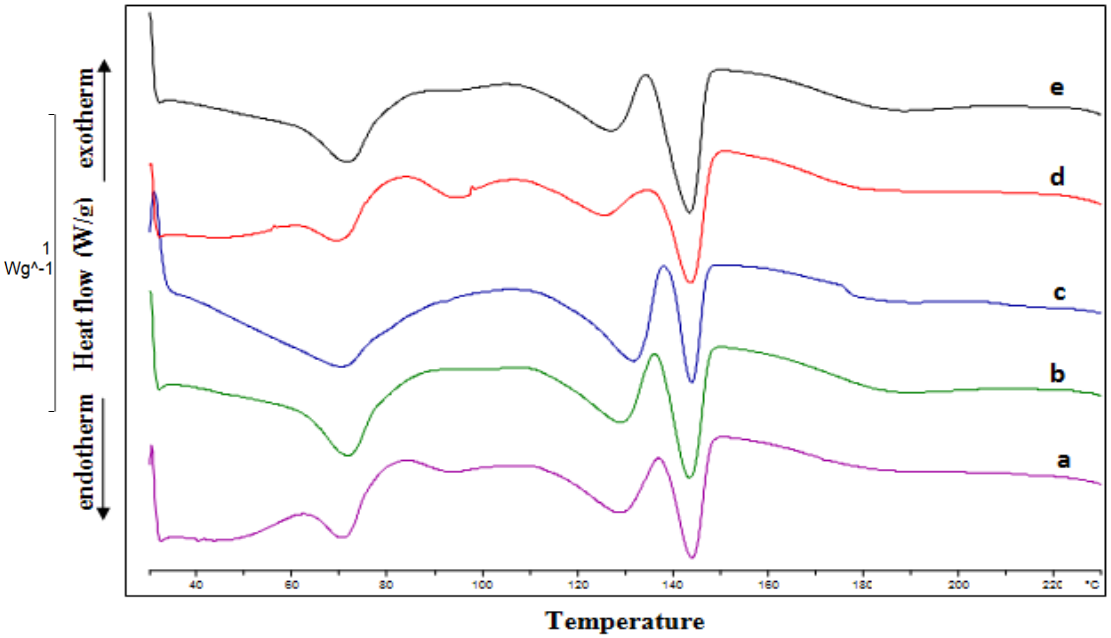

Figure 5.15: DSC of lyophilised ketoconazole-mannitol-SLS formulations sprayed with 4 ml of acetone/isopropyl alcohol (50/50% v/v) solvent system and dried for different times non-sprayed (a); 10 (b); 25 (c); 40 (d); 60 (e) minutes.

The corresponding XRPD patterns of the systems are represented in Figures 5.16-5.18. The diffractograms of glibenclamide and ketoconazole formulations dried for different times were similar to those of the corresponding non-sprayed formulations supporting the DSC results. This finding confirmed that drying time had no effect on the amorphous forms of both glibenclamide and ketoconazole included in their solid dispersions with the excipients. For spironolactone, it was found that drying time had no effect on the extent of spironolactone recrystallisation induced by the solvent system.

The corresponding FT-IR spectra are shown in Figures 5.19-5.21. The absorption spectra of the sprayed formulations for all three drugs were identical to those of the corresponding non-sprayed samples with no effect for the drying time observed. This finding confirmed that drying time did not affect the stability of the solid dispersions of the drugs with the excipients.

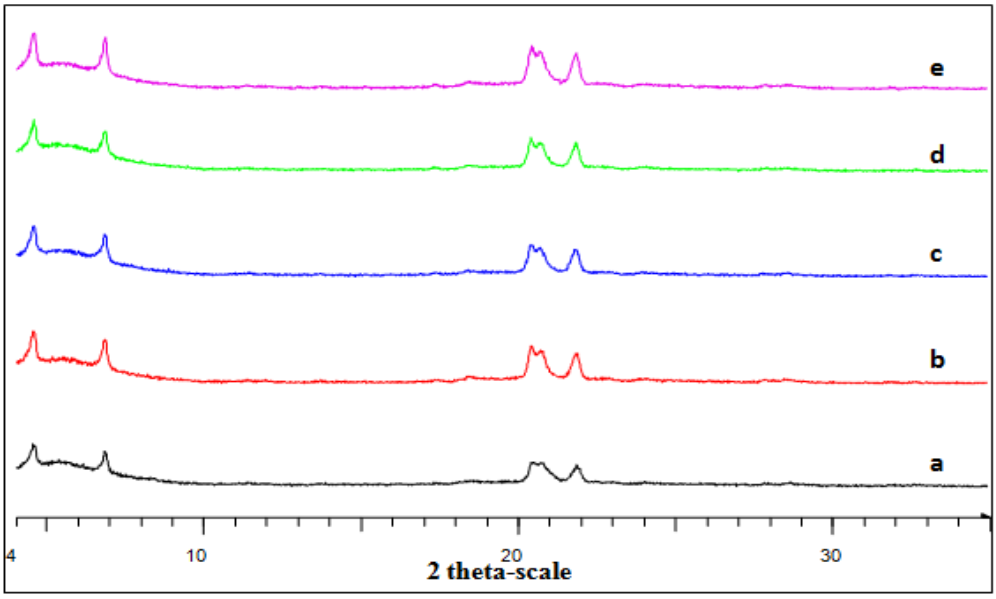

Figure 5.16: XRPD of lyophilised glibenclamide-SLS formulations sprayed with 4 ml of acetone/isopropyl alcohol (50/50% v/v) solvent system and dried for different times non-sprayed (a); 10 (b); 25 (c); 40 (d); 60 (e) minutes.

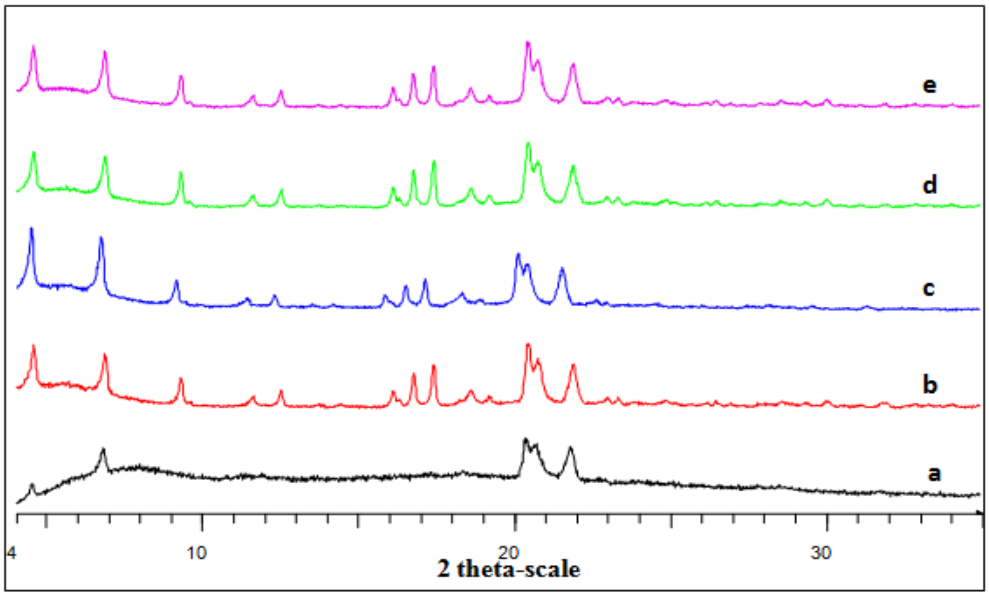

Figure 5.17: XRPD of lyophilised spironolactone-SLS formulations sprayed with 4 ml of acetone/isopropyl alcohol (50/50% v/v) solvent system and dried for different times non-sprayed (a); 10 (b); 25 (c); 40 (d); 60 (e) minutes.

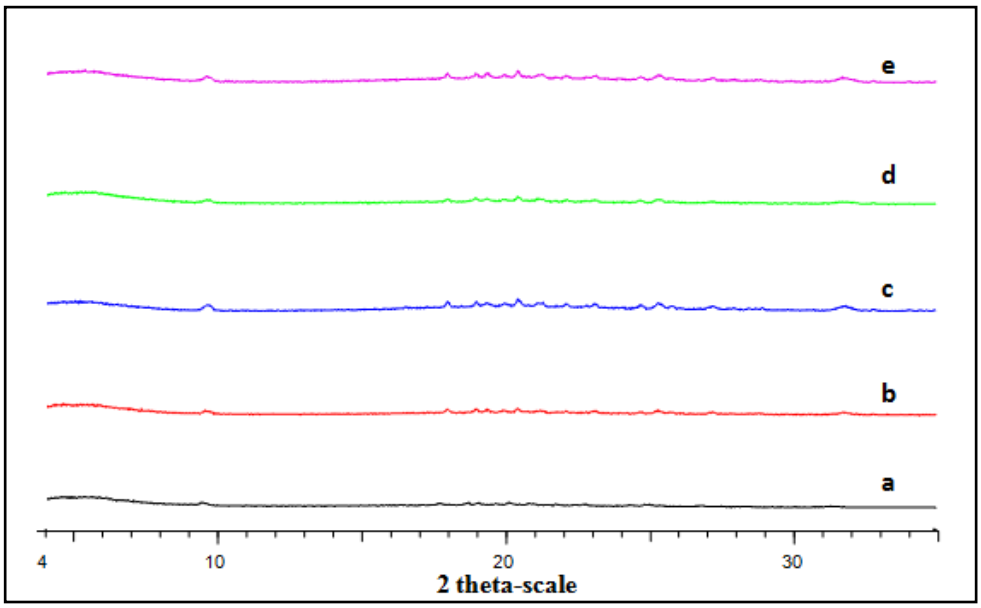

Figure 5.18: XRPD of lyophilised ketoconazole-mannitol-SLS formulations sprayed with 4 ml of acetone/isopropyl alcohol (50/50% v/v) solvent system and dried for different times non-sprayed (a); 10 (b); 25 (c); 40 (d); 60 (e) minutes.

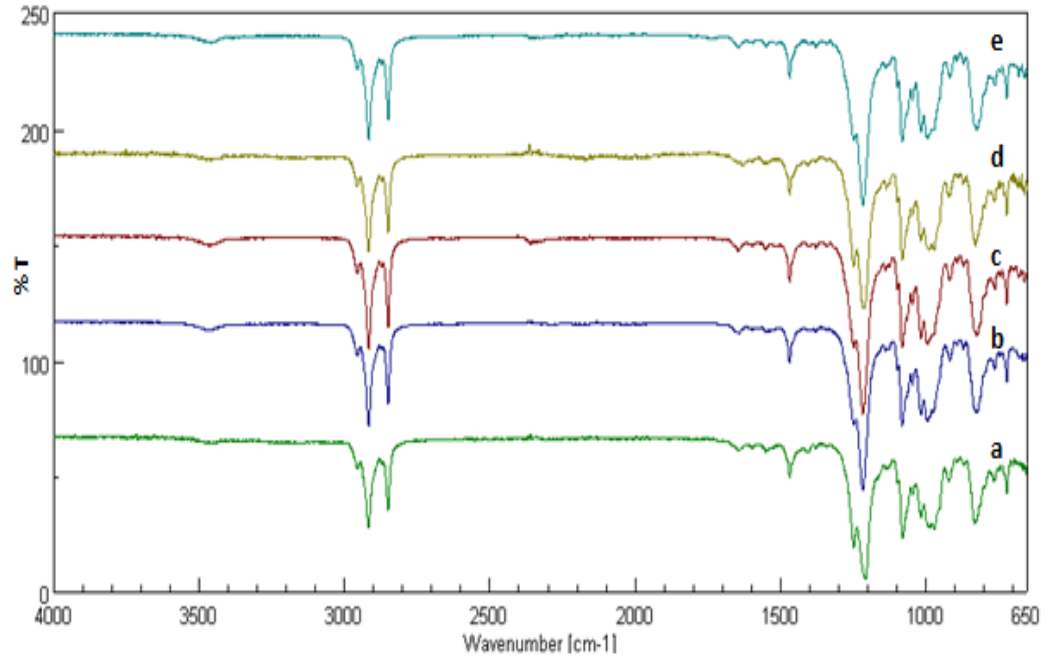

Figure 5.19: FT-IR of lyophilised glibenclamide-SLS formulations sprayed with 4 ml of acetone/isopropyl alcohol (50/50% v/v) solvent system and dried for different times non-sprayed (a); 10 (b); 25 (c); 40 (d); 60 (e) minutes.

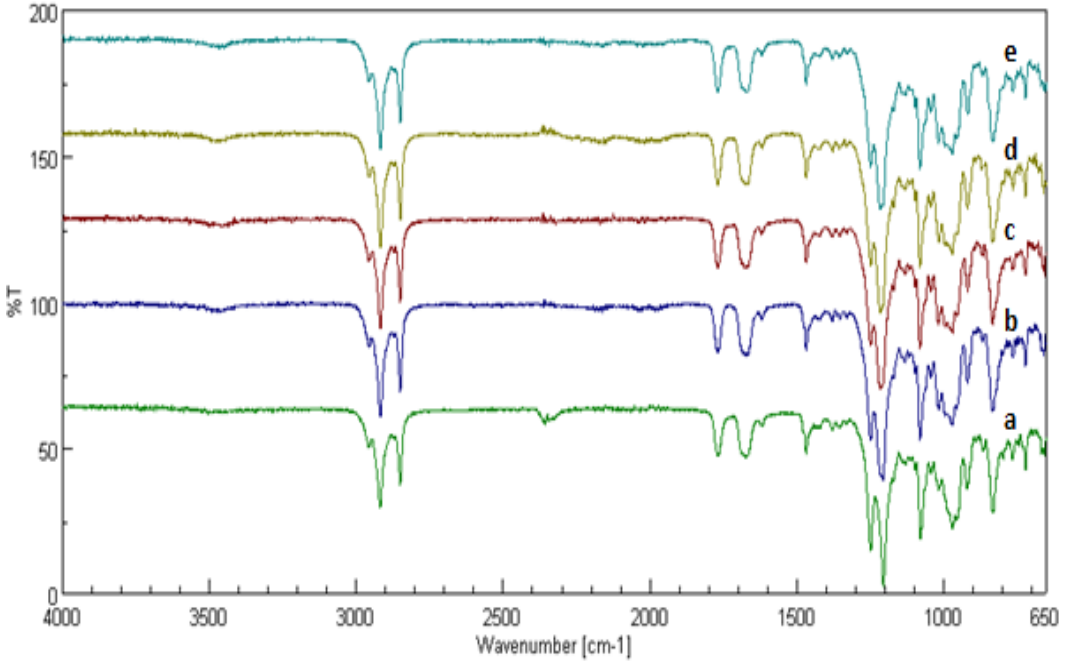

Figure 5.20: FT-IR of lyophilised spironolactone-SLS formulations sprayed with 4 ml of acetone/isopropyl alcohol (50/50% v/v) solvent system and dried for different times non-sprayed (a); 10 (b); 25 (c); 40 (d); 60 (e) minutes.

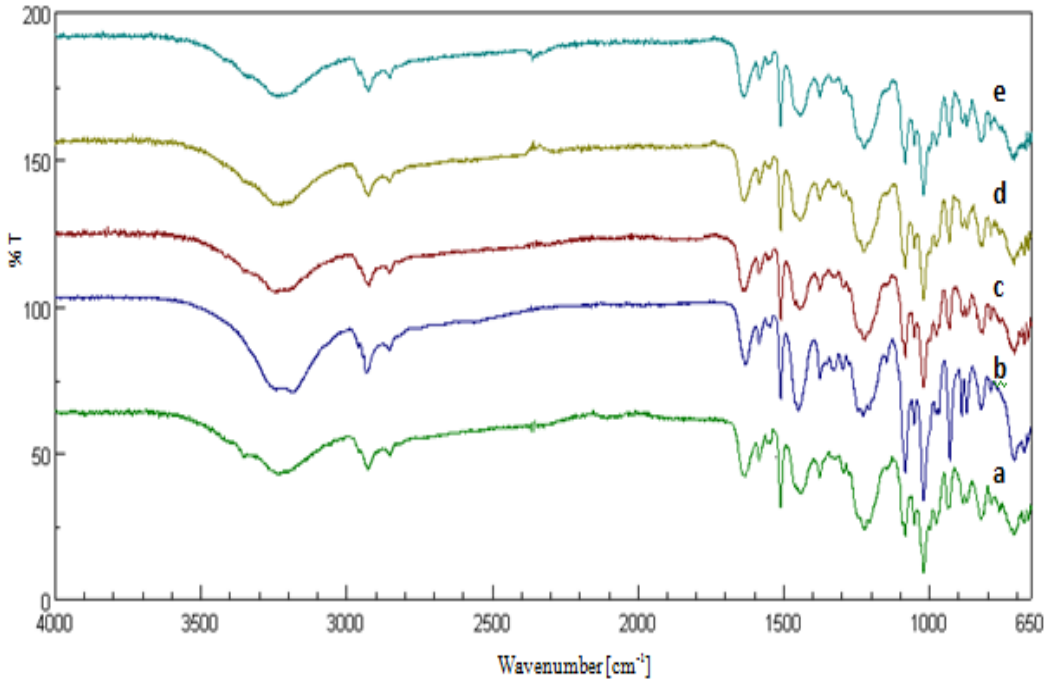

Figure 5.21: FT-IR of lyophilised ketoconazole-mannitol-SLS formulations sprayed with 4 ml of acetone/isopropyl alcohol (50/50% v/v) solvent system and dried for different times non-sprayed (a); 10 (b); 25 (c); 40 (d); 60 (e) minutes.

5.4.2 Ethanol/water (90/10% v/v)

5.4.2.1 Effect of application of different volumes of solvent on dissolution profiles of lyophilised glibenclamide, spironolactone and ketoconazole formulations

The dissolution profiles of glibenclamide, spironolactone and ketoconazole capsule formulations after spraying with different volumes of Ethanol/water (90/10% v/v) solvent system are illustrated in Figures 5.22-5.24 respectively. For all three drugs, the dissolution profiles were almost superimposed to those of the corresponding non-sprayed formulations with f_2 values > 50. This finding suggests the stability of their solid dispersions on being sprayed with this solvent system.

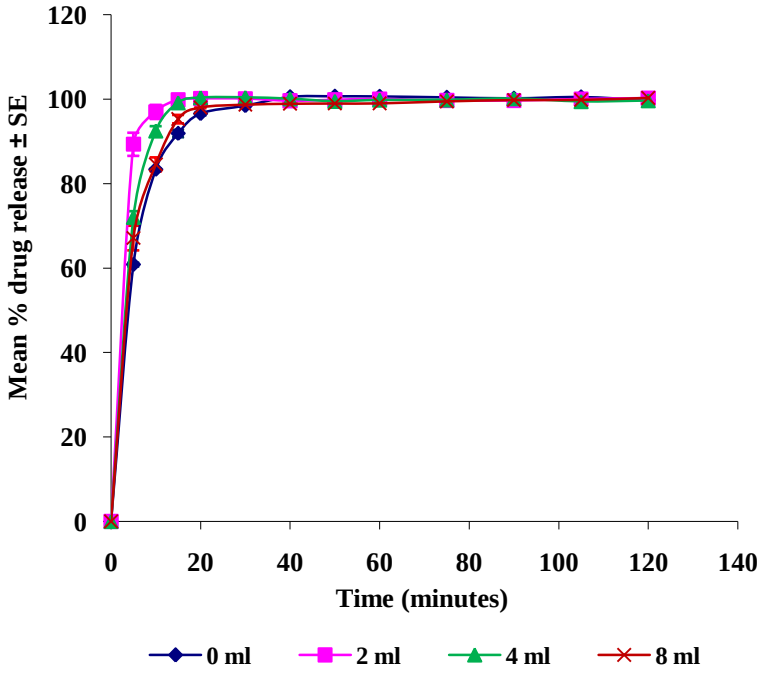

Figure 5.22: Effect of spraying different volumes of ethanol/water (90/10% v/v) solvent system on the dissolution profiles of lyophilised glibenclamide-SLS formulations (n=6).

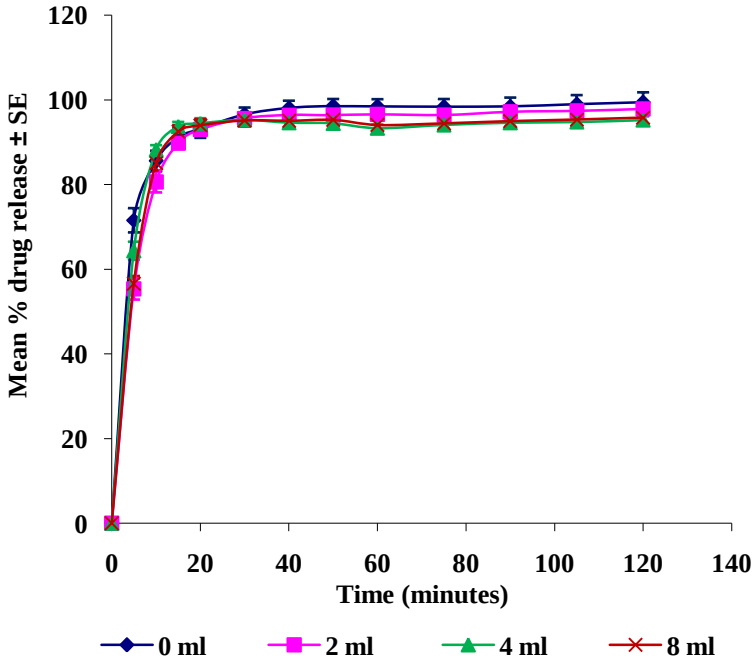

Figure 5.23: Effect of spraying different volumes of ethanol/water (90/10% v/v) solvent system on the dissolution profiles of lyophilised spironolactone-SLS formulations (n=6).

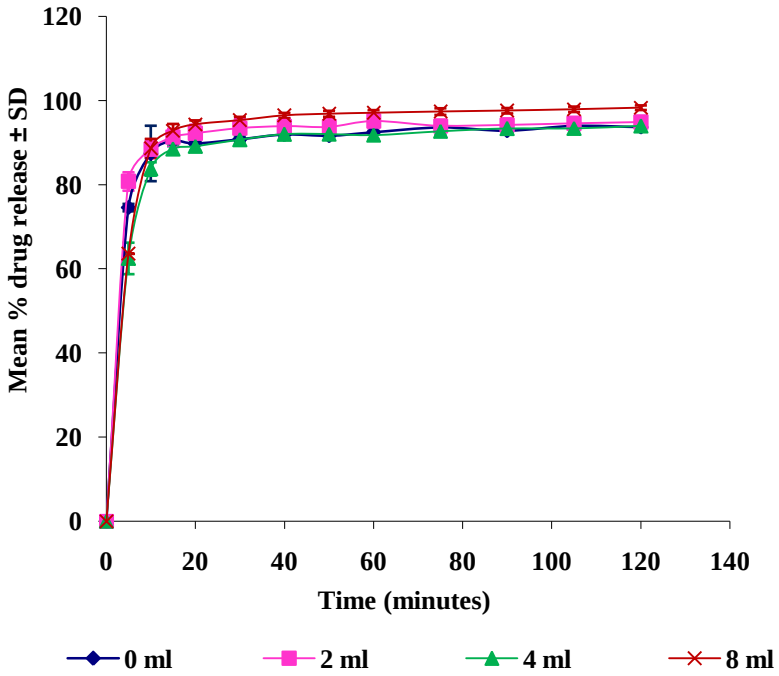

Figure 5.24: Effect of spraying different volumes of ethanol/water (90/10% v/v) solvent system on the dissolution profiles of lyophilised ketoconazole-mannitol-SLS formulations (n=6).

5.4.2.2 Physical characterisation of lyophilised glibenclamide, spironolactone and ketoconazole formulations that received different volumes of ethanol/water (90/10% v/v) solvent system

The DSC thermograms of lyophilised glibenclamide, spironolactone and ketoconazole formulations after spraying of the capsules with different volumes of ethanol/water (90/10% v/v) solvent system are illustrated in Figures 5.25-5.27 respectively. There were no differences observed between the thermograms of the sprayed formulations of glibenclamide and those of the corresponding non-sprayed samples. This finding suggests the stability of glibenclamide-SLS solid dispersion. The thermograms of the sprayed formulations of spironolactone displayed the appearance of a small shoulder for the drug melting endotherm (204ºC) which was more prominent in the case of spraying with 8 ml of the solvent system. This shoulder may represent the initiation of transformation to another polymorphic form of spironolactone as a result of exposure to the solvent vapour during the coating

process (see Section 5.4.1.2). It has been reported that spironolactone molecules can go through polymorphic transformation when crystallised from different solvents such as ethanol, acetone, ethyl acetate, methanol or acetonitrile (Agafonove et al, 1991, Neville et al., 1994; Beakstead et al., 1993; Berbenni et al., 1999). On the other hand, the thermograms of the sprayed ketoconazole formulations exhibited a shift in the melting endotherm at 144ºC towards the original melting temperature of ketoconazole crystals at 150ºC. This shift might be attributed to disturbance in the hydrogen bonding between the drug and the excipients in the solid dispersion formulations due to adsorption of the solvent system (especially water) during the spraying process. It has been reported that sorbed water had a drastic effect on the hydrogen bonding between felodipine and polyvinyl pyrrolidone leading to changes in the physical structures of their solid dispersion (Marsac et al., 2010). However, these changes had no effect on the dissolution rates of spironolactone or ketoconazole compared to the corresponding non-sprayed formulations (Section 5.4.2.1).

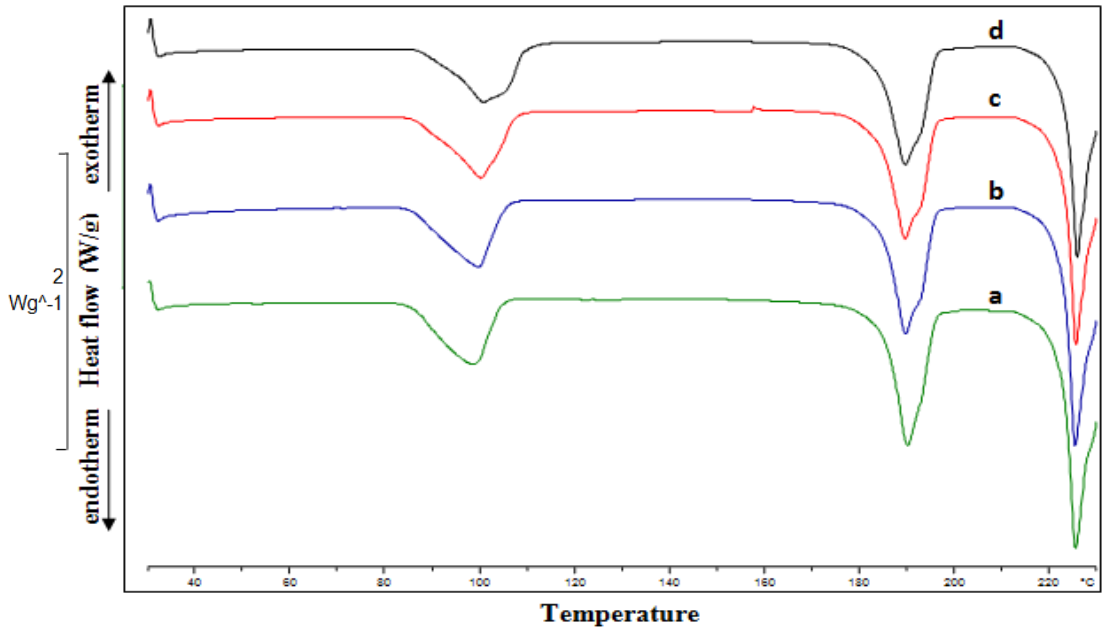

Figure 5.25: DSC of lyophilised glibenclamide-SLS formulations sprayed with different volumes of ethanol/water (90/10% v/v) solvent system 0 ml (a); 2 ml (b); 4 ml (c); or 8 ml (d).

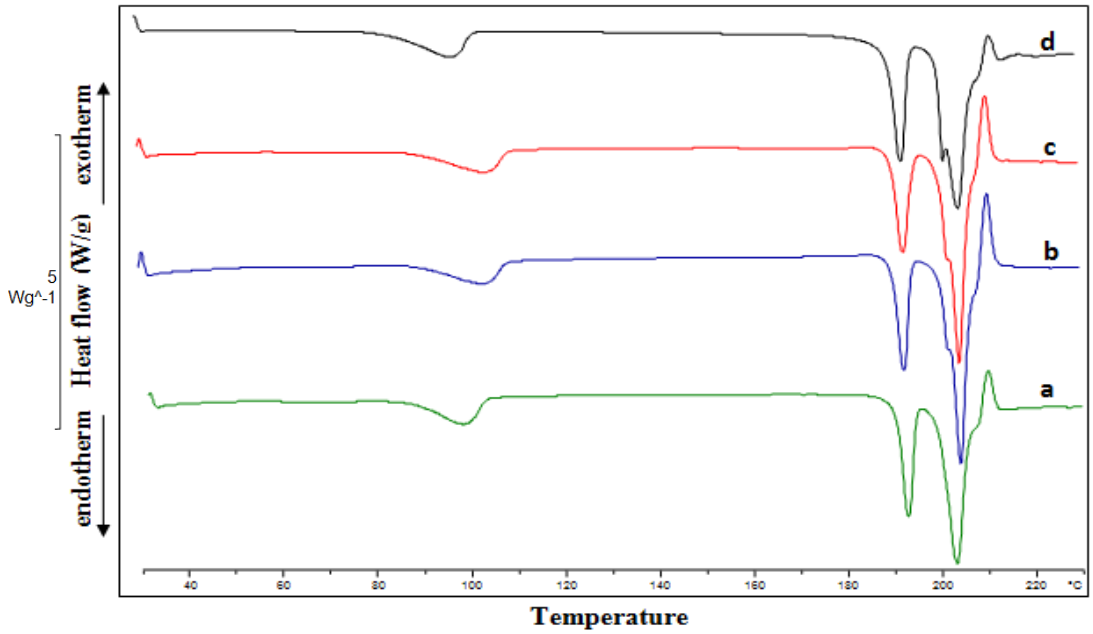

Figure 5.26: DSC of lyophilised spironolactone-SLS formulations sprayed with different volumes of ethanol/water (90/10% v/v) solvent system 0 ml (a); 2 ml (b); 4 ml (c); or 8 ml (d).

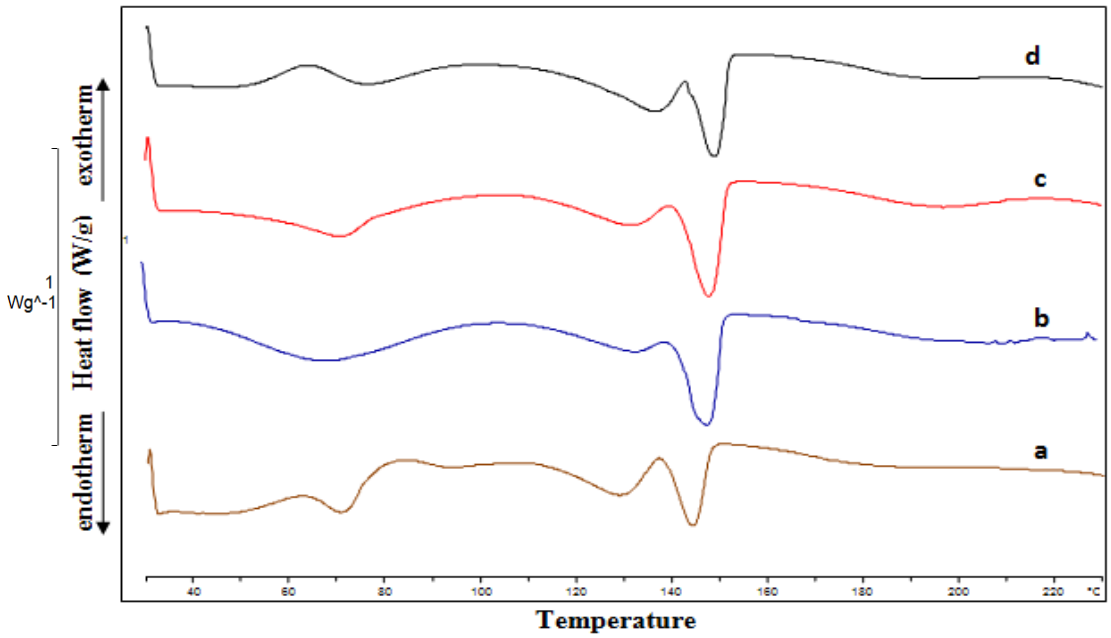

Figure 5.27: DSC of lyophilised ketoconazole-mannitol-SLS formulations sprayed with different volumes of ethanol/water (90/10% v/v) solvent system 0 ml (a); 2 ml (b); 4 ml (c); or 8 ml (d).

The corresponding XRPD patterns of the systems are represented in Figures 5.28-5.30. The diffractograms of the sprayed formulations of glibenclamide were identical to those of the non-sprayed samples with slight increase in the intensity of SLS peaks that may be attributed to low incidence of SLS recrystallisation. This finding supports the DSC results and suggests the stability of the amorphous form of glibenclamide in its solid dispersion with SLS upon spraying regardless the initial volume of the sprayed solvent system. The diffractograms of spironolactone formulations sprayed with 2 or 4 ml of the solvent system were similar to those of the corresponding non-sprayed samples showing no incidence of recrystallisation. This finding suggests the stability of spironolactone amorphous form in its solid dispersion with SLS upon being sprayed with small volumes of the solvent system. In contrast, the formulations sprayed with 8 ml of the solvent system displayed recrystallisation of spironolactone, highlighting the instability of the formulation after exposure to high volume of the solvent system. This finding supports the DSC results and is attributed to the effect of solvent vapour during the spraying process as explained in the DSC results. Yonemochi et al. (1999) has reported the recrystallisation of the amorphous (ground sample) form of deoxycholic acid on being heated or exposed to ethanol vapour. The diffractograms of the sprayed ketoconazole formulations were identical to those of the corresponding non-sprayed samples except for the appearance of few low intensity peaks suggesting a low incidence of recrystallisation. This finding confirmed the stability of the amorphous formulations of ketoconazole on being sprayed with different volumes of the solvent system. Van den Mooter et al. (2001) reported the stability of amorphous ketoconazole (glass) as it did not recrystallise even on being heated to 435 K at 5 K/min during DSC analysis.

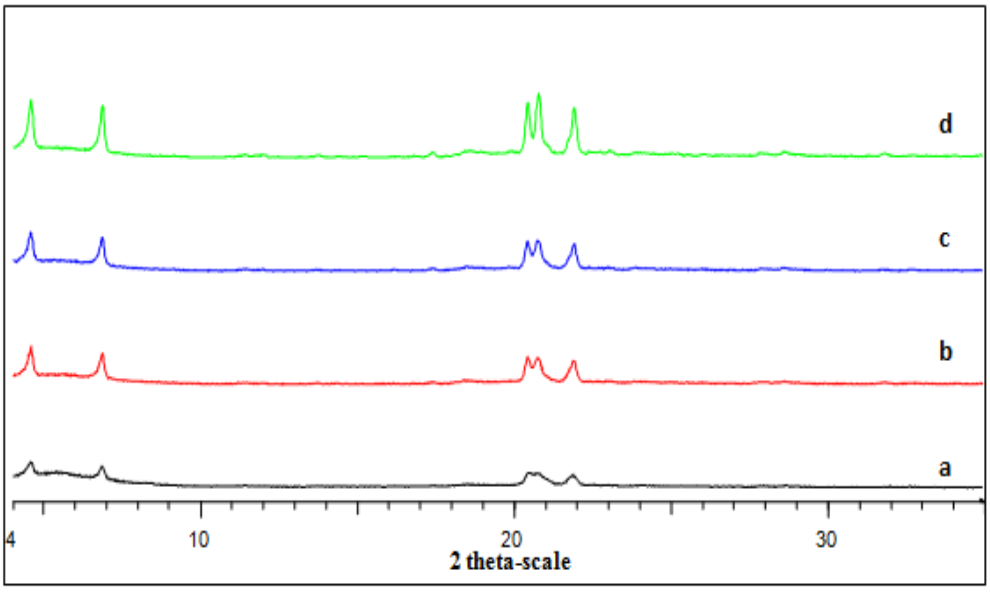

Figure 5.28: XRPD of lyophilised glibenclamide-SLS formulations sprayed with different volumes of ethanol/water (90/10% v/v) solvent system 0 ml (a); 2 ml (b); 4 ml (c); or 8 ml (d).

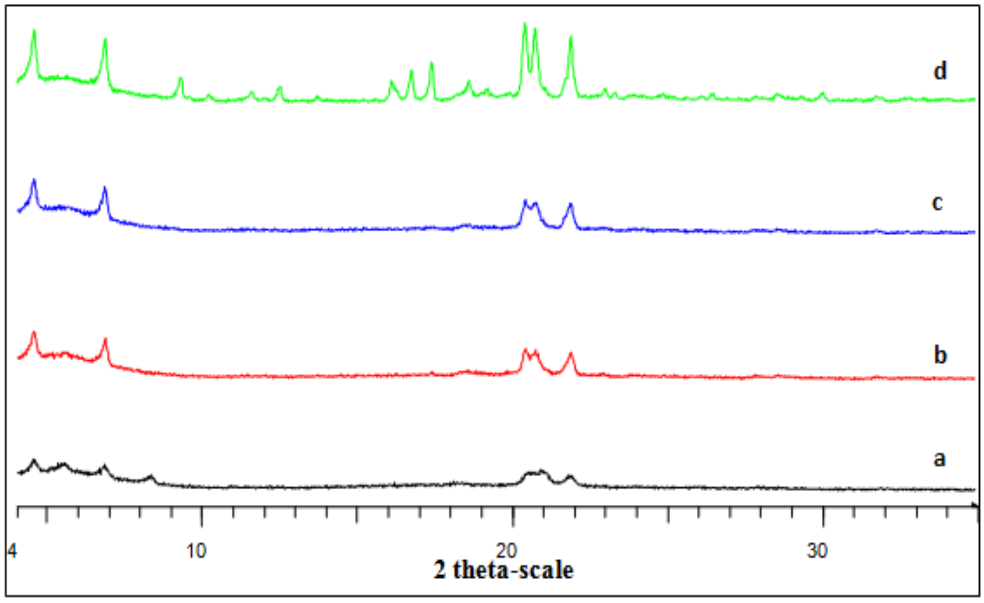

Figure 5.29: XRPD of lyophilised spironolactone-SLS formulations sprayed with different volumes of ethanol/water (90/10% v/v) solvent system 0 ml (a); 2 ml (b); 4 ml (c); or 8 ml (d).

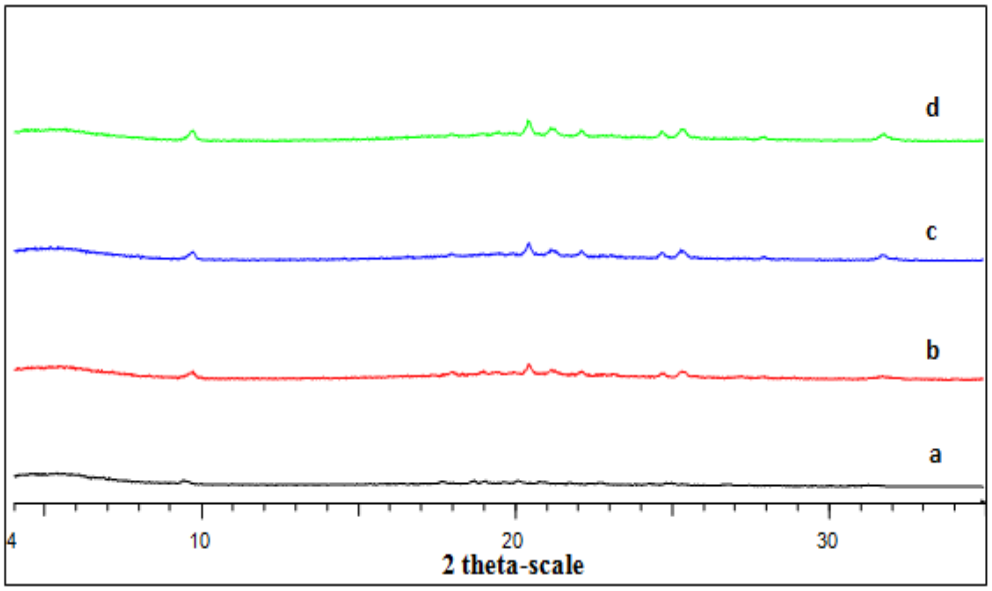

Figure 5.30: XRPD of lyophilised ketoconazole-mannitol-SLS formulations sprayed with different volumes of ethanol/water (90/10% v/v) solvent system 0 ml (a); 2 ml (b); 4 ml (c); or 8 ml (d).

Figures 5.31-5.33 show the corresponding FT-IR spectra. The absorption spectra of the sprayed formulations of glibenclamide were identical to that of the corresponding non-sprayed samples with no differences between different volumes of the solvent system applied. This finding supports the DSC and XRPD results indicating that spraying with different volumes of the solvent system did not affect the stability of the solid dispersion of glibenclamide with SLS. On the other hand, FT-IR spectra of spironolactone formulations sprayed with 2 or 4 ml of the solvent system displayed a shift of the characteristic C-O stretching vibrations of SLS from 1204 cm^{-1} to 1216 cm^{-1} (its original wave number in the spectrum of raw SLS) as well as an obvious decrease in the intensity of its shoulder. Furthermore, the spectrum showed the appearance of a broad peak around 3500 cm^{-1} highlighting water absorption. In addition to the above changes, the absorption spectrum of the formulations sprayed with 8 ml of the solvent system displayed the appearance of spironolactone characteristic peak at 1689 cm^{-1} corresponding to C=O stretching of the thioacetyl group and increase in the sharpness and intensity of spironolactone characteristic peak at 1672 cm^{-1} corresponding to C=O stretching of the C_6-ring. These changes may be attributed to the effect of the solvent vapour (during coating process) that

resulted in changes in the hydrogen bonding between spironolactone and SLS in the solid dispersion. This finding supports the DSC and XRPD results suggesting the instability of the spironolactone-SLS solid dispersion during spraying especially with 8 ml of the solvent system. For sprayed ketoconazole formulations, the absorption spectra were identical to those of the corresponding non-sprayed samples with no differences between the different volumes of the solvent system applied. This finding suggests that spraying with different solvent volumes did not affect the stability of the solid dispersion of ketoconazole with SLS.

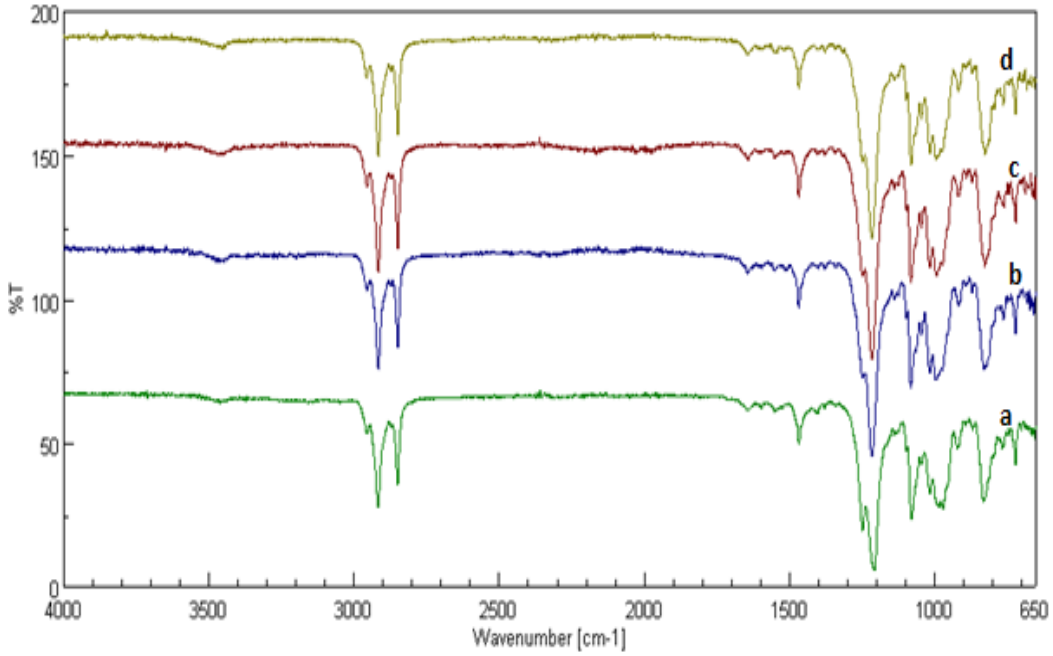

Figure 5.31: FT-IR of lyophilised glibenclamide-SLS formulations sprayed with different volumes of ethanol/water (90/10% v/v) solvent system 0 ml (a); 2 ml (b); 4 ml (c); or 8 ml (d).

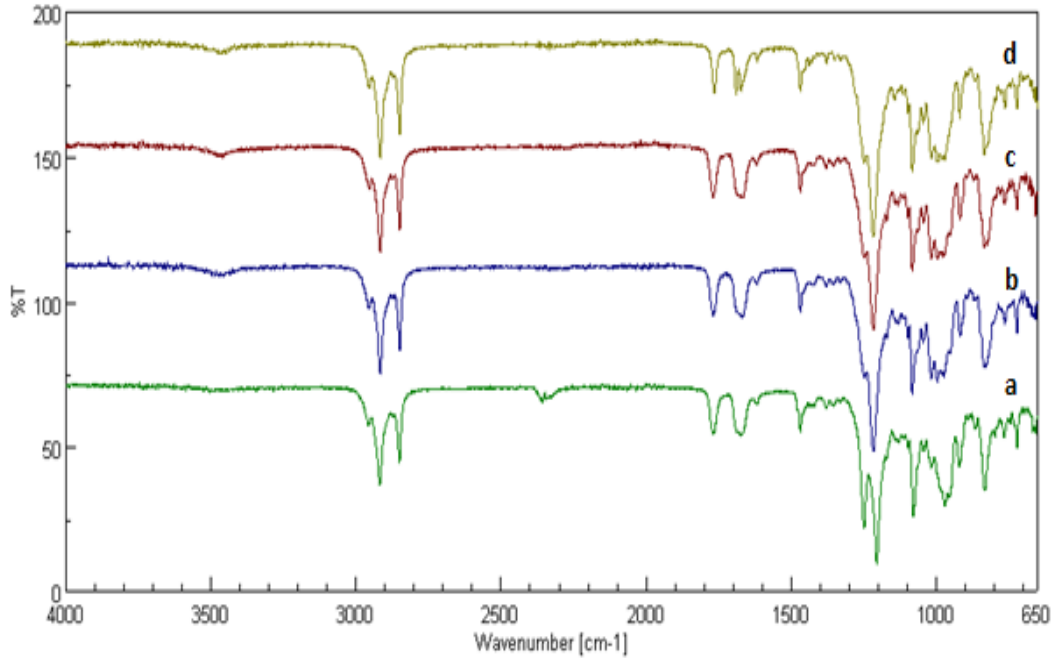

Figure 5.32: FT-IR of lyophilised spironolactone-SLS formulations sprayed with different volumes of ethanol/water (90/10% v/v) solvent system 0 ml (a); 2 ml (b); 4 ml (c); or 8 ml (d).

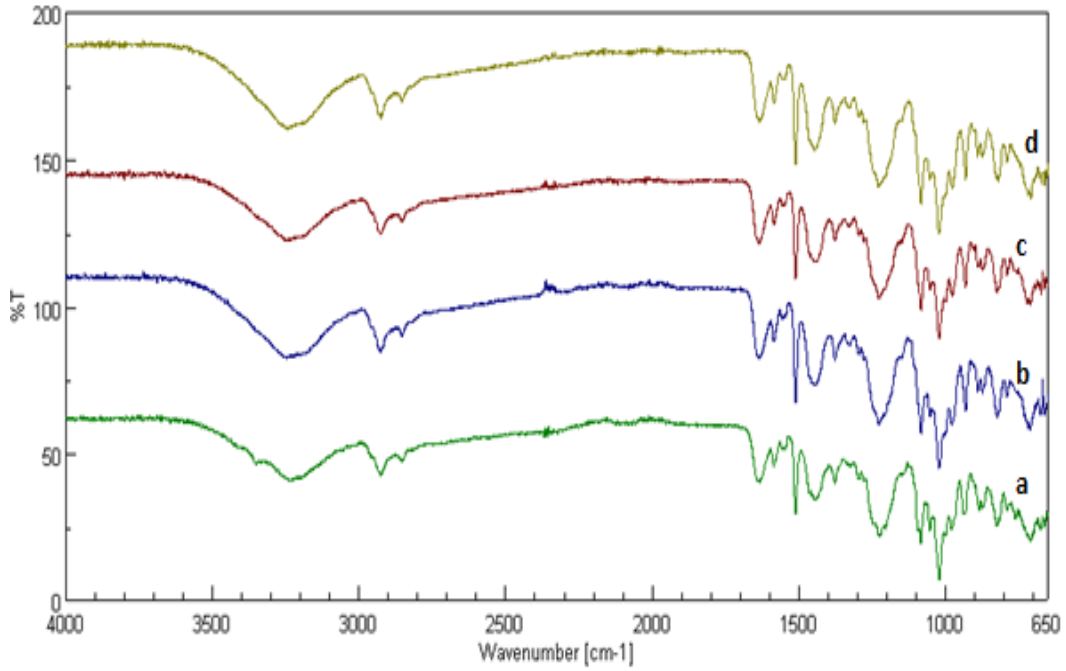

Figure 5.33: FT-IR of lyophilised ketoconazole-mannitol-SLS formulations sprayed with different volumes of ethanol/water (90/10% v/v) solvent system 0 ml (a); 2 ml (b); 4 ml (c); or 8 ml (d).

5.4.2.3 Effect of process drying time on physical characteristics of lyophilised glibenclamide, spironolactone and ketoconazole capsule formulations sprayed with ethanol/water (90/10% v/v) solvent system

The DSC thermograms of lyophilised glibenclamide, spironolactone and ketoconazole formulations after spraying capsules with 8 ml of ethanol/water (90/10% v/v) solvent system and drying for either 20, 60 or 90 minutes are illustrated in Figures 5.34-5.36. There were no differences between the thermograms of the glibenclamide formulations dried for different times and those of the corresponding non-sprayed samples. This finding confirms the stability of the glibenclamide-SLS solid dispersion. For spironolactone, the formulations dried for 20 minutes displayed the appearance of a shoulder for the drug melting endotherm (204ºC) while the formulations dried for 60 minutes exhibited dramatic decrease in the intensity of this shoulder (almost disappeared). This may be because longer time for drying facilitates evaporation of the majority of the solvent system decreasing its effect in initiating transformation of spironolactone to another polymorphic form. The reappearance of the shoulder in the thermograms of the formulations dried for 90 minutes may be attributed to prolonged exposure to the drying heat that reinitiate the transformation of spironolactone to another polymorphic form. These results are in accordance with what reported in literatures about the molecular flexibility of spironolactone and the ability of the drug to recrystallise in different polymorphic forms from different solvents and to go through structural rearrangement by the effect of heat (Neville et al., 1994; Beakstead et al., 1993; Berbenni et al., 1999). On the other hand, it was found that the thermograms of ketoconazole formulations dried for different times were identical. These thermograms showed a shift in the ketoconazole melting endotherm to 148ºC compared to the non-sprayed formulations (see Section 5.4.2.2). This finding indicates that prolongation of the drying time does not counteract the effect of solvent vapour inducing changes in the hydrogen bonding in ketoconazol-SLS solid dispersion.

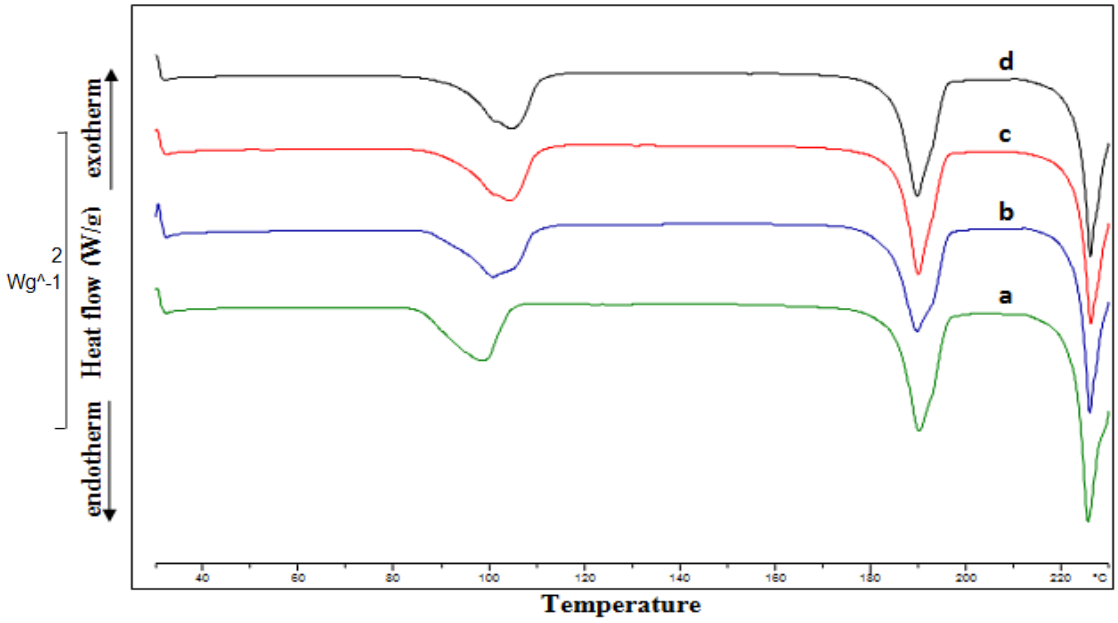

Figure 5.34: DSC of lyophilised glibenclamide-SLS formulations sprayed with 8 ml of ethanol/water (90/10% v/v) solvent system and dried for different times non-sprayed (a); 20 (b); 60 (c); 90 (d) minutes.

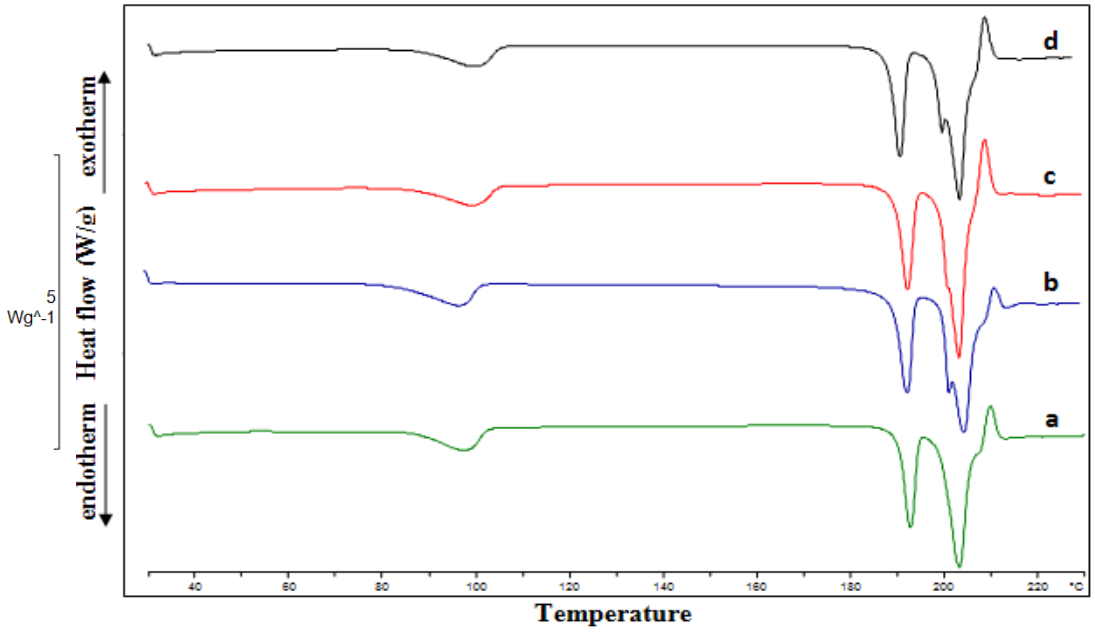

Figure 5.35: DSC of lyophilised spironolactone-SLS formulations sprayed with 8 ml of ethanol/water (90/10% v/v) solvent system and dried for different times non-sprayed (a); 20 (b); 60 (c); 90 (d) minutes.

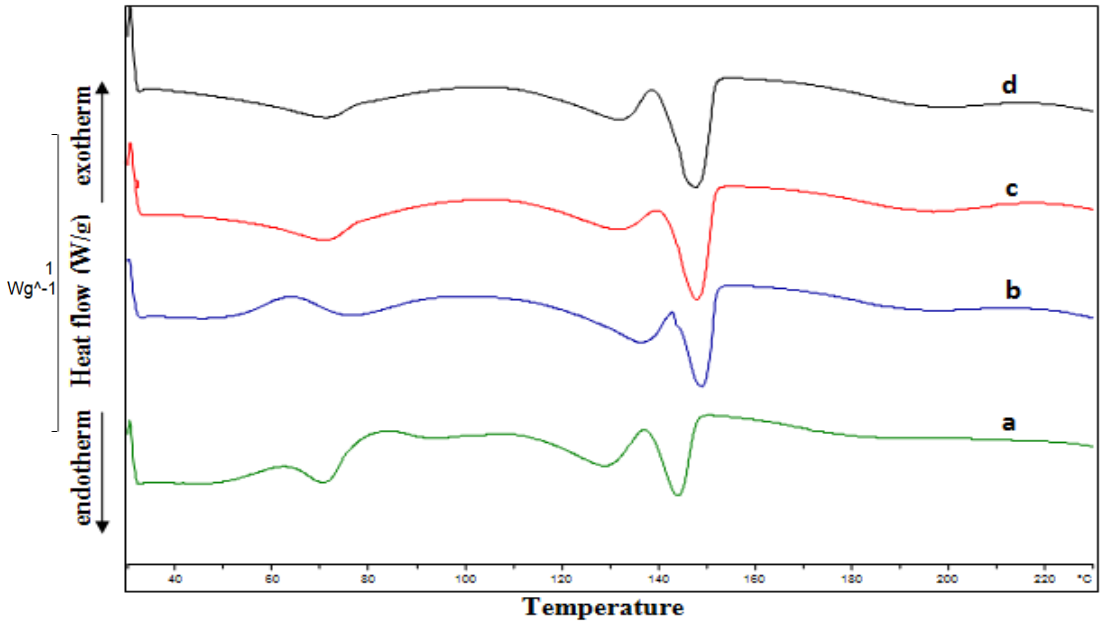

Figure 5.36: DSC of lyophilised ketoconazole-mannitol-SLS formulations sprayed with 8 ml of ethanol/water (90/10% v/v) solvent system and dried for different times non-sprayed (a); 20 (b); 60 (c); 90 (d) minutes.

The corresponding XRPD patterns of the systems are represented in Figures 5.37-5.39. For all three drugs, the diffractograms of the sprayed formulations dried for different times were identical. Therefore, increasing of the drying time did not affect the stability of glibenclamide solid dispersion or counteract spironolactone or ketoconazole recrystallisation induced by the effect of higher volume (8 ml) of the solvent system.

The above results are supported by the corresponding FT-IR spectra (Figures. 5.40-5.42). For all three drugs, it was found that the absorption bands of the formulations dried for different time periods were almost identical. However, increasing in the drying time did not prevent the changes in the spectrum of spironolactone formulations induced by spraying with high volume of the solvent system (8 ml).

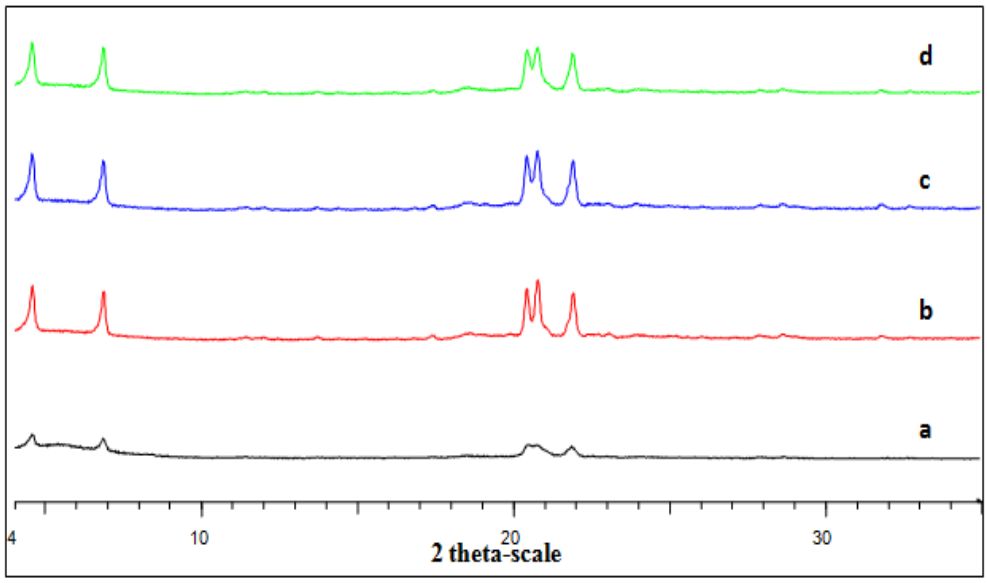

Figure 5.37: XRPD of lyophilised glibenclamide-SLS formulations sprayed with 8 ml of ethanol/water (90/10% v/v) solvent system and dried for different times non-sprayed (a); 20 (b); 60 (c); 90 (d) minutes.

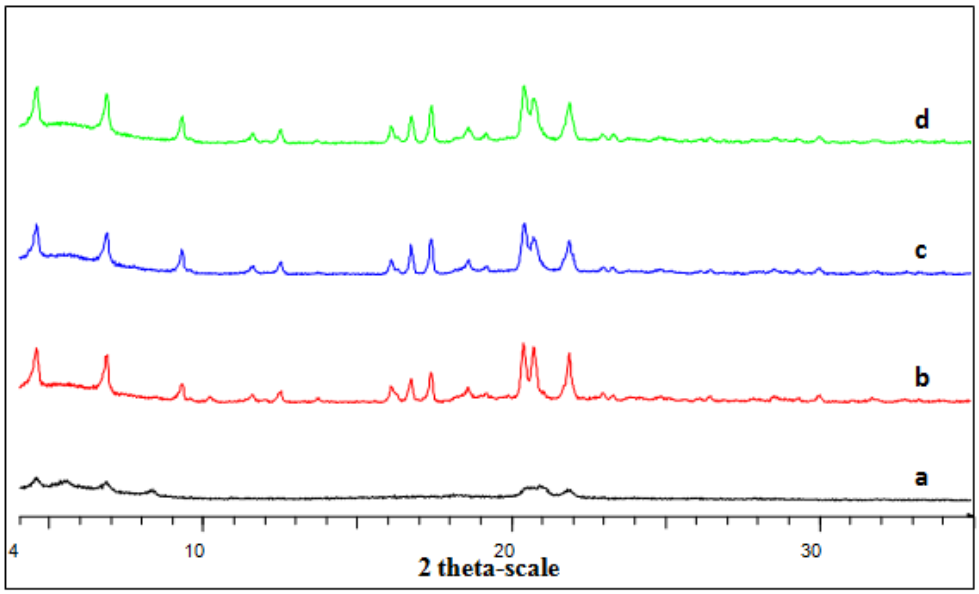

Figure 5.38: XRPD of lyophilised spironolactone-SLS formulations sprayed with 8 ml of ethanol/water (90/10% v/v) solvent system and dried for different times non-sprayed (a); 20 (b); 60 (c); 90 (d) minutes.

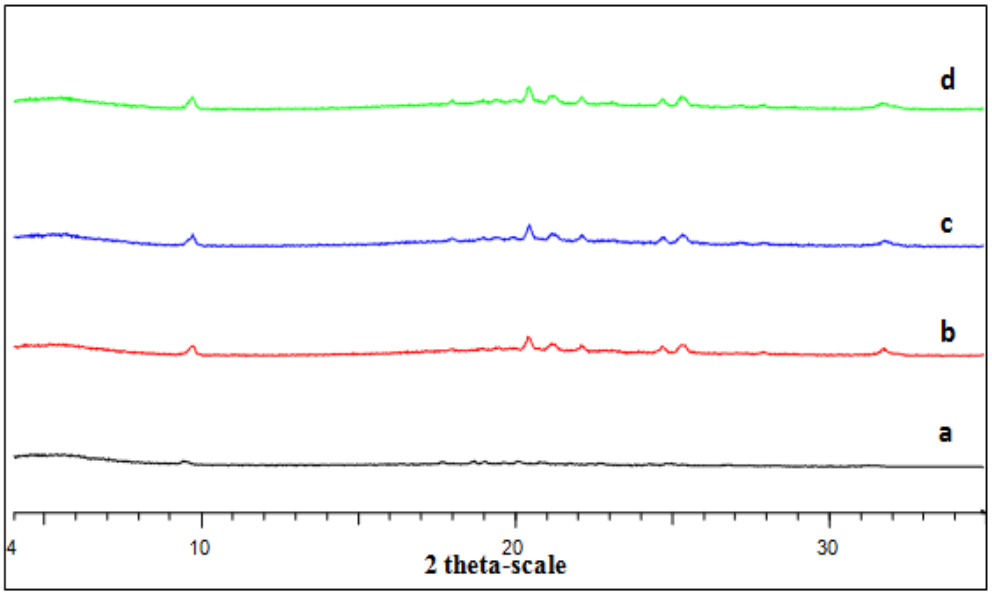

Figure 5.39: XRPD of lyophilised ketoconazole-mannitol-SLS formulations sprayed with 8 ml of ethanol/water (90/10% v/v) solvent system and dried for different times non-sprayed (a); 20 (b); 60 (c); 90 (d) minutes.

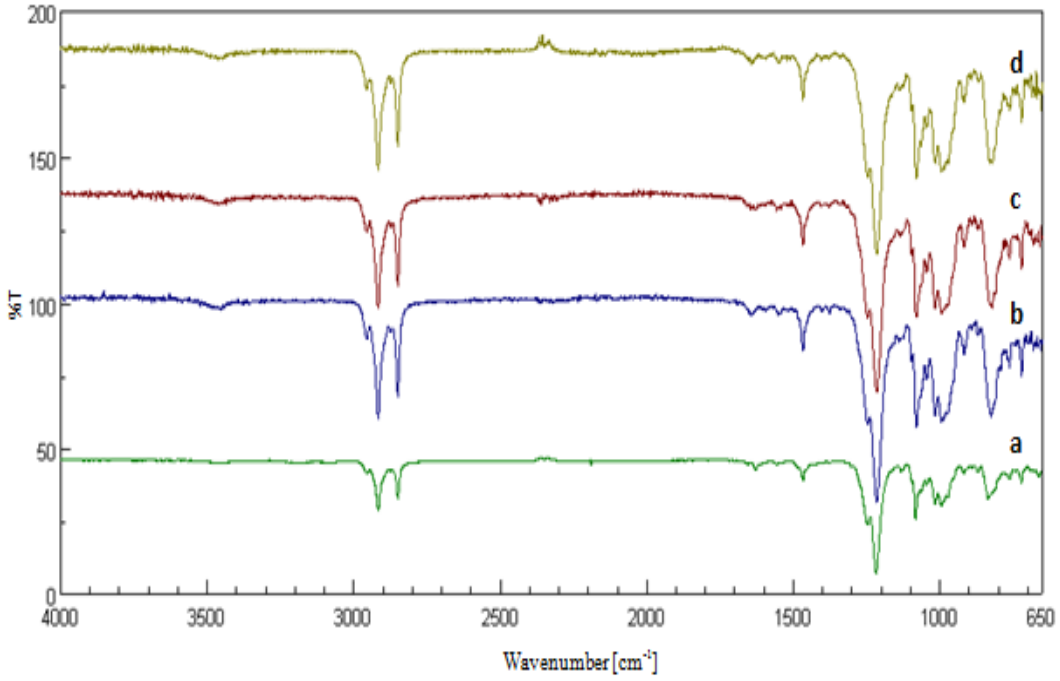

Figure 5.40: FT-IR of lyophilised glibenclamide-SLS formulations sprayed with 8 ml of ethanol/water (90/10% v/v) solvent system and dried for different times non-sprayed (a); 20 (b); 60 (c); 90 (d) minutes.

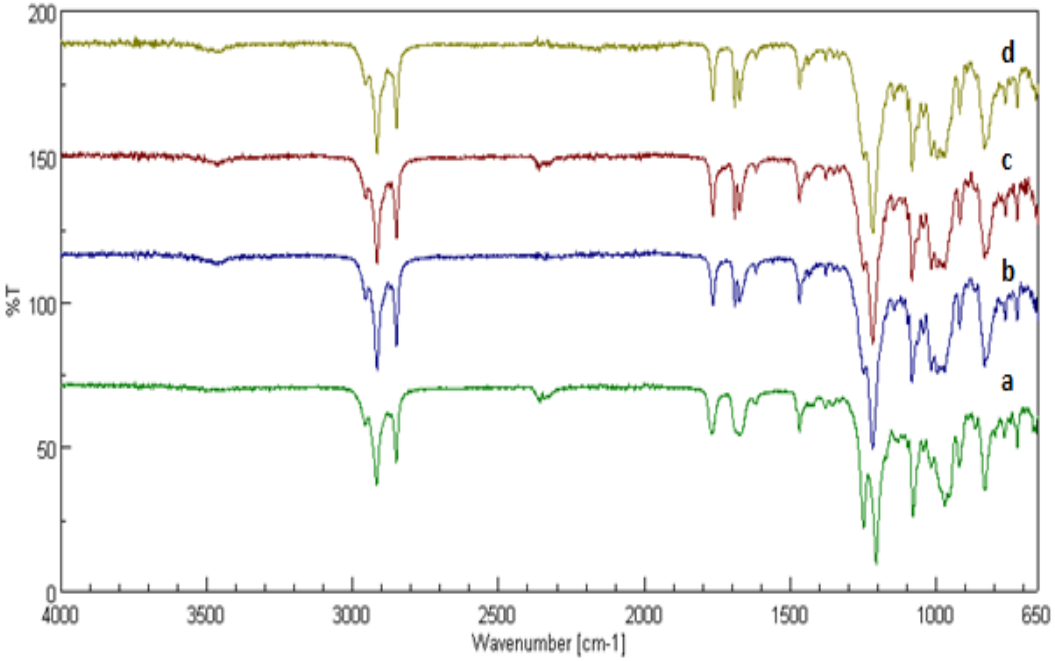

Figure 5.41: FT-IR of lyophilised spironolactone-SLS formulations sprayed with 8 ml of ethanol/water (90/10% v/v) solvent system and dried for different times non-sprayed (a); 20 (b); 60 (c); 90 (d) minutes.

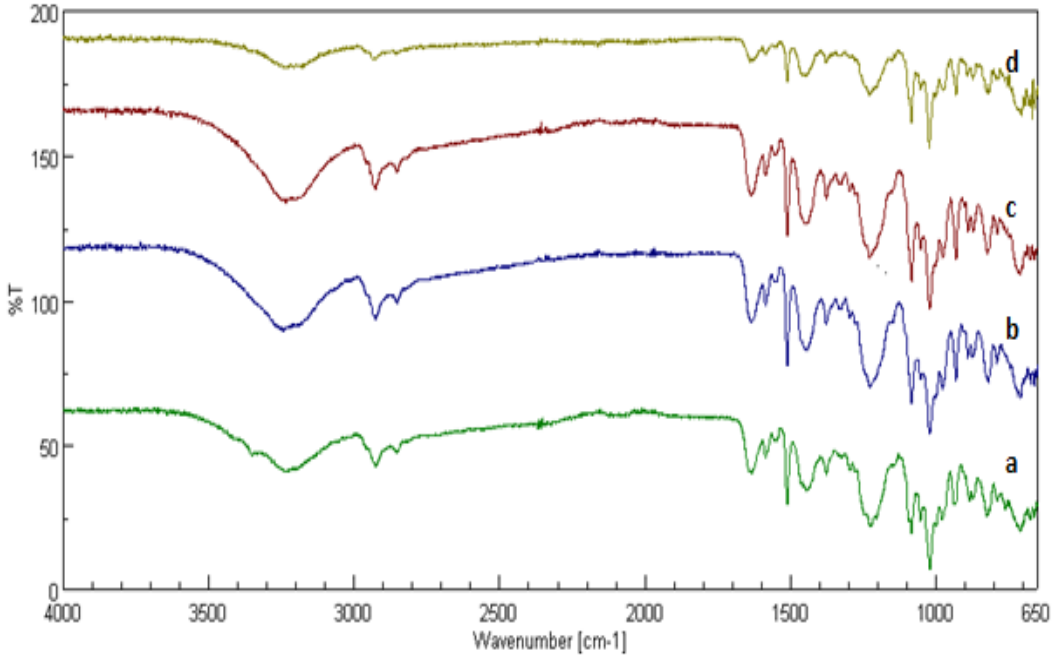

Figure 5.42: FT-IR of lyophilised ketoconazole-mannitol-SLS formulations sprayed with 8 ml of ethanol/water (90/10% v/v) solvent system and dried for different times non-sprayed (a); 20 (b); 60 (c); 90 (d) minutes.

5.4.3 Non-enteric coating

5.4.3.1 Effect of application of non-enteric coating system on dissolution profiles of lyophilised glibenclamide, spironolactone and ketoconazole capsule formulations

The dissolution profiles of lyophilised glibenclamide, spironolactone and ketoconazole formulations after coating with Opadry system are illustrated in Figures 5.43-5.45. Statistical analysis showed no significant differences between the dissolution profiles of the coated formulations of all three drugs and those of the corresponding non-coated formulations (f_2 > 50). Maintenance of the dissolution rates of the drugs after coating with Opadry coating system suggests the stability of their solid dispersions with the excipients.

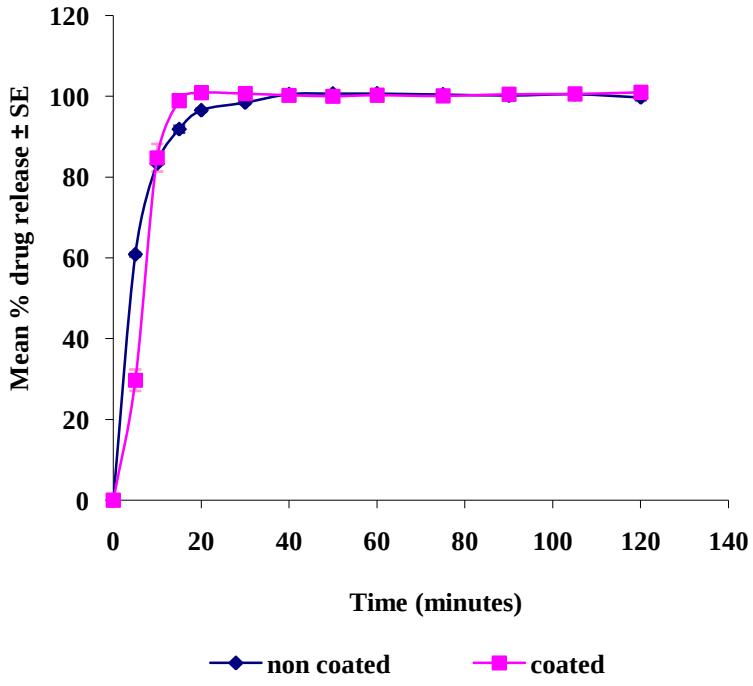

Figure 5.43: Dissolution profile of Opadry spray coated glibenclamide capsule formulations compared to the corresponding non-coated formulations (n=6).

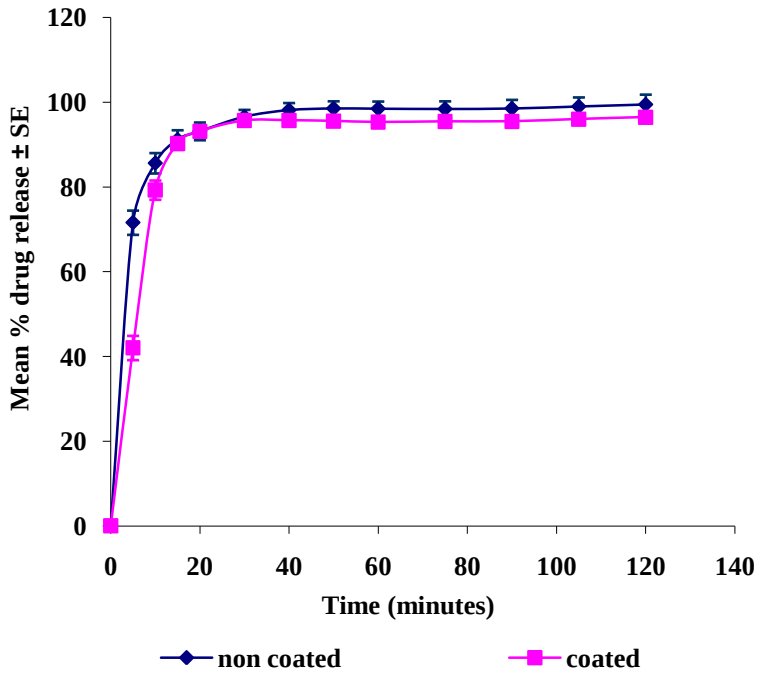

Figure 5.44: Dissolution profile of Opadry spray coated spironolactone capsule formulations compared to the corresponding non-coated formulations (n=6).

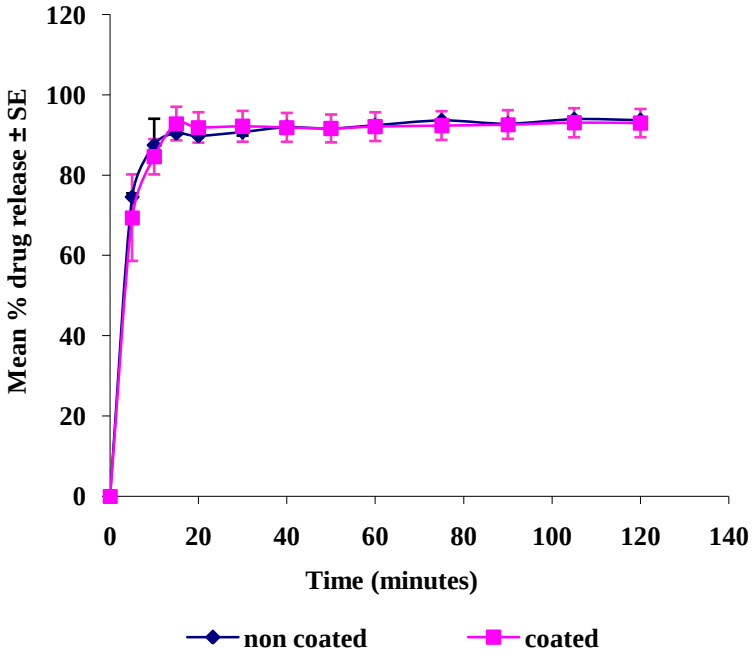

Figure 5.45: Dissolution profile of Opadry spray coated ketoconazole capsule formulations compared to the corresponding non-coated formulations (n=6).

5.4.3.2 Physical characterisation of lyophilised glibenclamide, spironolactone and ketoconazole formulations spray coated with non-enteric Opadry coating system

The DSC thermograms of glibenclamide, spironolactone and ketoconazole formulations after coating with Opadry system are illustrated in Figures 5.46-5.48. The thermograms of the coated glibenclamide or ketoconazole formulations were similar to those of the corresponding non-coated samples. This finding supports that the solid dispersion formulations of both drugs were stable on being coated with this system and explains the maintenance of the dissolution rate of glibenclamide and ketoconazole after the coating process (Section 5.4.3.1). The thermogram of the coated formulations of spironolactone displayed a severe decrease in the intensity of the melting endotherm of spironolactone at 204ºC as it appeared as a shoulder for another endotherm at 209ºC. This endotherm is close to that previously reported by Agafonove et al. (1991) and corresponds to the melting temperature of another polymorphic form of the drug (form II). This finding suggests the initiation of spironolactone transformation and supports the instability of the spironolactone-SLS solid dispersions on being coated with Opadry coating system. This was attributed to the effect of solvent vapour, during coating process, on the physical structure of the amorphous spironolactone. It has been reported that spironolactone molecules can go through polymorphic transformation when crystallised from different solvents such as ethanol, acetone, ethyl acetate, methanol or acetonitrile (Agafonove et al, 1991; Neville et al., 1994; Beakstead et al., 1993; Berbenni et al., 1999). Furthermore, the thermogram of the coated formulations showed a small endothermic peak at 162ºC which needs further investigations for interpretation. Similar endotherms has been reported by Agafonove et al. (1991) at 132ºC corresponding to desolvation of the spironolactone solvates that were produced during crystallisation of the drug from different solvents. Neville et al. (1994) have reported desolvation temperatures of some spironolactone solvates at 132.8ºC, 136.3ºC, 92.6ºC and 151.0ºC.

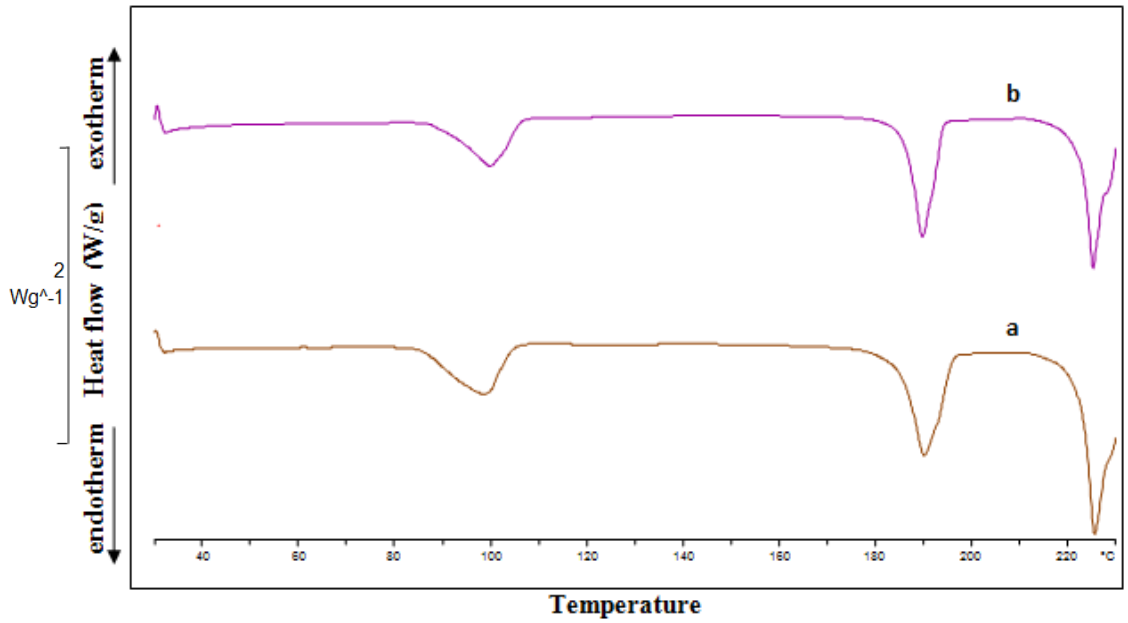

Figure 5.46: DSC of lyophilised glibenclamide-SLS formulations spray coated with non-enteric Opadry coating system (a) compared with the non-coated formulations (b).

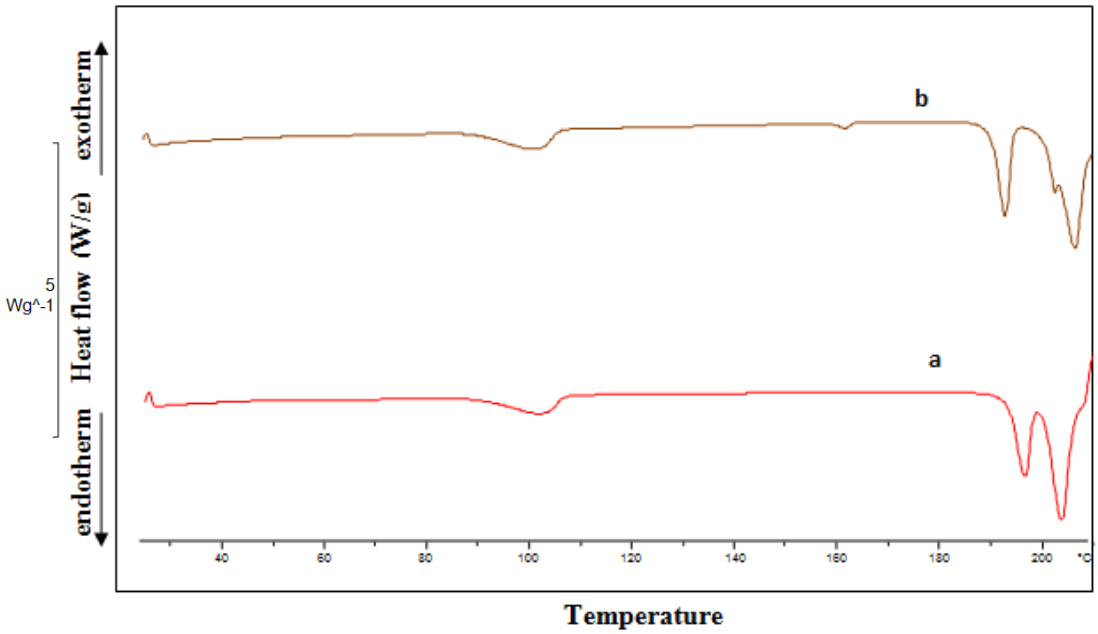

Figure 5.47: DSC of lyophilised spironolactone-SLS formulations spray coated with non-enteric Opadry coating system (a) compared with the non-coated formulations (b).

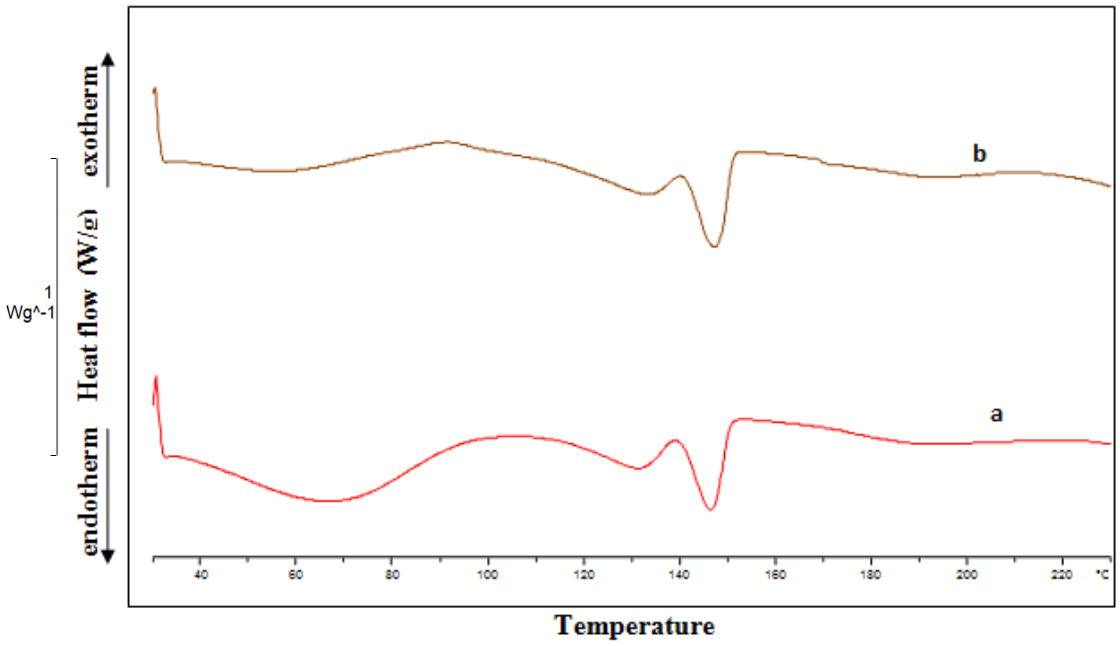

Figure 5.48: DSC of lyophilised ketoconazole-mannitol-SLS formulations spray coated with non-enteric Opadry coating system (a) compared with the non-coated formulations (b).

The corresponding XRPD patterns are shown in Figures 5.49-5.51. The diffractograms of the coated glibenclamide or ketoconazole formulations were similar to those of the corresponding non-coated samples. This result supports the DSC results and suggests the stability of the amorphous form of glibenclamide and ketoconazole in their solid dispersion formulations upon application of Opadry non-enteric coating system. On the other hand, the diffractogram of the coated spironolactone formulations showed a low incidence of recrystallisation which had no effect on the dissolution rate of spironolactone (Section 5.4.3.1).

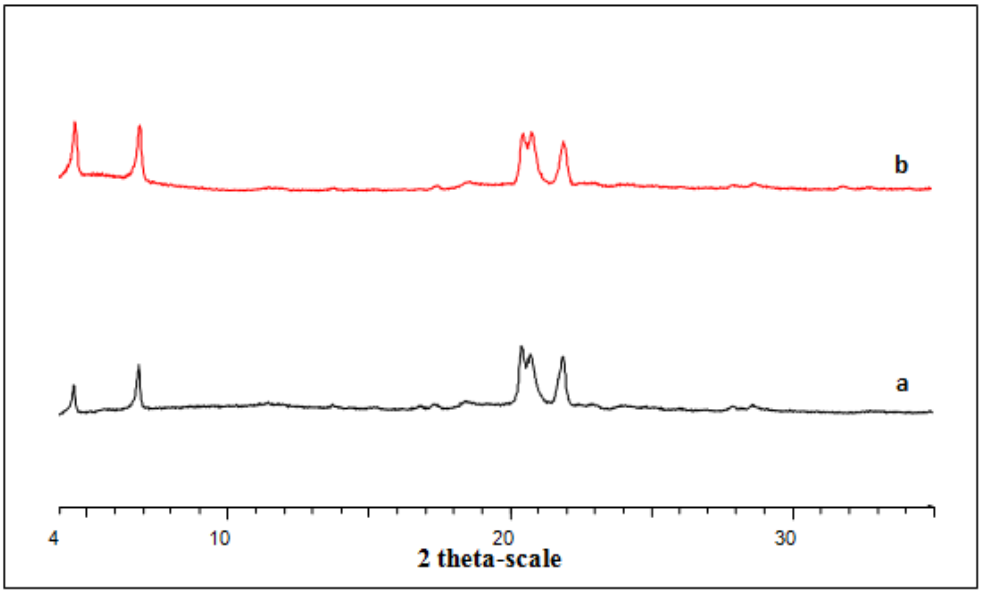

Figure 5.49: XRPD of lyophilised glibenclamide-SLS formulations spray coated with non-enteric Opadry coating system (a) compared with the non-coated formulations (b).

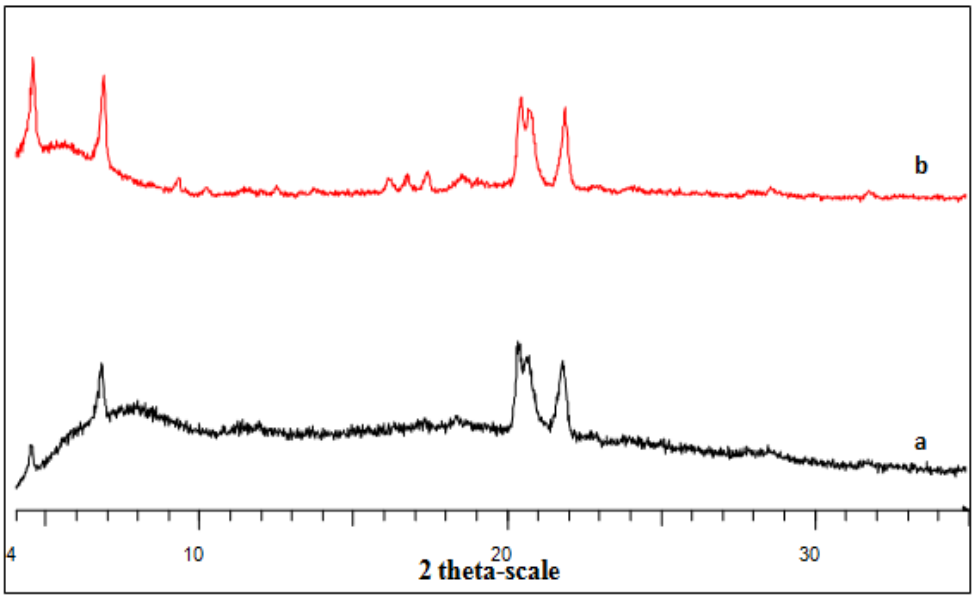

Figure 5.50: XRPD of lyophilised spironolactone-SLS formulations spray coated with non-enteric Opadry coating system (a) compared with the non-coated formulations (b).

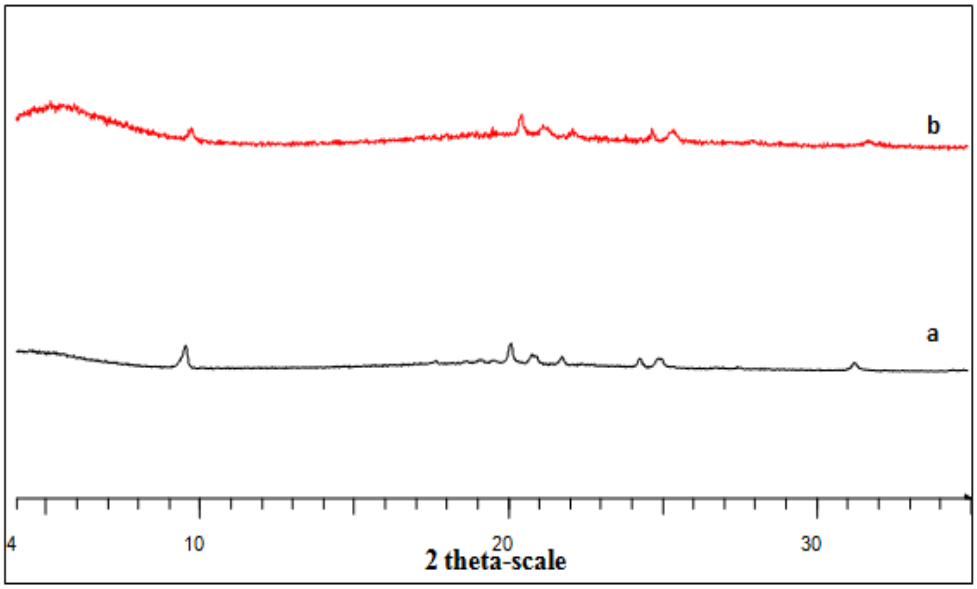

Figure 5.51: XRPD of lyophilised ketoconazole-mannitol-SLS formulations spray coated with non-enteric Opadry coating system (a) compared with the non-coated formulations (b).

Figures 5.52-5.54 show the corresponding FT-IR spectra. The spectrum of the coated formulations of glibenclamide was identical to that of the corresponding non-coated samples except for the appearance of a broad endotherm around 3500 cm^{-1} suggesting water absorption. This finding supports the DSC and XRPD results suggesting the stability of the amorphous form of glibenclamide in its solid dispersion with SLS on being coated with Opadry coating system. On the other hand, the FT-IR spectrum of the coated spironolactone formulations displayed a shift in the characteristic C-O stretching vibrations of SLS from 1204 cm^{-1} to 1216 cm^{-1} (its original wave number in the spectrum of raw SLS, Section 4.4.2.3). Furthermore, the spectrum showed the appearance of a broad peak around 3500 cm^{-1} highlighting water absorption. This finding supports the DSC and XRPD results suggesting that the amorphous form of spironolactone in its solid dispersion with SLS was physically changed as a result of the coating process in addition to disturbance in the drug/excipient interactions. For the coated ketoconazole formulations, the absorption spectrum was identical to those of the corresponding non-coated samples supporting the stability of the the ketoconazole/SLS solid dispersion.

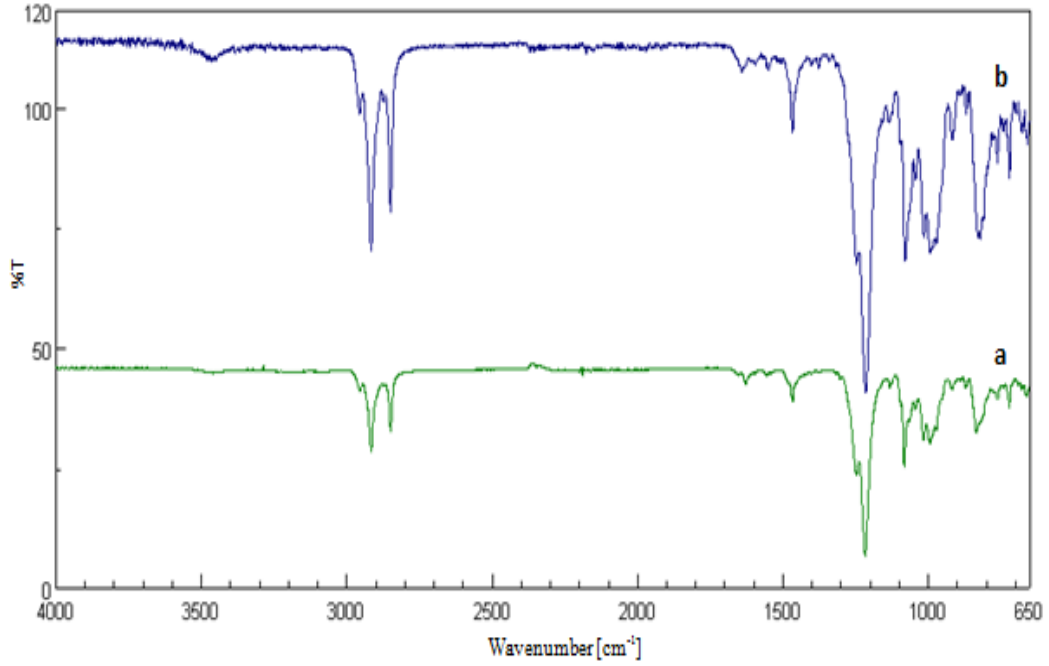

Figure 5.52: FT-IR of lyophilised glibenclamide-SLS formulations spray coated with non-enteric Opadry coating system (a) compared with the non-coated formulations (b).

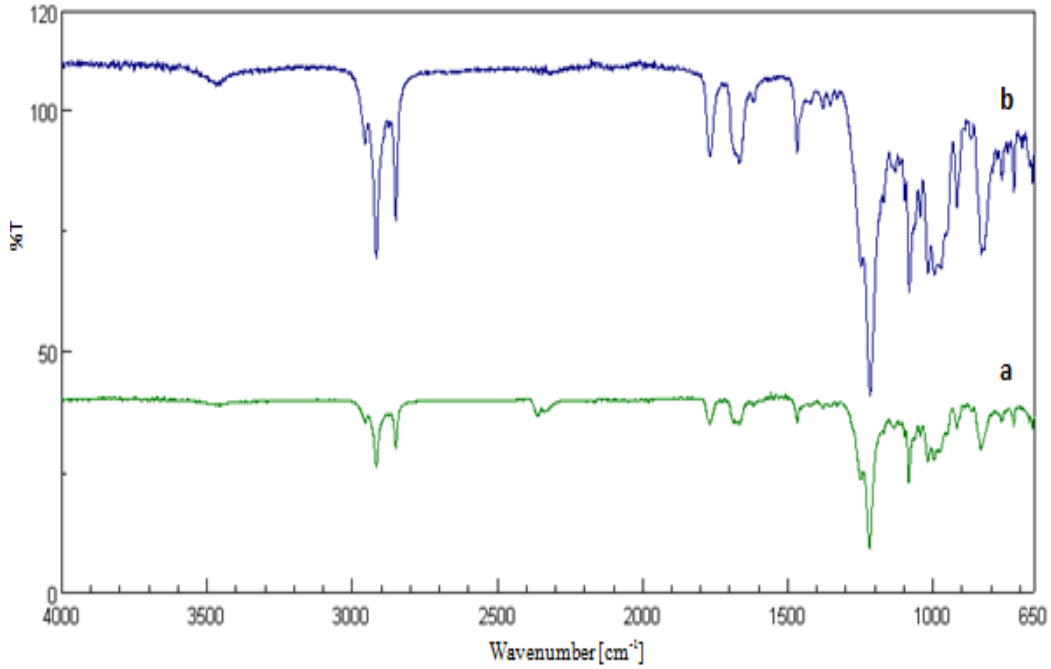

Figure 5.53: FT-IR of lyophilised spironolactone-SLS formulations spray coated with non-enteric Opadry coating system (a) compared with the non-coated formulations (b).

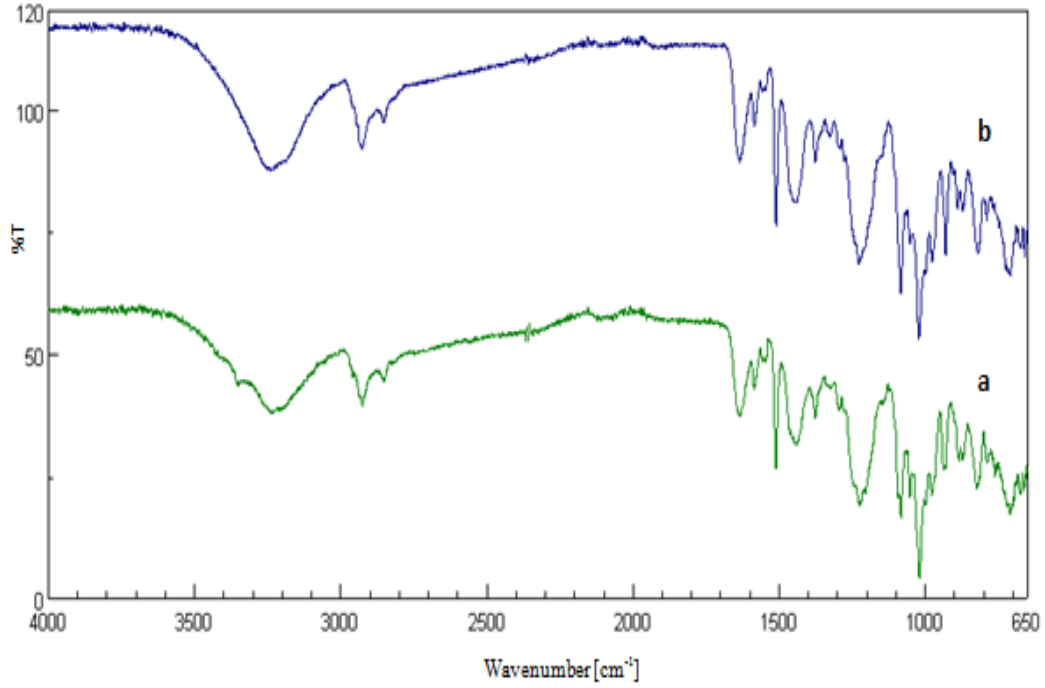

Figure 5.54: FT-IR of lyophilised ketoconazole-mannitol-SLS formulations spray coated with non-enteric Opadry coating system (a) compared with the non-coated formulations (b).

5.4.4 Enteric coating

5.4.4.1 Gastro-resistance study

The enteric coated glibenclamide capsule formulations exhibited good resistance to 0.1N HCL for 2 hours (Section 2.4.1) as indicated by the absence of any signs of disintegration, cracking, or diffusion of the blue dye included in the formulation (visually observed).

5.4.4.2 Effect of application of enteric coating system on dissolution profile of lyophilised glibenclamide capsule formulations

The dissolution profile of glibenclamide capsule formulations after coating with Opadry enteric system is illustrated in Figure 5.55. The dissolution profile of the coated formulations was found superimposable to that of the non-coated samples. Statistical analysis showed no significant differences between both profiles with an f_2

value of 67.5. Maintenance of the dissolution rate of glibenclamide suggests the stability of the amorphous form of glibenclamide in its solid dispersion with SLS after coating with Opadry enteric coating system.

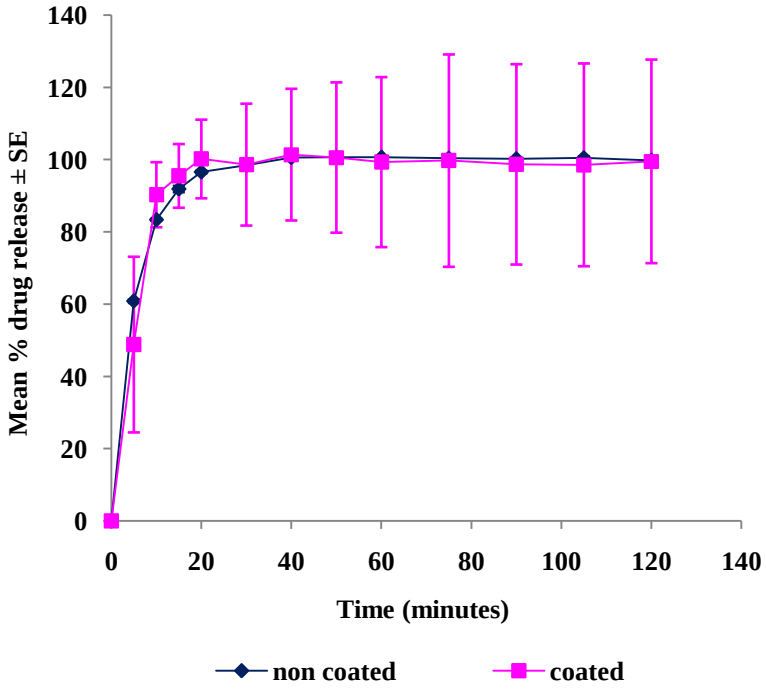

Figure 5.55: Dissolution profile of Opadry enteric spray coated glibenclamide capsule formulations compared to the corresponding non-coated formulations in phosphate buffer solution, pH 7.4 (n=6).

5.4.4.3 Physical characterisation of lyophilised glibenclamide formulations spray coated with Opadry enteric coating system

The DSC thermograms of glibenclamide formulations before and after coating with Opadry enteric system are illustrated in Figure 5.56. The thermogram of the coated formulations was similar to that of the corresponding non-coated samples. This finding suggests the stability of the solid dispersion formulations of glibenclamide with SLS after coating with Opadry enteric system.

The corresponding XRPD patterns are represented in Figures 5.57. The diffractogram of the coated glibenclamide formulations was similar to that of the

non-coated samples. It showed the absence of all the characteristic peaks of glibenclamide except a very low-intensity peak at 21.4º. This finding supports the DSC results suggesting the stability of the amorphous form of glibenclamide in its solid dispersion with SLS upon coating with the Opadry enteric system. This result explains the maintenance of the dissolution rate of glibenclamide after the coating process (Section 5.4.4.1).

Figure 5.58 shows the corresponding FT-IR spectra. The absorption spectrum of the coated glibenclamide formulations was identical to the spectrum of the non-coated samples except for a slight decrease in the shoulder intensity of the absorption band corresponding to C-O stretching vibrations of SLS at 1216 cm^{-1}. This confirms that the process of coating with Opadry enteric system did not affect the stability of the solid dispersion of glibenclamide with SLS.

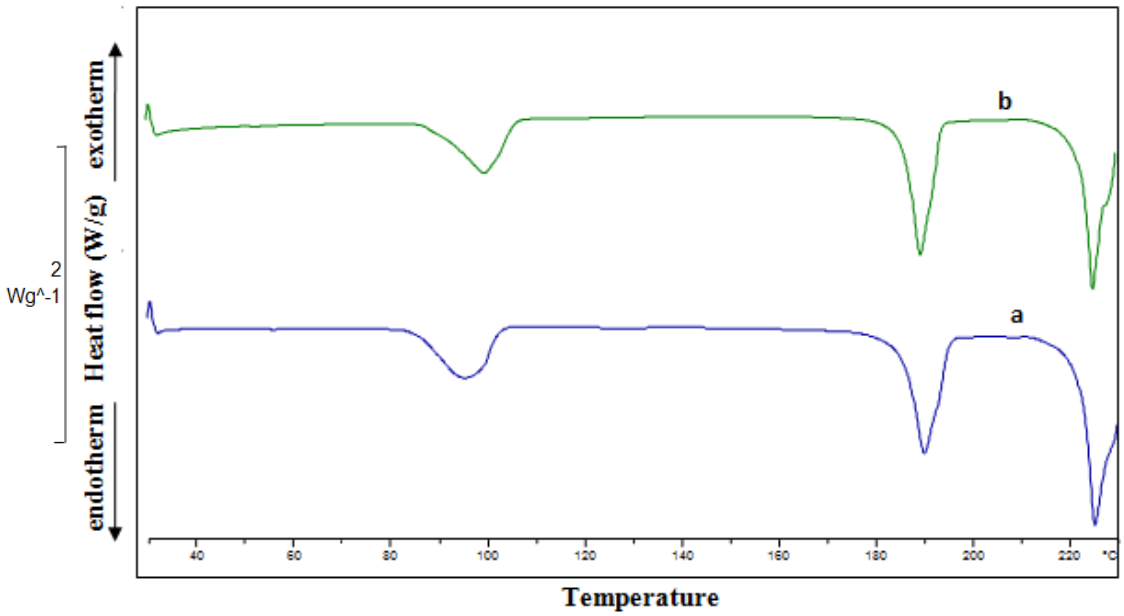

Figure 5.56: DSC of lyophilised glibenclamide-SLS formulations spray coated with Opadry enteric coating system (a) compared with the non-coated formulations (b).

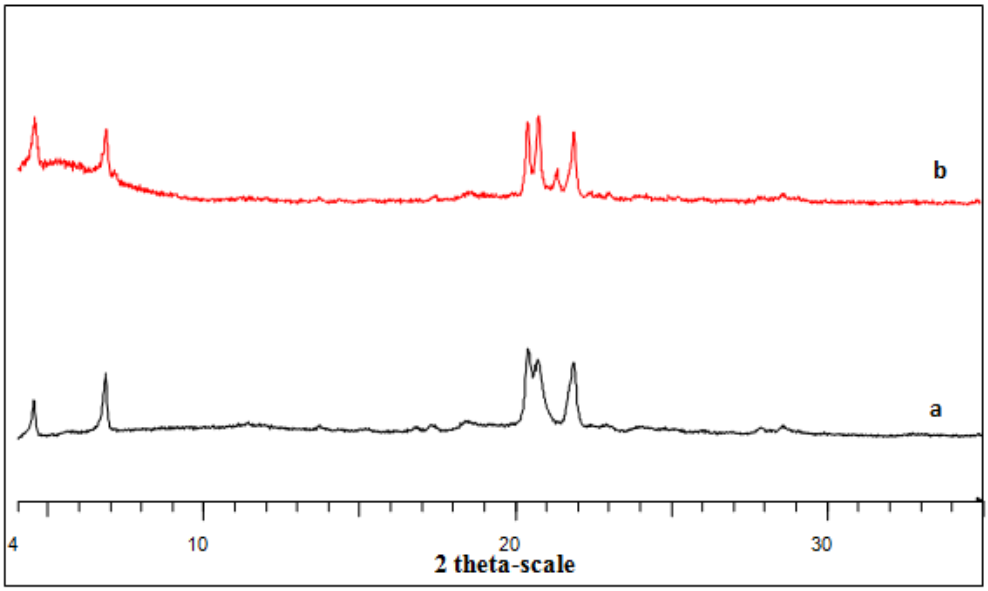

Figure 5.57: XRPD of lyophilised glibenclamide-SLS formulations spray coated with Opadry enteric coating system (a) compared with the non-coated formulations (b).

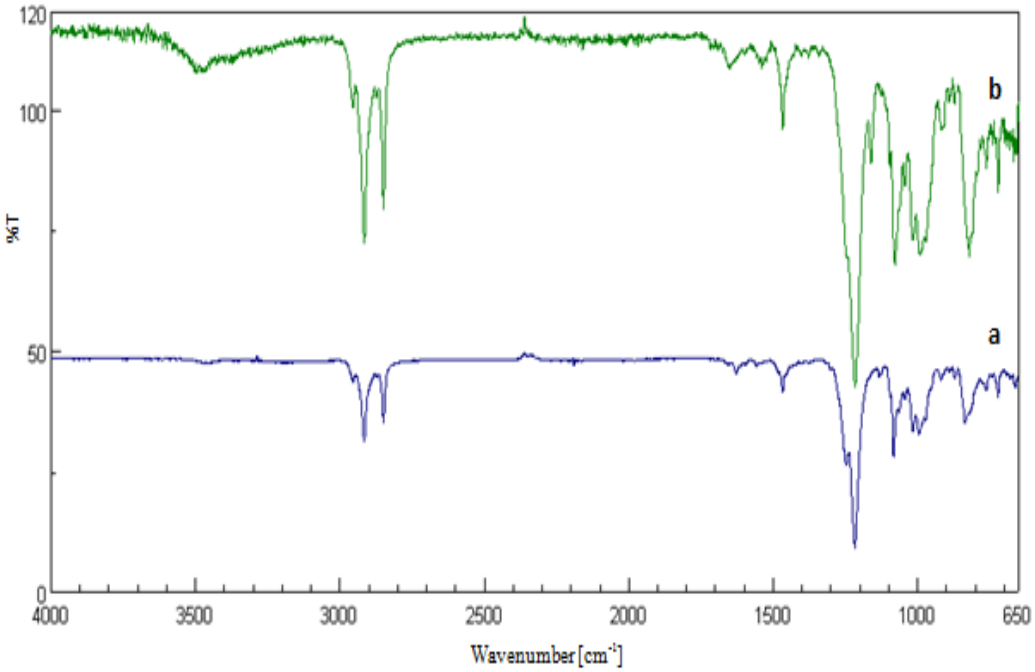

Figure 5.58: FT-IR of lyophilised glibenclamide-SLS formulations spray coated with Opadry enteric coating system (a) compared with the non-coated formulations (b).

5.5 Conclusion

It can be concluded from this chapter that:

- The amorphous form of glibenclamide in its lyophilised mixture with SLS showed good stability during the coating process regardless of the type or volume of the coating system or the drying time applied.
- The ketoconazole formulations sprayed with ethanol/water (90/10% v/v) solvent system showed a shift in the endothermic peaks in the DSC thermograms and a very low incidence of recrystallisation in the XRPD patterns compared to the non-sprayed formulations although no changes were detected in the corresponding FT-IR spectra or the dissolution profiles. This supports the stability of the amorphous form of the drug in its solid dispersion with the excipients following spray coating with this solvent system. The same formulations presented a good stability on being sprayed with 50% v/v acetone/isopropyl alcohol or coated with Opadry coating system.
- Higher volumes of solvent systems should be avoided for coating the lyophilised formulations of spironolactone as the solvent vapour may induce recrystallisation of the amorphous form of the drug. In addition, it is better to apply a short drying time as prolongation of the drying time after the coating process may initiate the polymorphic transformation of spironolactone.
- Although recrystallisation of the amorphous form of spironolactone appeared to take place during the coating process, as highlighted by the appearance of low intensity peaks in the XRPD diffractogram, dissolution rate of the drug was not unduly affected, supporting that recrystallisation was minimal.
- Generally, the changes observed in some of the sprayed or coated formulations could not be detected by all techniques applied. These changes had no effect on the dissolution profiles of the drugs which supports that these changes were minimal. Thus, the coating process had no detrimental effects on the lyophilised formulations of all three drugs.

Chapter 6

6. Stability studies of lyophilised systems of glibenclamide, spironolactone and ketoconazole

6.1 Introduction

Amorphous solids are systems in which there is no long-range order or repeating pattern in the positions of atoms or molecules. They are thermodynamically unstable due to the presence of excess free energy relative to crystalline solids (Bhugra & Pikal, 2008). This free energy is responsible for solubility and dissolution enhancement of amorphous forms, which consequently improve bioavailability especially if dissolution is the rate-limiting step (Hancock & Parks, 2000). Amorphous drug solids have a higher tendency to absorb moisture than their crystalline equivalents. Moisture can affect their physical and chemical characteristics causing plasticisation, and thus increases the opportunity for recrystallisation (Surana et al., 2004). Temperature also increases their molecular mobility and could influence crystal transformation (Strydom et al., 2009). Consequently, this may result in a marked decrease in their subsequent dissolution rate. Thus, during prolonged storage, many changes in the properties of amorphous systems may occur. These changes include chemical reactions, physical ageing, crystallization and protein destabilization resulting in loss of efficacy and/or quality of the system (Guo et al., 2000, Abdul-Fattah et al., 2007). Enhanced crystallisation has been previously reported for amorphous forms of many drugs such as indomethacin (Wu and Yu, 2006); nifedipine (Zhu et al., 2008); and Celecoxib (Gupta & Bansal, 2005).

6.2 Aims and objectives

The aim of this chapter is to investigate the effect of storage conditions on the stability of amorphous drug formulations after applying coating systems to the capsule.

6.3 Methods

6.3.1 Application of coating systems

The lyophilised formulations that exhibited a high dissolution rate enhancement (Sections 3.4.2.3, 3.4.2.9, 3.4.2.15) were coated with non-enteric (glibenclamide, spironolactone, ketoconazole) or enteric (glibenclamide) coating systems. These formulations are summarised in Table 6.1. Preparation of coating suspensions and spray coating details were provided in Section 5.3.3.

Table 6.1: Composition of the lyophilised formulations selected for coating

Drug	Excipient content in the formulation
Glibenclamide	93% w/w SLS
Spironolactone	67% w/w SLS
Ketoconazole	28% w/w mannitol and 14% w/w SLS

6.3.2 Stability studies

The effect of storage at different temperature and humidity conditions on the in-vitro dissolution and physical characteristics of the coated capsule formulations of the lyophilised systems were studied.

6.3.2.1 Effect of humidity

Saturated solutions of sodium nitrite or sodium chloride were prepared to obtain 65% and 75% relative humidity (RH) respectively (Hong et al., 1999; O'Brien, 1947). These saturated solutions were filled into the bottom of air tight desiccators. The formulations were kept in open jars on a perforated surface over the saturated solution (Figure 6.1). The desiccators were kept in a room maintained at a constant temperature of 25ºC. The non-enteric coated formulations of glibenclamide and spironolactone were physically characterised (DSC, FT-IR and XRPD, Sections 2.4.4, 2.4.5 and 2.4.7) and tested for dissolution immediately following coating and

after storage for 15, 30, 60 and 90 days. The enteric coated formulations of glibenclamide were tested for dissolution and physically characterised immediately following coating and after 30 and 60 days storage. The effect of humidity on the coated formulations of ketoconazole was determined by visual observation. The stored formulations of ketoconazole were photographed by a digital camera to follow the colour change in the formulation during storage.

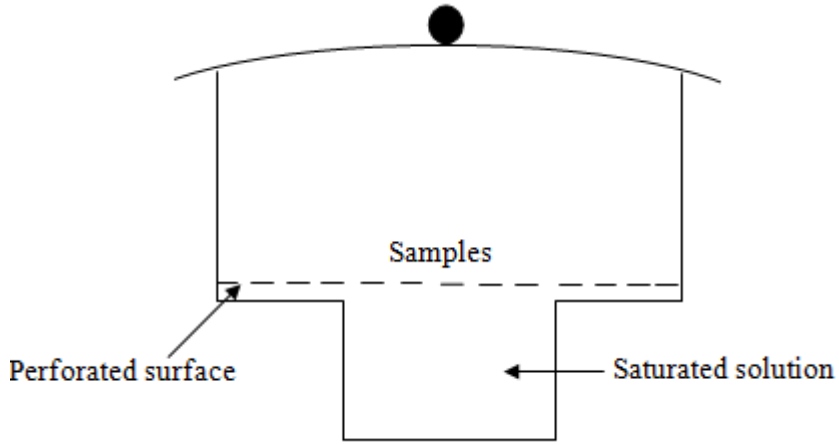

Figure 6.1: Diagram of air tight desiccators in which samples stored over saturated salt solutions

6.3.2.2 Effect of temperature

The coated formulations were put in air tight vials which placed in air tight desiccators containing moisture absorbing material (silica gel). The desiccators were stored in constant temperature rooms at 25ºC, 37ºC or 50ºC. The non-enteric coated formulations of glibenclamide and spironolactone were evaluated for physical properties and tested for dissolution after 15, 30, 60 or 90 days storage. The enteric coated formulations of glibenclamide were tested for dissolution and physically characterised after 30 and 60 days storage. The changes of the coated formulations of ketoconazole were determined as described in Section 6.3.2.1.

6.4 Results and discussion

6.4.1 Glibenclamide

6.4.1.1 Effect of storage at 25ºC/0% RH on the physicochemical characteristics of lyophilised glibenclamide-SLS formulations in non-enteric coated capsules

Figure 6.2 shows the dissolution profiles of the lyophilised mixtures of glibenclamide with 93% w/w SLS after storage at 25ºC/0% RH for up to 3 months. Statistical analysis showed no significant differences between the dissolution profiles of the freshly coated formulations and those of the samples stored for 15, 30, 60, and 90 days (f_2 values > 50).

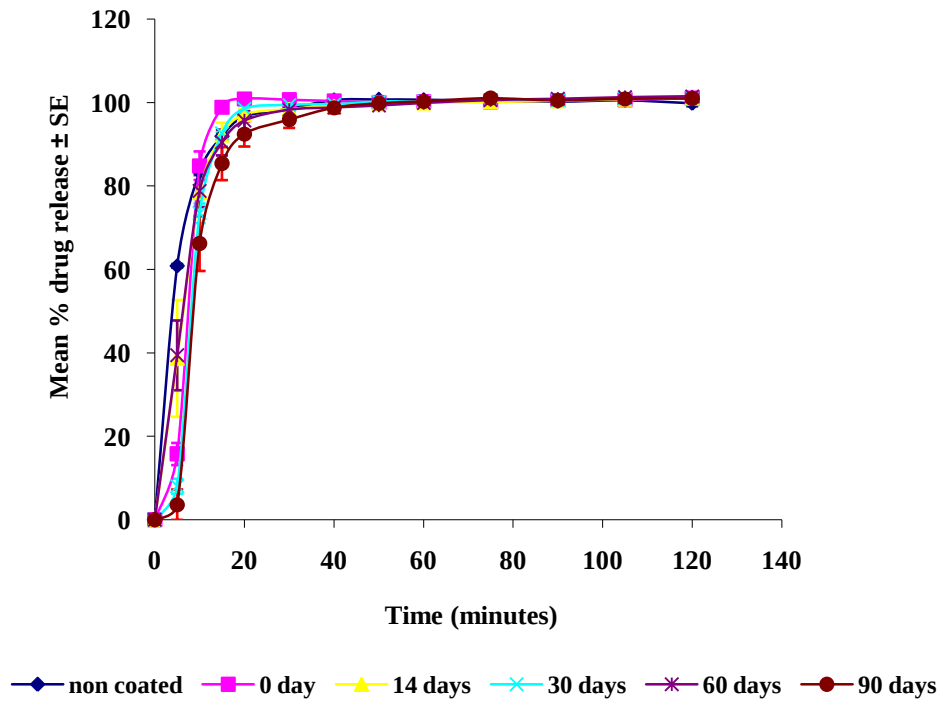

Figure 6.2: Effect of storage at 25ºC/0% RH on the dissolution profile of glibenclamide from non-enteric coated capsules of the lyophilised formulations (n=6).

The corresponding DSC thermograms are presented in Figure 6.3. The SLS endotherm at 99ºC and its melting endotherm at 192ºC were slightly shifted to higher

temperatures over time. This may be due to insignificant changes in glibenclamide/SLS hydrogen bonding in the solid dispersion during storage under these conditions. All thermograms exhibited the disappearance of the glibenclamide melting endotherm at 175ºC suggesting the stability of the amorphous form of glibenclamide in its lyophilised mixture with SLS up to 90 days when stored under these conditions.

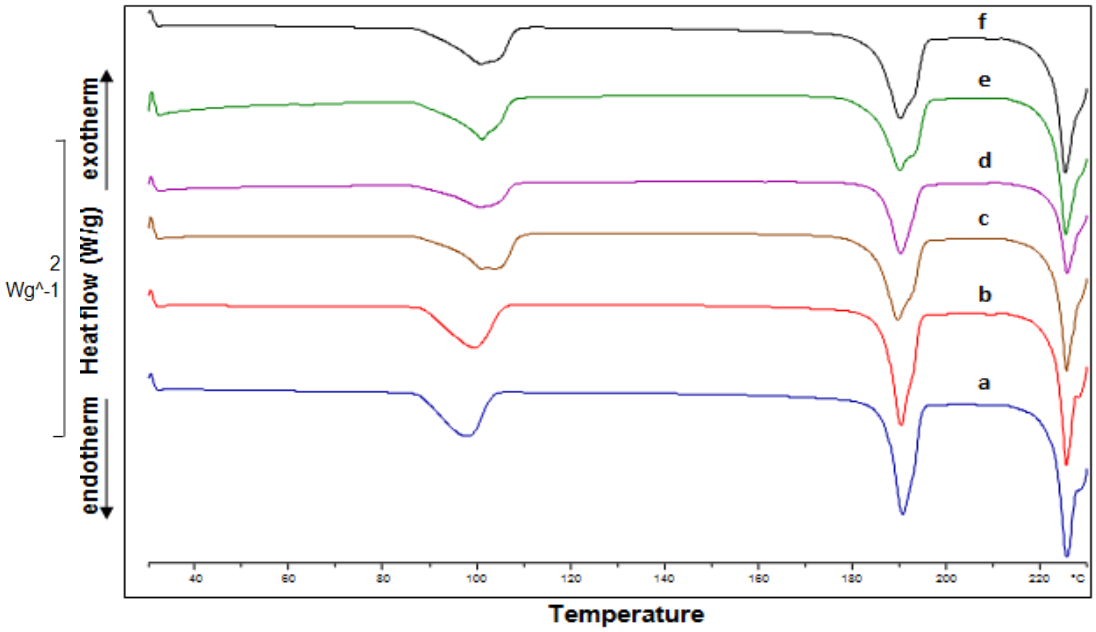

Figure 6.3: DSC of glibenclamide-SLS lyophilised mixture (non-enteric coated capsules) stored at 25ºC/0% RH; non-coated (a), freshly coated (b), 15 days (c), 30 days (d), 60 days (e), 90 days (f).

The fact that the amorphous form of glibenclamide was maintained in the solid dispersion during storage was confirmed by XRPD and FT-IR (Figures. 6.4 and 6.5) as the diffractograms and spectra of the stored samples show no difference from those of the freshly prepared formulations.

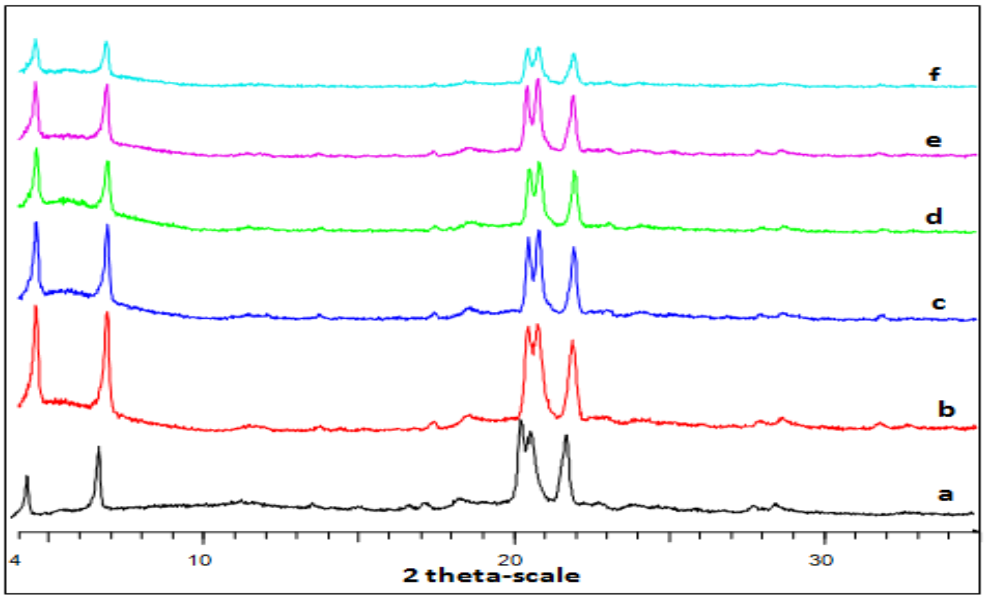

Figure 6.4: XRPD of glibenclamide-SLS lyophilised mixture (non-enteric coated capsules) stored at 25°C/0% RH; non-coated (a), freshly coated (b), 15 days (c), 30 days (d), 60 days (e), 90 days (f).

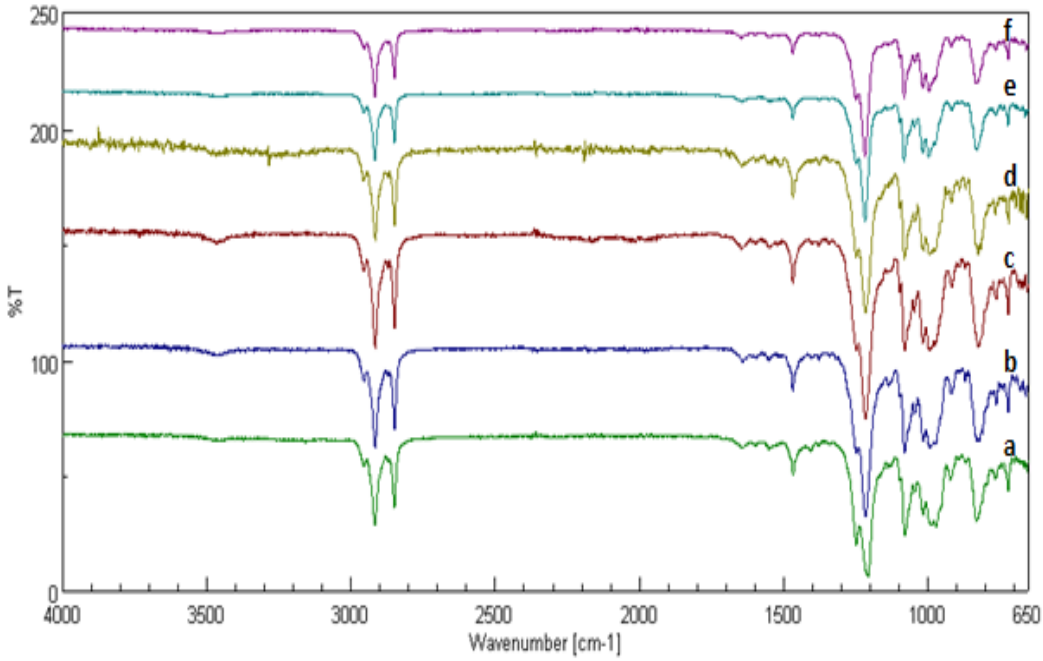

Figure 6.5: FT-IR of glibenclamide-SLS lyophilised mixture (non-enteric coated capsules) stored at 25°C/0% RH; non-coated (a), freshly coated (b), 15 days (c), 30 days (d), 60 days (e), 90 days (f).

6.4.1.2 Effect of storage at 25ºC/65% RH on the physicochemical characteristics of lyophilised glibenclamide-SLS formulations in non-enteric coated capsules

Figure 6.6 shows dissolution profiles of the lyophilised mixtures of glibenclamide with 93% w/w SLS after storage at 25ºC/65% RH up to 3 months. Statistical analysis showed no significant differences between the dissolution profiles of the formulations stored for 0, 15, 30, 60, and 90 days with f_2 values > 50.

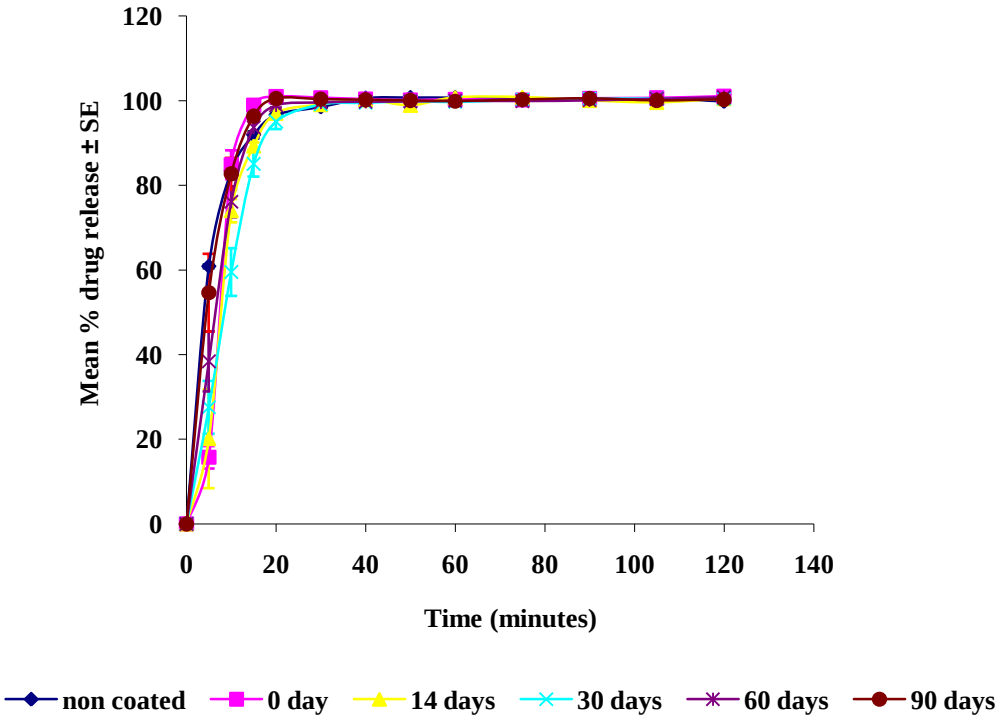

Figure 6.6: Effect of storage at 25ºC/65% RH on the dissolution profile of glibenclamide from non-enteric coated capsules of the lyophilised formulations (n=6).

The corresponding DSC thermograms are shown in Figure 6.7. Slight differences between the thermograms of different samples were noted. In addition to the slight shift in the SLS endotherms (see Section 6.4.1.1), a wide broad endotherm in the temperature range 30-60ºC was obviously detectable in the thermograms of the

samples stored. This endotherm could correspond to evaporation of water adsorbed during storage. Furthermore, all thermograms revealed the absence of the melting endotherm of glibenclamide at 175ºC. This finding suggests the stability of the amorphous form of glibenclamide in its solid dispersions with SLS up to 90 days.

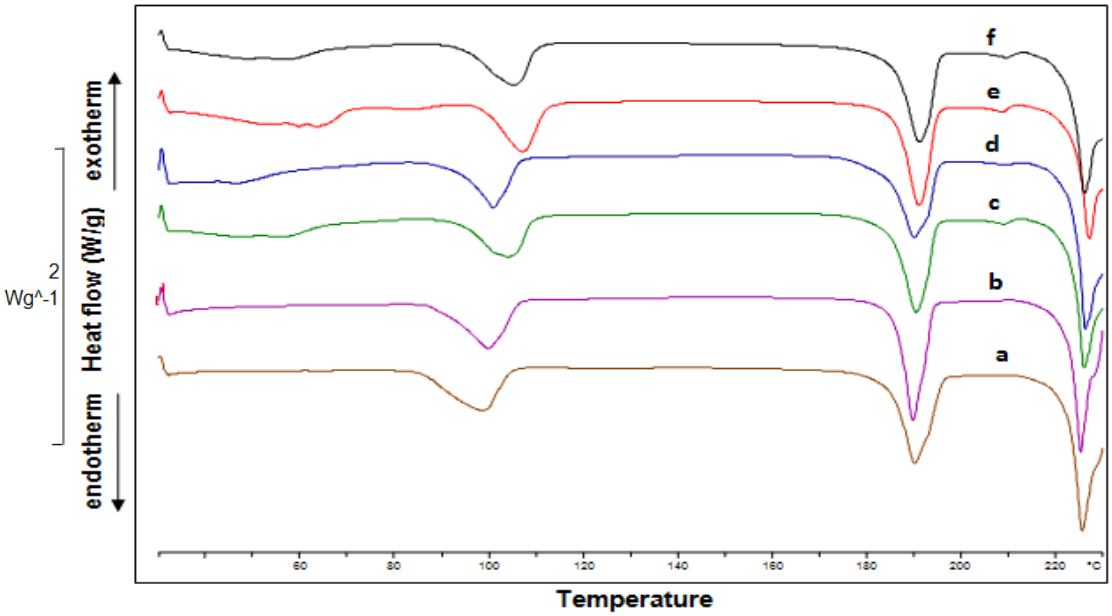

Figure 6.7: DSC of glibenclamide-SLS lyophilised mixture (non-enteric coated capsules) stored at 25ºC/65% RH; non-coated (a), freshly coated (b), 15 days (c), 30 days (d), 60 days (e), 90 days (f).

The above results were supported by XRPD (Figure 6.8) as the diffractograms show the absence of all the characteristic peaks of glibenclamide except for a very small peak at 21.4º 2θ. Drug-excipient interactions (investigated in Section 4.4.1.3) could be the factor responsible for the observed stability of glibenclamide as an amorphous form in its solid dispersion with SLS during storage under these conditions.

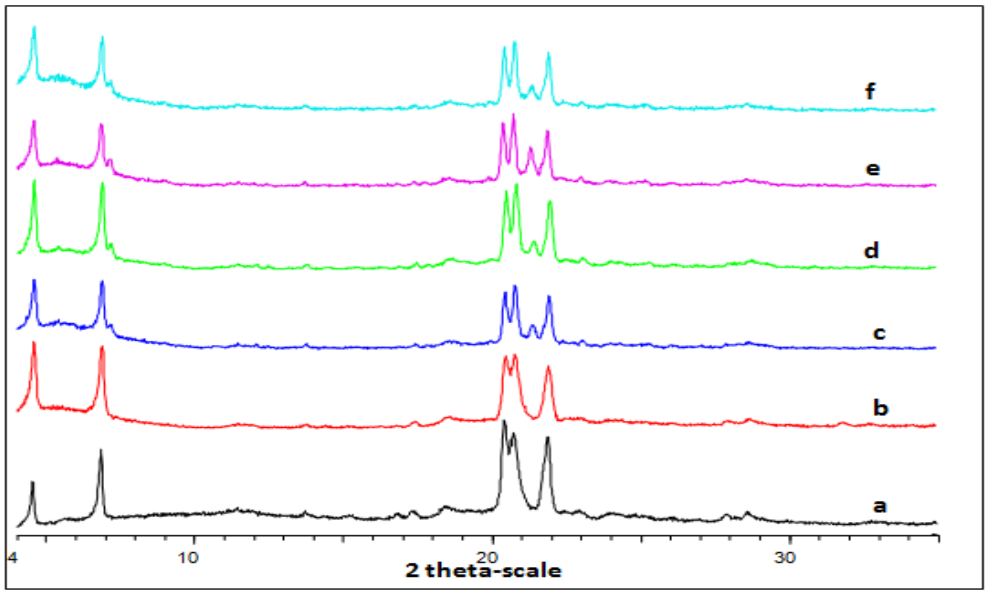

Figure 6.8: XRPD of glibenclamide-SLS lyophilised mixture (non-enteric coated capsules) stored at 25ºC/65% RH; non-coated (a), freshly coated (b), 15 days (c), 30 days (d), 60 days (e), 90 days (f).

The corresponding FT-IR spectra (Figure 6.9) did not display any significant difference except the appearance of a broad absorption band around 3500 cm^{-1} highlighting the presence of water. This finding confirms the fact of the stability of glibenclamide/SLS solid dispersion and maintenance of the drug amorphous form during storage which supports the DSC and XRPD results. It has been reported that the amorphous form of glibenclamide was maintained in its solid dispersion with Gelucire and silicon dioxide during ageing study at 30ºC/65% RH for 3 months (Chauhan et al., 2005). Similarly, the amorphous state of irbesartan (used in the treatment of hypertension) was maintained under accelerated stability conditions of 25ºC/75% RH or 40ºC/75% RH (Chawla & Bansal, 2009).

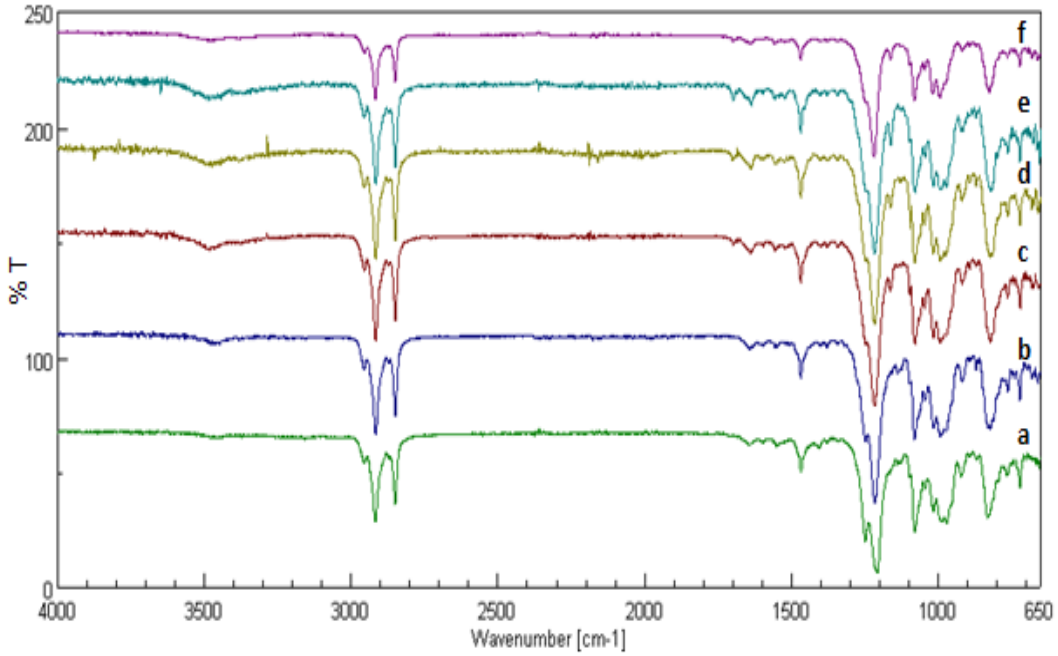

Figure 6.9: FT-IR of glibenclamide-SLS lyophilised mixture (non-enteric coated capsules) stored at 25ºC/65% RH; non-coated (a), freshly coated (b), 15 days (c), 30 days (d), 60 days (e), 90 days (f).

6.4.1.3 Effect of storage at 25ºC/75% RH on the physicochemical characteristics of lyophilised glibenclamide-SLS formulations in non-enteric coated capsules

Figures 6.10-6.13 show dissolution profiles, DSC, XRPD and FT-IR of the lyophilised mixtures of glibenclamide with 93% w/w SLS after storage at 25ºC/75% RH up to 3 months. The data show no differences from those obtained from the samples stored at 25ºC/65% RH. Thus, the amorphous form of glibenclamide in its solid dispersion with SLS (in non-enteric coated capsules) was stable during storage at 25ºC/65% or 75% RH up to 3 months without any tendency to recrystallisation.

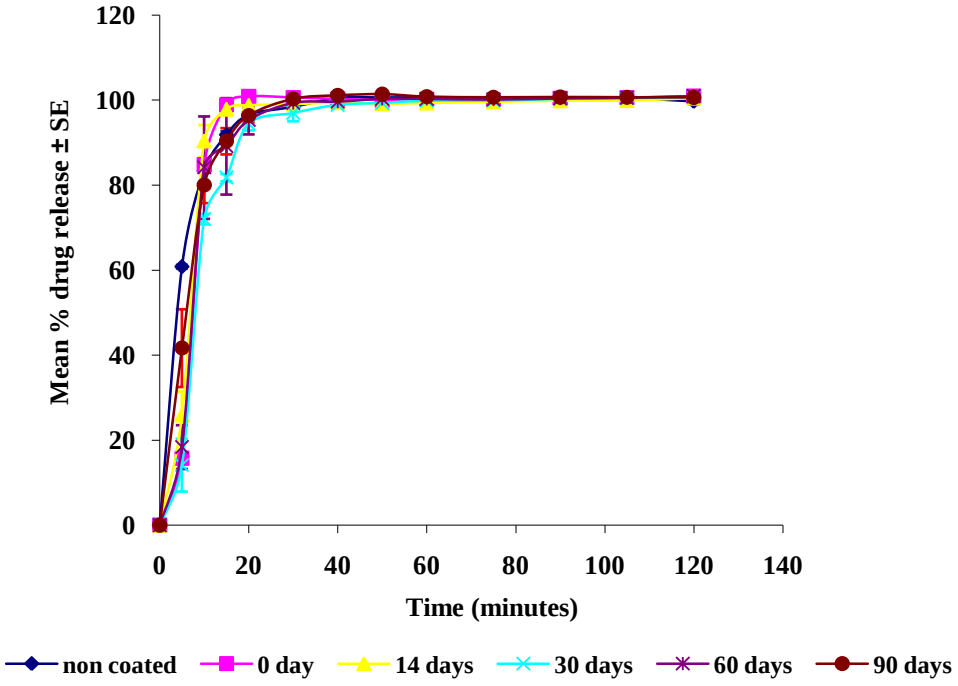

Figure 6.10: Effect of storage at 25°C/75% RH on the dissolution profile of glibenclamide from non-enteric coated capsules of the lyophilised formulations (n=6).

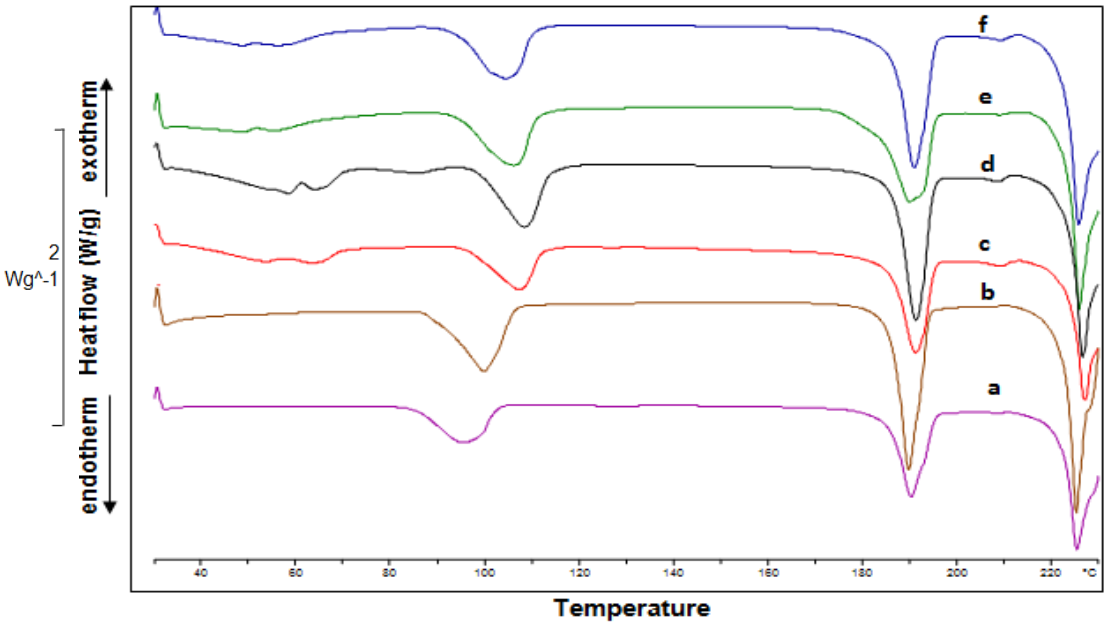

Figure 6.11: DSC of glibenclamide-SLS lyophilised mixture (non-enteric coated capsules) stored at 25°C/75% RH; non-coated (a), freshly coated (b), 15 days (c), 30 days (d), 60 days (e), 90 days (f).

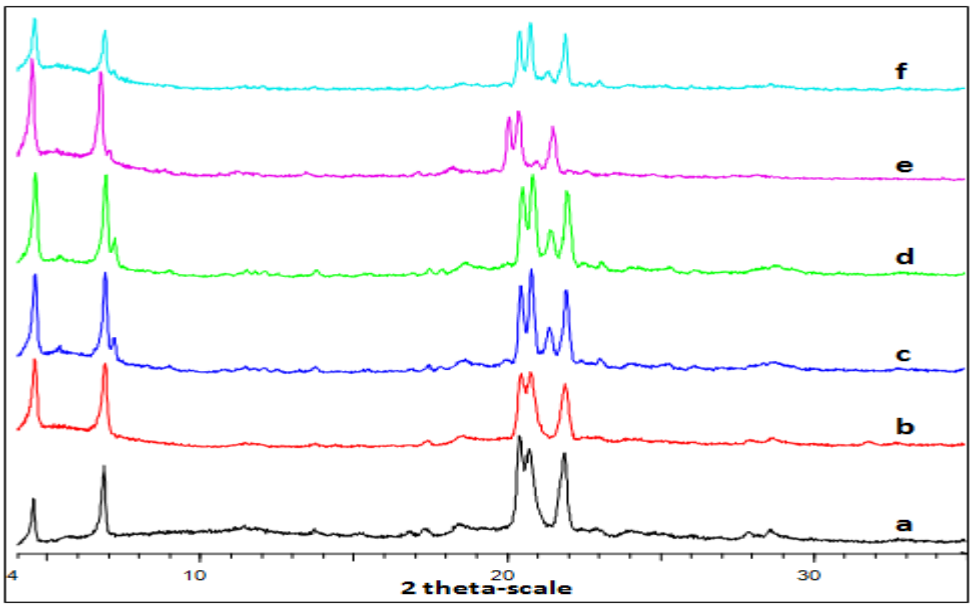

Figure 6.12: XRPD of glibenclamide-SLS lyophilised mixture (non-enteric coated capsules) stored at 25°C/75% RH; non-coated (a), freshly coated (b), 15 days (c), 30 days (d), 60 days (e), 90 days (f).

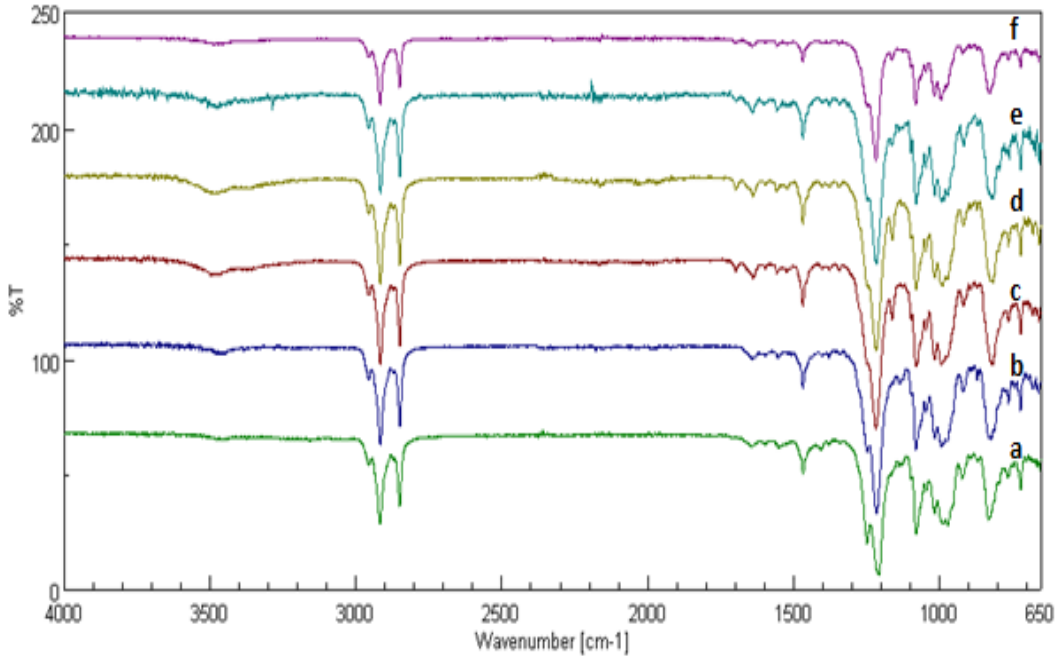

Figure 6.13: FT-IR of glibenclamide-SLS lyophilised mixture (non-enteric coated capsules) stored at 25°C/75% RH; non-coated (a), freshly coated (b), 15 days (c), 30 days (d), 60 days (e), 90 days (f).

6.4.1.4 Effect of storage at 37ºC/0% RH on the physicochemical characteristics of lyophilised glibenclamide-SLS formulations in non-enteric coated capsules

Figures 6.14-6.17 show dissolution profiles, DSC, XRPD and FT-IR of the lyophilised glibenclamide-SLS mixtures stored at 37ºC/0% RH up to 3 months. The data show no differences from those obtained from the formulations stored at 25ºC/0% RH (Section 6.4.1.1). Thus, the amorphous form of glibenclamide in its solid dispersions with SLS in non-enteric coated capsules was stable on being stored at 25ºC or 37ºC up to 3 months without any tendency to recrystallisation.

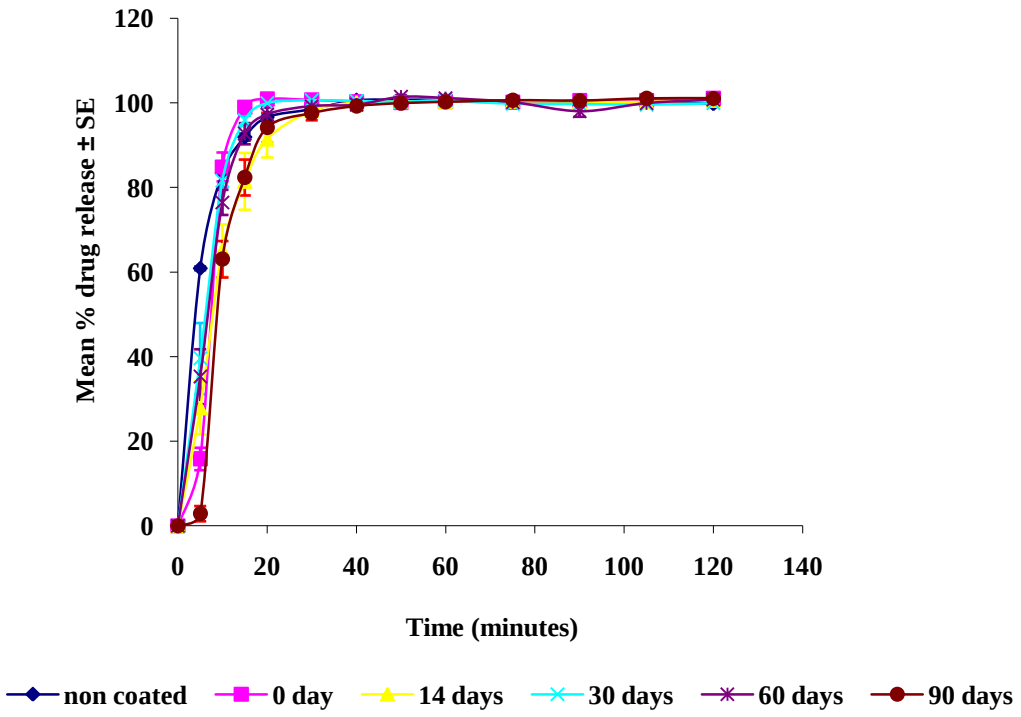

Figure 6.14: Effect of storage at 37ºC/0% RH on the dissolution profile of glibenclamide from non-enteric coated capsules of the lyophilised formulations (n=6).

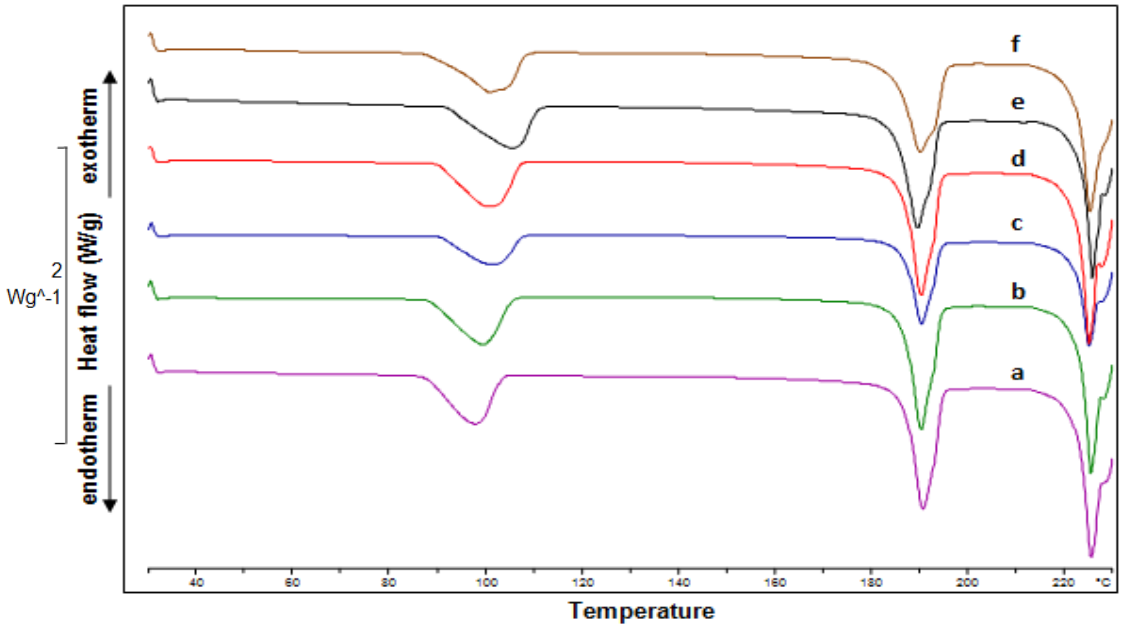

Figure 6.15: DSC of glibenclamide-SLS lyophilised mixture (non-enteric coated capsules) stored at 37ºC/0% RH; non-coated (a), freshly coated (b), 15 days (c), 30 days (d), 60 days (e), 90 days (f).

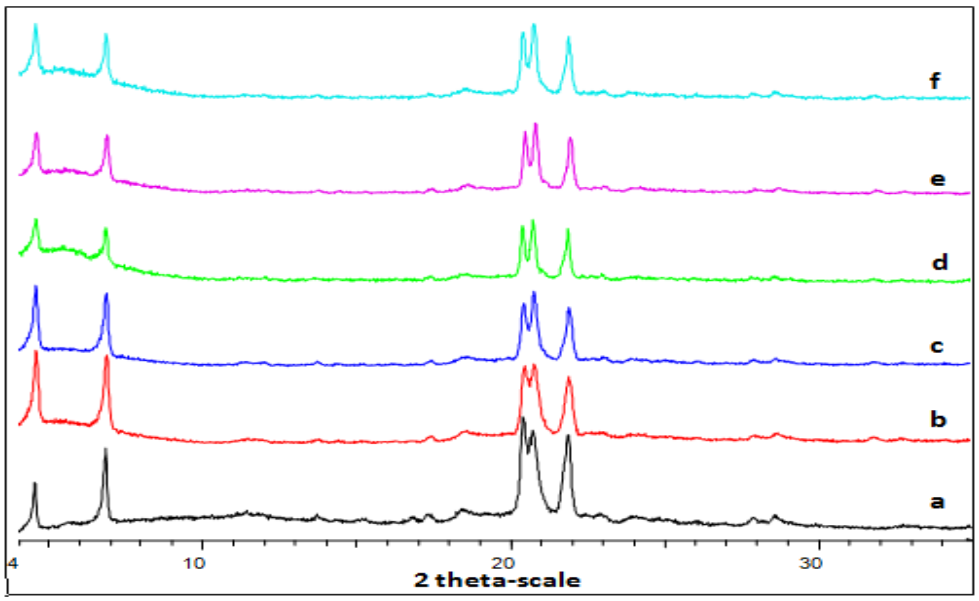

Figure 6.16: XRPD of glibenclamide-SLS lyophilised mixture (non-enteric coated capsules) stored at 37ºC/0% RH; non-coated (a), freshly coated (b), 15 days (c), 30 days (d), 60 days (e), 90 days (f).

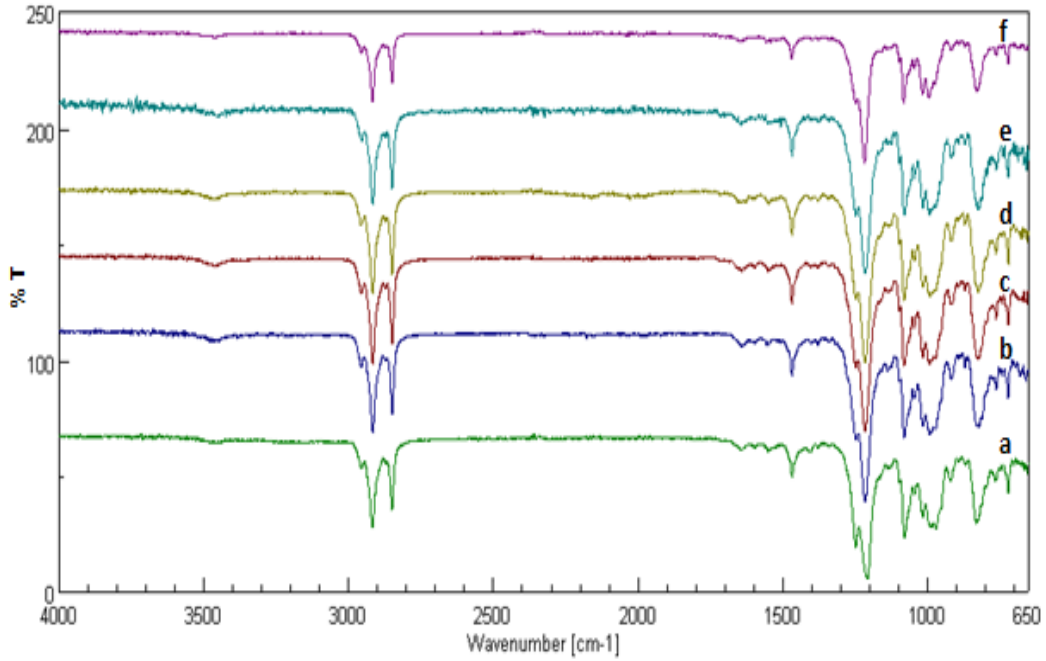

Figure 6.17: FT-IR of glibenclamide-SLS lyophilised mixture (non-enteric coated capsules) stored at 37ºC/0% RH; non-coated (a), freshly coated (b), 15 days (c), 30 days (d), 60 days (e), 90 days (f).

6.4.1.5 Effect of storage at 50ºC/0% RH on the physicochemical characteristics of lyophilised glibenclamide-SLS formulations in non-enteric coated capsules

The results obtained from the in-vitro dissolution studies and physicochemical characterisation of the samples stored at 50ºC/0% RH were similar to those obtained from the formulations stored at 25ºC/0% RH (6.4.1.1). This finding suggests the stability of the amorphous form of glibenclamide in its solid dispersion with SLS up to 3 months on being stored under these conditions (Figures. 6.18-6.21).

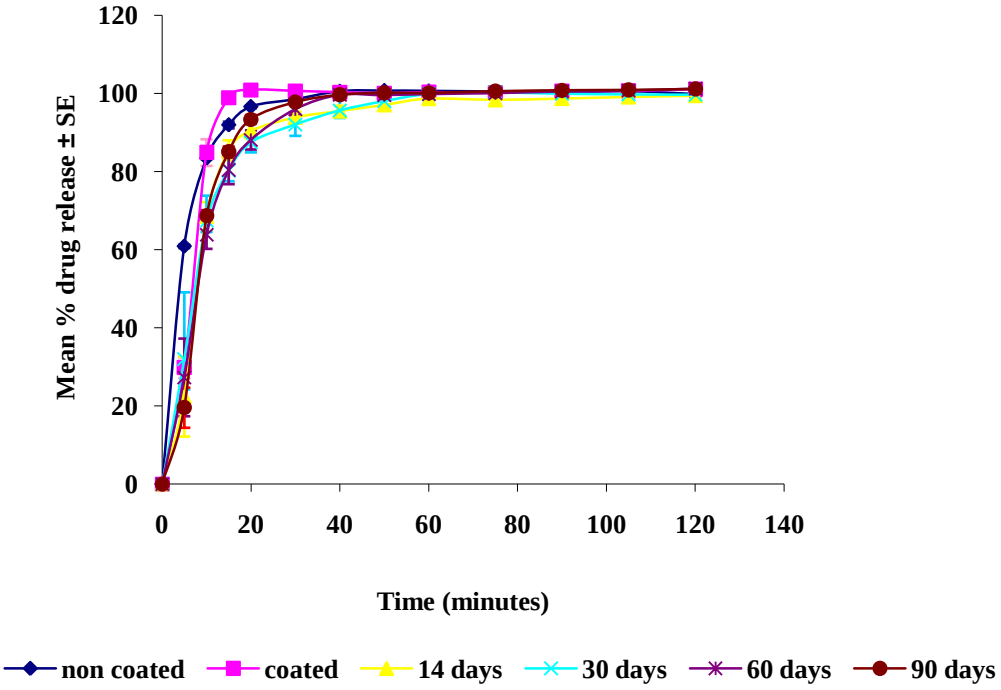

Figure 6.18: Effect of storage at 50ºC/0% RH on the dissolution profile of glibenclamide from non-enteric coated capsules of the lyophilised formulations (n=6).

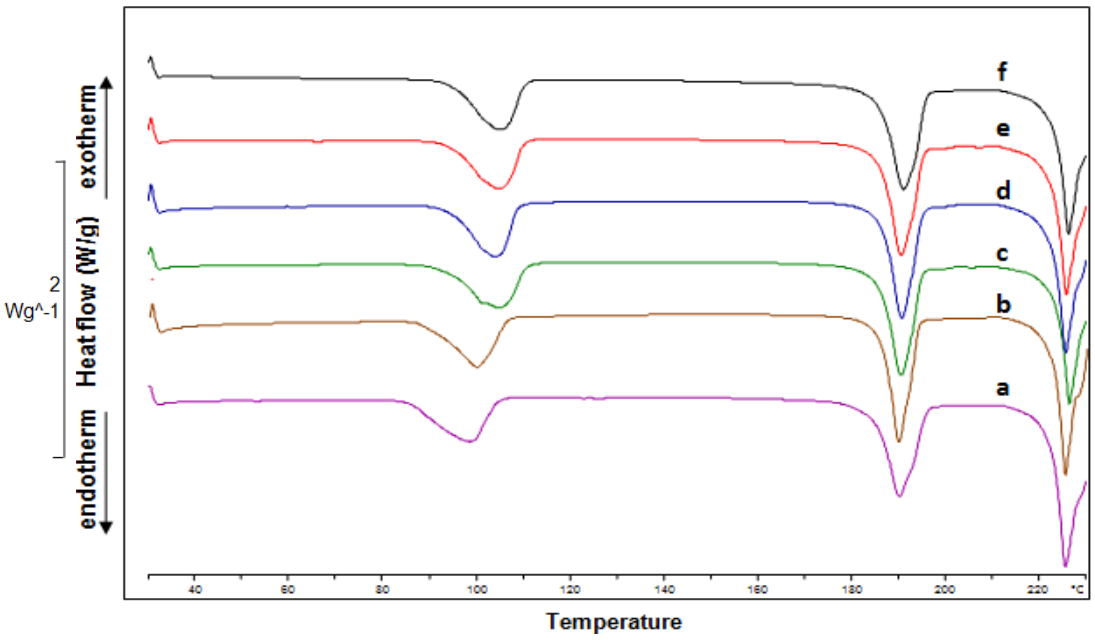

Figure 6.19: DSC of glibenclamide-SLS lyophilised mixture (non-enteric coated capsules) stored at 50ºC/0% RH; non-coated (a), freshly coated (b), 15 days (c), 30 days (d), 60 days (e), 90 days (f).

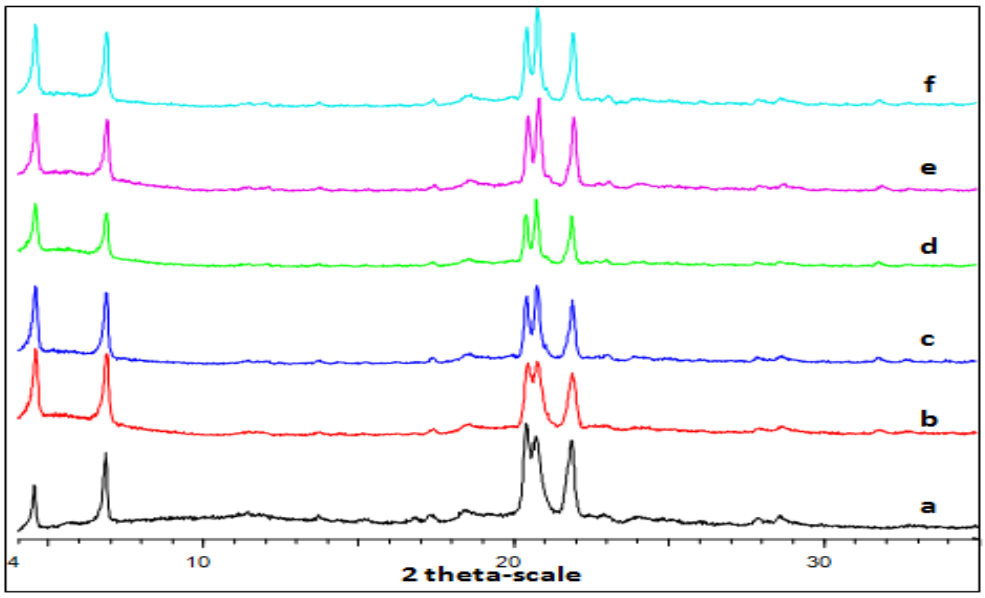

Figure 6.20: XRPD of glibenclamide-SLS lyophilised mixture (non-enteric coated capsules) stored at 50ºC/0% RH; non-coated (a), freshly coated (b), 15 days (c), 30 days (d), 60 days (e), 90 days (f).

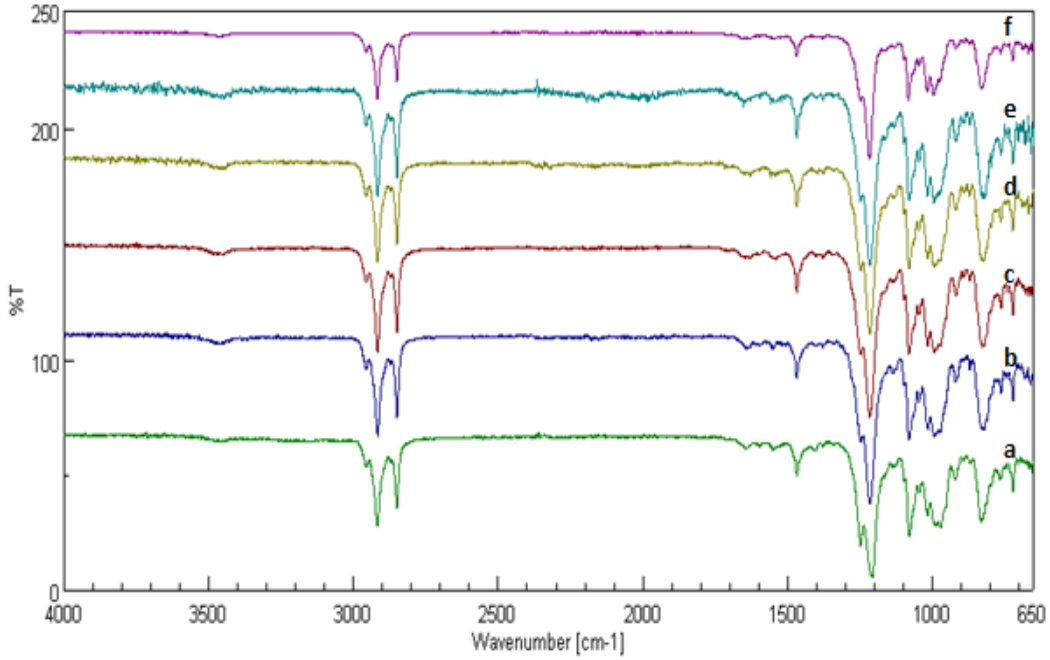

Figure 6.21: FT-IR of glibenclamide-SLS lyophilised mixture (non-enteric coated capsules) stored at 50ºC/0% RH; non-coated (a), freshly coated (b), 15 days (c), 30 days (d), 60 days (e), 90 days (f).

6.4.1.6 Effect of storage at 25ºC/0% RH on the physicochemical characteristics of lyophilised glibenclamide-SLS formulations in enteric coated capsules

Figures 6.22-6.25 present dissolution profiles, DSC thermograms, XRPD patterns, and FT-IR spectra of of the lyophilised mixtures of glibenclamide with 93% w/w SLS after storage at 25ºC/0% RH up to 2 months. The enteric coated formulations exhibited similar behaviours to the non-enteric coated formulations stored under the same conditions (see Section 6.4.1.1). This finding suggests that the amorphous form of glibenclamide when lyophilised with SLS is stable at day 60 when stored under these conditions (in enteric coated capsules).

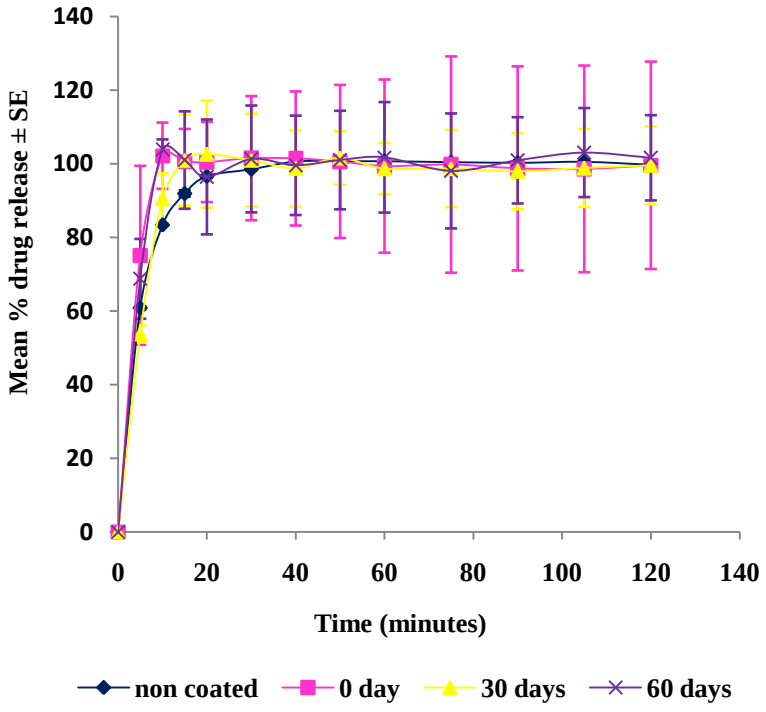

Figure 6.22: Effect of storage at 25ºC/0% RH on the dissolution profile of glibenclamide from enteric coated capsules of the lyophilised formulations (n=6).

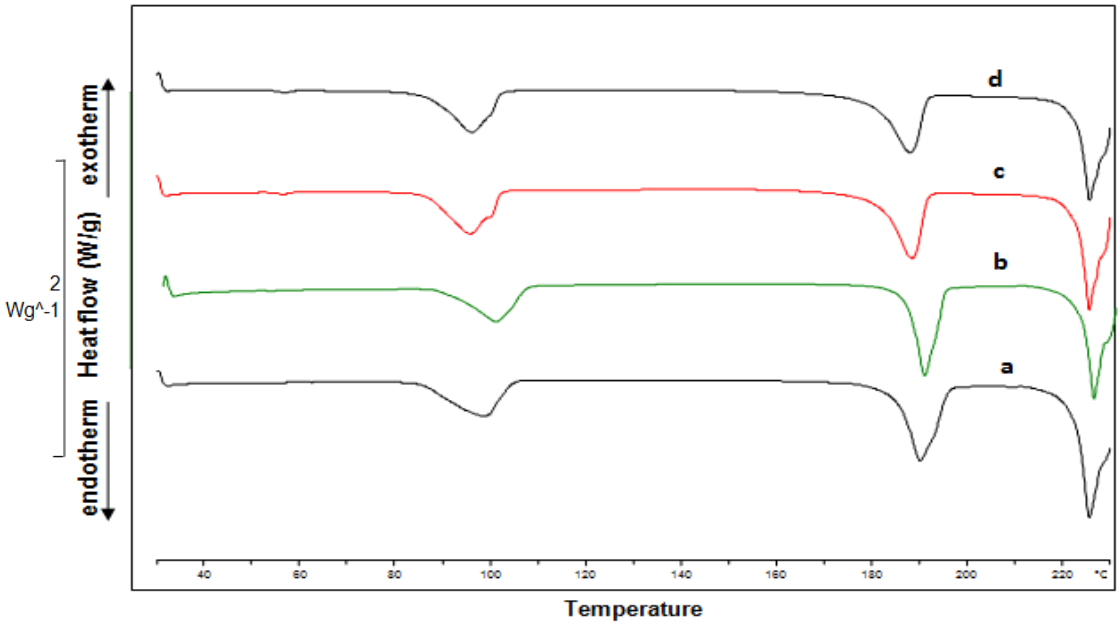

Figure 6.23: DSC of glibenclamide-SLS lyophilised mixture (enteric coated capsules) stored at 25°C/0% RH; non-coated (a), freshly coated (b), 30 days (c), 60 days (d).

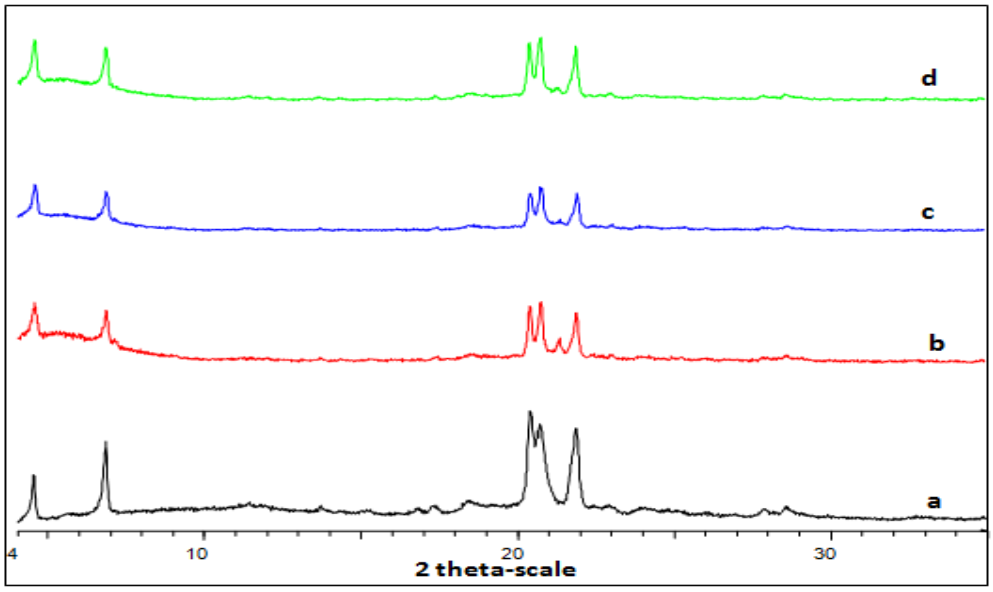

Figure 6.24: XRPD of glibenclamide-SLS lyophilised mixture (enteric coated capsules) stored at 25°C/0% RH; non-coated (a), freshly coated (b), 30 days (c), 60 days (d).

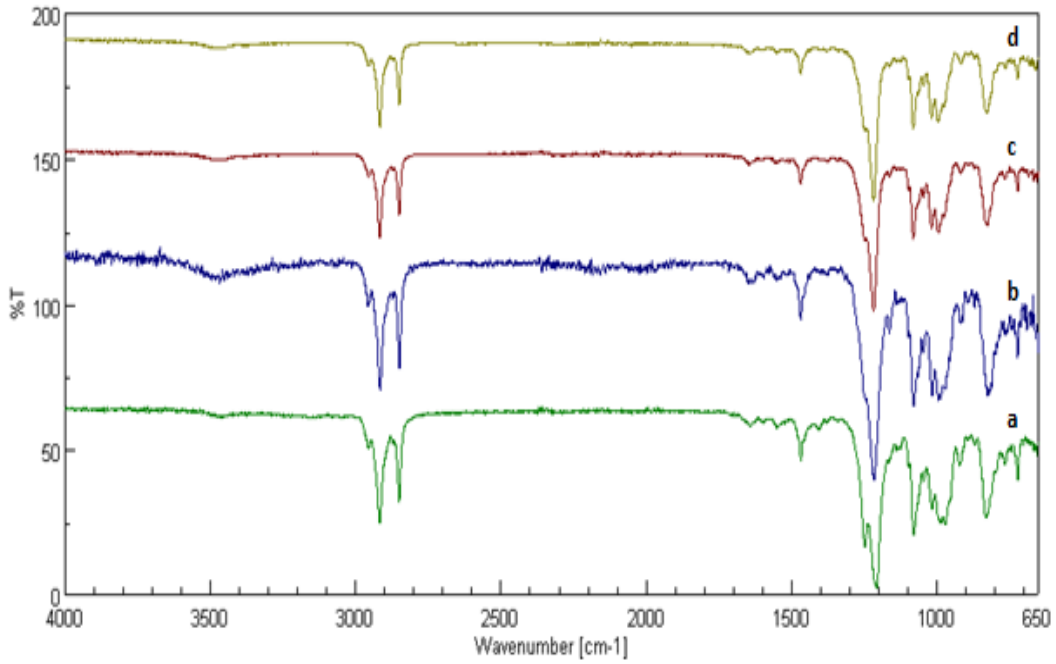

Figure 6.25: FT-IR of glibenclamide-SLS lyophilised mixture (enteric coated capsules) stored at 25°C/0% RH; non-coated (a), freshly coated (b), 30 days (c), 60 days (d).

6.4.1.7 Effect of storage at 25ºC/65% RH on the physicochemical characteristics of lyophilised glibenclamide-SLS formulations in enteric coated capsules

Figures 6.26-6.29 present dissolution profiles, DSC thermograms, XRPD patterns, and FT-IR spectra of of the lyophilised mixtures of glibenclamide with 93% w/w SLS after storage at 25ºC/65% RH up to 2 months. The enteric coated formulations exhibited similar behaviours to the non-enteric coated formulations stored under the same conditions (see Section 6.4.1.2). This finding suggests the stability of the amorphous form of glibenclamide in its lyophilised mixture with SLS at day 60 when stored under these conditions (in enteric coated capsules). The appearance of a small shoulder for the SLS melting endotherm and the decrease in its sharpness observed in the the thermograms of the stored formulations may reflect slight disruption in the crystalline structure of the excipient during storage.

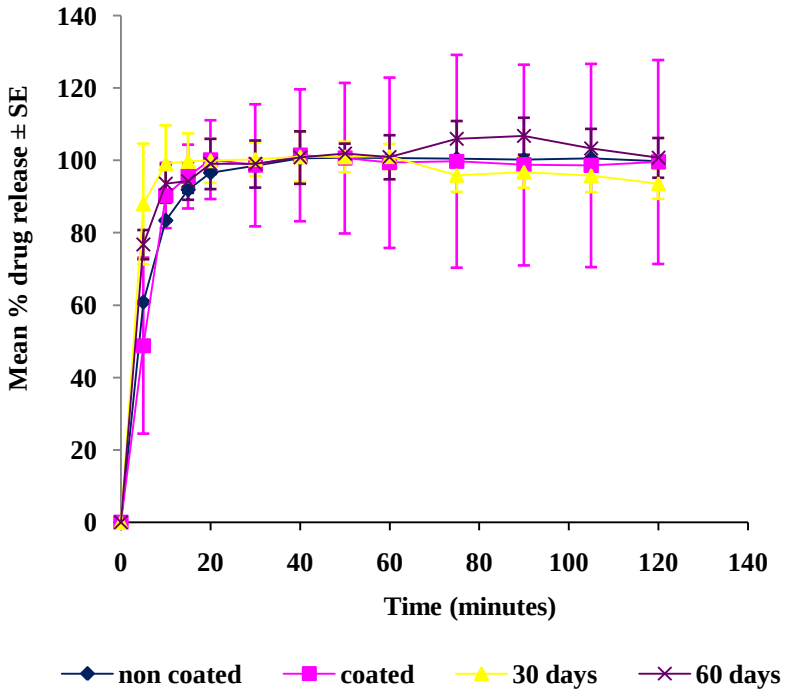

Figure 6.26: Effect of storage at 25ºC/65% RH on the dissolution profile of glibenclamide from enteric coated capsules of the lyophilised formulations (n=6).

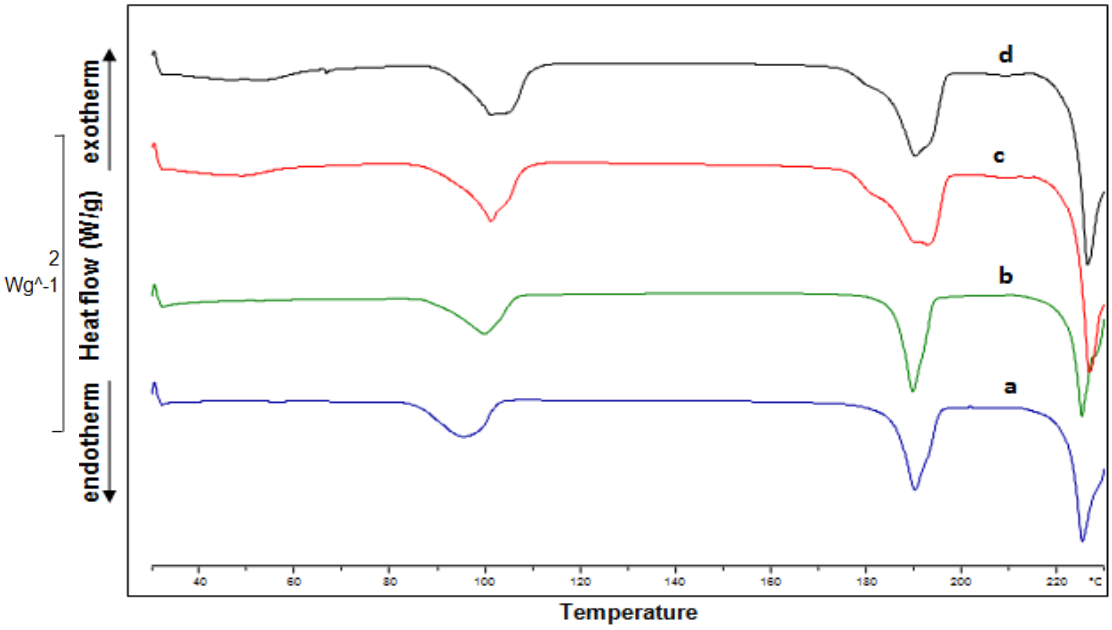

Figure 6.27: DSC of glibenclamide-SLS lyophilised mixture (enteric coated capsules) stored at 25ºC/65% RH; non-coated (a), freshly coated (b), 30 days (c), 60 days (d).

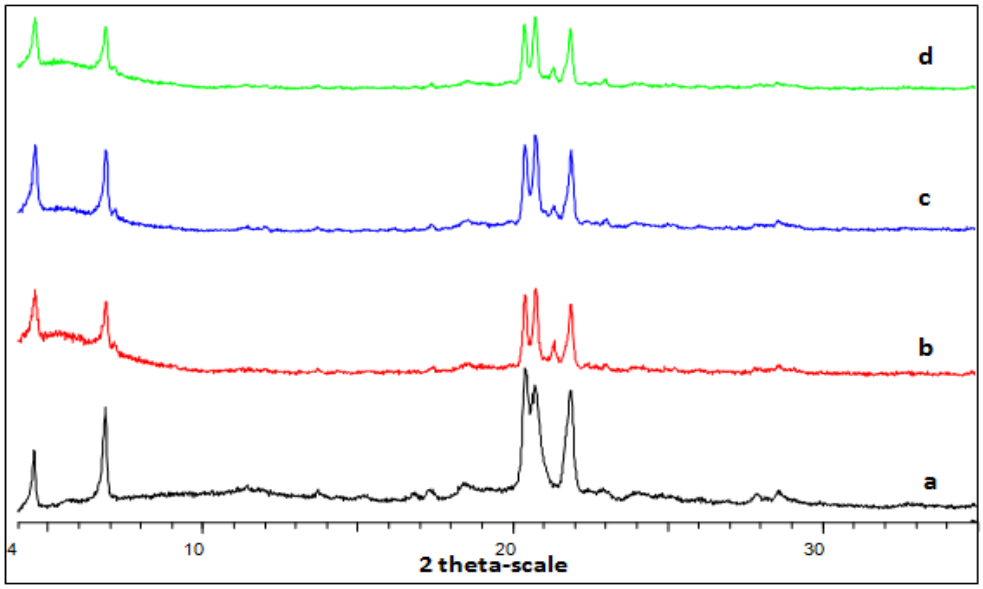

Figure 6.28: XRPD of glibenclamide-SLS lyophilised mixture (enteric coated capsules) stored at 25ºC/65% RH; non-coated (a), freshly coated (b), 30 days (c), 60 days (d).

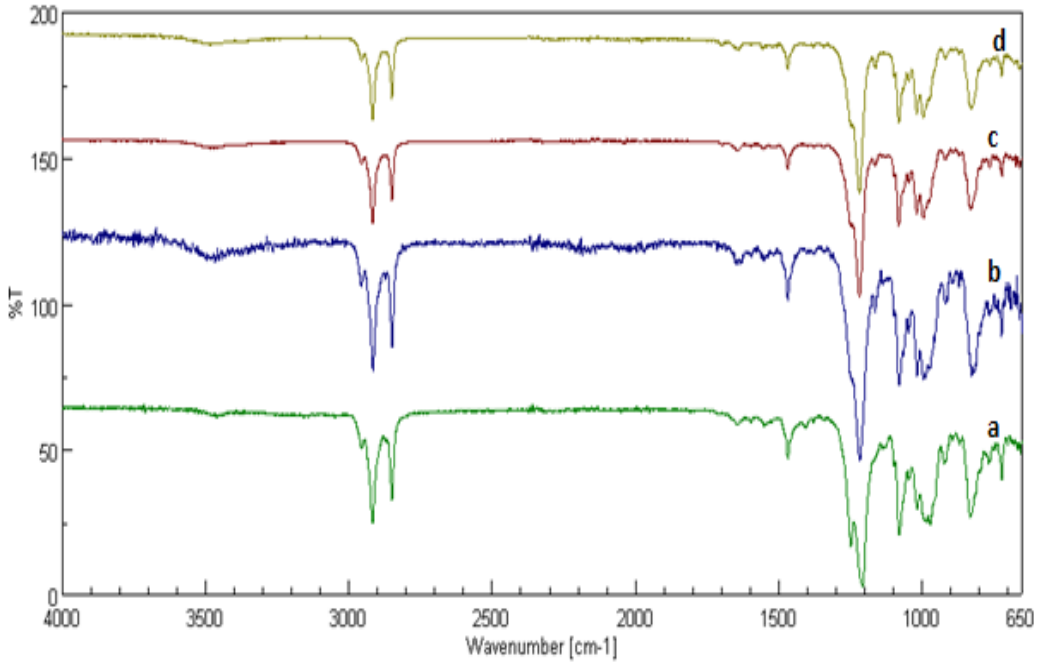

Figure 6.29: FT-IR of glibenclamide-SLS lyophilised mixture (enteric coated capsules) stored at 25ºC/65% RH; non-coated (a), freshly coated (b), 30 days (c), 60 days (d).

6.4.1.8 Effect of storage at 25ºC/75% RH on the physicochemical characteristics of lyophilised glibenclamide-SLS formulations in enteric coated capsules

Figures 6.30-6.33 show dissolution profiles, DSC, XRPD and FT-IR of the lyophilised mixtures of glibenclamide with SLS stored at 25ºC/75% RH up to two months. The data was similar to that obtained in Section 6.4.1.2. Hence, the amorphous form of glibenclamide in its lyophilised formulations (enteric coated capsules) was stable on being stored under these conditions without any tendency to recrystallisation.

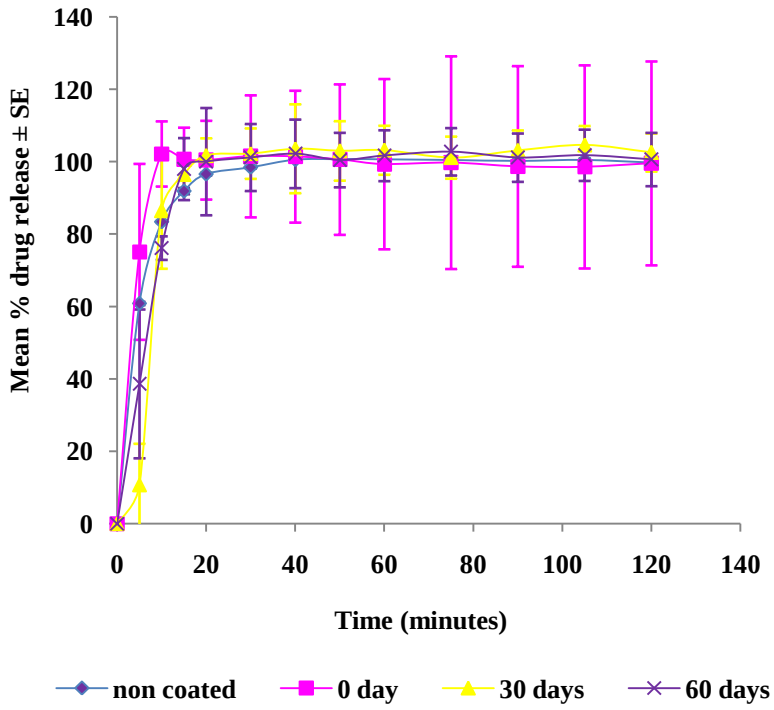

Figure 6.30: Effect of storage at 25ºC/75% RH on the dissolution profile of glibenclamide from enteric coated capsules of the lyophilised formulations (n=6).

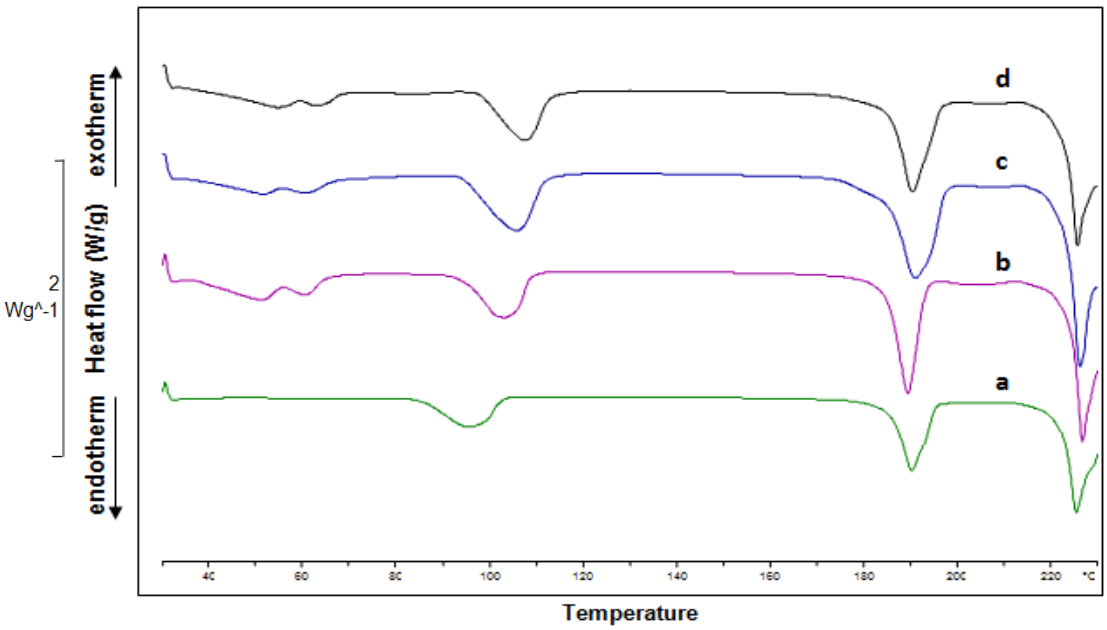

Figure 6.31: DSC of glibenclamide-SLS lyophilised mixture (enteric coated capsules) stored at 25ºC/75% RH; non-coated (a), freshly coated (b), 30 days (c), 60 days (d).

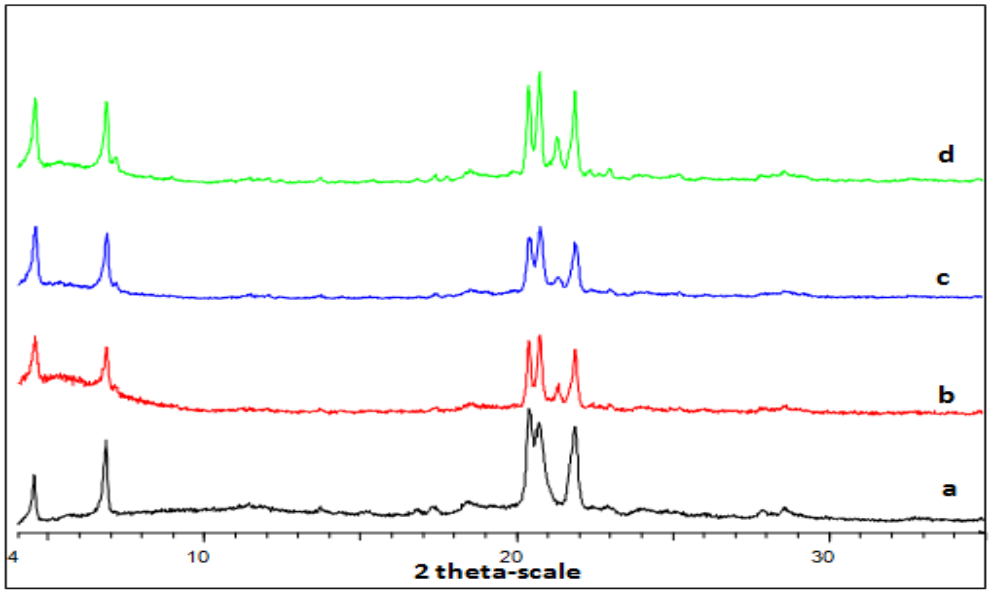

Figure 6.32: XRPD of glibenclamide-SLS lyophilised mixture (enteric coated capsules) stored at 25ºC/75% RH; non-coated (a), freshly coated (b), 30 days (c), 60 days (d).

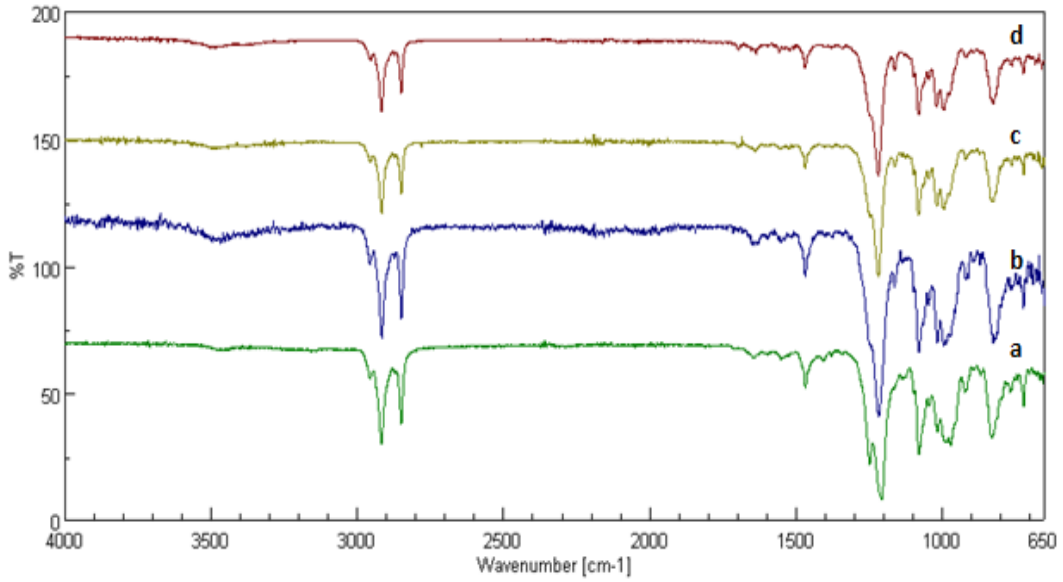

Figure 6.33: FTIR of glibenclamide-SLS lyophilised mixture (enteric coated capsules) stored at 25ºC/75 % RH; non-coated (a), freshly coated (b), 30 days (c), 60 days (d).

6.4.1.9 Effect of storage at 37ºC/0% RH on the physicochemical characteristics of lyophilised glibenclamide-SLS formulations in enteric coated capsules

Figures 6.34-6.37 show dissolution profiles, DSC, XRPD and FT-IR of the lyophilised mixtures of glibenclamide with SLS stored at 37ºC/0% RH up to two months. The data was similar to that obtained in Section 6.4.1.1. Hence, the amorphous form of glibenclamide in its lyophilised formulations (enteric coated capsules) was stable on being stored at under these conditions without any tendency for recrystallisation

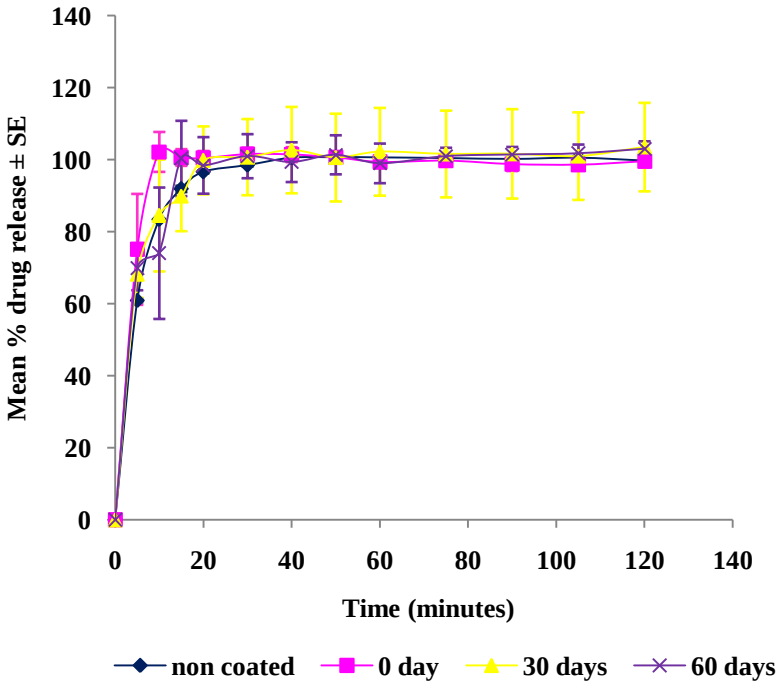

Figure 6.34: Effect of storage at 37ºC/0% RH on the dissolution profile of glibenclamide from enteric coated capsules of the lyophilised formulations (n=6).

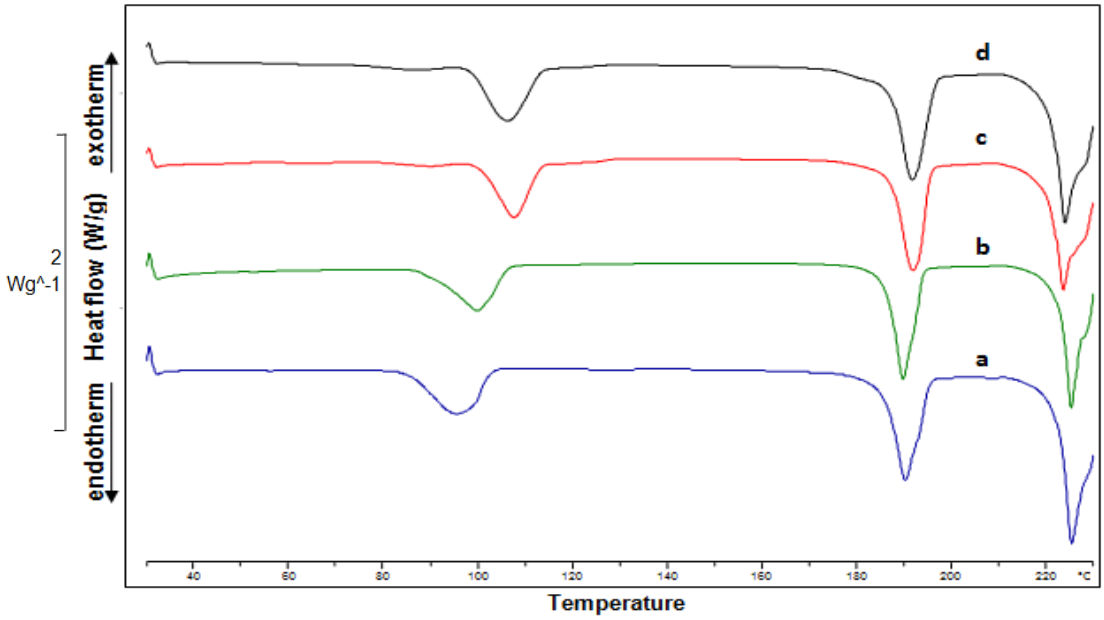

Figure 6.35: DSC of glibenclamide-SLS lyophilised mixture (enteric coated capsules) stored at 37ºC/0% RH; non-coated (a), freshly coated (b), 30 days (c), 60 days (d).

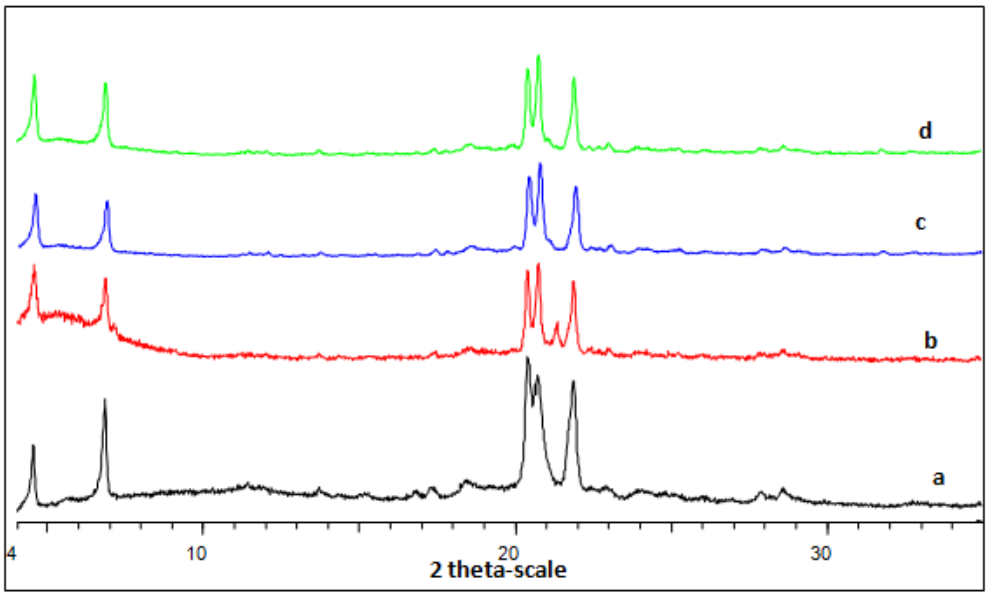

Figure 6.36: XRPD of glibenclamide-SLS lyophilised mixture (enteric coated capsules) stored at 37ºC/0% RH; non-coated (a), freshly coated (b), 30 days (c), 60 days (d).

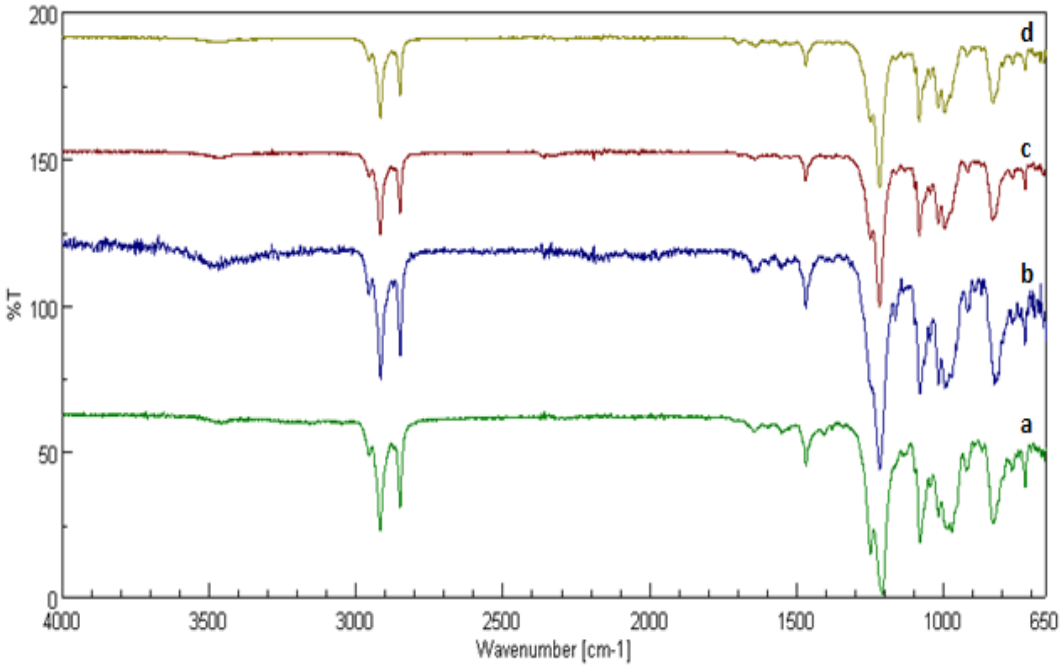

Figure 6.37: FT-IR of glibenclamide-SLS lyophilised mixture (enteric coated capsules) stored at 37ºC/0% RH; non-coated (a), freshly coated (b), 30 days (c), 60 days (d).

6.4.1.10 Effect of storage at 50ºC/0% RH on the physicochemical characteristics of lyophilised glibenclamide-SLS formulations in enteric coated capsules

Figures 6.38-6.41 show dissolution profiles, DSC, XRPD and FT-IR of the lyophilised mixtures of glibenclamide with SLS stored at 50ºC/0% RH up to two months. The data was similar to that obtained in Section 6.4.1.1 supporting the stability of the amorphous form of glibenclamide in its lyophilised formulations (enteric coated capsules) after storage under these conditions.

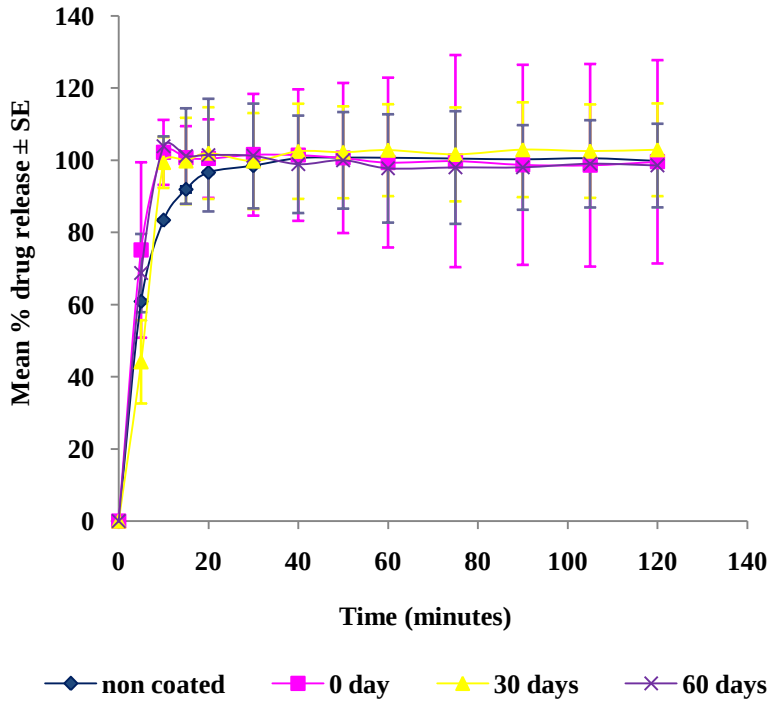

Figure 6.38: Effect of storage at 50ºC/0% RH on the dissolution profile of glibenclamide from enteric coated capsules of the lyophilised formulations (n=6).

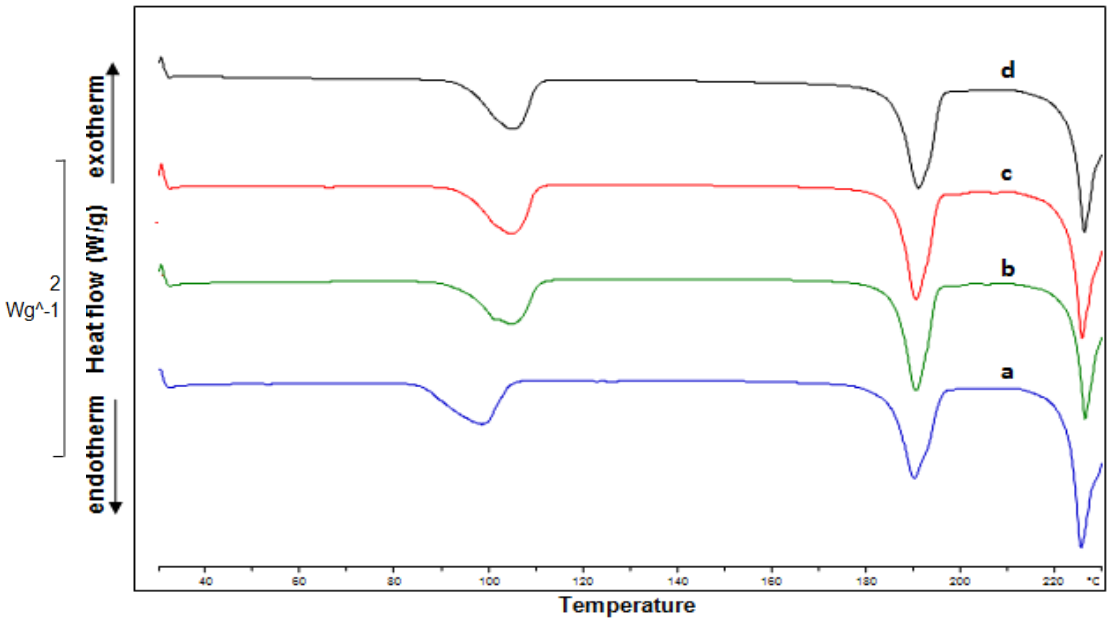

Figure 6.39: DSC of glibenclamide-SLS lyophilised mixture (enteric coated capsules) stored at 50ºC/0% RH; non-coated (a), freshly coated (b), 30 days (c), 60 days (d).

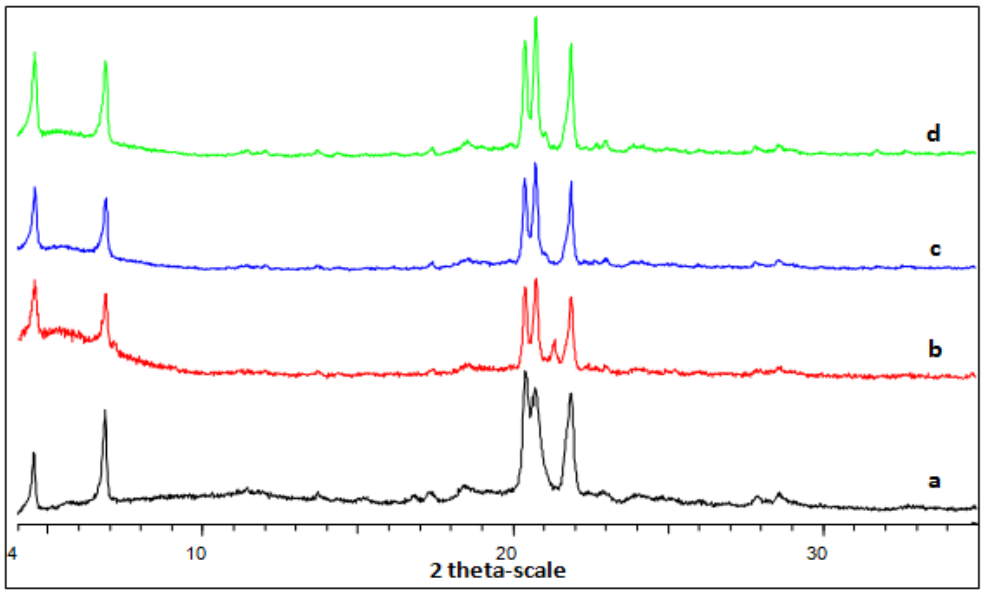

Figure 6.40: XRPD of glibenclamide-SLS lyophilised mixture (enteric coated capsules) stored at 50ºC/0% RH; non-coated (a), freshly coated (b), 30 days (c), 60 days (d).

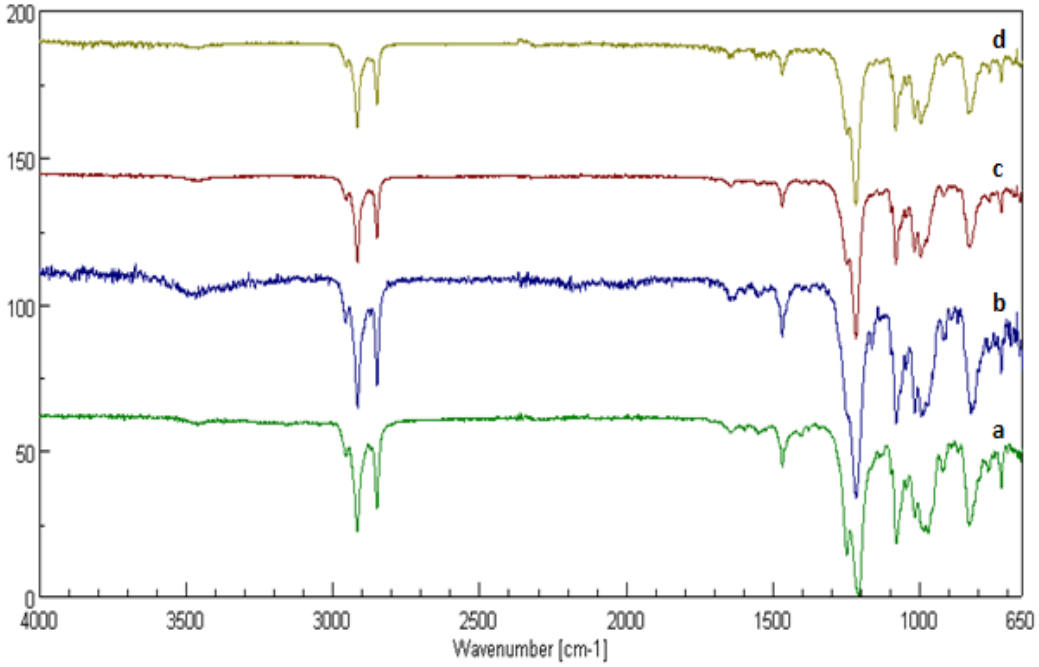

Figure 6.41: FT-IR of glibenclamide-SLS lyophilised mixture (enteric coated capsules) stored at 50ºC/0% RH; non-coated (a), freshly coated (b), 30 days (c), 60 days (d).

The stability of the amorphous form of glibenclamide in its lyophilised mixture with SLS under different conditions is not mainly attributed to the barrier effect of the coating system. This is because the absorption of moisture from the environment was evident in the DSC thermograms of the formulations stored in humid conditions. As the recrystallisation rate of the amorphous solid increases at temperatures above and directly below T_g (Guo et al., 2000), the high T_g of glibenclamide; 84.8ºC (Chauhan et al., 2005) had a significant role in the high stability of the amorphous form of glibenclamide during storage under different conditions. In addition, the decrease in the mobility of the drug molecules in the solid dispersion due to strong hydrogen bonding between glibenclamide and SLS may be another contributing factor. Sertsou et al. (2003) have reported the stability of the amorphous form of GWX, an analgesic drug, in its solid solution with hydroxypropyl methylcellulose phthalate when stored at 25ºC/75% RH or 40ºC/75 % RH due to decreased molecular mobility of the drug in the amorphous solid solution compared with the amorphous drug alone. Similarly, the amorphous form of indomethacin in its solid dispersion with polyvinyl pyrrolidone (PVP) remained stable on being stored for seven months

at 75% RH and 25ºC or 40ºC (Lim et al., 2010) due to the effect of PVP that prevented the recrystallisation of the drug through restricting the mobility of the drug molecules.

6.4.2 Spironolactone

6.4.2.1 Effect of storage at 25°C/0% RH on the physicochemical characteristics of lyophilised spironolactone-SLS formulations in non-enteric coated capsules

Figure 6.42 shows the dissolution profiles of the lyophilised mixtures of spironolactone with 67% w/w SLS after storage at 25ºC/0% RH up to 3 months. Statistical analysis showed no significant differences between the dissolution profiles of the formulations stored for different times and that of the freshly coated samples with f_2 values > 50.

The corresponding DSC thermograms are shown in Figure 6.43. The thermograms of the formulations stored up to 60 days displayed no differences from that of the freshly coated samples (see Section 5.4.3.2). On the other hand, the thermograms of the samples stored for 90 days showed a shift in the melting endotherm of spironolactone to 204ºC and almost complete disappearance of the shoulder pointing to presence of one polymorphic form of spironolactone (original crystals). The melting point of this polymorph is close to that previously reported by Agafonov et al. (1991) corresponding to form I polymorph of spironolactone. This could be attributed to the loss of the solvent molecules that were adsorbed on the surface of the formulation during the coating process and initiated the polymorphic transformation of the drug.

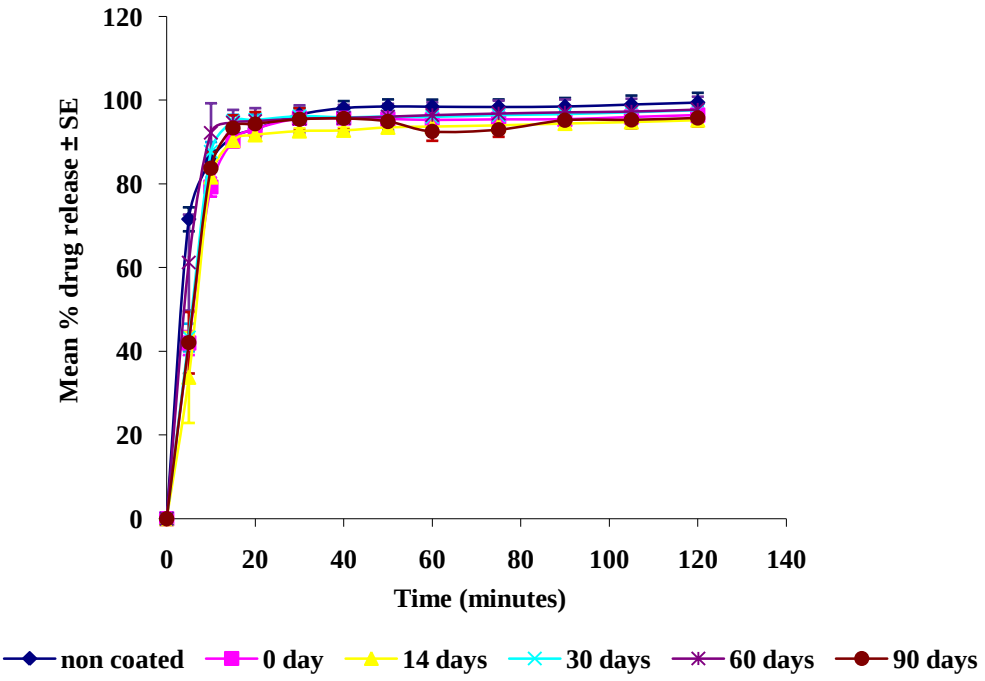

Figure 6.42: Effect of storage at 25°C/0% RH on the dissolution profile of spironolactone from non-enteric coated capsules of the lyophilised formulations (n=6).

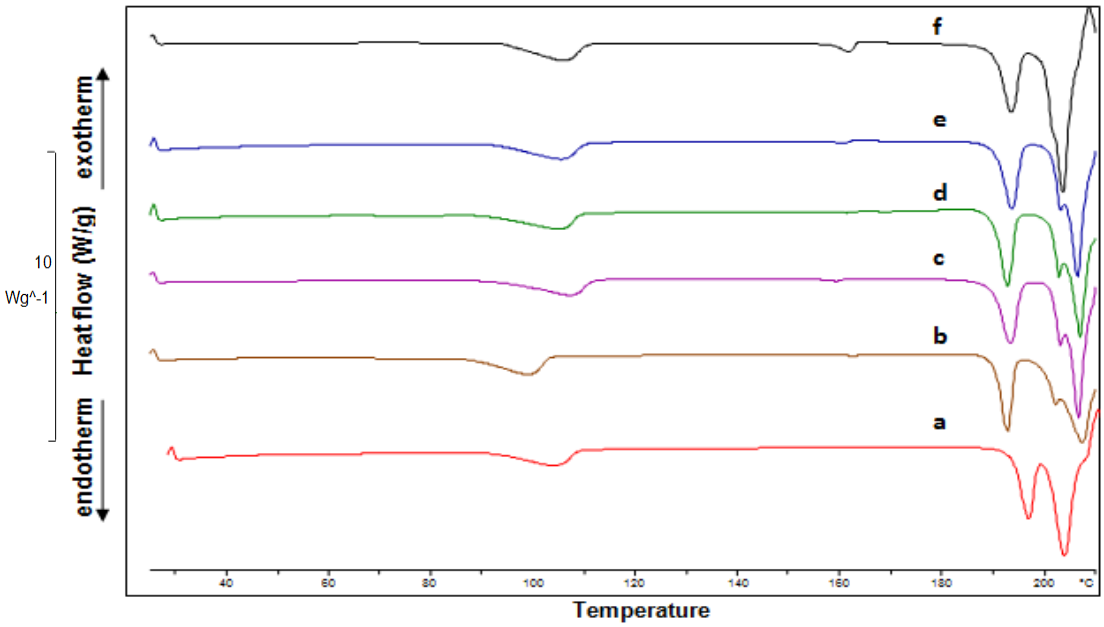

Figure 6.43: DSC of spironolactone-SLS lyophilised mixture (non-enteric coated capsules) stored at 25°C/0% RH; non-coated (a), freshly coated (b), 15 days (c), 30 days (d), 60 days (e), 90 days (f).

The corresponding XRPD patterns are represented in Figure 6.44. The diffractograms of the stored formulations showed no differences from that of the freshly coated samples suggesting maintenance of amorphous state of spironolactone on being stored under these conditions. These results explain the maintenance of the dissolution rate of the stored samples. These XRPD diffractograms contradict the previous DSC thermograms showing the melting endotherm of the drug due to the fact that spironolactone molecules are flexible and can go through structural rearrangement by heating (see Sections 3.4.2.2 and 4.4.2.1) during DSC analysis.

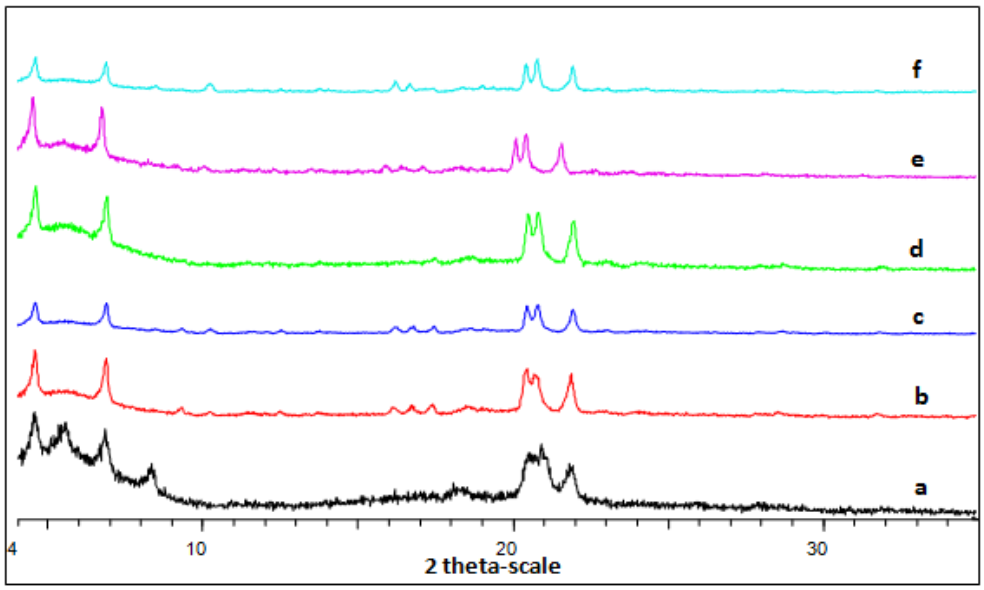

Figure 6.44: XRPD of spironolactone-SLS lyophilised mixture (non-enteric coated capsules) stored at 25ºC/0 % RH; non-coated (a), freshly coated (b), 15 days (c), 30 days (d), 60 days (e), 90 days (f).

The corresponding FT-IR spectra showed the appearance of spironolactone characteristic peak at 1689 cm^{-1} corresponding to C=O stretching of the thioacetyl group (Fig. 6.45). This finding may suggest disturbance in the hydrogen bonding between this group of spironolactone and SLS in their solid dispersion during storage. However, the changes had no effect on the dissolution rate of spironolactone from the lyophilised formulations.

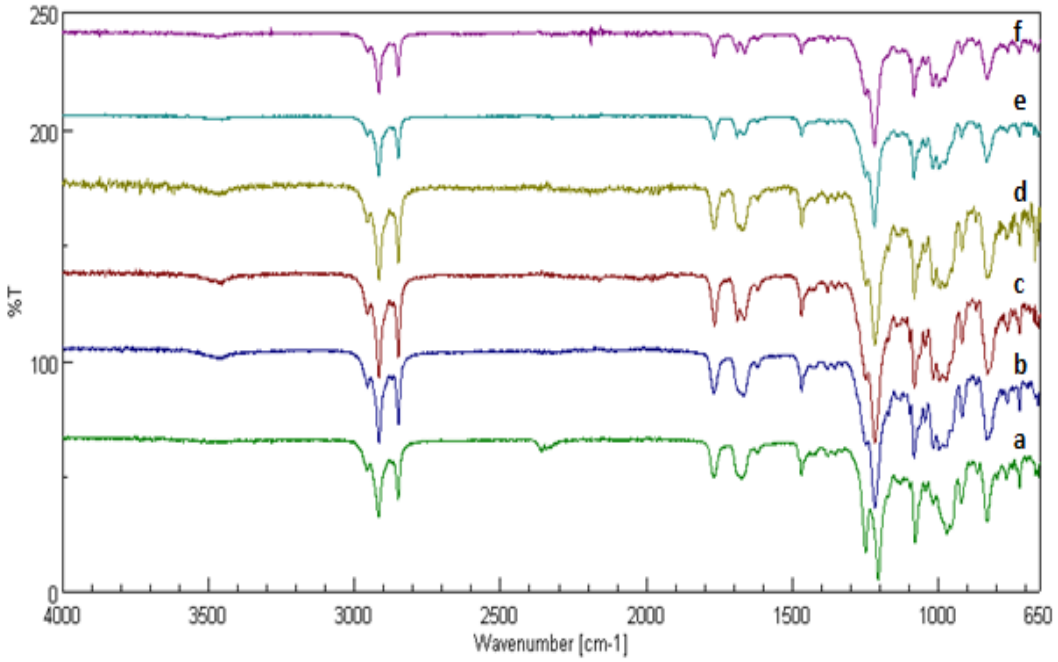

Figure 6.45: FT-IR of spironolactone-SLS lyophilised mixture (non-enteric coated capsules) stored at 25ºC/0% RH; non-coated (a), freshly coated (b), 15 days (c), 30 days (d), 60 days (e), 90 days (f).

6.4.2.2 Effect of storage at 25ºC/65% RH on the physicochemical characteristics of lyophilised spironolactone-SLS formulations in non-enteric coated capsules

Figure 6.46 shows the dissolution profiles of the lyophilised mixture of spironolactone with 67% w/w SLS after storage at 25ºC/65% RH up to 3 months. Statistical analysis revealed no significant differences between the different dissolution profiles with f_2 values > 50.

The corresponding DSC thermograms are presented in Figure 6.47. The thermograms of the stored samples were similar to that of the freshly coated samples (Section 5.4.3.2) except for the appearance of a shallow endotherm in the temperature range 40-70ºC representing removal of water that was absorbed during storage at these conditions.

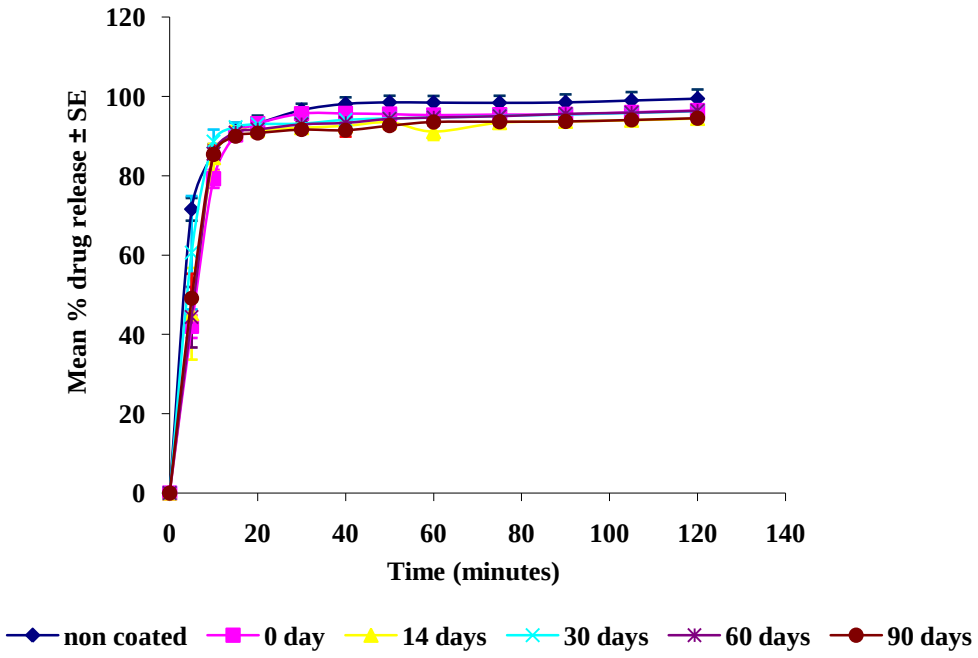

Figure 6.46: Effect of storage at 25ºC/65% RH on the dissolution profile of spironolactone from non-enteric coated capsules of the lyophilised formulations (n=6).

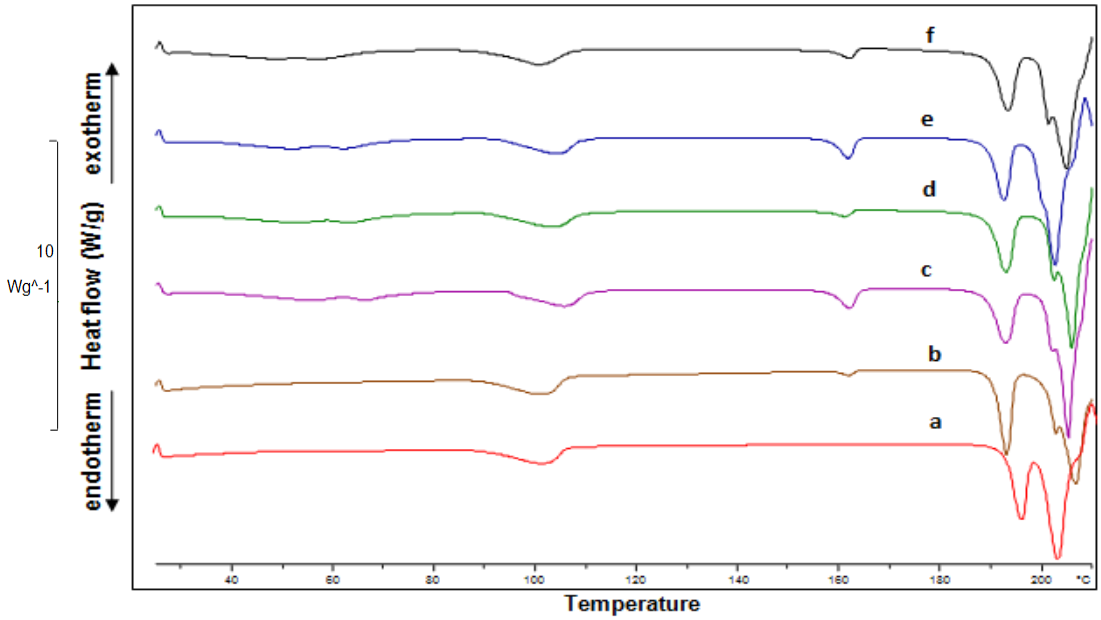

Figure 6.47: DSC of spironolactone-SLS lyophilised mixture (non-enteric coated capsules) stored at 25ºC/65% RH; non-coated (a), freshly coated (b), 15 days (c), 30 days (d), 60 days (e), 90 days (f).

The corresponding XRPD patterns are represented in Figure 6.48. Compared with the diffractogram of the freshly coated formulations (Section 5.4.3.2), those of the stored samples represent slight increase in the number and intensity of the crystal peaks. This finding suggests the instability of the amorphous form of spironolactone in its solid dispersion with SLS when stored under these conditions. This is in a good agreement with that previously reported in the literature about the plasticisation effect of moisture on the amorphous solids as it increases the molecular mobility and decreases T_g resulting in increased tendency for transformation to the crystalline form (Strydom et al., 2009; Ambike et al., 2004; Andronis & Zografi, 1998; Andronis et al., 1997).

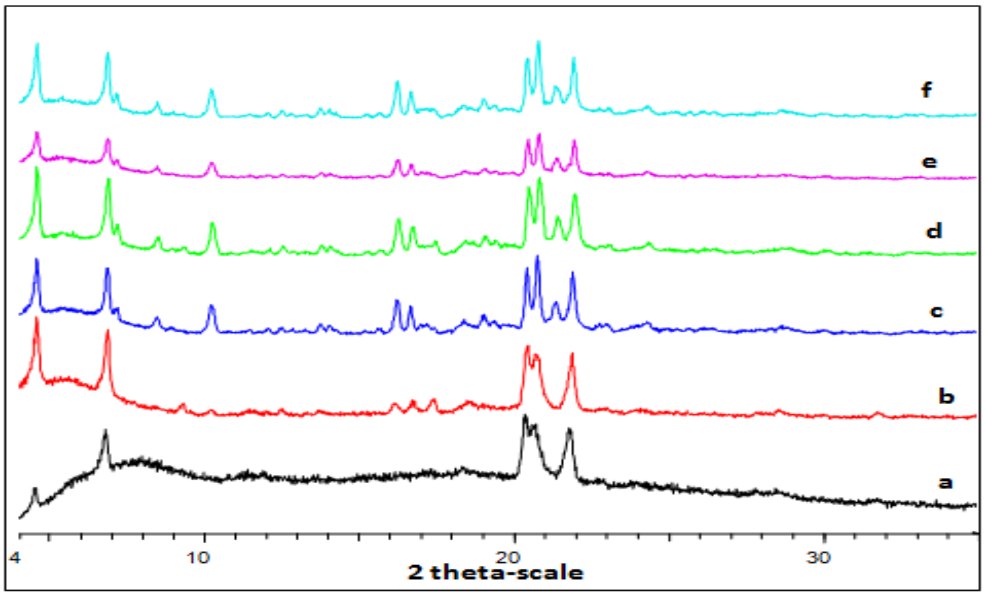

Figure 6.48: XRPD of spironolactone-SLS lyophilised mixture (non-enteric coated capsules) stored at 25ºC/65% RH; non-coated (a), freshly coated (b), 15 days (c), 30 days (d), 60 days (e), 90 days (f).

The corresponding FT-IR spectra are shown in Figure 6.49. The results were similar to those obtained in Section 6.4.2.1 supporting the fact of the change of hydrogen bonding between spironolactone and SLS in their solid dispersion after storage under these conditions. Marsac et al. (2010) have reported that the hydrogen bonding between felodopine and polyvinyl pyrrolidone in their solid dispersion were

weakened or less numerous when stored at different relative humidity (33, 43, 58, 75, 84 % RH) with more obvious effect in the case of 75% RH or higher leading to phase separation.

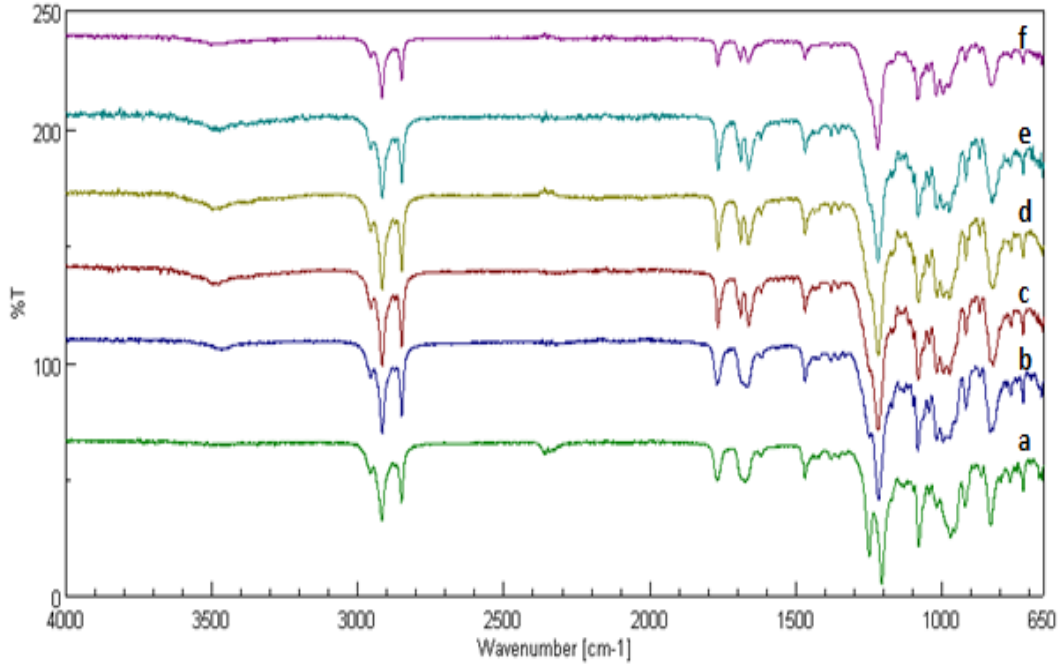

Figure 6.49: FT-IR of spironolactone-SLS lyophilised mixture (non-enteric coated capsules) stored at 25ºC/65% RH; non-coated (a), freshly coated (b), 15 days (c), 30 days (d), 60 days (e), 90 days (f).

6.4.2.3 Effect of storage at 25ºC/75% RH on the physicochemical characteristics of lyophilised spironolactone-SLS formulations in non-enteric coated capsules

Figures 6.50-6.53 show dissolution profiles, DSC thermograms, XRPD patterns and FT-IR spectra of the lyophilised mixtures of spironolactone with SLS after storage at 25ºC/75% RH up to 3 months. Statistical analysis revealed similarity between the dissolution profiles of the stored formulations and that of the freshly coated sample with f_2 values > 50.

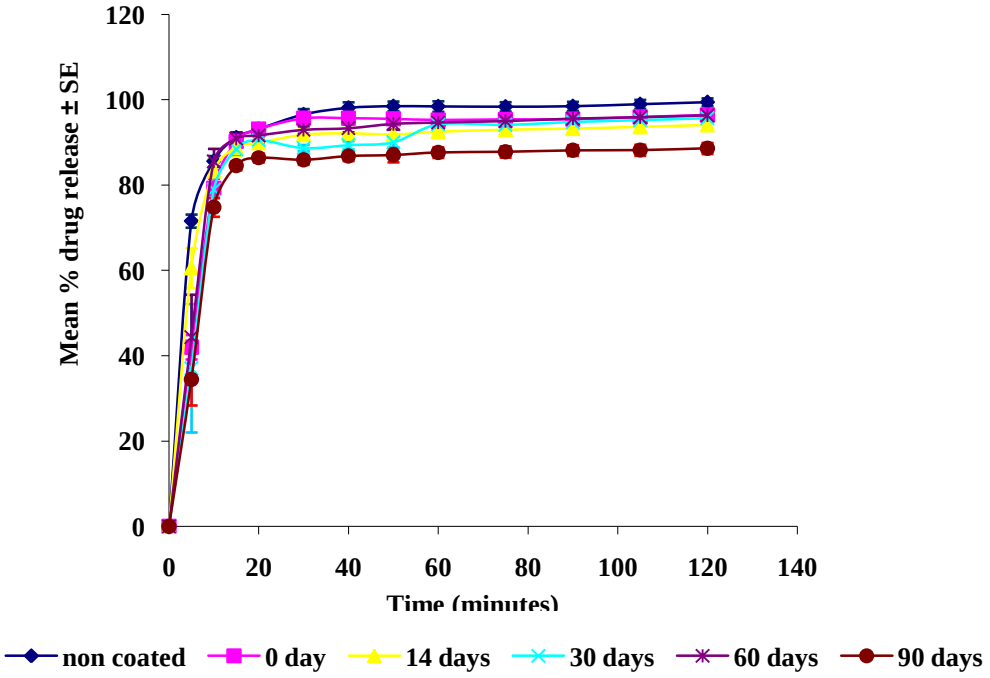

Figure 6.50: Effect of storage at 25ºC/75% RH on the dissolution profile of spironolactone from non-enteric coated capsules of the lyophilised formulations (n=6).

The corresponding DSC, XRPD and FT-IR show similar results to those obtained from the formulations stored at 25ºC/65% RH (6.4.2.2) supporting the incidence of physical changes in the lyophilised formulations of spironolactone during storage. This finding suggests the instability of the amorphous form of spironolactone in its solid dispersion with SLS when stored under these conditions. However, these changes had no impact on the dissolution profiles of the stored samples. In contrast to these results, Soliman et al. (1997) have reported the stability of the amorphous form of spironolactone in its complex with hydroxypropyl β-cyclodextrin for two months at storage conditions of 60ºC/75% RH. As an example for the effect of relative humidity on the amorphous solids, Jassens et al. (2008) have reported the recrystallisation of the amorphous form of itraconazole in its ternary solid dispersion with PEG 6000 and hydroxypropyl methylcellulose, on being stored at 25ºC/52% RH.

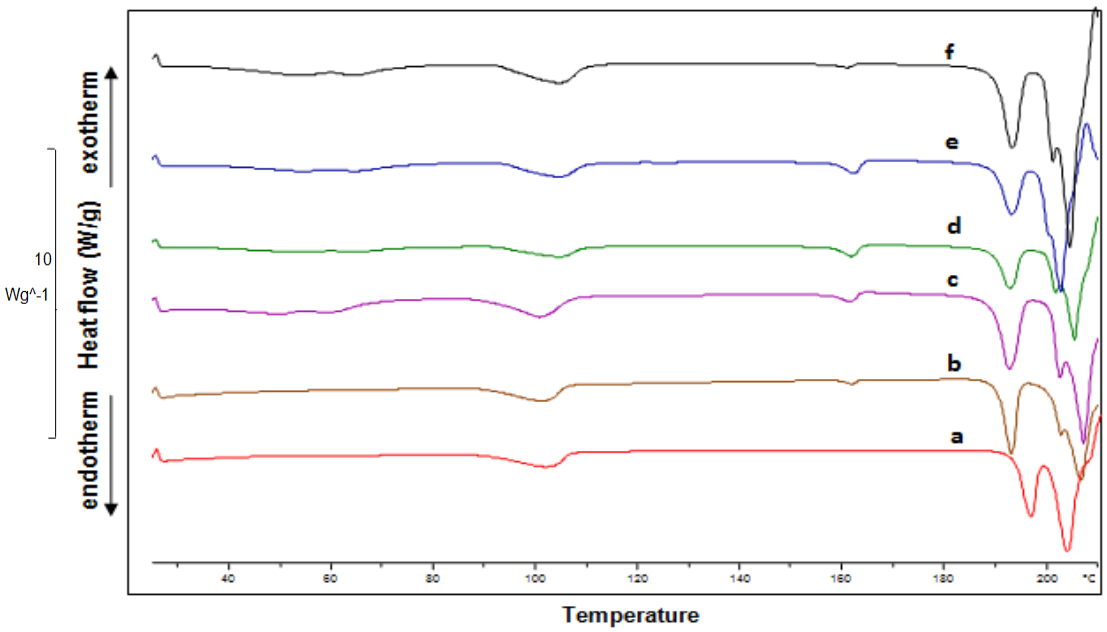

Figure 6.51: DSC of spironolactone-SLS lyophilised mixture (non-enteric coated capsules) stored at 25°C/75% RH; non-coated (a), freshly coated (b), 15 days (c), 30 days (d), 60 days (e), 90 days (f).

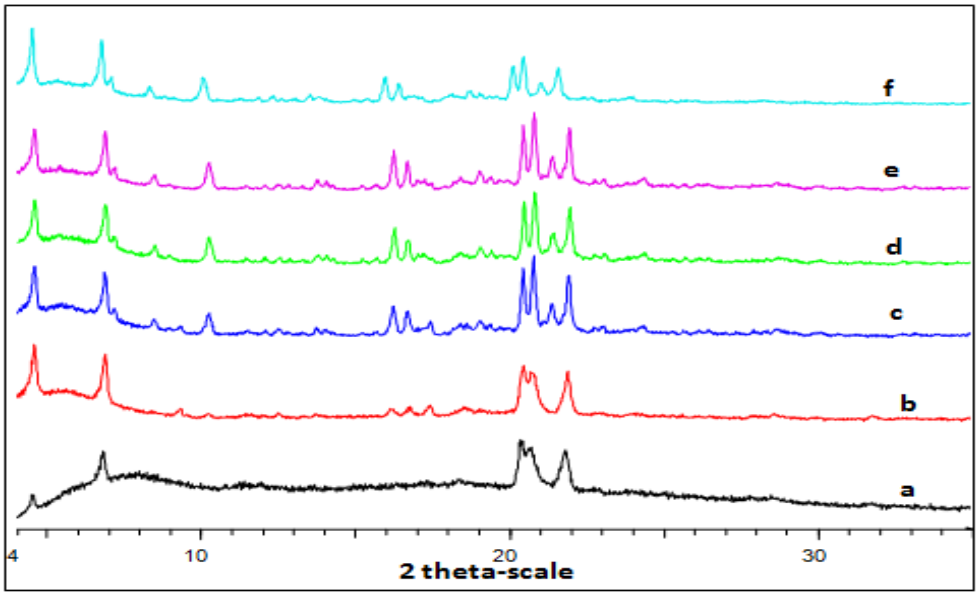

Figure 6.52: XRPD of spironolactone-SLS lyophilised mixture (non-enteric coated capsules) stored at 25°C/75% RH; non-coated (a), freshly coated (b), 15 days (c), 30 days (d), 60 days (e), 90 days (f).

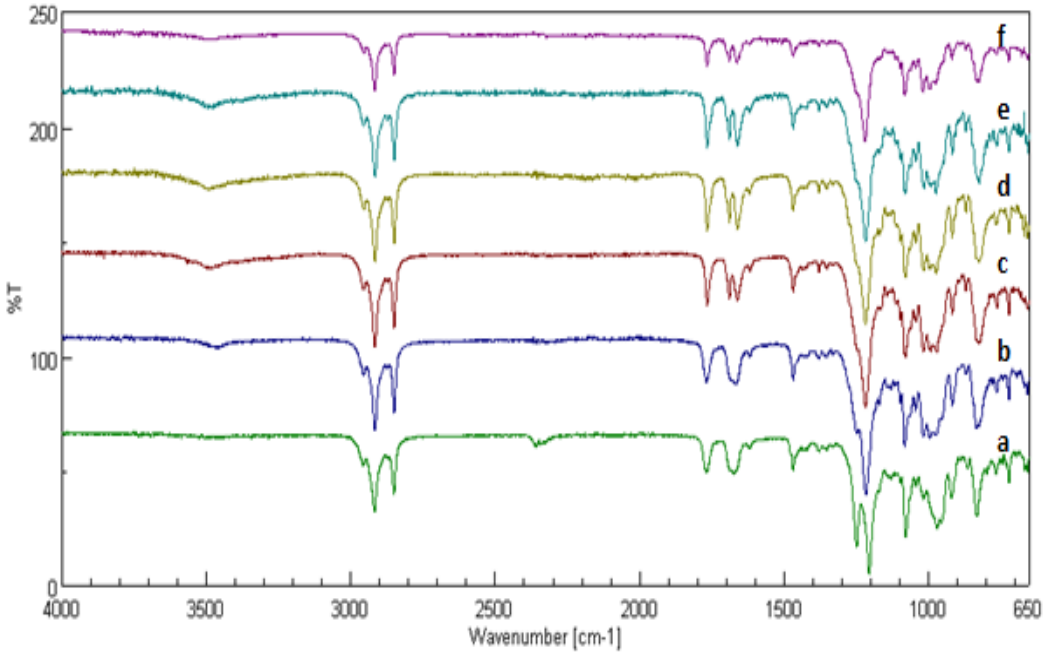

Figure 6.53: FT-IR of spironolactone-SLS lyophilised mixture (non-enteric coated capsules) stored at 25ºC/75% RH; non-coated (a), freshly coated (b), 15 days (c), 30 days (d), 60 days (e), 90 days (f).

6.4.2.4 Effect of storage at 37ºC/0% RH on the physicochemical characteristics of lyophilised spironolactone-SLS formulations in non-enteric coated capsules

The dissolution profiles of the formulations stored at 37ºC/0% RH up to 3 months are represented in Figure 6.54. There were no significant differences between the dissolution profiles of the stored formulations and that of the freshly coated samples with $f_2 > 50$.

Representative DSC thermograms are shown in Figure 6.55. Compared to the thermograms of the freshly coated formulations, those of the stored samples displayed a shift in the spironolactone melting endotherm at 209ºC (melting point of form II polymorph of spironolactone, section 5.4.3.2) to 204ºC corresponding to the melting point of form I polymorph of the drug. It also shows gradual decrease in the intensity of the endothermic shoulder till it disappeared in the thermogram of the samples stored for 90 days indicating the presence of only one polymorphic form. This is attributed to the effect of temperature in inducing structural rearrangement of spironolactone molecule (Neville et al., 1994; Berbenni et al., 1999). In addition,

storage under this temperature might lead to loss of the solvent molecules adsorbed on the surface of the amorphous formulations during the coating process as the solvent was the initiating factor for polymorphic transformation of the drug.

The corresponding XRPD patterns are represented in Figure 6.56. Compared to the diffractogram of the freshly coated formulations, those of the stored formulations showed less intense recrystallisation peaks that disappear in the diffractogram of the samples stored for 90 days. This finding supports the DSC results suggesting that storage under this temperature resulted in the removal of the residual solvent that induced polymorphic transformation of spironolactone during the coating process. Thus, the amorphous form of spironolactone was maintained during storage under 37ºC/0% RH up to 3 months.

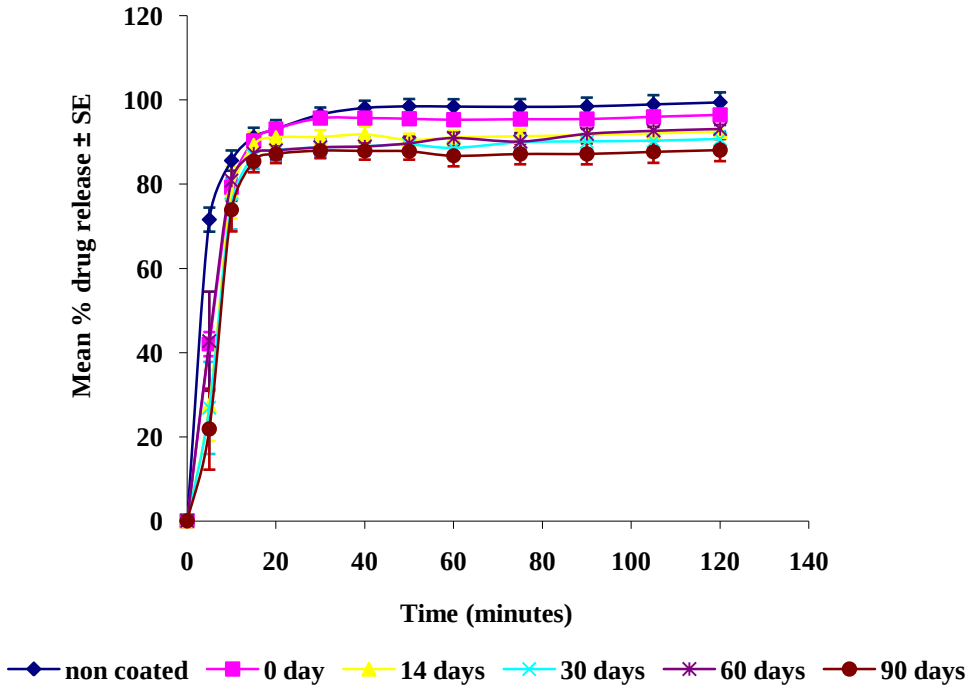

Figure 6.54: Effect of storage at 37ºC/0% RH on the dissolution profile of spironolactone from non-enteric coated capsules of the lyophilised formulations (n=6).

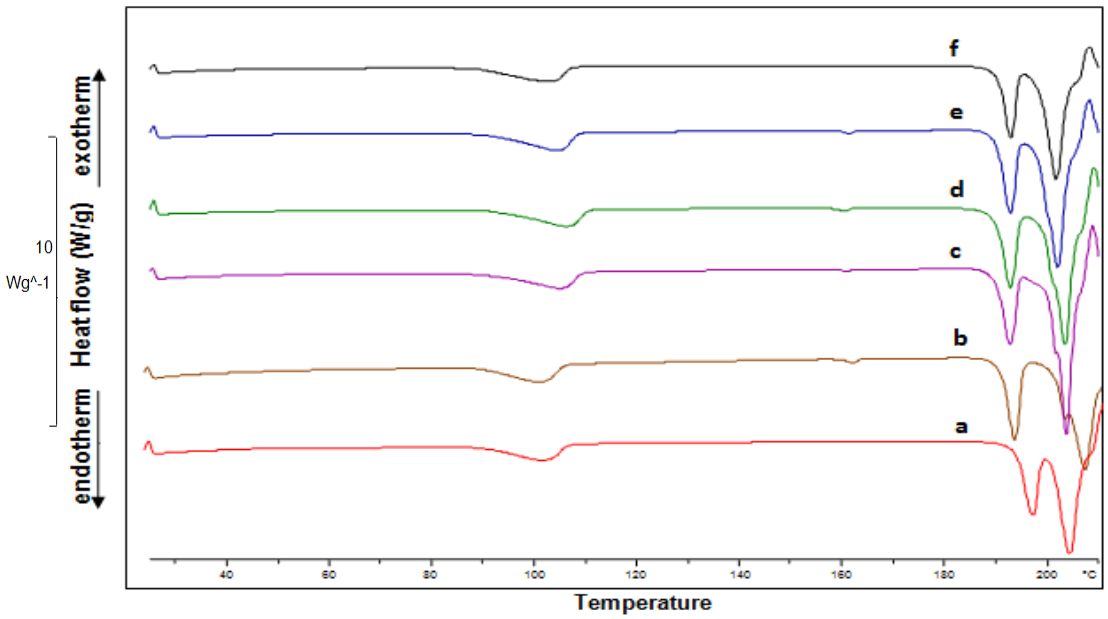

Figure 6.55: DSC of spironolactone-SLS lyophilised mixture (non-enteric coated capsules) stored at 37ºC/0% RH; non-coated (a), freshly coated (b), 15 days (c), 30 days (d), 60 days (e), 90 days (f).

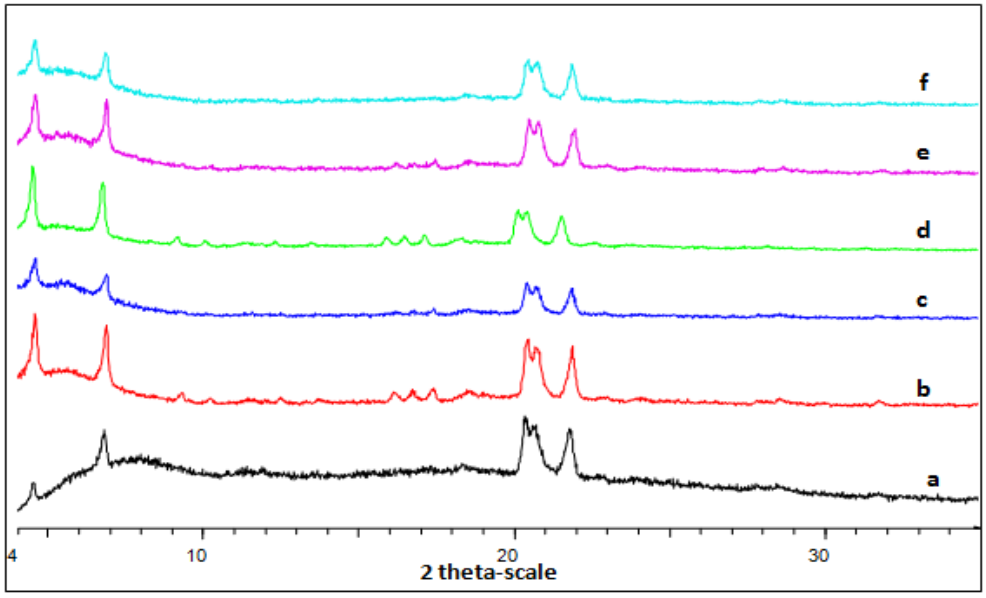

Figure 6.56: XRPD of spironolactone-SLS lyophilised mixture (non-enteric coated capsules) stored at 37ºC/0% RH; non-coated (a), freshly coated (b), 15 days (c), 30 days (d), 60 days (e), 90 days (f).

The corresponding FT-IR spectra were similar to that of the freshly coated samples supporting the fact of the stability of the coated samples on being stored at 37ºC/0% RH (Fig. 6.57).

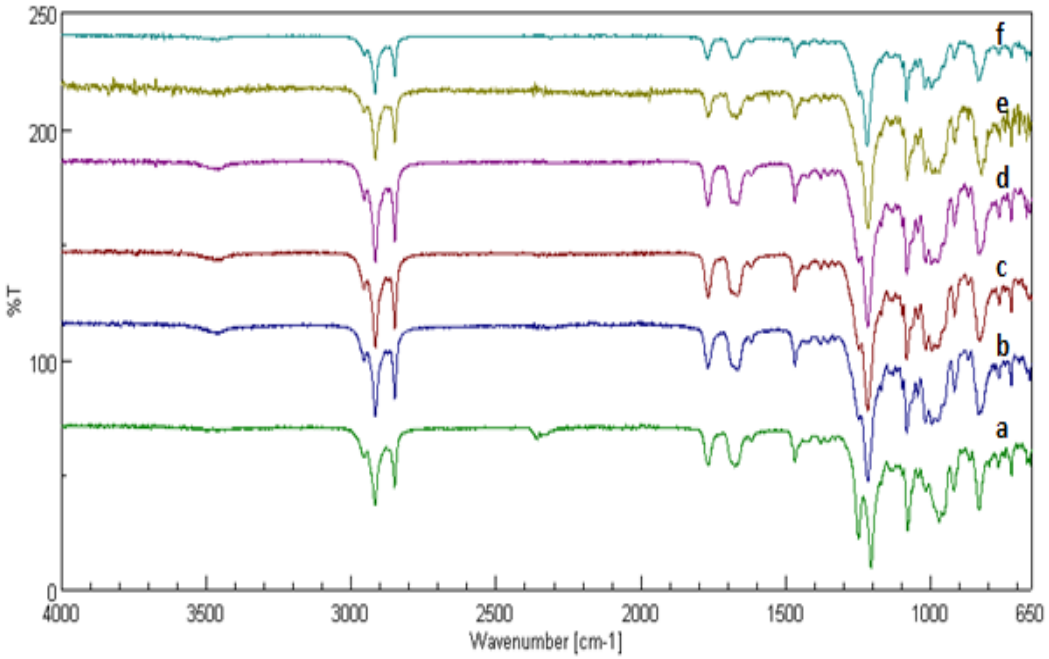

Figure 6.57: FT-IR of spironolactone-SLS lyophilised mixture (non-enteric coated capsules) stored at 37ºC/0% RH; non-coated (a), freshly coated (b), 15 days (c), 30 days (d), 60 days (e), 90 days (f).

6.4.2.5 Effect of storage at 50ºC/0% RH on the physicochemical characteristics of lyophilised spironolactone-SLS formulations in non-enteric coated capsules

Figures 6.58-6.61 show dissolution profiles, DSC, XRPD and FT-IR of the lyophilised spironolactone-SLS mixture stored at 50ºC/0% RH up to 3 months. The data show no differences from those obtained from the formulations stored at 37ºC/0% RH (Section 6.4.2.4). Thus, the amorphous form of spironolactone in its solid dispersions with SLS in non-enteric coated capsules was stable on being stored at 50ºC/0% RH up to 3 months without any tendency for recrystallisation.

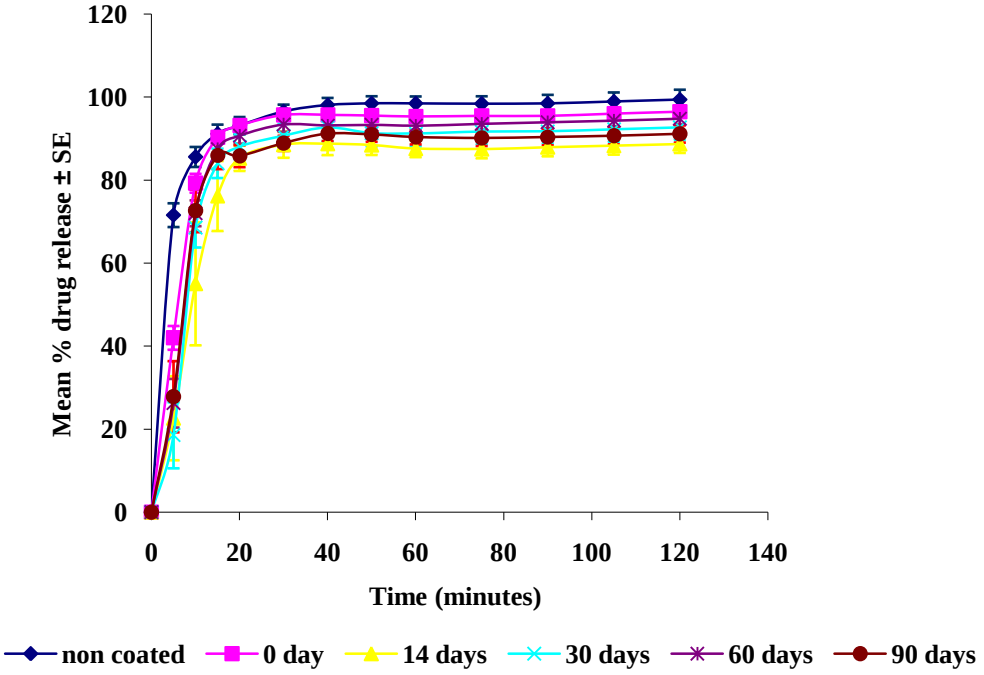

Figure 6.58: Effect of storage at 50ºC/0% RH on the dissolution profile of spironolactone from non-enteric coated capsules of the lyophilised formulations (n=6).

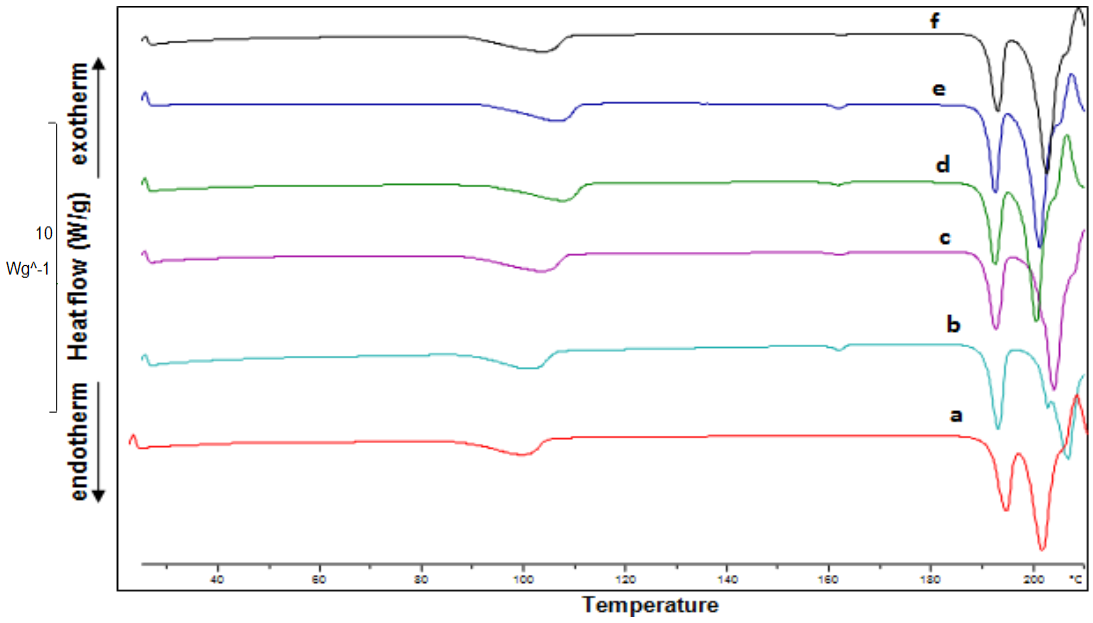

Figure 6.59: DSC of spironolactone-SLS lyophilised mixture (non-enteric coated capsules) stored at 50ºC/0% RH; non-coated (a), freshly coated (b), 15 days (c), 30 days (d), 60 days (e), 90 days (f).

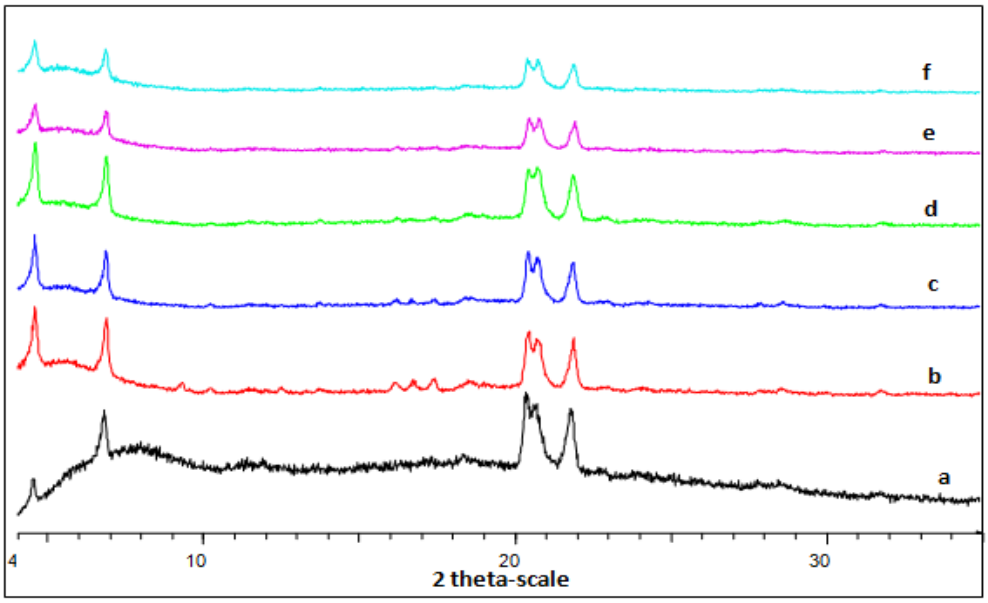

Figure 6.60: XRPD of spironolactone-SLS lyophilised mixture (non-enteric coated capsules) stored at 50ºC/0% RH; non-coated (a), freshly coated (b), 15 days (c), 30 days (d), 60 days (e), 90 days (f).

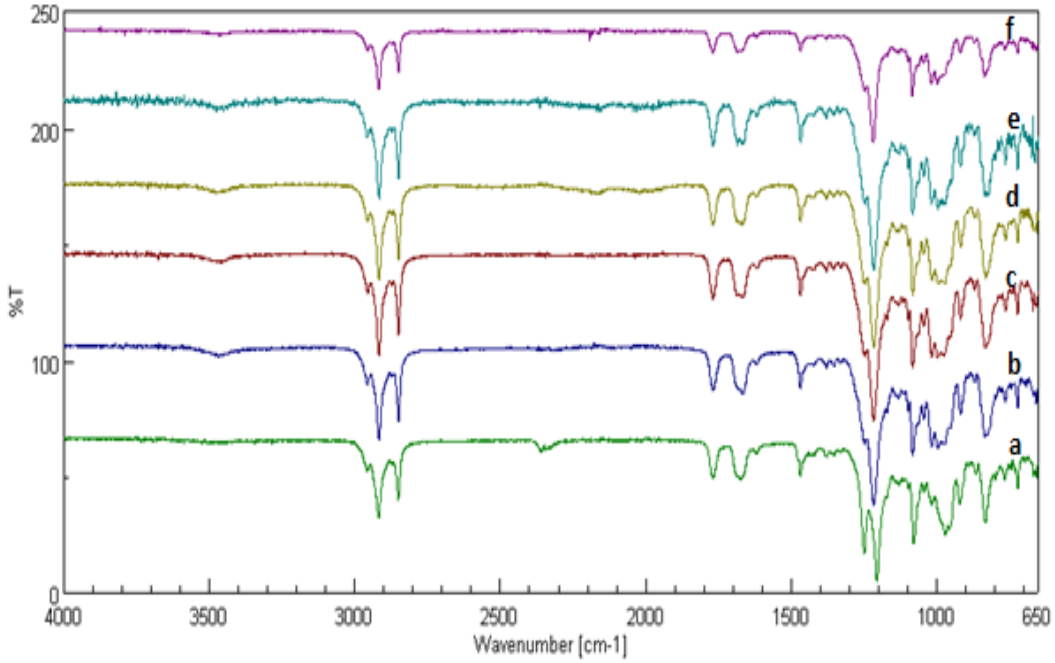

Figure 6.61: FT-IR of spironolactone-SLS lyophilised mixture (non-enteric coated capsules) stored at 50ºC/0% RH; non-coated (a), freshly coated (b), 15 days (c), 30 days (d), 60 days (e), 90 days (f).

As the amorphous form of spironolactone recrystallised on being stored in a humid environment while it was stable when stored at high temperatures, it can be concluded that humidity had a more influence on the amorphous formulations of spironolactone (non-enteric coated capsules) than did temperature. This is in accordance to Sertsou et al. (2003) who reported that high relative humidity (75%) had higher destabilising effect on the amorphous form of GWX, an analgesic drug, than that of a higher temperature (40°C). The stability of the amorphous form of spironolactone at high temperatures may be attributed to hydrogen bonding between the drug and SLS which decreases the mobility of the drug molecules in the solid dispersion.

6.4.3 Ketoconazole

The photographic images of ketoconazole formulations (non-enteric coated capsules) stored at different conditions are presented in Figures 6.62-5.67. These images showed a change in the colour of the formulations from white (freshly prepared and coated formulations) to red (stored formulations). It has been reported that the transformation of ketoconazole to the red colour is an indication for degradation of the drug (Staub & Bergold, 2004).

Figure 6.62: Photographic images of freshly prepared ketoconazole formulations (a) and freshly non-enteric coated formulations (b).

Figure 6.63: Photographic images of ketoconazole formulations stored at 25ºC/0% for 14 days (a), 30 days (b), 60 days (c), 90 days (d).

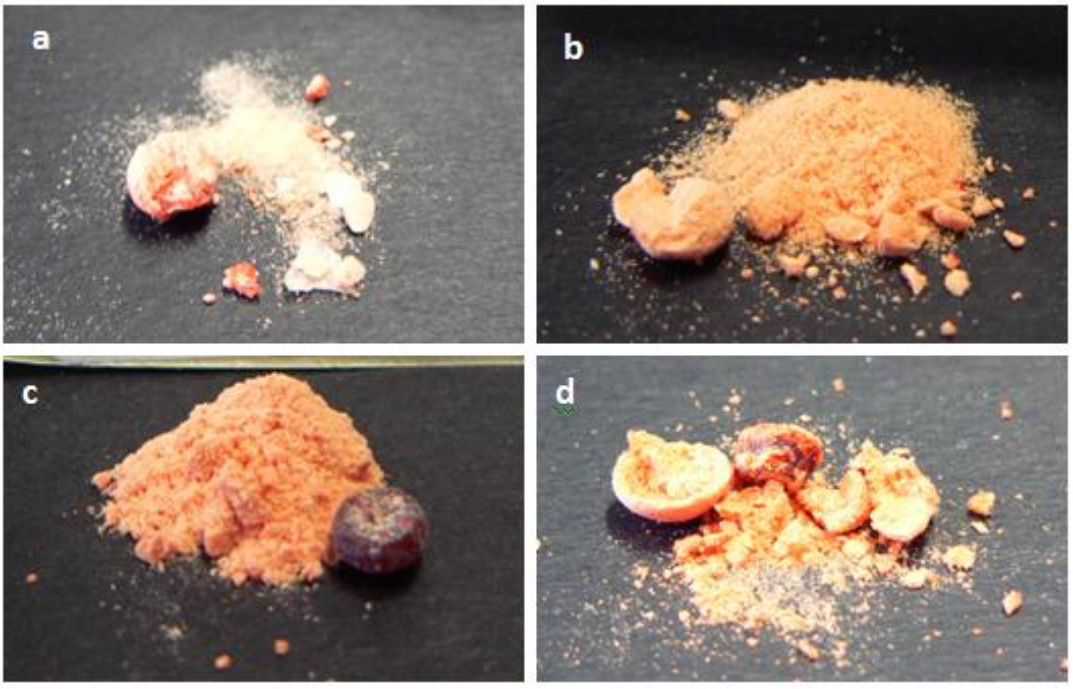

Figure 6.64: Photographic images of ketoconazole formulations stored at 37ºC/0% RH for 14 days (a), 30 days (b), 60 days (c), 90 days (d).

Figure 6.65: Photographic images of ketoconazole formulations stored at 50ºC/0% RH for 14 days (a), 30 days (b), 60 days (c), 90 days (d).

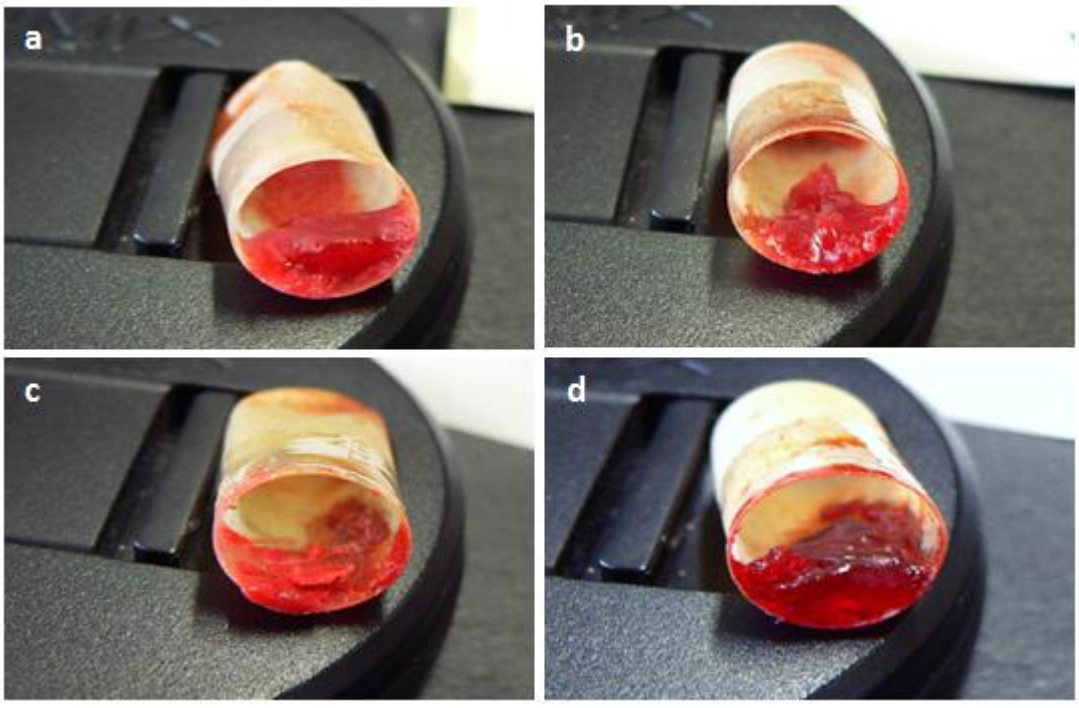

Figure 6.66: Photographic images of ketoconazole formulation stored at 25ºC/65% RH for 14 days (a), 30 days (b), 60 days (c), 90 days (d).

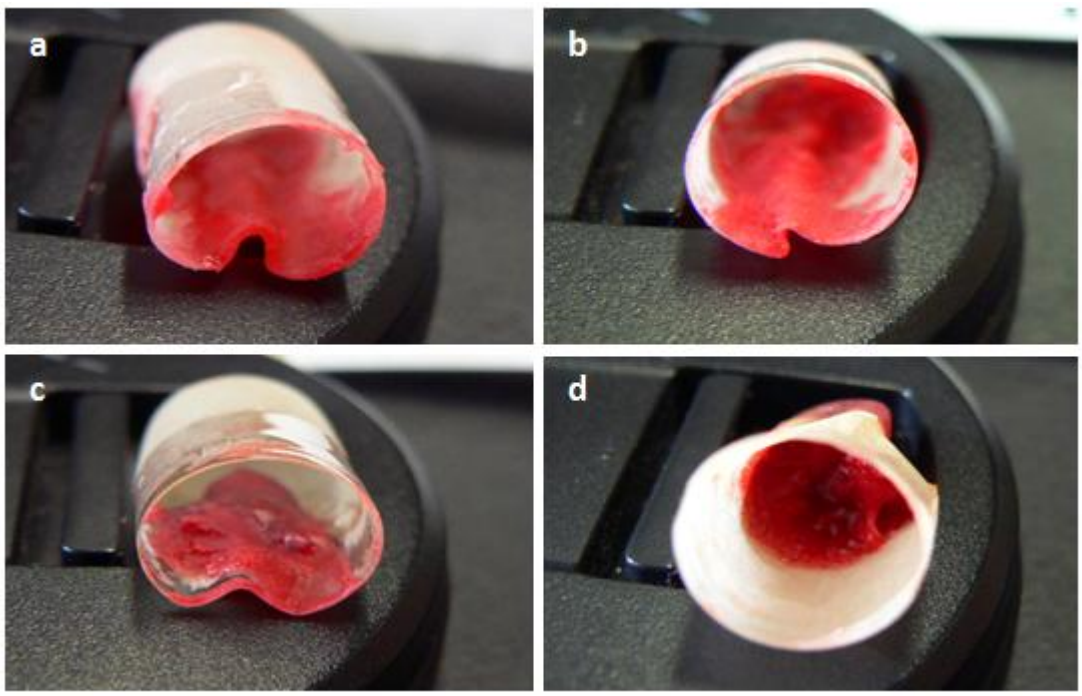

Figure 6.67: Photographic images of ketoconazole formulation stored at 25ºC/75% RH for 14 days (a), 30 days (b), 60 days (c), 90 days (d).

From the above images, it can be noticed that storage of non-enteric coated lyophilised ketoconazole formulations in different temperatures resulted in formation of clumps that turned into red colour over time and as the temperature increased. In addition, the formulations stored at high temperatures showed separation into two discrete phases; a dark red mass and light red powder. On the other hand, the formulations stored at high relative humidity absorbed moisture and converted into sticky semi solids suggesting the high hygroscopicity of the formulations. Thus, the physicochemical characterisation of the resultant formulations was difficult and their DSC thermograms were impossible to assign any thermal behaviour with accuracy. Photographic imaging was therefore used to record the changes in the lyophilised mixture during storage. These changes support the fact of a significant physical and chemical change in the lyophilised formulations of ketoconazole being stored under different temperatures and relative humidity. These observations need to be supported by further chemical analysis using appropriate techniques such as HPLC. Therefore, the lyophilised formulation of ketoconazole with mannitol and SLS was unstable under different storage conditions. This could be attributed to the low T_g of

the amorphous ketoconazole (44.5ºC, see Section 4.4.3.1) and to the high hygroscopic nature of the lyophilised system of the drug (see FT-IR in Section 4.4.3.3). This system had a high content of residual water that could initiate the chemical degradation of the drug in the low humidity storage conditions. In addition, this formulation readily absorbed moisture during storage at higher relative humidities resulting in enhanced degradation rates being visually observed. This finding was in agreement to that reported about the effect of moisture on the amorphous solids (see Section 5.1). Also, it has been reported that moisture and elevated temperatures can induce rapid degradation of some drugs through hydrolysis or oxidation reactions (Halbert, 2006).

6.5 Conclusion

From this chapter, it can be concluded that:

- The lyophilised formulation of glibenclamide (93% SLS) presented a high stability during storage under different conditions as the amorphous form of the drug was maintained. This was attributed to several factors. These factors include high T_g of the amorphous form of glibenclamide; hydrogen bonding between the drug and SLS that decreased the drug molecular mobility. For this reason, this formulation was selected for subsequent in-vivo study in chapter 7.
- The lyophilised formulation of spironolactone (67% SLS) was unstable during storage under 65% or 75% RH as the incidence and degree of recrystallisation increased. In contrast, storage at high temperatures (37, 50ºC) resulted in the removal of the solvent adsorbed during the coating process which favoured the maintenance of the amorphous form of the drug in the lyophilised formulations. Therefore, humid environments are not suitable for storage of the lyophilised spironolactone formulations even after application of a film coating to the capsule.
- As spironolactone molecules are flexible and can go through structural rearrangement by the effect of heat, some DSC results of the lyophilised formulations of spironolactone were not in agreement with the corresponding XRPD results.
- The lyophilised formulations of ketoconazole were unstable under different storage conditions as the drug went through apparent chemical degradation as indicated by the observed change in the colour and consistency of the stored formulations. This was attributed to the high residual water of the ketoconazole lyophilised system. Thus, the ketoconazole formulations could not be protected by film coating and the formulations need further development if they are to be stabilised.

Chapter 7

7. In-vivo performance of lyophilised glibenclamide capsule formulations in beagle dogs

7.1 Introduction

It is known that bioavailability studies of novel oral dosage forms are essential for the development of pharmaceutical products. However, it is difficult to predict the the absorption rate and the bioavailability of such dosage forms by using in-vitro release studies. Thus, in-vivo animal studies are important to provide data analogous to those obtained in human studies. Therefore, before the introduction of novel drug formulations into humans, they are often investigated in animals to establish their oral bioavailability (Akimoto et al., 1993, 1995) despite many physiological differences between animals and humans. A commonly used animal for this purpose is the beagle dog. These animals are suitable for evaluating oral dosage forms because they can be handled easily, along with their ability to swallow human-size dosage forms. Even if the dog is a convenient model for in-vivo studies, some examples represent a difference between the oral bioavailability detected in dogs and that detected in humans (Dressman, 1986). This could be explained on the basis of physiological differences in motility, pH, and surface area, between the GIT of dogs and humans (Kararli, 1995).

The short length of the small and large intestine and subsequent short overall GI transit time in dogs relative to humans is one of the most remarkable differences which can affect extended release oral formulations (Dressman & Yamada, 1991). This can also lead to miscalculation of the bioavailability of drugs that are absorbed mainly from the upper GIT due to passage of the dosage forms through the dog GIT before complete release of the drug is realised.

The villi of dogs are longer than those of humans which can compensate the shorter GI transit time. Moreover, the concentration and secretion rate of bile salts in dogs, have been reported to be higher than those in humans which possibly increases the permeability of the intestinal membrane for drug passage (Chiou et al., 2000). In

addition, the higher concentration of bile salts could facilitate the dissolution of poorly water-soluble drugs resulting in higher absorption rate.

The pH of the canine stomach has been reported to be either analogous to or higher than that of humans. However, more variability is documented in the dog (Akimoto et al., 2000). In general, the intestinal pH of the canine is about one pH unit higher than that of the human GIT at any comparable point (Lui et al., 1986).

Furthermore, in the fasting state, the canine GIT has an analogous migrating myoelectric complex (MMC) cycle to human (Dressman & Yamada, 1991). On the other hand, in the presence of food, the stomach of this species responds in a different way exhibiting longer gastric emptying time (Dressman, 1986). These differences may result in drug absorption data that are not predictive of humans. In spite of this, the dog is still considered the primary in-vivo investigational means for new oral formulations, and it has been used by many researchers as a useful animal model (Ghimire et al., 2007; McInnes et al., 2007). Moreover, some researchers suggest that dog gastric emptying is closer to that of human than other animal models (Aoyagi et al., 1992).

Most evaluation of dosage performance is derived from pharmacokinetic data as well as direct inspection of the dosage form performance employing gamma scintigraphy technique (see Section 2.7.1). The technique of gamma scintigraphy has been used in the dog by some researchers for tracking the behaviour of oral dosage forms in this animal model (Guan et al., 2010; Ghimire et al., 2007; McInnes et al., 2007). It presents helpful information about the position of a dosage form in the GIT at any point of a pharmacokinetic event in the plasma profiles. Subsequently, this facilitates interpretation of the pharmacokinetics of a drug on the basis of position or behaviour of the dosage form at any time. A dosage form including a formulation labelled with a radioactive isotope is administered to the animal, followed by imaging by a gamma camera for visual tracking of the dosage form. Commonly used radioactive isotopes and more details about the technique of gamma scintigraphy are discussed in Section 2.7.1.

Scintigraphic images along with pharmacokinetic data are invaluable techniques in explaining unusual pharmacokinetic profiles. The in-vivo data points are established by quantitative evaluation of the number of the radioactive counts in the region of interest (ROI) that surrounds the dosage form in the image (see Section 7.3.3).

7.2 Aims and objectives

The present chapter aims to investigate the bioavailability and performance of capsule formulations of lyophilised glibenclamide with 93% w/w SLS (equivalent to 5 mg glibenclamide) after oral administration in beagle dogs relative to a commercial 5 mg glibenclamide tablet using a cross-over study design with washout between evaluation of the separate dosage forms.

7.3 Methods

7.3.1 Preparation of radiolabelled formulations for gamma scintigraphy study

7.3.1.1 Preparation of ^{99m}Tc-DTPA labelled lactose

100 mg of lactose was weighed into a clean, tarred glass vial, and the actual weight was recorded. The activity of the supplied ^{99m}Tc-DTPA vial was recorded in MBq. ^{99m}Tc-DTPA was carefully added to the vial of lactose. The vial was clamped to a ring stand and the liquid was gradually evaporated with warm air till visibly dry. The activity was checked and recorded.

7.3.1.2 Preparation of bone cement

The liquid monomer was poured into a plastic beaker to which the powder was added. The contents were mixed together using a plastic spatula. The mixture was carefully stirred for 30-40 seconds until a dough-like mass was formed and used within 7 minutes.

7.3.1.3 Preparation procedures for tablets and capsules

Glibenclamide commercial tablets (APS, UK) were checked for any cracks or defects, and flawless tablets were chosen for use in the study. A hole of 2.4 mm depth and 1 mm diameter was made in the centre of the commercial tablet. The tablet hole or the capsule was carefully filled with ^{99m}Tc-DTPA-labelled lactose equivalent to 1 MBq of activity at the time of dosing using a micro spatula, ensuring no spillages occurred. The tablet hole was sealed with bone cement and the capsule was enclosed by 'clicking' the body and head of the capsule together. Dosage forms were placed in an individually labelled plastic vial within a lead pot until dosing.

7.3.2 In-vivo study conditions

Before each study, the dogs were fasted overnight with free access to water. A cannula was inserted into the saphenous vein in the hindleg for blood sampling during the study period. The cannula was maintained patent by washing out with heparinised normal saline when required, and was removed at the end of the study period. Markers containing about 0.1 MBq 99mTc were fixed on either side of the dog to act as a reference for the position between scintigraphic images. Each dog was placed in a sling that permitted the animal to stand comfortably. Immediately after oral administration of the formulations, the animals were placed under the gamma scintigraphic camera for imaging. After dosing, 2.6 ml blood samples were withdrawn from dogs into pre-labelled heparin beaded tubes at time points 0, 5, 10, 15, 30, 45, 60, 90, 120, 180, 240, 300, and 360 minutes. Blood samples were immediately tested for blood glucose level and centrifuged at 3500 rpm at 5ºC for 10 minutes, within the 6 hours of the sample collection time. The resultant plasma was separated from the centrifuged samples and transferred to fresh tubes that had labels indicating the animal name, date and time point. The tubes were stored in a freezer at -80ºC for subsequent analysis.

7.3.3 Gamma-scintigraphic imaging

60-second static images were acquired from the posterior aspect by a gamma scintigraphic camera with field of view of 533 x 387 mm, having a low energy parallel hole collimator (MIE Systems, Germany.) The frequency of imaging was every 2 minutes after dosing until 30 minutes, or until the formulation disappeared from the stomach, then every 10-20 minutes until 120 minutes and then every 60 minutes till the end of the study. Images were saved by the attached computer for analysis.

Analysis of scintigraphic images was carried out using the Scintron analysis software (MIE Systems, Germany). Regions of interest (ROI) were drawn on the images around the stomach using the positional markers as reference. ROI is a certain part in the computer image that has a specific number of pixels, with each pixel corresponds to a number of gamma rays released from the dosage form (Perkins, 1999). The radioactive counts in all regions were recorded and compared. The data was corrected for background activity and radioactive decay.

7.3.4 HPLC glibenclamide assay

Glibenclamide was assayed using a Dionex HPLC system described in Section 2.7.2.

7.3.4.1 Preparation of calibration curves in methanol and plasma

A stock standard solution of 1 mg/ml of glibenclamide in methanol was prepared. Serial dilutions of this solution in methanol were prepared to provide final concentrations of 0.1, 0.2, 0.5, 1, 2, 5 and 10 µg/ml.

Serum calibration standard samples were freshly prepared by spiking 0.950 ml of blank bovine serum with 50 µl of glibenclamide standard solutions of the following concentrations; 0.8, 2, 4, 8, 20 and 40 µg/ml to provide concentrations corresponding to 0.04, 0.1, 0.2, 0.4, 1 and 2 µg/ml. Glibenclamide was extracted from the spiked plasma as described in the following section.

7.3.4.2 Extraction of glibenclamide from plasma samples

The plasma samples of dogs were defrosted and equilibrated to room temperature. In a 2 ml polypropylene eppendorf tube, 0.5 ml of acetonitrile was added to 0.5 ml of plasma to induce protein precipitation and vortexed for 3 minutes at 2000 rpm. Samples were centrifuged for 10 minutes at 13000 rpm at 20ºC. 0.8 ml of the resultant supernatant was separated and to which 0.4 ml chloroform was added (for glibenclamide extraction) followed by vortexing for 1 minute at 2000 rpm. 0.3 ml of water was added followed by vortexing for 2 minutes at 2000 rpm. Samples were then centrifuged for 5 minutes at 13000 rpm at 4ºC after which the chloroform layer was separated and evaporated till dryness using an evaporative centrifuge (Speedvac SPD121P) at 35ºC and atmospheric pressure. The resultant residue was reconstituted in 80 µl of methanol, vortexed and then transferred to an autosampler vial where 20 µl was injected into the HPLC column.

7.3.4.3 Validation of HPLC methodology

The methodology procedures was validated regarding linearity, reproducability and recovery

- **Linearity**

A standard calibration curve was constructed by plotting the peak areas versus glibenclamide concentrations (three replicates for each concentration) and goodness of fit was estimated by linear regression. The mean best fit linear regression equation was used to calculate the concentrations of glibenclamide in the unknown plasma samples at different blood sampling time.

- **Precision and reproducability**

Inter and intra-day reproducibility studies were carried out. Three different concentrations of glibenclamide (in the linear range) were analysed three times in a successive manner to attain within-day reproducibility. The intra-day reproducibility was obtained by repeating the analysis of the same concentrations on 5 separate days.

Precision was determined by calculation of coefficient of variation (CV%) from measurement in the same day or on different days.

- **Recovery of glibenclamide**

The recovery of glibenclamide was determined by comparing the peak-heights measured in the extracts of blank bovine serum spiked with known amounts of glibenclamide with the peak-heights of the same concentrations measured in non extracted samples of glibenclamide in methanol. Percentage recovery of the drug was calculated from the following equation (Barakat et al., 2008):

$$\text{Recovery (\%)} = \frac{\text{peak height of glibenclamide in spiked bovine serum}}{\text{peak height of glibenclamide in methanol}} \times 100$$

7.3.4.4 Pharmacokinetic analysis

Pharmacokinetic parameters such as time of initial glibenclamide appearance in the plasma (T_{lag}), maximum plasma concentration (C_{max}) and time at which maximum plasma concentration was obtained (T_{max}) were estimated from the plasma concentration-time profile of each animal. Individual areas under the plasma concentration-time curve (extent of absorption) from the dosing time until the last blood sampling point (6 hours after administration) were determined by applying the trapezoidal method. All parameters were presented as individual values obtained from each dog. The statistical significance of differences between the basic pharmacokinetic parameters of glibenclamide capsules and commercial tablets was determined using a paired t-test with a 95% confidence interval using Minitab 15.

7.3.5 Dog blood glucose levels during the in-vivo study

The collected blood glucose measurements during the study (see Section 2.7.3) were used to plot blood glucose level versus time post administration of the glibenclamide formulations.

7.4 Results and discussion

7.4.1 Scintigraphic analysis

Glibenclamide dosage forms; either the capsule formulations or the commercial tablets were tracked throughout the GIT after oral administration to two healthy beagle dogs. The representative scintigraphic images of the dosage forms in the GIT and the gastric emptying profiles are represented in Figures 7.1 and 7.2 respectively. Both the glibenclamide commercial tablets and lyophilised glibenclamide-SLS capsule formulations disintegrated in the stomach. The disintegration time of the commercial tablet was 4 minutes in both dogs while that of the lyophilised glibenclamide-SLS capsule formulations was 2 minutes in dog 1 and 4 minutes in dog 2. The gastric emptying of both formulations was rapid (Figure, 7.2). The time required for the radioactive count of the commercial tablets to decrease to 50% in the stomach ($T_{50\%}$) was 13.6 and 24.7 minutes for dog 1 and dog 2 respectively while that of the capsule formulations was 8.5 and 21.5 minutes respectively. Thus, any difference in the in-vivo absorption profiles between both formulations, will reflect a difference in the dissolution rate of the drug formulations as most of the absorption of glibenclamide has been reported to take place in the upper GIT (Brockmeier et al., 1985).

7.4.2 HPLC method validation

Chromatographic presentation of glibenclamide was good with good peak shapes and acceptable retention time of about 7 minutes. The analytical procedures for glibenclamide in plasma was validated and the results are represented in Table 7.1.

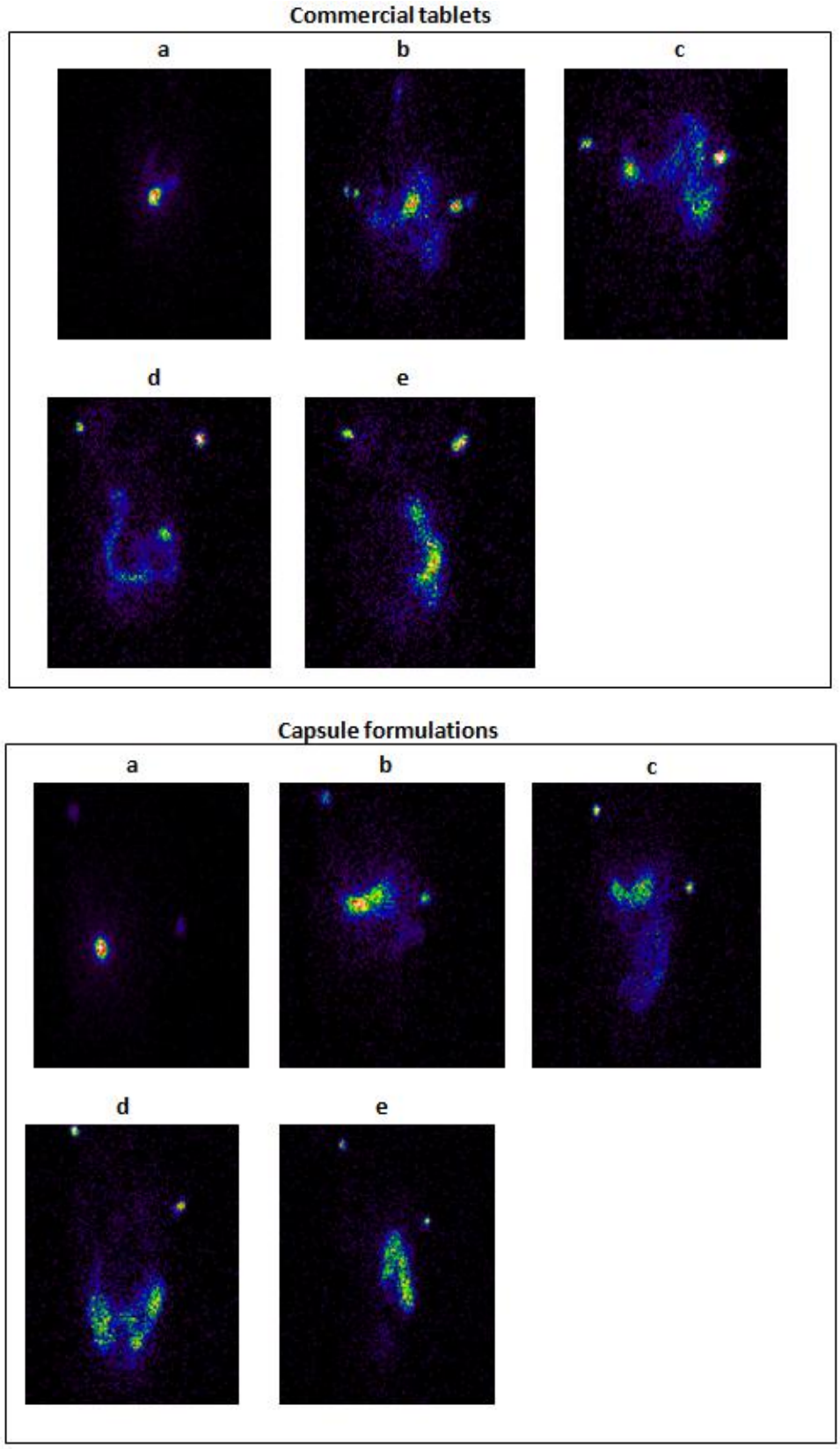

Figure 7.1: Scintigraphic images showing performance of glibenclamide dosage form in the GIT, immediately after dosing (a), in the stomach (b), in the duodenum (c), in the jejunum (d) and in the colon (e) of one beagle dog. (head position is on the right top while the tail position is on the left bottom).

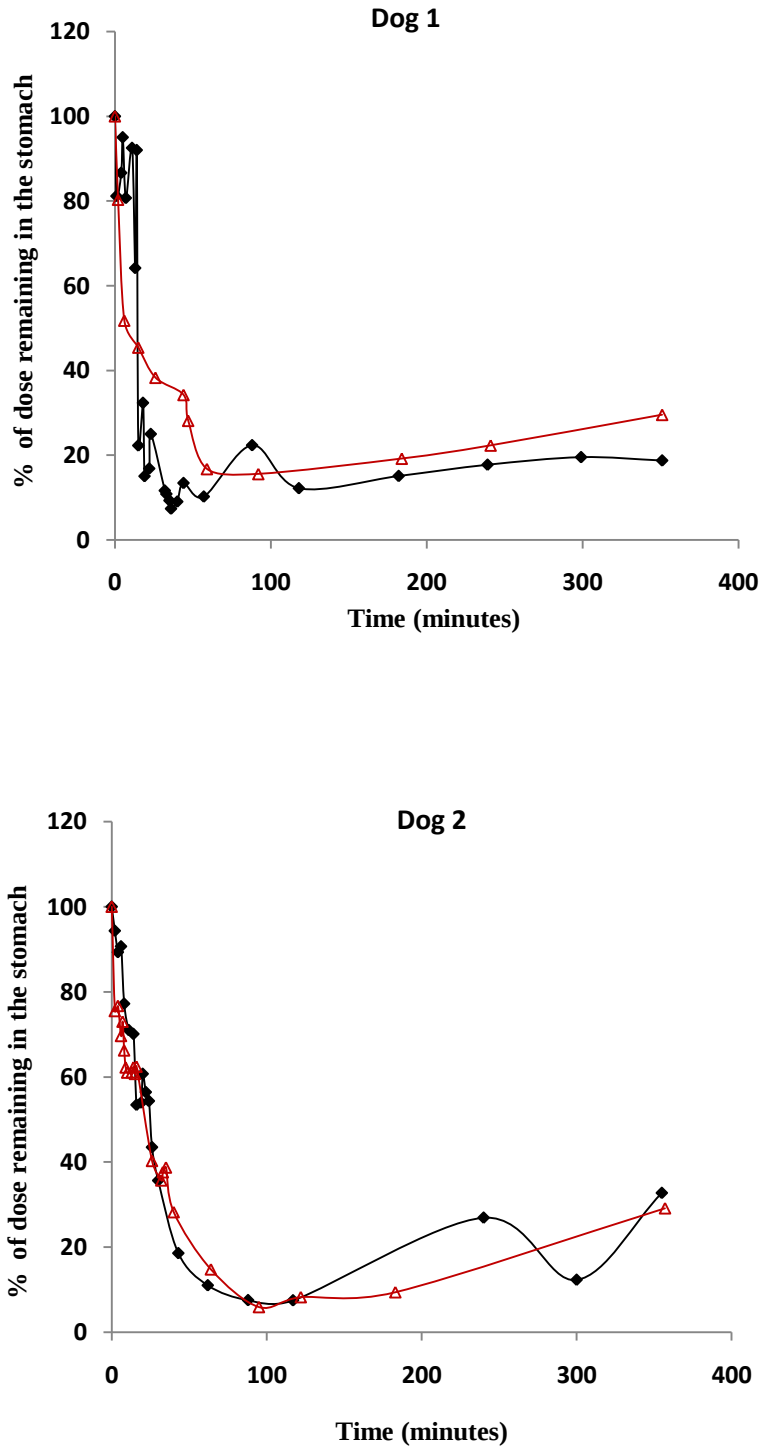

Figure 7.2: Gastric emptying profiles following oral administration of glibenclamide capsule formulations (triangle) and commercial tablets (square) to beagle dogs.

Table 7.1: Validation of HPLC methodology for the analysis of glibenclamide in plasma of beagle dogs

Parameter	Value
Regression equation	Y = 3.8786 x -0.0173
Correlation coefficient (R^2)	0.9995
Recovery (%)	91.64 ± 5.14
Inter-day CV%	12.35
Intra-day CV%	9.3774

7.4.3 Pharmacokinetic analysis

Lyophilised glibenclamide-SLS capsule formulations and commercial tablets were administered to beagle dogs to investigate the difference in in-vivo absorption profiles between the two formulations. The glibenclamide plasma concentration versus time curves following a single dose of 5 mg of the drug as capsules or commercial tablets are illustrated in Figure 7.3. It was found that the plasma levels of glibenclamide obtained from the drug capsule formulations were higher than those obtained from glibenclamide commercial tablets. The pharmacokinetic parameters of glibenclamide obtained from the drug plasma concentration-time curves are summarised in Table 7.2. In the case of lyophilised glibenclamide-SLS capsules, the first appearance of the drug in blood (the onset of absorption) was after a time period of 10-15 minutes. On the other hand, the onset of absorption of glibenclamide from commercial tablets was about 60-90 minutes.

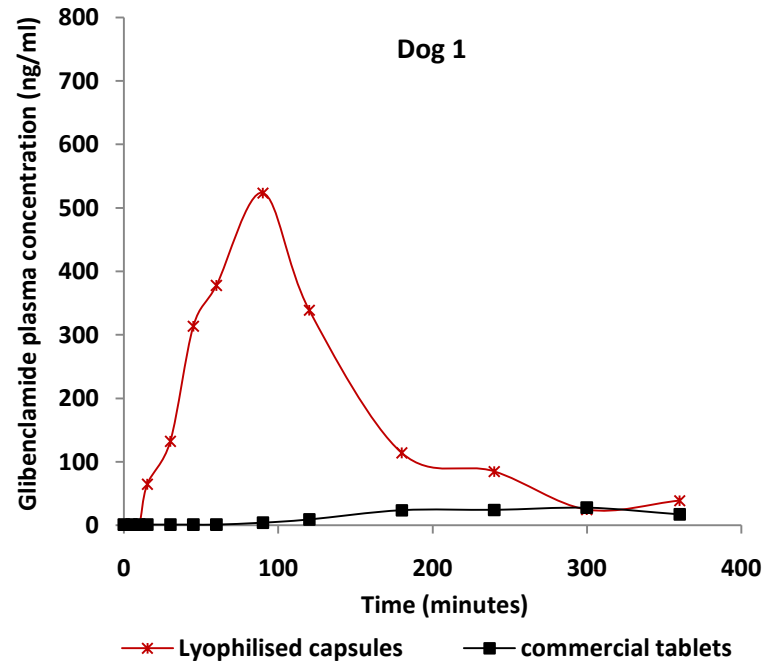

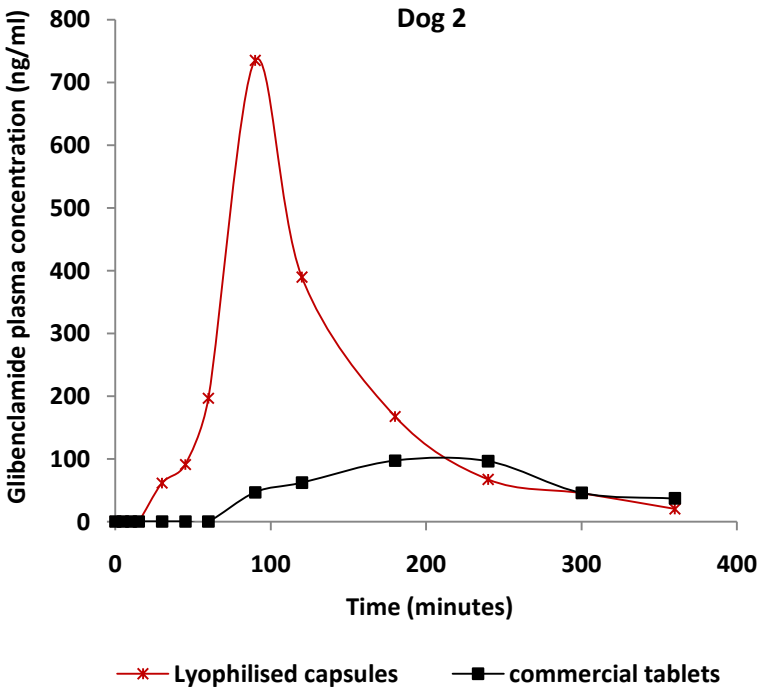

Figure 7.3: Mean plasma concentration-time curves of glibenclamide following oral administration of glibenclamide formulations to beagle dogs

The T_{max} obtained in the case of the lyophilised capsule formulations was significantly lower than that obtained in the case of the commercial tablets (p-value = 0.018). The C_{max} and area under the plasma concentration-time curve of glibenclamide (AUC_{0-360}) after administration of the lyophilised capsule formulations were significantly higher than those obtained after administration of the commercial tablets (p-values = 0.001). This finding suggests that the lyophilised glibenclamide formulations displayed a higher rate and extent of drug absorption than that displayed by the commercial tablets. These results may be attributed to the higher dissolution rate of glibenclamide from its lyophilised mixture with SLS compared to the commercial tablets.

Table 7.2: Pharmacokinetic parameters of glibenclamide obtained after oral administration of capsule formulations and commercial tablets to beagle dogs

Formulation	Parameter			
	T_{lag} (minutes)	AUC_{0-360} ($ng.min.ml^{-1}$)	C_{max} (ng/ml)	T_{max} (minutes)
Capsules	10 - 15	61362 - 63833	523.7 - 735.2	90
Commercial tablets	60 - 90	5641 - 19814	27.5 - 97.6	180 - 300

Savolainen et al. (1998) have reported significant enhancement in glibenclamide in-vivo absorption in beagle dogs after oral administration of capsules containing a complex of the drug with β-cyclodextrins and hydroxypropyle methyl cellulose (equivalent to 3 mg glibenclamide). In this study, close values of C_{max} (499.9-638.3 ng/ml) and T_{max} (108-120 minutes) to the present values have been obtained.

7.4.4 Blood glucose levels

The hypoglycaemic effect of glibenclamide after oral administration of lyophilised glibenclamide-SLS capsule formulations or commercial tablets is illustrated in Figure 7.4. The lyophilised glibenclamide-SLS capsule formulations were found to induce more and rapid decrease in blood glucose levels than the commercial tablets. Blood glucose levels began to decrease 15 minutes post administration of the lyophilised formulations in both dogs. Moreover, Glucogel® was given to the dogs 90 minutes post administration of the dosage form to control their blood glucose levels and the dogs were fed 15 minutes before withdrawing of the last blood sample. Thus, comparing the data in the time range 15-90 minutes revealed that there was an obvious difference between the blood glucose levels obtained after administration of the lyophilised glibenclamide-SLS capsule formulations and commercial tablets for dog 1 and dog 2. The onset of action of the lyophilised glibenclamide-SLS capsule formulations was rapid (10-15 minutes), reaching its maximum after 60 minutes as the blood glucose level was reduced to 1.3-1.4 mmol l^{-1} in comparison with 3.6-3.9 mmol l^{-1} at the beginning of the study. On the other hand, the onset of action of the commercial tablets was slow (45-90 minutes), reaching its maximum after 240 minutes with a blood glucose level of 1.85 mmol l^{-1} in comparison with 3.2-3.9 mmol l^{-1} at the beginning of the study.

It has been reported that solid dispersion of glibenclamide with microcrystalline cellulose achieved more reduction in blood glucose levels in Albino rabbits compared to the pure drug and the physical mixture after oral administrations. This result was attributed to the enhancement of the drug dissolution from the solid dispersion formulations (Dastmalchi et al., 2005). Compared to pure glibenclamide, more hypoglycaemic effect has been achieved in Swiss Albino mice from solid dispersion of the drug with polyglycolised glycerides and silicon dioxide due to enhanced dissolution rate (Chauhan et al., 2005).

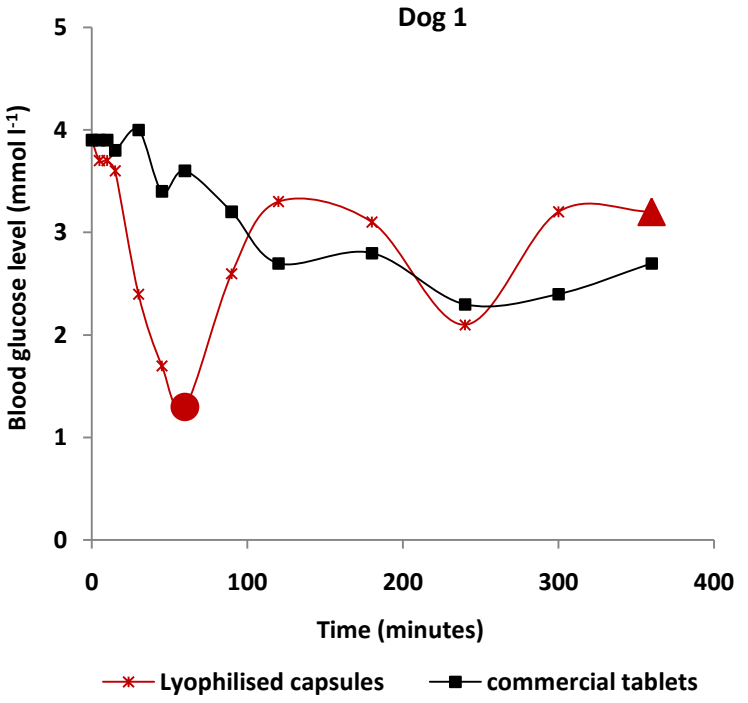

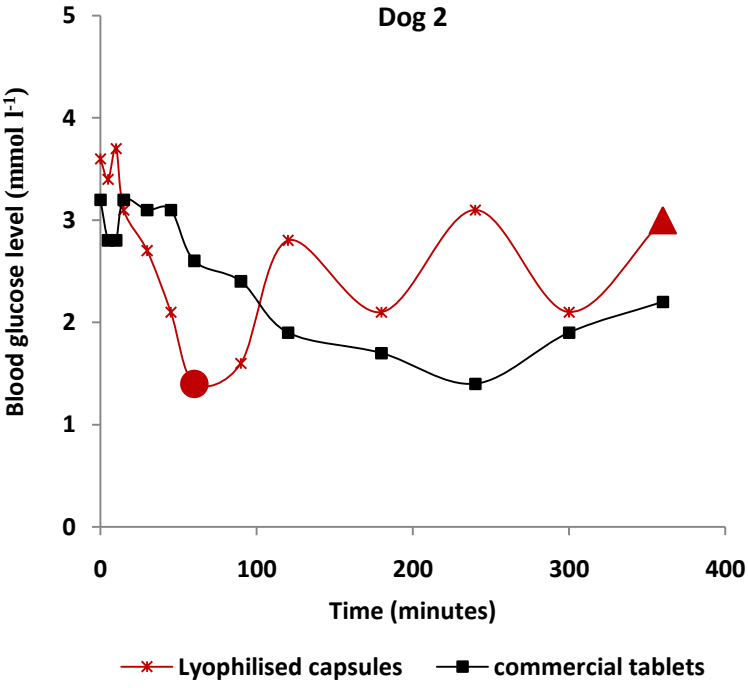

Figure 7.4: Blood glucose levels following oral administration of glibenclamide formulations to beagle dogs (the red circles highlight the time after which Glucogel® was given to the dogs and the red triangles highlights the time 15 minutes before which the dogs were fed)

7.4.5 In-vitro dissolution data versus in-vivo data

The mean in-vivo disintegration time for the lyophilised glibenclamide-SLS capsules was 3 minutes as shown by the scintigraphic study (Section 7.4.1). Similarly, the in-vivo disintegration time of the commercial tablets was 4 minutes. This finding is correlated with the observed in-vitro release as the percentage of glibenclamide dissolved at 5 minutes was 60.9% and 17.6% from the lyophilised glibenclamide-SLS capsule formulations and the commercial tablets respectively.

Table 7.3 shows a comparison between the concentrations of glibenclamide in the blood of one dog after oral administration of the lyophilised glibenclamide-SLS capsule or the commercial tablet and the percentages of glibenclamide dissolved from both formulations in-vitro. As the dissolution data was available for only 2 hours and the in-vivo study was done for 6 hours, the common time points were used for comparison. The dissolution rate and extent of glibenclamide from the lyophilised capsule formulations were higher than those obtained from the commercial tablets. Similarly, glibenclamide plasma concentrations and the extent of reduction in blood glucose level after administration of the lyophilised capsule formulations were absolutely higher than those obtained after administration of the commercial tablets. This could be attributed to the higher dissolution rates of the lyophilised formulations relative to the commercial tablets. Similar results have been obtained in previous studies as glibenclamide dissolution rate; blood concentration and hypoglycaemic effect (in albino rabbits) were enhanced from solid dispersion of the drug with microcrystalline cellulose prepared by solvent deposition technique (Dastmalchi et al., 2005).

Although 60% glibenclamide was dissolved from the lyophilised formulations (in-vitro) within the first 5 minutes, the first appearance of glibenclamide in plasma was after 15 minutes. Similarly, the maximum glibenclamide dissolved in-vitro was attained after 30 minutes while the maximum plasma concentration was attained after 90 minutes. As the dissolution rate of glibenclamide from the lyophilised formulations was rapid, the absorption of the drug is likely to be a function of the rate of gastric emptying and/or the intestinal permeability as in the case of immediate release products (Amidon et al., 1995). This fact explains the differences between

in-vitro and in-vivo results and suggests the absence of in-vitro/in-vivo correlation (Emami, 2006). Similarly, it has been reported that in-vitro dissolution studies of glibenclamide is undependable for prediction of the therapeutic efficacy of the orally administered dug and thus, the in-vivo study was necessary (Chalk et al., 1986).

Table 7.3: Comparison between percentages of glibenclamide dissolved in-vitro and its concentrations in blood after oral administration of lyophilised glibenclamide-SLS capsules or the commercial tablets in dog 2

Time (minutes)	Lyophilised capsule formulations		Commercial tablets	
	% drug dissolved in-vitro	Drug concentration in plasma (ng/ml)	% drug dissolved in-vitro	Drug concentration in plasma (ng/ml)
5	60.9	0	17.6	0
10	83.4	0	19.8	0
15	91.9	0	25.3	0
30	98.5	59.8	39.1	0
60	100.7	191.4	52.1	0
90	100.2	750.1	61.5	62.1
120	99.8	388	66.4	68.9

7.5 Conclusion

From this chapter, it can be concluded that:

- Both glibenclamide commercial tablets and lyophilised glibenclamide-SLS capsule formulations disintegrated in the stomach and their gastric emptying was rapid and similar to each other.
- C_{max} and AUC_{0-360} of glibenclamide after oral administration of the lyophilised glibenclamide-SLS capsule formulations were significantly higher than those obtained after administration of the drug commercial tablets. T_{max} in the case of lyophilised glibenclamide-SLS capsule formulations was significantly lower than that in the case of the commercial tablets. This finding suggests that the lyophilised glibenclamide-SLS formulations displayed a higher rate and extent of glibenclamide absorption than those displayed by the drug commercial tablets.
- The lyophilised glibenclamide-SLS capsule formulations were found to induce a rapid and more appreciable decrease in blood glucose levels compared to the commercial tablet formulations.
- The resultant enhancement of glibenclamide absorption from the lyophilised formulation was attributed to the higher dissolution rates and extent of the drug from these formulations compared to the commercial tablets. No correlation was found between the in-vitro and in-vivo data as the dissolution of the drug was rapid and the release was immediate.

GENERAL CONCLUSION

From the research presented in this thesis, it can be concluded that:

- The lyophilisation process may enhance the dissolution rate of some drugs such as glibenclamide, whilst it may have a negative effect on the dissolution rate of others such as spironolactone and ketoconazole, depending on the physical properties of the lyophilised products. Lyophilised spironolactone powder was electrically charged by the process of lyophilisation and consequently floated on the surface of the dissolution medium. In addition, lyophilised ketoconazole powder was highly hygroscopic and aggregated into a sticky clump that sank to the bottom of the dissolution medium. These effects resulted in retardation of the dissolution rate of both drugs.
- Incorporation of water-soluble excipients such as SLS, PEG 6000, tromethamine, fumaric acid and/or mannitol in the systems to be lyophilised significantly enhanced the dissolution rate of glibenclamide, spironolactone and ketoconazole compared with the corresponding commercial tablets and physical mixtures. This was attributed to the solubilisation effect of the excipients and the formation of solid dispersions of the drugs in the water-soluble excipients, resulting in a reduction in drug particle size. Alteration of the micro environmental pH or the chemical environment surrounding the drug particles may also have an important role in the dissolution enhancement observed in the case of addition of tromethamine or fumaric acid. The maximum dissolution rate enhancement of glibenclamide and spironolactone was achieved by SLS while that of ketoconazole was achieved by a mixture of mannitol and SLS.
- Citric acid is not a suitable excipient for the formulations to be lyophilised. This is because its high hygroscopicity had a detrimental effect on the lyophilised products, causing them to absorb ambient moisture and become difficult to handle under the normal laboratory conditions.
- Physicochemical characterisation of the lyophilised systems using DSC, XRPD and FT-IR techniques revealed that all three drugs transformed into

amorphous forms during the lyophilisation process. This was considered to be the main contributing factor in the dissolution rate enhancement of glibenclamide, spironolactone and ketoconazole. Drug/excipient interactions such as hydrogen bonding in the lyophilised mixtures were evident from the FT-IR results.

- For application of coating systems to the capsules containing the lyophilised products, use of high volumes of solvent systems and prolonged drying times should be avoided. This is because solvent vapour and prolonged drying time initiated recrystallisation of the amorphous form of spironolactone in its solid dispersion with SLS during the coating process.
- The amorphous form of glibenclamide and ketoconazole in lyophilised mixtures with SLS and mannitol-SLS respectively, showed high stability during the coating process which may be due to strong drug/excipient hydrogen bonding.
- The amorphous form of spironolactone in a lyophilised mixture with SLS exhibited low incidence of recrystallisation during the coating process
- Dissolution rates of glibenclamide, spironolactone or ketoconazole were maintained after the coating process.
- The amorphous form of glibenclamide in a lyophilised mixture with SLS displayed high stability during storage under different temperatures and relative humidities. This could be attributed to the intensive hydrogen bonding between the drug and SLS in the solid dispersion and due to the high glass transition temperature of the amorphous form of glibenclamide.
- The lyophilised formulations of spironolactone were unstable during storage at 25ºC/65% RH or 25ºC/75% RH while storage at high temperatures (37ºC/0% RH or, 50ºC/0% RH) favoured the maintenance of the amorphous form of the drug in the lyophilised formulations due to loss of the residual solvent after the coating process.
- Lack of correlation between DSC and XRPD analysis of some lyophilised formulations of spironolactone was thought to be due to the heat applied to the sample during DSC providing flexibility for spironolactone molecules to undergo structural rearrangement.

- Ketoconazole was unstable in lyophilised systems under different storage conditions, with the altered colour and consistency of the stored formulations suggesting drug degradation. This may be due to the high residual water and hygroscopic nature of lyophilised ketoconazole. Consequently, ketoconazole formulations need further development in order to be stabilised, and this will be investigated in the future work.
- The rate and extent of glibenclamide absorption from its lyophilised mixture with SLS in beagle dogs was significantly improved relative to the commercial tablets. This was mainly attributed to the enhancement of glibenclamide dissolution rate in the lyophilised system.
- Overall, this work has been successful in terms of using lyophilisation technology to provide a promising formulation strategy for poorly water-soluble compounds to enhance their dissolution and oral bioavailability.

References

REFERENCES

Abdelkader, H., Abdallah, O. Y. and Salem, H. S. **(2007)** Comparison of the effect of tromethamine and polyvinyl pyrrolidone on dissolution properties and analgesic effect of nimesulide. *AAPS PharmSciTech,* 65: E1-E5.

Abdul-Fattah, A. M., Dellerman, K. M., Bogner, R. H. and Pikal, M. J. **(2007)** The effect of annealing on the stability of amorphous solids: Chemical stability of freeze-dried moxalactam. *J. Pharm. Sci.,* 96: 1237-1250.

Abosehmah-Albidy, A. Z., York, P., Wong, V., Losowsky, M S. and Chrystyn, H. **(1997)** Improved bioavailability and clinical response in patients with chronic liver disease following the administration of a spironolactone: beta-cyclodextrin complex. *Br. J. Clin. Pharmacol.,* 44 :35-9.

Abshagen, U., Rennekamp, H. and Luszpinski, G. **(1976)** Pharmacokinetics of spironolactone in man. *Naunyn-Schmiedeberg's Arch. Pharmacol.,* 296: 37-45.

Aceves-Hernandez, J. M., Nicolás-Vázquez, I., Aceves, F. J., Hinojosa-Torres, J., Paz, M. and Castaño, V. M. **(2009)** Indomethacin polymorphs: Experimental and conformational analysis. *J. Pharm. Sci.,* 98: 2448-2463.

Agafonov, V., Legendre, B., Rodier, N., Wouessidjewe, D. and Cense, J. M. **(1991)** Polyphorphism of spironolactone. *J. Pharm. Sci.,* 80: 181-185.

Ahmed, I. S. and Nafadi, M. M. **(2006)** Formulation of a fast-dissolving ketoprofen Tablets using freeze-drying in blisters technique. *Drug Dev. Ind. Pharm.,* 32: 437-442.

Ahuja, N., Kata, O. P. and Singh, B. **(2007)** Studies on dissolution enhancement and mathematical modelling of drug dissolution of a poorly water-soluble drug using water-soluble carriers. *Eur. J. Pharm. Biopharm.,* 65: 26-38.

Akimoto, M. , Furuya, A., Maki, T., Yamada, K., Suwa, T. and Ogata, H. **(1993)** Evaluation of sustained- release granules of chlorphenesin carbamatein in dogs and humans. *Int. J. Pharm.,* 100: 133-142.

Akimoto, M., Furuya, A., Nakamura, M., Maki, T., Yamada, K., Suwa, T. and Ogata, H. **(1995)** Release and absorption characteristics of chlorphenesin carbamate sustained-release formulations: in vitro-in vivo and in vivo dog-human correlations. *Int. J. Pharm.,* 117: 31-39.

Akimoto, M., Nagahata, N., Furuya, A., Fukushima, K., Higuchi, S. and Suwa, T. **(2000)** Gastric pH profiles of beagle dogs and their use as an alternative to human testing. *Eur. J. Pharm. Biopharm.,* 49: 99–102.

Albers, J.,, Alles, R., Matthée, K., Knop, K., Nahrup, J. S. and Kleinebudde, P. **(2008)** Mechanism of drug release from polymethacrylate-based extrudates and milled strands prepared by hot-melt extrusion. *Eur. J. Pharm. Biopharm.,* 71: 387-394.

Aleem, O., Kuchekar, B., Pore, Y. and Late, S. **(2008)** Effect of B-cyclodextrin and hydroxypropyl B-cyclodextrin complexation on physicochemical properties and antimicrobial activity of cefdinir. *J. Pharm. Biomed. Anal.,* 47: 535-540.

Alhalaweh, A., Andersson, S. and Velaga, S. P. **(2009)** Preparation of zolmitriptan-chitosan microparticles by spray drying for nasal delivery. *Eur. J. Pharm. Sci.,* 38 : 206-214

Ambike, A. A., Mahadik, K. R. and Paradkar, A. **(2004)** stability study of amorphous valdecoxib. *Int. J. Pharm.,* 282: 151-162.

Amidon, G. L., Lennernas, H., Shah, V. P. and Crison, J. R. **(1995)** A theoretical basis for a biopharmaceutic drug classification: The correlation of in vitro drug product dissolution and in vivo bioavailability. *Pharm. Res.,* 12: 413-419.

Andronis, V. and Zografi, G. **(1998)** The molecular mobility of supercooled amorphous indomethacin as a function of temperature and relative humidity. *Pharm. Res.,* 15: 835-841.

Andronis, V., Yoshioka, M. and Zografi, G. **(1997)** Effects of sorbed water on the crystallization of indomethacin from the amorphous state. *J. Pharm. Sci.,* 86: 346-351.

Aoyagi, N., Ogata, H., Kaniwa, N., Uchiyama, M., Yasuda, Y. and Tanioka,Y. **(1992)** Gastric emptying of tablets and granules in humans, dogs, pigs, and stomach-emptying controlled rabbits. *J. Pharm. Sci.,* 81: 1170–1174.

Arias, M. J., Gines, J. M., Moyano, J. R. and Rabasco, A. M. **(1994)** The application of solid dispersion technique with D-mannitol to the improvement in oral absorption of triamterene. *J. Drug Target.,* 2: 45-51.

Ashford, M. **(2002)** Bioavailability-Physicochemical and dosage form factors. In: Pharmaceutics: the science of dosage form design. Aulton, M. E. (Ed.) 2nd ed., Churchill Livingston, London. Pp 234-252.

Asyarie, S. and Rashmawati, H. **(2007)** In vivo and in vitro evaluation of of solid dispersion system of gliclazide:PEG 6000. *PDA J. Pharm. Sci. Techn.,* 61: 400-410.

Aungst, B. J., Nguyen, N. H., Taylor, N. J. and Bindra, D. S. **(2002)** Formulation and food effects on the oral absorption of a poorly water soluble, highly permeable antiretroviral agent. *J. Pharm. Sci.,* 91: 1390-1395.

Avis, K. E., Shukla, A. J. and Chang, R. K. **(1999)** Pharmaceutical unit operations: coating. In: Film coating. Campbell, R. J. and Sackett G. L. (Eds.) IHS Health Group, Colorado. Pp 55-176.

Bachhav, Y. G. and Patravale, V. B. **(2009)** SMEDDS of glyburide: formulation, in vitro evaluation, and stability studies. *AAPS PharmSciTech.,* 10: 482-487.

Balakrichnan, A., Rege, B. D., Amidon, G. L. and Polli, J. E. **(2004)** Surfactant-mediated dissolution: contributions of solubility enhancement and relatively low micelle diffusivity. *J. Pharm. Sci.,* 93: 2064-2075.

Balan, G., Timmins, P., Greene, D. S. and Marathe, P. H. **(2000)** In-vitro In-vivo correlation models for glibenclamide after administration of metformin/glibenclamide tablets to healthy human volunteers. *J. Pharm. Pharmacol.,* 52: 831–838.

Barakat, N. S., Elbagory, I. M. and Almurshedi, A. S. **(2008)** Formulation, Release Characteristics and Bioavailability Study of Oral Monolithic Matrix Tablets Containing Carbamazepine. *AAPS PharmSciTech. ,* 9: 931-938.

Basa, S., Muniyappan, T., Karatgi, P., Prabhu, R. and Pillai, R. **(2008)** Production and in vitro characterization of solid dosage form incorporating drug nanoparticles. *Drug Dev. Ind. Pharm.,* 34: 1209-1218.

Bauer, J., Spanton, R., Henry, R., Quick, J., Dziki, W., Porter, W. and Morris, J. **(2001)** Ritonavir: an extraordinary example of conformational polymorphism. *Pharm. Res.,* 18: 859:866.

Beckstead, H. D., Neville, G. A. and Shurvell, H. F. **(1993)** Differentiation of solvated spironolactone samples by FT-Raman and FT-IR diffuse reflectance spectroscopy. *Fresenius J. Anal. Chem.,* 345: 727- 732.

Berbenni, V., Marini, A., Bruni, G., Maggioni, A., Riccardi, R. and Orlandi, A. **(1999)** Physico-chemical characterisation of different solid forms of spironolactone. *Thermochimica Acta,* 340-341: 117-129.

Bhugra, C. and Pikal, M. J. **(2008)** Role of thermodynamic, molecular, and kinetic factors in crystallization from the amorphous state. *J. Pharm. Sci.,* 97: 1329-1349.

Bley, H., Fussnegger, B. and Bodmeier, R. **(2010)** Characterization and stability of solid dispersions based on PEG/polymer blends. *Int. J. Pharm.,* 390: 165-173.

Brinkmann, M., Wittmann, J. C., Chaumont, C. and André, J. J. **(1997)** Effects of solvent on the morphology and crystalline structure of lithium phthalocyanine thin films and powders. *Thin Solid Films,* 292: 192-203.

Brockmeier, D., Grigoleit, H. G. and Leonhardt, H. **(1985)** Absorption of Glibenclamide from Different Sites of the Gastro-Intestinal Tract. *Eur. J. Clin. Pharmac.,* 29: 193-197.

Brouwers, J., Tack, J. and Augustijns, P. **(2007)** In-vitro behaviour of a phosphate ester prodrug of amprenavir in human intestinal fluids and in the Caco-2 system: illustration of intraluminal supersaturation. *Int. J. Pharm.,* 336: 302-309.

Brown, M. E., Antunes, E. M., Glass B. D., Lebete, M. and Walker, R. B. **(1999)** DSC screening of potential prochloroperazine-excipient interactions in preformulation studies. *J. Therm. Anal. Calorim.,* 56: 1317-1322.

Calafato N. R., Picó G. **(2006)** Griseofulvin and ketoconazole solubilization by bile salts studied using fluorescence spectroscopy. *Colloids Surf. B Biointerfaces.,* 47: 198-204.

Chakraborty S, Shukla D, Jain A, Mishra B and Singh S. **(2009)** Assessment of solubilization characteristics of different surfactants for carvedilol phosphate as a function of pH. *J. Colloid Interface Sci.,* 335: 242-249.

Chalk, J. B., Patterson, M., Smith, M. T. and Eadie, M. J. **(1986)** Correlations Between In Vitro Dissolution, In Vivo Bioavailability. *Eur. J. Clin. Pharmacol.,* 31 : 177-182.

Chang, R., Raghavan, K. S. and Hussain, M. A. **(1998)** A study on gelatin capsule brittleness: moisture transfer between the capsule shell and its content. *J. Pharm. Sci.,* 87: 556-558.

Charman, S. A. and Charman, W. N. **(2003)** Oral modified-release delivery systems. In: Modified-Release Drug Delivery Technology. Rathbone, M. J., Hadgraft, J. and Roberts, M. S. (Eds.) Marcel Dekker, New York. Pp. 1-10.

Chauhan, B., Shimpi, S. and Paradkar, A. **(2005)** Preparation and evaluation of glibenclamide-polyglycolized glycerides solid dispersions with silicon dioxide by spray drying technique. *Eur. J. Pharm. Sci.,* 26: 219-230.

Chawla, G. and Bansal, A. K. **(2008)** Improved dissolution of a poorly water soluble drug in solid dispersions with polymeric and non-polymeric hydrophilic additives. *Acta Pharm.,* 58: 257-274.

Chawla, G. and Bansal, A. k. **(2009)** Molecular mobility and physical stability of amorphous irbesartan. *Sci. Pharm.,* 77: 695–709.

Chen, Y., Zhang, G. G., Neilly, J., Marsh, K., Mawhinney, D. and Sanzgiri, Y. D. **(2004)** Enhancing the bioavailability of ABT-963 using solid dispersion containing Pluronic F-68. *Int. J. Pharm.,* 286: 69-80.

Chiou, W. L. and Riegelman, S. **(1971)** Pharmaceutical applications of solid dispersions. *J. Pharm. Sci*., 60: 1281–1302.

Chiou, W. L., Jeong, H. Y., Chung, S. M. and Wu, T. C. **(2000)** Evaluation of using dog as an animal model to study the fraction of oral dose absorbed of 43 drugs in humans. *Pharm. Res.,* 17 :135–140.

Chono, S., Takeda, E., Seki, T. and Morimoto, K. **(2008)** Enhancement of the dissolution rate and gastrointestinal absorption of pranlukast as a model poorly water-soluble drug by grinding with gelatin. *Int. J. Pharm.,* 347: 71-78.

Cirri, M., Maestrelli, F., Corti, G., Mura, P. and Valleri, M. **(2007)** Fast-dissolving tablets of glyburide based on ternary solid dispersions with PEG 6000 and surfactants. *Drug Deliv.,* 14: 247-255.

Cirri, M., Righi, M. F., Maestrelli, F., Mura, P. and Valleri, M. **(2009)** Development of glyburide fast-dissolving tablets based on the combined use of cyclodextrins and polymers. *Drug Dev. Ind. Pharm.,* 35: 73-82.

Clarke, G. M., Newton, J. M. and Short, M. B. **(1995)** Comparative gastrointestinal transit of pellet systems of varying density. *Int. J. Pharm.,* 114: 1–11.

Corrigan, O. I. **(1985)** Mechanisms of dissolution of fast release solid dispersions. *Drug Dev. Ind. Pharm.,* 11: 697–724.

Crowley, K. J. and Zografi, G. **(2002)** Water vapour absorption into amorphous hydrophobic drug/poly(vinylpyrrolidone) dispersions. *J. Pharm. Sci.,* 91: 2150–2165.

Cui, C. Y., Lu, W. L., Xiao, L., Zhang, S. Q., Huang, Y. B., Li, S. L., Zhang, R. J., Wang, G. L., Zhang, X. and Zhang, Q. **(2005)** Sublingual delivery of insulin: effects of enhancers on the mucosal lipid fluidity and protein conformation, transport, and in-vivo hypoglycaemic activity. *Biol. Pharm. Bull.,* 28: 2279-2288.

Custodio, J. M., Wu, C. Y. and Benet, L. Z. **(2008)** Predicting drug disposition, absorption/elimination/transporter interplay and the role of food on drug absorption. *Adv. Drug Del. Rev.,* 60: 717-733.

Dahan, A. S. and Amidone, G. L. **(2008)** Gastrointestinal dissolution and absorption of Class II drugs. In: Drug bioavailability: Estimation of Solubility, Permeability, Absorption and Bioavailability. Waterbeemd, H. and Testa, B. (Eds.) WILEY-VCH, Weinheim. Pp 33-45.

Dahan, A. and Hoffman, A. **(2007)** Enhanced Gastrointestinal Absorption of Lipophilic Drugs. In: Enhancement in Drug delivery. Touitou, E. and Barry, B. W. (Eds.) CRC press, Taylor& francis Group, London. Pp111-131.

Dastmalchi, S., Garjani, A., Maleki, N., Sheikhee, G., Baghchevan, V., Jafari-Azad, P., Valizadeh, H. and Barzegar-Jalali, M. **(2005)** Enhancing dissolution, serum concentrations and hypoglycaemic effect of glibenclamide using solvent deposition technique. *J. Pharm. Sci.,* 8: 175-181.

Digenis, G. A., Sandefer, E. P., Page, R. C. and Doll, W. J. **(1998)** Gamma scintigraphy: an evolving technology in pharmaceutical formulation development-part 1. *Pharm. Sci. Tech. Today,* 1: 100-108.

Dong, Y., Ng, W. K., Hu, J., Shen, S., Tan, R. B. H. **(2010)** A continuous and highly effective static mixing process for antisolvent precipitation of nanoparticles of poorly water-soluble drugs. *Int. J. Pharm.,* 386: 256-261.

Dong, Y., Ng, W. K., Shen, S., Kim, S. and Tan, R. B. H. **(2009)** Preparation and characterization of spironolactone nanoparticles by antisolvent precipitation. *Int. J. Pharm.,* 375: 84–88.

Dora, C. P., Singh, S. K., Kumar, S., Datusalia, A. K. and Deep, A. **(2010)** Development and characterization of nanoparticles of glibenclamide by solvent displacement method. *Acta Pol. Pharm.,* 67: 283-290.

Drake, A. **(2004)** Infra-red spectroscopy. In: Clark's analysis of Drugs and Poisons. Moffat, A. C., Osselton, M. D. and Widdop, B. (Eds.) volume I, Pharmaceutical Press, London. Pp. 328-357.

Dressman, J. B. **(1986)** Comparison of canine and human gastrointestinal physiology, *Pharm. Res.,* 3: 123-131.

Dressman, J. B. and Reppas, C. **(2000)** In-vitro-in-vivo correlations for lipophilic poorly water soluble drugs. *Eur. J. Pharm. Sci.,* 11: S73- S80.

Dressman, J. B. and Yamada. K. **(1991)** Animal models for oral drug absorption. In: Pharmaceutical Bioequivalence. Welling, P. G. (Ed.) Marcel Dekker, New York. Pp. 235–266.

Dressman, J. B., Amidon, G. L., Reppas, C. and Shah, V. P. **(1998)** Dissolution testing as a prognostic tool for oral drug absorption: immediate release dosage forms. *Pharm. Res.,* 15: 11-22.

Dressman, J. B., Vertzoni, M., goumas, K. and Reppas, C. **(2007)** Estimating drug solubility in the gastrointestinal tract. *Adv. Drug Del. Rev.,* 59: 591-602.

Dunmire, D., Freedman, T. B., Nafie, L. A., Aeschlimann, C., Gerber, J. G. and Gal, J. **(2005)** Determination of the absolute configuration and solution conformation of the antifungal agents ketoconazole, itraconazole, and miconazole with vibrational circular dichroism. *Chirality, 17 Suppl:* S 101-108.

Elder, E. J., Evans, J. C., Scherzer, B. D., Hitt, J. E., Kupperblatt, G. B., Saghir, S. A. and Markham, D. A. **(2007)** Preparation, characterization, and scale-up of ketoconazole with enhanced dissolution and bioavailability. *Drug Dev. Ind. Pharm.*, 33: 755-765.

Elder, E. J., Scherzer, B. D., Saghir, S., Kupperblatt, G. B., Hitt, J. E., Evans, J. C., Wilson, D. L. and Becker, J. N. **(2003)** Particle Engineering by Ultra-Rapid Freezing for Improved Bioavailability of Ketoconazole. *AAPS abstract*.

El-Zein, H., Riad, L. and El-Bary, A. A. **(1998)** Enhancement of carbamazepine dissolution: in-vitro and in-vivo evaluation. *Int. J. Pharm.*, 168: 209-220.

Emami, J. **(2006)** In vitro - In vivo correlation: from theory to applications. *J. Pharm. Pharmaceut Sci.*, 9: 169-189.

Esclusa-Díaz, M. T., Guimaraens-Méndez, M., Pérez-Marcos, M. B., Vila-Jato, J. L. and Torres-Labandeira, J. J. **(1996)** Characterization and in vitro dissolution behaviour of ketoconazole/β- and 2-hydroxypropyl-β-cyclodextrin inclusion compounds. *Int. J. Pharm.*, 143: 203-210.

European Pharmacopoeia, 3rd ed., **(1997)** European Department for the Quality of Medicines Council of Europe. Strasbourg, France. Pp. 1072–1073.

Fadda, H. M., McConnell, E. L., Short, M. D. and Basit, A. W. **(2009)** Meal-induced acceleration of tablet transit through the human small intestine. *Pharm Res.*, 26: 356-360.

Fagerholm, U. **(2007)** Evaluation and suggested improvements of biopharmaceutics classification system (BCS). *J. Pharm. Pharmacol.*, 59: 751-757.

Felix, F. **(2007)** Primary Drying: The sublimation of Ice. In: Lyophilisation of Pharmaceuticals and Biopharmaceuticals. RSC, London. Pp 105-120.

Fleisher, D., Bong, R. and Stewart, B. H. **(1996)** Improved oral drug delivery: solubility limitations overcome by the use of prodrugs. *Adv. Drug Deliv. Rev.*, 19: 115-130.

Fukushima, K., Terasak, S., Haraya, K., Kodera, S., Seki, Y., Wada, A., Ito, Y., Shibata, N., Sugiok, N. and Takada, K. **(2007)** Pharmaceutical approach to HIV protease inhibitor atazanavir for bioavailability enhancement based on solid dispersion system. *Biol. Pharm. Bull.*, 30: 733-738.

Galia, E., Nicolaides, E., Hörter, D., Löbenberg, R., Reppas, C. and Dressman, J. B. **(1998)** Evaluation of various dissolution media for predicting in-vivo performance of class I and II drugs. *Pharm. Res.,* 15: 698-705.

Gao, P. **(2008)** Amorphous pharmaceutical solids: characterization, stabilization, and development of marketable formulations of poorly soluble drugs with improved oral absorption. *Mol. Pharm.,* 5: 903-904.

Garmise, R. J., Mar, K., Crowder, T. M., Hwang, C. R., Ferriter, M., Huang, J., Mikszta, J. A., Sullivan, V. J. and Hickey, A. J. **(2006)** Formulation of dry powder influenza vaccine for nasal delivery. *AAPS PharmSciTech*. 7: E_1-E_7.

Ghimire, M., McInnes, F. J., Watson, D. G., Mullen, A. B.and Stevens, H. N. E. **(2007)** In-vitro/in-vivo correlation of pulsatile drug release from press-coated tablet formulations: A pharmacoscintigraphic study in the beagle dog. *Eur. J. Pharm. Biopharm.,* 67: 515-523.

Grant, D. J. W. and Brittain, H. J. **(1995)** Solubility of pharmaceutical solids. In: Physical characterisation of pharmaceutical solids. (Brittain, H. C. ed.), Marcel Dekker, New York. Pp 321-386.

Gröning, R., Cloer, C., Georgarakis, M. and Müller, R. S. **(2007)** Compressed collagen sponges as gastroretentive dosage forms: in vitro and in vivo studies. *Eur J Pharm Sci.*, 30: 1-6.

Guan, J., Zhou, L., Nie, S., Yan T., Tang, X. and Pan, W. **(2010)** A novel gastric-resident osmotic pump tablet: in vitro and in vivo evaluation. *Int. J. Pharm.,* 383: 30-36.

Guo, Y., Byrn, S. R. and Zografi, G. **(2000)** Physical characterization and chemical degradation of amorphous quinapril hydrochloride. *J. Pharm. Sci.* 89: 1–16.

Gupta, P. and Bansal A. K. **(2005)** Devitrification of Amorphous Celecoxib. *AAPS PharmSciTech.,* 6: E223-E230.

Halbert, G. **(2006)** Pharmaceutical development. In: The text book of pharmaceutical medicin. Griffin, J. P. and O'Grady, J. (Eds.), 1st ed., Blackwell Publishing Ltd., USA. Pp 87-110.

Hamid, R. A., Al-Akayleh, F., Shubair, M., Rashid, I., Remawi, M. A. and Badwan, A. **(2010)** Evaluation of three chitin metal silicate co-precipitates as a potential multifunctional single excipient in tablet formulations. *Mar. Drugs*, 8: 1699-1715.

Hancock, B. C. and Parks, M. **(2000)** what is the true solubility advantage for amorphous pharmaceuticals? *Pharm. Res.*, 17: 397-404.

Haque, M. D. K. and Roos, Y. H. **(2005)** Crystallisation and x-ray diffraction of spray-dried and freeze-dried amorphous lactose. *Carbohydr. Res.,* 340: 293-301.

Hashmat, D., Shoaib, M. H., Mehmood, Z. A., Bushra, R., Yousuf, R. I. and Lakhani, F. **(2007)** Development of enteric coated flurbiprofen tablets using opadry/acryl-eze System—A Technical Note. *AAPS PharmSciTech,* 9: 116-121.

Hassan, M. A., Najib, N. M. and Suleiman, M. S. **(1991)** Characterization of glibenclamide glassy state. *Int. J. Pharm.,* 67: 131-137.

Hatakeyama, T. and Quinn, F. X. **(1999)** Thermal analysis, In: Thermal analysis: fundamentals and applications to polymer science. John Wiley & Sons Ltd., West Sussex, Pp. 1-4.

Hawe, A. and Frieß, W. **(2006)** Impact of freezing procedure and annealing on the physico-chemical properties and the formation of mannitol hydrate in mannitol-sucrose-NaCl formulations. *Eur. J. Pharm. Biopharm.,* 64: 316-25.

He, W., Fan, L., Du, Q., Xiang, B., Li, C., Bai, M., Chang, Y. and Cao, D. **(2009)** Design and in vitro/in vivo evaluation of multi-layer film coated pellets for omeprazole. *Chem. Pharm. Bull.*, 57: 122-128.

Heo, M. Y., Piao, Z. Z., Kim, T. W., Cao, Q. R., Kim, A., and Lee, B. J. **(2005)** Effect of solubilizing and microemulsifying excipients in polyethylene glycol 6000 solid dispersion on enhanced dissolution and bioavailability of ketoconazole. *Arch. Pharm. Res.*, 285: 604-611.

Hodges, L. A., Elkordy, A. A. and Mullen, A. B. **(2006)** Dissolution enhancement of spironolactone by in situ lyophilisation. *J. Pharm. Pharmacol.*, 58: A14.

Hogan, J. **(2002)** Coating of tablets and multiparticulates. In: Pharmaceutics The Science of Dosage Form Design. Aulton, M. E. (Ed.), Churchill Livingstone, London. Pp 441-448.

Hong, T. D., Ellis, R. H., Buitink, J., Walterso, C., Hoekstra, F. A. and Crane, J. **(1999)** A model of the effect of temperature and moisture on pollen longevity in airdry storage environments. *Annal.s of Botany*, 83: 167-173.

Hoppu, P., Jouppila, K., Rantanen, J., Schantz, S. and Juppo, A. M. **(2007)** Characterisation of blends of paracetamol and citric acid. *J. Pharm. Pharmacol.*, 59: 373-381.

Hörter, D. and Dressman, J. B. **(2001)** Influence of physicochemical properties on dissolution of drugs in the gastrointestinal tract. *Adv. Drug Del. Rev.*, 46: 75-87.

Ikegami, K., Tagawa K. and Osawa T**. (2006)** Bioavailability and in-vivo release behaviour of controlled-release multiple-unit theophylline dosage forms in beagle dogs, cynomolgus monkeys, and göttingen minipigs. *J. Pharm. Sci.*, 95: 1888-1895.

Izutsu, K., Ocheda, S. O., Aoyagi, N. and Kojima, S. **(2004)** Effects of sodium tetraborate and boric acid on nonisothermal mannitol crystallisation in frozen solutions and lyophilised solids. *Int. J. Pharm.*, 273: 85-93.

Janssens, S., Roberts, C., Smith, E. F. and Van den Mooter, G. **(2008)** Physical stability of ternary solid dispersions of itraconazole in polyethyleneglycol 6000/hydroxypropylmethylcellulose 2910 E5 blends. *Int. J. Pharm.,* 355: 100-107.

Javadzadeh, Y., Jafari-Navimipour, B. and Nokhodchi, A. **(2007)** Liquisolid technique for dissolution rate enhancement of a high dose water-insoluble drug (carbamazepine). *Int. J. Pharm.,* 341: 26-34.

Jones, B. E. **(2004)** The history of medicinal capsule In: Pharmaceutical capsules. Podczeck, F. and Jones, B. E. (Eds.) 2nd ed., Pharmaceutical Press, UK. Pp 1-20.

Juppo, A. M., Boissier, C. and Khoo, C. **(2003)** Evaluation of solid dispersion particles prepared with SEDS. *Int . J. Pharm.,* 250: 385-401.

Kadoya, S., Izutsu, K., Yonemochi, E., Terada, K., Yomota, C. and Kawanishi, T. **(2008)** Glass-state amorphous salt solids formed by freeze-drying of amines and hydroxyl carboxylic acids: Effect of hydrogen-bonding and electrostatic interactions. *Chem. Pharm. Bull.,* 56: 821-826.

Kagkadis, K. A., Rekkas, D. M., Dallas, P. P. and Choulis, N. H. **(1996)** A freeze-dried injectable form of ibuprofen: Development and optimization using response surface methodology. *PDA J. Pharm. Sci. Technol.,* 50: 317-323.

Kalantzi, L., Goumas, K., Kalioras, V., Abrahamsson, B., Dressman, J. and Reppas, C. **(2006a)** Characterization of the human upper gastrointestinal contents under conditions simulating bioavailability/bioequivalence studies. *Pharm. Res.,* 23: 165-176.

Kalantzi, L., Person, E., Polentarutti, B., Abrahamsson, B., Goumas, K., Dressman, J. and Reppas, C. **(2006b)** Canine intestinal contents vs. Simulated media for the assessment of solubility of two weak bases in the human small intestinal contents. *Pharm. Res.*, 23: 1373-13781.

Kallinteri, P. and Antimisiaris, S. G. **(2001)** Solubility of drugs in the presence of gelatin: effect of drug lipophilicity and degree of ionization. *Int. J. Pharm.,* 221: 219–226.

Kang, Y., Yin, G., Ouyang, P., Huang, Z., Yao, Y., Liao, X., Chen, A. and Pu, X. **(2008)** Preparation of PLLA/PLGA microparticles using solution enhanced dispersion by supercritical fluids (SEDS). *J. Colloid Interface Sci.,* 322: 87-94.

Kararli, T. T. **(1995)** Comparison of the gastrointestinal anatomy, physiology, and biochemistry of humans and commonly used laboratory animals. *Biopharm. Drug. Dispos.* 16: 351-380.

Karavas, E., Ktistis, G., Xenakis, A. and Georgarakis, E. **(2005)** Miscibility behaviour and formation mechanism of stabilized felodipine polyvinyl pyrrolidone amorphous solid dispersions. *Drug Dev. Ind. Pharm.,* 31: 473-489.

Karavas, E., Ktistis, G., Xenakis, A. and Georgarakis, E. **(2006)** Effect of hydrogen bonding interactions on the release mechanism of felodipine from nanodispersions with polyvinyl pyrrolidone. *Eur. J. Pharm.,* 63: 103-114.

Kasraian, K. and Deluca, P. P. **(1995)** The effect of tertiary butyl alcohol on the resistance of the dry product layer during primary drying. *Pharm. Res.,* 12: 491-495.

Kennedy, M., Hu, J., Gao, P., Li, L., Ali-Reynolds, A., Chal, B., Gupta, V., Ma, C., Mahajan, N., Akrami, A., Surapaneni, S. **(2008)** Enhanced bioavailability of a poorly soluble VR1 antagonist using an amorphous solid dispersion approach: a case study. *Mol Pharm.,* 5: 981-93.

Kenyon, C. J., Hooper, G., Tierney, D., Butler, J., Devane, J. and Wilding, I. R. **(1995)** The effect of food on the gastrointestinal transit and systemic absorption of naproxen from a novel sustained release formulation. *J. Control. Release.* 34: 31-36.

Kim, A. I., Akers, M. J. and Nail, S. L. **(1998)** The physical state of mannitol after freeze-drying: Effects of Mannitol Concentration, Freezing Rate, and a Noncrystallizing Cosolute. *J. Pharm. Sci.,* 87: 931-935.

Kim, C. K. and Park, J. S. **(2004)** Solubility Enhancers for Oral Drug Delivery: Can Chemical Structure Manipulation Be Avoided? Am. *J. Drug Deliv.,* 2: 113-130.

Klein, S., Wempe, M. F., Zoeller, T., Buchanan, N. L., Lambert, J. L., Ramsey, M. G., Edgar, K. J. and Buchanan, C. M. **(2009)** Improving glyburide solubility and dissolution by complexation with hydroxybutenyl-beta-cyclodextrin. *J. Pharm. Pharmacol.,* 61: 23-30.

Kohri, N., Yamayaoshi, Y., Xin, H., Iseki, K., Sato, N., Todo, S. and Miyazaki, K. **(1999)** Improving the oral bioavailability of albendazole in rabbits by the solid dispersion technique. *J. Pharm. Pharmacol.,* 51: 159-164.

Konno, H., Handa, T., Alonzo, D. E. and Taylor, L. S. **(2008)** Effect of polymer type on the dissolution profile of amorphous solid dispersions containing felodipine. *Eur. J. Pharm. Biopharm.,* 70: 493-499.

Kostewicz, E. S., Brauns, U., Becker, R. and Dressman, J. B. **(2002)** Forecasting the oral absorption behaviour of poorly soluble weak bases using solubility and dissolution studies in biorelevant media. *Pharm. Res.,* 19: 345-349.

Kumar, R., Gupta, R. B. and Betageri, G. V. **(2001)** Formulation, characterization, and in vitro dissolution of glyburide from proliposomal beads. *Drug Delivery,* 8: 25-27.

Lai, F., Sinico, C., Ennas, G., Marongiu, F., Marongiu, G. and Fadda, A. M. **(2009)** Diclofenac nanosuspensions: influence of preparation procedure and crystal form on drug dissolution behaviour. *Int. J. Pharm.,* 373: 124-132.

Laitinen R., Suihko, E., Toukola, K., Björkqvist, M., Riikonen, J., Lehto, V. P., Järvinen, K. and Ketolainen, J. **(2009)** Intraorally fast-dissolving particles of a poorly soluble drug: Preparation and in-vitro characterization. *Eur. J. Pharm. Biopharm.,* 71: 271-281.

Lakshman, J. P., Cao, Y., Kowalski, J. and Serajuddin, A. T. **(2008)** Application of melt extrusion in the development of a physically and chemically stable high-energy amorphous solid dispersion of a poorly water-soluble drug. *Mol. Pharm.,* 5: 994-1002.

Law, D., Krill, S. L., Schmitt, E. A., Fort, J. J., Qiu, Y., Wang, W. and Porter, W. R. **(2001)** Physicochemical considerations in the preparation of amorphous ritonavir-poly(ethylene glycol) 8000 solid dispersions. *J. Pharm. Sci.,* 90: 1015-1025.

Lennernas, H. and Reghard, C. G. **(1993)** Evidence from an interaction between the beta-blocker pafenolol and bile salts in the intestinal lumen of the rat leading to dose dependent oral absorption and double peaks in the plasma concentration time profile. *Pharm. Res.,* 10: 879-883.

Leuner, C. and Dressman, J. **(2000)** Improving drug solubility for oral delivery using solid dispersions. *Eur. J. Pharm., Biopharm.,* 50: 47-60.

Lim, R. T. Y., Ng, W. K. and Tan, R. B. H. **(2010)** Amorphization of pharmaceutical compound by co-precipitation using supercritical anti-solvent (SAS) process (Part I). *J. Supercrit. Fluid,* 53: 179–184.

Liu, R., **(2008)** Water-Insoluble Drug Formulations. In: Development of Solid Dispersions for Poorly Water-Soluble Drugs. Vasanthavada, M., Tong, W. Q. and Serajuddin, A. T. M. (Eds.) Informa Health-care, New York. Pp 149-184.

Löbenberg, R., Kramer, J., Shah, V. P., Amidon, G. L. and Dressman, J. B. **(2000)** Dissolution testing as a prognostic tool for oral drug absorption: dissolution behaviour of glibenclamide. *Pharm. Res.,* 17: 439- 444.

Long, M. and Chen, Y. **(2009)** Dissolution testing of solid products. In: Developing solid oral dosage forms: Pharmaceutical theory and practice. Qiu, Y., Chen, Y., Zhang, G. G. Z., Liu, L. and Porler, W. R. (Eds.), 1st ed., Academic Press, USA. Pp 319-337.

Lula, I., Gomes, M. F., Pilo-Veloso, D., Noronha, A. L. D., Duarte, H. A., Sanatos, R. A. S. and Sinisterra, R. D. **(2006)** Spironolactone and its Complexes with β-cyclodextrin: Modern NMR Characterization and Structural DFTB-SCC Calculations. *J. Inc. Phenom. Macro. Chem.,* 56: 293–302.

Luner, P. E. **(2000)** Wetting properties of bile salt solutions and dissolution media. *J. Pharm. Sci.,* 89: 382-395.

Luner, P. E. and Kamp, D. V. **(2001)** wetting behaviour of bile salt-lipid dispersions and dissolution media patterned after intestinal fluids. *J. Pharm. Sci.,* 90: 348-359.

Mackin, L., Zanon, R., Park. J. M., Foster, K., Opalenik, H. and Demonte, M. **(2002)** Quantification of low levels (<10%) of amorphous content in micronised active batches using dynamic vapour sorption and isothermal microcalorimetry. *Int. J. Pharm.,* 231: 227-236.

Maggi, L., Segale, .L, Ochoa Machiste, E., Faucitano, A., Buttafava, A. and Conte, U. **(2004)** Polymers-gamma ray interaction. Effects of gamma irradiation on modified release drug delivery systems for oral administration. *Int. J. Pharm.,* 269: 343-51.

Mannila, J., Järvinen, K., Holappa, J., Matilainen, L., Auriola, S. and Jarho, P. **(2009)** Cyclodextrins and chitosan derivatives in sublingual delivery of low solubility peptides: A study using cyclosporin A, alpha-cyclodextrin and quaternary chitosan N-betainate. *Int. J. Pharm.* 381: 19-24.

Mannila, J., Järvinen, T., Järvinen, K. and Jarho, P. **(2007)** Precipitation complexation method produces cannabidiol/beta-cyclodextrin inclusion complex suitable for sublingual administration of cannabidiol. *J. Pharm. Sci.,* 96: 312-319.

Mannila, J., Järvinen, T., Järvinen, K., Tervonen, J. and Jarho, P. **(2006)** Sublingual administration of Delta9-tetrahydrocannabinol/beta-cyclodextrin complex increases the bioavailability of Delta9-tetrahydrocannabinol in rabbits. *Life Sci.,* 78: 1911-1914.

Marcotty, T., Berkvens, D., Besa, R. K., Losson, B., Dolan, T. T., Madder, M., Chaka, G., Bossche, P. and Brandt, J. **(2003)** Lyophilisation and resuscitation of sporozoites of Theileria Parva: Preliminary experiments. *Vaccine,* 22: 213-216.

Margulis-Goshen, K. and Magdassi, S. **(2009)** Formation of simvastatin nanoparticles from microemulsion. *Nanomedicine,* 5: 274-281.

Marques, M. R. C., Cole, E., Kruep, D., Gray, V., Murachanian, D., Brown, W. E. and Giancaspro, G. I. **(2009)** Liquid-filled gelatin capsules. *Pharmacopeial Forum*, 35: 1029-1041.

Marsac, P. J., Rumondor, A. C., Nivens, D. E., Kestur, U. S., Stanciu, L. and Taylor, L. S. **(2010)** Effect of temperature and moisture on the miscibility of amorphous dispersions of felodipine and poly(vinyl pyrrolidone). *J. Pharm. Sci.,* 99: 169–185.

Marvola, J., Kanerva, H., Slot, L., Lipponen, M., Kekki, T., Hietanen, H., Mykkänen, S., Ariniemi, K., Lindevall, K. and Marvola, M. **(2004)** Neutron activation-based gamma scintigraphy in pharmacoscintigraphic evaluation of an Egalet constant-release drug delivery system. *Int. J. Pharm.,* 281: 3-10.

McGloughlin, R. M. R. and Corrigan, O. I. **(1992)** Dissolution characteristics of benzoic acid-Tris mixtures. *Int. J. Pharm.,* 82: 135-143.

McInnes, F. J., Thapa, P., Baillie, A. J., Welling, P. G., Watson, D. G., Gibson, I., Nolan, A. and Stevens, H. N. E. **(2005)** In-vivo evaluation of nicotine lyophilized nasal insert in sheep. *Int. J. Pharm.,* 304: 72-82.

McInnes, F., Clear, N., James, G., Stevens, H. N. E.,Vivanco, U. and Humphrey, M. **(2008)** Evaluation of the Clearance of a Sublingual Buprenorphine Spray in the Beagle Dog Using Gamma Scintigraphy. *Pharm. Res.,* 25: 869-874.

McInnes, F., Clear, N., Humphrey, M. and Stevens, H. N. **(2007)** In vivo performance of an oral MR matrix tablet formulation in the beagle dog in the fed and fasted state: assessment of mechanical weakness. *Pharm. Res.,* 25: 1075-1084.

Mehta, A. M.. **(2008)** Processing and equipment considerations for aqueous coatings. In: Aqueous polymeric coatings for pharmaceutical dosage forms. McGinity, J. W. (Ed.) 3rd ed., Marcel Dekker Inc., New York. Pp 287-326.

Merisko-Liversidge, E., Liversidge, G. G., Cooper, E. R. **(2003)** Nanosizing: a formulation approach for poorly-water-soluble compounds. *Eur. J. Pharm. Sci.,* 18: 113-120.

Mi, F. L. **(2005)** Synthesis and characterization of a novel chitosan-gelatin bioconjugate with fluorescence emission. *Biomacromolecules,* 6: 975-87.

Mididoddi, P. K. and Repka, M. A. **(2007)** Characterization of hot-melt extruded drug delivery systems for onychomycosis. *Eur. J. Pharm. Biopharm.,* 66: 95–105.

Millard, J. W., Alvarez-Nunez, F. A. and Yalkowsky, S. H. **(2002)** Solubilisation by co-solvents-establishing useful constants for the log-linear model. *Int. J. Pharm.,* 245: 153-166.

Modi A. and Tayade, P. **(2006)** Enhancement of dissolution profile by solid dispersion (kneading) technique. *AAPS PharmSciTech,* 7: E1-E6.

Moffat, A. C., Osselton, M. D. and Widdop, B. **(2004)** Clark's analysis of Drugs and Poisons, In: monographs, volume II , Pharmaceutical Press, London.

Mohammed, A. R., Bramwell, V. W., Coombes, A. G. A. and Perrie, Y. **(2006)** Lyophilisation and sterilization of liposomal vaccines to produce stable and sterile products. *Methods,* 40: 30-38.

Mooter, G., Weuts, I., De Ridder, T. and Blaton, N. **(2006)** Evaluation of Inutec SP1 as a new carrier in the formulation of solid dispersions for poorly soluble drugs. *Int. J. Pharm.,* 316: 1-6.

Murgatroyd, K. **(1997)** The freeze drying process. In: Good Pharmaceutical freeze-drying Practice. Cameron, P. (Ed.) Interpharm Press, Inc., Buffalo Grove, USA. Pp 1-57.

Német, Z., Sztatisz, J. and Demeter, A. **(2008)** Polymorph transitions of bicalutamide: a remarkable example of mechanical activation. *J. Pharm. Sci.,* 97: 3222-3232.

Neville, G. A., Becksteadlf, H. D. and Cooney, J. D. **(1994)** Thermal analyses (TGA and DSC) of some spironolactone solvates. *Fresenius J. Anal. Chem.,* 349: 746-750.

Newa, M., Bhandari, K. H., Kim, J. O., Im, J. S., Kim, J. A., Yoo, B. K., Woo, J. S., Choi, H. G. and Yong, C. S. **(2008)** Enhancement of solubility, dissolution and bioavailability of ibuprofen in solid dispersion systems. *Chem. Pharm. Bull.,* 56: 569-574.

Newa, M., Bhandari, K. H., Li, D. X., Kwon, T. H., Kim, J. A., Yoo, B. K., Woo, J. S., Lyoo, W. S., Yong, C. S. and Choi, H. G. **(2007)** Preparation, characterization and in vivo evaluation of ibuprofen binary solid dispersions with poloxamer 188. *Int. J. Pharm.*,343: 228-237.

Nunes, C., Suryanarayanan, R., Botez, C. E., Stephens, P. W. **(2004)** Characterization and crystal structure of D-mannitol hemihydrate. *J. Pharm. Sci.,* 93: 2800-2809.

O'Brien, F. M. E. **(1947)** The control of humidity by saturated salt solutions. *J. Sci. Instrum.,* 25: 73-76.

Obara, S., Maruyama, N., Nishiyama, Y. and Kokubo, H. **(1999)** Dry coating: an innovative enteric coating method using a cellulose derivative. *Eur . J. Pharm. Biopharm.,* 47: 51-59.

Onoue, S., Sato, H., Kawabata, Y., Mizumoto, T., Hashimoto, N. and Yamada, S. **(2009)** In vitro and in vivo characterization on amorphous solid dispersion of cyclosporine A for inhalation therapy. *J. Control. Dissolution.,* 138: 16-23.

Pagliara, A., Reist, M., Geinoz, S., Carrupt, P. and Testa, B. **(1999)** Evaluation and Prediction of Drug Permeation. *J. Pharm. Pharmacol.,*51: 1339-1357.

Panagopoulou-Kaplani, A. and Malamataris, S. **(2000)** Preparation and characterisation of a new insoluble polymorphic form of glibenclamide. *Int. J. Pharm.,* 195: 239-246.

Pang, K. S. **(2004)** Physiological modeling of the small intestine in drug absorption. In: Advanced methods of pharmacokinetic and pharmacodynamic systems analysis. (D'Argenio, D. Z. ed.), Kluwer academic publishers, USA, Pp 3-32.

Patel, A. R. and Joshi, V. Y. **(2008)** Evaluation of SLS: APG mixed surfactant systems as carrier for solid dispersion. *AAPS PharmSciTech,* 9: 583-590.

Pathak, D., Dahiya, S. and Pathak, K. **(2008)** Solid dispersion of meloxicam: factorially designed dosage form for geriatric population. *Acta Pharm.,* 58: 99-110.

Patterson, J. E., james, M. B., Forster, A. H., Lancaster, R. W., Butler, J. M. and Rades, T. **(2005)** The influence of thermal and mechanical preparative techniques on the amorphous state of four poorly soluble compounds. *J. Pharm. Sci.,* 94: 1998-2012.

Perkins, A. C. **(1999)** Instrumentation, imaging, data analysis and display. In: Nuclear Medicin in Pharmaceutical Research. Perkins, A. C. & Frier, M. (Eds.) Taylor & Francis Ltd, London. Pp 15-29.

Petereit, H. and Weisbord, W. **(1999)** formulation and process considerations affecting the stability of solid dosage forms formulated with methacrylate copolymers. *Eur. J. Pharm. Biopharm.,* 47: 15-25.

Pikal, M. J. and Shah S. **(1990)** The collapse temperature in freeze drying: dependence on measurement methodology and rate of water removal from the glassy phase. *Int. J. Pharm.,* 62: 165-186.

Pina, M. E., Sousa, A. T. and Brojo, A. P. **(1997)** Enteric coating of hard gelatin capsules. Part 2 Bioavailability of formaldehyde treated capsules. *Int. J. Pharm.,* 148: 73-84.

Pokharkar, V. B., Mandpe, L. P., Padamwar, M. N., Ambike, A. A., Mahadik, K. R. and Paradkar, A. **(2006)** Development, characterization and stabilization of amorphous form of a low T_g drug. *Powder Technology*, 167: 20–25.

Pouton, C. W. **(2006)** Formulation of poorly water-soluble drugs for oral administration: physicochemical and physiological issues and the lipid formulation classification system. *Eur. J. Pharm. Sci.,* 29: 278-287.

Pudipeddi, M. and Serajuddin, A. T. **(2004)** Trends in solubility of polymorphs. *J. Pharm. Sci.,* 94: 929-939.

Pyne, A., Surana, R. and Suryanarayanan, R. **(2002)** Crystallisation of Mannitol below T_g_during Freeze-Drying in Binary and Ternary Aqueous Systems. *Pharm. Res.,* 19: 901-908.

Quintanar-Guerrero, D., Allemann, E., Fessi, H. and Doelker, E. **(1999)** Pseudolatex preparation using a novel emulsion-diffusion process involving direct displacement of partially water-miscible solvents by distillation. *Int. J. Pharm.,* 188: 155-164.

Rajabi, O., Tayyari, F., Salari, R. and Tayyari, F. S. **(2008)** Study of interaction of spironolactone with hydroxypropyl-b-cyclodextrin in aqueous solution and in solid state. *J. Mol. Struct.,* 878: 78–83.

Rasenack , N. and Müller, B. W. **(2002)** Dissolution rate enhancement by in situ micronization of poorly water-soluble drugs. *Pharm. Res.,* 19: 1894-1900.

Rodriguez , L., Cavallari, C., Passerini, N., Albertini , B., Gonza´lez-Rodrı´guez , M. L. and Fini, A. **(2002)** Preparation and characterization by morphological analysis of diclofenac/PEG 4000 granules obtained using three different techniques. *Int. J. Pharm.,* 242: 285-289.

Sakellariou, P. and Rowe, R. C. **(1995)** Interactions in cellulose derivative films for oral drug delivery. *Prog. Polym. Sci.,* 20: 889-942.

Savolainen, J., Järvinen, k., Taipale, h., Jarho, P., Loftsson, T. and Järvinen, T. **(1998)** Co-administration of a water-soluble polymer increases the usfuleness of cyclodextrins in solid oral dosage forms. *Pharm. Res.,* 15: 1696-1701.

Savolainen, M., Heinz, A., Strachan, C.,, Gordon, K. .C, Yliruusi, J., Rades, T. and Sandler, N. **(2007)** Screening for differences in the amorphous state of indomethacin using multivariate visualization. *Eur. J. Pharm. Sci.,* 30: 113-123.

Schwudke, D., Stößer, R. and Scholz, F. **(2000)** Solid-state electrochemical, X-ray and spectroscopic characterization of substitutional solid solutions of iron–copper hexacyanoferrates. *Electrochem. Commun.,* 2: 301–306.

Sertsou, G., Butler, J., Hempenstall, J. and Rades, T. **(2002)** Physical stability and enthalpy relaxation of drug–hydroxypropyl methylcellulose phthalate solvent change co-precipitates. *JPP.,* 55: 35–41.

Shah, V. P., Tsong, Y., Sathe, P. and Liu, J. **(1998)** In vitro dissolusion profile comparison-statistics and analysis of the similarity factor, f_2. *Pharm. Res.,*15: 889-896.

Sheng, J. J., Kasim, N. A., Chandrasekharan, R. and Amidon, G. L. **(2006)** Solubilisation and dissolution of insoluble weak acid, ketoprofen: effects of pH combined with surfactant. *Eur. J. Pharm., Sci.,* 29: 306-314.

Shinde, V. R., Shelake, M. R., Shetty, S. S., Chavan-Patil, A. B., Pore, Y. V. and Late, S. G. **(2008)** Enhanced solubility and dissolution rate of lamotrigine by inclusion complexation and solid dispersion technique. *J. Pharm. Pharmacol.,* 60: 1121-1129.

Singhal, D. and Curatalo, W. **(2004)** Drug polymorphism and dosage form design: a practical prespective. *Adv. Drug Delv. Rev.,* 56: 335-347.

Skiba, M., Skiba-Lahiani, M., Marchais, H., Duclos, R. and Arnaud, P. **(2000)** Stability assessment of ketoconazole in aqueous formulations. *Int. J. Pharm.,* 198: 1-6.

Smith, B. C. **(2000)** fundamentals of fourier transform infrared spectroscopy. CRC Press LLC , Florida. Pp 15-53.

Soliman, O. A., Kimura, K., Hirayama, F., Uekama, K., E1-Sabbagh, H. M., Abd E1-Gawad, A. H. and Hashim, F. M. **(1997)** Amorphous spironolactone-hydroxypropylated cyclodextrin complexes with superior dissolution and oral bioavailability. *Int. J. Pharm.,* 149: 73-83.

Staub, I. and Bergold, A. M. **(2004)** Determination of Ketoconazole in Shampoo by High Performance Liquid Chromatography. *Acta Farm. Bonaerense,* 23 :387-390.

Stella, V. J. and He, Q. **(2008)** Cyclodextrins. *Toxicol. Pathol.,* 36: 30-42.

Stendal, C. **(1997)** Practical Guide to gastrointestinal Function testing. In: anatomy of the digestive system. Blackwell Science Ltd., London. Pp 1-25.

Streubel, A., Siepmann, J. and Bodmeier, R. **(2006)** Drug delivery to the upper small intestine window using gastroretentive technologies. *Curr. Opin. Pharmacol.,* 6: 501–508.

Strydom, S., Liebenberg, W., Yu, L., de Villiers, M. **(2009)** The effect of temperature and moisture on the amorphous-to-crystalline transformation of stavudine. *Int. J. Pharm.,* 379:72-81.

Suleiman, M. S. and Najib, N. **(1989)** Isolation and physicochemical characterization of solid forms of glibenclamide. *Int. J. Pharm.,* 50: 103-109.

Surana, R., pyne, A. and Suryanarayanan, R. **(2004)** Effect of Aging on the Physical Properties of Amorphous Trehalose. *Pharm. Res.,* 21: 867-874.

Szejtli, S. **(1997)** Utilization of cyclodextrins in industrial products and processes. *J. Mater. Chem.,* 7: 575–587.

Takada, A., Nail, S. L. and Yonese, M. **(2009)** Influence of ethanol on physical state of freeze-dried mannitol. *Pharm. Res.,* 5: 1112-1120.

Takano, R., Sugano, K., Higashida, A., Hayashi, Y., Machida, M., Aso, Y. and Yamashita, S. **(2006)** Oral absorption of poorly water-soluble drugs: computer simulation of fraction absorbed in humans from a miniscale dissolution test. *Pharm. Res.,* 23: 1144-1156.

Takeuchi, H., Nagira, S., Yamamoto, H., Kawashima, Y. **(2005)** Solid dispersion particles of amorphous indomethacin with fine porous silica particles by using spray-drying method. *Int. J . Pharm.,* 293: 155-164.

Taneri, F., Güneri, T., Aigner, Z. N. and Kata, M. **(2002)** Improvement in the physicochemical properties of ketoconazole through complexation with cyclodextrin derivatives. *J. Incl. Phenom. and Macro. Chem.,* 44: 257–260.

Tang, X. and Pikal, M. J. **(2004)** Design of freeze drying processes for pharmaceuticals: Practical Advice. *Pharm. Res.,* 21: 191-200.

Tashtoush, B. M., Al-Qashi, Z. S. and Najib, N. M. **(2004)** In vitro and in vivo evaluation of glibenclamide in solid dispersion systems. *Drug Dev. Ind. Pharm.* 30: 601-607.

Telang, C., Mujumdar, S. and Mathew, M. **(2009)** Improved physical stability of amorphous state through acid base interactions. *J. Pharm. Sci.,* 98: 2149-2159.

Temesvàri, I., Liptay, G. and Pungor, E. **(1971)** Determination of maleic acid and fumaric acid in the presence of each other by thermal analysis. *J. Therm. Anal.,* 3: 293-295.

Ticehurst, M. D., Basford, P. A., Dallman, C. I., Lukas, T. M., Marshall, P. V., Nichols, G. and Smith, D. **(2000)** Characterisation of the influence of micronisation on the crystallinity and physical stability of revatropate hydrobromide. *Int. J. Pharm.,* 193: 247-259.

Timmins, P., Marathe, P. H., Cave, G., Arnold, M. E., Dennis, A. B. and Greene, D. S. **(2006)** Development of a glyburide-metformin fixed combination tablet with optimized glyburide particle size. *Drug Dev. Ind. Pharm.,* 66: 25–35.

Torres-Labandeira, J. J. **(1996)** Characterization and in vitro dissolution behaviour of ketoconazole/β-cyclodextrin and 2-hydroxypropyl-β-cyclodextrin inclusion compounds. *Int. J. Pharm.,* 143: 203-210.

Tortora, G. J. and Grabowski, S. R. **(2003)** The digestive system In: Principles of anatomy and physiology., 10 th ed., John Wiley & Sons, Inc., USA. Pp 851-891.

Tran, T. T., Tran, P. H., Choi, H. G., Han, H. K., Lee, B. J. **(2010)** The roles of acidifiers in solid dispersions and physical mixtures. *Int. J. Pharm.,* 384: 60-66.

Tsong,, V. P., Sathe, Y. and Liu, J. **(1998)** In-vitro dissolution profile comparison-statistics and analysis of the similarity factor, f_2. *Pharm. Res.,* 15: 889-896.

Uchino, T., Yasuno, N., Yanagihara, Y. and Suzuki, H. **(2007)** Solid dispersion of spironolactone with porous silica prepared by the solvent method. *Pharmazie,* 62: 599–603.

Valleri, M., Mura, P., Maestrelli, F., Cirri, M. and Ballerini, R. **(2004)** Development and evaluation of glyburide fast dissolving tablets using solid dispersion technique. *Drug Dev. Ind. Pharm.,* 30: 525-534.

Van den Mooter, G., Wuyts, M., Blaton, N., Busson, R., Grobet, P., Augustijns, P., and Kinget, R. **(2001)** Physical stabilisation of amorphous ketoconazole in solid dispersions with polyvinylpyrrolidone K25. *Eur. J. Pharm.,* 12: 261–269.

van Drooge, D. J., Hinrichs, W. L., Dickhoff, B. H., Elli, M. N., Visser, M. R., Zijlstra, G. S. and Frijlink, H. W. **(2005)** Spray freeze drying to produce a stable Delta(9)-tetrahydrocannabinol containing inulin-based solid dispersion powder suitable for inhalation. *Eur. J. Pharm. Sci.,* 26: 231-240.

van Drooge, D. J., Hinrichs, W. L., Frijlink, H. W. **(2004a)** Anomalous dissolution behaviour of tablets prepared from sugar glass-based solid dispersions. *J. Control. Release.,* 97: 441-452.

van Drooge, D. J., Hinrichs, W. L., Wegman, K. A., Visser, M. R., Eissens, A. C. and Frijlink, H. W. **(2004b)** Solid dispersions based on inulin for the stabilisation and formulation of delta 9-tetrahydrocannabinol. *Eur. J. Pharm. Sci.*, 21: 511-518.

van, Drooge, D. J., Hinrichs, W. L., Visser, M. R. and Frijlink, H. W. **(2006)** Characterization of the molecular distribution of drugs in glassy solid dispersions at the nano-meter scale, using differential scanning calorimetry and gravimetric water vapour sorption techniques. *Int. J. Pharm.*, 310: 220-229.

Vanderhoff, J. W. **(1993)** Recent advances in the preparation of latexes. *Chem. Eng. Sci.*, 48: 203-217.

Vasanthavada, M., Tong, W. Q. and Serajuddin, A. T. M. **(2008)** Development of Solid Dispersions for Poorly Water-Soluble Drugs. In: Water-Insoluble Drug Formulations. Liu, R., (Ed.) Informa Health-care, New York. Pp 149-184.

Vasconcelos, T., Sarmento, B. and Costa, P. **(2007)** Solid dispersion as a strategy to improve oral bioavailability of poor water soluble drugs. *Drug Discovery Today*, 12: 1068-1075.

Verma, R. k. and Garg, S. **(2005)** Selection of excipients for extended release formulations of glipizide through drug–excipient compatibility testing. *J. Pharm. Biomed. Ana.*, 38: 633–644.

Vippagunta, S. R., Wang, Z., Hornung, S. and Krill, S. L. **(2007)** Factors affecting the formation of eutectic solid dispersions and their dissolution behaviour. *J. Pharm. Sci.*, 96: 294-304.

Viseras, C. , Salem, I. I., Galan, I. C. R., Galan, A. C. and Galindo, A. L. **(1995)** The effect of recrystallisation on the crystal growth, melting point and solubility of ketoconazole. *Thermochimica Acta*, 268: 143-151.

Waard, H., Hinrichs, W. L. J., Visser, M. R., Bologna, C. and Frijlink, H. W. **(2008)** Unexpected differences in dissolution behaviour of Tablets prepared from solid dispersions with a surfactant physically mixed or incorporated. *Int. J. Pharm.*, 349: 66–73.

Waghmare, A., Pore, Y. and Kuchekar, B. **(2008)** Development and Characterization of Zaleplon Solid Dispersion Systems: A Technical Note. *AAPS PharmSciTech*, 9: 536-543.

Wang, X., Michoel, A. and Mooter, G. **(2005)** Solid state characteristics of ternary solid dispersions composed of PVP VA64, Myrj 52 and itraconazole. *Int. J. Pharm.*, 303: 54-61.

Wang, X., Michoel, A. and Van den Mooter, G. **(2004)** Study of the phase behaviour of polyethylene glycol 6000-itraconazole solid dispersions using DSC. *Int. J. Pharm.*, 27: 181-187.

Webb, S. D., Page, R. C., Jay, M., Bummer, P. M. **(2002)** Characterization and validation of the gamma-scintigraphic method for determining liquid holdup in foam. *Appl. Radiat. Isot.*, 57: 243-55.

Wei, H., Dalton, C., Maso, M. D., Kanfer, I. and Löbenberg, R. **(2008)** Physicochemical characterization of five glyburide powders: a BCS based approach to predict oral absorption. *Eur. J. Pharm. Biopharm.*, 69: 1046–1056.

Wesseling, M. and Bodmeier, R. **(1999)** Drug release from beads coated with an aqueous colloidal ethylcellulose dispersion, Aquacoat, or an organic ethylcellulose solution. *Eur. J. Pharm. Biopharm.*, 47: 33–38.

Wilding, I. **(1999)** Evolution of biopharmaceutics classification system (BCS) to oral modified release (MR) formulations, what do we need to consider? *Eur. J. Pharm. Sci.*, 8: 157-159.

Wilding, I. R., Coupe, A. J. and Davis, S. S. **(2001)** The role of gamma-scintigraphy in oral drug delivery. *Adv. Drug Deliv. Rev.*, 46: 103-124.

Wilson, C. G. **(2000)** gastrointestinal transit and drug absorption. In: Oral drug Absorption: Prediction and Assessment. Dressman, J. B. (Ed.) Volume 106, Marcel Dekker, Inc., New York. Pp 1-11.

Winstanley, P. A. and Orme, M. L. E. **(1989)** The effects of food on drug bioavailability. *Br. J. Clin. Pharmac.,* 28: 621-628.

Wu, T., Yu, L., **(2006)** Surface crystallization of indomethacin below T_g. *Pharm. Res.,* 23, 2350–2355.

Yalkowsky, S. H. **(1999)** Solubility and solubilisation in aqueous media. Oxford University Press, New York.

Yamashita, K., Nakate, T., Okimoto, K., Ohike, A., Tokunaga, Y., Ibuki, R., Higaki, K., Kimura, T. **(2003)** Establishment of new preparation method for solid dispersion formulation of tacrolimus. *Int. J. Pharm.,* 267: 79-91.

Yassin, A. E., Alanazi, F. K., El-Badry, M., Alsarra, I. A., Barakat, N. S. and Alanazi, F. K. **(2009)** Preparation and characterization of spironolactone-loaded gelucire microparticles using spray-drying technique. *Drug Dev. Ind. Pharm.,* 35: 297-304.

Yonemochi, E., Inoue, Y., Buckton, G., Moffat, A., Oguchi, T. and Yamamoto, K. **(1999)** Differences in crystallisation behaviour between quenched and ground amorphous ursodeoxycholic acid. *Pharm. Res.,* 16: 835-840.

Yoshioka, S. and Stella, V. J. **(2000)** Stability of drugs and dosage forms. Kluwer Academic/Plenum Publishers, New York. Pp 139-186.

Yu, L. X. and Amidon, G. L. **(1999)** A compartmental absorption and transit model for estimating oral drug absorption. *Int. J. Pharm.,* 186: 119-25.

Yu, L. X., Crison, J. R. and Amidon, G. L. **(1996)** Compartmental transit and dispersion model analysis of small intestinal transit flow in humans. *Int. J. Pharm.,* 140: 111-118.

Zahedi, P. and Lee, P. I. **(2007)** Solid molecular dispersions of poorly water-soluble drugs in poly(2-hydroxyethyl methacrylate) hydrogels. *Eur. J. Pharm. Biopharm.,* 65: 320-328.

Zajc, N., Obreza, A., Bele, M. and Srcic, S. **(2005)** Physical properties and dissolution behaviour of nifedipine/mannitol solid dispersions prepared by hot melt method. *Int. J. Pharm.,* 291: 51-58.

Zerrouk, N., Chemtob, C., Arnaud, P., Toscani, S. and Dugue, J. **(2001)** In vitro and in vivo evaluation of carbamazepine-PEG 6000 solid dispersions. *Int. J. Pharm.,* 225: 49-62.

Zerrouk, N., Corti, G., Ancillotti, S., Maestrelli, F., Cirri, M. and Mura, P. **(2006)** Influence of cyclodextrins and chitosan, separately or in combination, on glyburide solubility and permeability. *Eur. J. Pharm. Biopharm.,* 62: 241-246.

Zhang, G. G., Law, D., Schmitt, E. A. and Qiu, Y. **(2004)** Phase transformation considerations during process development and manufacture of solid oral dosage forms. *Adv. Drug Deliv. Rev.,* 56: 371-390.

Zhou, D., Grant, D. J., Zhang, G. G., Law, D. and Schmitt, E. A. **(2007)** A calorimetric investigation of thermodynamic and molecular mobility contributions to the physical stability of two pharmaceutical glasses. *J. Pharm. Sci.,* 96: 71-83.

Zhou, R., Moench, P., Heran, C., Lu, X., Mathias, N., Faria, T. N., Wall, D. A., Hussain, M. A., Smith, R. L. and Sun, D. **(2005)** pH-dependent dissolution in vitro and absorption in vivo of weakly basic drugs: development of a canine model. *Pharm. Res.,* 22: 188-192.

Zhu, Q., Taylor, L. S. and Harris, M. T. **(2010)** Evaluation of the Microstructure of Semicrystalline Solid Dispersions. *Mol. Pharm.,* 7: 1291-1300.